EMERGING INFECTIOUS DISEASES®

CDC
Centers for Disease Control and Prevention

High-Consequence Pathogens

May 2019

Giovanni Battista Foggini (1652–1725), *Laocöon* (c. 1720). Bronze, 22 1/16 in × 17 5/16 in × 8 5/8 in/56 cm × 44 cm x 21.9 cm. Digital image courtesy of the Getty's Open Content Program, The J. Paul Getty Museum, Los Angeles, CA, USA.

EMERGING INFECTIOUS DISEASES®

Emerging Infectious Diseases is published monthly by the Centers for Disease Control and Prevention, 1600 Clifton Rd NE, Mailstop H16-2, Atlanta, GA 30329-4027, USA. Telephone 404-639-1960, fax 404-639-1954, email eideditor@cdc.gov.

EMERGING INFECTIOUS DISEASES®

High-Consequence Pathogens **May 2019**

On the Cover

Giovanni Battista Foggini (1652–1725), *Laocöon* (c. 1720). Bronze, 22 1/16 in × 17 5/16 in × 8 5/8 in/56 cm × 44 cm x 21.9 cm. Digital image courtesy of the Getty's Open Content Program, The J. Paul Getty Museum, Los Angeles, CA, USA.

About the Cover p. 1035

Synopsis

Research

EMERGING INFECTIOUS DISEASES®
May 2019

Dispatches

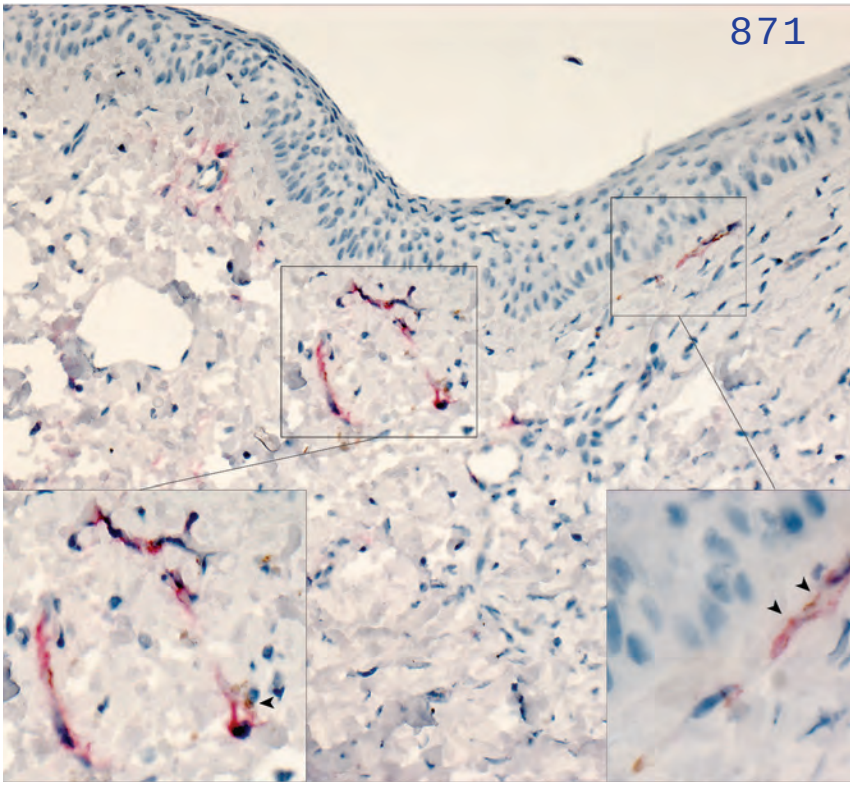

EMERGING INFECTIOUS DISEASES®
May 2019

Letters

About the Cover

Etymologia

Corrections

Vol. 24, No. 10

A grant number was listed incorrectly in Human Pegivirus in Patients with Encephalitis of Unclear Etiology, Poland (I. Bukowska-Ośko et al.).

Vol. 25, No. 2

The number of cases of West Nile neuroinvasive disease was listed incorrectly in the abstract of Acute and Delayed Deaths after West Nile Virus Infection, Texas, USA, 2002–2012 (D.C.E. Philpott et al.).

Online Reports

The World Unseen:
Intersections of Art and Science
May 20–August 30, 2019

Amie Esslinger, *Collisions*, mixed media, 2016

The World Unseen: Intersections of Art and Science gathers the work of 10 international artists who draw upon microbiology, biotechnology, anatomy, and texts in their investigations of microbes and cells, DNA, history of disease and science, the body, and beauty. Through paintings, drawings, installations, and videos, these artists ponder the humanistic and scientific implications of knowing and seeing what we normally cannot see.

DAVID J. SENCER
CDC MUSEUM
History·Legacy·Innovation

The David J. Sencer CDC Museum, a Smithsonian Affiliate, uses award-winning exhibitions, dynamic educational programming, and physical and web archives to educate visitors about the value of public health, while presenting the rich heritage and vast accomplishments of CDC.

Hours

Monday–Wednesday: 9 a.m.–5 p.m.
Thursday: 9 a.m.–7 p.m.
Friday: 9 a.m.–5 p.m.
Closed weekends and federal holidays

Location

1600 Clifton Road, NE
Atlanta, GA
30329-4021
Phone (404) 639-0830

Admission and parking free
Vehicle inspection required
Government-issued photo ID required for adults over the age of 18
Passport required for non-U.S. citizens

Outbreak of Nontuberculous Mycobacteria Joint Prosthesis Infections, Oregon, USA, 2010–2016

Genevieve L. Buser,[1,2] Matthew R. Laidler,[1] P. Maureen Cassidy, Heather Moulton-Meissner, Zintars G. Beldavs, Paul R. Cieslak

We investigated a cluster of *Mycobacterium fortuitum* and *M. goodii* prosthetic joint surgical site infections occurring during 2010–2014. Cases were defined as culture-positive nontuberculous mycobacteria surgical site infections that had occurred within 1 year of joint replacement surgery performed on or after October 1, 2010. We identified 9 cases by case finding, chart review, interviews, surgical observations, matched case–control study, pulsed-field gel electrophoresis of isolates, and environmental investigation; 6 cases were diagnosed >90 days after surgery. Cases were associated with a surgical instrument vendor representative being in the operating room during surgery; other potential sources were ruled out. A tenth case occurred during 2016. This cluster of infections associated with a vendor reinforces that all personnel entering the operating suite should follow infection control guidelines; samples for mycobacterial culture should be collected early; and postoperative surveillance for <90 days can miss surgical site infections caused by slow-growing organisms requiring specialized cultures, like mycobacteria.

Rapidly growing environmental nontuberculous mycobacteria (NTM), including *Mycobacterium abscessus*, *M. chelonae*, and *M. fortuitum*, are uncommon but recognized causes of difficult-to-eradicate implant-associated infections (*1*–*3*). NTM prosthetic joint surgical site infections are associated with severe disease and require debridement, prosthesis excision, and prolonged administration of intravenous and broad spectrum antimicrobial drugs before prosthesis reimplantation (*3*,*4*). Such infections can result from inoculation of the surgical field or prosthesis during a surgical or medical procedure or from environmental contamination during the early postoperative period (*5*). A common potential source of infection, contaminated water, is not always identified despite thorough investigation (*6*). A less common source of implant-associated infections is transient NTM colonization of human hair and body sites (*7*,*8*). Rahav et al. showed how a hirsute surgeon, colonized with *M. jacuzzii* through frequent hot tub use, shed organisms during multiple breast implant surgeries (*7*). The investigators halted the outbreak by decolonizing the surgeon's skin and hair and increasing operative infection control barriers.

In Oregon, USA, nonpulmonary, non–*Mycobacterium avium* complex NTM invasive isolates are uncommonly identified. During 2005–2006, a statewide laboratory survey of clinical microbiology isolates identified 28 *M. fortuitum*–group and 3 *M. goodii* isolates (*9*). During 2011, however, infection preventionists from 2 hospitals in the same region of Oregon reported 2 *M. goodii* prosthetic hip infections in close succession (cases 1 and 2; Table). A lack of additional cases that year precluded finding a statistical association with a common source. On January 1, 2014, extrapulmonary NTM isolates became reportable in Oregon (*10*). In May 2014, the same 2 hospitals and a third hospital in the region reported 4 *M. fortuitum* infections after prosthetic hip and knee implantations performed during July–December 2013 (cases 3, 4, 6, and 7). Root-cause analysis did not identify a common source. We launched an epidemiologic investigation to describe the cluster, determine the infection source, and guide control measures.

Methods

Case Definition and Ascertainment

We reviewed surgical site infection cases reported by Oregon hospitals to the National Healthcare Safety Network (NHSN) during January 2009–May 2014 (*11*). A case was defined as a culture-positive NTM prosthetic joint surgical site infection within 1 year of joint replacement surgery performed in an Oregon patient on or after October 1, 2010.

Author affiliations: Oregon Health Authority, Portland, Oregon, USA (G.L. Buser, M.R. Laidler, P.M. Cassidy, Z.G. Beldavs, P.R. Cieslak); Centers for Disease Control and Prevention, Atlanta, Georgia, USA (H. Moulton-Meissner)

DOI: https://doi.org/10.3201/eid2505.181687

[1]These authors were co-principal investigators and contributed equally to this article.

[2]Current affiliation: Providence Health and Services, Portland, Oregon, USA.

Table. Characteristics of 9 nontuberculous mycobacterial knee and hip prosthetic joint SSIs at multiple hospitals, Oregon, 2010–2014*

Case no.	Prosthesis type	Procedure year	SSI type	*Mycobacterium* species	Time to SSI, d†	SSI to culture, d‡	Time to culture, d§
1	Hip	2010	Unknown	*M. goodii*	157	0	157
2	Hip	2010	Organ space	*M. goodii*	35	35	70
3	Knee	2013	Deep incision	*M. fortuitum*	70	22	92
4	Knee	2013	Superficial incisional	*M. fortuitum*	85	0	85
5	Hip	2013	Organ space	*M. fortuitum*	78	54	132
6	Knee	2013	Organ space	*M. fortuitum*	69	34	103
7	Knee	2013	Organ space	*M. fortuitum*	69	30	99
8	Hip	2014	Suture abscess	*M. fortuitum*	86	14	100
9	Hip	2014	Organ space	*M. fortuitum*	83	1	84

*SSI identification date: National Health Safety Network event date, chart review, or specimen culture collection date. Case 10 not included in analysis. SSI, surgical site infection.
†From time of surgery to SSI identification date. Median 78 d.
‡From time of SSI identification to mycobacterial specimen culture collection date. Median 22 d.
§From time of surgery to mycobacterial specimen culture collection date. Median 99 d.

NHSN uses standardized definitions to harmonize healthcare-associated infection surveillance across US medical facilities. Oregon hospitals have been required to report knee prosthesis infections since 2009 and hip prosthesis infections since 2011. To identify cases not captured by NHSN surveillance, we queried healthcare providers within Oregon by using the Oregon Health Alert Network (*12*) and nationally by using *Epi-X* (*13*) and MedWatch (*14*).

Chart Review

Case medical charts were reviewed by epidemiologists who used a modified version of the Centers for Disease Control and Prevention (CDC) healthcare-associated infection chart abstraction form to identify common exposures (e.g., hospital, surgery date, surgery type, prosthesis type and brand, surgeon, anesthesiologist, surgical assistants, vendor representatives, medications, surgical joint cement, and location to which patient was discharged) (*15*,*16*). We reviewed the following patient characteristics and exposures: municipal water source by address, postoperative wound care, and rehabilitation facility. To delineate the timeline of NTM surgical site infection identifications, we calculated 1) time from implantation surgery date to surgical site infection identification date, 2) time from surgical site infection identification date to mycobacterial culture specimen collection date, and 3) total time from implantation surgery date to mycobacterial culture specimen collection date (Figure 1). Surgical site infection identification date was defined as 1) NHSN event date; 2) date of clinical diagnosis as determined by chart review, if NHSN event date unavailable; or 3) specimen collection date, if information for the first 2 criteria was unavailable. Rapidly growing NTM are typically detected after 7–10 days of incubation on mycobacterial growth media.

Interviews and Observations

To ascertain surgical instrument sterilization and implant inventory management practices, we interviewed infection preventionists in the 4 hospitals where case surgeries had been performed. We observed 3 joint prosthesis surgeries to assess general surgical procedures, generate hypotheses, and identify potential sources of surgical site contamination.

Case–Control Study

To test associations between infection and exposures ascertained from chart review, including surgery records, we performed a 1:4 matched case–control study. We matched controls by hospital and type of prosthesis surgery (hip vs. knee) and restricted controls to surgeries performed within 6 months of the matched-case surgery date. Variables evaluated included surgeon, other operating room staff, time of day of surgery, patient age (>65 vs. ≤65 years), orthopedic device manufacturer, and surgeon orthopedic practice. We conducted analysis by using exact methods for matched data (SAS version 9.3, https://www.sas.com).

Investigation of Clinical Specimens and Environment

Clinical isolates were available from all patients. Identification of isolates was confirmed by 16s rRNA gene sequencing. Pulsed-field gel electrophoresis (PFGE) was performed at CDC (National Center for Emerging and Zoonotic Infectious Diseases, Division of Healthcare Quality Promotion) as follows: chromosomal DNA was digested with the restriction endonuclease AseI (*17*), and restriction fragments were separated with a CHEF Mapper XA Pulsed-Field Electrophoresis System (Bio-Rad Laboratories, http://www.bio-rad.com) and analyzed for relatedness by BioNumerics software (Applied Maths, http://www.applied-maths.com). Similarity of PFGE patterns was based on Dice coefficients, and a

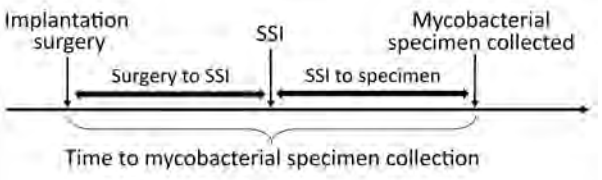

Figure 1. Time interval definitions used in investigation of mycobacterial prosthetic joint SSIs, Oregon, USA, 2010–2016. SSI, surgical site infection.

dendrogram was built by using the unweighted pair group method. The Tenover criteria were used to classify comparisons of patient isolate PFGE patterns as indistinguishable (100% similarity), closely related (1–3-band difference), possibly related (4–6 band difference), or unrelated (≥7 band difference) (*18*). Environmental investigation was based on investigation results, findings from published NTM investigations (*7*,*8*), and expert consultation with CDC.

Results

Descriptive Epidemiology

In addition to the 2 cases of unknown exposure source from 2011 and the 4 cases reported during May 2014, review of NHSN data identified a previously unreported case of *M. fortuitum* prosthetic hip infection from the same Oregon healthcare region during 2013 (case 5). Queries of the Oregon Health Alert Network, *Epi-X*, and MedWatch did not identify additional cases or prosthesis recalls in Oregon or other US states. Cases 8 and 9 occurred during the investigation (Table).

We identified a total of 7 *M. fortuitum* and 2 *M. goodii* surgical site infections involving 4 knee and 5 hip prostheses; 5 were deep organ space infections. Patients were 46–79 (median 68) years of age, and 5 were female and 4 male; none had signs of infection at the time of prosthesis placement. Surgeries were performed at 4 hospitals by 6 different surgeons. Surgeries were performed during October 2010–June 2014; corresponding infection onsets occurred during January 2011–September 2014. Cases clustered in July (3 cases) and October (3 cases); others occurred in May, June, November, and December (1 case each) (Figure 2). Time from implantation surgery to surgical site infection identification was 35–157 (median 78) days (Table), from surgical site infection identification to mycobacterial specimen collection was 0–54 (median 22) days, and from implantation to specimen collection for mycobacterial culture was 70–157 (median 99) days. For 6 (67%) patients, ≥90 days elapsed between implantation and collection of the specimen for mycobacterial culture that yielded NTM.

Case–Control Study

NTM surgical site infections were significantly associated with implantation of a brand A prosthesis (unadjusted matched odds ratio [mOR] 27.7, 95% CI 5.3–∞; p = 0.0002), with surgeon A (mOR 15.4, 95% CI 2.3–∞; p = 0.016), and with the presence of person A (a brand A vendor) in the operating room during surgery (mOR 32.4, 95% CI 6.3–∞; p = 0.0001). All case-patients had brand A prostheses implanted, but the devices and lot numbers differed. Surgeon A was present at only 3 of the 9 surgeries and did not perform any surgeries at 2 of the hospitals. Person A was the brand A prosthesis vendor representative at all 4 hospitals, and operating room records documented person A's presence at all surgeries except that of case 5 (8 [89%] of 9 patients).

Interviews and Observations

During 3 observed surgeries (not attended by person A), lapses in operating room infection control standards by other prosthesis vendor representatives were observed. Lapses included uncovered arms, uncovered hair and beards, and breaches of the vertical sterile field boundary over the surgical instrument table.

Infection preventionists reported that vendors regularly transport loaner instruments for prosthetic surgeries between

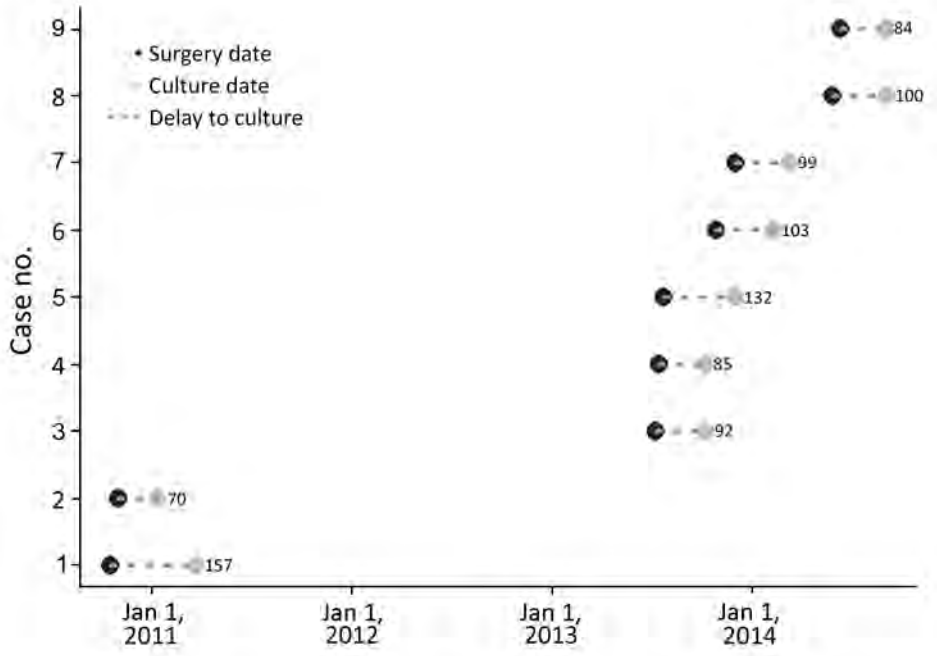

Figure 2. Time intervals between knee and hip prosthetic joint surgery to collection of surgical site mycobacterial cultures yielding related nontuberculous mycobacteria, multiple hospitals, Oregon, 2010–2014 (n = 9). Numbers indicate total number of days from surgery (black dots) to culture collection (gray dots). Case 10 is not included.

hospitals; hospital policies require, and infection preventionists confirmed, that before surgical use such instruments are reprocessed according to each facility's internal standards. Person A reported similar loaner instrument practices and did not report using or transporting other undocumented tools or instruments into the surgeries involved in the outbreak reported here. None of the 4 hospitals reported failures of biological indicators of sterilization during the period investigated.

Clinical Specimens

PFGE indicated that *M. goodii* isolates from cases 1 and 2 were closely related. *M. fortuitum* isolates from cases 7 and 9 were indistinguishable (100% similarity). Isolates from cases 3, 4, 5, and 6 were closely related to isolates from cases 7 and 9 (1–3 band differences, >89% similarity); and the isolate from case 8 was possibly related to isolates from cases 3, 4, 5, 6, 7, and 9 (4–6 band differences, >87% similarity) (Figure 3).

Environmental Specimens

On the basis of the above findings, on 1 day we collected environmental and human samples from the home of person A. Environmental samples were collected from person A's hot tub water, filter, cover, and headrest; bathroom showerhead and faucet aerators; washing machine; cell phone; and touch computer screen. Human samples from person A included skin; scalp hair; eyebrows; facial hair; and swab specimens of nares, ears, and hands. Specimens were shipped directly to CDC for immediate processing and culture. Acid-fast isolates were identified by 16s rRNA sequencing. On the same day as sample collection, a registered environmental health specialist reviewed person A's hot tub maintenance processes on site.

In total, we collected 16 environmental samples from person A's residence and 9 samples directly from person A. *M. fortuitum* was isolated from person A's hands, but the strain was genetically unrelated to the outbreak isolates (Figure 3). Culture of environmental samples yielded heavy growth of non-NTM bacteria, and none yielded slow-growing NTM. Person A reported doing yard work and using a personal outdoor hot tub daily; however, hot tub water chlorination and pH were not routinely monitored. At the time of specimen collection, hot tub water pH was >8.0 (optimal pH for chlorinated tubs is 7.4–7.6) (*19*).

Infection Control Response

When cases 8 and 9 were reported during the investigation, the Oregon Health Authority Public Health Division recommended immediate sequestration of remaining unused, packaged brand A products and that person A complete infection control training consistent with guidance from the Association of periOperative Registered Nurses before returning to the operating suite (*20*). Hospitals involved in the outbreak required infection control training for all persons entering the operating rooms, including vendors. Operating room audits were increased to monitor guideline compliance of all staff. Person A was advised to use hot tub disinfection and chlorination practices consistent with the manufacturer's recommendations. Person A returned to work 2 months later.

Follow-Up

After 28 months of no reported outbreak cases, hospital B identified an *M. fortuitum* superficial surgical site infection 37 days after a knee prosthesis replacement surgery in which a brand B prosthetic was used (case 10). The new isolate was closely related to that of the outbreak by PFGE (3-band difference), suggesting epidemiologic linkage to the outbreak cases (Figure 3). Surgeons other than those involved in the original outbreak series performed the surgery; however, the vendor present was person A.

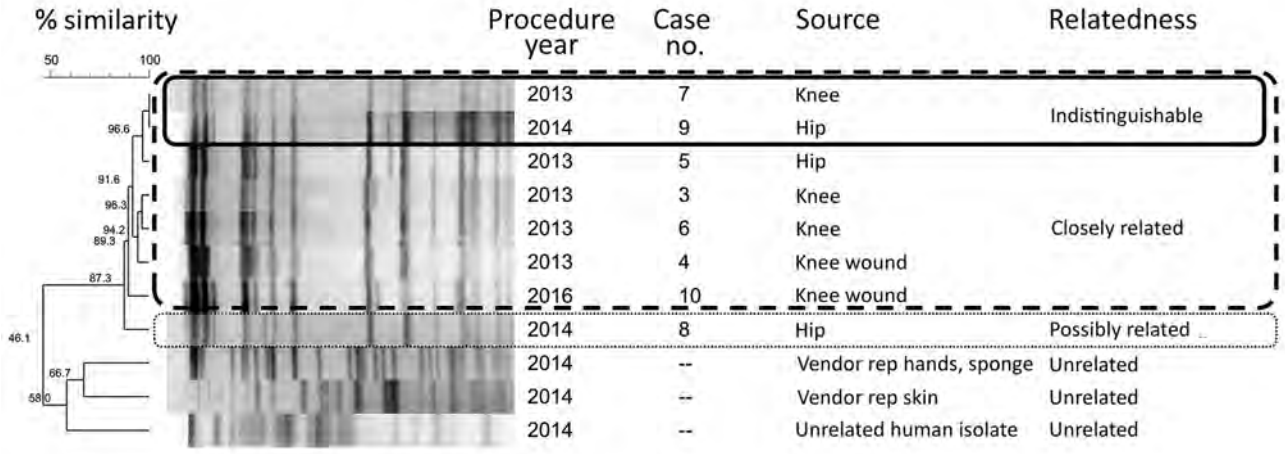

Figure 3. Dendrogram of 8 *Mycobacterium fortuitum* isolates associated with prosthetic joint surgical site infections, multiple hospitals, Oregon, 2013–2016. Boxes indicate group relatedness according to pulsed-field gel electrophoresis: solid lines, indistinguishable (no band difference); dashed lines, closely related (1–3 band difference); dotted lines, possibly related (4–6 band difference). Differences of ≥7 bands indicate not related. Rep, representative.

Discussion

Although we identified no common intraoperative water or fomite source, this uncommon geotemporal and PFGE-linked cluster of NTM prosthetic joint surgical site infections was statistically associated with the presence of a non–hospital employee (the prosthetic joint vendor, person A). Although the outbreak strain was not isolated from person A, epidemiologic evidence suggests repeated introduction of the NTM outbreak strains into multiple knee and hip prosthetic joint surgeries over 6 years and across 4 facilities. Other reports have suggested the possibility of NTM human colonization—made possible by repeated exposure to hot tub water, which, when coupled with lapses in infection control practices, leads to the entry of NTM via squamous epithelial cells or body hair shed into the sterile field (*7*,*8*,*21*,*22*). Other hypotheses include an as-yet-unidentified instrument fomite associated with person A, for which the usual hospital policy for loaner instrument sterilization was circumvented (*23*). However, sterilization process failures were not identified at any of the facilities, making simultaneous contamination of an instrument or instruments at 4 different hospitals implausible.

Most NTM surgical site infection investigations have focused on contamination by nonsterile water but did not identify a contaminated water source (*4*,*6*,*24*). Modern operating suites are constructed to avoid this known risk. Of note, isolation of an NTM strain from person A's hands supports the biological plausibility of transmission via healthcare worker contact. Persistent hand and skin colonization with NTM organisms could occur after contact with soil and water sources and other outdoor activities. Hot tubs are a known source of NTM infections, including *M. fortuitum* infections, presumably via water droplets (*25*). There is evidence that NTM can be transmitted via colonized persons, from contaminated water sources such as hot tubs, to the sterile surgical field, leading to surgical site infections (*7*,*8*). Of note, the pH of person A's hot tub water at the time of the environmental investigation was >8, which is ineffective for disinfection (*19*).

Because NTM are widespread and colonization can occur at any time, adherence to perioperative infection control guidelines by all operating suite personnel, including vendors, is necessary (*20*,*23*). Vendors are active members of the operating team and should be required to complete infection control training that meets hospital standards for other operating room personnel. Hospitals should consider sharing surgical site infection rates with product vendors to highlight their accountability in preventing surgical site infections. Even without direct patient contact, vendors could be vectors that transmit pathogens into the operating room environment via rectal or nasal colonization, spread shed skin and hair cells via air currents, or transport contaminated fomites into the operating suite (*26*,*27*).

The unusual organisms involved enabled detection of this outbreak of prosthetic joint–associated surgical site infection and the subsequent search for a source. If the pathogens had been more common surgical site infection–associated skin colonizers, such as coagulase-negative staphylococci, this outbreak could have remained undetected and persisted indefinitely. Indeed, it is possible that more typical surgical site infections stem from the operating room presence of vendors or others for whom infection prevention standards are overlooked.

Identifying and linking NTM surgical site infections is challenging for multiple reasons. Surgical teams, including vendors, can rotate among multiple hospitals, decreasing the likelihood that epidemiologically related cases will be recognized as such. Although culture on mycobacteria-specific media improves yield, mycobacterial cultures are often not sent until after the initial bacterial cultures are negative, resulting in an apparent delay in identification of NTM surgical site infection; in 6 of 9 cases in this outbreak, mycobacteria were first grown from specimens obtained >90 days postoperatively. In 2015, when NHSN shortened the postoperative infection surveillance period after knee and hip prosthesis implantation surgeries from 365 to 90 days, surveillance may have shifted toward detection of acute bacterial infections and away from detection of slow-growing NTM infections, which require special culture media.

Since January 2014, Oregon has required laboratories to report extrapulmonary NTM infections, and cases are routinely investigated by public health officials (*10*). From January 2014 through December 2017, a total of 150 cases were reported, including 2 clusters: *M. fortuitum* infections associated with abdominoplasty in an ambulatory surgery center and *M. haemophilum* infections associated with using water from a water cooler to dilute tattoo ink before subcutaneous injection (*28*,*29*). To assist surveillance in other states and territories, in 2017 the Council for State and Territorial Epidemiologists adopted a standardized case definition for extrapulmonary NTM infections (*30*). In the presence of a 90-day postoperative surveillance period, state surveillance of nonpulmonary NTM infections may provide a method for identifying these uncommon but medically complex surgical site infections.

This investigation has several limitations. Cases might have been missed despite NHSN surveillance before nonpulmonary NTM infections became reportable in Oregon in January 2014, because NHSN definitions do not include superficial surgical site infections identified >30 days after surgery (e.g., case 10). The likelihood of missing cases during the investigation was small because of extensive case finding by multiple methods, including mandatory reporting by Oregon laboratories and direct communication with infection preventionists.

Although early analysis indicated that the presence of surgeon A was significant, surgeon A did not have operating privileges at 2 of the hospitals and therefore could not have been a source of exposure for those cases. Although loaner instrument storage is not regulated outside of the hospital, all hospitals had strict reprocessing policies in place for cleaning and sterilizing trays received. In the case–control analysis, the association between person A and surgical site infection was confounded by brand A; no NTM surgical site infections linked to the brand were reported elsewhere in Oregon or nationally, suggesting that brand A per se was not a factor in the outbreak. In addition, case 10 occurred when person A was a vendor for a different prosthetic company. Although unidentified fomites associated with person A can never be summarily excluded without a direct microbiological link from an environmental source via person A to the surgical site, we believe that the totality of the epidemiologic and observational evidence leaves the most likely source of these infections to be human colonization.

All persons, including vendors, who enter operating suites should recognize that environmental exposures (e.g., hot tub bathing, gardening, field work) can colonize their hands, skin, and hair with infectious organisms such as NTM, which can then cause surgical site infections. All personnel and vendors in the operating suite should adhere to published guidelines about perioperative infection prevention, surgical attire, and environmental controls (*20*,*23*) and should be required to undergo annual infection control training. Infection preventionists should regularly observe operating room staff to verify compliance and to promptly apply any necessary corrective measures. When evaluating device-associated surgical site infections, clinicians should obtain mycobacterial along with bacterial and fungal cultures. Extrapulmonary NTM infection surveillance is an option for public health jurisdictions to increase detection of these slow-moving, but morbid, outbreaks. Finally, specialized measures like environmental and human sampling to isolate fastidious NTM organisms are recommended during investigations and could reveal the elusive microbiological link.

Acknowledgments

We acknowledge Charlene Stewart, Ruth Rabinovitch, Annette M. Stefan, Chad Peterson, Jackson Baures, Jim Shames, and Mary T. Post for assistance with the investigation; Kevin Winthrop for NTM expertise; Judith Noble-Wang and her laboratorians for assistance with specimen collection and processing; and Joseph Perz for healthcare-associated infection expertise.

CDC supported this work through the Epidemiology and Laboratory Capacity cooperative agreement with the Oregon Health Authority Public Health Division.

About the Author

Dr. Buser completed her 2011 Epidemic Intelligence Service fellowship at the Oregon Health Authority, then remained to join the Healthcare-Associated Infections team, during which time she completed this investigation. She currently works in pediatric infectious diseases and population health in Portland, Oregon.

References

1. Brown-Elliott BA, Wallace RJ Jr. Infections due to nontuberculous mycobacteria other than *Mycobacterium avium-intracellulare*. In: Mandell GL, Bennett JE, Dolin R, editors. Bennett's Principles and practice of Infectious Diseases. 7th ed. Philadelphia: Churchill Livingstone; 2009. p. 3191–98.
2. Herold RC, Lotke PA, MacGregor RR. Prosthetic joint infections secondary to rapidly growing *Mycobacterium fortuitum*. Clin Orthop Relat Res. 1987;(216):183–6.
3. Vinh DC, Rendina A, Turner R, Embil JM. Breast implant infection with Mycobacterium fortuitum group: report of case and review. J Infect. 2006;52:e63–7. http://dx.doi.org/10.1016/j.jinf.2005.07.004
4. Wang S-X, Yang C-J, Chen Y-C, Lay C-J, Tsai C-C. Septic arthritis caused by *Mycobacterium fortuitum* and *Mycobacterium abscessus* in a prosthetic knee joint: case report and review of literature. Intern Med. 2011;50:2227–32. http://dx.doi.org/10.2169/internalmedicine.50.5610
5. Cheung I, Wilson A. *Mycobacterium fortuitum* infection following total knee arthroplasty: a case report and literature review. Knee. 2008;15:61–3. http://dx.doi.org/10.1016/j.knee.2007.08.007
6. Cornelius L, Reddix R, Burchett C, Bond G, Fader R. Cluster of *Mycobacterium fortuitum* prosthetic joint infections. J Surg Orthop Adv. 2007;16:196–8.
7. Rahav G, Pitlik S, Amitai Z, Lavy A, Blech M, Keller N, et al. An outbreak of *Mycobacterium jacuzzii* infection following insertion of breast implants. Clin Infect Dis. 2006;43:823–30. http://dx.doi.org/10.1086/507535
8. Scheflan M, Wixtrom RN. Over troubled water: an outbreak of infection due to a new species of *Mycobacterium* following implant-based breast surgery. Plast Reconstr Surg. 2016;137:97–105. http://dx.doi.org/10.1097/PRS.0000000000001854
9. Cassidy PM, Hedberg K, Saulson A, McNelly E, Winthrop KL. Nontuberculous mycobacterial disease prevalence and risk factors: a changing epidemiology. Clin Infect Dis. 2009;49:e124–9. http://dx.doi.org/10.1086/648443
10. Oregon Health Authority. Extrapulmonary nontuberculous mycobacterium (NTM) Investigative Guidelines, December 2017 [cited 2018 Jun 17]. http://www.oregon.gov/oha/PH/DISEASESCONDITIONS/COMMUNICABLEDISEASE/REPORTINGCOMMUNICABLEDISEASE/REPORTINGGUIDELINES/Documents/ntm.pdf
11. Centers for Disease Control and Prevention. Surveillance for surgical site infection (SSI) events [cited 2018 Jun 17]. http://www.cdc.gov/nhsn/acute-care-hospital/ssi/index.html
12. Oregon Health Authority. Oregon Health Alert Network and HOSCAP [cited 2018 Jun 17]. http://www.healthoregon.org/han
13. Centers for Disease Control and Prevention. Epidemic Information Exchange (Epi-X) [cited 2018 Jun 17]. http://www.cdc.gov/epix
14. Food and Drug Administration. MedWatch: The FDA Safety Information and Adverse Event Reporting Program [cited 2018 Jun 17]. http://www.fda.gov/safety/medwatch/default.htm
15. Centers for Disease Control and Prevention. Healthcare-Associated Infection Outbreak Investigation Toolkit [cited 2018 Jun 17]. https://www.cdc.gov/hai/outbreaks/outbreaktoolkit.html
16. Centers for Disease Control and Prevention. Healthcare-Associated Infection Outbreak Investigation Abstraction Form [cited

2018 Jun 17]. https://www.cdc.gov/hai/pdfs/outbreaks/Response_Toolkit_Abstraction_Form-508.pdf
17. Wallace RJ Jr, Zhang Y, Brown BA, Fraser V, Mazurek GH, Maloney S. DNA large restriction fragment patterns of sporadic and epidemic nosocomial strains of *Mycobacterium chelonae* and *Mycobacterium abscessus*. J Clin Microbiol. 1993;31:2697–701.
18. Tenover FC, Arbeit RD, Goering RV, Mickelsen PA, Murray BE, Persing DH, et al. Interpreting chromosomal DNA restriction patterns produced by pulsed-field gel electrophoresis: criteria for bacterial strain typing. J Clin Microbiol. 1995;33:2233–9.
19. Centers for Disease Control and Prevention. Healthy swimming [cited 2018 Jun 17]. https://www.cdc.gov/healthywater/swimming
20. Association of periOperative Registered Nurses (AoRN) guidelines and clinical resources [cited 2018 Jun 17]. https://www.aorn.org/guidelines
21. Groenewold M, Russell ES, Konkle SL, Rice J, Giesbrecht K, Moulton-Meissner H, et al. Investigation of a cluster of rapidly-growing mycobacteria infections associated with joint replacement surgery in a Kentucky hospital. Presented at: Council of State and Territorial Epidemiologists Annual Conference; 2014 Jun 22–26; Nashville, Tennessee, USA [cited 2018 Dec 11]. https://cste.confex.com/cste/2014/webprogram/Paper3211.html
22. Lee KH, Heo ST, Choi S-W, Park DH, Kim YR, Yoo SJ. Three cases of postoperative septic arthritis caused by *Mycobacterium conceptionense* in the shoulder joints of immunocompetent patients. J Clin Microbiol. 2014;52:1013–5. http://dx.doi.org/10.1128/JCM.02652-13
23. International Association of Healthcare Central Services and Material Management. IAHCSMM loaner instrument paper [cited 2018 Jun 17]. https://www.iahcsmm.org/resource-documents/loaner-instrument-template.html
24. Porat MD, Austin MS. Bilateral knee periprosthetic infection with *Mycobacterium fortuitum*. J Arthroplasty. 2008;23:787–9. http://dx.doi.org/10.1016/j.arth.2007.07.010
25. Mangione EJ, Huitt G, Lenaway D, Beebe J, Bailey A, Figoski M, et al. Nontuberculous mycobacterial disease following hot tub exposure. Emerg Infect Dis. 2001;7:1039–42. http://dx.doi.org/10.3201/eid0706.010623
26. Mastro TD, Farley TA, Elliott JA, Facklam RR, Perks JR, Hadler JL, et al. An outbreak of surgical-wound infections due to group A Streptococcus carried on the scalp. N Engl J Med. 1990;323:968–72. http://dx.doi.org/10.1056/NEJM199010043231406
27. Centers for Disease Control and Prevention (CDC). Nosocomial group A streptococcal infections associated with asymptomatic health-care workers—Maryland and California, 1997. MMWR Morb Mortal Wkly Rep. 1999;48:163–6.
28. Centers for Disease Control and Prevention (CDC). Tattoo-associated nontuberculous mycobacterial skin infections—multiple states, 2011–2012. MMWR Morb Mortal Wkly Rep. 2012;61:653–6.
29. Conaglen PD, Laurenson IF, Sergeant A, Thorn SN, Rayner A, Stevenson J. Systematic review of tattoo-associated skin infection with rapidly growing mycobacteria and public health investigation of a cluster in Scotland, 2010. Euro Surveill. 2013;18:20553. http://dx.doi.org/10.2807/1560-7917.ES2013.18.32.20553
30. Council for State and Territorial Epidemiologists. Standardized case definition for extrapulmonary nontuberculous mycobacteria infections (17-ID-17) [cited 2018 Dec 14]. http://www.cste.org/resource/resmgr/2017PS/2017PSFinal/17-ID-07.pdf

Address for correspondence: Genevieve L. Buser, Providence St. Vincent Medical Center, 9427 SW Barnes Rd, Ste 395, Portland, OR 97225, USA; email: genevieve.buser@gmail.com

Recurrent Cholera Outbreaks, Democratic Republic of the Congo, 2008–2017

Brecht Ingelbeen,[1] David Hendrickx,[1] Berthe Miwanda, Marianne A.B. van der Sande, Mathias Mossoko, Hilde Vochten, Bram Riems, Jean-Paul Nyakio, Veerle Vanlerberghe, Octavie Lunguya, Jan Jacobs, Marleen Boelaert, Benoît Ilunga Kebela, Didier Bompangue, Jean-Jacques Muyembe

In 2017, the exacerbation of an ongoing countrywide cholera outbreak in the Democratic Republic of the Congo resulted in >53,000 reported cases and 1,145 deaths. To guide control measures, we analyzed the characteristics of cholera epidemiology in DRC on the basis of surveillance and cholera treatment center data for 2008–2017. The 2017 nationwide outbreak resulted from 3 distinct mechanisms: considerable increases in the number of cases in cholera-endemic areas, so-called hot spots, around the Great Lakes in eastern DRC; recurrent outbreaks progressing downstream along the Congo River; and spread along Congo River branches to areas that had been cholera-free for more than a decade. Case-fatality rates were higher in nonendemic areas and in the early phases of the outbreaks, possibly reflecting low levels of immunity and less appropriate prevention and treatment. Targeted use of oral cholera vaccine, soon after initial cases are diagnosed, could contribute to lower case-fatality rates.

The Democratic Republic of the Congo (DRC) accounts for an estimated 189,000 (5%–14%) of the 1.34–4.01 million cholera cases worldwide annually (*1*,*2*). *Vibrio cholerae* repeatedly reappeared in the DRC throughout the 1970s and became endemic around the Great Lakes in eastern DRC in 1978, resulting in part from favorable conditions for the bacterium's environmental survival (*3*–*6*). Complex emergencies in eastern DRC have since enabled the regular spread of cholera along the lake banks and to surrounding health zones, driven by water supply interruptions, high population densities, and population movement (*5*,*7*–*9*). In 2017, a countrywide cholera outbreak totaling >53,000 cases and 1,145 deaths was reported in DRC, affecting 20 out of 26 provinces, some of which had not seen cholera cases for more than a decade (*10*).

Cholera prevention and control rely on rapid outbreak detection, access to clean water, safe sanitation, dedicated treatment centers, and the targeted use of oral cholera vaccines (OCV) (*11*). We describe major cholera outbreaks that occurred in DRC during 2008–2017 to explore possible drivers for the spread of cholera in DRC and provide guidance for prevention and control interventions.

Methods

Study Design

We performed a retrospective analysis of cholera outbreaks from national cholera surveillance data and reference laboratory data collected from January (week 1) 2008 through November (week 46) 2017. In addition, we analyzed case management data collected during outbreaks in 2015–2017 from a selection of cholera isolation and treatment wards, called cholera treatment centers (CTCs).

Surveillance Data

Cholera is a notifiable disease in DRC and is therefore included in the national Integrated Disease Surveillance and

Author affiliations: Santé Publique France, Paris, France (B. Ingelbeen); European Centre for Disease Prevention and Control, Stockholm, Sweden (B. Ingelbeen, D. Hendrickx); Institute of Tropical Medicine, Antwerp, Belgium (B. Ingelbeen, M.A.B. van der Sande, V. Vanlerberghe, J. Jacobs, M. Boelaert); Landesgesundheitsamt Baden-Württemberg, Stuttgart, Germany (D. Hendrickx); Institut National de Recherche Biomedicale, Kinshasa, Democratic Republic of the Congo (B. Miwanda, O. Lunguya, J.-J. Muyembe); Utrecht University, Utrecht, the Netherlands (M.A.B. van der Sande); Ministère de la Santé, Kinshasa (M. Mossoko, B.I. Kebela, D. Bompangue); Médecins sans Frontières, Kinshasa (H. Vochten, B. Riems, J.-P. Nyakio); Université de Kinshasa, Kinshasa (D. Bompangue)

DOI: https://doi.org/10.3201/eid2505.181141

[1]These authors contributed equally to this article.

Response System (IDSRS). The IDSRS is a syndromic surveillance system that compiles weekly morbidity and mortality reports, aggregated at the health zone level. These reports include weekly counts of suspected cholera cases and deaths, stratified into 2 age categories, <5 years and ≥5 years.

The IDSRS uses 2 case definitions for a suspected cholera case, depending on whether a cholera outbreak has been declared by the Ministry of Health. During an outbreak, the definition is acute watery diarrhea with or without vomiting in a patient ≥1 year of age; in nonoutbreak situations, the definition is severe dehydration or death following acute watery diarrhea in a patient ≥5 years of age.

Other Definitions

The World Health Organization (WHO) defines cholera hot spots as geographically limited areas where environmental, cultural, or socioeconomic conditions make transmission of disease easier and where cholera persists or reappears regularly (*11*). In DRC, hot spots are defined at the health zone level; 26 (5.0%) of 518 health zones across 6 of 26 DRC provinces are labeled as cholera hot spots according to WHO classification (D. Legros, World Health Organization, pers. comm., 2017 Nov 17). We considered a health zone's hot spot status to be stable throughout the study period. We defined a hot spot province as a province that included ≥1 hot spot health zones (Figure 1, panel A). A non–hot spot

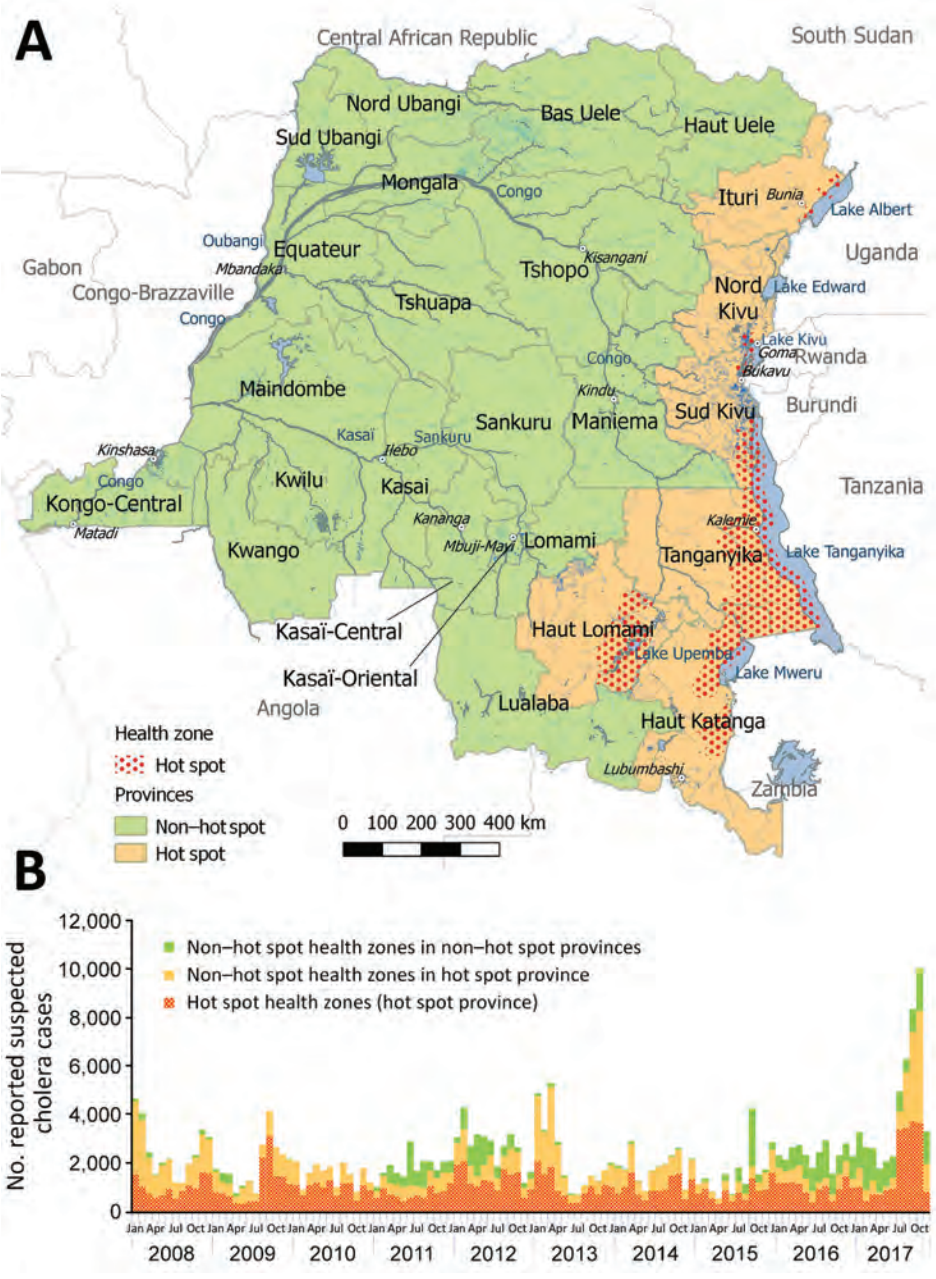

Figure 1. Hot spot and non–hot spot locations for cholera and number of suspected cases by location, Democratic Republic of the Congo, 2008–2017. A) Locations of cholera hot spot and non–hot spot provinces and hot spot health zones (2017 classification). B) Weekly number of suspected cholera cases. Case counts for 2017 are through week 46.

province was any province that did not contain any hot spot health zones.

We generally defined an outbreak as follows: ≥1 laboratory-confirmed cholera case and an increase in the number of suspected cases for ≥3 consecutive weeks. In the 3 provinces that consistently reported cholera cases all year (North Kivu, South Kivu, and Tanganyika), we applied a minimum threshold of 1,000 cases/week for ≥3 consecutive weeks. In the 2 provinces where sampling for laboratory confirmation was lacking (Ituri and Haut Lomami), we defined a major outbreak as any increase in the number of suspected cases for ≥3 consecutive weeks, reported by ≥3 different health zones.

Microbiological Data

The DRC national cholera reference laboratory, located at the Institut National de Recherche Biomédicale (INRB) in Kinshasa, carried out routine culture confirmation testing for national surveillance and outbreak confirmation purposes during the entire study period. Fecal samples or rectal swabs from patients with suspected cholera, which are usually collected at the beginning or end of suspected cholera outbreaks (*12*), were placed in either Carry-Blair transport medium or on filter paper and transported to the INRB for laboratory confirmation by culture. The following data were extracted from the laboratory database at INRB for each documented clinical sample: age, sex, health zone of residence, date of symptom onset, date of sample collection, date of sample receipt at the reference laboratory, and serotype result. Antimicrobial susceptibility testing was performed, from 2011 onward, by disk-diffusion testing according to Clinical and Laboratory Standards Institute M45-Ed3 (*13*), with testing of erythromycin instead of azithromycin and additional testing of fluoroquinolone antimicrobial drugs. Intermediate-susceptible isolates were grouped with resistant ones.

Case Management Data

Case management data were provided by 19 CTCs that Médecins sans Frontières had deployed in support of Ministry of Health cholera outbreak response activities, all in non–hot spot health zones, during 2015–2017. Médecins sans Frontières defines a case as >3 liquid stools in the previous 24 hours. From these line lists, we extracted age, sex, health zone of residence, date of symptom onset, date of admission to the CTC, and treatment outcome.

Population Data

We used population estimates by health zone for 2006 and 2016 provided by the Expanded Programme of Immunization to extrapolate the population of individual health zones for each year during 2008–2017, under the assumption of stable population growth. To ensure comparability of our data throughout the study period, we also used the DRC administrative divisions that were adopted in 2015 (26 provinces, instead of the previous 11) for 2008–2014 data.

Data Analysis

We analyzed weekly trends in the number of suspected cholera cases reported to the IDSRS, age and sex distributions, and case-fatality rates (CFRs) over the entire period, stratified by cholera hot spot status. We also calculated age and sex distributions for confirmed cases and cases admitted to CTCs, based on the reference laboratory register and CTC data. CFRs for persons with suspected cholera and for admitted patients were calculated with the cholera deaths as numerator (IDSRS data) and the suspected or admitted cholera cases as denominator (CTC data). We described the geographic spread of suspected cholera cases over time by mapping annual cumulative incidence rates by health zone. All reported cumulative incidence rates were expressed as suspected cholera cases per 100,000 population.

We performed data collation, cleaning, and analysis using Microsoft Excel (Microsoft, http://www.microsoft.com), Stata 12.0 (StataCorp LP, https://www.stata.com/stata12), and R (The R Project for Statistical Computing, https://www.r-project.org) software. Maps were generated in QGIS 2.18 (Open Source Geospatial Foundation, https://www.osgeo.org) using OpenStreetMap shapefiles.

Ethics Statement

We analyzed databases that contained routinely collected and aggregated surveillance data and anonymized laboratory and patient admission data. For the use of patient admission data, we obtained ethics approval (ref. ESP/CE/034/2017) from the Kinshasa University Ethics Committee.

Results

General Description of Cholera Cases

During January 1, 2008–November 19, 2017, a total of 270,852 suspected cholera infections and 5,231 cholera-related deaths (CFR 1.9%) were reported in DRC in all 26 provinces. The largest cholera outbreaks were reported in 2008, 2009, late 2011 through 2012, early 2013, and late 2015 through 2017 (Table 1; Figure 1, panel B). Of the 9,510 (3.5%) suspected cholera cases for which the national reference laboratory received samples, 2,941 (30.9%), or 1.1% of all suspected cholera cases reported to the IDSRS, were laboratory confirmed for cholera.

Almost half of all suspected cholera cases (127,642; 47.1%) were reported in the 26 hot spot health zones and 224,212 (82.8%) in hot spot provinces. Of the remaining 46,640 suspected cases that were reported in non–hot spot provinces, 42,340 (90.8%) were reported during the outbreaks in 2011–2012 and 2015–2017.

Table 1. Suspected cases reported and number of samples collected, tested, and confirmed, countrywide, during cholera outbreaks, Democratic Republic of the Congo, 2008–2017

Location	Period	No. suspected cases			No. samples collected (% positive)			Serotype		
		Age <5 y	Age ≥5 y	Total	Age <5 y	Age ≥5 y	Total	Inaba	Ogawa	Hikojima
DRC	Jan 2008–Nov 2017	66,008	204,483	270,852	2,028 (34)	7,482 (30)	9,510 (31)	2,612	274	7
Reported outbreaks* in hot spot provinces										
North Kivu, South Kivu, Tanganyika	Aug–Nov 2009	1,935	9,641	11,652	20 (50)	189 (33)	209 (35)	11	63	0
North Kivu, South Kivu, Tanganyika	Aug–Nov 2017	6,653	14,709	21,362	5 (20)	41 (27)	46 (26)	5	7	0
Haut Katanga	Jan–Mar 2008	1,278	4,712	5,990	3 (67)	16 (50)	19 (53)	7	0	0
Haut Katanga	Jan–Apr 2013	1,935	6,504	8,441	1 (100)	11 (55)	12 (58)	4	3	0
Haut Lomami	Jan–Dec 2014	1,285	3,359	4,644	0	0	0	0	0	0
Ituri	Jan–Sep 2012	828	3,868	4,696	0	0	0	0	0	0
Reported outbreaks* in non–hot spot provinces										
Congo River	Jan 2011–Dec 2012	2,809	11,878	14,686	89 (30)	578 (26)	667 (27)	179	0	0
Congo River	Sep 2015–2017	4,991	20,330	25,422	123 (7)	633 (19)	756 (17)	118	10	0
Kwilu, Kwango, Kasai, Lomami, Sankuru	Jul–Nov 2017	374	2,123	2,497	0	10 (20)	10 (20)	1	1	0

*Defined as >1 laboratory-confirmed cholera cases with evidence of local transmission and an increase in the number of suspected cases for >3 consecutive weeks, or weekly incidence >1,000 cases for >3 consecutive weeks for provinces reporting cases all year round, or increasing number of suspect cases for >3 consecutive weeks if no cholera samples were submitted to the national reference laboratory for testing.

Demographic Characteristics of Cholera Case-Patients

In hot spot health zones, 33,477 (26.2%) suspected cholera cases and 589 (28.4%) confirmed cholera cases were in children <5 years of age. In this age group, 23,615 (24.4%) suspected and 44 (14.4%) confirmed cases were reported in non–hot spot health zones in hot spot provinces and 8,916 (19.1%) suspected and 48 (10.8%) confirmed cholera cases in non–hot spot provinces. The median age of patients with confirmed cholera was 10 (interquartile range [IQR] 4–26) years in hot spot health zones, 20 (IQR 8–32) years in non–hot spot health zones in hot spot provinces, and 22 (IQR 10–36) years in non–hot spot provinces. Among CTC admissions in non–hot spot provinces, median age of the patients was 17 (IQR 5–32) years; 23% of those patients were <5 years of age. We observed an increase in the proportion of children <5 years of age admitted to a CTC: 19.0% in the first 4 weeks of the outbreak, >24.7% in weeks 5–8, 27.1% in weeks 9–12, and 34.5% in weeks 13–15. Male patients accounted for 51.4% of confirmed cholera cases and 50.2% of CTC admissions.

CFRs

The CFR among suspected cholera cases was higher in non–hot spot provinces (4.5%) than in hot spot health zones (1.1%) and non–hot spot health zones located in hot spot provinces (1.8%). The CFR for suspected cases was lower for patients <5 years of age (911/66,008; 1.4%) than for those ≥5 years of age (4,331/204,483; 2.1%). We observed comparable distributions in CFRs by age for suspected cases when stratified by hot spot status (Table 2). Among CTC admissions in non–hot spot provinces, CFRs increased by age, from 2.4% (43/1,759) among children <5 years of age to 4.3% (32/752) among patients ≥50 years of age. CFRs decreased throughout an outbreak, from 5.1% (23/452) among CTC admissions in the first week of an outbreak to 4.4% (35/793) in the fifth week and 0.7% (3/429) in the tenth week.

Geographic Spread in Hot Spot Provinces

Suspected cholera cases were reported all year in 3 of 6 hot spot provinces: North and South Kivu and Tanganyika, along Kivu and Tanganyika Lakes. Major outbreaks occurred in these provinces in 2009 and 2017. Both outbreaks started in August, peaked 6–8 weeks later, and decreased in intensity until the regions went back to baseline levels 5 months after the peak. Hot spot health zones constituting the lakeside cities of Goma (North Kivu) and Kalémie (Tanganyika) were first to report increasing case numbers, followed by adjacent non–hot spot health zones. The highest annual cumulative incidence among hot spot health zones was reported in Goma in 2017 (1,015 cases/100,000 inhabitants).

In the other 3 hot spot provinces, Ituri, Haut Lomami, and Haut Katanga, more sporadic outbreaks occurred.

Table 2. Case-fatality rate among suspected cholera cases, 2008–2017, and among patients admitted to a cholera treatment center, 2015–2017, Democratic Republic of the Congo

Criterion and location	Patient age, y	No. deaths	No. (%) cases	Case-fatality rate, %
Suspected cholera cases				
Overall		5,231	270,852 (100)	1.9
Hot spot health zones	Total	1,407	127,642 (100)	1.1
	<5	292	33,477 (26)	0.9
	≥5	1,116	94,082 (74)	1.2
Non–hot spot health zones in hot spot provinces	Total	1,745	96,570 (100)	1.8
	<5	301	23,615 (24)	1.3
	≥5	1,440	72,777 (75)	2.0
Non–hot spot provinces	Total	2,079	46,640 (100)	4.5
	<5	318	8,916 (19)	3.6
	>5	1,775	37,624 (81)	4.7
CTC admissions				
Overall		267	9,076 (100)	2.9
Non–hot spot health zones in hotspot provinces	Total	3	1,294 (100)	0.2
	<5	0	357 (28)	0.0
	5–19	1	625 (48)	0.2
	20–49	1	241 (19)	0.4
	≥50	1	63 (5)	1.6
Non–hot spot provinces	Total	264	7,782 (100)	3.4
	< 5	43	1,759 (23)	2.4
	5–19	68	2,442 (31)	2.8
	20–49	104	2,609 (34)	4.0
	≥50	32	752 (10)	4.3

The largest outbreaks were observed in Haut Katanga in 2008 and 2013. Both outbreaks occurred during January–March; the 2008 outbreak counted 5,990 suspected cases and the 2013 outbreak 7,533 suspected cases. In both instances, most outbreak cases were reported in non–hot spot zones, in the cities of Lubumbashi and Likasi: 5,645 (94%) in 2008 and 6,534 (87%) in 2013. Haut Lomami Province reported smaller, but more frequent, outbreaks (every year, except in 2011); the number of suspected cases varied from 690 in 2009 to 4,644 in 2014. Of the 19,975 suspected cases reported in Haut Lomami Province, 17,043 (85%) were from hot spot health zones around Upemba Lake. In 2017, non–hot spot health zones along the Lualaba River, a tributary of the Congo, also started to report cases. Ituri Province experienced a large outbreak during January–September 2012. Initial cases were reported in hot spot health zones along Lake Albert, followed by marked case increases in neighboring health zones.

Geographic Spread in Non–Hot Spot Provinces

In non–hot spot provinces, 2 major recurrent outbreaks occurred along the Congo River, the first in 2011–2012 and the second in 2015–2017. The outbreaks started in 2 different towns located in eastern, upstream provinces through which the Congo River flows: Kisangani (Tshopo) in March 2011 and Kindu (Maniema) in August 2015. From there, both outbreaks gradually progressed downstream in a westerly direction, consecutively reaching health zones in the provinces of Mongala, Equateur, Mai-Ndombe, Kinshasa, and Kongo Central (Figure 2). The elapsed time between the first reported outbreak cases in upstream provinces and those reported in Kongo Central, at the mouth of the Congo River, was 11 months for the 2011–2012 outbreak and 14 months for the 2015–2017 outbreak. Several provinces affected by the 2 outbreaks experienced a second, less intensive peak in suspected cholera cases approximately 1 year after the initial outbreak peaks. This dynamic was observed in several non–hot spot provinces: Tshopo in March 2011 and April 2012, Equateur in June 2011 and April 2012, and Mai-Ndombe in June 2011 and March 2012. Maniema Province experienced 2 such postoutbreak increases following an initial outbreak peak in September 2015: the first in January 2017 and a second in September 2017.

In 2017, in addition to the downstream spread along the Congo, suspected cholera cases were reported in inland non–hot spot provinces where no cases had previously been reported during the study timeframe (Figures 2. 3). In July 2017, cases were reported in Kwango Province, followed by Kasaï, Lomami, and Sankuru Provinces, upstream along the Kasaï and Sankuru Rivers.

Along the Congo River, we observed the highest annual cumulative incidence rates in 3 different locations in 3 different years. The first came in 2011 in Bolobo (Mai-Ndombe, 1,107/100,000 population), the second in 2015 in Alunguli (Maniema, 1,088/100,000 population), and the last in 2017 in Kimpese (Kongo Central, 1,335/100,000 population).

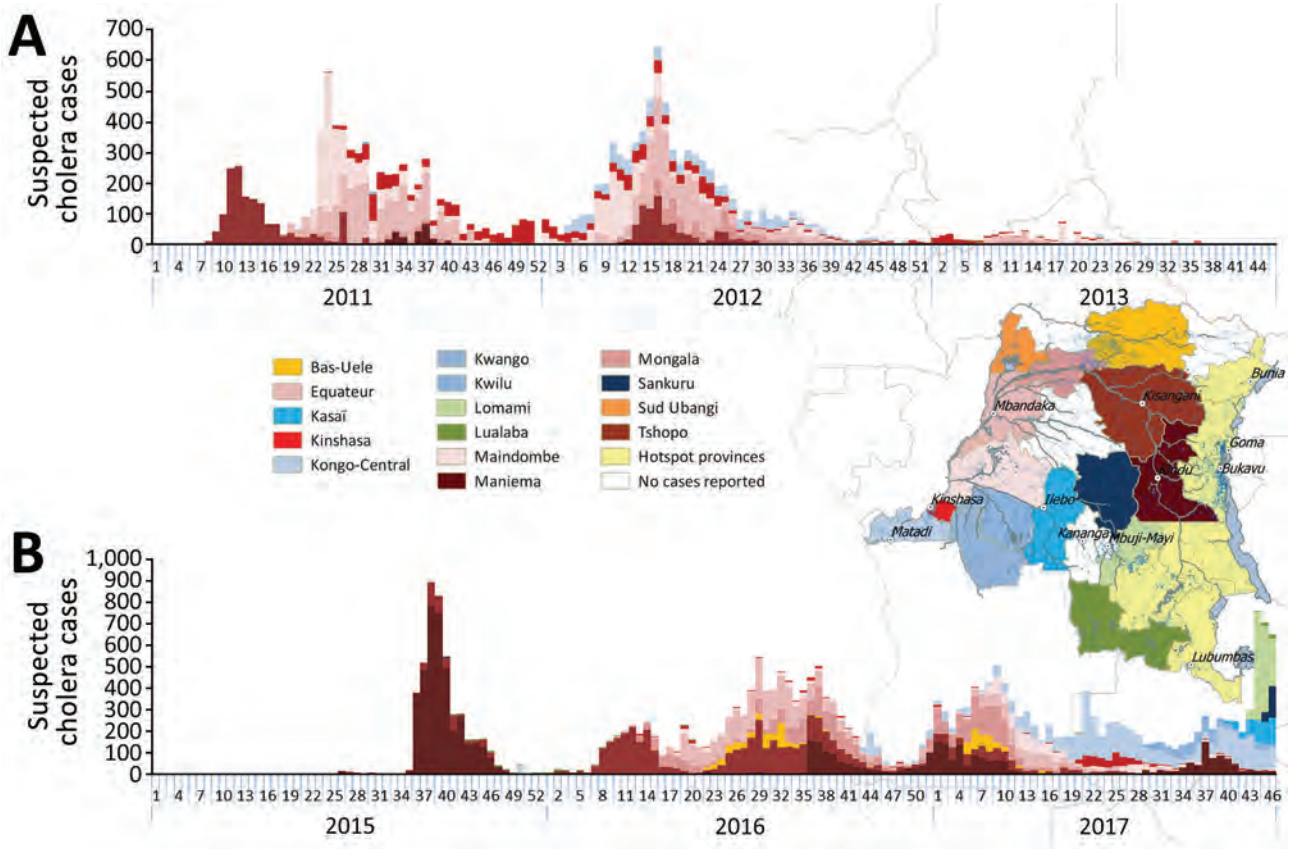

Figure 2. Weekly number of suspected cholera cases for non–hot spot provinces, Democratic Republic of Congo, 2011–2013 (A) and 2015–2017 (B). Colors differentiate provinces and correspond to the colors used in the overlaid map. Case counts for 2017 are through week 46.

Distribution of Cholera Serotypes

Serotyping data were available for 2,893 (98.4%) laboratory-confirmed samples. Overall, Inaba was the most common serotype (90.3%), followed by Ogawa (9.5%) and Hikojima (0.2%) (Table 1). In the 2009 cholera outbreak in North and South Kivu and Tanganyika, the Ogawa serotype was detected in 84.0% of confirmed samples; in the 2017 outbreak, the Ogawa serotype was detected in 58.3% of confirmed samples. In the non–hot spot province outbreaks, the Inaba serotype was detected in 96.4% of confirmed samples. Although Inaba was the dominant serotype in the 2015–2017 nationwide cholera outbreak, Ogawa serotype cases were identified from August 2016 onward, initially in the upstream Maniema Province, followed by reports further downstream in Tshopo Province in October 2016 and Kinshasa in July 2017.

Antimicrobial Resistance

Antimicrobial resistance testing yielded the following results: 99.2% (2,011 of 2,028 tested) were susceptible to doxycycline, 32.6% (642/1,993) to erythromycin, 99.1% (1,628/1,642) to tetracycline, 0.4% (8/2,029) to cotrimoxazole, and 96.9% (2,009/2,024) to ciprofloxacin. Of the 15 isolates that were resistant to ciprofloxacin, 14 were reported during 2016–2017.

Discussion

This 10-year retrospective analysis established 3 mechanisms of geographic spread contributing to the acute escalation of cholera in DRC in 2017: strong increases in the number of cases in cholera-endemic areas, the so-called hot spots, around the Great Lakes in eastern DRC; recurrent outbreaks spreading downstream along the Congo River; and the spread along branches of the Congo River that had been cholera free for at least the preceding 10 years. The observed geographic spread supports the hypothesis that the increased numbers of cases in cholera hot spots located along the Great Lakes functioned as incubators for major countrywide outbreaks (*14–17*). Coordinated and sustained cholera control interventions in these hot spot areas could be crucial for achieving cholera prevention, control, and elimination in DRC.

The 2011–2012 and 2015–2017 outbreaks followed a similar pattern: a spread from hot spots in the Great Lakes region to major cities located in the upstream section of the Congo River, then progressively spreading downstream,

eventually reaching the country's densely populated capital of Kinshasa and Kongo-Central Province at the mouth of the Congo River. These outbreaks recurred in the same health zones over several years with peaks 1 year apart. Cholera propagation along major rivers has also been observed in Mali, Niger, Sudan, and the Central African Republic (*17*). Population movement and seasonal activities that increase human traffic and trade along the Congo River, and on the Great Lakes in particular, are likely to be key factors in such spread (*16–18*).

The range of circulating cholera strains in DRC, their origin, and their contribution to the epidemic remain unclear. During the 2011–2012 outbreak in nonendemic areas along the Congo River, fecal samples collected 1 year apart belonged to a single serotype and multilocus variable number tandem repeat analysis haplotype (*19*), suggesting that this outbreak was caused by a single cholera strain. Samples collected during the first year of the 2015–2017 outbreak affecting the same areas along the Congo River belonged to one serotype. The different serotype isolated 1 year later,

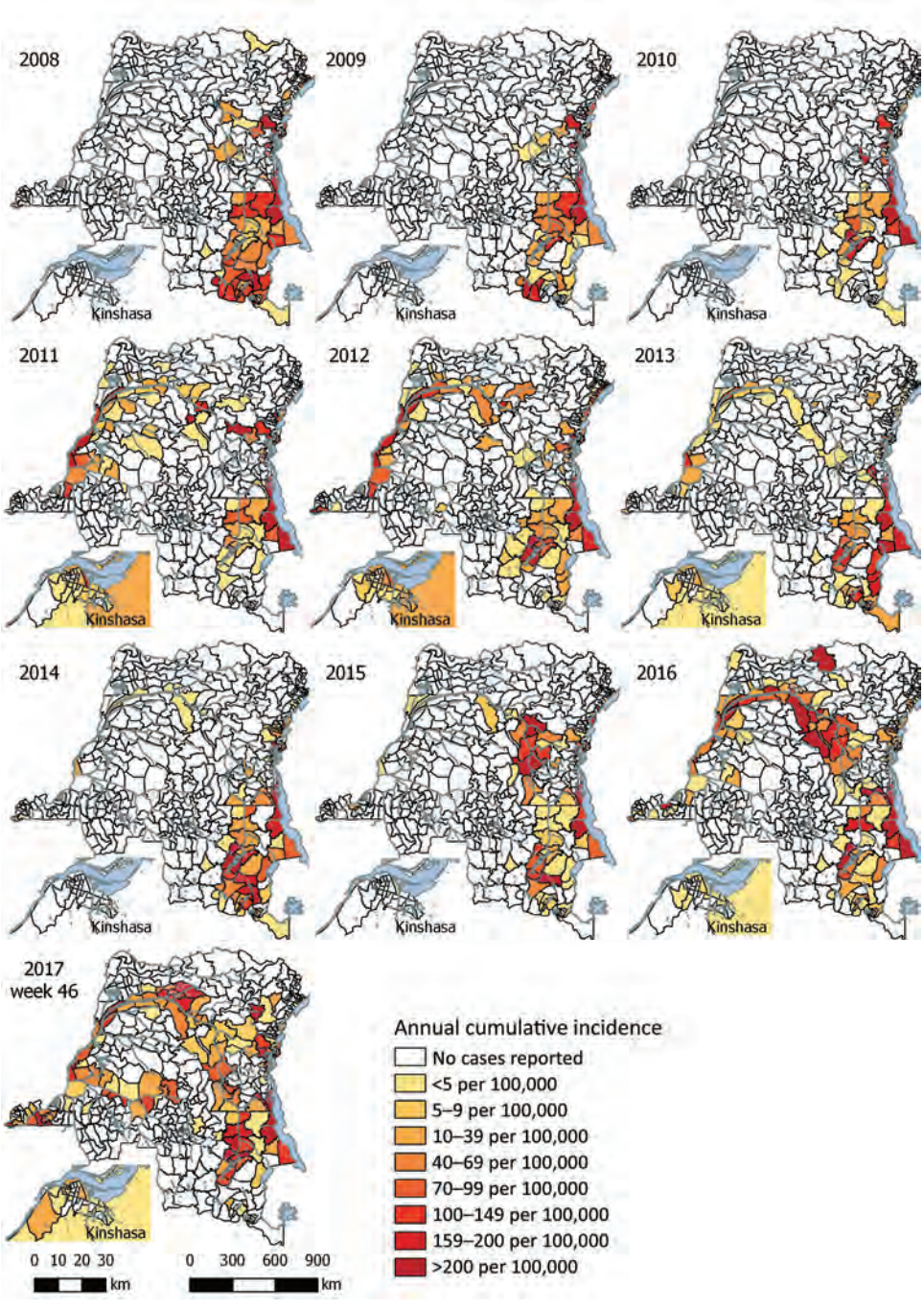

Figure 3. Annual cumulative incidence of suspected cholera cases reported per health zone, Democratic Republic of the Congo, 2008–2017. Case counts for 2017 are through week 46.

which followed the same downstream spread to reach Kinshasa only after a year, probably suggests reintroduction of *V. cholerae*, rather than continued presence of the original *V. cholerae* through asymptomatic human carriers or an environmental reservoir in each of these communities living along the Congo River. In the hot spot provinces of DRC, several *V. cholerae* serotypes were simultaneously identified throughout the study period (Table 1), and isolates from several years grouped in 2 distinct multilocus variable-number tandem-repeat analysis haplotypes (*19*). This finding confirms the presence and role in these provinces of a *V. cholerae* reservoir, either the lakes or potential asymptomatic human carriers (*7*). In addition to gaining further insight into *V. cholerae* circulation, whole-genome sequencing studies could elucidate whether diversification of circulating strains contributed to the intensification of cases in cholera-endemic areas in 2017.

Our findings indicated that cholera outbreaks more disproportionately affected young children, particularly in hot spot provinces where preexisting immunity in the older population was possible. We also found that, although outbreaks along the Congo River affected all ages at the start of the outbreak, the adult population became gradually less affected in the subsequent weeks compared with young children. This finding might suggest that children continued to be exposed more intensely than adults, that fewer adults remained susceptible to become ill after being infected, or that the case definition was less specific for children with watery diarrhea of other origin (non-*Vibrio*).

In a 2017 position paper, WHO recommended the targeted use of OCV in cholera-endemic regions, in humanitarian crises, and during outbreaks (*11*). The use of OCV in DRC has been limited so far to small-scale interventions: 120,000 persons in Kalémie (Tanganyika) in 2015 and 375,000 persons in 5 health zones along the Congo River in Kinshasa in 2016, attaining 90.0% vaccination coverage after a single OCV dose (A. Blake, Epicentre, Paris, pers. comm., 2017 Nov 14). OCV could be considered in several situations in DRC: in cholera hot spot health zones that report a notable increase in reported cases; in non–hot spot health zones adjacent to hot spot health zones, when such increases occur; in health zones along the Congo River, when surveillance reports cholera in upstream communities; during acute emergencies in non–cholera endemic areas of DRC where suspected cases are reported and confirmed; and in settings with particularly poor water and sanitation conditions. In 2015, only 31% of the population in rural DRC used a drinking water source protected from outside contamination, and 29% used sanitation facilities (*20*); targeted OCV can provide an effective additional means to control cholera in areas without good water and sanitation conditions.

Antimicrobial resistance testing results support the continued use of doxycycline to treat severe cholera (*21*) but indicate that cotrimoxazole and erythromycin (and probably azithromycin), which are alternate treatment choices, are unlikely to be very effective treatment options. Ciprofloxacin remains an alternate option to treat children (*22*), but the recent emergence of ciprofloxacin resistance needs to be monitored.

Some limitations apply to our study. Although the reporting of suspected cholera likely does not accurately reflect the full burden of cholera in DRC, it does allow for the documenting of trends and outbreaks. Zero case reporting is not required in the IDSRS, possibly leading to an underestimation of suspected cholera in our analysis, particularly for non–cholera endemic areas where health services might not as readily clinically diagnose and report cholera. Logistical constraints, the lack of an established and systematically implemented national sampling protocol, and limited resources (including an inconsistent availability of transport media) resulted in variable sampling and laboratory confirmation rates over time and place. A more systematic sampling and laboratory confirmation protocol could be developed on the basis of existing international guidelines (*23*) and possibly through the implementation of a decentralized cholera confirmation laboratory network. Our study considered hot spots to be stable throughout 10 years. When observing the affected provinces over the years, we found no indications that hot spots at the province level changed. However, at the health zone level, hot spots could have changed, which could have influenced some of our findings.

Focusing control efforts in DRC on hot spots would be an effective approach to reach elimination only if it can be done rapidly and effectively. Considering the context of conflict and instability in some of the hot spot health zones, a critical portion of the population in the hot spots may continue to be infected, and traveling of cases to nonendemic health zones will then give rise to new outbreaks every few years. Our study was able to identify several such highly vulnerable health zones that are at risk of recurrent outbreaks that could be avoided through the use of OCV, providing population immunity.

In conclusion, 2017 was characterized by an intensified epidemic along the Great Lakes of DRC, recurrence of an outbreak downstream of the Congo River, and an unexpected increase in cholera cases in inland regions of DRC where no cases had been reported for 15 years. Furthermore, ongoing conflicts in the cholera-endemic provinces remain a concern, hampering control efforts at the presumptive origins of outbreaks. Surveillance data adequately describe geographic spread and differences in CFRs, which can be used for targeting of cholera prevention and control actions. A policy for targeted vaccination

of at risk populations is needed. Epidemiologic and phylogenetic studies of historical and circulating cholera strains could provide further insight into how cholera spreads from one community to others.

This study was financed by the Outbreak Research Team of the Institute of Tropical Medicine, Antwerp, Belgium, and the ECDC Fellowship Programme.

About the Author

Mr. Ingelbeen is a pharmacist and infectious disease epidemiologist at the Institute of Tropical Medicine. His research interests include emerging infectious diseases and antimicrobial resistance. Dr. Hendrickx is a social scientist and epidemiologist and currently works as a consultant. His research activities in DRC have focused on African sleeping sickness and cholera. Both carried out this research as part of a European Programme for Intervention Epidemiology Training (EPIET) fellowship.

References

1. Global Task Force on Cholera Control. Ending cholera. A global roadmap to 2030. 2017 [cited 2017 Oct 9]. http://www.who.int/cholera/publications/global-roadmap.pdf?ua=1
2. Ali M, Nelson AR, Lopez AL, Sack DA. Updated global burden of cholera in endemic countries. PLoS Negl Trop Dis. 2015;9:e0003832. http://dx.doi.org/10.1371/journal.pntd.0003832
3. Schyns C, Fossa A, Mutombo-Nfenda, Kabuyahiya, Hennart P, Piot P, et al. Cholera in Eastern Zaire, 1978. Ann Soc Belg Med Trop. 1979;59:391–400.
4. Lutz C, Erken M, Noorian P, Sun S, McDougald D. Environmental reservoirs and mechanisms of persistence of *Vibrio cholerae*. Front Microbiol. 2013;4:375. http://dx.doi.org/10.3389/fmicb.2013.00375
5. Bompangue D, Giraudoux P, Piarroux M, Mutombo G, Shamavu R, Sudre B, et al. Cholera epidemics, war and disasters around Goma and Lake Kivu: an eight-year survey. PLoS Negl Trop Dis. 2009;3:e436. http://dx.doi.org/10.1371/journal.pntd.0000436
6. Eeckels R. Cholera. In: Janssens PG, Kivits M, Vuylsteke J, editors. Health in Central Africa since 1885; past, present and future. Brussels: King Baudouin Foundation; 1997. p. 1075–183.
7. Bompangue Nkoko D, Giraudoux P, Plisnier PD, Tinda AM, Piarroux M, Sudre B, et al. Dynamics of cholera outbreaks in Great Lakes region of Africa, 1978–2008. Emerg Infect Dis. 2011;17:2026–34.
8. Jeandron A, Saidi JM, Kapama A, Burhole M, Birembano F, Vandevelde T, et al. Water supply interruptions and suspected cholera incidence: a time-series regression in the Democratic Republic of the Congo. PLoS Med. 2015;12:e1001893. http://dx.doi.org/10.1371/journal.pmed.1001893
9. Goma Epidemiology Group. Public health impact of Rwandan refugee crisis: what happened in Goma, Zaire, in July, 1994? Lancet. 1995;345:339–44. http://dx.doi.org/10.1016/S0140-6736(95)90338-0
10. World Health Organization Regional Office for Africa. Weekly bulletin on outbreaks and other emergencies—week 1 2018. 2018 [cited 2018 Jan 09]. http://apps.who.int/iris/bitstream/10665/259809/1/OEW1-2018.pdf
11. World Health Organization. Cholera vaccines: WHO position paper—August 2017. Wkly Epidemiol Rec. 2017;92:477–98.
12. Muyembe JJ, Bompangue D, Mutombo G, Akilimali L, Mutombo A, Miwanda B, et al. Elimination of cholera in the Democratic Republic of the Congo: the new national policy. J Infect Dis. 2013;208(suppl1):S86–91. http://dx.doi.org/10.1093/infdis/jit204
13. Clinical and Laboratory Standards Institute. Methods for antimicrobial dilution and disk susceptibility testing of infrequently isolated or fastidious bacteria. 3rd ed. CLSI guideline M45. Wayne (PA): The Institute; 2015.
14. Bwire G, Munier A, Ouedraogo I, Heyerdahl L, Komakech H, Kagirita A, et al. Epidemiology of cholera outbreaks and socio-economic characteristics of the communities in the fishing villages of Uganda: 2011–2015. PLoS Negl Trop Dis. 2017;11:e0005407. http://dx.doi.org/10.1371/journal.pntd.0005407
15. Bwire G, Mwesawina M, Baluku Y, Kanyanda SSE, Orach CG. Cross-border cholera outbreaks in sub-Saharan Africa, the mystery behind the silent illness: what needs to be done? PLoS One. 2016;11:e0156674. http://dx.doi.org/10.1371/journal.pone.0156674
16. Bompangue D, Vesenbeckh SM, Giraudoux P, Castro M, Muyembe JJ, Kebela Ilunga B, et al. Cholera ante portas—the re-emergence of cholera in Kinshasa after a ten-year hiatus. PLoS Curr. 2012;4:RRN1310. http://dx.doi.org/10.1371/currents.RRN1310
17. Rebaudet S, Sudre B, Faucher B, Piarroux R. Environmental determinants of cholera outbreaks in inland Africa: a systematic review of main transmission foci and propagation routes. J Infect Dis. 2013;208(suppl1):S46–54. http://dx.doi.org/10.1093/infdis/jit195
18. Birmingham ME, Lee LA, Ndayimirije N, Nkurikiye S, Hersh BS, Wells JG, et al. Epidemic cholera in Burundi: patterns of transmission in the Great Rift Valley Lake region. Lancet. 1997;349:981–5. http://dx.doi.org/10.1016/S0140-6736(96)08478-4
19. Moore S, Miwanda B, Sadji AY, Thefenne H, Jeddi F, Rebaudet S, et al. Relationship between distinct African cholera epidemics revealed via MLVA haplotyping of 337 *Vibrio cholerae* isolates. PLoS Negl Trop Dis. 2015;9:e0003817. http://dx.doi.org/10.1371/journal.pntd.0003817
20. United Nations Statistics Division. Millennium Development Goals Indicators. 2015 [cited 2018 Oct 3]. http://mdgs.un.org/unsd/mdg/Data.aspx
21. World Health Organization. Cholera outbreak. Assessing the outbreak response and improving preparedness. 2004 [cited 2017 Oct 3]. https://apps.who.int/iris/bitstream/handle/10665/43017/WHO_CDS_CPE_ZFk_2004.4_eng.pdf
22. World Health Organization. WHO model list of essential medicines for children. 6th list. 2017 [cited 2017 Oct 3]. http://apps.who.int/iris/bitstream/handle/10665/273825/EMLc-6-eng.pdf
23. World Health Organization. Interim guidance document on cholera surveillance, Global Task Force on Cholera Control (GTFCC) Surveillance Working Group. 2017 [cited 2018 Jan 10]. http://www.who.int/cholera/task_force/GTFCC-Guidance-cholera-surveillance.pdf

Address for correspondence: Brecht Ingelbeen, Institute of Tropical Medicine, Nationalestraat 155, 2000 Antwerp, Belgium; email: brechtingelbeen@gmail.com

Lassa Virus Targeting of Anterior Uvea and Endothelium of Cornea and Conjunctiva in Eye of Guinea Pig Model

Joy M. Gary, Stephen R. Welch, Jana M. Ritter, JoAnn Coleman-McCray, Thanhthao Huynh, Markus H. Kainulainen, Brigid C. Bollweg, Vaunita Parihar, Stuart T. Nichol, Sherif R. Zaki, Christina F. Spiropoulou, Jessica R. Spengler

Lassa virus (LASV), a hemorrhagic fever virus endemic to West Africa, causes conjunctivitis in patients with acute disease. To examine ocular manifestations of LASV, we histologically examined eyes from infected guinea pigs. In fatal disease, LASV immunostaining was most prominent in the anterior uvea, especially in the filtration angle, ciliary body, and iris and in and around vessels in the bulbar conjunctiva and peripheral cornea, where it co-localized with an endothelial marker (platelet endothelial cell adhesion molecule). Antigen was primarily associated with infiltration of T-lymphocytes around vessels in the anterior uvea and with new vessel formation at the peripheral cornea. In animals that exhibited clinical signs but survived infection, eyes had little to no inflammation and no LASV immunostaining 6 weeks after infection. Overall, in this model, LASV antigen was restricted to the anterior uvea and was associated with mild chronic inflammation in animals with severe disease but was not detected in survivors.

Lassa virus (LASV) is the etiologic agent of Lassa fever (LF), a viral hemorrhagic fever endemic to West Africa. Incidence of LF in areas to which it is endemic is ≈100,000–300,000 cases annually, of which ≈5,000 are fatal (*1*). After an incubation period of 7–21 days (*2*,*3*), disease onset is gradual and includes fever, weakness, myositis, and ulcerative pharyngitis that may progress to myocarditis, pneumonitis and pleuritis, and encephalopathy and hemorrhage (*2*). The most well-documented sequela of LF is hearing loss (*4*–*8*).

Ocular involvement in acute LF includes conjunctivitis and conjunctival edema (*9*). In addition, transient blindness has been described in humans recovering from LASV infection (*3*,*10*). The extent of viral presence in the eye, the ocular structures targeted by LASV, and the clinical implications of ocular infection are unknown.

In viral hemorrhagic fever disease, ocular manifestations are not limited to LF and are well described for infection with Ebola virus (EBOV) (*11*,*12*), Marburg virus (*13*), and Rift Valley fever virus (RVFV) (*14*–*16*). Recently, the implications of viral persistence in the eye and other immunoprivileged sites have been highlighted in Ebola virus disease (EVD) (*12*,*17*). The possibility of LASV persistence in the eye is unknown, as is the extent of chronic pathologic changes secondary to infection that could result in long-term functional abnormalities.

Inbred Strain 13 guinea pigs almost uniformly die of disease after LASV infection with the prototypic 1976 Josiah strain without requiring serial adaptation (*18*). In addition, we recently described nonlethal disease in Strain 13 guinea pigs infected with a 2015 isolate from a person with LF imported to New Jersey, USA, from Liberia (LASV 812673-LBR-USA-2015, or LASV-NJ2015 [*19*]). To investigate ocular manifestations of LASV infection in animals that died of or survived infection, we collected samples from animals infected with either LASV-Josiah or LASV-NJ2015. LASV loads and distribution, and associated ocular histopathology, were assessed in these animals.

Material and Methods

Ethics Statement

All animal procedures were approved by the Centers for Disease Control and Prevention (CDC; Atlanta, GA, USA) Institutional Animal Care and Use Committee (IACUC; #2833SPEGUIC) and conducted in accordance with the Guide for the Care and Use of Laboratory Animals (*20*). CDC is fully accredited by the Association for Assessment and Accreditation of Laboratory Animal

Author affiliation: Centers for Disease Control and Prevention, Atlanta, Georgia, USA

DOI: https://doi.org/10.3201/eid2505.181254

Care International. Procedures conducted with LASV or LASV-infected animals were performed in the CDC Biosafety Level 4 laboratory.

Virus

Recombinant LASV-Josiah, based on the sequence of an isolate obtained in 1976 from the serum of a 40-year-old man hospitalized at Songo Hospital in Sebgwena, Sierra Leone (*21*,*22*), was rescued in BSR-T7/5 cells and passaged twice in Vero-E6 cells (GenBank accession nos. HQ688673.1, HQ688675.1). Recombinant LASV 812673-LBR-USA-2015 (LASV-NJ2015), based on the sequence of an isolate obtained in 2015 from a 55-year-old man who died of LF in New Jersey after returning from Liberia, was rescued in BSR-T7/5 cells and passaged twice in Vero-E6 cells (*19*) (GenBank accession nos. MG 812650, MG812651). We determined focus-forming units and 50% tissue culture infectious dose ($TCID_{50}$) titers in Vero-E6 cells by immunofluorescence assays using an in-house anti-LASV monoclonal antibody mix targeting nucleoprotein and glycoprotein 2 (SPR628), with $TCID_{50}$ titers calculated using the method of Reed and Muench (*23*).

Guinea Pig Infections

Sixteen strain 13/N guinea pigs (8 male, 8 female, 6 months to >3 years of age) were obtained from our breeding colony at CDC. Age- and sex-matched 13/N guinea pigs were inoculated subcutaneously with 10^4 focus-forming units (equivalent to $\approx 2 \times 10^4$ $TCID_{50}$) of LASV, either LASV-Josiah (10 animals) or LASV-NJ2015 (6 animals). Four animals infected with LASV-Josiah served as unvaccinated controls in parallel studies (*24*). All animals were housed individually and given daily fresh vegetable enrichment, hay, commercial guinea pig chow, and water as desired. Experienced CDC veterinarians or animal health technicians assessed animal health. Animals were humanely euthanized with isoflurane vapors and sodium pentobarbital (SomnaSol Euthanasia-III solution; Henry Schein Animal Health, https://www.henryscheinvet.com) once clinical illness scores (including piloerection, ocular discharge, weight loss >25%, changes in mentation, ataxia, dehydration, dyspnea, or hypothermia) indicated the animal was in the terminal stages of disease, or at the completion of study 41 days postinfection (dpi).

Quantitative Reverse Transcription PCR

RNA was extracted from blood and homogenized tissue samples using the MagMAX-96 Total RNA Isolation Kit (Thermo Fisher Scientific, https://www.thermofisher.com) on a 96-well ABI MagMAX extraction platform with a DNase-I treatment step, according to the manufacturer's instructions. RNA was quantified by a quantitative reverse transcription PCR (qRT-PCR) targeting a strain-specific nucleoprotein gene sequence (primer and probe sequences available on request from the authors), and normalized to 18S RNA levels. We determined viral small (S) segment copy numbers using standards prepared from in vitro–transcribed S segment RNA.

Histochemical Staining and Immunohistochemical Analysis

Tissue specimens were fixed in 10% neutral buffered formalin and subjected to gamma irradiation (2×10^6 rad). Formalin-fixed tissues from all guinea pigs were routinely processed, embedded in paraffin, sectioned at 4 μm, and stained with hematoxylin and eosin. A veterinary pathologist visually assessed inflammation within the eye as minimal (few scattered lymphocytes around vessels), mild (small clusters of lymphocytes around vessels or within the filtration angle), or moderate (noticeably more intense infiltrates of lymphocytes within the eye). A marked response, which we did not observe in these animals, would have comprised tissue architecture disrupted by inflammatory cells.

We conducted immunohistochemical (IHC) assays using indirect immunoalkaline phosphatase detection on 4-μm sections. Colorimetric detection of attached antibodies was performed using the Mach 4 AP polymer kit (Biocare Medical, https://biocare.net) at room temperature, except for heat-induced epitope retrieval. Using either Reveal or EDTA buffer, we conducted heat-induced epitope retrieval using the NxGen decloaker (Biocare Medical) at 110°C for 15 min. All slides were blocked in Background Punisher (Biocare Medical) for 10 min and incubated with primary antibody for 30 min. Antibodies used were anti-CD3 (diluted 1:100 in EDTA buffer [#NCL-L-CD3–565; Leica Biosystems, https://www.leicabiosystems.com), anti-CD79a (1:100, EDTA buffer [#NCL-L-CD79a-22; Leica Biosystems]), and a mouse monoclonal antibody targeting LASV glycoprotein 2 at 1:1,000 (CDC). Mach 4 Probe was applied for 10 min, followed by Mach 4 AP polymer for 15 min (Biocare Medical). The antibody/polymer conjugate was visualized by applying Fast Red Chromogen dissolved in Naphthol Phosphate substrate buffer to tissue sections for 20 min (Thermo Fisher Scientific). Appropriate negative control serum was run in parallel. Slides were counterstained with Mayer's hematoxylin (Poly Scientific, https://www.polyrnd.com) and blued in lithium carbonate (Poly Scientific). Positive controls included formalin-fixed, paraffin-embedded Vero-E6 cells infected with LASV, tissue from a human with LF, and guinea pig spleen and liver (for inflammatory cell and cell lineage markers). A veterinary pathologist scored IHC staining on a scale of 0 (no IHC staining seen) to 4 (abundant, intense IHC staining within structures in the eye).

Table. Summary of ocular LASV staining and histopathologic findings in LASV-infected guinea pigs in study of LASV targeting of anterior uvea and endothelium of cornea and conjunctiva in eye*

Guinea pig	Age at D0/sex	dpi	Viral RNA†	IHC distribution	IHC score	H&E
Jos-1‡	3 y 10 mo/F	14	4.55×10^5	Conjunctival endothelium and anterior uvea; eyelid epithelium and endothelium	+++/++++	Mild conjunctivitis and anterior uveitis
Jos-2	3 y 10 mo/M	41	2.50×10^1	None	–	Mild perivascular mononuclear inflammation, sclera
Jos-3‡	2 y 5 mo/F	20	1.32×10^5	Anterior uvea, peripheral corneal endothelium	++	Neovascularization at corneal margin, mild conjunctivitis
Jos-4‡	2 y 4 mo/F	17	7.87×10^5	Endothelium, conjunctiva, and peripheral cornea; anterior uvea	+++	Neovascularization at corneal margin, mild conjunctivitis
Jos-5‡	0 y 6 mo/M	17	1.02×10^6	Anterior uvea	++	Mild anterior uveitis
Jos-6‡	0 y 6 mo/M	18	5.32×10^5	Anterior uvea	+	Mild neovascularization at corneal margin
Jos-7‡	3 y 7 mo/F	23	5.23×10^6	Conjunctival endothelium and anterior uvea	++	Neovascularization at corneal margin, mild conjunctivitis, anterior uveitis
Jos-8‡	3 y 3 mo/F	21	2.02×10^6	Anterior uvea, peripheral corneal endothelium	++	Neovascularization at corneal margin, anterior uveitis
Jos-9‡	3 y 6 mo/M	20	6.71×10^6	Conjunctival and peripheral corneal endothelium and anterior uvea, eyelid and lacrimal gland	+++	Neovascularization at corneal margin, moderate conjunctivitis, anterior uveitis
Jos-10‡	>2 y/M	23	2.26×10^6	Conjunctival and peripheral corneal endothelium and anterior uvea	++	Mild neovascularization at corneal margin, minimal anterior uveitis
NJ2015-1	3 y 11 mo/F	41	BLD	None	–	Minimal heterophilic infiltrate at corneal margin
NJ2015-2	3 y 8 mo/M	41	BLD	None	–	NSF
NJ2015-3	2 y 5 mo/F	41	BLD	None	–	NSF
NJ2015-4	2 y 4 mo/F	41	BLD	None	–	NSF
NJ2015-5	0 y 6 mo/M	41	1.54×10^2	None	–	Minimal heterophilic infiltrate at corneal margin, minimal chronic anterior uveitis
NJ2015-6	0 y 6 mo/M	41	4.28×10^2	None	–	Mild anterior uveitis

*All survivors were euthanized at end of study (41 dpi). BLD, below limit of detection (<5 copies); D0, day 0; dpi, days postinfection; H&E, hematoxylin and eosin staining; IHC, immunohistochemical; Jos, guinea pig infected with recombinant LASV-Josiah; LASV, Lassa virus; NJ2015, guinea pig infected with recombinant LASV 812673-LBR-USA-2015; NSF, no significant findings; –, negative results at staining; +, mild immunostaining; ++, moderate immunostaining; +++/++++, abundant immunostaining.
†LASV small segment copies in the eye quantified per millileter of eluted RNA.
‡Guinea pig euthanized because of disease.

We performed double staining of antigens after heat-induced epitope retrieval using the EnVision G|2 Doublestain System Rabbit/Mouse (DAB+/Permanent Red; Agilent, https://www.agilent.com) according to the manufacturer's instructions. We incubated slides in Endogenous Enzyme block for 5 min, primary antibody for 30 min, horseradish peroxidase-polymer for 10 min, and diaminobenzidine (DAB) working solution for 10 min. Double-stain block was then applied for 3 min, and the second stain procedure consisted of applying the other primary antibody for 30 min, followed by addition of the Rabbit/Mouse Link, AP-Polymer, and Permanent Red working solution for 10 min each. Slides were double-stained with the LASV monoclonal antibody (labeled in Permanent Red) and platelet endothelial cell adhesion molecule (PECAM; 1:10 dilution in EDTA buffer [#MU241-UC; BioGenex, https://www.biogenex.com]; labeled with DAB). Appropriate negative control serum was run in parallel. Slides were counterstained, and coverslips were applied.

Results

Detection of LASV in Eyes of Animals with Terminal Disease but Not in Survivors

All animals from which samples were obtained demonstrated ≥1 clinical signs of LASV infection, including elevated body temperature, weight loss, hunched posture, ruffled fur, and altered mentation. Swollen, red conjunctiva with associated ocular discharge was observed in most of the animals, coinciding with onset of clinical signs. To determine whether LASV infects the eye, we collected 1 eye from each of 16 guinea pigs (10 infected with LASV-Josiah and 6 infected with LASV-NJ2015) for PCR to detect viral nucleic acids. The other eye from each animal was used to create full ocular sections that were IHC stained to assess presence and localization of viral antigens.

We detected viral nucleic acids in the eyes of all guinea pigs that died of infection (9 of 10 guinea pigs infected

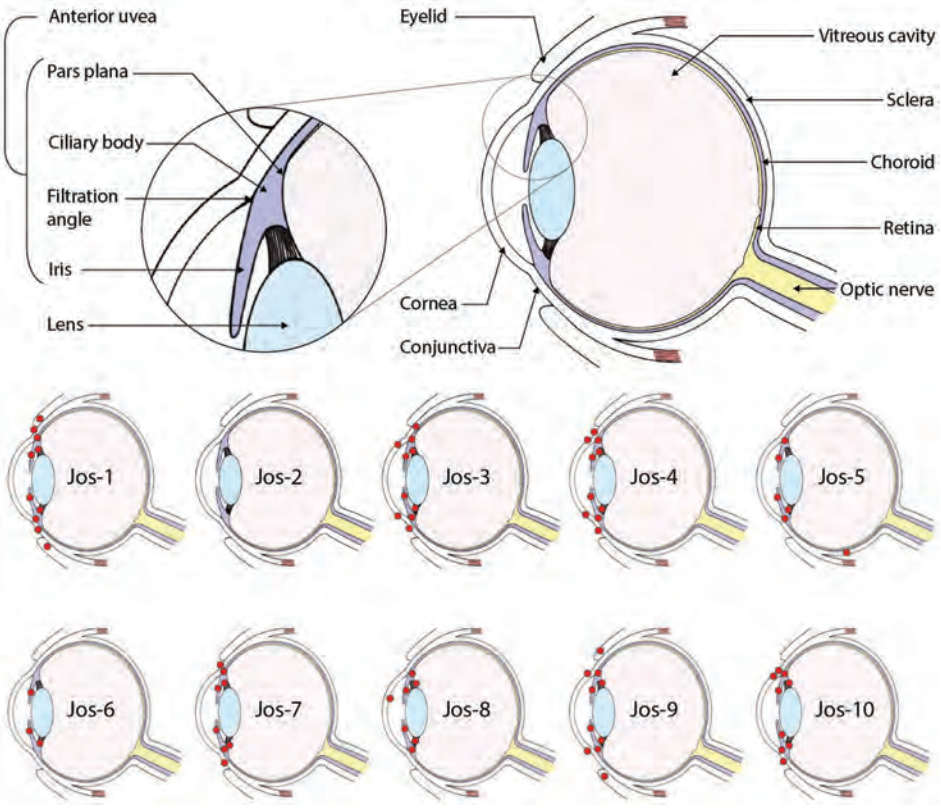

Figure 1. Lassa virus (LASV) localization in guinea pigs that died of or survived infection with LASV-Josiah in study of LASV targeting of anterior uvea and endothelium of cornea and conjunctiva in eye. Primary diagram at top shows major structures of the eye; smaller diagrams detail the general regions in which LASV antigen (red circles) was detected in the eye of each animal by immunohistochemical analysis. All animals were euthanized because of disease (14–23 days postinfection) except Jos-2, which did not exhibit overt clinical signs (no weight loss or elevated body temperature) and was euthanized at study completion (41 days postinfection).

with LASV-Josiah), ranging from 1.32×10^5 to 6.71×10^6 S-segment copies per μL of eluted RNA. Three of the 7 surviving animals, 1 infected with LASV-Josiah (Jos-2) and 2 infected with LASV-NJ2015, had detectable viral RNA within the eye, ranging from 2.50×10^1 to 4.28×10^2 copies per μL of eluted RNA. Viral RNA was below the limit of detection in the remaining survivors (4 guinea pigs infected with LASV-NJ2015).

We saw no IHC staining in the eyes of any animals that survived infection and detected little to no viral RNA within the eye, including in 1 animal infected with LASV-Josiah (Jos-2) and all animals infected with LASV-NJ2015 (infection confirmed by serology [*19*]). In contrast, IHC staining revealed LASV antigen in the eyes of all animals that died of infection and had detectable viral RNA in the range of 10^5–10^6 viral copies. LASV antigen staining was primarily concentrated within anterior regions of the eye (Table; Figures 1, 2). Specifically, we saw staining in the anterior uvea, mostly in the trabecular meshwork at the filtration angle (in 9/9 animals; Figure 2, panels A, D); in the iris, particularly in the pigmented epithelium along the posterior margin, as well as along the anterior margin (in 9/9 animals; Figure 2, panels A, F); and multifocally in the ciliary body epithelium (in 7/9 animals; Figure 2, panels A, E). In addition, we observed perivascular and endothelial staining within the sclera (5/9 animals) and bulbar conjunctiva (5/9 animals) and occasionally in new vessels forming at the peripheral cornea (5/9 animals) (Figure 2, panels A–C). In 5 animals, we noted patchy IHC staining in the corneal endothelium deep to Descemet's membrane. In 2 animals (Jos-1 and -9), patchy but strong LASV staining was observed in epithelial cells in the surface epithelium of the eyelid, as well as within the dermal vessels, and within acini of the lacrimal glands (Figure 2, panels G, H). In animal Jos-5, we saw staining around scleral vessels at the midline of the eye, in association with mild inflammation.

LASV Infection in Endothelial Cells in the Eye

The distribution of IHC staining in animals with severe disease indicated a predilection for LASV infection of endothelial cells (in the cornea, sclera, conjunctiva, and deep to Descemet's membrane) and in cells of neural crest and mesenchymal origin (in the iris, ciliary body, and filtration angle [*25*]); we noted viral antigen in endothelial cells and perivascular connective tissues in the conjunctiva and sclera of 5 of 9 animals with terminal disease. In 8 of the 9 animals, we observed mild new vessel formation at the peripheral cornea, with minimal associated inflammation (Figure 2, panel B; Figure 3, panels A–C); LASV staining was noted in endothelial cells of the new vessels in 5 of these guinea pigs (Jos-3, Jos-4, Jos-8, Jos-9, and Jos-10; Figure 2, panels A, B).

To confirm that LASV targets endothelial cells within the eye, we conducted IHC costaining with an anti-PECAM

(anti-CD31) antibody and the anti-LASV antibody. In 50% of animals tested (3/6), we observed viral antigen and PECAM co-staining within vessels in the bulbar conjunctiva and in the newly formed vessels in the peripheral cornea (Figure 4).

Lymphocytic Ocular Inflammation Caused by LASV Infection

On histopathologic investigation, 56% (5/9) of animals that reached endpoint criteria had mild mononuclear anterior uveitis, with perivascular inflammation composed of lymphocytes primarily in the pars plana of the ciliary body, located near the iridoscleral junction, and scattered within the margins of the trabecular meshwork of the filtration angle (representative animal Jos-1; Table; Figure 3, panels D, H). Inflammation rarely extended into the stroma of the iris. Another prominent feature in 6 of 9 animals that died of LASV infection was mild to moderate lymphocytic inflammation around vessels in the bulbar conjunctiva and the anterior sclera, especially at the corneoscleral junction, and adjacent to the filtration angle (Figure 3, panels D, E). Mild conjunctival hemorrhage was noted in these animals

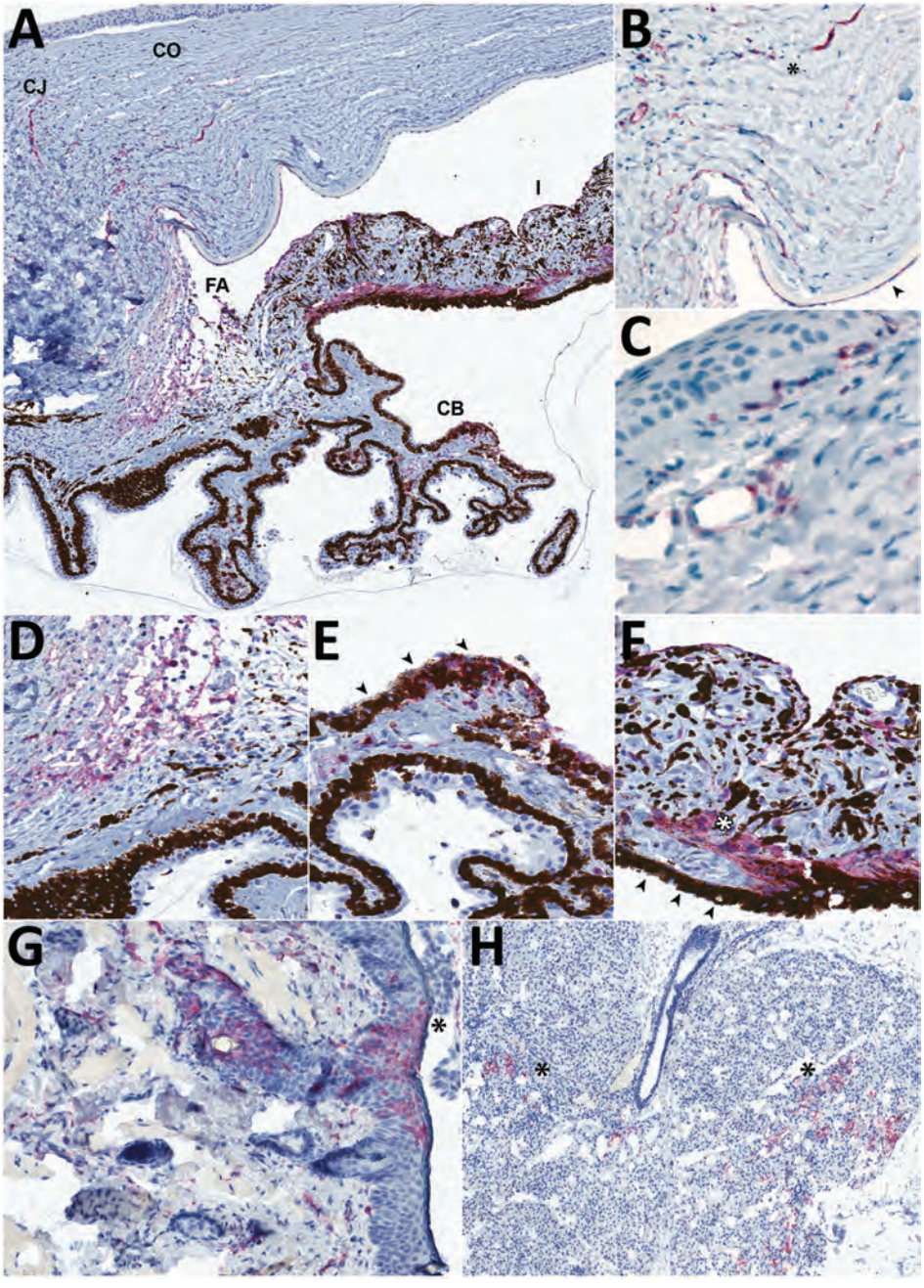

Figure 2. Detection of Lassa virus (LASV) antigen in the anterior uvea and endothelium within the eye of guinea pigs infected with LASV-Josiah and in the epithelium of structures adjacent to the eye in study of LASV targeting of anterior uvea and endothelium of cornea and conjunctiva in eye. A) Anterior uvea with LASV antigen immunolabeled (red) within the peripheral CO and CJ vessels, the FA, CB, and I. Original magnification ×4. B) Immunohistochemical (IHC) staining in the endothelium and adjacent stroma of the corneal margin (asterisk) and in the endothelium deep to Descemet's membrane (arrowhead). Original magnification ×20 with 1.25 Optivar. C) Perivascular and endothelial staining in the bulbar conjunctiva. Original magnification ×63. D) IHC staining in the filtration angle. Original magnification ×20. E) Photomicrograph of the ciliary body highlighting the labeling in the pigmented epithelium (arrowheads) and stroma. Original magnification ×30. F) Photomicrograph of the iris showing IHC staining of LASV antigen in the stroma, smooth muscle (dilator muscle, white asterisk) and posterior pigmented epithelium (arrowheads). Original magnification ×40. G) IHC staining in eyelid epithelium (asterisk) and dermal vessels in the eyelid. Representative animal Jos-9. Original magnification ×15. H) IHC staining for LASV antigen in the acini of the lacrimal gland (asterisks). Representative animal Jos-9. Original magnification ×5. Representative animals: A–F, Jos-4; F, G, Jos-9. CB, ciliary body; CJ, conjunctival; CO, corneal; FA, filtration angle; I, iris; IHC, immunohistochemical.

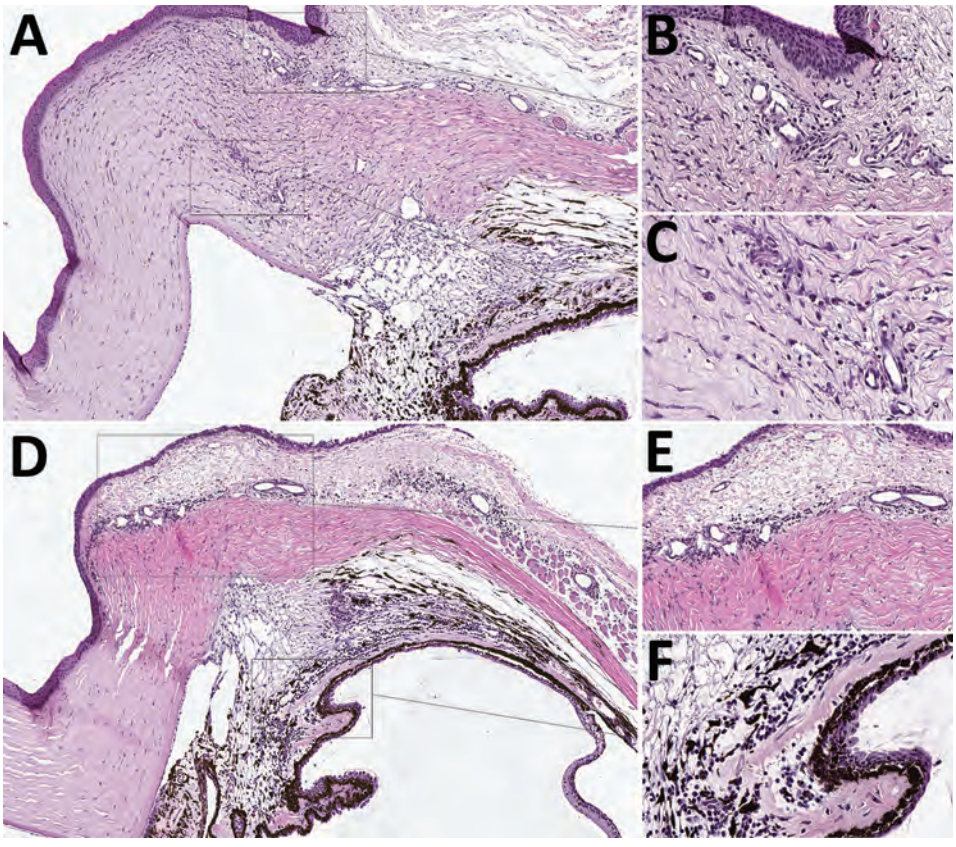

Figure 3. Mild mononuclear anterior uveitis in eyes of guinea pigs infected with Lassa virus (LASV) Josiah by hematoxylin and eosin stain in study of LASV targeting of anterior uvea and endothelium of cornea and conjunctiva in eye. A) Anterior uvea, conjunctiva, and cornea highlighting the mild inflammation and new vessel formation in the peripheral cornea. Original magnification ×4. B) New vessel formation of the peripheral cornea. Original magnification ×12. C) New vessel formation within the cornea highlighting the endothelial swelling and mixed inflammation. Original magnification ×20. D) The ciliary body, filtration angle, peripheral cornea, and a portion of the conjunctiva with mixed, mild, primarily lymphocytic inflammation in the filtration angle and around vessels in the conjunctiva, peripheral cornea, and sclera. Representative animal Jos-1. Original magnification ×6. E) Inflammation around conjunctival vessels at the margin of the cornea. Original magnification ×20. F) Mononuclear inflammation in the filtration angle and at the base of the ciliary body. Original magnification ×20. Representative animals: A–C, Jos-3; D–F, Jos-1.

histologically. Almost all (8/9) animals with terminal disease had mild, mixed inflammation composed of heterophils and lymphocytes at the peripheral cornea, as well as mild peripheral corneal neovascularization (representative animal Jos-4; Figure 3, panels A–C); 4 of these animals had a small amount of associated necrotic nuclear debris (Figure 3, panel C). The lymphocytic inflammation in the anterior uvea was most prominent in Jos-1, the guinea pig that had the most acute clinical course and died 14 dpi.

To characterize the inflammatory cell populations in animals with terminal disease, we conducted IHC staining targeting CD3+ T-lymphocytes and CD79a+ B-lymphocytes. The composition of inflammatory cells varied based on disease duration. The inflammatory milieu comprised T-lymphocytes and B-lymphocytes in Jos-1, which died of disease 14 dpi (Figure 5, panels A, B), but consisted primarily of T-lymphocytes in all animals that died ≥17 dpi (representative animal Jos-5; Figure 5, panels C–F). T-lymphocytes were most abundant in the trabecular meshwork and in the perivascular connective tissue in the sclera and bulbar conjunctiva. Scattered T-lymphocytes also were seen in the peripheral corneal stroma and epithelium in animals with corneal neovascularization (Figure 5, panel E).

Despite the absence of detectable viral antigen, we observed inflammation in all animals infected with LASV-NJ2015, but not in Jos-2, which survived LASV-Josiah infection. However, the degree of inflammation in surviving animals was notably less than in animals with terminal disease. Survivors demonstrated minimal to mild lymphocytic inflammation in the eye, compared with mild to moderate inflammation in animals with terminal disease. The lymphocytic inflammation in the eyes of surviving animals was accompanied by minimal heterophilic infiltrate around vessels of the peripheral cornea in 2 animals (NJ2015-1 and -5; Table). In addition, mild lymphocytic anterior uveitis was seen in NJ2015-6, which had the highest viral RNA copy number among surviving animals.

Discussion

Long-term ocular manifestations are not well described in LASV infection, but given the importance and persistence of ocular lesions after infection with other hemorrhagic fever viruses, the pathogenesis of LASV in immune-privileged sites such as the eye must be fully characterized. In the few reported cases of ocular involvement in acute LF, clinical findings have primarily been described

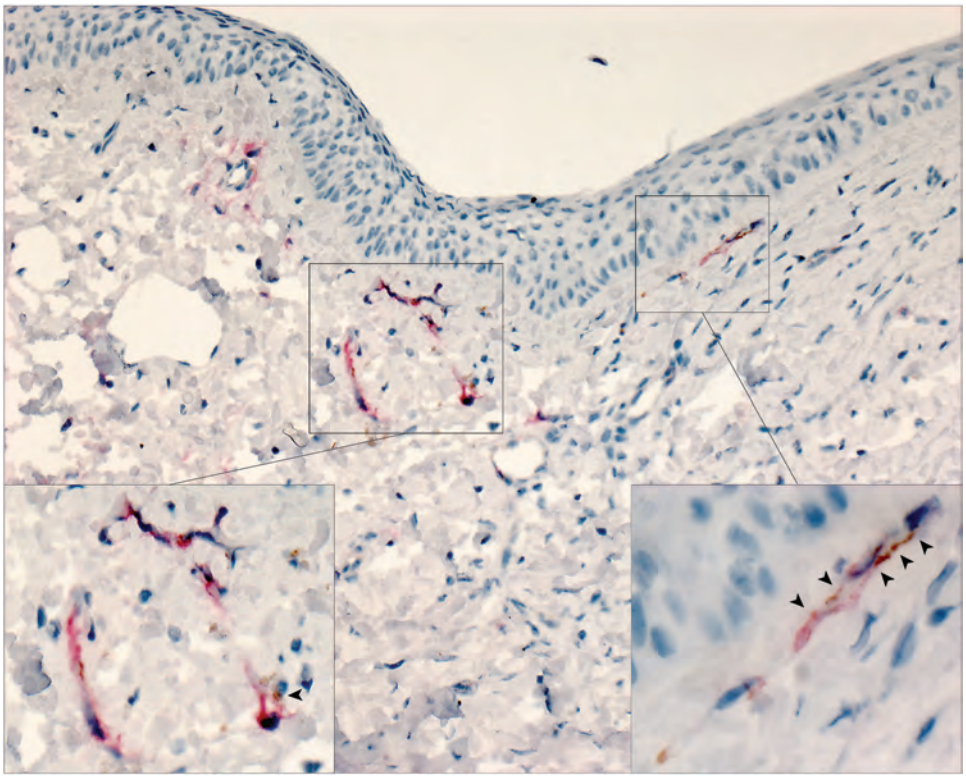

Figure 4. Lassa virus (LASV) targeting endothelial cells in the eye in study of LASV targeting of anterior uvea and endothelium of cornea and conjunctiva in eye. Co-staining for LASV antigen (red) and platelet endothelial cell adhesion molecule (an endothelial marker, brown) in vessels at the margin of the cornea and within the conjunctiva show co-localization of LASV and endothelial antigens (arrowheads). Original magnification ×10; insets enlarged to ×63.

as conjunctivitis and conjunctival edema (*9*), although uveitis resulted in transient blindness in 1 case (*3*). In this study, we observed conjunctivitis and conjunctival edema clinically in infected guinea pigs, as described in human patients with acute disease. LASV RNA was detected by PCR in the eye, and LASV antigen was detected by IHC within the anterior uvea of animals that died of infection, particularly in the endothelium and perivascular stromal cells, and occasionally within epithelium. Similar LASV immunostaining was previously noted in other tissues in this animal model, as were the histologic features of mild lymphocytic inflammation and rare cell death (*26*).

Other animal models of LF also demonstrate infection in the eye. For example, the aqueous humor of the anterior chamber of the eye was found to be heavily infected in rhesus macaques that died of experimental LASV infection (*27*). Perivascular infiltrates of plasma cells and lymphocytes were described in the choroid, sclera, iris, filtration angle, and ciliary body of most of the animals, similar to what we observed here in guinea pigs.

In contrast to the findings in humans with LF and in animal models of LF, ocular manifestations during infection with several other hemorrhagic fever viruses, including filoviruses and phenuiviruses, include a broader tissue tropism in the eye and some viral persistence within the eyes of survivors. During the most recent EVD outbreak, infectious virus was detected months after clinical resolution in the intraocular aqueous humor of 1 person (*11*), and uveitis was reported in 18% of a group of EVD survivors in Sierra Leone (*12*). Uveitis, both anterior and posterior, was described in a series of survivors of the 1995 EVD epidemic in the Democratic Republic of the Congo (*12*,*28*). Anterior uveitis was also described after infection with the related Marburg virus, and the virus was subsequently cultured from the aqueous fluid of this patient (*13*). Macular, paramacular, or extramacular retinal lesions, with hemorrhage, edema, vasculitis, and retinitis, often occurring bilaterally, have been reported in association with RVFV infection. Patients were monitored during a 6-month convalescence after RVFV infection, and though lesions were resorbed, approximately half of the patients permanently lost visual acuity (*15*,*16*). Subsequent studies from an RVFV outbreak in Saudi Arabia in 2000 reported similar findings (*14*).

Recent studies have focused heavily on ocular involvement in EVD, resulting in detailed clinical descriptions in patients and prioritization for evaluation in animal models. In primates with an acute course of disease that resulted in death, EBOV RNA was not detected in the parenchymal ocular tissues but was consistently detected in the blood vessels of the choroid or ciliary processes or in the optic nerve leptomeninges (*29*). In this nonhuman primate EVD model, EBOV persisted in the vitreous humor, in cells attached to the retinal inner limiting membranes, and in the ciliary body, with a predilection for CD68+ macrophage/

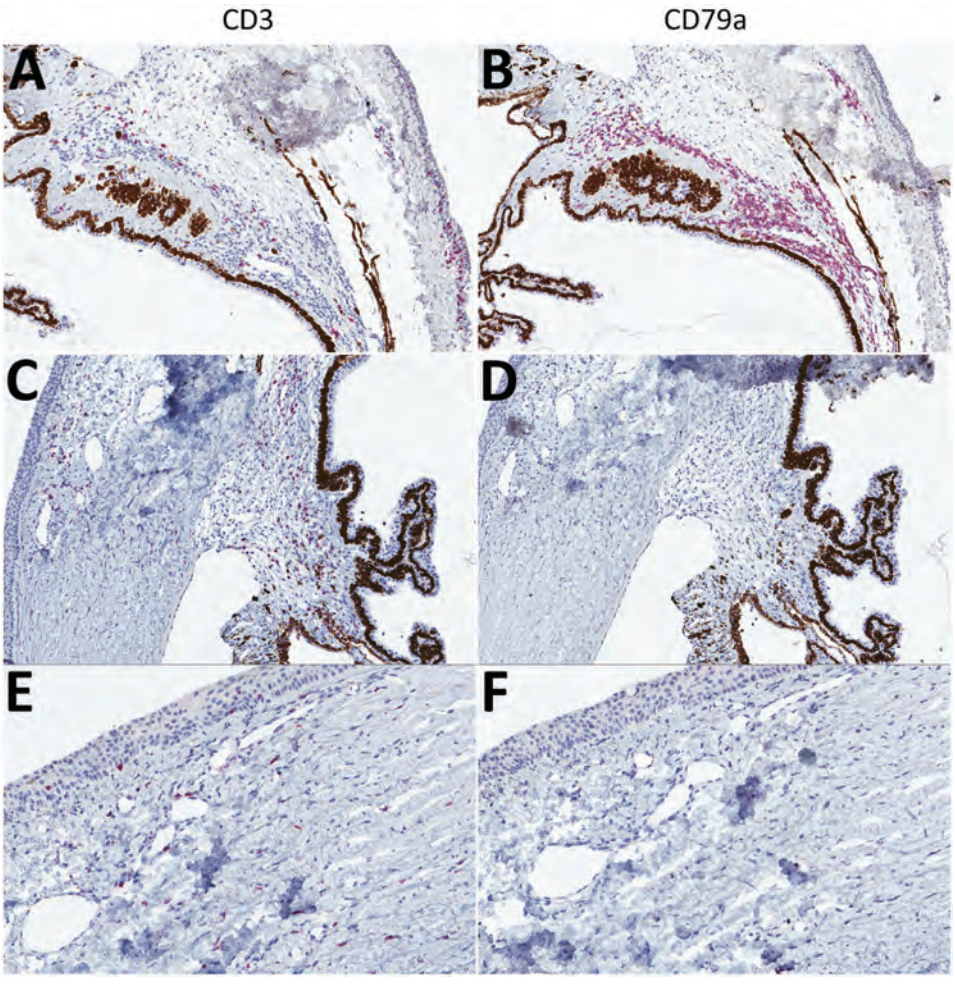

Figure 5. T-lymphocyte inflammation predominant in the eyes of animals that died of Lassa virus (LASV) infection >17 days postinfection in study of LASV targeting of anterior uvea and endothelium of cornea and conjunctiva in eye. CD3+ (left) and CD79a+ (right) lymphocyte antigens targeted by immunohistochemical (IHC) analysis are stained red. A) Inflamed filtration angle and sclera highlighting CD3+ T-lymphocytes. Original magnification ×10. B) Inflamed filtration angle and sclera highlighting the predominant population of CD79a+ B-lymphocytes. Original magnification ×10. C) Mildly inflamed filtration angle and sclera showing the predominance of CD3+ T-lymphocytes within the region. Original magnification ×10. D) Absence of CD79a+ B-lymphocytes. Original magnification ×10. E) New vessel formation at the margin of the cornea, indicating scattered CD3+ T-lymphocytes. Original magnification ×20. F) Minimal CD79a+ B-lymphocytes. Original magnification ×20. Representative animals: A, B, Jos-1; C–F, Jos-5.

monocytes, and with associated uveitis, retinitis, and vitritis (*29*). In contrast, we found that guinea pigs that died of LASV infection had viral antigen only in anterior regions of the eye, whereas surviving animals did not have LASV antigen and only showed minimal inflammation within the eye.

One major site of viral localization in this study was within endothelial cells in the conjunctiva and peripheral cornea. This finding correlated with studies describing the ability of LASV to replicate to high levels in endothelial cells and alter cytokine expression in cell culture (*30*). Another feature of ocular LASV infection noted in this study was the associated chronic inflammation, composed primarily of T-lymphocytes, in the anterior uvea, conjunctiva, and cornea in animals that died at later time points in the infection (>17 dpi). Lymphocytic anterior uveitis has been described in ocular infections with other viruses (e.g., rubella virus, cytomegalovirus, herpes simplex virus, and chikungunya virus) and can indicate a secondary immune response to viral antigens (*31*,*32*), although the pyknotic debris and swollen endothelium in the new vessels at the corneal margin in LASV-infected guinea pigs suggest a more acute insult. A predominantly T-lymphocyte response has been documented as a particularly important component of the systemic immune response to LASV infection (*33*).

Our studies in the strain 13/N guinea pig model indicate that LASV is present in the eye and elicits an inflammatory response primarily during acute clinical disease that is only minimally detected in convalescence. These features echo clinical findings in LF survivors, in whom ocular disease has not been described. The lack of reported ocular disease in LF survivors, along with the presence of only minimal or mild pathology in surviving animals, suggests less frequent or less severe ocular sequelae of LF than described in other viral hemorrhagic fever diseases. However, because similar mild inflammation has been associated with iris atrophy and ocular hypertension in other viral infections (*31*,*32*), the low degree of inflammation seen in our study is not necessarily innocuous. Although these data and the few clinical reports of ocular involvement in survivors of human LF disease support minimal long-term

effects on vision, careful ophthalmologic observation of LF survivors is warranted, along with further longitudinal studies in the subpopulation of animal models that survive LASV infection despite clinical signs. These studies would aid in determining whether the presence of LASV and the resultant inflammation, even after clearance, produce long-term sequelae in the eye.

Acknowledgments

We thank César G. Albariño for designing and generating recombinant viruses and Tatyana Klimova for assistance in editing the manuscript.

This work was supported in part by CDC emerging infectious disease research core funds.

About the Author

Dr. Gary is a veterinary pathologist with the Infectious Disease Pathology Branch, Division of High-Consequence Pathogens and Pathology, National Center for Emerging and Zoonotic Infectious Diseases, CDC. Her research interests include comparative pathology, zoonotic diseases, and digital pathology.

References

1. McCormick JB, Webb PA, Krebs JW, Johnson KM, Smith ES. A prospective study of the epidemiology and ecology of Lassa fever. J Infect Dis. 1987;155:437–44. http://dx.doi.org/10.1093/infdis/155.3.437
2. Frame JD, Baldwin JM Jr, Gocke DJ, Troup JM. Lassa fever, a new virus disease of man from West Africa. I. Clinical description and pathological findings. Am J Trop Med Hyg. 1970;19:670–6. http://dx.doi.org/10.4269/ajtmh.1970.19.670
3. McCormick JB, King IJ, Webb PA, Johnson KM, O'Sullivan R, Smith ES, et al. A case-control study of the clinical diagnosis and course of Lassa fever. J Infect Dis. 1987;155:445–55. http://dx.doi.org/10.1093/infdis/155.3.445
4. Mateer EJ, Huang C, Shehu NY, Paessler S. Lassa fever–induced sensorineural hearing loss: a neglected public health and social burden. PLoS Negl Trop Dis. 2018;12:e0006187. http://dx.doi.org/10.1371/journal.pntd.0006187
5. Yun NE, Ronca S, Tamura A, Koma T, Seregin AV, Dineley KT, et al. Animal model of sensorineural hearing loss associated with Lassa virus infection. J Virol. 2015;90:2920–7. http://dx.doi.org/10.1128/JVI.02948-15
6. Okokhere PO, Ibekwe TS, Akpede GO. Sensorineural hearing loss in Lassa fever: two case reports. J Med Case Reports. 2009;3:36. http://dx.doi.org/10.1186/1752-1947-3-36
7. Cummins D, McCormick JB, Bennett D, Samba JA, Farrar B, Machin SJ, et al. Acute sensorineural deafness in Lassa fever. JAMA. 1990;264:2093–6. http://dx.doi.org/10.1001/jama.1990.03450160063030
8. Rybak LP. Deafness associated with Lassa fever. JAMA. 1990;264:2119. http://dx.doi.org/10.1001/jama.1990.03450160089037
9. White HA. Lassa fever. A study of 23 hospital cases. Trans R Soc Trop Med Hyg. 1972;66:390–401. http://dx.doi.org/10.1016/0035-9203(72)90269-6
10. Jahrling PB, Hesse RA, Eddy GA, Johnson KM, Callis RT, Stephen EL. Lassa virus infection of rhesus monkeys: pathogenesis and treatment with ribavirin. J Infect Dis. 1980;141:580–9. http://dx.doi.org/10.1093/infdis/141.5.580
11. Varkey JB, Shantha JG, Crozier I, Kraft CS, Lyon GM, Mehta AK, et al. Persistence of Ebola virus in ocular fluid during convalescence. N Engl J Med. 2015;372:2423–7. http://dx.doi.org/10.1056/NEJMoa1500306
12. Yeh S, Shantha JG, Hayek B, Crozier I, Smith JR. Clinical manifestations and pathogenesis of uveitis in Ebola virus disease survivors. Ocul Immunol Inflamm. 2018;26:1128–1134.
13. Kuming BS, Kokoris N. Uveal involvement in Marburg virus disease. Br J Ophthalmol. 1977;61:265–6. http://dx.doi.org/10.1136/bjo.61.4.265
14. Al-Hazmi A, Al-Rajhi AA, Abboud EB, Ayoola EA, Al-Hazmi M, Saadi R, et al. Ocular complications of Rift Valley fever outbreak in Saudi Arabia. Ophthalmology. 2005;112:313–8. http://dx.doi.org/10.1016/j.ophtha.2004.09.018
15. Siam AL, Meegan JM, Gharbawi KF. Rift Valley fever ocular manifestations: observations during the 1977 epidemic in Egypt. Br J Ophthalmol. 1980;64:366–74. http://dx.doi.org/10.1136/bjo.64.5.366
16. Siam AL, Meegan JM. Ocular disease resulting from infection with Rift Valley fever virus. Trans R Soc Trop Med Hyg. 1980;74:539–41. http://dx.doi.org/10.1016/0035-9203(80)90074-7
17. Shantha JG, Mattia JG, Goba A, Barnes KG, Ebrahim FK, Kraft CS, et al. Ebola virus persistence in ocular tissues and fluids (EVICT) study: reverse transcription–polymerase chain reaction and cataract surgery outcomes of Ebola survivors in Sierra Leone. EBioMedicine. 2018;30:217–24. http://dx.doi.org/10.1016/j.ebiom.2018.03.020
18. Jahrling PB, Smith S, Hesse RA, Rhoderick JB. Pathogenesis of Lassa virus infection in guinea pigs. Infect Immun. 1982;37:771–8.
19. Welch SR, Scholte FEM, Albariño CG, Kainulainen MH, Coleman-McCray JD, Guerrero LW, et al. The S genome segment is sufficient to maintain pathogenicity in intra-clade Lassa virus reassortants in a guinea pig model. Front Cell Infect Microbiol. 2018;8:240. http://dx.doi.org/10.3389/fcimb.2018.00240
20. National Research Council of the National Academies. Guide for the care and use of laboratory animals. 8th ed. Washington (DC): The National Academies Press; 2011.
21. Wulff H, Johnson KM. Immunoglobulin M and G responses measured by immunofluorescence in patients with Lassa or Marburg virus infections. Bull World Health Organ. 1979;57:631–5.
22. Albariño CG, Bird BH, Chakrabarti AK, Dodd KA, Erickson BR, Nichol ST. Efficient rescue of recombinant Lassa virus reveals the influence of S segment noncoding regions on virus replication and virulence. J Virol. 2011;85:4020–4. http://dx.doi.org/10.1128/JVI.02556-10
23. Reed LJ, Muench H. A simple method for estimating fifty percent endpoints. Am J Hyg. 1938;27:493–7.
24. Kainulainen MH, Spengler JR, Welch SR, Coleman-McCray JD, Harmon JR, Klena JD, et al. Use of a scalable replicon-particle vaccine to protect against lethal Lassa virus infection in the guinea pig model. J Infect Dis. 2018;217:1957–66. http://dx.doi.org/10.1093/infdis/jiy123
25. Cvekl A, Tamm ER. Anterior eye development and ocular mesenchyme: new insights from mouse models and human diseases. BioEssays. 2004;26:374–86. http://dx.doi.org/10.1002/bies.20009
26. Bell TM, Shaia CI, Bearss JJ, Mattix ME, Koistinen KA, Honnold SP, et al. Temporal progression of lesions in guinea pigs infected with Lassa virus. Vet Pathol. 2017;54:549–62. Erratum in: Corrigendum. Vet Pathol. 2018. http://dx.doi.org/10.1177/0300985816677153
27. Walker DH, Johnson KM, Lange JV, Gardner JJ, Kiley MP, McCormick JB. Experimental infection of rhesus monkeys with Lassa virus and a closely related arenavirus, Mozambique

virus. J Infect Dis. 1982;146:360–8. http://dx.doi.org/10.1093/infdis/146.3.360
28. Kibadi K, Mupapa K, Kuvula K, Massamba M, Ndaberey D, Muyembe-Tamfum JJ, et al. Late ophthalmologic manifestations in survivors of the 1995 Ebola virus epidemic in Kikwit, Democratic Republic of the Congo. J Infect Dis. 1999;179 Suppl 1:S13–4.
29. Zeng X, Blancett CD, Koistinen KA, Schellhase CW, Bearss JJ, Radoshitzky SR, et al. Identification and pathological characterization of persistent asymptomatic Ebola virus infection in rhesus monkeys. Nat Microbiol. 2017;2:17113. http://dx.doi.org/10.1038/nmicrobiol.2017.113
30. Lukashevich IS, Maryankova R, Vladyko AS, Nashkevich N, Koleda S, Djavani M, et al. Lassa and Mopeia virus replication in human monocytes/macrophages and in endothelial cells: different effects on IL-8 and TNF-alpha gene expression. J Med Virol. 1999;59:552–60. http://dx.doi.org/10.1002/(SICI)1096-9071(199912) 59:4<552::AID-JMV21>3.0.CO;2-A
31. Jap A, Chee S-P. Cytomegalovirus-associated anterior segment infection. Expert Rev Ophthalmol. 2011;6:517–28. http://dx.doi.org/10.1586/eop.11.49
32. De Groot-Mijnes JDF, Chan ASY, Chee S-P, Verjans GMGM. Immunopathology of virus-induced anterior uveitis. Ocul Immunol Inflamm. 2018;26:338–46. http://dx.doi.org/10.1080/09273948.2018.1439069
33. Yun NE, Walker DH. Pathogenesis of Lassa fever. Viruses. 2012;4:2031–48. http://dx.doi.org/10.3390/v4102031

Address for correspondence: Jessica R. Spengler, Centers for Disease Control and Prevention, 1600 Clifton Rd NE, Mailstop H18-SB, Atlanta, GA 30329-4027, USA; email: JSpengler@cdc.gov

Age-Dependent Increase in Incidence of *Staphylococcus aureus* Bacteremia, Denmark, 2008–2015

Louise Thorlacius-Ussing, Haakon Sandholdt, Anders Rhod Larsen, Andreas Petersen, Thomas Benfield

Medscape EDUCATION ACTIVITY

In support of improving patient care, this activity has been planned and implemented by Medscape, LLC and Emerging Infectious Diseases. Medscape, LLC is jointly accredited by the Accreditation Council for Continuing Medical Education (ACCME), the Accreditation Council for Pharmacy Education (ACPE), and the American Nurses Credentialing Center (ANCC), to provide continuing education for the healthcare team.

Medscape, LLC designates this Journal-based CME activity for a maximum of 1.00 ***AMA PRA Category 1 Credit(s)™***. Physicians should claim only the credit commensurate with the extent of their participation in the activity.

Successful completion of this CME activity, which includes participation in the evaluation component, enables the participant to earn up to 1.0 MOC points in the American Board of Internal Medicine's (ABIM) Maintenance of Certification (MOC) program. Participants will earn MOC points equivalent to the amount of CME credits claimed for the activity. It is the CME activity provider's responsibility to submit participant completion information to ACCME for the purpose of granting ABIM MOC credit.

All other clinicians completing this activity will be issued a certificate of participation. To participate in this journal CME activity: (1) review the learning objectives and author disclosures; (2) study the education content; (3) take the post-test with a 75% minimum passing score and complete the evaluation at http://www.medscape.org/journal/eid; and (4) view/print certificate. For CME questions, see page 1036.

Release date: April 12, 2019; Expiration date: April 12, 2020

Learning Objectives

Upon completion of this activity, participants will be able to:

- Assess epidemiologic characteristics of *Staphylococcus aureus* bacteremia (SAB) cases in Denmark
- Distinguish age groups experiencing the biggest changes in the epidemiology of SAB
- Evaluate hospitalization data for SAB in Denmark
- Analyze mortality outcomes associated with SAB

CME Editor

Deborah Wenger, MBA, Copyeditor, Emerging Infectious Diseases. *Disclosure: Deborah Wenger, MBA, has disclosed no relevant financial relationships.*

CME Author

Charles P. Vega, MD, Health Sciences Clinical Professor of Family Medicine, University of California, Irvine School of Medicine, Irvine, California. Disclosure: *Charles P. Vega, MD, has disclosed the following relevant financial relationships: served as an advisor or consultant for Johnson & Johnson Pharmaceutical Research & Development, L.L.C.; Genentech; GlaxoSmithKline; served as a speaker or a member of a speakers bureau for Shire.*

Authors

Disclosures: ***Louise Thorlacius-Ussing, MD; Håkon Sandholdt, MSc; Anders Rhod Larsen, PhD;*** *and* ***Andreas Petersen, PhD,*** *have disclosed no relevant financial relationships.* ***Thomas Benfield, MD, DMSc,*** *has disclosed the following relevant financial relationships: served as a speaker or a member of a speakers bureau for Boehringer Ingelheim Pharmaceuticals, Inc.; GlaxoSmithKline; Pfizer Inc.; received grants for clinical research from GlaxoSmithKline; Pfizer Inc.; owns stock, stock options, or bonds from ViroGates.*

Author affiliations: Hvidovre Hospital, University of Copenhagen, Copenhagen, Denmark (L. Thorlacius-Ussing, H. Sandholdt, T. Benfield); Statens Serum Institut, Copenhagen (A. Larsen, A. Petersen)

DOI: https://doi.org/10.3201/eid2505.181733

Staphylococcus aureus bacteremia (SAB) is a major cause of illness and death worldwide. We analyzed temporal trends of SAB incidence and death in Denmark during 2008–2015. SAB incidence increased 48%, from 20.76 to 30.37 per 100,000 person-years, during this period ($p<0.001$). The largest change in incidence was observed for persons ≥80

years of age: a 90% increase in the SAB rate (p<0.001). After adjusting for demographic changes, annual rates increased 4.0% (95% CI 3.0–5.0) for persons <80 years of age, 8.4% (95% CI 7.0–11.0) for persons 80–89 years of age, and 13.0% (95% CI 9.0–17.5) for persons >90 years of age. The 30-day case-fatality rate remained stable at 24%; crude population death rates increased by 53% during 2008–2015 (p<0.001). Specific causes and mechanisms for this rapid increase in SAB incidence among the elderly population remain to be clarified.

Staphylococcus aureus is the most frequent gram-positive bacterium to cause invasive bloodstream infection (*1*). *S. aureus* bacteremia (SAB) is associated with considerable illness and death, yielding a case-fatality rate of 20%–25% (*2*). The occurrence of SAB has changed over time (*3*–*5*). Increasing incidence rates of SAB have been reported worldwide throughout the past few decades (*3*,*5*). However, more recent studies have reported stable or decreasing rates of SAB, as well as improved short-term death rates (*1*,*2*,*4*,*6*). As a result of demographic changes, including a rapidly increasing elderly population, contemporary analysis of the epidemiology of SAB is necessary to prioritize and allocate healthcare resources. Because concurrent conditions are more common with age, the changing demographics are of particular concern; older age and concurrent conditions are strongly associated with an increased risk for SAB (*2*,*4*,*7*).

Population-based studies are necessary to obtain valid epidemiologic data regarding SAB (*8*). Using surveillance data from the ongoing national registration of SAB in Denmark, we conducted a nationwide cohort study of temporal changes in SAB. The aims of this study were 2-fold. First, we analyzed temporal changes in SAB incidence; second, we assessed short-term death rates and associated risk factors.

Methods

Study Setting

We conducted a nationwide study of SAB in Denmark during 2008–2015. The population of Denmark comprised 5,475,791 residents in 2008 and 5,659,715 residents in 2015; all had free access to tax-financed healthcare. This study was approved by the Danish Data Protection Agency (approval nos. 2009-41-4179 and 2014-41-3376). Legislation in Denmark does not require informed consent for register-based studies.

Study Population

We identified cases of SAB using data from the continuous national SAB surveillance in Denmark (*5*). Inclusion in the register was based on the identification of *S. aureus* in ≥1 blood culture. We defined cases in the study as those in patients with a first-time episode of SAB recorded during January 1, 2008–December 31, 2015.

Data Sources

The unique civil registration number assigned to residents of Denmark by the Civil Registration System tracks information on vital and immigrant status and enables linkage of nationwide administrative healthcare registers on an individual level (*9*). The registry is updated daily.

The Danish National Patient Registry contains discharge diagnoses (from the International Classification of Diseases, 10th Revision) for residents regarding all hospital contacts (inpatient and outpatient) (*10*). The Danish National Bureau of Statistic provides data on the resident population and number of hospital admission and days in the hospital. The Danish Microbiology Database has conducted national surveillance on infectious diseases and microorganisms since 2010 (*11*).

Variables of Interest

We analyzed and stratified age by 11 age groups: <1, 1–9; 10–19; 20–29; 30–39; 40–49; 50–59; 60–69; 70–79; 80–89 and ≥90 years. We used the Charlson Comorbidity Index (CCI) was used as a general measure of concurrent conditions; this index has previously been validated for SAB (*12*). We categorized CCI score into 3 levels: no concurrent conditions (CCI score = 0), intermediate (CCI score = 1–2), or high (CCI score ≥3) (*2*).

Recent hospital contact within 90 days before SAB was applied as a proxy of healthcare- and hospital-acquired SAB. We have previously validated this approach with a positive predictive value of 83% of distinguishing between healthcare/hospital- and community-associated SAB (*13*).

Statistics

We reported counts by median and interquartile range (IQR). We computed crude incidence rates of SAB overall and by age, sex, and calendar year and calculated the incidence rates as the number of SAB cases per 100,000 person-years at risk and estimated person-years at risk assuming a uniform death rate throughout the year in the background population. We assessed temporal trends by comparing the incidence rate ratio (IRR) in 3 time periods, 2008–2010, 2011–2012, and 2013–2015. In addition, we used a Poisson regression model to evaluate the association of calendar year and incidence of SAB and added all available variables to the model hypothesized as confounders for the outcome in question. We validated the model assumptions using a quasi-Poisson model.

We performed several sensitivity analyses to assess whether changes in SAB incidence were associated with the rate of *S. aureus* isolates per 10,000 blood cultures,

per 100,000 hospital admissions, or per 100,000 hospital days; changes in the relative difference of CCI score during 2008–2014 between cases and the population controls, by randomly matching 10 population controls by age and gender to each SAB case; and the proportion of SAB cases during 2008–2014 with hospital contact within 90 days before the diagnosis of SAB. We reported all-cause death rates for SAB cases as a 30-day case-fatality rate (CFR) and deaths as a percentage of the number of cases. In addition, we calculated crude population death rates as deaths of SAB cases per 100,000 person-years in the background population and applied a mortality rate ratio (MRR) to assess temporal trends in death rates. We used logistic regression models to identify any association between risk factors and 30-day death rates and adjusted for the following covariates: age, gender, calendar year, CCI score, and 90-day prior hospital contact. We present risk estimates as odds ratio (OR) with 95% CIs, and for all analyses, we considered a p value ≤0.05 to be significant. We performed statistical analyses using R software version 3.2.3 (R Project for Statistical Computing, https://www.r-project.org).

Results

Demographics

We identified a total of 11,054 incident cases of SAB during the study period. Demographics of the study population are provided in Table 1. In brief, the median age was 68 years (IQR 56–79 years); 62% of patients were male and 38% female. More than 75% of SAB case-patients had ≥1 concurrent condition recorded before the SAB episode. Methicillin-resistant *S. aureus* (MRSA) accounted for 1.3% of cases.

Incidence Rates

The number of patients with SAB increased from 1,131 in 2008 to 1,731 in 2015, corresponding to a 48% increase in incidence, from 20.76 (95% CI 19.57–22.01) to 30.73 (95% CI 29.30–32.21) (IRR 1.48 [95% CI 1.37–1.59]), compared with an average annual incidence rate of 24.93 (95% CI, 24.47–25.40) cases/100,000 person-yeras. The highest incidence rates were observed among male patients, the elderly, and infants <1 year of age (Table 2; Figure 1; Appendix Tables 1–3, http://wwwnc.cdc.gov/EID/article/25/5/18-1733-App1.pdf).

For persons ≥80 years of age, the incidence rate increased consistently throughout the 8-year study period (Figure 1). As such, during 2008–2015, the relative proportion of cases in persons ≥80 years of age increased from 19.72% (95% CI 17.40–22.04) to 26.17% (95% CI 24.10–28.24) of all cases. Further, the age-specific incidence rate increased significantly, by an estimated 56% (IRR 1.56 [95% CI 1.41–1.72]) for persons 80–89 years of age and 92% (IRR1.92 [95% CI 1.57–2.37]) for patients ≥90 years of age in 2013–2015 compared with 2008–2010. For persons <80 years of age, only rates for patients 50–79 years of age increased in 2013–2015 compared with 2008–2010 (50–59 years, IRR 1.24 [95% CI 1.09–1.40]; 60–69 years, IRR 1.20 [95% CI 1.10–1.32]; 70–79 years, IRR 1.26 [95% CI 1.15–1.38]) (Appendix Table 1). For 2011–2012, the incidence rate for persons <80 years of age did not differ compared with the rates for 2008–2010. Gender did not affect the age-specific trends in SAB rate (Appendix Tables 2, 3).

Regression analysis indicated that age was strongly associated with SAB incidence (Table 2). Additionally, male case-patients had a 2-fold higher risk (IRR 2.00 [95% CI 1.92–2.08]) of acquiring SAB than female case-patients. After adjustment for demographic changes, the estimated annual rates of SAB increased by 4% (IRR 1.04 [95% CI 1.03–1.05]) for persons <80 years of age, 8% (IRR 1.08 [95% CI 1.07–1.11]) for persons 80–89 years of age, and 13% (IRR 1.13 [95% CI 9.0–17.5]) for persons ≥90 years (Figure 2; Appendix Figure 1).

Blood Culture Activity, Hospital Admission, and Hospital Stays

The number of blood cultures performed in the healthcare system in Denmark increased from 367,884 in 2010 to 480,892 in 2015. The positivity rate of *S. aureus* per 10,000 blood cultures increased from 33.43 (95% CI 31.59–35.36) to 36.00 (95% CI 34.32–37.73) during that period, corresponding to an increase of 8% (95% CI 0%–16%) (Appendix Table 4). The rate of SAB cases per 10,000 blood

Table 1. Demographic characteristics of patients with *Staphylococcus aureus* bacteremia, Denmark, 2008–2015*

Characteristic	Value
Sex	
F	4,161 (37.6)
M	6,893 (62.4)
Age, y	
<1	282 (2.6)
1–9	157 (1.4)
10–19	208 (1.9)
20–29	204 (1.8)
30–39	374 (3.4)
40–49	792 (7.2)
50–59	1,326 (12.0)
60–69	2,486 (22.4)
70–79	2,561 (23.2)
80–89	2,121 (19.2)
≥90	543 (4.9)
Median (IQR)	68 (56.0–79.0)
Mean (SD)	64 (63.9–64.7)
CCI score	
0	2,599 (23.5)
1–2	4,171 (37.7)
>3	4,284 (38.8)
MSSA	10,911 (98.7)
MRSA	143 (1.3)

*Values are no. (%) patients except as indicated. CCI, Charlson Comorbidity Index; IQR, interquartile range; MRSA, methicillin-resistant *S. aureus;* MSSA, methicillin-susceptible *S. aureus*.

Table 2. Incidence rate and incidence rate ratio of *Staphylococcus aureus* bacteremia stratified by sex and age, Denmark, 2008–2015*

Characteristic	IR, SAB/100.000 PY (95% CI)	IRR (95% CI)†	p value
Sex			
F	18.62 (18.06–19.19)	Referent	NA
M	31.35 (30.61–32.10)	2.00 (1.92–2.08)	<0.001
Age, y			
<1	57.96 (51.28–65.12)	17.37 (14.28–21.13)	<0.001
1–9	3.35 (2.84–3.91)	Referent	NA
10–19	3.75 (3.26–4.30)	1.12 (0.91–1.38)	0.281
20–29	3.84 (3.33–4.41)	1.15 (0.91–1.38)	0.199
30–39	6.50 (5.85–7.19)	1.96 (1.63–2.34)	<0.001
40–49	12.21 (11.37–13.09)	3.66 (3.09–4.34)	<0.001
50–59	22.92 (21.70–24.18)	6.88 (5.84–8.12)	<0.001
60–69	46.14 (44.35–47.99)	13.93 (11.86–16.36)	<0.001
70–79	81.26 (78.15–84.47)	24.93 (21.23–29.28)	<0.001
80–89	145.17 (139.05–151.45)	40.02 (33.35–48.03)	<0.001
≥90	197.03 (180.80–214.32)	49.97 (39.19–63.72)	<0.001
Period, per-year increment	NA	1.04 (1.03–1.05)	<0.001

*IR, incidence rate; IRR, incidence rate ratio; NA, not applicable; PY, person-years; SAB, *Staphylococcus aureus* bacteremia.
†Adjusted for sex, age, and period.

cultures remained stable for all age groups across the study period (Appendix Figure 2, Table 5). Annual hospital admissions increased from 1,175,452 to 1,347,563, but the total number of hospital days admitted decreased from 4,854,060 to 4,067,222 during 2008–2015. After adjustment, the number of SAB cases per 100,000 hospital admissions increased by 33% (95% CI 24%–44%) and SAB cases per 100,000 hospital days increased by 83% (95% CI 69%–97%) (Appendix Table 4).

Concurrent Conditions and Recent Hospital Contact before SAB

Patients with SAB had significantly more concurrent conditions than the matched population controls (mean CCI 2.43 for case-patients compared with 0.81 for population controls; p<0.001). SAB case-patients and population controls both had increasingly more concurrent conditions during the study period, but the changes over time were similar for case-patients and population controls overall and stratified by age (Appendix Figure 3). Approximately 75% (n = 6,707) of case-patients had had hospital contact within 90 days before their SAB diagnosis. The proportion of SAB cases with recent hospital contact remained unchanged over the years (Appendix Figure 4, panel A). Stratification by age did not affect this result (Appendix Figure 4, panel B).

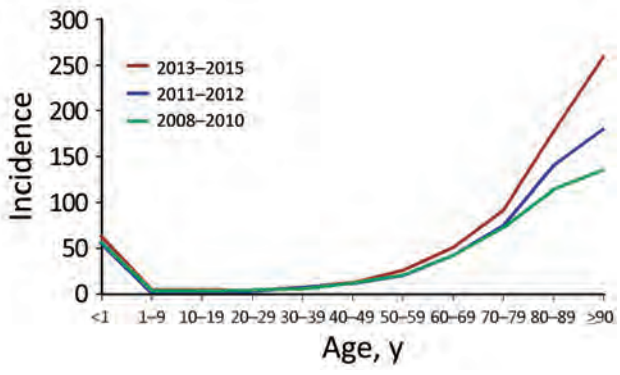

Figure 1. Temporal changes in *Staphylococcus aureus* bacteremia incidence (cases per 100,000 person-years), by age group and years, Denmark, 2008–2015.

CFR, Population Death Rate, and Associated Risk Factors

In the 8-year study period, 30-day all-cause deaths increased from 271 in 2008 to 428 in 2015. The population death rate for SAB rose significantly, from 4.97 (95% CI 4.40–5.60) to 7.60 (95% CI 6.90–8.35), corresponding to an estimated increase of 53% (MRR 1.53 [95% CI 1.31–1.78]) (Figure 3, panel A). Stratification by age group showed great variation in trends of the age-specific death rate, with the most rapid increase in death rate for the oldest age groups (Figure 3, panel B). For persons <80 years of age, the death rate increased by 25% (MRR 1.25 [95% CI 1.03-1.51]).

The overall 30-day CFR for the study period was 24% (95% CI 23%–25%) and remained unchanged over the years (Table 3; Figure 3, panel A). A higher 30-day CFR was observed with increasing age and CCI score, and for female compared with male case-patients (Table 3; Appendix Table 6). The 30-day CFR did not differ over time by gender or age (Appendix Figures 5, 6). Multivariate analysis indicated that age was strongly associated with 30-day CFR (Table 3). Any concurrent condition before SAB was also associated with higher risk of death. Compared with persons with no concurrent conditions, the risk for death increased for persons with increasing CCI scores (OR 1.32 [95% CI 1.14–1.55] for CCI score 1–2 and OR 1.67 [95% CI 1.43–1.94] for CCI score ≥3). Female sex was an independent risk factor for death compared with male sex (OR 1.20 [95% CI 1.08–1.33]). In contrast, prior hospital contact and time period were not associated with 30-day CFR.

Discussion

In this nationwide study, we evaluated trends of SAB incidence in the population of Denmark in an 8-year period, corresponding to >40 million patient-years. We report a 48% increase in SAB incidence during 2008–2015. Although the short-term death rate remained unchanged throughout the period, population-based death rates increased more than 50% because of the increase in SAB incidence.

The reported increase in SAB incidence was, in particular, a result of the major and consistent increase among persons ≥80 years of age: the SAB rate among the oldest old (≥80 years) rose with an alarming 90% during 2008–2015, corresponding to an estimated annual increase of 8%–13% in incidence rate. In comparison, a 36% increase in the incidence rate was found for persons <80 years of age.

The differential increase in the SAB rate among age groups stresses the importance of comprehensive data that enable age-stratified analyses when investigating temporal trends in infectious diseases. Significant changes in death and incidence rates within subgroups of a population may otherwise not be apparent.

The increasing incidence rate observed in this study is contrary to most other recent studies. Stable or decreasing rates of SAB were reported in several large observational studies (*2*,*4*–*6*,*14*,*15*). However, increasing rates of both community- and healthcare-acquired SAB were reported in a recent study in Finland (*16*). A higher occurrence of SAB is somewhat to be expected in an increasingly elderly population. However, our data showed an increase in SAB occurrence that exceeded contemporary changes in the population demographic profile.

Multiple factors may have influenced the changes in SAB incidence. Concurrent conditions form a strong risk factor associated with development of SAB; the increasing burden of concurrent conditions associated with aging could explain the higher SAB rate among the oldest elderly (*2*). The study population generally developed more concurrent conditions during the study period; thus, the number of persons at risk of acquiring SAB increased. However, because concurrent conditions increased similarly for SAB cases and population controls, the increasing incidence of SAB could not be explained solely by an increase in these conditions.

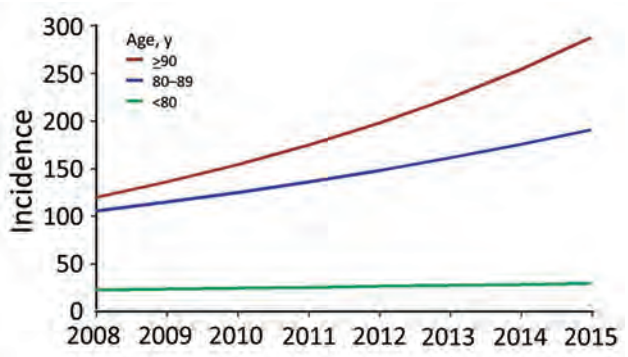

Figure 2. Increase in incidence of *Staphylococcus aureus* bacteremia for persons >80 years of age compared with younger persons, Denmark, 2008–2015.

A more liberal use of invasive hospital procedures and immune modulating treatments may also contribute to a higher occurrence of SAB. Although the proportion of SAB cases with 90-day prior hospital contact remained unchanged throughout the study, we do not know whether rates of invasive procedures and immune-suppressive medication increased in the same period. Thus, rates of hospital contacts might not be an accurate measure; recent reports showed an increasing use of chemotherapy and invasive procedures over time, in particular among the elderly (*17*,*18*).

The average life expectancy in Denmark increased during the study period, leading to an increasingly older and potentially more fragile population (*19*). There may be biologic risk factors of infectious diseases associated with aging that have not yet been identified. Physiologic age-dependent changes, such as immunological senescence, are likely attributable, in part, to the higher vulnerability to infectious diseases among elderly persons (*20*,*21*).

Higher rates of hospitalization and test activity and longer in-hospital stays may be other potential explanations for the increasing SAB rate (*22*). Blood culture activity

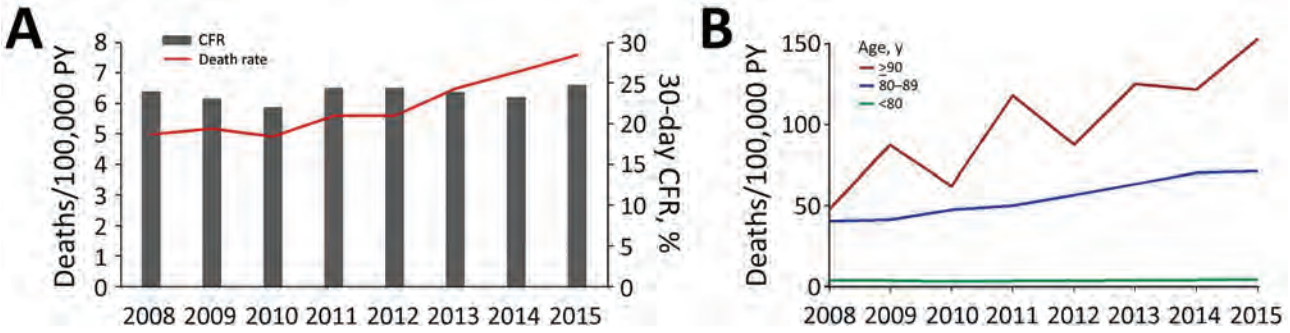

Figure 3. *Staphylococcus aureus* bacteremia deaths, Denmark, 2008–2015. A) Overall population death rate and 30-day CFR. B) Population death rates for persons >80 years of age compared with younger persons. PY, person-years.

Table 3. CFR and associated risk of *Staphylococcus aureus* bacteremia, Denmark, 2008–2015*

Characteristic	30-d CFR (95% CI)	Multivariate OR (CI 95%)	p value
Sex			
M	21.88 (20.79–23.01)	Referent	NA
F	26.92 (25.36–28.54)	1.20 (1.08–1.33)	<0.001
Age, y			
≤1	6.74 (4.06–10.52)	4.68 (1.05–20.85)	0.043
1–9	2.55 (0.69–6.52)	Referent	NA
10–19	1.92 (0.52–4.92)	1.71 (0.31–9.50)	0.538
20–29	2.94 (1.08–6.40)	2.22 (0.44–11.20)	0.333
30–39	2.13 (0.92–4.21)	1.36 (0.28–6.64)	0.705
40–49	9.47 (7.45–11.87)	6.37 (1.54–26.34)	0.011
50–59	16.44 (14.33–18.77)	10.79 (2.64–44.06)	<0.001
60–69	19.79 (18.08–21.62)	13.00 (3.19–52.89)	<0.001
70–79	27.80 (25.80–29.92)	19.69 (4.85–79.94)	<0.001
80–89	38.10 (35.51–40.82)	32.26 (7.94–131.03)	<0.001
≥90	51.93 (46.05–58.36)	58.48 (14.26–239.82	<0.001
CCI score			
0	14.20 (12.79–15.72)	Referent	NA
1–2	23.90 (22.44–25.43)	1.32 (1.14–1.55)	<0.001
≥3	29.46 (27.86–31.13)	1.67 (1.43–1.94)	<0.001
Hospital contact within 90 d			
No	22.21 (20.34–24.23)	Referent	NA
Yes	23.98 (22.82–25.18)	1.10 (0.97–1.24)	0.130
Period, per-year increment	NA	0.99 (0.97–1.01)	0.044

*CCI, Charlson Comorbidity Index; CFR, case-fatality rate; NA, not applicable; OR, odds ratio.

increased by 31% during the study period but the increase in the SAB positivity rate was 8%, suggesting that the increase in activity alone could not explain the observed changes. Further, a systematic increase in culture activity or higher sensitivity of culture systems would not explain a differential increase in incidence among age groups. Higher test rates would likely lead to the identification of milder cases of SAB. If so, a contemporary decline in the overall 30-day CFR would be expected, given higher survival rates among the less severe cases, but this was not the case.

Annual hospital admission rates increased by 15% and the number of days hospitalized declined by 16% during the study period, suggesting that changes in hospitalizations did not explain the increased rates of SAB. The increase in rates of SAB remained after adjustment for hospitalizations and hospital days. An increase in hospital-acquired infections is an unlikely explanation for the increased SAB rates because the proportion of SAB patients with and without 90-day prior hospital contact remained unchanged throughout the study.

A recent study found that the increase in sepsis rates and decline in death rates in California were associated with up-capture of less severely ill patients after introduction of guidance on coding based on the International Classification of Diseases, Ninth Revision (*23*). Our study, however, relied on blood culture positive cases of SAB; therefore, changes in coding practices are an unlikely explanation of our finding. Further, death rates were unchanged over time in our study.

In spite of a recent report of a decline in death associated with infectious diseases in general, SAB survival has not improved markedly during the past decades (*24*). The 30-day CFR of 24% found in our study is in line with other reports (*25*–*27*). However, the population death rate rose 1.5-fold, to 7.60/100,000 person-years by 2015, because of the contemporary increase in SAB incidence. Thus, population death rates may represent a more accurate measure of the actual disease burden, as changes in incidence are reflected despite an unchanged 30-day CFR. Few studies have reported SAB death rates as population death rates for comparison and none have reported age-specific death rates (*28*,*29*). Tom et al. reported a death rate from community-acquired SAB of 3.4/100,000 person-years (*28*). A recent study from Norway on bloodstream infections found a death rate for SAB similar to ours, of 7/100,000 person-years (*29*).

A particular finding in our study was the close association between the changes in the overall death rate and the increase in the age-specific death rate for the oldest age groups. The higher incidence rates for the oldest age groups were directly reflected by higher population death rates. Death rates from SAB will likely increase even more over the next decades owing to the increasingly older population, which may also be the case for other invasive bloodstream infections. However, temporal population death rates from nonstaphylococcal bloodstream infections have not been reported; further studies are warranted to address this matter.

Contrary to the case with most bloodstream infections, female sex has been associated with an inferior outcome in SAB (*25*). In agreement with several previous observations, we found a significantly higher death rate among women compared with men (*7*,*25*,*30*,*31*). The mechanisms underlying the observed gender differences in SAB death rates are not fully understood; a recent study did not find any gender-specific differences in clinical management,

patient characteristics, or severity of the disease between men and women (*32*).

This study benefits from the large number of observational years, nationwide settings, and standardized registration. Nonetheless, some limitations must be noted. First, the increasing life expectancy during the study period could have led to an increasing median age within age groups and, consequently, an underestimation of the effect of age on incidence rates, in particular for the oldest persons. Second, the SAB definition was based solely on microbiological findings and not related to criteria of clinical infection such as systemic inflammatory response syndrome and sequential organ failure assessment score. Thus, we cannot preclude that a minor proportion of the positive blood cultures may be from contamination rather than clinical infection. Still, this possibility does not explain the age-dependent increase in SAB. Third, we were not able to stratify SAB origin by community-, healthcare-, and hospital-acquired infections, because these data were not accessible. Instead, we used a validated approach to access temporal changes in healthcare/hospital- and community-acquired infections. Fourth, data on blood culture activity were not available for 2008–2009; thus, we were not able to analyze trends in culture rates for the whole study period. Finally, we did not have access to clinical data regarding the primary focus of the infection, the severity of the disease, and the applied treatment strategies, as well as the effect of these potential risk factors on SAB death.

MRSA bacteremia is infrequent in Denmark (1.3% of all SAB cases), which could theoretically limit the validity of the results of this study to settings with higher MRSA prevalence. Nevertheless, in most populations, methicillin-susceptible *S. aureus* (MSSA) bacteremia has remained prevalent despite the emergence of MRSA and, as such, several studies have concluded that MRSA bacteremia adds to the total burden of SAB rather than replacing MSSA bacteremia (*16*,*33*). Thus, we believe that the observed changes in MSSA bacteremia in our study may be applicable to other populations.

In conclusion, SAB incidence in Denmark increased by 48% during 2008–2015. SAB rates increased the most among the oldest age group, for whom the age-specific incidence rate nearly doubled and where increases in rates exceeded the contemporary changes in the population demographic profile. Furthermore, the short-term prognosis of SAB did not improve within the study period and, combined with the increasing incidence, population death rates rose significantly. Our results stress that infection prevention initiatives and improved care are warranted to reduce SAB incidence and improve outcomes. In addition, examinations of the burden of bloodstream infections caused by MSSA must be prioritized in future research; a specific focus should be on the frail elderly population.

Acknowledgments

The authors thank the departments of clinical microbiology throughout Denmark who contributed data to the national surveillance program.

About the Author

Dr. Thorlacius-Ussing is a physician and PhD student at Department of Infectious Diseases, Hvidovre Hospital, Copenhagen University, Denmark. Her primary research interests are epidemiology and management of invasive bloodstream infections.

References

1. Nielsen SL, Pedersen C, Jensen TG, Gradel KO, Kolmos HJ, Lassen AT. Decreasing incidence rates of bacteremia: a 9-year population-based study. J Infect. 2014;69:51–9. http://dx.doi.org/10.1016/j.jinf.2014.01.014
2. Mejer N, Westh H, Schønheyder HC, Jensen AG, Larsen AR, Skov R, et al.; Danish Staphylococcal Bacteraemia Study Group. Stable incidence and continued improvement in short term mortality of *Staphylococcus aureus* bacteraemia between 1995 and 2008. BMC Infect Dis. 2012;12:260. http://dx.doi.org/10.1186/1471-2334-12-260
3. Lyytikäinen O, Ruotsalainen E, Järvinen A, Valtonen V, Ruutu P. Trends and outcome of nosocomial and community-acquired bloodstream infections due to *Staphylococcus aureus* in Finland, 1995–2001. Eur J Clin Microbiol Infect Dis. 2005; 24:399–404. http://dx.doi.org/10.1007/s10096-005-1345-3
4. Laupland KB, Lyytikäinen O, Søgaard M, Kennedy KJ, Knudsen JD, Ostergaard C, et al.; International Bacteremia Surveillance Collaborative. The changing epidemiology of *Staphylococcus aureus* bloodstream infection: a multinational population-based surveillance study. Clin Microbiol Infect. 2013; 19:465–71. http://dx.doi.org/10.1111/j.1469-0691.2012.03903.x
5. Benfield T, Espersen F, Frimodt-Møller N, Jensen AG, Larsen AR, Pallesen LV, et al. Increasing incidence but decreasing in-hospital mortality of adult *Staphylococcus aureus* bacteraemia between 1981 and 2000. Clin Microbiol Infect. 2007;13:257–63. http://dx.doi.org/10.1111/j.1469-0691.2006.01589.x
6. Khatib R, Sharma M, Iyer S, Fakih MG, Obeid KM, Venugopal A, et al. Decreasing incidence of *Staphylococcus aureus* bacteremia over 9 years: greatest decline in community-associated methicillin-susceptible and hospital-acquired methicillin-resistant isolates. Am J Infect Control. 2013;41:210–3. http://dx.doi.org/10.1016/j.ajic.2012.03.038
7. Braquet P, Alla F, Cornu C, Goehringer F, Piroth L, Chirouze C, et al.; VIRSTA-AEPEI study group. Factors associated with 12 week case-fatality in *Staphylococcus aureus* bacteraemia: a prospective cohort study. Clin Microbio l Infect. 2016;22:948.e1–7. http://dx.doi.org/10.1016/j.cmi.2016.07.034
8. Laupland KB. Incidence of bloodstream infection: a review of population-based studies. Clin Microbiol Infect. 2013;19:492–500. http://dx.doi.org/10.1111/1469-0691.12144
9. Schmidt M, Pedersen L, Sørensen HT. The Danish Civil Registration System as a tool in epidemiology. Eur J Epidemiol. 2014;29:541–9. http://dx.doi.org/10.1007/s10654-014-9930-3
10. Lynge E, Sandegaard JL, Rebolj M. The Danish National Patient Register. Scand J Public Health. 2011;39(suppl7):30–3. http://dx.doi.org/10.1177/1403494811401482
11. Voldstedlund M, Haarh M, Mølbak K,; MiBa Board of Representatives. The Danish Microbiology Database (MiBa) 2010 to 2013. Euro Surveill. 2014;19:20667. http://dx.doi.org/10.2807/1560-7917.ES2014.19.1.20667

12. Lesens O, Methlin C, Hansmann Y, Remy V, Martinot M, Bergin C, et al. Role of comorbidity in mortality related to *Staphylococcus aureus* bacteremia: a prospective study using the Charlson weighted index of comorbidity. Infect Control Hosp Epidemiol. 2003;24:890–6. http://dx.doi.org/10.1086/502156
13. Gotland N, Uhre ML, Mejer N, Skov R, Petersen A, Larsen AR, et al.; Danish Staphylococcal Bacteremia Study Group. Long-term mortality and causes of death associated with *Staphylococcus aureus* bacteremia. A matched cohort study. J Infect. 2016;73:346–57. http://dx.doi.org/10.1016/j.jinf.2016.07.005
14. Mitchell BG, Collignon PJ, McCann R, Wilkinson IJ, Wells A. A major reduction in hospital-onset *Staphylococcus aureus* bacteremia in Australia—12 years of progress: an observational study. Clin Infect Dis. 2014;59:969–75. http://dx.doi.org/10.1093/cid/ciu508
15. David MZ, Daum RS, Bayer AS, Chambers HF, Fowler VG Jr, Miller LG, et al. *Staphylococcus aureus* bacteremia at 5 US academic medical centers, 2008–2011: significant geographic variation in community-onset infections. Clin Infect Dis. 2014; 59:798–807. http://dx.doi.org/10.1093/cid/ciu410
16. Jokinen E, Laine J, Huttunen R, Lyytikäinen O, Vuento R, Vuopio J, et al. Trends in incidence and resistance patterns of *Staphylococcus aureus* bacteremia. Infect Dis (Lond). 2018;50:52–8. http://dx.doi.org/10.1080/23744235.2017.1405276
17. van der Geest LGM, Haj Mohammad N, Besselink MGH, Lemmens VEPP, Portielje JEA, van Laarhoven HWM, et al.; Dutch Pancreatic Cancer Group. Nationwide trends in chemotherapy use and survival of elderly patients with metastatic pancreatic cancer. Cancer Med. 2017;6:2840–9. http://dx.doi.org/10.1002/cam4.1240
18. Pagé M, Doucet M, Eisenberg MJ, Behlouli H, Pilote L. Temporal trends in revascularization and outcomes after acute myocardial infarction among the very elderly. CMAJ. 2010;182:1415–20. http://dx.doi.org/10.1503/cmaj.092053
19. Statistics Denmark. Life expectancy [cited 2018 Oct 10]. https://www.dst.dk/en/Statistik/emner/befolkning-og-valg/doedsfald-og-middellevetid/middellevetid
20. Gavazzi G, Krause K-H. Ageing and infection. Lancet Infect Dis. 2002;2:659–66. http://dx.doi.org/10.1016/S1473-3099(02)00437-1
21. Butcher S, Chahel H, Lord JM. Ageing and the neutrophil: no appetite for killing? Immunology. 2000;100:411–6. http://dx.doi.org/10.1046/j.1365-2567.2000.00079.x
22. Laupland KB, Niven DJ, Pasquill K, Parfitt EC, Steele L. Culturing rate and the surveillance of bloodstream infections: a population-based assessment. Clin Microbiol Infect. 2018;24:910.e1–4. http://dx.doi.org/10.1016/j.cmi.2017.12.021
23. Gohil SK, Cao C, Phelan M, Tjoa T, Rhee C, Platt R, et al. Impact of policies on the rise in sepsis incidence, 2000–2010. Clin Infect Dis. 2016;62:695–703. http://dx.doi.org/10.1093/cid/civ1019
24. El Bcheraoui C, Mokdad AH, Dwyer-Lindgren L, Bertozzi-Villa A, Stubbs RW, Morozoff C, et al. Trends and patterns of differences in infectious disease mortality among US counties, 1980–2014. JAMA. 2018;319:1248–60. http://dx.doi.org/10.1001/jama.2018.2089
25. Smit J, López-Cortés LE, Kaasch AJ, Søgaard M, Thomsen RW, Schønheyder HC, et al. Gender differences in the outcome of community-acquired *Staphylococcus aureus* bacteraemia: a historical population-based cohort study. Clin Microbiol Infect. 2017;23:27–32. http://dx.doi.org/10.1016/j.cmi.2016.06.002
26. Allard C, Carignan A, Bergevin M, Boulais I, Tremblay V, Robichaud P, et al. Secular changes in incidence and mortality associated with *Staphylococcus aureus* bacteraemia in Quebec, Canada, 1991–2005. Clin Microbiol Infect. 2008;14:421–8. http://dx.doi.org/10.1111/j.1469-0691.2008.01965.x
27. Søgaard M, Nørgaard M, Dethlefsen C, Schønheyder HC. Temporal changes in the incidence and 30-day mortality associated with bacteremia in hospitalized patients from 1992 through 2006: a population-based cohort study. Clin Infect Dis. 2011;52:61–9. http://dx.doi.org/10.1093/cid/ciq069
28. Tom S, Galbraith JC, Valiquette L, Jacobsson G, Collignon P, Schønheyder HC, et al.; International Bacteraemia Surveillance Collaborative. Case fatality ratio and mortality rate trends of community-onset *Staphylococcus aureus* bacteraemia. Clin Microbiol Infect. 2014;20:O630–2. http://dx.doi.org/10.1111/1469-0691.12564
29. Mehl A, Åsvold BO, Lydersen S, Paulsen J, Solligård E, Damås JK, et al. Burden of bloodstream infection in an area of mid-Norway 2002–2013: a prospective population-based observational study. BMC Infect Dis. 2017;17:205. http://dx.doi.org/10.1186/s12879-017-2291-2
30. Yahav D, Yassin S, Shaked H, Goldberg E, Bishara J, Paul M, et al. Risk factors for long-term mortality of *Staphylococcus aureus* bacteremia. Eur J Clin Microbiol Infect Dis. 2016;35:785–90. http://dx.doi.org/10.1007/s10096-016-2598-8
31. Mansur N, Hazzan R, Paul M, Bishara J, Leibovici L. Does sex affect 30-day mortality in *Staphylococcus aureus* bacteremia? Gend Med. 2012;9:463–70. http://dx.doi.org/10.1016/j.genm.2012.10.009
32. Forsblom E, Kakriainen A, Ruotsalainen E, Järvinen A. Comparison of patient characteristics, clinical management, infectious specialist consultation, and outcome in men and women with methicillin-sensitive *Staphylococcus aureus* bacteremia: a propensity-score adjusted retrospective study. Infection. 2018;46:837–45. http://dx.doi.org/10.1007/s15010-018-1216-3
33. Mostofsky E, Lipsitch M, Regev-Yochay G. Is methicillin-resistant *Staphylococcus aureus* replacing methicillin-susceptible *S. aureus*? J Antimicrob Chemother. 2011;66:2199–214. http://dx.doi.org/10.1093/jac/dkr278

Address for correspondence: Louise Thorlacius-Ussing, Hvidovre Hospital Department of Infectious Diseases, Kettegaard Allé 30, 2650 Hvidovre, Denmark; email: louise.thorlacius-ussing@regionh.dk

Novel Sequence Type in *Bacillus cereus* Strains Associated with Nosocomial Infections and Bacteremia, Japan

Reiko Akamatsu, Masato Suzuki, Keiji Okinaka, Teppei Sasahara, Kunikazu Yamane, Satowa Suzuki, Daisuke Fujikura,[1] Yoshikazu Furuta, Naomi Ohnishi,[2] Minoru Esaki, Keigo Shibayama, Hideaki Higashi

Medscape EDUCATION ACTIVITY

In support of improving patient care, this activity has been planned and implemented by Medscape, LLC and Emerging Infectious Diseases. Medscape, LLC is jointly accredited by the Accreditation Council for Continuing Medical Education (ACCME), the Accreditation Council for Pharmacy Education (ACPE), and the American Nurses Credentialing Center (ANCC), to provide continuing education for the healthcare team.

Medscape, LLC designates this Journal-based CME activity for a maximum of 1.00 ***AMA PRA Category 1 Credit(s)™***. Physicians should claim only the credit commensurate with the extent of their participation in the activity.

Successful completion of this CME activity, which includes participation in the evaluation component, enables the participant to earn up to 1.0 MOC points in the American Board of Internal Medicine's (ABIM) Maintenance of Certification (MOC) program. Participants will earn MOC points equivalent to the amount of CME credits claimed for the activity. It is the CME activity provider's responsibility to submit participant completion information to ACCME for the purpose of granting ABIM MOC credit.

All other clinicians completing this activity will be issued a certificate of participation. To participate in this journal CME activity: (1) review the learning objectives and author disclosures; (2) study the education content; (3) take the post-test with a 75% minimum passing score and complete the evaluation at http://www.medscape.org/journal/eid; and (4) view/print certificate. For CME questions, see page 1035.

Release date: April 17, 2019; Expiration date: April 17, 2020

Learning Objectives

Upon completion of this activity, participants will be able to:

- Describe findings from genotype analysis of *Bacillus cereus* strains isolated from recent nosocomial infections in Japan in 2006, 2012, 2013, and 2016
- Determine findings from multilocus sequence typing analysis of *B. cereus* strains isolated from recent nosocomial infections in Japan in 2006, 2012, 2013, and 2016
- Explain findings from phylogenetic analysis of *B. cereus* strains isolated from recent nosocomial infections in Japan in 2006, 2012, 2013, and 2016.

CME Editor

Thomas J. Gryczan, MS, Technical Writer/Editor, Emerging Infectious Diseases. *Disclosure: Thomas J. Gryczan, MS, has disclosed no relevant financial relationships.*

CME Author

Laurie Barclay, MD, freelance writer and reviewer, Medscape, LLC. *Disclosure: Laurie Barclay, MD, has disclosed no relevant financial relationships.*

Authors

Disclosures: ***Reiko Akamatsu, DVM; Masato Suzuki, PhD; Keiji Okinaka, MD; Teppei Sasahara, MD, PhD; Kunikazu Yamane, MD, PhD; Satowa Suzuki, MD, PhD, MPH; Daisuke Fujikura, DVM, PhD; Yoshikazu Furuta, PhD; Naomi Ohnish, PhD; Minoru Esaki, MD, PhD; Keigo Shibayama, MD, PhD;*** *and* ***Hideaki Higashi, PhD,*** *have disclosed no relevant financial relationships.*

Author affiliations: Hokkaido University, Sapporo, Japan (R. Akamatsu, D. Fujikura, Y. Furuta, N. Ohnishi, H. Higashi); National Institute of Infectious Diseases, Tokyo, Japan (M. Suzuki, S. Suzuki, K. Shibayama); National Cancer Center Hospital, Tokyo (K. Okinaka, M. Esaki); Jichi Medical University, Tochigi, Japan (T. Sasahara); Yonago Medical Center, Tottori, Japan (K. Yamane)

DOI: https://doi.org/10.3201/eid2505.171890

[1]Current affiliation: Asahikawa Medical University, Asahikawa, Japan.

[2]Current affiliation: Japanese Foundation for Cancer Research, Tokyo, Japan

Bacillus cereus is associated with foodborne illnesses characterized by vomiting and diarrhea. Although some *B. cereus* strains that cause severe extraintestinal infections and nosocomial infections are recognized as serious public health threats in healthcare settings, the genetic backgrounds of *B. cereus* strains causing such infections remain unknown. By conducting pulsed-field gel electrophoresis and multilocus sequence typing, we found that a novel sequence type (ST), newly registered as ST1420, was the dominant ST isolated from the cases of nosocomial infections that occurred in 3 locations in Japan in 2006, 2013, and 2016. Phylogenetic analysis showed that ST1420 strains belonged to the Cereus III lineage, which is much closer to the Anthracis lineage than to other Cereus lineages. Our results suggest that ST1420 is a prevalent ST in *B. cereus* strains that have caused recent nosocomial infections in Japan.

Bacillus cereus causes foodborne illness that is characterized by vomiting because of production of emetic toxin and diarrhea because of production of enterotoxin (*1*). In addition to foodborne illness, *B. cereus* causes severe nongastrointestinal infections, such as bacteremia (*2*), endocarditis (*3*), meningoencephalitis (*4*), and pneumonia (*5*). Severe infections occur particularly in immunocompromised patients, sometimes resulting in nosocomial infections. Such nosocomial infections with *B. cereus* have been reported to be associated with *B. cereus* contamination of ventilator equipment (*6*), intravenous catheters (*7*), and linens (*8*).

Multilocus sequence typing (MLST) is a molecular typing technique based on 7 housekeeping genes (*9*). The phylogenetic tree of isolates of *B. cereus* group species, which include *B. anthracis*, *B. thuringiensis*, and several *B. cereus* subspecies (*10*), clusters into clades 1, 2, and 3. Clade 1 consists of 4 lineages defined by Priest et al. (*9*). Previous MLST studies have shown that clinical isolates of *B. cereus* are phylogenetically diverse and clustered mainly in clades 1 and 2 (*11*), suggesting that specific clones or lineages of *B. cereus* are associated with specific illnesses and severe infections. For example, Zhang et al. showed that isolates from outbreaks of nosocomial infections were closely related to *B. anthracis* by phylogenetic analysis using MLST (*12*).

There have been only a few reports on MLST analysis of *B. cereus* isolates that have caused nosocomial infections (*12*,*13*). The objective of our study was to elucidate the genetic characteristics of *B. cereus* strains that were isolated from recent nosocomial infections in 4 hospitals in Japan during 2006, 2012, 2013, and 2016. A novel sequence type (ST) was dominant in isolates from 3 of the hospitals, suggesting a strong association of the ST with recent nosocomial infections in Japan.

Materials and Methods

Bacterial Strains

We used 4 groups of B. cereus strains in our study (Table 1, https://wwwnc.cdc.gov/EID/article/25/5/17-1890-T1.htm; Table 2, https://wwwnc.cdc.gov/EID/article/25/5/17-1890-T2.htm; Tables 3, 4). A total of 69 strains were isolated from equipment and patients in a hospital in Tokyo that had *B. cereus* infections in 2013. These strains were designated Tokyo strains. Two blood cultures were prepared per patient. A patient was considered to have bacteremia when a B. cereus strain was isolated from both cultures. A patient was designated as having pseudobacteremia when a B. cereus strain was isolated from only 1 of the 2 cultures. A total of 65 strains were isolated from equipment and patients in a hospital in Tochigi that had B. cereus infections in 2006. These strains were designated Tochigi strains (*14*). During 2012, four strains were isolated from patients in hospitals in Kochi. These strains were designated Kochi strains. During 2016, ten strains were isolated from patients in hospitals in Tottori. These strains were designated Tottori strains. The Tokyo, Tottori, and Kochi strains were isolated by medical institutions in Japan (Tokyo, Tottori, and Kochi, respectively), and the Tochigi strains were isolated by Jichi Medical University (Tochigi, Japan).

Pulsed-Field Gel Electrophoresis

We performed pulsed-field gel electrophoresis (PFGE) for the Tokyo, Tochigi, and Tottori strains to determine their genetic relatedness. DNA was digested with *Sma*I. We used the CHEF Mapper Pulsed Field Electrophoresis Systems (Bio-Rad Laboratories, https:///www.bio-rad.com) for electrophoresis. We analyzed resulting photographic images by using the GelCompar II software (Applied Maths, http://www.applied-maths.com). Isolates with a PFGE fingerprint similarity >80% were clustered into the same PFGE cluster type (*15*).

Repetitive-Element PCR

We isolated DNA by using the Ultraclean Microbial DNA Isolation Kit (MO BIO Laboratories, https://mobio.com) and performed DNA amplification by using a DiversiLab *Bacillus* Fingerprinting Kit (bioMérieux, https://www.biomerieux.com). We separated repetitive-element PCR (rep-PCR) amplicons in a microfluidics DNA chip by using an Agilent 2100 Bioanalyzer (Agilent Technologies, Inc., https://www.agilent.com) and performed analysis by using DiversiLab version 3.4 software (bioMérieux), which uses the Pearson product-moment correlation and the unweighted pair group method with arithmetic averages. Isolates with a rep-PCR fingerprint similarity >96% were categorized as being in the same rep-PCR cluster type (*16*).

Table 3. Sequence types and source of 10 *Bacillus cereus* Tottori strains, Japan*

Sequence type	Sample name
1420†	Tottori_ID2
	Tottori_ID4_#2‡
	Tottori_ID5
	Tottori_ID6
	Tottori_ID8
1431†	Tottori_ID3
1828†	Tottori_ID1
163	Tottori_ID4_#1‡
368	Tottori_ID7
953	Tottori_ID9

*All strains were isolated from patient blood.
†Sequence types found in this study.
‡Samples isolated from the same patients at different time points.

Multilocus Sequence Typing

For the Tokyo, Kochi and Tottori strains, 7 sets of primers in the *B. cereus* MLST database (http://www.pubmlst.org/bcereus) were used to perform PCR analysis for the 7 MLST gene loci (*glpF*, *gmk*, *ilvD*, *pta*, *pur*, *pycA*, and *tpi*). We purified PCR products by using QIAquick PCR Purification (QIAGEN, https://www.qiagen.com), followed by sequencing with the 3130xl Genetic Analyzer (Life Technologies, https://www.thermofisher.com), after performing a reaction using the BigDye Terminator v3.1 Cycle Sequencing Kit (Life Technologies). Sequences of the 7 genes were trimmed to the lengths described in the database. Each unique sequence was assigned an allele number according to the *B. cereus* MLST database. We determined the ST by combining the allele numbers for all 7 loci. For the Tochigi strains, we determined STs by using results of whole-genome sequencing with the Illumina MiSeq Platform (Illumina, https://www.illumina.com). Sequences were de novo assembled by using Platanus_B version 1.1.0) (*17*). STs were determined from the de novo assembled genomes by using MLST2.0 (*18*).

We constructed phylogenetic trees by using MEGA7 (*19*) and aligned sequences produced by concatenating the sequence of each locus for MLST by using the neighbor-joining method (*19*,*20*). Branch quality was evaluated by using a bootstrap test with 1,000 replicates. We obtained sequences of each locus in the representative strains of *B. cereus*, *B. anthracis*, *B. thuringiensis*, *B. mycoides*, *B. pseudomycoides*, and *B. weihenstephanensis* from the *B. cereus* MLST database and used as references.

Table 4. Sequence types and source of 4 *Bacillus cereus* Kochi strains, Japan*

Sequence type	Sample name
1432†	Kochi_ID3
368	Kochi_ID1_#1‡
	Kochi_ID1_#2‡
427	Kochi_ID2

*All strains were isolated from patient blood.
†Sequence type found in this study.
‡Samples isolated from the same patients at different time points.

Results

Genotype Profile of Tokyo Strains

During June–August 2013, a hospital in Tokyo had nosocomial infections attributed to *B. cereus* that caused bacteremia in 13 patients and led to the death of 2 patients. To genetically characterize *B. cereus* isolated from patients and equipment in the hospital, which we named Tokyo strains, we performed PFGE analysis and rep-PCR fingerprinting. Among the Tokyo strains, we detected 19 PFGE cluster types and 11 rep-PCR cluster types. We found by PFGE analysis that more than one third of the Tokyo strains were in a single PFGE cluster, which was denoted cluster e (Figure 1). Rep-PCR fingerprinting showed results consistent with those of PFGE analysis, in which all but 1 of the isolates in cluster e identified by PFGE were in the same cluster type identified by rep-PCR (Figure 1).

MLST Analysis of Tokyo, Tochigi, Tottori, and Kochi Strains

To identify the genetic characteristics of the Tokyo strains, we performed MLST analysis for the Tokyo strains. For the 69 isolates, Tokyo strains had 18 distinct STs, including 7 novel STs (Table 1). The strains in the largest cluster, which was based on PFGE and rep-PCR analyses, were all determined to have the same novel ST that had been newly registered as ST1420. Therefore, results indicated the presence of a major cluster in the Tokyo strains (Figure 1).

Thirteen strains from blood samples isolated from 12 patients with bacteremia had the following 4 STs: 1420, 1421, 1428, and 368 (Table 1). Nine isolates with ST1420 were isolated from 8 of the 12 patients. We observed that strains that caused bacteremia were identified as ST1420 at a significantly high rate ($p = 0.03$ by Fisher exact test), suggesting an association between ST1420 and bacteremia cases with Tokyo strains.

To evaluate the relationship between ST1420 and other *B. cereus* isolates associated with nosocomial infections, we performed MLST for the Tochigi, Tottori and Kochi strains. The strains were also isolates from nosocomial infections by *B. cereus* in Japan but occurred in different prefectures and different years. The Tochigi strains were determined to have 19 distinct STs (Table 2), 8 of which were novel. Fifteen isolates from blood samples of 9 patients with bacteremia had the following 5 STs: 1420, 1425, 167, 365, and 368. Eight strains with ST1420 were isolated from 4 of 9 patients with bacteremia. The Tottori strains, all isolated from blood samples of patients with bacteremia, had the following 6 STs: 1420, 1431, 163, 368, 953, and 1828 (Table 3). ST1420 was isolated from 5 patients. ST1420 was also a dominant ST among isolates from patients with bacteremia

involving the Tochigi and Tottori strains, similar to that for the Tokyo strains. The Kochi strains, which were also isolated from 4 blood samples of 3 patients with bacteremia, had the following 3 STs: 1432, 368, and 427 (Table 4). Although it was not possible to rule out the likelihood that strains with other STs were associated

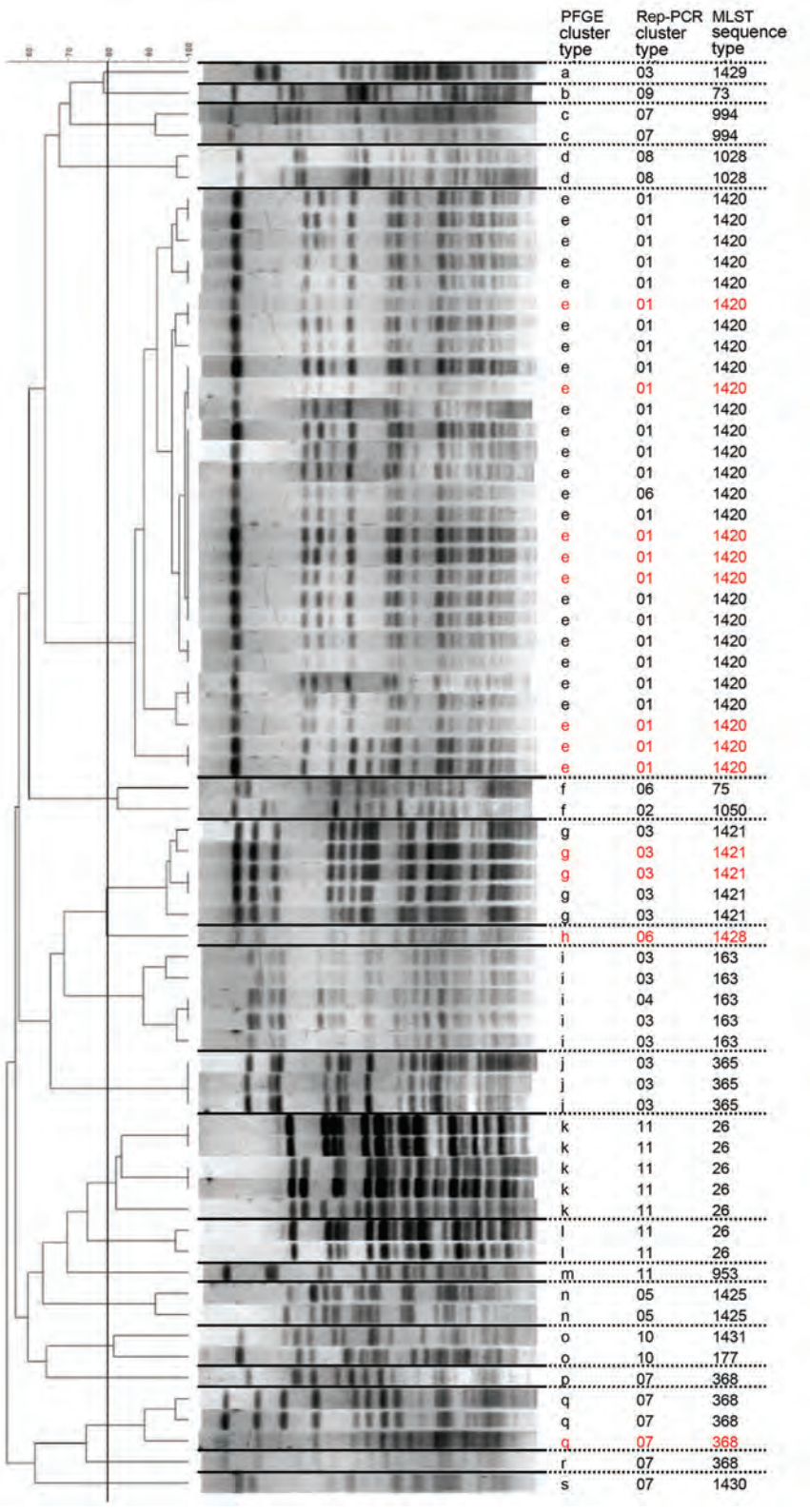

Figure 1. PFGE of the Tokyo strains of *Bacillus cereus* isolates, Japan. The 80% similarity cutoff for PFGE cluster typing is shown as a vertical line in the phylogenetic tree. Red letters and numbers represent samples isolated from patients with bacteremia. Rep-PCR cluster type and MLST sequence types are also shown. The Tokyo_ID31 strain was not analyzed. Scale bar indicates percent similarity. MLST, multilocus sequence typing; PFGE, pulsed-field gel electrophoresis; Rep-PCR, repetitive-element PCR.

with the bacteremia cases in Kochi, in general, samples from different hospitals suggested a significant relationship between ST1420 and bacteremia (p = 0.0006 by Fisher exact test) even when the Kochi strains were taken into account.

ST1420 was a novel ST that had a new *tpi* allele number, registered as 210 (Table 5). ST1420 had a combination of allele numbers that was the most similar to that of ST366 in the MLST database. ST1420 and ST366 had the same allele numbers at 5 (*glpF*, *gmk*, *pta*, *pur*, and *pycA*) of 7 loci used in the MLST analysis. Allele *tpi* 210 of ST1420 differed from *tpi* allele 83 of ST366 by only 1 nt. In addition, a search of genome sequences of *B. cereus* strains in the National Center for Biotechnology Information (https://www.ncbi.nlm.nih.gov/) database showed that ST1420 had an allele profile closest to *B. cereus* strain 2M5. ST1420 and *B. cereus* strain 2M5 had the same allele numbers at 6 loci (*glpF*, *gmk*, *ilvD*, *pta*, *pur*, and *tpi*), including the *tpi* allele 210 detected in this study.

To determine if ST1420 strains isolated from the different hospitals were derived from a single clone, we performed PFGE analysis for ST1420 strains from the Tochigi and Tottori strains and compared the results with those for Tokyo strains (Figure 2). All ST1420 strains formed

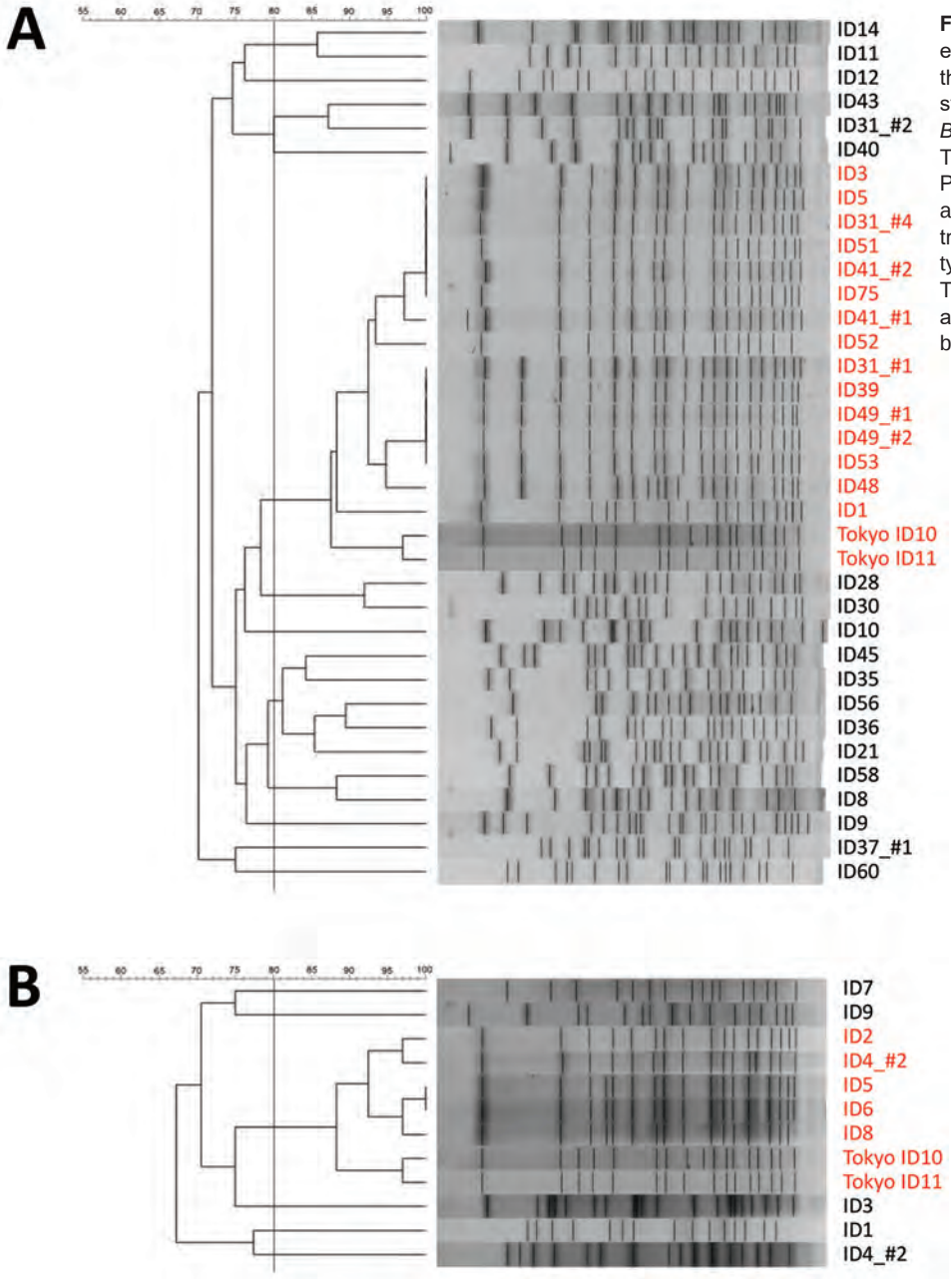

Figure 2. Pulsed-field gel electrophoresis (PFGE) results of the ST1420 strains of A) Tochigi strains and B) Tottori strains of *Bacillus cereus* isolates, Japan. The 80% similarity cutoff for PFGE cluster typing is shown as a vertical line in the phylogenetic tree. Names of strains of sequence type 1420 are indicated in red. The Tochigi_ID31_#3 was not analyzed. ID, identification. Scale bars indicate percent similarity.

Table 5. Allele profiles of ST1420 and similar sequence types of *Bacillus cereus*, Japan*

Strain	ST	Gene allele							Country of origin
		glpF	*gmk*	*ilvD*	*pta*	*pur*	*pycA*	*tpi*	
ST1420 strains found in this study	1420†	62	1	93	109	55	102	210‡	Japan
BC1	366	62	1	113	109	55	102	83	Japan
2M5	NA	62	1	93	109	55	37	210‡	Burkina Faso

*NA, not available; ST, sequence type.
†ST found in this study.
‡New alleles in the Multilocus Sequencing Typing Database (https://pubmlst.org).

a single cluster but some differences were observed in the band pattern. Therefore, although the ST is the same, these strains are not derived from a recently emerged single clone.

Phylogenetic Analysis

To investigate the relationship between *B. cereus* isolates in the present study and other strains of the *B. cereus* group, we constructed phylogenetic trees by using concatenated

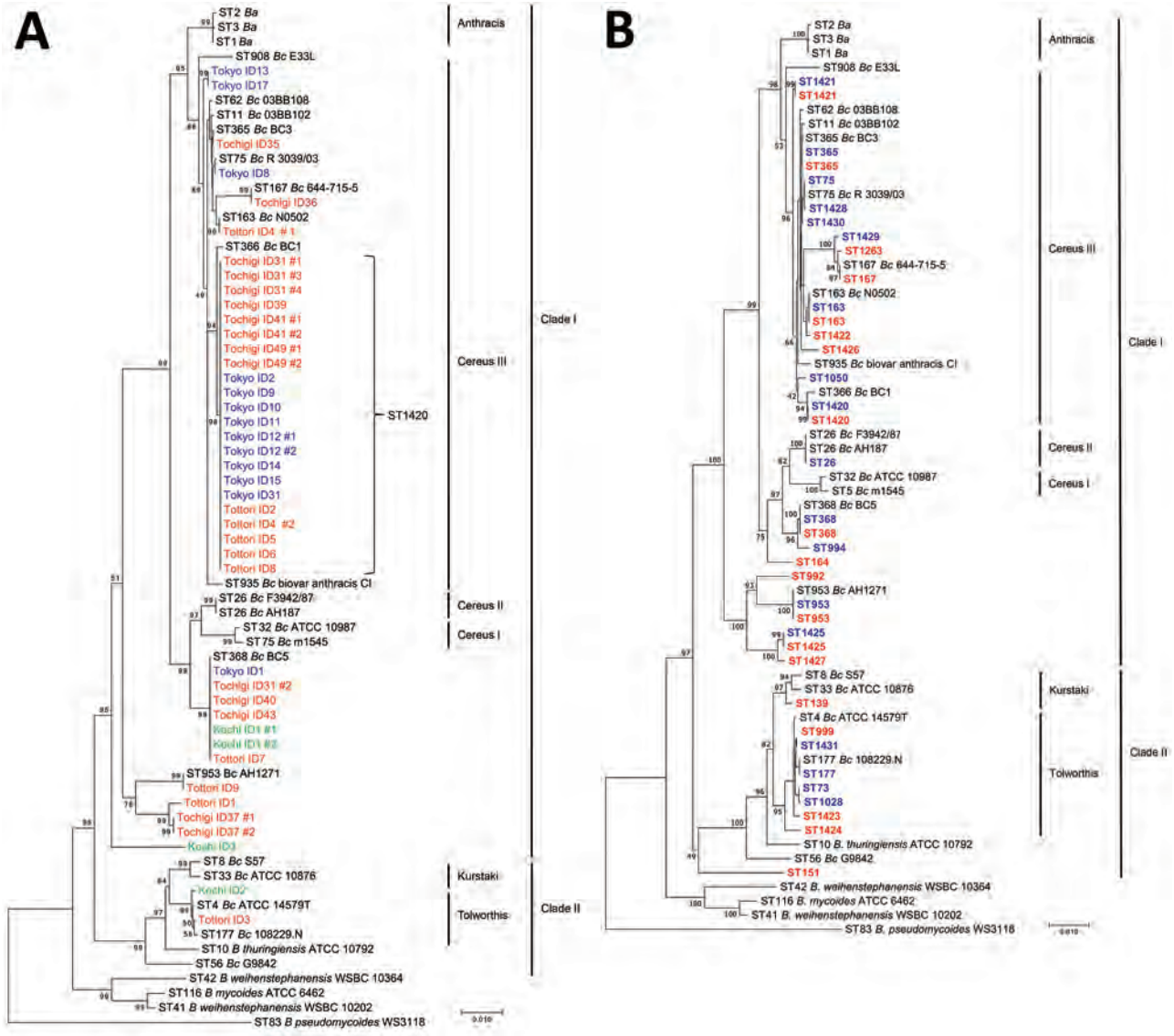

Figure 3. Multilocus sequence typing (MLST)–based phylogenetic trees of strains and STs of *Bacillus cereus* isolates, Japan. Reference sequences were obtained from the MLST database (https://pubmlst.org). Definitions of clades and lineage names followed those of Priest et al. (*9*). A) Phylogenetic tree of isolates from patients with bacteremia. Blue indicates Tokyo strains, red indicates Tochigi stains, orange indicates Tottori strains, and green indicates Kochi strains. B) Phylogenetic tree of STs detected in Tokyo and Tochigi strains. Blue indicates STs detected in Tokyo strains, and red indicates STs detected in Tochigi strains. Scale bars indicates nucleotide substitutions per site. Ba, *B. anthracis*; Bc, *B. cereus*; ID, identification; ST, sequence type.

sequences from 7 housekeeping genes used in MLST. ST1420 was classified into the Cereus III lineage, which is more closely related to the Anthracis lineage than to Cereus I and II lineages (Figure 3, panel A). Most strains isolated from patients with bacteremia were grouped into the Cereus III lineage, suggesting closer relationships with *B. anthracis*. Among Tokyo and Tochigi strains, isolates from patients with bacteremia were classified only into clade I, which includes Cereus I, Cereus II, Cereus III, and Anthracis lineages, whereas isolates from the environment were distributed not only in clade I but also in clade II (Figure 3, panel B).

Discussion

We performed MLST analysis to identify genotypic characteristics of *B. cereus* clinical isolates from recent nosocomial infections in Japan. We established that ST1420, which has a novel combination of allele numbers of the 7 loci used in MLST, was the major ST in strains isolated from patients with bacteremia. The strains were isolated from hospitals in different prefectures of Japan in which nosocomial infections by *B. cereus* occurred during 2006, 2012, and 2016. Our analyses suggested that ST1420 is a high-risk clone that has a major association with recent nosocomial infections and bacteremia cases caused by *B. cereus* in Japan.

Tokyo and Tochigi are in the greater Tokyo area. However, the distance between the 2 hospitals in these cities is so large that nosocomial case-patients with the same *B. cereus* ST are rarely found. Nosocomial infections in Tochigi were associated with contaminated hospital linens (*14*). However, the linen suppliers are often quite localized, and it is unlikely that hospitals in Tochigi and Tokyo had the same suppliers. Although ST1420 was not found in Kochi strains, further studies are required to investigate the distribution of ST1420 clones in Japan by testing more strains of nosocomial infections in various places and years.

Phylogenetic relationships among reference strains of the *B. cereus* group showed that ST1420 strains were found in the Cereus III lineage. The Cereus III lineage is closely related to the Anthracis lineage, suggesting a close genetic background with *B. anthracis*. In a previous report, clinical isolates classified into the Cereus III lineage were also associated with systemic diseases (*11*); *B. cereus* 03BB102 (ST11), which was isolated from a patient who died from pneumonia, and *B. cereus* D4214 (ST62), which was isolated from a patient with septicemia, belonged to the Cereus III lineage. *B. cereus* strains isolated from other severe infection outbreaks in hospitals have been found to belong to the Cereus III lineage (*12*,*21*). The fact that ST1420, which is believed to be associated with bacteremia, belongs to the Cereus III lineage is consistent with the previously reported relationships between *B. cereus* strains causing severe symptoms.

To determine relationships between *B. cereus* strains belonging to the Cereus III lineage and *B. anthracis*, we analyzed isolates from our study for a genetic marker for *B. anthracis*. Ba813 is a 277-bp chromosomal DNA sequence present in *B. anthracis* and has been used for differentiation of *B. anthracis* from *B. cereus* (*22*). However, it has been reported that some *B. cereus* strains contain Ba813 (*12*,*23*). We found that some of the *B. cereus* isolates in our study were in the Cereus III lineage, including ST1420, contained Ba813. These results indicate close relationships among some *B. cereus* strains belonging to the Cereus III lineage with *B. anthracis* and suggest that Ba813 is not a suitable chromosomal genetic marker for identification of *B. anthracis*.

For other STs, ST167, ST365, and ST368 were detected in bacteremia cases in Tochigi. ST368 was also detected in strains isolated from patients with bacteremia in Tokyo, Tottori, and Kochi. ST167 has been reported in patients with bacteremia, ST365 has been reported in patients with sepsis, and ST368 has been reported in patients with pyrexia in Japan (*13*,*24*). ST365 and ST368 have been reported in a person with a nosocomial infection (*13*). In previous studies, some pathogenic *B. cereus* isolates associated with emetic illness were classified as ST26, and some isolates associated with pneumonia were classified as ST78 (*11*). Our findings suggest that specific STs are associated with nosocomial infections or severe infections.

In conclusion, we have shown that *B. cereus* ST1420, a novel ST, was a major ST among nosocomial infections and bacteremia cases in Japan that occurred in different hospitals and different years. ST1420 could be a prevalent ST in recent *B. cereus* nosocomial infections in Japan. Further investigations are required to elucidate its distribution.

Acknowledgments

We thank Yoshitoshi Ogura, Rei Kajitani, and Keisuke Katsura for their advice regarding bioinformatics analysis.

This study was supported by the Program for Leading Graduate Schools, Ministry of Education, Culture, Sports, Science and Technology and partly supported by the Japan Initiative for Global Research Network on Infectious Diseases.

About the Author

Ms. Akamatsu is a PhD student at Hokkaido University, Sapporo, Japan. Her research interests include genomics and pathogenesis of the *B. cereus* group.

References

1. Bottone EJ. *Bacillus cereus*, a volatile human pathogen. Clin Microbiol Rev. 2010;23:382–98. http://dx.doi.org/10.1128/CMR.00073-09

2. Schaefer G, Campbell W, Jenks J, Beesley C, Katsivas T, Hoffmaster A, et al. Persistent *Bacillus cereus* bacteremia in 3 persons who inject drugs, San Diego, California, USA. Emerg Infect Dis. 2016;22:1621–3. http://dx.doi.org/10.3201/eid2209.150647
3. Thomas BS, Bankowski MJ, Lau WK. Native valve *Bacillus cereus* endocarditis in a non-intravenous-drug-abusing patient. J Clin Microbiol. 2012;50:519–21. http://dx.doi.org/10.1128/JCM.00657-11
4. Marley EF, Saini NK, Venkatraman C, Orenstein JM. Fatal *Bacillus cereus* meningoencephalitis in an adult with acute myelogenous leukemia. South Med J. 1995;88:969–72. http://dx.doi.org/10.1097/00007611-199509000-00017
5. Hoffmaster AR, Ravel J, Rasko DA, Chapman GD, Chute MD, Marston CK, et al. Identification of anthrax toxin genes in a *Bacillus cereus* associated with an illness resembling inhalation anthrax. Proc Natl Acad Sci U S A. 2004;101:8449–54. http://dx.doi.org/10.1073/pnas.0402414101
6. Bryce EA, Smith JA, Tweeddale M, Andruschak BJ, Maxwell MR. Dissemination of *Bacillus cereus* in an intensive care unit. Infect Control Hosp Epidemiol. 1993;14:459–62. http://dx.doi.org/10.2307/30145517
7. Hernaiz C, Picardo A, Alos JI, Gomez-Garces JL. Nosocomial bacteremia and catheter infection by *Bacillus cereus* in an immunocompetent patient. Clin Microbiol Infect. 2003;9:973–5. http://dx.doi.org/10.1046/j.1469-0691.2003.00682.x
8. Barrie D, Hoffman PN, Wilson JA, Kramer JM. Contamination of hospital linen by *Bacillus cereus.* Epidemiol Infect. 1994;113:297–306. http://dx.doi.org/10.1017/S0950268800051724
9. Priest FG, Barker M, Baillie LW, Holmes EC, Maiden MC. Population structure and evolution of the *Bacillus cereus* group. J Bacteriol. 2004;186:7959–70. http://dx.doi.org/10.1128/JB.186.23.7959-7970.2004
10. Zwick ME, Joseph SJ, Didelot X, Chen PE, Bishop-Lilly KA, Stewart AC, et al. Genomic characterization of the *Bacillus cereus* sensu lato species: backdrop to the evolution of *Bacillus anthracis.* Genome Res. 2012;22:1512–24. http://dx.doi.org/10.1101/gr.134437.111
11. Hoffmaster AR, Novak RT, Marston CK, Gee JE, Helsel L, Pruckler JM, et al. Genetic diversity of clinical isolates of *Bacillus cereus* using multilocus sequence typing. BMC Microbiol. 2008;8:191. http://dx.doi.org/10.1186/1471-2180-8-191
12. Zhang J, van Hung P, Hayashi M, Yoshida S, Ohkusu K, Ezaki T. *DnaJ* sequences of *Bacillus cereus* strains isolated from outbreaks of hospital infection are highly similar to *Bacillus anthracis.* Diagn Microbiol Infect Dis. 2011;70:307–15. http://dx.doi.org/10.1016/j.diagmicrobio.2011.02.012
13. Dohmae S, Okubo T, Higuchi W, Takano T, Isobe H, Baranovich T, et al. *Bacillus cereus* nosocomial infection from reused towels in Japan. J Hosp Infect. 2008;69:361–7. http://dx.doi.org/10.1016/j.jhin.2008.04.014
14. Sasahara T, Hayashi S, Morisawa Y, Sakihama T, Yoshimura A, Hirai Y. *Bacillus cereus* bacteremia outbreak due to contaminated hospital linens. Eur J Clin Microbiol Infect Dis. 2011;30:219–26. http://dx.doi.org/10.1007/s10096-010-1072-2
15. McDougal LK, Steward CD, Killgore GE, Chaitram JM, McAllister SK, Tenover FC. Pulsed-field gel electrophoresis typing of oxacillin-resistant *Staphylococcus aureus* isolates from the United States: establishing a national database. J Clin Microbiol. 2003;41:5113–20. http://dx.doi.org/10.1128/JCM.41.11.5113-5120.2003
16. Fluit AC, Terlingen AM, Andriessen L, Ikawaty R, van Mansfeld R, Top J, et al. Evaluation of the DiversiLab system for detection of hospital outbreaks of infections by different bacterial species. J Clin Microbiol. 2010;48:3979–89. http://dx.doi.org/10.1128/JCM.01191-10
17. Kajitani R, Toshimoto K, Noguchi H, Toyoda A, Ogura Y, Okuno M, et al. Efficient de novo assembly of highly heterozygous genomes from whole-genome shotgun short reads. Genome Res. 2014;24:1384–95. http://dx.doi.org/10.1101/gr.170720.113
18. Larsen MV, Cosentino S, Rasmussen S, Friis C, Hasman H, Marvig RL, et al. Multilocus sequence typing of total-genome-sequenced bacteria. J Clin Microbiol. 2012;50:1355–61. http://dx.doi.org/10.1128/JCM.06094-11
19. Kumar S, Stecher G, Tamura K. MEGA7: Molecular Evolutionary Genetics Analysis Version 7.0 for Bigger Datasets. Mol Biol Evol. 2016;33:1870–4. http://dx.doi.org/10.1093/molbev/msw054
20. Saitou N, Nei M. The neighbor-joining method: a new method for reconstructing phylogenetic trees. Mol Biol Evol. 1987;4:406–25.
21. Ogawa H, Fujikura D, Ohnuma M, Ohnishi N, Hang'ombe BM, Mimuro H, et al. A novel multiplex PCR discriminates *Bacillus anthracis* and its genetically related strains from other *Bacillus cereus* group species. PLoS One. 2015;10:e0122004. http://dx.doi.org/10.1371/journal.pone.0122004
22. Ramisse V, Patra G, Garrigue H, Guesdon JL, Mock M. Identification and characterization of *Bacillus anthracis* by multiplex PCR analysis of sequences on plasmids pXO1 and pXO2 and chromosomal DNA. FEMS Microbiol Lett. 1996;145:9–16. http://dx.doi.org/10.1111/j.1574-6968.1996.tb08548.x
23. Ramisse V, Patra G, Vaissaire J, Mock M. The Ba813 chromosomal DNA sequence effectively traces the whole *Bacillus anthracis* community. J Appl Microbiol. 1999;87:224–8. http://dx.doi.org/10.1046/j.1365-2672.1999.00874.x
24. Vassileva M, Torii K, Oshimoto M, Okamoto A, Agata N, Yamada K, et al. Phylogenetic analysis of *Bacillus cereus* isolates from severe systemic infections using multilocus sequence typing scheme. Microbiol Immunol. 2006;50:743–9. http://dx.doi.org/10.1111/j.1348-0421.2006.tb03847.x

Address for correspondence: Hideaki Higashi, Research Center for Zoonosis Control, Hokkaido University North 20, West 10, Kita 20, Nishi 10, Kita-ku, Hokkaido, Sapporo, 001-0020, Japan; email: hidea-hi@czc.hokudai.ac.jp

Infectious Dose of African Swine Fever Virus When Consumed Naturally in Liquid or Feed

Megan C. Niederwerder, Ana M.M. Stoian, Raymond R.R. Rowland, Steve S. Dritz, Vlad Petrovan, Laura A. Constance, Jordan T. Gebhardt, Matthew Olcha, Cassandra K. Jones, Jason C. Woodworth, Ying Fang, Jia Liang, Trevor J. Hefley

African swine fever virus (ASFV) is a contagious, rapidly spreading, transboundary animal disease and a major threat to pork production globally. Although plant-based feed has been identified as a potential route for virus introduction onto swine farms, little is known about the risks for ASFV transmission in feed. We aimed to determine the minimum and median infectious doses of the Georgia 2007 strain of ASFV through oral exposure during natural drinking and feeding behaviors. The minimum infectious dose of ASFV in liquid was 10^0 50% tissue culture infectious dose ($TCID_{50}$), compared with 10^4 $TCID_{50}$ in feed. The median infectious dose was $10^{1.0}$ $TCID_{50}$ for liquid and $10^{6.8}$ $TCID_{50}$ for feed. Our findings demonstrate that ASFV Georgia 2007 can easily be transmitted orally, although higher doses are required for infection in plant-based feed. These data provide important information that can be incorporated into risk models for ASFV transmission.

African swine fever virus (ASFV) is an emerging threat to swine production in North America and Europe. During the past decade, ASFV has spread into Eastern Europe and Russia (*1*,*2*) and most recently into China (*3*,*4*) and Belgium (*5*). Disease caused by ASFV is characterized by severe disseminated hemorrhage, and case-fatality rates approach 100% (*6*). The virus is a member of the *Asfarviridae* family and is the only known vectorborne DNA virus (*7*). Challenges to disease control include the lack of available vaccines and the potential for ASFV to become endemic in feral swine and ticks (*8*). Because no effective vaccine or treatment exists, preventing ASFV introduction is the primary goal of disease-free countries. Mitigation strategies during an African swine fever (ASF) outbreak are centered around restricting pig movement and conducting large-scale culling of infected herds. It is estimated that the introduction of ASFV into the United States would cost producers >$4 billion in losses (*9*).

Author affiliation: Kansas State University, Manhattan, Kansas, USA

DOI: https://doi.org/10.3201/eid2505.181495

Historical outbreaks, including the introduction of ASFV into the Caucasus region in 2007 and subsequent spread into Russia, have been attributed to feeding contaminated pork products (*1*) or direct contact with pigs (*10*). ASFV survives in meat and blood at room temperature for several months (*11*,*12*) and is resistant to temperature and pH extremes (*13*). Molecular characterization of the more recent ASFV incursions into China (*4*) and Siberia (*14*) demonstrate similarity in viral isolates to the Georgia 2007 strain of ASFV. These outbreaks have occurred in herds separated by thousands of kilometers (*15*). For example, ASFV spread ≈2,100 km from the city Shenyang in northern China to the city Wenzhou, south of Shanghai, in ≈3 weeks (*16*). Also, an ASFV incursion has been reported recently in a large-scale, high-biosecurity farm in Romania (*17*). Contaminated water from the Danube River has been implicated in introducing ASF onto the ≈140,000-pig breeding farm (*18*). Contaminated feed as a transmission vehicle for introducing transboundary animal diseases onto high-biosecurity swine operations has been recognized as a major risk factor since the introduction of porcine epidemic diarrhea virus into the United States in 2013 (*19*–*24*). The lesson learned from porcine epidemic diarrhea virus underscores the need to quantitate the risk that feed plays in the introduction of other transboundary animal diseases. Nonetheless, data defining the risk for ASFV transmission through feed or feed ingredients are limited.

In 2014, the introduction and spread of ASFV in Latvia was associated with the feeding of virus-contaminated fresh grass or crops to naive pigs (*25*). Furthermore, recent work has demonstrated that ASFV survives in feed ingredients, such as conventional soybean meal, organic soybean meal, soy oil cake, and choline, under conditions simulating trans-Atlantic shipment from Eastern Europe to the United States (*21*). These reports suggest that the spread of ASFV might be attributed to less-recognized transmission routes, such as feed or water.

ASFV can be transmitted experimentally through several routes, including intramuscularly, oronasally, or through direct contact (*6*). In many of the studies on oronasal transmission, however, ASFV was placed directly in the mouth or on the tonsils. The infectious dose of ASFV in plant-based feed or liquid consumed naturally is lacking; moreover, nothing has been reported regarding ASFV Georgia 2007 transmission in feed. Although field-based epidemiologic reports provide information suggesting routes of transmission, they provide little information about infectious dose. Thus, our objectives were to 1) define the relationship between infection probability and dose, 2) identify the minimum infectious dose (MID) or lowest dose required to result in ASFV infection of ≥1 pig, and 3) identify the median infectious dose (ID_{50}) or dose required to result in ASFV infection of 50% of pigs for ASFV Georgia 2007 when consumed naturally in contaminated feed or liquid.

Materials and Methods

ASFV Inoculum Preparation

We used an ASFV Georgia 2007/1 isolate (*2*) for this study. Viral stocks were created from spleen tissue collected from pigs during acute infection with ASFV Georgia 2007 (*26*). We minced splenic tissue and passed it through a cell strainer in the presence of phosphate-buffered saline (PBS) supplemented with penicillin/streptomycin and fungizone. We centrifuged the suspension at 4,000 × *g* for 30 min and stored the supernatant at 4°C. We then resuspended the pellet in sterile PBS with antibiotics and antimycotics and obtained additional virus by 3 freeze-thaw cycles. The suspension was centrifuged and clarified supernatant stored at 4°C.

For virus titration, we collected porcine alveolar macrophages (PAMs) by using lung lavage of 3–5-week-old pigs. We cultured PAMs for 2 days in RPMI media supplemented with 10% fetal bovine serum and antibiotics in a 37°C 5% CO_2 incubator. We then prepared 10-fold serial dilutions of virus in triplicate and added the dilutions to PAMs in a 96-well plate. After 3 days at 37°C, cells were fixed by using 80% acetone for 10 min. Cells were stained using a p30 monoclonal antibody (*27*) diluted 1:6,000. We incubated the plate at 37°C for 1 h and washed it 3 times with PBS. Bound antibody was detected by using a goat-antimouse antibody (AlexaFluor 488; Thermo Fisher Scientific, https://www.thermofisher.com) diluted 1:400 and incubated for 1 h at 37°C. We observed stained cells under an inverted fluorescence microscope (Evos FL; Thermo Fisher Scientific) and calculated the $\log_{10}$ 50% tissue culture infectious dose per milliliter ($TCID_{50}$/mL) according to the method of Reed and Muench (*28*).

We made dilutions of the clarified ASFV Georgia 2007 splenic homogenate by using RPMI media, with doses ranging from 10^0 $TCID_{50}$ to 10^8 $TCID_{50}$ added to a final volume of 100 mL RPMI or 100 g complete feed. The feed was a typical corn soybean meal–based diet formulated to be nutritionally adequate according to the National Research Council recommendations for pigs weighing 10–25 kg (*29*). The diet did not contain any animal-based feed ingredients. For mixing virus with feed, we allowed 10 mL of virus to absorb onto 100 g of feed in a 500 mL, wide-mouth, high-density polyethylene round bottle (Nalgene, Thermo Fisher Scientific) for 30 s before homogenization by rolling and gently mixing the bottle by hand.

Animals and Housing

The use of pigs and viruses in research was performed in accordance with the Federation of Animal Science Societies Guide for the Care and Use of Agricultural Animals in Research and Teaching and the US Department of Agriculture's Animal Welfare Act and Animal Welfare Regulations. The research was approved by the Kansas State University Institutional Animal Care and Use Committee and the Institutional Biosafety Committee.

We obtained 84 crossbred pigs (average age, 51.8 ± 2.2 days) from a single high-health commercial source. Pigs were housed in 3 identical 66 m^2 rooms at the Kansas State University Biosecurity Research Institute and maintained under Biosafety Level 3 agriculture containment conditions. Rooms were environmentally controlled, and complete exchange of air occurred 14.5 times/hour in each room. Pigs were maintained individually in 1.9 m^2 pens, and each pen was separated by ≥1.5 m in the room. The stainless-steel pens were raised and contained slotted fiberglass flooring. Three sides of the pen were solid, with a fourth side consisting of bars and a gate. All efforts were made to prevent aerosol spread of virus. Negative control pigs were maintained in the room as a means to monitor the potential for cross-contamination between pens.

Experimental Design

We adapted the experimental design and approach for determining the median infectious dose of ASFV Georgia 2007 from previous work on porcine reproductive and respiratory syndrome virus (*30*,*31*). We conducted 7 replicates for both liquid and feed, each composed of 6 pigs for liquid and 6 pigs for feed. In each replicate for feed or liquid, we administered 5 pigs a specific dose of ASFV; 1 pig served as the negative control. An adaptive study design was incorporated throughout the course of the experiment to result in the most precise estimate of the ID_{50} while maximizing the information gained from the trial (*32*,*33*). The most likely ID_{50} was based on a review of the available literature (*34*–*40*). We used this information to identify the initial infectious dose tested of 10^3 $TCID_{50}$ for liquid and 10^4 $TCID_{50}$ for feed. After completion of the first replicate, we used the continual reassessment method to update the ID_{50} estimate (*32*,*33*). The results of each replicate were used to select dosages for

subsequent replicates; in general, this process resulted in liquid doses decreasing and feed doses increasing after the initial replicates were completed. All replicates and pig numbers for each dose are shown in Table 1.

For drinking, pigs consumed ASFV mixed in a 100-mL volume of RPMI media. Liquid was provided through a gravity-fed restricted-flow nipple drinker (Arato 76 Piglet Drinker; Ag Works International, http://www.agworksintl.com) attached to an adjustable galvanized wall bracket (1.3 cm × 61 cm pipe; SMB Manufacturing, https://www.smbmfg.com). If pigs became averse to drinking from a nipple, liquid medium was placed in a small stainless-steel bowl for pigs to drink. For feeding, pigs consumed ASFV mixed in a 100-g volume of complete feed provided in a 23-cm stainless-steel creep feeder (Vittetoe Inc., http://www.vittetoe.com). Infectious titers of each virus dilution were back-titrated on PAMs by endpoint titration assay ($TCID_{50}$/mL) to confirm accurate dosing. Negative control pigs received the same volumes of sterile media or complete feed without virus.

Pigs were acclimated to the drinkers or feeders for 3–4 days before ASFV inoculation. During this acclimation period, water and feed (drinking) or feed alone (feeding) were withheld for 10–14 hours before liquid media or feed was offered. Pigs were monitored during the drinking or eating process. Once pigs had consumed the specified volume of liquid or feed, pigs were given unrestricted access to feed and water until the next withholding period. After acclimation, 5 pigs in each replicate were offered the same substrate containing a specific dose of ASFV followed by unrestricted access to feed and water.

We evaluated the pigs for clinical signs of ASF twice daily and collected blood from each pig at 0 and 5 days postinoculation (dpi). Pigs showing clinical signs before 5 dpi were humanely euthanized, and blood and tissues were collected. The remaining pigs were humanely euthanized on 5 dpi, and complete necropsies were performed. We determined infection status on the basis of real-time PCR detection of ASFV in the serum or spleen and virus isolation from the spleen. We constructed dose-response curves and calculated ID_{50}, as described further in this article.

ASFV PCR

We extracted nucleic acid from serum or splenic homogenate by using the MagMAX-96 Viral RNA Isolation Kit (Thermo Fisher Scientific). For nucleic acid isolation, we combined 50 μL of sample with 20 μL of Bead mix (containing lysis/binding solution, carrier RNA, and 100% isopropanol) on a U-bottom 96-well plate. Cells were lysed by using 130 μL lysis/binding solution and mixed for 5 minutes on a shaker. The beads were captured on a magnetic stand and washed twice using 150 μL Wash Solution 1 and 2 with a final elution volume of 50 μL.

We performed PCR amplification of p72 according to King et al. (*41*). The primer and probe mixture was commercially synthesized by using PrimeTime Mini qPCR Assay (IDT Technologies, https://www.idtdna.com): probe (5′-[6-FAM]- CCA CGG GAG ZEN GAA TAC CAA CCC AGT G-3′-[IBFQ]), sense primer (5′-CTG CTC ATG GTA TCA ATC TTA TCG A-3′), and anti-sense primer (5′-GAT ACC ACA AGA TCR GCC GT-3′). The 15 μL PCR mixture consisted of 10 μL 2X iTaq Universal Probes Supermix (Bio-Rad Laboratories, http://www.bio-rad.com), 1 μL 1X PrimeTime Mini (500 nM primers and 250 nM probe), and 4 μL nuclease-free water. We dispensed this mastermix into a Hard-Shell optical 96-well reaction plate (Bio-Rad Laboratories), added DNA samples, and briefly centrifuged the plate to remove air bubbles. We then performed real-time PCR on a CFX96 Real-Time System (Bio-Rad Laboratories) under the following conditions: 95°C for 2 min, followed by 45 cycles of 94°C for 30 s, 58°C for 1 min, and 60°C for 30 s. We performed data analysis by using CFX96 software and reported results as cycle threshold values.

Data Analysis

We assessed infectivity by using 3 diagnostic methods (PCR of spleen, PCR of serum, and virus isolation of spleen), which resulted in 3 binary response variables (i.e., positive

Table 1. Replicates of pigs orally exposed to ASFV in liquid or feed based on a sequential adaptive experimental design to determine the infectious dose of ASFV when consumed naturally*

Dose ASFV,	Liquid media replicates, no. tested (no. positive)							Plant-based feed replicates, no. tested (no. positive)						
$TCID_{50}$	1	2	3	4	5	6	7	1	2	3	4	5	6	7
10^0	–	–	–	–	3 (3)	–	5 (0)	–	–	–	–	–	–	–
10^1	–	–	5 (3)	5 (1)†	–	–	–	–	–	–	–	–	–	–
10^2	–	4 (2)	–	–	2 (2)	2 (2)	–	–	–	–	–	–	–	–
10^3	5 (5)	1 (0)	–	–	–	–	–	–	5 (0)	–	–	–	–	–
10^4	–	–	–	–	–	3 (3)	–	5 (2)	–	–	–	–	–	–
10^5	–	–	–	–	–	–	–	–	–	5 (2)	5 (2)†	–	–	–
10^6	–	–	–	–	–	–	–	–	–	–	–	3 (0)	–	5 (2)
10^7	–	–	–	–	–	–	–	–	–	–	–	2 (0)	3 (2)	–
10^8	–	–	–	–	–	–	–	–	–	–	–	–	2 (1)	–

*Data are shown for the 5 infected pigs. In each replicate, 1 negative control pig was present. ASFV, African swine fever virus; $TCID_{50}$, 50% tissue culture infectious dose; –, no pigs tested.
†One pig in each of these replicates died before 5 days postinoculation for causes other than ASF and was eliminated from the data analysis.

or negative) for each individual pig. We categorized ASFV infection as positive if ≥1 diagnostic test indicated evidence of infection. We analyzed all binary responses simultaneously to account for imperfect test agreement (*42*–*44*).

Without assuming a functional form for the relationship between dose and probability of infection, we used a constrained spline regression model. The constraints used were limited to the assumptions that infection probability increases as dose increases and that the relationship is continuous. We used a constrained regression spline within a Bayesian hierarchical model to estimate the infection probability at each dose for a single exposure based on the results of the 3 diagnostic methods. On the basis of the single exposure, we also modeled repeated exposures, assuming repeated exposures are independent events. Thus, we calculated the infection probability for multiple exposures as $1 - (1 - p)^q$, where p is the single-exposure infection probability and q is the number of exposures. Repeated exposures can be viewed interactively online (https://trevorhefley.shinyapps.io/asfv). We used previously described algorithms for statistical model implementation (*45*,*46*) by using the cgam package in R (*47*). We have provided a tutorial with the computational details, annotated computer code to assist readers implementing similar models, and the necessary code to reproduce results and figures related to the analysis (Appendix, https://wwwnc.cdc.gov/EID/article/25/5/18-1495-App1.pdf).

Results

A summary of the infection results is shown in Table 2. A total of 68 pigs were included in the study. No evidence of ASFV infection was detected in the 14 negative control pigs. Therefore, adequate biosecurity was maintained throughout the study. Of the 32 pigs with evidence of ASFV infection, 16 (50%) were positive on virus isolation and PCR of spleen, 8 (25%) were positive on virus isolation of spleen alone, and 8 (25%) were positive on all 3 tests. The 34 pigs in the feeding trial consumed the 100 g of feed in a mean ± SD of 14.8 ± 5.5 min (minimum 7 min, maximum 30 min). For the liquid trial, the 34 pigs consumed the 100 mL of ASFV-inoculated media in a mean ± SD of 21.1 ± 18.2 min (minimum 3 min, maximum 63 min). A small number of pigs (3/34 [8.8%]) averse to the restricted-flow nipples consumed media from a bowl.

Overall, the probability of infection increased as the dose increased for both feed and liquid (Figure 1). Reported as the lowest dose required to result in ASFV infection of ≥1 pig, the MID after liquid consumption was 10^0 $TCID_{50}$, whereas 10^4 $TCID_{50}$ was the MID required to result in infection after consumption of contaminated complete feed. For a single exposure, liquid had a higher infection probability compared with feed at doses up to $10^{7.5}$ $TCID_{50}$ where the 95% CIs overlap (Figure 1, panel A). At the highest dose tested in liquid (10^4 $TCID_{50}$), 100% of pigs were infected with ASFV; in contrast, no feed dose resulted in a 100% infection rate in this experiment.

When multiple exposures are considered, the infection probability increases at all dose levels for both liquid and feed (Figure 1, panels B and C). By 10 exposures with liquid, the probability of infection increases to near 1 at the lowest dose of 1 $TCID_{50}$ ASFV. For feed with multiple exposures, we observed an increase in the width of the 95% CI at the lower dosages, indicating that with repeated exposures, the uncertainty in the infection probability increased. This result was attributable to fewer pigs being infected with lower doses and the lower infection probability for a single exposure. The distribution of plausible doses that could produce infection in 50% of pigs is shown in Figure 2. The ID_{50} was $10^{1.0}$ (95% CI 10^0–$10^{2.3}$) for liquid and $10^{6.8}$ (95% CI $10^{4.6}$–10^{8+}) for feed.

Discussion

Our study confirms the efficient transmission of ASFV by the oral route in liquid and feed lacking contaminated pork products and provides quantitative data for the Georgia 2007 strain. Early studies indicated a minimum dose of 10^5 50% hemadsorption doses (HAD_{50}) of ASFV KWH/12 was required to cause infection when administered orally in milk (*38*). Later, Howey et al. (*35*) determined the infectious potential of 3 doses of ASFV Malawi 1983 delivered intraoropharyngeally to commercial pigs. Although a low dose of 10^2 HAD_{50} did not induce infection (0/2), moderate (10^4 HAD_{50}) and high (10^6 HAD_{50}) doses were sufficient to cause infection in 100% of the pigs (4/4) (*35*). More recently,

Table 2. Summary of results for pigs orally exposed to ASFV in liquid or feed to determine the infectious dose of ASFV when consumed naturally*

Dose ASFV,	Liquid media			Plant-based feed		
$TCID_{50}$	No. tested	No. positive	% Positive	No. tested	No. positive	% Positive
10^0	8	3	37.5	–	–	–
10^1	9	4	44.4	–	–	–
10^2	8	6	75	–	–	–
10^3	6	5	83.3	5	0	0
10^4	3	3	100	5	2	40
10^5	–	–	–	9	4	44.4
10^6	–	–	–	8	2	25
10^7	–	–	–	5	2	40
10^8	–	–	–	2	1	50

*ASFV, African swine fever virus; $TCID_{50}$, 50% tissue culture infectious dose; –, no pigs tested.

a study demonstrated that even lower doses of a contemporary ASFV isolate related to ASFV Georgia 2007 was capable of inducing infection. Specifically, Pietschmann et al. (*34*) showed that oronasal doses as low as 3 and 25 hemadsorption units of ASFV Armenia 2008, when delivered in 2 mL of splenic suspension, caused infection in wild boar. Increased susceptibility was demonstrated in wild boar described as weak with poor condition (*34*).

In our study, we confirmed the high infectivity of ASFV Georgia 2007 through liquid by the oral route. Of note, the pigs in our study consumed the contaminated liquid naturally through drinking and were considered healthy and robust. Productive infection resulted in almost 40% of the pigs exposed to an ASFV liquid inoculum containing as little as 1 $TCID_{50}$. The low infectious dose of ASFV through natural liquid consumption should be considered as a possible factor in the spread of ASF through water, consistent with the epidemiologic evidence linking the Danube River with ASF spread in Romania (*18*).

ASFV delivered through liquid by the oronasal or intraoropharyngeal route might result in infection because of virus exposure of the nasopharynx, including the tonsils, or of the gastrointestinal tract. Because of the high stability of ASFV in a wide range of pH values (from 4 to 10) (*13*), survival in the acidic gastric environment is possible but unlikely. More likely is that liquid medium provides an ideal substrate for virus contact with the tonsils, where primary virus replication occurs after natural exposure to ASFV (*38*).

Reports documenting experimental ASFV infection through contaminated feed involve consumption of tissues from infected animals. As early as 1954, it was reported that transmission of ASFV by oral feeding required a minimum dose of 10^5 (*40*). Parker et al. failed to infect pigs with homogenized tissues from warthogs containing $10^{3.7}$–$10^{6.1}$ HAD_{50} of ASFV administered in solid feed (*37*). In contrast, Colgrove et al. (*39*) successfully infected domestic pigs by adding 50 g of minced spleen and liver from an infected pig to solid feed. Each gram of tissue contained $10^{7.0}$–$10^{7.5}$ HAD_{50} of ASFV isolate Hinde WH II (*39*). Our experimental studies using the contemporary isolate Georgia 2007 show that ASFV infection through the consumption of plant-based feed requires a higher dose compared with liquid. Compared with liquid media, feed might stimulate salivary proteases that degrade virus integrity. Furthermore, the feed matrix might inhibit tonsillar contact, reducing virus exposure to lymphoid and epithelial tissues before gastrointestinal entry (*36*).

Despite the higher MID in feed compared with liquid observed in this study, we hypothesize that feed might actually pose a higher risk compared with water sources in modern swine production systems. Feed delivery is a high-frequency event, and feed production is highly centralized; thus, contaminated feed can be easily distributed across a substantial number of pig farms. Pigs would also likely consume the contaminated feed in higher volumes (>100 g) and at higher frequencies (>1 exposure) than what was tested in our study. The likelihood of productive infection after consumption of ASFV-contaminated complete feed increases significantly after 3 or 10 exposures (Figure 1, panels B, C). Therefore, despite infection after consumption of ASFV in contaminated feed being a lower-probability event compared with liquid, the high frequency of exposure might make feed a more important risk factor for transmission. Adding to this risk is the fact that highly centralized feed mills use ingredients from a global distribution supply chain. For example, inventory from a midwestern US

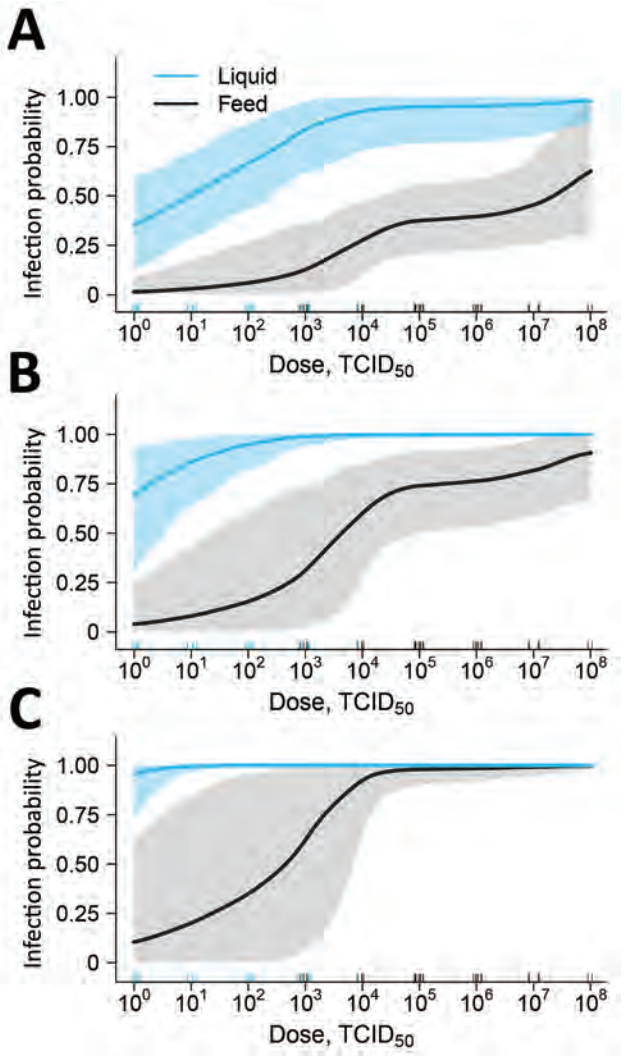

Figure 1. Estimated liquid (blue line) and feed (black line) infection probability at different oral doses of ASFV based on experimental data to determine the infectious dose of ASFV when consumed naturally. Data are shown for 1 exposure (A), 3 exposures (B), and 10 exposures (C). Shading indicates 95% CIs. Numbers of individual pig dosages are represented by the blue and black tick marks above the horizontal axis. Repeated exposures can be viewed interactively online (https://trevorhefley.shinyapps.io/asfv).

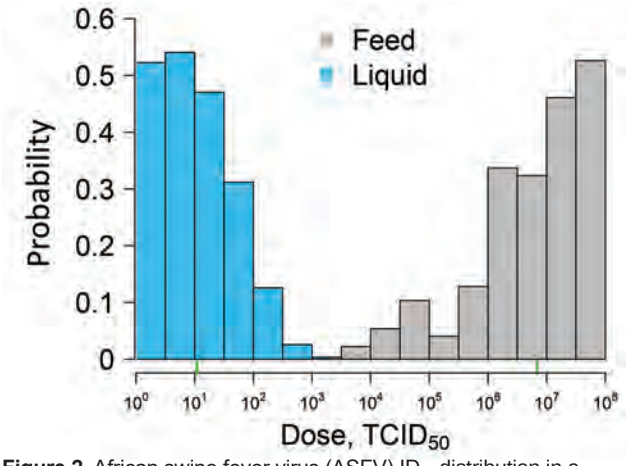

Figure 2. African swine fever virus (ASFV) ID_{50} distribution in a study determining the infectious dose of ASFV when consumed naturally in liquid or feed. For liquid, ID_{50} was $10^{1.0}$, and for feed, ID_{50} was $10^{6.8}$ (represented by green tick marks along baseline). ID_{50}, median infectious dose (dose required to result in ASFV infection of 50% of pigs); $TCID_{50}$, 50% tissue culture infectious dose.

swine farm indicated feed ingredients originating from 12 countries in North America, Asia, and Europe (S.S. Dritz, unpub. data, 2018 Sep 6).

As of February 2019, ASFV had spread to a high-biosecurity farm in Romania (*17*) and had been detected in pig herds located in ≥25 provinces of China, including the capital Beijing (*48*), with thousands of kilometers separating affected herds. How ASFV is moving across such vast areas within the largest pork-producing country in the world is unknown; however, movement of the virus within feed or feed ingredients should be considered. The results of our study demonstrate that ASFV can be easily transmitted orally through natural consumption of both liquid and feed, supporting the potential role of feed in the emergence of this virus in new pig populations throughout the world.

Acknowledgments

We thank the staff of the Biosecurity Research Institute for their assistance in completing this research. The authors also acknowledge Scott Dee, Diego Diel, and Jeff Zimmerman for their collaborative efforts in understanding the risk of viruses in feed. The ASFV Georgia 2007/1 isolate used in this study was kindly provided by Linda Dixon of the Pirbright Institute and through the generosity of David Williams of the Commonwealth Scientific and Industrial Research Organization's Australian Animal Health Laboratory.

Funding for this study was provided by the National Pork Checkoff grant no. 17-057 and the State of Kansas National Bio and Agro-defense Facility Fund. L.A.C. and M.O. were partially funded by the US Department of Homeland Security's Science and Technology Directorate under contract no. D15PC00276.

About the Author

Dr. Niederwerder is an assistant professor of virology in the Department of Diagnostic Medicine/Pathobiology at Kansas State University, Manhattan, Kansas. Her research interests are in the pathogenesis, prevention, and control of emerging and endemic viral diseases of swine.

References

1. Gogin A, Gerasimov V, Malogolovkin A, Kolbasov D. African swine fever in the North Caucasus region and the Russian Federation in years 2007-2012. Virus Res. 2013;173:198–203. http://dx.doi.org/10.1016/j.virusres.2012.12.007
2. Rowlands RJ, Michaud V, Heath L, Hutchings G, Oura C, Vosloo W, et al. African swine fever virus isolate, Georgia, 2007. Emerg Infect Dis. 2008;14:1870–4. http://dx.doi.org/10.3201/eid1412.080591
3. Ge S, Li J, Fan X, Liu F, Li L, Wang Q, et al. Molecular characterization of African swine fever virus, China, 2018. Emerg Infect Dis. 2018;24:2131–3. http://dx.doi.org/10.3201/eid2411.181274
4. Zhou X, Li N, Luo Y, Liu Y, Miao F, Chen T, et al. Emergence of African swine fever in China, 2018. Transbound Emerg Dis. 2018;65:1482–4. http://dx.doi.org/10.1111/tbed.12989
5. Swine Health Information Center. Swine Disease Global Surveillance Report: African swine fever (ASF) has been confirmed in Belgium [cited 2018 Sep 13]. https://www.swinehealth.org/wp-content/uploads/2018/09/Sept.2018_Belgium_ASF-vf_.pdf
6. Blome S, Gabriel C, Beer M. Pathogenesis of African swine fever in domestic pigs and European wild boar. Virus Res. 2013;173:122–30. http://dx.doi.org/10.1016/j.virusres.2012.10.026
7. Dixon LK, Alonso C, Escribano JM, Martins C, Revilla Y, Salas ML, et al. *Asfarviridae*. In: King A, Lefkowitz E, Adams MJ, Carstens EB, editors. Virus taxonomy: ninth report of the International Committee on Taxonomy of Viruses. Oxford: Elsevier; 2011. p. 153–62.
8. McVicar JW, Mebus CA, Becker HN, Belden RC, Gibbs EPJ. Induced African swine fever in feral pigs. J Am Vet Med Assoc. 1981;179:441–6.
9. Rendleman CM, Spinelli FJ. An economic assessment of the costs and benefits of African swine fever prevention. Animal Health Insight. 1994;Spring/Summer:18–27.
10. Guinat C, Gogin A, Blome S, Keil G, Pollin R, Pfeiffer DU, et al. Transmission routes of African swine fever virus to domestic pigs: current knowledge and future research directions. Vet Rec. 2016;178:262–7. http://dx.doi.org/10.1136/vr.103593
11. Mebus C, Arias M, Pineda JM, Taiador J, House C, Sanchez-Vizcaino JM. Survival of several porcine viruses in different Spanish dry-cured meat products. Food Chem. 1997; 59:555–9. http://dx.doi.org/10.1016/S0308-8146(97)00006-X
12. Montgomery RE. On a form of swine fever occurring in British East Africa (Kenya Colony). J Comp Pathol Ther. 1921;34:243–62.
13. Niederwerder MC, Rowland RR. Is there a risk for introducing porcine reproductive and respiratory syndrome virus (PRRSV) Through the Legal Importation of Pork? Food Environ Virol. 2017;9:1–13. http://dx.doi.org/10.1007/s12560-016-9259-z
14. Kolbasov D, Titov I, Tsybanov S, Gogin A, Malogolovkin A. African swine fever virus, Siberia, Russia, 2017. Emerg Infect Dis. 2018;24:796–8. http://dx.doi.org/10.3201/eid2404.171238
15. United Kingdom Department for Environment, Food, and Rural Affairs. Updated outbreak assessment #2: African swine fever in China [cited 2018 Sep 6]. https://assets.publishing.service.gov.uk/government/uploads/system/uploads/attachment_data/file/737662/asf-china-update2.pdf
16. Swine Health Information Center. Swine Disease Global Surveillance Report: African swine fever in China [cited 2018

Aug 23]. https://www.swinehealth.org/wp-content/uploads/2018/08/Report-ASF-China-8.23.18.pdf
17. World Organization for Animal Health (OIE). African swine fever, Romania [cited 2018 Aug 28]. https://www.oie.int/wahis_2/public/wahid.php/Reviewreport/Review?page_refer=MapFullEventReport&reportid=27687
18. Boklund A, Cay B, Depner K, Földi Z, Guberti V, Masiulis M, et al. Epidemiological analyses of African swine fever in the European Union (November 2017 until November 2018). EFSA J. 2018;16:5494.
19. Pasick J, Berhane Y, Ojkic D, Maxie G, Embury-Hyatt C, Swekla K, et al. Investigation into the role of potentially contaminated feed as a source of the first-detected outbreaks of porcine epidemic diarrhea in Canada. Transbound Emerg Dis. 2014; 61:397–410. http://dx.doi.org/10.1111/tbed.12269
20. Bowman AS, Krogwold RA, Price T, Davis M, Moeller SJ. Investigating the introduction of porcine epidemic diarrhea virus into an Ohio swine operation. BMC Vet Res. 2015;11:38. http://dx.doi.org/10.1186/s12917-015-0348-2
21. Dee SA, Bauermann FV, Niederwerder MC, Singrey A, Clement T, de Lima M, et al. Survival of viral pathogens in animal feed ingredients under transboundary shipping models. PLoS One. 2018;13:e0194509. http://dx.doi.org/10.1371/journal.pone.0194509
22. Schumacher LL, Woodworth JC, Jones CK, Chen Q, Zhang J, Gauger PC, et al. Evaluation of the minimum infectious dose of porcine epidemic diarrhea virus in virus-inoculated feed. Am J Vet Res. 2016;77:1108–13. http://dx.doi.org/10.2460/ajvr.77.10.1108
23. Dee S, Clement T, Schelkopf A, Nerem J, Knudsen D, Christopher-Hennings J, et al. An evaluation of contaminated complete feed as a vehicle for porcine epidemic diarrhea virus infection of naïve pigs following consumption via natural feeding behavior: proof of concept. BMC Vet Res. 2014;10:176. http://dx.doi.org/10.1186/s12917-014-0176-9
24. Dee S, Neill C, Singrey A, Clement T, Cochrane R, Jones C, et al. Modeling the transboundary risk of feed ingredients contaminated with porcine epidemic diarrhea virus. BMC Vet Res. 2016;12:51. http://dx.doi.org/10.1186/s12917-016-0674-z
25. Oļševskis E, Guberti V, Seržants M, Westergaard J, Gallardo C, Rodze I, et al. African swine fever virus introduction into the EU in 2014: Experience of Latvia. Res Vet Sci. 2016;105:28–30. http://dx.doi.org/10.1016/j.rvsc.2016.01.006
26. Popescu L, Gaudreault NN, Whitworth KM, Murgia MV, Nietfeld JC, Mileham A, et al. Genetically edited pigs lacking CD163 show no resistance following infection with the African swine fever virus isolate, Georgia 2007/1. Virology. 2017;501:102–6. http://dx.doi.org/10.1016/j.virol.2016.11.012
27. Petrovan V, Fang Y, Rowland RR. Diagnostic application of monoclonal antibodies against African swine fever virus (ASFV). In: Abstracts of Diagnostics of Endemic and Emerging Diseases: Beyond The Status Quo, June 11–13, 2018. Manhattan (KS): Center of Excellence for Emerging and Zoonotic Animal Diseases and Kansas State Veterinary Diagnostic Laboratory; 2018. p 30.
28. Reed LJ, Muench H. A simple method of estimating fifty per cent endpoints. Am J Hyg. 1938;27:493–7.
29. National Research Council. Nutrient requirements of swine. 11th edition. Washington: National Academies Press; 2012.
30. Hermann JR, Muñoz-Zanzi CA, Roof MB, Burkhart K, Zimmerman JJ. Probability of porcine reproductive and respiratory syndrome (PRRS) virus infection as a function of exposure route and dose. Vet Microbiol. 2005;110:7–16. http://dx.doi.org/10.1016/j.vetmic.2005.06.012
31. Hermann JR, Muñoz-Zanzi CA, Zimmerman JJ. A method to provide improved dose-response estimates for airborne pathogens in animals: an example using porcine reproductive and respiratory syndrome virus. Vet Microbiol. 2009;133:297–302. http://dx.doi.org/10.1016/j.vetmic.2008.07.002
32. O'Quigley J, Pepe M, Fisher L. Continual reassessment method: a practical design for phase 1 clinical trials in cancer. Biometrics. 1990;46:33–48. http://dx.doi.org/10.2307/2531628
33. O'Quigley J, Iasonos A, Bornkamp B. Handbook of methods for designing, monitoring, and analyzing dose-finding trials. 1st edition. Boca Raton (FL): CRC Press; 2017.
34. Pietschmann J, Guinat C, Beer M, Pronin V, Tauscher K, Petrov A, et al. Course and transmission characteristics of oral low-dose infection of domestic pigs and European wild boar with a Caucasian African swine fever virus isolate. Arch Virol. 2015;160:1657–67. http://dx.doi.org/10.1007/s00705-015-2430-2
35. Howey EB, O'Donnell V, de Carvalho Ferreira HC, Borca MV, Arzt J. Pathogenesis of highly virulent African swine fever virus in domestic pigs exposed via intraoropharyngeal, intranasopharyngeal, and intramuscular inoculation, and by direct contact with infected pigs. Virus Res. 2013;178:328–39. http://dx.doi.org/10.1016/j.virusres.2013.09.024
36. McVicar JW. Quantitative aspects of the transmission of African swine fever. Am J Vet Res. 1984;45:1535–41.
37. Parker J, Plowright W, Pierce MA. The epizootiology of African swine fever in Africa. Vet Rec. 1969;85:668–74.
38. Greig A. Pathogenesis of African swine fever in pigs naturally exposed to the disease. J Comp Pathol. 1972;82:73–9. http://dx.doi.org/10.1016/0021-9975(72)90028-X
39. Colgrove GS, Haelterman EO, Coggins L. Pathogenesis of African swine fever in young pigs. Am J Vet Res. 1969;30:1343–59.
40. Heuschele WP. Studies on the pathogenesis of African swine fever. I. Quantitative studies on the sequential development of virus in pig tissues. Arch Gesamte Virusforsch. 1967;21:349–56. http://dx.doi.org/10.1007/BF01241735
41. King DP, Reid SM, Hutchings GH, Grierson SS, Wilkinson PJ, Dixon LK, et al. Development of a TaqMan PCR assay with internal amplification control for the detection of African swine fever virus. J Virol Methods. 2003;107:53–61. http://dx.doi.org/10.1016/S0166-0934(02)00189-1
42. Tyre AJ, Tenhumberg B, Field SA, Niejalke D, Parris K, Possingham HP. Improving precision and reducing bias in biological surveys: estimating false-negative error rates. Ecol Appl. 2003;13:1790–801. http://dx.doi.org/10.1890/02-5078
43. Minuzzi-Souza TTC, Nitz N, Cuba CAC, Hagström L, Hecht MM, Santana C, et al. Surveillance of vector-borne pathogens under imperfect detection: lessons from Chagas disease risk (mis)measurement. Sci Rep. 2018;8:151. http://dx.doi.org/10.1038/s41598-017-18532-2
44. Brost BM, Mosher BA, Davenport KA. A model-based solution for observational errors in laboratory studies. Mol Ecol Resour. 2018;18:580–9. http://dx.doi.org/10.1111/1755-0998.12765
45. Shaby BA, Fink D. Embedding black-box regression techniques into hierarchical Bayesian models. J Stat Comput Simul. 2011;82:1–14.
46. Dorazio RM, Rodríguez DT. A Gibbs sampler for Bayesian analysis of site-occupancy data. Methods Ecol Evol. 2012;3:1093–8. http://dx.doi.org/10.1111/j.2041-210X.2012.00237.x
47. R Development Core Team. R: a language and environment for statistical computing. Version 2.13.1. Vienna: R Foundation for Statistical Computing; 2008 [cited 2018 May 28]. http://cran.r-project.org/doc/manuals/refman.pdf
48. Swine Health Information Center. Swine Disease Global Surveillance Report: African swine fever [cited 2018 Aug 3]. https://www.swinehealth.org/wp-content/uploads/2018/01/SHIC-109-SGDS-December-report-12-3-18-Final.pdf

Address for correspondence: Megan C. Niederwerder, L-227 Mosier Hall, College of Veterinary Medicine, Kansas State University, 1800 Denison Ave, Manhattan, KS 66506, USA; email: mniederwerder@vet.k-state.edu

Management of Central Nervous System Infections, Vientiane, Laos, 2003–2011

Audrey Dubot-Pérès, Mayfong Mayxay, Rattanaphone Phetsouvanh,[1] Sue J. Lee, Sayaphet Rattanavong, Manivanh Vongsouvath, Viengmon Davong, Vilada Chansamouth, Koukeo Phommasone, Catrin Moore, Sabine Dittrich, Olay Lattana, Joy Sirisouk, Phonelavanh Phoumin, Phonepasith Panyanivong, Amphonesavanh Sengduangphachanh, Bountoy Sibounheuang, Anisone Chanthongthip, Manivone Simmalavong, Davanh Sengdatka, Amphaivanh Seubsanith, Valy Keoluangkot, Prasith Phimmasone, Kongkham Sisout, Khamsai Detleuxay, Khonesavanh Luangxay, Inpanh Phouangsouvanh, Scott B. Craig, Suhella M. Tulsiani, Mary-Anne Burns, David A.B. Dance, Stuart D. Blacksell, Xavier de Lamballerie, Paul N. Newton

During 2003–2011, we recruited 1,065 patients of all ages admitted to Mahosot Hospital (Vientiane, Laos) with suspected central nervous system (CNS) infection. Etiologies were laboratory confirmed for 42.3% of patients, who mostly had infections with emerging pathogens: viruses in 16.2% (mainly Japanese encephalitis virus [8.8%]); bacteria in 16.4% (including *Orientia tsutsugamushi* [2.9%], *Leptospira* spp. [2.3%], and *Rickettsia* spp. [2.3%]); and *Cryptococcus* spp. fungi in 6.6%. We observed no significant differences in distribution of clinical encephalitis and meningitis by bacterial or viral etiology. However, patients with bacterial CNS infection were more likely to have a history of diabetes than others. Death (26.3%) was associated with low Glasgow Coma Scale score, and the mortality rate was higher for patients with bacterial than viral infections. No clinical or laboratory variables could guide antibiotic selection. We conclude that high-dependency units and first-line treatment with ceftriaxone and doxycycline for suspected CNS infections could improve patient survival in Laos.

Author affiliations: Lao-Oxford-Mahosot Hospital-Wellcome Trust Research Unit, Mahosot Hospital, Vientiane, Laos (A. Dubot-Pérès, M. Mayxay, R. Phetsouvanh, S. Rattanavong, M. Vongsouvath, V. Davong, V. Chansamouth, K. Phommasone, C. Moore, S. Dittrich, O. Lattana, J. Sirisouk, P. Phoumin, P. Panyanivong, A. Sengduangphachanh, B. Sibounheuang, A. Chanthongthip, M. Simmalavong, D. Sengdatka, A. Seubsanith, D.A.B. Dance, P.N. Newton); University of Oxford Nuffield Department of Clinical Medicine Center for Tropical Medicine and Global Health, Oxford, UK (A. Dubot-Pérès, S.J. Lee, C. Moore, S. Dittrich, D.A.B. Dance, S.D. Blacksell, P.N. Newton); Unité des Virus Émergents (UVE: Aix-Marseille Univ-IRD 190-INSERM 1207-IHU Méditerranée Infection), Marseille, France (A. Dubot-Pérès, X. de Lamballerie); University of Health Sciences Institute of Research and Education Development, Vientiane (M. Mayxay); Mahidol University Faculty of Tropical Medicine Mahidol–Oxford Tropical Medicine Research Unit, Bangkok, Thailand (S.J. Lee, S.D. Blacksell); Mahosot Hospital, Vientiane (V. Keoluangkot, P. Phimmasone, K. Sisout, K. Detleuxay, K. Luangxay, I. Phouangsouvanh); Queensland Health Forensic and Scientific Service World Health Organization Collaborating Centre for Reference and Research on Leptospirosis, Brisbane, Queensland, Australia (S.B. Craig, S.M. Tulsiani, M.-A. Burns); London School of Hygiene and Tropical Medicine Faculty of Infectious and Tropical Diseases, London, UK (D.A.B. Dance, P.N. Newton)

DOI: https://doi.org/10.3201/eid2505.180914

Central nervous system (CNS) infections, which can be caused by a number of different viruses, bacteria, fungi, and parasites, cause substantial disease and death in Southeast Asia (*1*). The etiologies of these infections are usually confirmed in <50% patients globally (*2*,*3*). Conventionally, most CNS infections are classified as meningitis or encephalitis by using a diverse set of clinical and laboratory definitions. The main causes of meningitis reported in Asia are *Mycobacterium tuberculosis*, *Streptococcus pneumoniae*, *Streptococcus suis*, *Neisseria meningitidis*, and *Cryptococcus* spp. (Appendix Table 1, https://wwwnc.cdc.gov/EID/article/25/5/18-0914-App1.pdf). Physicians rarely consider rickettsial and leptospiral pathogens, but interest in these reemerging treatable etiologies is resurfacing (*4*). Emerging viruses are important causes of CNS infections

[1]Deceased.

in Asia. Japanese encephalitis virus (JEV) causes ≈68,000 cases of encephalitis a year (*5*), and dengue virus is increasingly reported as a cause of neurologic disease, occurring in 0.5%–6.2% of dengue patients (*6*–*9*). Other common viral causes of encephalitis include enterovirus and herpes simplex viruses (HSVs) 1 and 2 (*10*).

Few data globally are available to guide policy on the prevention, diagnosis, and treatment of CNS infections, and the diversity of definitions for different CNS infection syndromes is confusing (*11*); some case definitions use clinical criteria only (*12*,*13*), and others include additional laboratory variables (*10*,*14*). Meningitis (i.e., meningeal infection) and encephalitis (i.e., parenchymal infection) presumably represent a continuum, but the diversity of clinical and laboratory features and etiologies across this wide spectrum is poorly understood. The standard for differentiating encephalitis from meningitis is histopathology, but biopsies and autopsies are rarely performed in Asia.

In Laos, the only comprehensive routine cerebrospinal fluid (CSF) diagnostic service available is in the capital city, Vientiane, at Mahosot Hospital (*15*–*17*). After a publication reporting rickettsial and leptospiral pathogens as important causes of CNS infections in Laos (*4*), we present the results of the full investigation conducted on the causes of CNS infection in this hospital to guide public health policy and treatment guidelines.

Methods

Study Site and Patient Recruitment

This study was prospectively conducted (January 2003–August 2011) with inpatients on all wards of Mahosot Hospital in Vientiane (17.959431°N, 102.613144°E, 188 m above mean sea level), an ≈400-bed hospital providing primary, secondary, and tertiary care and admitting ≈2,000 patients/month. We recruited inpatients of all ages for whom diagnostic lumbar puncture was indicated for suspicion of CNS infection because of altered consciousness or neurologic findings and for whom lumbar puncture was not contraindicated. For patient inclusion, we used no formal definition for CNS infection; patient recruitment was at the discretion of the responsible physician, reflecting local clinical practice. We recorded patient history and examination findings on standardized forms.

Ethics Statement

We obtained verbal (2003–2006) or written (2006–2011) informed consent from all recruited patients or close relatives. Ethics clearance was granted by the Ethical Review Committee of the Faculty of Medical Sciences, National University of Laos (Vientiane, Laos), and the Oxford University Tropical Ethics Research Committee (Oxford, UK).

Encephalitis and Meningitis Clinical Case Definitions

We classified febrile patients meeting the World Health Organization (WHO) criteria for encephalitis or meningitis (Figure 1) (*18*) as patients with WHO clinical CNS (hereafter WHO CNS) infection. Because of the overlapping WHO case definitions for encephalitis and meningitis, which both include a Glasgow Coma Scale (GCS) score <15 as criteria, we created additional classifications for febrile patients: those with stiff neck; reduced GCS score (<15), seizures, or both; stiff neck and reduced GCS score, seizures, or both; no stiff neck but reduced GCS score, seizures, or both; and stiff neck, a GCS score of 15, and no seizures (Table 1).

Laboratory Tests

Cerebrospinal fluid (CSF) was collected from patients (≈8 mL for adults [defined as patients ≥15 years of age], ≈3.5

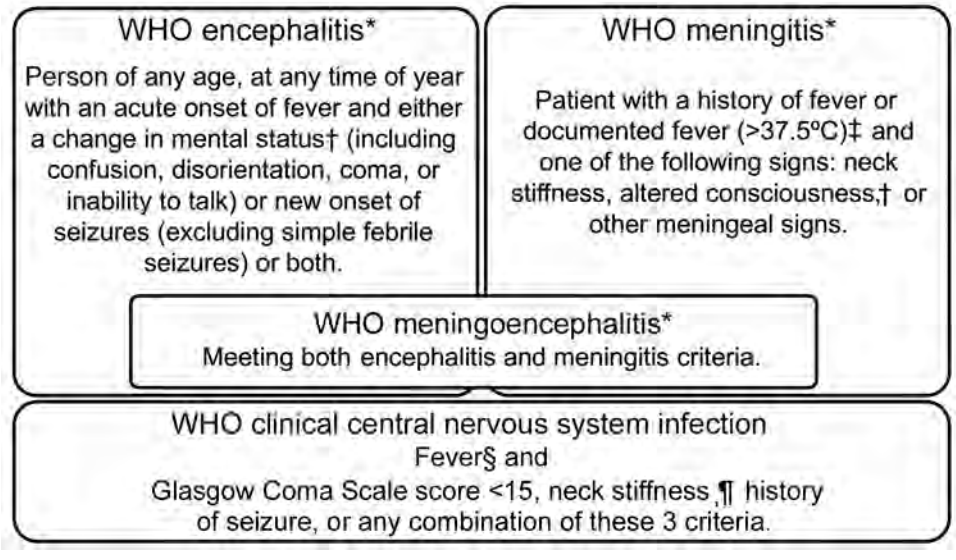

Figure 1. WHO encephalitis and meningitis case definitions. *Definitions from WHO (*18*). †Defined here as a Glasgow Coma Scale score <15. ‡Not "with sudden onset of fever >38.5°C" as recommended by the WHO because we saw patients, especially young children, with meningitis but with temperatures below the WHO temperature criterion. §Patients with history of fever or documented fever (>37.5°C). ¶History of neck stiffness or neck stiffness on examination. WHO, World Health Organization.

Table 1. Classifications of febrile patients with clinical central nervous system infection (n = 771), Laos, January 2003–August 2011*

Clinical sign				WHO classification, %†			Additional classification, %				
								GCS score <15, seizure, or both			Stiff neck + GCS score 15 + no seizure
Stiff neck	GCS score <15	Seizure	No. (%) patients	MEN	E	ME	Stiff neck	All	Stiff neck	No stiff neck	
+			191 (24.8)	96.2			83.5				24.8
+	+		244 (31.6)		75.2	71.5		75.2	58.8		
+	+	+	171 (22.2)								
+		+	38 (4.9)								
	+	+	57 (7.4)							16.5	
	+		41 (5.3)								
		+	29 (3.8)								

*Each line of the table corresponds to a given combination of criteria presented on the left side of the table. Each combination is then assigned (shaded cell) to ≥1 classifications (WHO and additional classifications) as defined in the Methods section. Green-shaded cells are the additional classifications used throughout our study. E, encephalitis; GCS, Glasgow Coma Scale; ME, meningoencephalitis; MEN, meningitis; WHO, World Health Organization; +, clinical sign present.
†Definitions of WHO classification provided in Figure 1.

mL for children 1–14 years of age, and ≈2.5 mL for children <1 year of age), and opening pressure was recorded. Venous blood (≈18.5 mL for adults, 10 mL for children 1–14 years of age, and 5.5 mL for children <1 year of age) was drawn on the same day. We aimed to collect ≈2 mL follow-up serum 7–10 days after lumbar puncture. Specimens were transported to the laboratory within ≈30 minutes, and we aliquoted and immediately tested or stored them at −80°C. We submitted all patient samples for a panel of laboratory tests: complete blood count; biochemistry panel; culture; and serologic and molecular assays for a range of bacteria, viruses, parasites, and fungi (Table 2; Appendix). HIV-1 and HIV-2 rapid diagnostic tests were performed when indicated by the physician. Computed tomography brain scan was available starting in 2002 but rarely used, especially for intensive care patients, because of difficulties transferring patients. Magnetic resonance imaging and electroencephalographic facilities were not available.

Interpretation

The confirmed etiology was determined by the results of a panel of diagnostic tests (Table 2), which included tests for the direct detection of pathogens in CSF or blood, specific IgM in CSF, seroconversion, or a 4-fold rise in antibody titer between admission and follow-up serum samples. Pathogen detection was confirmed after critical analysis of test results to rule out possible contamination. When evidence of >1 pathogen was obtained for a patient, we defined the confirmed etiology as detection by direct tests over indirect tests (antibody-based tests) and prioritized CSF detection over blood detection (*39*). We defined a confirmed co-infection as the direct (or indirect, if only indirect tests were positive) detection of >1 pathogen in the same matrix (CSF or blood).

Statistical Analyses

We compared patients with confirmed bacterial infection (including co-infections involving only bacteria) and patients with confirmed viral infection (including co-infections involving only viruses) with all other patients, excluding those with mixed co-infections (i.e. co-infections with fungi or infections with both bacteria and viruses). We investigated the factors associated with death (died in hospital or discharged moribund), bacterial infection, or viral infection by univariate analysis using the χ^2 or Fisher exact test for categorical variables or the Mann-Whitney U test for continuous variables. We analyzed the independent predictors of death, bacterial infection, and viral infection using multivariate logistic regression models. In multivariate analyses, we included all factors having a p value <0.010 in the univariate analysis.

For variables with 6%–20% of the values missing, we executed multiple imputation models using chained equations and used a number of imputations that exceeded the highest proportion of missing values (*40*). We added age and sex to imputation models as auxiliary variables. We specified the imputation methods as linear for continuous normally distributed variables, logistic for binary variables, ordered logistic for ordinal variables, and predictive mean matching for continuous skewed variables. We performed logistic regression with the dependent variable (death, bacterial or viral infection) and all relevant covariates on each imputed data set and combined results using Rubin rules to take into account the variability in estimates among imputed data sets (*41*). Only variables that were significant (p<0.050) were retained in the final models. For comparison of analysis methods, we provided the results using the corresponding complete case analysis. We conducted analyses using Stata/SE version 14.0 (StataCorp, https://www.stata.com).

Results

Patients

In total, 1,065 inpatients with suspected CNS infection consented to study participation (Appendix Figure 1); 80% were recruited from the pediatric and adult intensive care wards and adult infectious disease ward. On each ward, ≈8 physicians were in charge of patient recruitment. All were general

hospital or infectious disease physicians; none were neurologists. We collected information on patient demographics, clinical presentation, and blood and CSF parameters (Table 3–4; Figure 2). More patients were recruited during the rainy season (Figure 3). The median time between admission and follow-up blood collection was 9 (interquartile range [IQR] 6–16) days. One third (33.6%, 358/1,065) were children <15 years of age (Table 3; Appendix Table 2).

Table 2. Diagnostic laboratory tests used to confirm etiology in patients with suspected central nervous system infection, by sample type, Laos, January 2003–August 2011*

Pathogens tested	Cerebrospinal fluid†	Blood
Malaria pathogens	None	Giemsa thick and thin smear (if patient from endemic area)
Leptospira spp.	Hydrolysis probe real-time PCR (*19*)	Culturing of blood clot on EMJH medium; microscopic agglutination test of admission and follow-up serum samples (4-fold rise considered positive result) (*20*); hydrolysis probe real-time RT-PCR from buffy coat (*19*)
Cryptococcus spp.	Indian ink stain; if HIV suspected, *Cryptococcus* Antigen Latex Agglutination Test (IMMY, http://www.immy.com); if Indian ink positive and HIV suspected, culture on Sabouraud agar	None
Mycobacterium tuberculosis	Lowenstein-Jensen culture; auramine and Ziehl-Neelsen stains	None
Rickettsia spp.‡	Hydrolysis probe real-time PCR (*21*,*22*)	Hydrolysis probe real-time and conventional PCR from buffy coat (*21*,*22*); sequencing
R. typhi, *Orientia tsutsugamushi*‡	Hydrolysis probe real-time PCR (*21*,*23*)	Hydrolysis probe real-time PCR on buffy coat (*21*,*23*); IgM and IgG indirect immunofluorescent assay of admission and follow-up serum samples (4-fold rise considered positive result) (*24*)
Community-acquired bacterial infection	Gram stain; culture in blood agar and chocolate agar	Blood culture bottle
Streptococcus pneumoniae, Streptococcus suis, Haemophilus influenzae, *Neisseria meningitidis*	Culture on blood agar, chocolate agar, and MacConkey plates (for patients <1 year of age); hydrolysis probe real-time RT-PCR (*25*–*27*)	Blood culture bottle
Dengue virus	Hydrolysis probe real-time RT-PCR (*28*); NS1 ELISA (Dengue Early ELISA, Panbio, https://www.alere.com); ELISA IgM (Japanese Encephalitis/Dengue IgM Combo ELISA, Panbio)	Hydrolysis probe real-time RT-PCR on serum samples (*28*); NS1 ELISA on serum samples; ELISA IgM on admission and follow-up serum samples (assessed seroconversion)
JEV§	ELISA IgM (Japanese Encephalitis/Dengue IgM Combo ELISA, Panbio)	ELISA IgM on admission and follow-up serum samples (assessed seroconversion)
Enterovirus, West Nile virus, influenza viruses A and B, Henipavirus	Hydrolysis probe real-time RT-PCR (*29*–*31*) (in house)	Hydrolysis probe real-time RT-PCR on serum samples (*29*–*31*) (in house)
Flavivirus¶	SYBR Green real-time RT-PCR (*32*,*33*)	SYBR Green real-time RT-PCR on serum samples (*32*,*33*)
Herpes simplex virus 1 and 2, Varicella zoster virus, human cytomegalovirus	Hydrolysis probe real-time RT-PCR (*34*–*36*)	None
Measles virus, mumps virus	Hydrolysis probe real-time RT-PCR (*37*,*38*); if seropositive in blood sample, IgM ELISA with Enzygnost Anti-Measles Virus/IgM or Enzygnost Anti-Parotidis/IgM kits (Dade Behring, https://www.healthcare.siemens.com)	Hydrolysis probe real-time RT-PCR on serum samples (*37*,*38*); IgM and IgG ELISAs: Enzygnost Anti-Measles Virus/IgM, Enzygnost Anti-Measles Virus/IgG, Enzygnost Anti-Parotidis/IgM, and Enzygnost Anti-Parotidis/IgG kits (Dade Behring) (assessed seroconversion)
HIV	None	Determine HIV-1/2 Combo (Alere, https://www.alere.com) or Uni-Gold HIV (Trinity Biotech, https://www.trinitybiotech.com)

*See Appendix (https://wwwnc.cdc.gov/EID/article/25/5/18-0914-App1.pdf) for further details on methods. Cerebrospinal fluid and serum samples were inoculated on Vero and buffalo green monkey kidney cells for viral isolation. The median (interquartile range) interval between admission and follow-up serum sample collection was 9 (6–16) days. EMJH, Ellinghausen-McCullough-Johnson-Harris; JEV, Japanese encephalitis virus; NS1, nonstructural protein 1; RT-PCR, reverse transcription PCR.

†Contraindications for lumbar puncture included focal neurologic signs on examination, clinical evidence for raised intracranial pressure, skin or soft tissue sepsis at the proposed puncture site, severe coagulopathy, or severe thrombocytopenia.

‡Buffy coats were inoculated on Vero and L929 cells for *O. tsutsugamushi* and *Rickettsia* sp isolation.

§Detection of JEV IgM in a single sample of serum is considered as laboratory confirmation according to World Health Organization criteria. However, in this study, to be conservative and consistent with interpretation of other test results, a single detection of JEV IgM in serum was not counted as confirming JEV central nervous system infection.

¶Flavivirus RT-PCR would have likely detected the main flaviviruses circulating in Laos.

Of 476 adults tested for HIV, 118 (24.8%) were seropositive; of 227 children tested, 1 (0.4%) was seropositive. More than half (61.9%, 590/953) of patients had a history or hospital chart evidence of antibiotic use before lumbar puncture. Most (90.8%, 962/1,059) patients had a history of fever or documented admission fever. The median length of fever at admission was 4 (IQR 2–8) days. The most frequent symptoms and signs were headache (88.1%, 787/893); neck stiffness (64.2%, 683/1,064); confusion (57.4%, 608/1,060); GCS score <15 (52.6%, 551/1,047); and vomiting, diarrhea, or both (54%, 575/1,064). All symptoms and signs were more frequent in children than adults ($p<0.05$), except headache, which was more frequent in adults ($p = 0.023$). Most (93.6%, 832/889) patients had CSF findings outside reference ranges (elevated CSF white cell count, elevated CSF lactate, elevated CSF protein, low CSF glucose, or any combination of these parameters) (Table 4; Appendix Table 3, Figure 2).

Etiology was confirmed in 450 (42.3%) patients; 413 (38.8%) had monoinfections and 37 (3.5%) co-infections (Appendix Tables 4–8). The identified monoinfections were JEV (8.8%, 94/1,065), *Cryptococcus* spp. (6.6%, 70/1,065; 9 *C. gattii*), *Orientia tsutsugamushi* (2.9%, 31/1,065), dengue virus (2.5%, 27/1,065), *Leptospira* spp. (2.3%, 25/1,065), *Rickettsia* spp. (2.3%, 24/1,065), *S. pneumoniae* (2.1%, 22/1,065), *M. tuberculosis* (1.9%, 20/1,065), HSV-1 or HSV-2 (1.4%, 15/1,065), human cytomegalovirus (1.1%, 12/1,065), enterovirus (0.9%, 10/1,065), varicella

Table 3. Demographic and clinical data at admission of patients with suspected CNS infection, by age group and etiology, Laos, January 2003–August 2011*

	Age group			Etiology			
Characteristic	All, n = 1,065	Children, n = 358	Adults, n = 707	Confirmed, n = 450	None confirmed, n = 615	Confirmed viral, n = 172	Confirmed bacterial, n = 175
Demographic							
M	666 (62.5)	207 (57.8)	459 (64.9)	288 (64.0)	378 (61.5)	111 (64.5)	117 (66.9)
F	399 (37.5)	151 (42.2)	248 (35.1)	162 (36.0)	237 (38.5)	61 (35.5)	58 (33.1)
Age, y, median (IQR)	23 (8–38)	3 (0.41–8)	32 (24–47)	23 (10–38)	24 (6–40)	16 (7–28)	23 (9–45)
History							
HIV seropositive, n = 703	119 (16.9)	1 (0.4)	118 (24.8)	75 (27.1)	44 (10.33)	8 (8.0)	6 (6.2)
Diabetes, n = 850	24 (2.8)	0	24 (4.2)	12 (3.5)	12 (2.4)	1 (0.8)	10 (7.5)
Antibiotic use before lumbar puncture, n = 953	590 (61.9)	238 (71.9)	352 (56.6)	252 (64.0)	338 (60.5)	109 (69.9)	100 (62.5)
Signs and symptoms							
Days of fever at admission, median (IQR), n = 1,058	4 (2–8)	4 (2–6)	5 (2–10)	5 (3–10)	4 (1–7)	5 (3–7)	5 (3–8)
Fever, n = 1,059	962 (90.8)	340 (95.2)	622 (88.6)	425 (94.9)	537 (87.9)	162 (95.3)	171 (97.7)
Headache,† n = 893	787 (88.1)	155 (83.3)	632 (89.4)	369 (92.5)	418 (84.6)	139 (90.9)	135 (91.2)
Hearing loss,† n = 893	51 (5.7)	10 (5.4)	41 (5.8)	20 (5.0)	31 (6.3)	8 (5.2)	7 (4.7)
Dysuria,† n = 891	28 (3.1)	4 (2.2)	24 (3.4)	10 (2.5)	18 (3.7)	3 (2.0)	3 (2.0)
Visual loss,† n = 885	66 (7.5)	14 (7.7)	52 (7.4)	23 (5.8)	43 (8.8)	11 (7.2)	5 (3.4)
Diplopia,† n = 889	36 (4.1)	4 (2.2)	32 (4.5)	15 (3.4)	21 (4.3)	6 (4.0)	6 (4.1)
Photophobia, n = 850	52 (5.8)	14 (7.4)	38 (5.4)	23 (5.8)	29 (5.9)	7 (4.6)	10 (6.8)
Focal neurologic signs, n = 939	22‡ (2.3)	5 (1.6)	17 (2.7)	8 (2.1)	14 (2.5)	1 (0.7)	6 (4.1)
Neck stiffness, n = 1,064	683 (64.2)	245 (68.4)	438 (62.0)	316 (70.2)	367 (59.8)	130 (75.6)	128 (73.1)
Confusion, n = 1,060	608 (57.4)	232 (65.5)	376 (53.3)	254 (56.7)	354 (57.8)	114 (66.3)	103 (59.5)
Convulsions, n = 1,063	319 (30.0)	233 (65.3)	86 (12.2)	119 (26.5)	200 (32.6)	65 (37.8)	44 (25.3)
GCS score, median (IQR), n = 1,010	14 (11–15)	14 (10–15)	15 (11–15)	15 (11–15)	14 (10–15)	13 (10–15)	14 (11–15)
GCS score <15,§ n = 1,047	551 (52.6)	220 (63.4)	331 (47.3)	225 (50.5)	326 (54.2)	101 (59.4)	94 (54.0)
WHO clinical CNS infection,¶ n = 1,040	771 (74.1)	313 (90.7)	458 (65.9)	341 (77.0)	430 (72.0)	143 (85.1)	140 (80.9)
Outcome							
Days of hospitalization, n = 846, median (IQR)	9 (5–14)	8 (5–13)	10 (5–15.5)	11 (6–17)	8 (5–13)	10 (6–14)	11 (7–17)
Death,# n = 893	235 (26.3)	70 (22.5)	165 (28.4)	94 (25.0)	141 (27.3)	23 (15.7)	43 (27.9)

*Values are no. (%) unless indicated otherwise. We defined children as patients <15 years of age and adults ≥15 years of age. History or physical examination or both, were taken into account for confusion, neck stiffness, photophobia, fever (history of fever or >37.5ºC during physical examination). In total, 8 women in the patient population were pregnant; 26 (2.4%) patients had computed tomography brain scans, and 2 of these scans demonstrated brain abscesses. The confirmed viral group includes patients infected with multiple viruses, and the confirmed bacterial group includes patients infected with multiple bacteria. CNS, central nervous system; GCS, Glasgow Coma Scale; IQR, interquartile range; WHO, World Health Organization.
†Data from children <3 years of age were considered not reliable and were thus excluded from analysis.
‡Of these patients, 7 had hemiplegia, 11 had limb weakness, and 1 had paraplegia; 13 patients had admission or discharge diagnoses of Guillain-Barre syndrome. Retrospective evaluation of the likelihood of this diagnosis by using the Brighton system suggested that 4 patients met level 3 criteria for Guillain-Barre syndrome diagnostic certainty (*42*).
§Includes confused and disoriented patients.
¶Defined as fever with GCS score <15, neck stiffness (history of or present during examination), or history of seizures or any of these signs in combination. Patients with missing data for 1 of these criteria were not counted.
#Includes patients who died at the hospital and those taken home to die.

zoster virus (0.6%, 6/1,065), mumps virus (0.5%, 5/1,065), and *Plasmodium falciparum* (0.4%, 4/1,065). Other bacteria were detected in 48 (4.5%) patients (Figure 4; Appendix Table 5). All samples were negative for West Nile virus, influenza A and B, Henipavirus, and measles virus by PCR. Infection by *M. tuberculosis*, *Cryptococcus* spp., or varicella zoster virus was not detected in children (Appendix Table 8). The median age of children with enterovirus infection was 4.5 (IQR 1–11) years and JEV infection 13 (IQR 8–20) years. The proportion of patients with JEV infection was higher for children (14%, 50/358) than adults (6%, 44/707, p<0.001). Significantly more enterovirus patients (80%) than nonenterovirus patients (33%; p = 0.002) were children.

Factors Associated with Bacterial and Viral Infections

We compared patients with single (n = 170) or multiple (n = 5) bacterial infections (excluding co-infections with viruses or fungi) with all other patients (n = 875). Factors significantly associated with bacterial infections on univariate analysis (p<0.01; Appendix Table 9) were included in multivariate analysis. Diabetes (adjusted odds ratio [aOR] 3.1, 95% CI 1.2–7.7), history of fever or fever at admission (aOR 3.9, 95% CI 1.4-11.1), higher serum C-reactive protein (aOR 1.08, 95% CI 1.05-1.11), and higher CSF lactate (aOR 3.5, 95% CI 2.3–5.4) were independent predictors of bacterial infection (Appendix Table 10).

We compared patients with single (n = 169) or multiple (n = 3) viral infections (excluding co-infections with bacteria or fungi) with all other patients (n = 867). Factors significantly associated with viral infections on univariate analysis (p<0.01; Appendix Table 11) were included in multivariate analysis. Neck stiffness (aOR 1.9, 95% CI 1.3-2.8) and higher hematocrit (aOR 1.4, 95% CI 1.1-1.9) were associated with viral infection, whereas higher CSF lactate (aOR 0.3, 95% CI 0.1–0.5), older age (aOR 0.8, 95% CI 0.7–0.9), and longer interval between admission and lumbar puncture (aOR 0.9, 95% CI 0.8–1.0) were negatively associated with viral infection (Appendix Table 12).

Relationships between Clinical Presentation and Etiology

In total, 771 (74.1%) of 1,040 patients had WHO CNS infection; 44.2% of these patients had confirmed etiologies compared with 37.9% of patients not fulfilling WHO CNS infection criteria (p = 0.063; Appendix Table 13). Because of the considerable overlap between the WHO encephalitis and meningitis definitions, 551 (71.5%) patients were classified as having meningoencephalitis. Therefore, we analyzed the frequency of neck stiffness, reduced GCS score, and seizures among febrile patients with clinical CNS infection (Table 1).

Table 4. Characteristics of peripheral blood and cerebrospinal fluid at admission of patients with suspected central nervous system infection, by age group and etiology, Laos, January 2003–August 2011*

	Age group			Etiology			
Sample type and parameter	All, n = 1,065	Children, n = 358	Adults, n = 707	Confirmed, n = 450	None confirmed, n = 615	Confirmed viral, n = 172	Confirmed bacterial, n = 175
Peripheral blood							
Elevated white cell count,† n = 952	449 (47.2)	150 (47.9)	299 (46.8)	198 (49.0)	251 (45.8)	84 (53.9)	84 (53.5)
Low white cell count, n = 952	45 (4.7)	22 (7.0)	23 (3.6)	22 (5.5)	23 (4.2)	6 (3.9)	7 (4.5)
Anemia, n = 948	355 (37.5)	112 (35.7)	243 (38.3)	160 (39.8)	195 (35.7)	44 (28.2)	68 (43.9)
Thrombocytopenia, n = 649	55 (8.5)	16 (6.8)	39 (9.4)	22 (7.8)	33 (9.0)	4 (3.5)	12 (10.6)
Elevated C-reactive protein, n = 868	547 (63.0)	145 (51.6)	402 (68.5)	265 (69.2)	282 (58.1)	98 (64.9)	114 (79.7)
Hyperglycemia,† n = 991	237 (23.9)	81 (25.8)	156 (23.0)	105 (24.5)	132 (23.5)	40 (24.0)	53 (32.3)
Severe hyperglycemia,† n = 991	72 (7.3)	26 (8.3)	46 (6.8)	35 (8.2)	37 (6.6)	12 (7.2)	22 (13.4)
Elevated serum sodium,‡ n = 807	225 (27.9)	45 (17.8)	180 (32.5)	82 (22.8)	143 (31.9)	40 (28.6)	26 (19.4)
Low serum sodium,‡ n = 807	63 (7.8)	31 (12.3)	32 (5.8)	31 (8.6)	32 (7.1)	8 (5.7)	16 (11.9)
Cerebrospinal fluid							
Turbid, n = 999	145 (14.5)	40 (12.2)	105 (15.7)	80 (18.4)	65 (11.5)	21 (12.4)	38 (23.2)
Elevated opening pressure, n = 977	334 (34.2)	86 (27.6)	248 (37.3)	155 (36.4)	179 (32.5)	42 (24.9)	60 (37.3)
Elevated white cell count,§ n = 975	729 (74.8)	237 (74.8)	492 (74.8)	341 (80.2)	388 (70.6)	141 (84.9)	129 (80.1)
Elevated lymphocyte count, n = 890	467 (52.5)	149 (51.2)	318 (53.1)	234 (59.5)	233 (46.9)	106 (68.4)	91 (62.3)
Elevated neutrophil count, n = 889	644 (72.4)	213 (73.5)	431 (72.0)	309 (78.8)	335 (67.4)	130 (83.9)	116 (80.0)
Elevated eosinophil count,¶ n = 1,001	46 (4.6)	7 (2.1)	39 (5.8)	11 (2.5)	35 (6.2)	9 (5.3)	2 (1.2)
Elevated protein, n = 955	601 (62.9)	177 (57.3)	424 (65.6)	281 (66.9)	320 (59.8)	112 (66.3)	108 (69.7)
Decreased glucose, n = 957	280 (29.3)	58 (18.8)	222 (34.3)	138 (32.8)	142 (26.5)	45 (26.6)	51 (32.9)
Decreased cerebrospinal fluid: venous glucose ratio, n = 929	540 (58.1)	159 (54.8)	381 (59.6)	253 (61.7)	287 (55.3)	97 (58.8)	97 (64.2)
Elevated lactate, n = 985	650 (66.0)	217 (67.8)	433 (65.1)	298 (69.8)	352 (63.1)	93 (56.0)	132 (80.5)

*Values are no. (%). We defined children as patients <15 years of age and adults ≥15 years of age. The confirmed viral group includes patients infected with multiple viruses, and the confirmed bacterial group includes patients infected with multiple bacteria. Elevated and low parameters mean above or below reference ranges. Anemia is defined as hematocrit below reference range. Thrombocytopenia is defined as platelet count below reference range. See Appendix Table 3 (https://wwwnc.cdc.gov/EID/article/25/5/18-0914-App1.pdf) for reference ranges. CSF, cerebrospinal fluid.
†Hyperglycemia was defined as a blood glucose level of >7.7 mmol/L and severe hyperglycemia as a blood glucose level >11.1 mmol/L.
‡Serum sodium levels >150 mmol/L were considered elevated and <130 mmol/L considered low; 5 patients (0.6%) had serum sodium <115 mmol/L.
§Samples with high turbidity could not be counted and were thus not included.
¶An eosinophil count >10% was considered elevated.

When comparing viral and bacterial infections, we observed no significant differences (p>0.05) in the proportions of encephalitis and meningitis syndromes, although differences were observed for some specific etiologies (Figure 4). In total, 90 (53.6%) febrile patients with viral infection and 86 (49.7%) with bacterial infection had neck stiffness and reduced GCS score, seizures, or both; 17 (10.1%) patients with viral infection and 16 (9.3%) with bacterial infection had reduced GCS score, seizures, or both without neck stiffness; and 36 (21.4%) patients with viral infection and 38 (22.0%) with bacterial infection had neck stiffness, a GCS score of 15, and no seizures (Figure 4). We obtained similar results using the WHO definitions. In total, 25 (14.9%) patients with viral infection and 33 (19.1%) with bacterial infection did not fulfill the WHO CNS infection definition.

In comparison with the distribution of syndromes observed for all patients, the distribution in patients with some etiologies were significantly different (p<0.05). Of the 89 JEV patients with WHO CNS infection, 75.3% had fever; neck stiffness; and reduced GCS score, seizures, or both. Of the 26 *O. tsutsugamushi* patients with WHO CNS infection, 50% had fever, neck stiffness, a GCS score of 15, and no seizures. Of note, almost half (47.8%) of the patients with cryptococcal infection did not fulfill the definition for WHO CNS infection, and of the 36 who did, 55.6% had fever, neck stiffness, a GCS score of 15, and no seizures.

Risk Factors for Death

Of 893 patients, 235 (26.3%) died, including those discharged moribund; we compared them to the 658 (73.7%) patients discharged alive and not moribund. For factors significantly associated with death (p<0.01; Appendix Table 14) in the univariate analysis, we conducted multivariate analysis. The variables strongly associated with death were higher CSF lactate (aOR 1.1, 95% CI 1.0–1.1) and reduced GCS score (aOR 0.8, 95% CI 0.8–0.9). Patients with viral infection were less likely to die than those with other

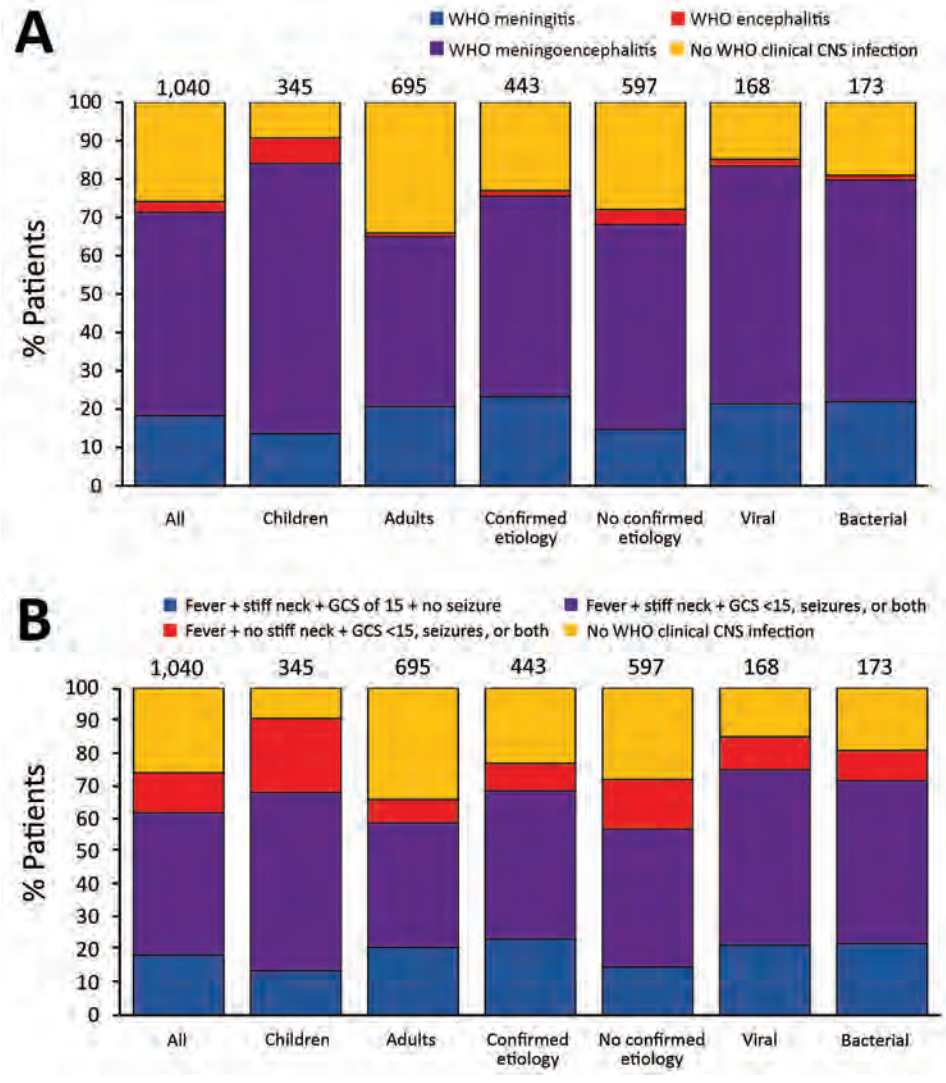

Figure 2. Distribution of clinical manifestations among patients with suspected CNS infection, by age group and etiology, Laos, January 2003–August 2011. A) WHO criteria; B) additional criteria (Table 1). Children were patients <15 years of age and adults patients ≥15 years of age. Numbers above bars indicate number of patients in group. CNS, central nervous system; GCS, Glasgow Coma Scale; WHO, World Health Organization.

diagnoses (aOR 0.4, 95% CI 0.3–0.7) (Appendix Table 15). Diabetes and hyperglycemia (glucose >7.7 mmol/L) at admission were not associated with death.

Indications for Antibiotic Treatment

In total, 56 patients (12.4% of the 450 patients with confirmed etiologies) were infected with bacteria treatable by ceftriaxone and 64 patients (14.2% of the patients with confirmed etiologies) with bacteria treatable by doxycycline but not ceftriaxone (Table 5). Twenty-eight patients were infected with a *Leptospira* spp. treatable by ceftriaxone or doxycycline, but 2 were co-infected with *O. tsutsugamushi* not treatable by ceftriaxone. Of 142 patients infected by bacteria treatable by ceftriaxone or doxycycline, 89 (62.7%) received appropriate treatment, 17% (13/77) of whom died. In comparison, 25% (12/48) of the patients who did not receive appropriate treatment died (p = 0.270).

Including the 450 patients with confirmed diagnoses, we analyzed the criteria for bacterial meningitis commonly considered when making decisions on antibiotic treatment: elevated CSF white cell count, elevated CSF lactate, elevated CSF protein, decreased CSF glucose, reduced GCS score, turbid CSF, and neck stiffness. A low percentage (<23%) of patients with any 1 of these criteria (except turbid CSF, 38.8%) or a combination of these criteria had bacterial infections treatable by ceftriaxone or doxycycline (Appendix Table 16). Furthermore, only 1 combination of criteria (elevated C-reactive protein, elevated CSF protein, or elevated CSF lactate or any combination of these criteria) could identify all patients infected with bacteria treatable by ceftriaxone (Table 5). However, because only 5% of our patient series did not display this combination of criteria, none of the analyzed clinical and biological results can be reliably used to guide decisions on antibiotic use.

Discussion

Etiology was confirmed in 42.3% of patients with suspected CNS infection, consistent with regional published data (Appendix Table 1); 16.2% had viral infections, and 16.4% had bacterial infections. We observed no significant differences in the distribution of clinical encephalitis and meningitis syndromes by bacterial or viral etiology; the most common infections in this patient population were JEV (8.8%) and *Cryptococcus* spp. (6.6%).

The results of this study provided evidence for the implementation of pneumococcal immunization in 2011

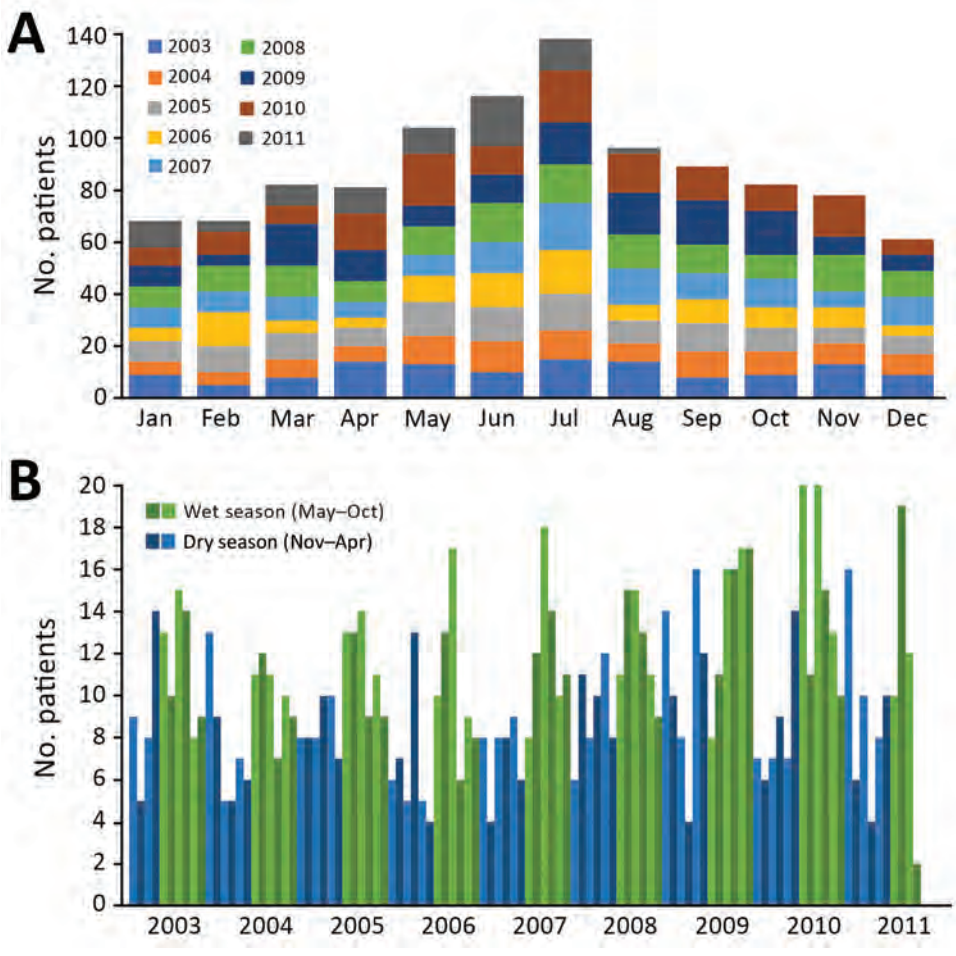

Figure 3. Recruited patients with suspected central nervous system infection, by month, Laos, January 2003–August 2011. A) Total patients recruited by month cumulating all studied years. B) Patients recruited each month of each year. Light and dark shades of colors were used in an alternating pattern to facilitate graph reading.

and JEV immunization in 2013 in Laos (*16*,*17*). Although the main etiology reported among patients with suspected CNS infection was JEV, this finding might be an overestimate; we have noted that the detection of JEV IgM in CSF has low predictive value (*44*). On the other hand, bacterial causes were probably underestimated; 61.9% of patients were known or thought to have received an antibiotic before lumbar puncture, potentially rendering bacteria uncultivable or reducing the bacterial load below the threshold needed for molecular detection.

The mortality rate we report in our study (26.3%) was higher than those reported in similar studies in neighboring countries (≈10%; Appendix Table 1). Ineffective patient management or inappropriate treatment through lack of previous local data might have caused this higher mortality rate. The epidemiology of CNS infection varies by geography; therefore, regional evidence should be used to build regional policies on prevention, diagnosis, and treatment of these infections.

In this study, 17% (119/703) of the patients tested were HIV seropositive. The highest proportion of HIV-seropositive patients was among those with cryptococcal infection (79%; Appendix Table 7). However, only 66% (703/1,065) of patients were tested. More patients need to receive HIV testing in Laos, and more investigations on the relationship between HIV and other infections are needed.

Our study had a number of limitations, including the partial use of stored samples; missing values; a low frequency of computed tomography brain scans and HIV testing; and a lack of magnetic resonance imaging, brain or postmortem examination, and diagnostics for autoimmune and eosinophilic CNS disease (*45*,*46*) and other

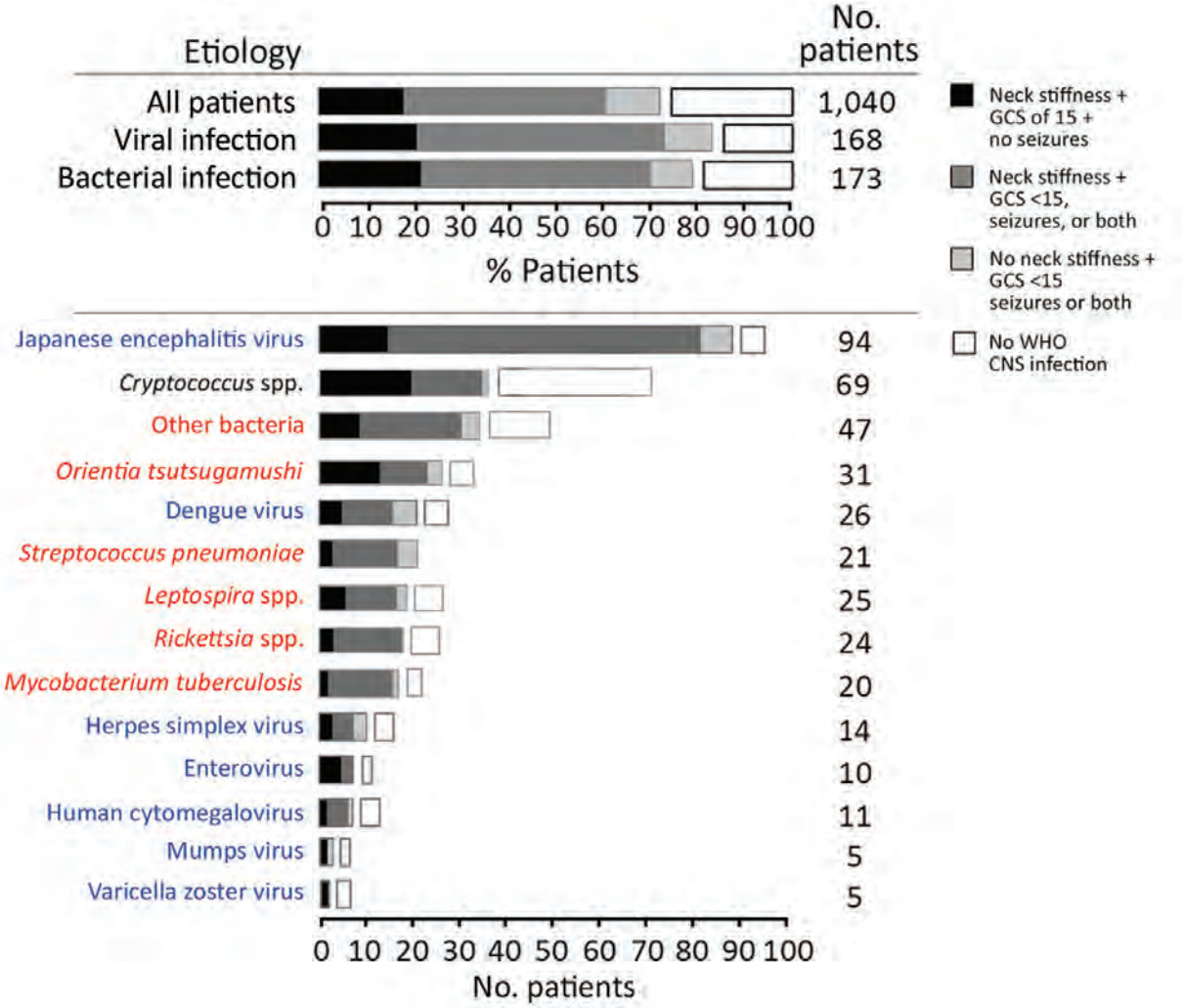

Figure 4. Distribution of clinical presentations in patients with suspected central nervous system infection, by confirmed etiology, Laos, January 2003–August 2011. Analysis per pathogen includes only patients with monoinfections. Other bacteria include 7 *Escherichia coli*, 4 *Streptococcus agalactiae*, 4 *Neisseria meningitidis*, 1 *Salmonella enterica* group D, 1 *S. enterica* group B or C, 5 *S. enterica* serovar Typhi, 4 *Streptococcus suis*, 3 *Klebsiella pneumoniae*, 7 *Haemophilus influenzae* type b, 5 *Burkholderia pseudomallei*, 6 *Staphylococcus aureus*, and 1 *Morganella morganii.* Blue font indicates viruses, red font indicates bacteria, and black font indicates fungi. CNS, central nervous system; GCS, Glasgow Coma Scale; WHO, World Health Organization.

pathogens (e.g., *Toxoplasma gondii*, *Mycoplasma* spp., and Zika virus). The absence of strict criteria for the inclusion of patients could have resulted in recruitment bias; however, the data reflect real-life medical practice. The proportion of patients who declined lumbar puncture is unknown. Almost all patients (93.6%) had CSF findings outside reference ranges. Although published data on this combined index are few, the proportion of patients with abnormal CSF findings is generally lower in routine practice (e.g., <40% at La Timone Hospital, Marseille; L. Ninove and J. Fromonot, La Timone Hospital, pers. comm., March 2017). This finding suggests a relatively low frequency of lumbar puncture at Mahosot Hospital, reflecting current practice but representing an unknown proportion of all patients admitted with CNS disease. The sample size was too small for a comparison of mortality rates between treated and nontreated patients.

Table 5. Frequency of criteria consistent with bacterial meningitis among patients with suspected central nervous system infection, by etiology and antibiotic susceptibility, Laos, January 2003–August 2011*

	Patients with confirmed etiology, n = 450							
		Patients infected by bacteria treatable by†						
		Ceftriaxone		Doxycycline				
Variables	All	Not including *Leptospira* infections, n = 56‡	Including *Leptospira* infections, n = 84	Not including *Leptospira* infections, n = 64§	Including *Leptospira* infections, n = 90	Other, n = 305	Patients without confirmed etiology, n = 615	Total, n = 1,065
Neck stiffness¶	316 (70.2)	41 (73.2)	60 (71.4)	46 (71.9)	63 (70.0)	213 (69.8)	367 (59.8)	683 (64.2)
GCS score <15	225 (50.5)	34 (61.8)	47 (56.6)	27 (42.2)	40 (44.4)	152 (50.3)	326 (54.2)	551 (52.6)
Elevated CRP	265 (69.2)	44 (91.7)	60 (87.0)	36 (70.6)	51 (72.9)	171 (64.3)	282 (58.1)	547 (63.0)
CSF turbid	80 (18.4)	27 (49.1)	31 (37.8)	6 (10.7)	9 (11.1)	45 (15.1)	65 (11.5)	145 (14.5)
Elevated CSF lactate	298 (69.8)	44 (83.0)	63 (78.8)	44 (74.6)	62 (73.8)	193 (66.3)	352 (63.1)	650 (66.0)
Elevated CSF protein	281 (66.9)	44 (81.5)	57 (73.1)	32 (62.7)	43 (58.9)	195 (66.3)	320 (59.8)	601 (62.9)
Decreased CSF glucose	138 (32.8)	23 (42.6)	26 (33.3)	12 (23.5)	15 (20.5)	101 (34.2)	142 (26.5)	280 (29.3)
Decreased CSF:venous glucose ratio	253 (61.7)	40 (76.9)	49 (64.5)	27 (54)	35 (48.6)	179 (62.4)	287 (55.3)	540 (58.1)
Elevated CSF leukocyte count#	341 (80.2)	44 (86.3)	64 (82.1)	39 (69.6)	57 (70.4)	241 (82.0)	388 (70.6)	729 (74.8)
Combinations of ≥1 of the above findings								
Elevated CSF lactate, protein, leukocyte count; decreased CSF glucose; CSF turbid#	418 (95.9)	53 (96.4)	76 (93.8)	54 (90.0)	75 (89.3)	291 (97.7)	534 (93.2)	952 (94.4)
Elevated CRP; elevated CSF lactate, protein; CSF turbid	427 (96.4)	56 (100)	82 (100)	59 (92.2)	83 (94.3)	289 (96.3)	526 (93.4)	953 (94.7)
Elevated CRP; elevated CSF lactate, protein	425 (95.4)	56 (100)	82 (100)	58 (92.1)	82 (94.3)	288 (96.3)	525 (93.4)	950 (94.7)
Elevated CRP; elevated CSF lactate	385 (91.2)	54 (98.2)	78 (98.7)	56 (91.8)	78 (94.0)	254 (89.1)	478 (88.5)	863 (89.7)
Elevated CRP; elevated CSF protein	382 (90.1)	54 (98.2)	75 (94.9)	49 (89.1)	68 (88.3)	261 (89.1)	442 (84.2)	824 (86.8)
Elevated CRP; GCS score <15	348 (83.9)	50 (100.0)	72 (98.6)	49 (86.0)	70 (89.7)	229 (79.5)	448 (83.1)	796 (83.4)
GCS score <15; elevated CSF protein	348 (81.1)	49 (90.7)	68 (85.0)	44 (77.2)	61 (75.3)	239 (81.0)	454 (80.8)	802 (80.9)
GCS score <15; elevated CSF lactate	361 (84.1)	48 (88.9)	69 (85.2)	50 (83.3)	70 (82.4)	244 (83.8)	466 (80.3)	827 (82.0)
GCS score <15; elevated CSF lactate, protein	404 (92.9)	52 (94.5)	75 (91.5)	53 (88.3)	74 (87.1)	279 (94.3)	515 (89.4)	919 (90.9)

*All values are no. (%). See Appendix Table 3 (https://wwwnc.cdc.gov/EID/article/25/5/18-0914-App1.pdf) for reference ranges. Only patients with confirmed etiology strictly sensitive to ceftriaxone or doxycycline are included in the analysis. Classification was based on a combination of susceptibility testing of isolates from patients and information from Principles and Practice of Infectious Diseases (*43*). Patients who were confused or disoriented who had their GCS score missing were considered to have a GCS score <15. CRP, C-reactive protein; CSP, cerebrospinal fluid; GCS, Glasgow Coma Scale.
†In total, 28 patients were infected with *Leptospira* spp. treatable by either ceftriaxone or doxycycline, but 2 were also co-infected with *Orientia tsutsugamushi* not treatable with ceftriaxone. One patient co-infected with *Streptococcus suis* and *Rickettsis typhi* required therapy with both ceftriaxone and doxycycline.
‡Includes 24 patients infected with *Streptococcus pneumoniae* and 32 infected with other bacteria (7 *Escherichia coli*, 4 Group B *Streptococcus*, 4 *Neisseria meningitidis*, 1 *Salmonella enterica* group D, 1 *S. enterica* group B or C, 5 *S. suis*, 5 *S. enterica* serovar Typhi, 2 *Klebsiella pneumoniae*, 2 *Haemophilus influenzae*, and 1 *Edwardsiella tarda*).
§Includes 31 patients with *Rickettsia* spp. infection and 33 with *O. tsutsugamushi* infection.
¶History of neck stiffness or neck stiffness on examination.
#Samples with high turbidity could not be counted and were thus not included.

Although CNS infection is a global public health burden, global consensus on the case definition is lacking (Appendix Table 17). In clinical studies, encephalitis and meningitis have been studied separately or together (*11*), and CSF findings might or might not be taken into account (e.g., CSF findings are not part of the WHO criteria). There is confusion regarding the clinical and laboratory definitions of encephalitis and meningitis, so we suggest pairing clinical, laboratory, or clinicolaboratory with these terms to reduce confusion. Further, altered consciousness and altered mental status, shared by encephalitis and meningitis in many definitions, are undefined in the WHO definitions. We used GCS score <15 to define both objectively, but this practice resulted in considerable overlap in clinical definitions: 71.4% of patients had WHO-defined meningitis and 53% WHO-defined meningoencephalitis. When we restricted the definition of meningitis to the presence of fever and neck stiffness, 61.9% of patients fulfilled those criteria; 43.6% had neck stiffness combined with low GCS score, seizures, or both.

Studies on the clinical and etiologic characteristics of patients requiring lumbar puncture in Asia have usually focused on particular pathogens or just meningitis or encephalitis (Appendix Table 1) (*47*). Although needed for treatment trials and pathophysiologic research, our data call into question the validity of defining criteria for patient management differently between encephalitis and meningitis (Figure 4; Appendix Table 13). In Laos, evidence suggests that brain (encephalitis) and meningeal (meningitis) infections have no clear distinguishable clinical manifestations relating to the responsible pathogen and that these classifications should be used with caution in the Asia tropics for guiding patient management.

We found that history of diabetes was independently associated with bacterial CNS infection. Indeed, some evidence suggests that diabetes is a risk factor for bacterial CNS disease (*48*) and poor outcome in tuberculous meningitis (*49*). In univariate analysis, higher blood glucose level was also associated with bacterial infection ($p<0.001$). Of 237 patients with hyperglycemia at admission (>7.7 mmol/L), 16 (6.8%) had a history of diabetes and 164 (69.2%) did not. Without convalescent glucose and hemoglobin A1c assays, however, we were unable to distinguish hyperglycemia resulting from severe disease or undiagnosed diabetes that might have predisposed to CNS infection. Intensive euglycemia management is difficult; can lead to hypoglycemia, especially in unconscious patients; and requires skilled dedicated nursing that is not available in hospitals in rural Asia. Whether such intensive therapy would save lives remains uncertain, but the development of an inexpensive computerized algorithm technology for resource-poor settings to facilitate safe euglycemia management (*50*) should be a priority for investigation of efficacy. The burgeoning global prevalence of diabetes calls for research regarding the relationship between hyperglycemia and CNS infections and optimizing their combined management (*48*).

Our data suggest that patient survival could be improved through 2 patient management interventions, the implementation of antibiotic use guidelines and strengthening of high-dependency units. The finding that poor outcomes were associated with a decreased GCS score at admission suggests that high-dependency units (a likely cost-effective intervention) could be used to enhance supportive care for unconscious patients with CNS infection. Creating these units and incorporating them into care could improve outcomes and reduce the burden of intensive care unit treatment for these patients. More investigation is needed on the efficacy and cost-effectiveness of high-dependency units in different contexts.

Ceftriaxone is conventionally used in Laos as a first-line treatment for CNS bacterial infection but lacks efficacy for emerging rickettsial pathogens, for which doxycycline is recommended (*4*). Because delays in antibiotic therapy could result in severe consequences for patients, the decision for administering these drugs is made on the basis of clinical signs and laboratory results at admission. However, in Laos, we found that no variable, even in combination, could permit objective selection of appropriate antibiotics. Therefore, the administration of early first-line empiric treatment with ceftriaxone and doxycycline for all patients with suspected CNS infection might save patient lives in Laos and elsewhere in rural Asia (*4*).

Acknowledgments

We thank the patients, Bounthaphany Bounxouei (Associate Professor and Director), and staff of Mahosot Hospital, especially the microbiology laboratory staff and the ward staff for their technical help and support. We also thank Bounnack Saysanasongkham (Associate Professor and Director of Department of Health Care, Ministry of Health) and Bounkong Syhavong (Associate Professor and Minister of Health), Laos, for their kind help and support. We thank the staff of the Meningococcal Reference Unit of the Health Protection Agency (Manchester, UK) for *N. meningitidis* typing and the staff of the Respiratory and Vaccine Preventable Bacteria Reference Unit of Public Health England (Colindale, UK) for *Haemophilus influenzae* typing. We also thank Mavuto Mukaka for his help with statistical analysis and Nicholas Day for comments on the paper.

This work was supported by the Wellcome Trust of Great Britain, the Institute of Research for Development, Aix-Marseille University, and the European Union's Horizon 2020 research and innovation program European Virus Archive global (grant agreement no. 653316).

About the Author

Dr. Dubot-Pérès is a virologist serving as the Head of Partnerships and Programmes of South Countries for the Unité des Virus Émergents (Aix-Marseille University, IRD 190, INSERM 1207, IHU Méditerranée Infection) in Marseille, France. She is an Honorary Visiting Research Fellow at the Nuffield Department of Medicine, University of Oxford, Oxford, UK, and the Head of Virology at the Lao-Oxford-Mahosot Hospital-Wellcome Trust Research Unit in Vientiane, Laos. Her main research topics of interest are the study of undifferentiated fever, dengue epidemiology, infections of the CNS, and respiratory infections.

References

1. Tarantola A, Goutard F, Newton P, de Lamballerie X, Lortholary O, Cappelle J, et al. Estimating the burden of Japanese encephalitis virus and other encephalitides in countries of the Mekong Region. PLoS Negl Trop Dis. 2014;8:e2533. http://dx.doi.org/10.1371/journal.pntd.0002533
2. Glaser CA, Gilliam S, Schnurr D, Forghani B, Honarmand S, Khetsuriani N, et al. In search of encephalitis etiologies: diagnostic challenges in the California Encephalitis Project, 1998—2000. Clin Infect Dis. 2003;36:731–42. http://dx.doi.org/10.1086/367841
3. Glaser CA, Honarmand S, Anderson LJ, Schnurr DP, Forghani B, Cossen CK, et al. Beyond viruses: clinical profiles and etiologies associated with encephalitis. Clin Infect Dis. 2006;43:1565–77. http://dx.doi.org/10.1086/509330
4. Dittrich S, Rattanavong S, Lee SJ, Panyanivong P, Craig SB, Tulsiani SM, et al. *Orientia, Rickettsia,* and *Leptospira* pathogens as causes of CNS infections in Laos: a prospective study. Lancet Glob Health. 2015;3:e104–12. http://dx.doi.org/10.1016/S2214-109X(14)70289-X
5. World Health Organization. Japanese encephalitis. 2015 Dec 31 [cited 2018 Jun 6]. https://www.who.int/en/news-room/fact-sheets/detail/japanese-encephalitis
6. Solomon T, Dung NM, Vaughn DW, Kneen R, Thao LT, Raengsakulrach B, et al. Neurological manifestations of dengue infection. Lancet. 2000;355:1053–9. http://dx.doi.org/10.1016/S0140-6736(00)02036-5
7. Puccioni-Sohler M, Orsini M, Soares CN. Dengue: a new challenge for neurology. Neurol Int. 2012;4:e15. http://dx.doi.org/10.4081/ni.2012.e15
8. Cam BV, Fonsmark L, Hue NB, Phuong NT, Poulsen A, Heegaard ED. Prospective case-control study of encephalopathy in children with dengue hemorrhagic fever. Am J Trop Med Hyg. 2001;65:848–51. http://dx.doi.org/10.4269/ajtmh.2001.65.848
9. Hendarto SK, Hadinegoro SR. Dengue encephalopathy. Acta Paediatr Jpn. 1992;34:350–7. http://dx.doi.org/10.1111/j.1442-200X.1992.tb00971.x
10. Ho Dang Trung N, Le Thi Phuong T, Wolbers M, Nguyen Van Minh H, Nguyen Thanh V, Van MP, et al.; VIZIONS CNS Infection Network. Aetiologies of central nervous system infection in Viet Nam: a prospective provincial hospital-based descriptive surveillance study. PLoS One. 2012;7:e37825. http://dx.doi.org/10.1371/journal.pone.0037825
11. Flett KB, Rao S, Dominguez SR, Bernard T, Glode MP. Variability in the diagnosis of encephalitis by pediatric subspecialists: the need for a uniform definition. J Pediatric Infect Dis Soc. 2013;2:267–9. http://dx.doi.org/10.1093/jpids/pis094
12. Xie Y, Tan Y, Chongsuvivatwong V, Wu X, Bi F, Hadler SC, et al. A population-based acute meningitis and encephalitis syndromes surveillance in Guangxi, China, May 2007-June 2012. PLoS One. 2015;10:e0144366. http://dx.doi.org/10.1371/journal.pone.0144366
13. Touch S, Hills S, Sokhal B, Samnang C, Sovann L, Khieu V, et al. Epidemiology and burden of disease from Japanese encephalitis in Cambodia: results from two years of sentinel surveillance. Trop Med Int Health. 2009;14:1365–73. http://dx.doi.org/10.1111/j.1365-3156.2009.02380.x
14. Olsen SJ, Campbell AP, Supawat K, Liamsuwan S, Chotpitayasunondh T, Laptikulthum S, et al.; Thailand Encephalitis Surveillance Team. Infectious causes of encephalitis and meningoencephalitis in Thailand, 2003–2005. Emerg Infect Dis. 2015;21:280–9. http://dx.doi.org/10.3201/eid2102.140291
15. Dittrich S, Sunyakumthorn P, Rattanavong S, Phetsouvanh R, Panyanivong P, Sengduangphachanh A, et al. Blood-brain barrier function and biomarkers of central nervous system injury in rickettsial versus other neurological infections in Laos. Am J Trop Med Hyg. 2015;93:232–7. http://dx.doi.org/10.4269/ajtmh.15-0119
16. Moore CE, Sengduangphachanh A, Thaojaikong T, Sirisouk J, Foster D, Phetsouvanh R, et al. Enhanced determination of *Streptococcus pneumoniae* serotypes associated with invasive disease in Laos by using a real-time polymerase chain reaction serotyping assay with cerebrospinal fluid. Am J Trop Med Hyg. 2010;83:451–7. http://dx.doi.org/10.4269/ajtmh.2010.10-0225
17. Moore CE, Blacksell SD, Taojaikong T, Jarman RG, Gibbons RV, Lee SJ, et al. A prospective assessment of the accuracy of commercial IgM ELISAs in diagnosis of Japanese encephalitis virus infections in patients with suspected central nervous system infections in Laos. Am J Trop Med Hyg. 2012;87:171–8. http://dx.doi.org/10.4269/ajtmh.2012.11-0729
18. World Health Organization. Recommended standards for surveillance of selected vaccine-preventable diseases. 2003 [cited 2018 Jun 6]. http://www.measlesrubellainitiative.org/wp-content/uploads/2013/06/WHO-surveillance-standard.pdf
19. Thaipadungpanit J, Chierakul W, Wuthiekanun V, Limmathurotsakul D, Amornchai P, Boonslip S, et al. Diagnostic accuracy of real-time PCR assays targeting 16S rRNA and *lipL32* genes for human leptospirosis in Thailand: a case-control study. PLoS One. 2011;6:e16236. http://dx.doi.org/10.1371/journal.pone.0016236
20. Cole JR Jr, Sulzer CR, Pursell AR. Improved microtechnique for the leptospiral microscopic agglutination test. Appl Microbiol. 1973;25:976–80.
21. Jiang J, Chan T-C, Temenak JJ, Dasch GA, Ching W-M, Richards AL. Development of a quantitative real-time polymerase chain reaction assay specific for *Orientia tsutsugamushi*. Am J Trop Med Hyg. 2004;70:351–6. http://dx.doi.org/10.4269/ajtmh.2004.70.351
22. Jiang J, Stromdahl EY, Richards AL. Detection of *Rickettsia parkeri* and *Candidatus* Rickettsia andeanae in *Amblyomma maculatum* Gulf Coast ticks collected from humans in the United States. Vector Borne Zoonotic Dis. 2012;12:175–82. http://dx.doi.org/10.1089/vbz.2011.0614
23. Henry KM, Jiang J, Rozmajzl PJ, Azad AF, Macaluso KR, Richards AL. Development of quantitative real-time PCR assays to detect *Rickettsia typhi* and *Rickettsia felis,* the causative agents of murine typhus and flea-borne spotted fever. Mol Cell Probes. 2007;21:17–23. http://dx.doi.org/10.1016/j.mcp.2006.06.002
24. Phetsouvanh R, Blacksell SD, Jenjaroen K, Day NPJ, Newton PN. Comparison of indirect immunofluorescence assays for diagnosis of scrub typhus and murine typhus using venous blood and finger prick filter paper blood spots. Am J Trop Med Hyg. 2009;80:837–40. http://dx.doi.org/10.4269/ajtmh.2009.80.837
25. Carvalho MG, Tondella ML, McCaustland K, Weidlich L, McGee L, Mayer LW, et al. Evaluation and improvement of real-time PCR assays targeting *lytA, ply,* and *psaA* genes for detection of pneumococcal DNA. J Clin Microbiol. 2007;45:2460–6. http://dx.doi.org/10.1128/JCM.02498-06

26. Corless CE, Guiver M, Borrow R, Edwards-Jones V, Fox AJ, Kaczmarski EB. Simultaneous detection of *Neisseria meningitidis, Haemophilus influenzae,* and *Streptococcus pneumoniae* in suspected cases of meningitis and septicemia using real-time PCR. J Clin Microbiol. 2001;39:1553–8. http://dx.doi.org/10.1128/JCM.39.4.1553-1558.2001
27. Mai NTH, Hoa NT, Nga TVT, Linh D, Chau TTH, Sinh DX, et al. *Streptococcus suis* meningitis in adults in Vietnam. Clin Infect Dis. 2008;46:659–67. http://dx.doi.org/10.1086/527385
28. Leparc-Goffart I, Baragatti M, Temmam S, Tuiskunen A, Moureau G, Charrel R, et al. Development and validation of real-time one-step reverse transcription-PCR for the detection and typing of dengue viruses. J Clin Virol. 2009;45:61–6. http://dx.doi.org/10.1016/j.jcv.2009.02.010
29. Watkins-Riedel T, Woegerbauer M, Hollemann D, Hufnagl P. Rapid diagnosis of enterovirus infections by real-time PCR on the LightCycler using the TaqMan format. Diagn Microbiol Infect Dis. 2002;42:99–105. http://dx.doi.org/10.1016/S0732-8893(01)00330-3
30. Lanciotti RS, Kerst AJ, Nasci RS, Godsey MS, Mitchell CJ, Savage HM, et al. Rapid detection of West Nile virus from human clinical specimens, field-collected mosquitoes, and avian samples by a TaqMan reverse transcriptase-PCR assay. J Clin Microbiol. 2000;38:4066–71.
31. van Elden LJ, Nijhuis M, Schipper P, Schuurman R, van Loon AM. Simultaneous detection of influenza viruses A and B using real-time quantitative PCR. J Clin Microbiol. 2001;39:196–200. http://dx.doi.org/10.1128/JCM.39.1.196-200.2001
32. Moureau G, Temmam S, Gonzalez JP, Charrel RN, Grard G, de Lamballerie X. A real-time RT-PCR method for the universal detection and identification of flaviviruses. Vector Borne Zoonotic Dis. 2007;7:467–77. http://dx.doi.org/10.1089/vbz.2007.0206
33. Moureau G, Ninove L, Izri A, Cook S, De Lamballerie X, Charrel RN. Flavivirus RNA in phlebotomine sandflies. Vector Borne Zoonotic Dis. 2010;10:195–7. http://dx.doi.org/10.1089/vbz.2008.0216
34. Kessler HH, Mühlbauer G, Rinner B, Stelzl E, Berger A, Dörr HW, et al. Detection of herpes simplex virus DNA by real-time PCR. J Clin Microbiol. 2000;38:2638–42.
35. Bousbia S, Papazian L, Saux P, Forel JM, Auffray J-P, Martin C, et al. Repertoire of intensive care unit pneumonia microbiota. PLoS One. 2012;7:e32486. http://dx.doi.org/10.1371/journal.pone.0032486
36. Griscelli F, Barrois M, Chauvin S, Lastere S, Bellet D, Bourhis JH. Quantification of human cytomegalovirus DNA in bone marrow transplant recipients by real-time PCR. J Clin Microbiol. 2001;39:4362–9. http://dx.doi.org/10.1128/JCM.39.12.4362-4369.2001
37. Hummel KB, Lowe L, Bellini WJ, Rota PA. Development of quantitative gene-specific real-time RT-PCR assays for the detection of measles virus in clinical specimens. J Virol Methods. 2006;132:166–73. http://dx.doi.org/10.1016/j.jviromet.2005.10.006
38. Uchida K, Shinohara M, Shimada S, Segawa Y, Doi R, Gotoh A, et al. Rapid and sensitive detection of mumps virus RNA directly from clinical samples by real-time PCR. J Med Virol. 2005;75:470–4. http://dx.doi.org/10.1002/jmv.20291
39. Phommasone K, Paris DH, Anantatat T, Castonguay-Vanier J, Keomany S, Souvannasing P, et al. Concurrent infection with murine typhus and scrub typhus in southern Laos—the mixed and the unmixed. PLoS Negl Trop Dis. 2013;7:e2163. http://dx.doi.org/ 10.1371/journal.pntd.0002163
40. White IR, Royston P, Wood AM. Multiple imputation using chained equations: issues and guidance for practice. Stat Med. 2011;30:377–99. http://dx.doi.org/10.1002/sim.4067
41. Rubin DB. Multiple imputation for nonresponse in surveys. New York: John Wiley and Sons; 1987.
42. Sejvar JJ, Kohl KS, Gidudu J, Amato A, Bakshi N, Baxter R, et al.; Brighton Collaboration GBS Working Group. Guillain-Barré syndrome and Fisher syndrome: case definitions and guidelines for collection, analysis, and presentation of immunization safety data. Vaccine. 2011;29:599–612. http://dx.doi.org/10.1016/j.vaccine.2010.06.003
43. Bennett JE, Dolin R, Blaser MJ. Principles and practice of infectious diseases. 8th ed. Philadelphia: Elsevier Saunders; 2014.
44. Dubot-Pérès A, Sengvilaipaseuth O, Chanthongthip A, Newton PN, de Lamballerie X. How many patients with anti-JEV IgM in cerebrospinal fluid really have Japanese encephalitis? Lancet Infect Dis. 2015;15:1376–7. http://dx.doi.org/10.1016/S1473-3099(15)00405-3
45. Eamsobhana P. Angiostrongyliasis in Thailand: epidemiology and laboratory investigations. Hawaii J Med Public Health. 2013;72(Suppl 2):28–32.
46. Newman MP, Blum S, Wong RCW, Scott JG, Prain K, Wilson RJ, et al. Autoimmune encephalitis. Intern Med J. 2016;46:148–57. http://dx.doi.org/10.1111/imj.12974
47. Taylor WR, Nguyen K, Nguyen D, Nguyen H, Horby P, Nguyen HL, et al. The spectrum of central nervous system infections in an adult referral hospital in Hanoi, Vietnam. PLoS One. 2012;7:e42099. http://dx.doi.org/10.1371/journal.pone.0042099
48. Schut ES, Westendorp WF, de Gans J, Kruyt ND, Spanjaard L, Reitsma JB, et al. Hyperglycemia in bacterial meningitis: a prospective cohort study. BMC Infect Dis. 2009;9:57. http://dx.doi.org/10.1186/1471-2334-9-57
49. Erdem H, Ozturk-Engin D, Tireli H, Kilicoglu G, Defres S, Gulsun S, et al. Hamsi scoring in the prediction of unfavorable outcomes from tuberculous meningitis: results of Haydarpasa-II study. J Neurol. 2015;262:890–8. http://dx.doi.org/10.1007/s00415-015-7651-5
50. Blaha J, Barteczko-Grajek B, Berezowicz P, Charvat J, Chvojka J, Grau T, et al. Space GlucoseControl system for blood glucose control in intensive care patients-a European multicentre observational study. BMC Anesthesiol. 2016;16:8. http://dx.doi.org/10.1186/s12871-016-0175-4

Address for correspondence: Audrey Dubot-Pérès, UVE, Faculté de Médecine, 27 Blvd Jean Moulin, 13005 Marseille, France; email: audrey@tropmedres.ac

Serologic Prevalence of Ebola Virus in Equatorial Africa

Imke Steffen,[1] Kai Lu, Lauren K. Yamamoto, Nicole A. Hoff, Prime Mulembakani, Emile O. Wemakoy, Jean-Jacques Muyembe-Tamfum, Nicaise Ndembi, Catherine A. Brennan, John Hackett Jr., Susan L. Stramer, William M. Switzer, Sentob Saragosti, Guy O. Mbensa, Syria Laperche, Anne W. Rimoin, Graham Simmons

We conducted a serologic survey of 2,430 serum samples collected during 1997–2012 for various studies to determine the prevalence of the hemorrhagic fever virus Ebola virus (EBOV) in equatorial Africa. We screened serum samples for neutralizing antibodies by using a pseudotype microneutralization assay and a newly developed luciferase immunoprecipitation system assay. Specimens seroreactive for EBOV were confirmed by using an ELISA. Our results suggest a serologic prevalence of 2%–3.5% in the Republic of the Congo and the Democratic Republic of the Congo, which have reported outbreaks of infection with EBOV. In addition we detected a seroprevalence of 1.3% in southern Cameroon, which indicated a low risk for exposure in this region.

The 2014 outbreak of Ebola virus disease in West Africa has changed our understanding of viral hemorrhagic fever epidemiology. What was previously thought to be a sporadic, localized disease is now perceived as a more widespread threat to public health in heavily populated regions. The reemerging epidemic illustrated the need for epidemiologic investigations of the serologic prevalence and geographic range of hemorrhagic fever viruses, as well as development of novel serologic assays for their detection and surveillance.

Three species in the genus *Ebolavirus* and 1 species in the genus *Marburgvirus* within the family *Filoviridae* cause hemorrhagic fever in humans and have triggered several outbreaks with high case-fatality rates (*1*). Ebola viruses (EBOVs) have been found to asymptomatically infect different bat species and are known to cause fatal infections in great apes and other wildlife in the Congo Basin (*2*,*3*). Consequently, it has been proposed that bush-meat hunting, butchering, and consumption, as well as mining and caving, are potential risk factors associated with EBOV infection (*4*,*5*). However, epidemiologic links are not always well established (*6*), and the risk for exposure to hemorrhagic fever viruses for the general population in Central and West Africa remains unclear. Data are limited in that previous serologic surveys for filoviruses date back several decades (*7*–*9*) or have focused on specific populations and locations with high exposure to potential risk factors (*6*,*10*).

We conducted a widespread serologic survey for EBOV-specific antibodies in 5 countries in central Africa, including known filovirus-endemic regions (the Democratic Republic of the Congo [DRC], the Republic of the Congo, and Uganda), as well as areas without previously reported filovirus infections (Ghana and Cameroon). We tested 2,430 serum samples for specific antibodies to EBOV proteins to determine the seroprevalence of this virus in the respective populations. Serologic assays for detection of antibodies against EBOV glycoprotein (EBOV-GP), matrix protein (VP40), and nucleoprotein (NP) included novel microneutralization and luciferase immunoprecipitation system (LIPS) assays, as well as a commercially available ELISA.

Materials and Methods

Samples

The deidentified serum samples tested in this study were obtained from several different studies in 5 countries in

Author affiliations: Vitalant Research Institute, San Francisco, California, USA (I. Steffen, K. Lu, L.K. Yamamoto, G. Simmons); University of California, San Francisco (I. Steffen, K. Lu, G. Simmons); University of California, Los Angeles, California, USA (N.A. Hoff, A.W. Rimoin); University of Kinshasa, Kinshasa, Democratic Republic of the Congo (P. Mulembakani, E.O. Wemakoy); Institut National de Recherche Biomedicale, Kinshasa (J.-J. Muyembe-Tamfum); Institute of Human Virology, Abuja, Nigeria (N. Ndembi); Abbott Diagnostics, Abbott Park, Illinois, USA (C.A. Brennan, J. Hackett Jr.); American Red Cross Scientific Support Office, Gaithersburg, Maryland, USA (S.L. Stramer); Centers for Disease Control and Prevention, Atlanta, Georgia, USA (W.M. Switzer); Institut National de la Santé et de la Recherche Médicale Unité 941, Paris, France (S. Saragosti); Centre National de Transfusion Sanguine, Kinshasa (G.O. Mbensa); Institut National de la Transfusion Sanguine, Paris (S. Laperche)

DOI: https://doi.org/10.3201/eid2505.180115

[1]Current affiliation: University of Veterinary Medicine, Hannover, Germany.

Africa and were collected during different periods as part of unrelated surveillance projects using approved human subjects protocols. We obtained sampling locations, numbers, and collection dates (Table; Figure 1).

Cell Lines

Human embryonic kidney 293T, human rhabdosarcoma RD, and African green monkey COS-1 cells were grown in Dulbecco modified essential medium supplemented with 10% fetal bovine serum, L-glutamine, nonessential amino acids, and antimicrobial drugs (penicillin and streptomycin). Cells were incubated at 37°C in a humidified atmosphere containing 5% CO_2.

Plasmids

Expression plasmids were constructed by restriction-ligation cloning of viral glycoprotein sequences into multiple cloning site of the pCAGGS expression vector. We obtained the HIV pNL4–3 R^-E^- plasmid containing the firefly luciferase gene (pNL-Luc) from the National Institutes of Health AIDS Reagent Program (https://www.aidsreagent.org). The corresponding plasmid encoding *Renilla* luciferase (pNL-Ren) was generated by swapping the firefly luciferase gene for *Renilla* luciferase (*11*). We also used the pRen2 vector for expression of *Renilla* luciferase fusion proteins (*12*).

Pseudotype Preparation

We generated pseudotypes as described (*11*) by using 25 μg EBOV-GP expression plasmid or 30 μg Machupo virus glycoprotein (MACV-GP) expression plasmid and 10 μg pNL-Luc or pNL-Ren. Before use in neutralization assays, we titered pseudotypes for RD cells to normalize input relative light units.

Pseudotype Microneutralization Assay

We diluted heat-inactivated human serum samples in culture medium, mixed with viral inoculum, and incubated at room temperature for 1 h. We used final serum dilutions of 1:50 and 1:500 in the high-throughput screen and dilutions ranging from 1:10 to 1:31,250 in titrations. Subsequently, 30,000 RD cells/well were added and plates incubated at 37°C for 48 h. The MACV-GP, which is from an unrelated arenavirus prevalent only in South America, was included as a negative control. All infections were performed in duplicate, and each plate contained identical controls, including uninfected cells, cells infected in absence of serum, and cells infected with virus incubated with negative control serum (US blood donor) or positive control serum from a survivor of Ebola virus disease.

We lysed cells and measured luciferase activities in cell lysates by using the Dual-Glo Luciferase Assay System (Promega, https://www.promega.com). Infection rates in

Table. Assay results for study of serologic prevalence of Ebola virus in equatorial Africa*

Country	City	Risk group	Collection period	No. samples	No. (%) EBOV neut+	No. (%) EBOV LIPS+	No. (%) EBOV ELISA+/no. tested	No. (%) EBOV confirmed	95% CI, %†
Uganda	Unknown	AIDS	1997	106	0	1 (0.9)	0/1	0	0–1 (0–0.9)
Cameroon	Unknown	AIDS	1997	96	0	4 (4.2)	0/4	0	0–4 (0–4.2)
Ghana	Unknown	AIDS	1997	48	0	0	0/0	0	0
Cameroon	All locations	Illness of unknown etiology	2011–2012	160	2 (1.3)	4 (2.5)	2/6 (33.3)	2 (1.3)	0–6 (0–3.8)
Cameroon	Djoum	Illness of unknown etiology	2011–2012	35	0	1 (2.9)	0/1	0	0–1 (0–2.9)
Cameroon	Ebolowa	Illness of unknown etiology	2011–2012	80	0	1 (1.3)	0/1	0	0–1 (0–1.3)
Cameroon	Sangmelima	Illness of unknown etiology	2011–2012	45	2 (4.4)	2 (4.4)	2/4 (50.0)	2 (4.4)	2–4 (4.4–8.9)
ROC	All locations	HIV surveillance	1999	458	4 (0.9)	9 (2.0)	9/13 (69.2)	9 (2.0)	0–13 (0–2.8)
ROC	Madingou	HIV surveillance	1999	149	1 (0.7)	1 (0.7)	1/2 (50.0)	1 (0.7)	0–2 (0–1.3)
ROC	Nkayi	HIV surveillance	1999	149	0	3 (2.0)	3/3 (100.0)	3 (2.0)	0–3 (0–2.0)
ROC	Owando	HIV surveillance	1999	160	3 (1.9)	5 (3.1)	5/8 (62.5)	5 (3.1)	0–8 (0–5.0)
DRC	Kinshasa	Blood donors	2011–2012	752	12 (1.6)	38 (5.1)	8/38 (21.1)	15 (2.0)	5–38 (0.7–5.1)
DRC	Kasaï Oriental	Monkeypox surveillance	2007	810	15 (1.9)	52 (6.4)	15/54 (27.8)	27 (3.3)	1–54 (0.1–6.7)
Total	NA	NA	1997–2012	2,430	33 (1.4)	108 (4.4)	34/116 (29.3)	53 (2.2)	6–116 (0.3–4.8)

*Confirmed seroprevalence rates are based on reactivity in ≥2 different assay formats. DRC, Democratic Republic of the Congo; EBOV, Ebola virus; LIPS, luciferase immunoprecipitation system; NA, not applicable; neut, neutralization assay; ROC, Republic of the Congo; +, positive.
†Based on number of samples reactive in all 3 assays to number of samples reactive in a single assay (values in parentheses).

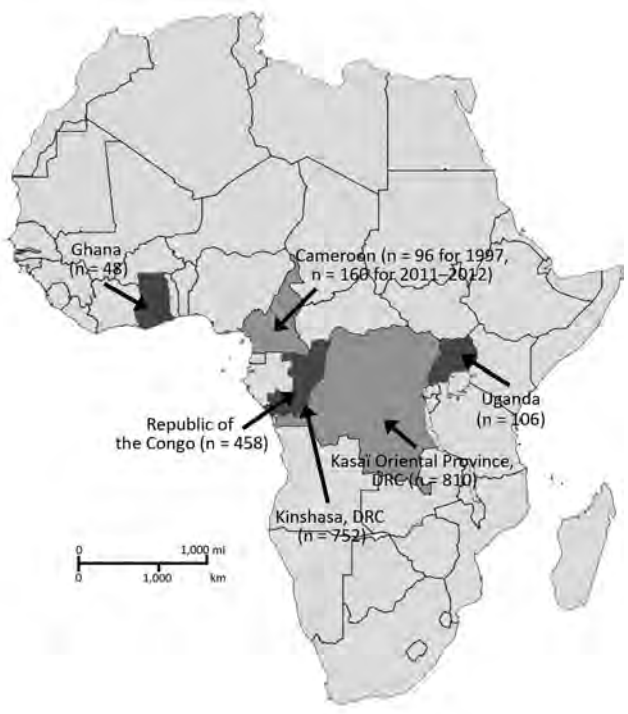

Figure 1. Numbers of serum samples collected from Ghana, Cameroon, Republic of the Congo, DRC, and Uganda in study of serologic prevalence of Ebola virus in equatorial Africa. DRC, Democratic Republic of the Congo.

the presence of serum samples were expressed as percentage of infection in the presence of negative control serum.

Heat-inactivated human serum samples were diluted in culture medium, mixed with viral inoculum, and incubated at room temperature for 1 hour. Final serum dilutions of 1:50 and 1:500 were used in the high-throughput screen, and dilutions ranging from 1:10 to 1:31,250 were used in titrations. Subsequently, 30,000 RD cells/well were added and plates incubated at 37°C for 48 hours. The MACV-GP, which is from an unrelated arenavirus prevalent only in South America, was included as a negative control. All infections were performed in duplicates and each plate contained identical controls, including uninfected cells, cells infected in absence of serum, and cells infected with virus incubated with negative control serum (US blood donor) or positive control serum from a survivor of Ebola virus disease. Cells were lysed, and luciferase activities in cell lysates were measured by using the Dual-Glo Luciferase Assay System (Promega, https://www.promega.com). Infection rates in the presence of serum samples were expressed as percentage of infection in the presence of negative control serum.

Luciferase Immunoprecipitation System

For expression of *Renilla* luciferase antigen fusion proteins, we cloned the C-terminal domain of EBOV VP40 (bp positons 583–981) into the pRen2 plasmid and transfected it into Cos-1 cells by using a 10-cm culture dish, 10 μg plasmid DNA, and the TransIT 2020 Transfection Reagent (Mirusbio, https://www.mirusbio.com). Cell lysates containing the fusion proteins were harvested at 48-h post-transfection. The LIPS assay was performed as described (*12*). We measured luciferase activities by using the *Renilla* Luciferase Assay System Substrate (Promega).

ELISA

We obtained ELISA kits for detection of human IgG against Zaire EBOV NP from Alpha Diagnostics International (https://www.4adi.com). We performed assays according to the manufacturer's instructions at 1:200 sample dilutions and read absorbance at 450 nm.

Data Analysis and Assay Cutoff Determination

We considered serum samples that reduced infection with EBOV pseudoviruses by >50% in the high-throughput screen compared with a negative serum control to be potential neutralizing samples and confirmed this assessment by titration over a 5-fold sample dilution series. MACV-GP pseudotypes served as internal control for nonspecific neutralization activity. Only 1 sample showed nonspecific neutralization of MACV pseudotypes at the 50% cutoff value, demonstrating the general specificity of the micro-neutralization assay (Figure 2).

We determined reactivity in the EBOV VP40 LIPS assay by calculating the cutoff for each experiment on the basis of the average + 3 SDs of 10 presumed negative samples from Kinshasa, DRC, included in each experiment to monitor plate-by-plate variations. We defined the cutoff value for the commercial EBOV-NP ELISA as 4.62 U/mL on the basis of the average + 3 SDs of the background signal in 47 presumed negative samples from Kinshasa. In addition, assay specifications require that the resultant 4 calibrator optical density values are plotted against concentration and that a linear fit be applied to the data. An R^2 value >0.90 must be observed for the plate to pass this test.

All assays included 3 serum samples from recently confirmed EBOV survivors as positive controls. Serum samples reactive in ≥2 separate assays were considered confirmed seropositive. We calculated prevalence rates on the basis of the number of confirmed seropositive specimens. We defined 95% CIs on the basis of the number of samples reactive in ≥1 assay (high) or reactive in all 3 assays (low).

Results

We tested all samples for EBOV-specific antibodies against VP40 by using the LIPS assay (Figure 3) and for neutralizing antibodies by using a pseudotype neutralization assay (Figure 2). We then conformed seroreactivity in either

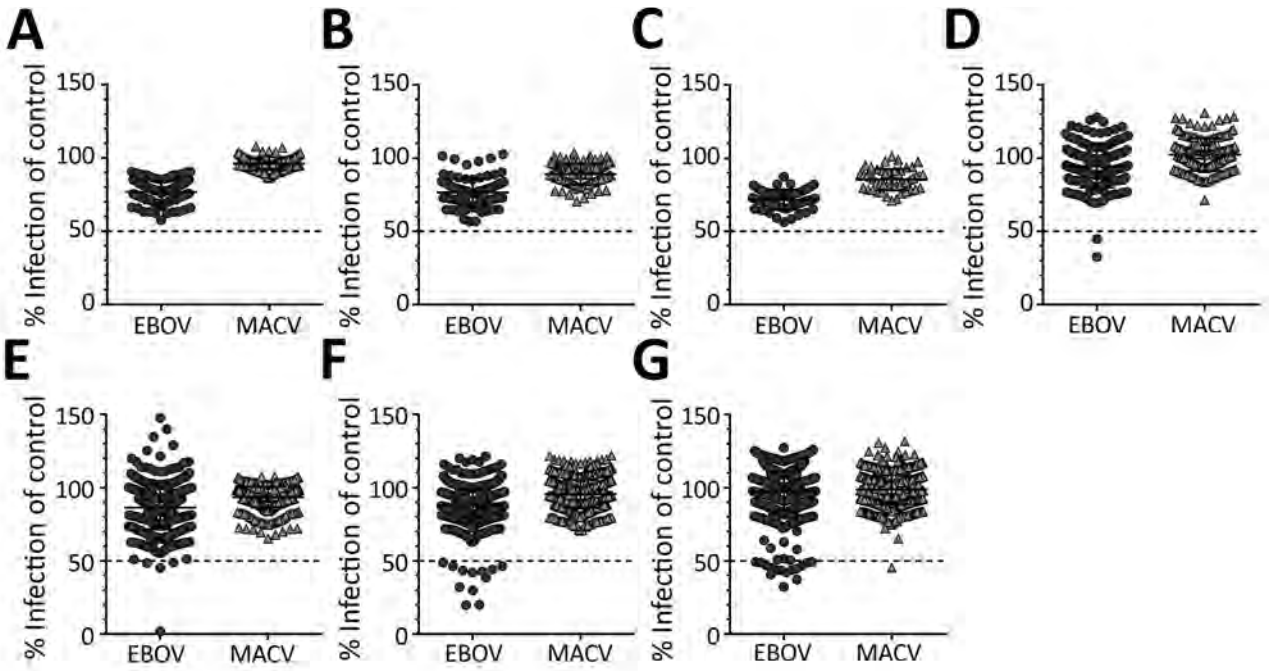

Figure 2. High-throughput screening data for neutralizing antibodies against EBOV and MACV glycoprotein pseudotypes in serum samples in study of serologic prevalence of Ebola virus in equatorial Africa. A) Uganda; B) Cameroon; C) Ghana; D) southern Cameroon; E) Republic of the Congo; F) Kinshasa, Democratic Republic of the Congo; G) Kasaï Oriental Province, Democratic Republic of the Congo. Serum samples were tested at a 1:50 dilution against the different pseudotypes. Samples that reduced pseudotype infectivity by ≥50% compared with a negative serum control were considered positive and confirmed by titration. Error bars indicate 95% CIs. EBOV, Ebola virus; MACV, Machupo virus.

assay by using an EBOV-NP–specific ELISA (Figure 4). No antibody-positive samples for EBOV were detected in the 1997 HIV surveillance samples from Ghana (n = 48) by any of the assays (Figure 2, panel C). The VP40 LIPS assay detected 1 (0.9%) of 160 reactive cases in Uganda and 4 (4.2%) of 96 reactive cases in Cameroon (Figure 3). However, none of these reactive samples were confirmed by neutralization assay or EBOV-NP ELISA (Figure 2, panels A, B; Figure 4). In contrast, samples collected in Cameroon during 2011–2012 contained 2 (1.3%) of 160 EBOV-neutralizing serum samples (Figure 2, panel D) and 4 (2.5%) of 160 VP40 antibody–positive samples (Figure 3). Both neutralizing serum samples were confirmed by EBOV-NP ELISA, but the 4 VP40-positive samples were nonreactive in other assays (Figure 4). Both neutralizing samples and 2 of the VP40-reactive serum samples were collected in Sangmelima, and the 2 other VP40-reactive samples were collected in Djoum and Ebolowa (Table).

Although analysis of the 1997 HIV surveillance samples from Ghana, Uganda, and Cameroon yielded inconclusive results, we determined an overall EBOV seroprevalence in Cameroon of 1.3% (95% CI 1.3%–3.8%) on the basis of the 2011–2012 samples (Table). Because both confirmed seropositive samples originated from Sangmelima, this finding resulted in a local seroprevalence rate of 4.4% (Table).

We tested 458 samples from 3 locations in the Republic of the Congo (Nkayi, n = 149; Madingou, n = 149; and Owando, n = 160) by using the VP40-LIPS and pseudotype neutralization assays. Four (0.9%) samples showed EBOV pseudotype neutralization activity: 1 sample from Madingou and 3 samples from Owando (Figure 2, panel E). Nine (2.0%) samples showed reactivity to VP40 in the LIPS assay: 5 from Owando, 3 from Nkayi, and 1 from Madingou (Figure 3). Although none of the 4 neutralizing samples could be confirmed, all 9 of the VP40-reactive specimens showed positive results in the EBOV-NP ELISA (Figure 4). The overall serologic prevalence for EBOV in the Republic of the Congo was 2.0% (95% CI 2.0%–2.8%) (Table). Local prevalence rates were 3.1% in Owando, 2.0% in Nkayi, and 0.7% in Madingou.

Of 752 blood donor samples from Kinshasa, 12 (1.6%) showed neutralizing activity specific for EBOV-GP and were positive for VP40-specific antibodies by the LIPS assay (Figure 2, panel F; Figure 3). Five (41.7%) of 12 neutralizing specimens were confirmed by EBOV-NP ELISA, and they showed positive results in all 3 assays (Figure 4; Figure 5, panel B). Of the nonneutralizing samples, an additional 26 samples were reactive in the VP40 LIPS (total VP40 reactive = 5.1%), but only 3 samples were confirmed by EBOV-NP ELISA (Figure 3; Figure 5,

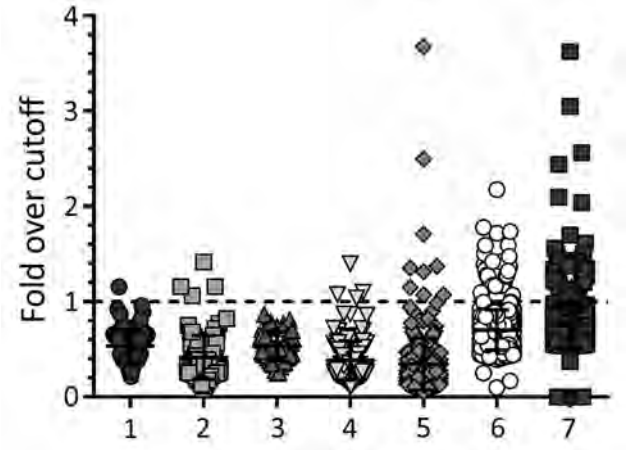

Figure 3. Antibody reactivity against Ebola virus matrix protein as measured by luciferase immunoprecipitation system assay for the different sample sets in study of serologic prevalence of Ebola virus in equatorial Africa. Data were normalized against individual cutoff values determined for each experiment. Samples yielding reactivity >1 were counted as positive specimens. Error bars indicate 95% CIs. 1, Uganda 2007; 2, Cameroon 2007; 3, Ghana 2007; 4, Cameroon 2011–2012; 5, Republic of the Congo; 6, Kinshasha, Democratic Republic of the Congo; 7, Kasaï Oriental Province, Democratic Republic of the Congo.

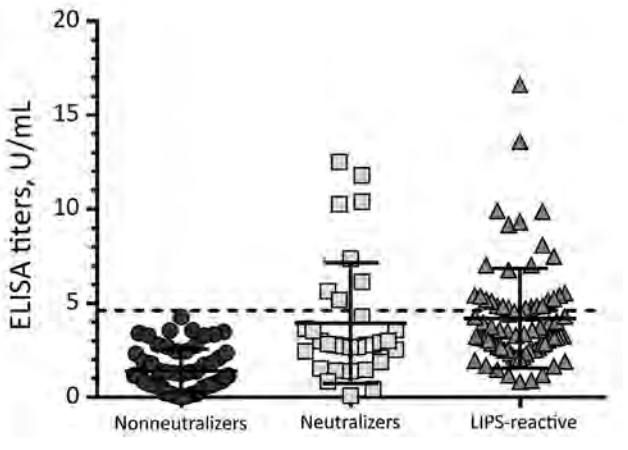

Figure 4. Summarized Ebola virus nucleoprotein ELISA data for confirmation of neutralizing and LIPS-reactive specimens across all sample sets in study of serologic prevalence of Ebola virus in equatorial Africa. For comparison, 57 random nonneutralizers were included. The ELISA cutoff value of 4.62 U/mL (dashed line) was determined on the basis of background reactivity for 47 serum samples from the local general population. Error bars indicate 95% CIs. LIPS, luciferase immunoprecipitation system.

panel B). The serologic prevalence for EBOV in this population was 2.0% (95% CI 1.1%–5.1%) (Table).

Similarly, of 810 samples from Kasaï Oriental Province, 15 (1.9%) samples neutralized EBOV-GP pseudotypes, but only 1 was confirmed by EBOV-NP ELISA (Figure 2, panel G; Figure 4). Thirteen of the 15 neutralizing samples (including the ELISA-positive sample) and 39 nonneutralizing samples were reactive with VP40 (total VP40-reactive = 6.4%) (Figure 3; Figure 5, panel C). Fourteen of the nonneutralizing VP40-reactive samples showed positive results in the EBOV-NP ELISA, which resulted in a triple-positive rate of 0.1% and a double-positive rate of 3.2% (Figure 4; Figure 5, panel C). The serologic EBOV prevalence in this population was 3.3% (95% CI 0.1%–6.4%) (Table).

We found a serologic prevalence for EBOV of 1.3% in Cameroon, a country without previously reported cases of EBOV infections, and prevalence rates ranging from 2.0% in the Republic of the Congo and Kinshasa (DRC) to 3.3% in Kasaï Oriental Province (DRC). We found no serologically reactive specimens in Ghana and Uganda in the samples available for this study (Table).

Discussion

To better investigate the distribution of hemorrhagic fever viruses across Africa, we tested a large number of serum samples from 5 countries in East (Uganda), Central (Republic of the Congo and DRC), West (Ghana), and West Central (Cameroon) Africa, including samples collected during different decades. Our main concern after reviewing previously published serologic studies was an overestimation of seropositivity on the basis of data generated by assays with limited specificity. Therefore, we chose our testing strategy and defined our assay cutoff values in the most conservative way. The detection of neutralizing antibodies against viral glycoproteins is one of the most specific serologic tests for most viruses.

The microneutralization test enables simultaneous testing of serum samples against 2 distinct viral glycoproteins, thereby providing internal specificity controls. In our study, detection of EBOV antibodies by microneutralization might have led to an underestimation of seroprevalence because of a minor role of neutralizing antibodies in filovirus disease (*13*). However, one of our recent studies in EBOV disease survivors found neutralizing antibodies 40 years after exposure (*14*), suggesting a long-lived and robust response. Filovirus NPs resemble each other in amino acid sequence, organization, and structure among the different filoviral species and even show partial similarities to NPs of paramyxoviruses (*15*). Accordingly, studies have reported cross-reactive antibodies against NP with the highest frequency (*16*). In our study, we observed a high background signal in the EBOV NP ELISA when serum samples from areas with low risk for EBOV exposure were tested. This result led us to adjust the cutoff value for the NP ELISA to increase the specificity, which in turn reduced the sensitivity of this assay. Some studies suggest that antibodies against VP40 are more prevalent than antibodies against GP and NP in asymptomatic

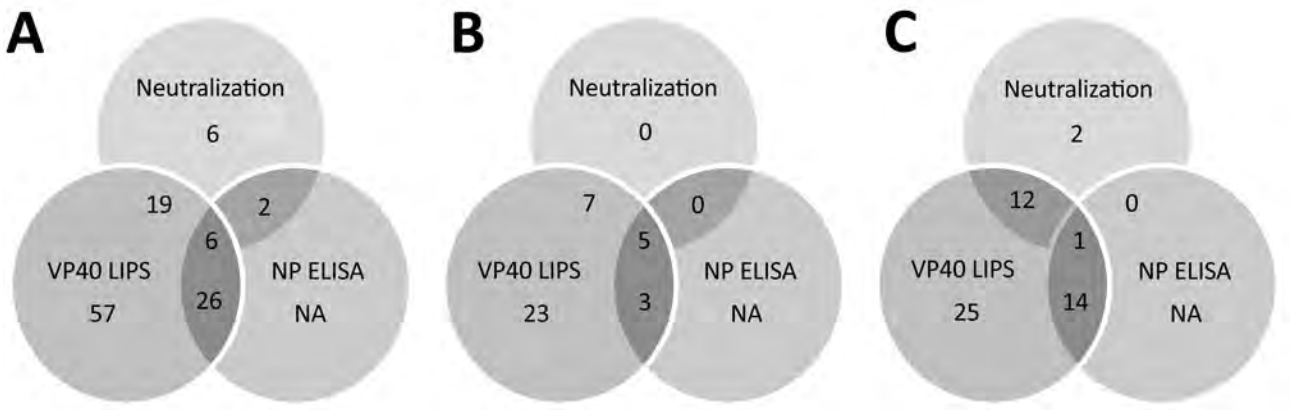

Figure 5. Overlap of different assay results for Ebola virus serology across all samples in study of serologic prevalence of Ebola virus in equatorial Africa. A) Total sample set; B) sample sets from Kinshasha, Democratic Republic of the Congo; C) sample set from Kasaï Oriental Province, Democratic Republic of the Congo. LIPS, luciferase immunoprecipitation system; NA, not applicable (ELISA was performed only for samples with positive results in other assays); NP, nucleoprotein; VP40, matrix protein.

infections (*17*). However, there have also been reports of VP40 antibody responses in nonimmunized, presumably nonexposed humans, indicating some background immunity against EBOV in human populations (*18*). Our results suggest the presence of VP40 antibodies in persons who could not be confirmed to be specific for EBOV with any of the other antigens.

All samples were also screened for antibodies against Marburg virus (MARV) glycoprotein (MARV-GP); only 1 sample showed cross-reactivity against both filovirus glycoproteins. A small number of samples from all 5 countries included in this study were reactive against MARV-GP in a pseudotype neutralization assay and MARV-GP ELISA. However, these data could not be confirmed because of the lack of positive controls and available assays. Even so, this finding might suggest a wide geographic range of MARV or related viruses and their natural reservoir hosts. Serologic evidence for MARV infection of several bat species has been found in northern Republic of the Congo and Gabon, which have borders with Cameroon (*19*), and MARV RNA has recently been detected in bats in Sierra Leone (A. Liah et al., pers. comm.; [*20*]). Furthermore, a study that modeled the risk for zoonotic MARV transmission across sub-Saharan Africa found a substantial threat for MARV transmission in Cameroon and identified southern Cameroon as a beneficial target site for future surveillance efforts (*21*).

Serologic evidence for EBOV exposure was detected in the Republic of the Congo, the DRC, and the 2011–2012 samples from southern Cameroon. Although 10 outbreaks of Ebola virus disease have been reported in the DRC since its discovery in 1976 to its latest reappearance in 2018 (*22*), and a series of 4 separate outbreaks are known to have occurred in the Republic of the Congo during 2001–2005 (*23*,*24*), Ebola virus disease has not been diagnosed in Cameroon to date. However, a serologic survey conducted in 1983 in different areas of Cameroon suggested Ebola virus disease prevalence rates on the basis of indirect immunofluorescence (now known to be rather unspecific) ranging from 3.0% to 14.5%, depending on ethnicity and location (*7*). In comparison, we found a lower EBOV prevalence of 1.3% (95% CI 1.3%–3.8%) on the basis of reactivity with ≥2 virus antigens and different assay formats in a small set of samples from southern Cameroon. This finding illustrates the dependence of serologic data on sampling method, time, location, and assay specificities.

We also found EBOV prevalence rates of ≈2.0% for the Republic of the Congo and a blood donor cohort in Kinshasa, DRC. These results are consistent with those of a serologic survey of blood donors in the Republic of the Congo during 2011, which reported an EBOV prevalence rate of 2.5% (*5*). A serologic survey conducted during the 1995 EBOV outbreak in Kikwit, DRC, reported prevalence rates of 2.2% for workers in Kikwit and an average of 9.3% in surrounding villages, suggesting a higher risk for EBOV exposure in rural settings (*25*). Similarly, we identified a higher prevalence rate of 3.5% in villages in Kasaï Oriental Province in the central region of the country compared with a prevalence rate of 2.0% in the urban capital of Kinshasa. However, samples from the 2 cohorts in the DRC were collected as part of unrelated studies, under separate protocols, and at different time points, which limited the validity of direct comparison. Moreover, many persons living in Kinshasa have migrated to the capital from other parts of the country that have lower or higher risks for exposure to EBOV.

A study in the northeastern Watsa region of the DRC during 2002 reported one of the highest reported EBOV prevalence rates (18.7%) in the local Efé pygmy

population, which included traditional primate hunters (*6*). These results, combined with our data, suggest that EBOV exposure risks might vary greatly in different locations and populations across Central Africa. Furthermore, the choice of serologic assay(s) and methods for setting assay cutoff values vary widely between different studies, which might contribute to the broad range of reported EBOV prevalence rates.

In conclusion, we used a conservative approach of multiple serologic assays with stringent assay cutoff values normalized by background assay reactivity for the general local population to determine that EBOV exposure outside recognized outbreaks is likely a rare event. Nevertheless, serologic evidence of past EBOV exposure was detected throughout different regions of central Africa. This finding could be explained by migration of persons from areas with known risk for exposure or thus far undetected presence of the virus in these regions. In addition, specific regions might experience increased levels of human exposure to EBOV or undiscovered related viruses because of ongoing environmental, societal, and behavioral changes.

Acknowledgments

We thank Edward Murphy for help and advice in specimen acquisition and Peter Burbelo for providing the pRen2 vector for expression of *Renilla* luciferase fusion proteins.

This study was supported by National Institutes of Health/National Institute of Allergy and Infectious Diseases grant R21 AI107420-01A1 to G.S. and K.L. and German Research Foundation (Deutsche Forschungsgemeinschaft) fellowship STE 2237-1-1 to I.S.

About the Author

At the time of this study, Dr. Steffen was a postdoctoral fellow at the Vitalant Research Institute (formerly called the Blood Systems Research Institute) and the Department of Laboratory Medicine, University of California, San Francisco, CA. She is currently the head of a Junior Research Group at the University of Veterinary Medicine, Hannover, Germany. Her research interests are newly identified and emerging RNA viruses with a focus on viral entry, neutralization, glycoprotein characterization, and development of serologic assays.

References

1. Murray MJ. Ebola virus disease: a review of its past and present. Anesth Analg. 2015;121:798–809. http://dx.doi.org/10.1213/ANE.0000000000000866
2. Leroy EM, Kumulungui B, Pourrut X, Rouquet P, Hassanin A, Yaba P, et al. Fruit bats as reservoirs of Ebola virus. Nature. 2005;438:575–6. http://dx.doi.org/10.1038/438575a
3. Leroy EM, Rouquet P, Formenty P, Souquière S, Kilbourne A, Froment JM, et al. Multiple Ebola virus transmission events and rapid decline of central African wildlife. Science. 2004;303:387–90. http://dx.doi.org/10.1126/science.1092528
4. Bausch DG, Borchert M, Grein T, Roth C, Swanepoel R, Libande ML, et al. Risk factors for Marburg hemorrhagic fever, Democratic Republic of the Congo. Emerg Infect Dis. 2003;9:1531–7. http://dx.doi.org/10.3201/eid0912.030355
5. Moyen N, Thirion L, Emmerich P, Dzia-Lepfoundzou A, Richet H, Boehmann Y, et al. Risk factors associated with Ebola and Marburg viruses seroprevalence in blood donors in the Republic of Congo. PLoS Negl Trop Dis. 2015;9:e0003833. http://dx.doi.org/10.1371/journal.pntd.0003833
6. Mulangu S, Borchert M, Paweska J, Tshomba A, Afounde A, Kulidri A, et al. High prevalence of IgG antibodies to Ebola virus in the Efé pygmy population in the Watsa region, Democratic Republic of the Congo. BMC Infect Dis. 2016;16:263. http://dx.doi.org/10.1186/s12879-016-1607-y
7. Bouree P, Bergmann JF. Ebola virus infection in man: a serological and epidemiological survey in the Cameroons. Am J Trop Med Hyg. 1983;32:1465–6. http://dx.doi.org/10.4269/ajtmh.1983.32.1465
8. Johnson ED, Gonzalez JP, Georges A. Haemorrhagic fever virus activity in equatorial Africa: distribution and prevalence of filovirus reactive antibody in the Central African Republic. Trans R Soc Trop Med Hyg. 1993;87:530–5. http://dx.doi.org/10.1016/0035-9203(93)90075-2
9. Tomori O, Fabiyi A, Sorungbe A, Smith A, McCormick JB. Viral hemorrhagic fever antibodies in Nigerian populations. Am J Trop Med Hyg. 1988;38:407–10. http://dx.doi.org/10.4269/ajtmh.1988.38.407
10. Becquart P, Wauquier N, Mahlakõiv T, Nkoghe D, Padilla C, Souris M, et al. High prevalence of both humoral and cellular immunity to Zaire ebolavirus among rural populations in Gabon. PLoS One. 2010;5:e9126. http://dx.doi.org/10.1371/journal.pone.0009126
11. Zhou Y, Steffen I, Montalvo L, Lee TH, Zemel R, Switzer WM, et al. Development and application of a high-throughput microneutralization assay: lack of xenotropic murine leukemia virus-related virus and/or murine leukemia virus detection in blood donors. Transfusion. 2012;52:332–42. http://dx.doi.org/10.1111/j.1537-2995.2011.03519.x
12. Burbelo PD, Goldman R, Mattson TL. A simplified immunoprecipitation method for quantitatively measuring antibody responses in clinical sera samples by using mammalian-produced *Renilla* luciferase-antigen fusion proteins. BMC Biotechnol. 2005;5:22. http://dx.doi.org/10.1186/1472-6750-5-22
13. Lennemann NJ, Herbert AS, Brouillette R, Rhein B, Bakken RA, Perschbacher KJ, et al. Vesicular stomatitis virus pseudotyped with Ebola virus glycoprotein serves as a protective, non-infectious vaccine against Ebola virus challenge in mice. J Virol. 2017;91:JVI.00479-17. http://dx.doi.org/10.1128/JVI.00479-17
14. Rimoin AW, Lu K, Bramble MS, Steffen I, Doshi RH, Hoff NA, et al. Ebola virus neutralizing antibodies detectable in survivors of the Yambuku, Zaire outbreak 40 years after infection. J Infect Dis. 2018;217:223–31. http://dx.doi.org/10.1093/infdis/jix584
15. Sanchez A, Kiley MP, Klenk HD, Feldmann H. Sequence analysis of the Marburg virus nucleoprotein gene: comparison to Ebola virus and other non-segmented negative-strand RNA viruses. J Gen Virol. 1992;73:347–57. http://dx.doi.org/10.1099/0022-1317-73-2-347
16. Natesan M, Jensen SM, Keasey SL, Kamata T, Kuehne AI, Stonier SW, et al. Human survivors of disease outbreaks caused by Ebola or Marburg virus exhibit cross-reactive and long-lived antibody responses. Clin Vaccine Immunol. 2016;23:717–24. http://dx.doi.org/10.1128/CVI.00107-16
17. Becquart P, Mahlakõiv T, Nkoghe D, Leroy EM. Identification of continuous human B-cell epitopes in the VP35, VP40, nucleoprotein and glycoprotein of Ebola virus. PLoS One. 2014;9:e96360. http://dx.doi.org/10.1371/journal.pone.0096360

18. Alpha Diagnostics International. Ebola detection using rapid tests and ELISA kits for humans and animals [cited 2018 Oct 8]. https://www.4adi.com/objects/catalog/product/extras/Ebola_Marburg_Vaccines_ELISA_Flr.pdf
19. Pourrut X, Souris M, Towner JS, Rollin PE, Nichol ST, Gonzalez JP, et al. Large serological survey showing cocirculation of Ebola and Marburg viruses in Gabonese bat populations, and a high seroprevalence of both viruses in *Rousettus aegyptiac*us. BMC Infect Dis. 2009;9:159. http://dx.doi.org/10.1186/1471-2334-9-159
20. Fox M. Deadly Ebola cousin Marburg found in West African bats; 2018 [cited 2019 Jan 4]. https://www.nbcnews.com/health/health-news/ deadly-ebola-cousin-marburg-found-west-african-bats-n950331
21. Pigott DM, Golding N, Mylne A, Huang Z, Weiss DJ, Brady OJ, et al. Mapping the zoonotic niche of Marburg virus disease in Africa. Trans R Soc Trop Med Hyg. 2015;109:366–78. http://dx.doi.org/10.1093/trstmh/trv024
22. Rosello A, Mossoko M, Flasche S, Van Hoek AJ, Mbala P, Camacho A, et al. Ebola virus disease in the Democratic Republic of the Congo, 1976–2014. eLife. 2015;4:4. http://dx.doi.org/10.7554/eLife.09015
23. Nkoghe D, Kone ML, Yada A, Leroy E. A limited outbreak of Ebola haemorrhagic fever in Etoumbi, Republic of Congo, 2005. Trans R Soc Trop Med Hyg. 2011;105:466–72. http://dx.doi.org/10.1016/j.trstmh.2011.04.011
24. Pourrut X, Kumulungui B, Wittmann T, Moussavou G, Délicat A, Yaba P, et al. The natural history of Ebola virus in Africa. Microbes Infect. 2005;7:1005–14. http://dx.doi.org/10.1016/j.micinf.2005.04.006
25. Busico KM, Marshall KL, Ksiazek TG, Roels TH, Fleerackers Y, Feldmann H, et al. Prevalence of IgG antibodies to Ebola virus in individuals during an Ebola outbreak, Democratic Republic of the Congo, 1995. J Infect Dis. 1999;179(Suppl 1):S102–7. http://dx.doi.org/10.1086/514309

Address for correspondence: Graham Simmons, Vitalant Research Institute, 270 Masonic Ave, San Francisco, CA, 94118-4417, USA: email: gsimmons@vitalant.org

Formaldehyde and Glutaraldehyde Inactivation of Bacterial Tier 1 Select Agents in Tissues

Jennifer Chua,[1] Joel A. Bozue,[1] Christopher P. Klimko, Jennifer L. Shoe, Sara I. Ruiz, Christopher L. Jensen, Steven A. Tobery, Jared M. Crumpler, Donald J. Chabot, Avery V. Quirk, Melissa Hunter, David E. Harbourt, Arthur M. Friedlander, Christopher K. Cote

For safety, designated Select Agents in tissues must be inactivated and viability tested before the tissue undergoes further processing and analysis. In response to the shipping of samples of "inactivated" *Bacillus anthracis* that inadvertently contained live spores to nonregulated entities and partners worldwide, the Federal Register now mandates in-house validation of inactivation procedures and standardization of viability testing to detect live organisms in samples containing Select Agents that have undergone an inactivation process. We tested and validated formaldehyde and glutaraldehyde inactivation procedures for animal tissues infected with virulent *B. anthracis*, *Burkholderia pseudomallei*, *Francisella tularensis*, and *Yersinia pestis*. We confirmed that our fixation procedures for tissues containing these Tier 1 Select Agents resulted in complete inactivation and that our validated viability testing methods do not interfere with detection of live organisms. Institutions may use this work as a guide to develop and conduct their own testing to comply with the policy.

Despite being a disease of antiquity, anthrax remains a public health concern and is considered a reemerging threat in developed countries, in part because of bioterrorism (*1*). Threats of bioterrorism and the ease of global travel have led nations to also be concerned about diseases such as tularemia, plague, and melioidosis (*1*). In addition, natural outbreaks and the global distribution and endemic nature of these bacteria continue to be subjects of public health and biodefense research.

In the United States, biological agents and toxins with the potential to pose a severe threat to public health and safety are overseen by the Federal Select Agents Program (https://www.selectagents.gov), a joint program of the Centers for Disease Control and Prevention/Division of Select Agents and Toxins and the US Department of Agriculture Animal and Plant Health Inspection Service/Agriculture Select Agent Services. Agents that pose a particularly high risk to humans are classified as Tier 1 Select Agents; *Bacillus anthracis* is a Tier 1 Select Agent.

Work with Select Agents necessitates complete inactivation because these organisms can cause serious illness or death and could potentially endanger public health through accidental infection of laboratory workers. In 2015, virulent *B. anthracis* samples thought to be completely inactivated by irradiation were unwittingly sent to unregistered laboratories (*2*). These samples, containing spores produced to support research and development for detection and medical countermeasures, were sent to domestic and international entities not under the purview of the Federal Select Agent Program. Although the samples contained low numbers of live organisms and did not pose a serious risk, this event was a breach in a regulation intended to restrict access to the pathogen and safeguard public health. Investigations at the transgressing facility revealed that *B. anthracis* could be cultured from multiple γ-irradiated batches of spores (*2*). Another troubling aspect was the failure of viability tests, performed after irradiation, to detect viable organisms. Thus, the US Department of Defense developed a well-characterized and reproducible method for inactivating *B. anthracis* spores with irradiation (*3*). In addition, all validation of inactivation procedures and viability testing involving Tier 1 Select Agents at each institution is now mandated by federal regulation (*4*).

A common way to inactivate infectious agents in tissues before histologic analysis is formaldehyde fixation, coincidentally first characterized in 1893 with the fixation of *B. anthracis*–infected tissue (*5*). Glutaraldehyde, the use of which was described decades later in 1963 (*6*), is commonly used to inactivate samples for electron microscopy (EM) analysis. These related aldehydes cross-link primary amines and other reactive groups in proteins, fatty acids, and nucleic acids, thereby halting biochemical reactions and placing cellular structures in permanent stasis

Author affiliation: United States Army Medical Research Institute of Infectious Diseases, Frederick, Maryland, USA

DOI: https://doi.org/10.3201/eid2505.180928

[1]These authors contributed equally to this article.

resembling structures found in living tissue (*5*,*7*–*9*). Formaldehyde molecules are small and diffuse quickly but fix tissue slowly (*7*,*10*). An attractive property of formaldehyde fixation is that it is partially reversible and some denatured antigens can be retrieved to be again recognized by antibodies (*11*). In contrast, the larger glutaraldehyde molecules fix tissues quickly and irreversibly but do not penetrate thick tissues well.

Despite a century of use, formaldehyde inactivation of tissues containing Select Agents has been described in few reports (*12*,*13*). Frequently, studies test only a small fraction of tissue for complete inactivation (*14*), which carries a risk of concealing low numbers of viable organisms in the remaining sample. The process of fixation, and concurrently that of inactivation, is dependent on variables such as time, pH, temperature, fixative concentration, and tissue size/composition (*10*,*15*–*17*). The desire to accelerate the fixation process for faster workflow (*15*,*17*) increases the risk for incomplete inactivation. Because *B. anthracis* spores in particular are hardy (i.e., resistant to heat, radiation, and chemicals) (*1*,*18*), their inactivation is more difficult.

The detection of viable organisms in partially inactivated tissues relies on the organisms' ability to proliferate when placed in rich growth media. However, fixative is probably retained internally in tissues, potentially interfering with growth during viability testing. The key function of a viability test is to detect viable organisms by encouraging the proliferation of any organisms, live or injured, that may have survived the inactivation procedure. Testing for viability requires the removal or neutralization of the inactivating agent that may interfere with growth. Removing or neutralizing chemical fixatives is particularly important because their presence might restrict organism proliferation at low, nonlethal concentrations. Similar to the time required for penetration into thick tissues (*10*), adequate time for washing must be provided to allow for outward diffusion. As an alternative, fixative in tissue, including any inhibitory components from the tissue itself, can be diluted in a large volume of medium used for the viability test. Tissue disaggregation or homogenization also exposes potentially live organisms deep within tissues to nutrient-rich medium, allowing growth.

We tested and validated inactivation procedures that used formaldehyde with or without glutaraldehyde on lung, liver, spleen, and skin from infected animals destined for microscopic analyses. Our validation procedure is aligned with requirements set forth by the Centers for Disease Control and Prevention (CDC), under the US Health and Human Services, as mandated in the Federal Register (42 CFR §73) (*4*). We confirmed that our inactivation procedures for tissue fixation resulted in complete inactivation and validated neutralization procedures for viability testing. This work specifically focused on the agents that cause anthrax, melioidosis, tularemia, and plague but could be applicable to others. Because we demonstrated fixation of highly resistant spores, this work could also be applied to unknown or undetermined etiologic agents with uncharacterized properties that cause other emerging infectious diseases.

Materials and Methods

Bacterial Strains and Culture

We placed spores of *B. anthracis* Ames (pXO1+/pXO2+), Sterne, and ANR (pXO1+/pXO2–) in Leighton and Doi broth (*19*) or on NBY agar plates (*20*) and purified them with Omnipaque (GE Healthcare, https://www.gehealthcare.com) as previously described (*21*). All spores were heated for 30 min at 65°C before animal infection. Bacilli were grown in brain heart infusion broth (Difco; Becton, Dickinson and Company, http://www.bd.com), on tryptic soy agar, or on sheep blood agar (SBA) plates (Remel ThermoFisher Scientific, https://www.thermofisher.com) at 37°C. *Burkholderia pseudomallei* 1026b and *B. pseudomallei* 82 (purine auxotroph) were grown in Luria Bertani (Lennox) broth (Difco) with 4% glycerol (Sigma Aldrich, https://www.sigmaaldrich.com) (*22*) or on SBA plates. *Francisella tularensis* Schu S4 and live vaccine strain were grown in either brain heart infusion broth with 1% IsoVitaleX (Becton, Dickinson and Company) or on chocolate agar plates (Remel) at 37°C. *Yersina pestis* CO92 and *Y. pestis* Pgm–/pPst– were grown in heart infusion broth with 0.2% xylose (Sigma Aldrich) or on SBA plates at 28°C. All bacterial strains were from the collection at the US Army Medical Research Institute of Infectious Diseases (Frederick, MD, USA).

Chemical Fixatives

The standard fixative for tissue destined for light microscopy analyses is 4% formaldehyde, which is used interchangeably with 10% neutral buffered formalin, 10% buffered formalin phosphate (Fisher Chemical, https://www.fishersci.com), or 4% paraformaldehyde. Immediately before its use, we used phosphate-buffered saline (PBS), pH 7.4, to dilute 16% paraformaldehyde (Electron Microscopy Sciences, https://www.emsdiasum.com) to 4% paraformaldehyde. We fixed tissues destined for EM with 4% paraformaldehyde and 1% glutaraldehyde (Electron Microscopy Sciences) in 0.1 M sodium cacodylate (Sigma Aldrich) buffer (*14*). This combination is referred to as EM fixative.

Fixative Removal from Tissue and Formaldehyde Sensitivity Assays

Because of their size and the amount of tissue that can be obtained, we used guinea pigs for these assays. We harvested spleen, liver, outer ear pinna, and skin from euthanized guinea pigs. To enable effective penetration of fixative,

Table 1. Formaldehyde fixation of *Bacillus anthracis* Ames–infected skin tissue from guinea pigs in study of inactivation of bacterial Tier 1 Select Agents*

Fixation time, d, no. samples	Maximum tissue weight, g	Maximum tissue size, mm	Total CFU recovered/g	Sample inactivation†	Positive control inactivation†
7, 3	2.04	20 × 30 × 3	6.15×10^7	+/+‡	+/+
14, 3	1.94	23 × 28 × 3	5.41×10^7	–/–	+/+
21, 3	2.55	28 × 28 × 3	4.86×10^7	–/–	+/+

*Infected skin tissues from 3 guinea pigs were fixed for 7, 14, or 21 d in 4% paraformaldehyde, rinsed for 30 min in phosphate-buffered saline, and then homogenized. The maximum tissue weight, size, and CFU recovered per group are listed. +/– indicates presence or absence of growth in broth/on plates.
†100% of sample tested.
‡Of 3 samples, 1 was positive for growth.

we excised tissues ≤10 mm in 1 dimension. Samples were incubated in fixative (≥1:10 wt/vol) at ambient temperature for various times. To allow for outward diffusion of fixative, we soaked samples in PBS/water; ear and spleen required longer submersion to support bacterial growth. Tissues were cut into smaller pieces, ground with a homogenizer (Pro200; Pro Scientific, https://proscientific.com), and then transferred to broth (≥1:50 wt/vol). In accordance with CDC policy on the neutralization method, we split the broth into 2 aliquots: 1 was inoculated with 5×10^3 Sterne spores and the other was left as is. The 7-day broth-to-plate viability test for *B. anthracis* was performed by culturing in broth (≥1:10 wt/vol) followed by solid medium (≥100 μL), each incubated for 7 days at 37°C (*23*). To detect growth in broth, we read optical densities at 620 nm by using a spectrophotometer (Genesys 20, ThermoFisher Scientific).

To test genus-specific sensitivity to formaldehyde, we used *B. pseudomallei* 1026b, *B. anthracis* Sterne, *B. pseudomallei* 82, *F. tularensis* live vaccine strain, and *Y. pestis* Pgm–/pPst–. Strains were incubated in broth with formaldehyde (10% neutral buffered formalin diluted 10-fold from 1:10 to 1:10,000) and shaken for up to 5 days. The starting inoculum was plated for CFU.

Animal Challenges

To limit the number of animals used, we repurposed Hartley guinea pig survivors (Table 1); repurposing was deemed appropriate because of the short duration of the study and because dissemination of bacteria into organs was not required. After administering an intramuscular injection of ketamine, acepromazine (both from Vedco, https://www.vedco.com), and xylazine (Akorn, Inc., http://www.akorn.com), we injected the guinea pigs intradermally at several demarcated locations with 2×10^8 *B. anthracis* Ames spores. To maximize the number of ungerminated spores, we collected whole-skin samples at 2 hours after challenge.

For spleen, liver, and lung tissue collection, we used ≤4 naive Strain 13 guinea pigs per Select Agent (Tables 2,3). To maximize spores in the lungs, we administered *B. anthracis* Ames spores to the guinea pigs by the inhalation route (*24*); to enable rapid dissemination to the spleen and liver, we also administered them by the intramuscular route

Table 2. Formaldehyde fixation of infected spleen, liver, and lung tissue from guinea pigs in study of inactivation of bacterial Tier I Select Agents*

Infectious agent, tissue type	Maximum tissue weight, g	Maximum tissue size, mm	Maximum CFU/g	Fixation time, d	Sample inactivation	Positive control inactivation
Bacillus anthracis Ames (inhalational and intramuscular), n = 3						
Spleen	1.04	20 × 20 × 6	1.1×10^9	13	–/–†	+
Liver	1.78	20 × 10 × 10	9.8×10^7	13	–/–†	+
Lung	1.14	20 × 20 × 10	2.1×10^8; 5.5×10^4 (heat resistant)	13	–/–†	+
Burkholderia pseudomallei 1026b, n = 4						
Spleen	0.81	20 × 15 × 10	7.5×10^8	13	–/–‡	+
Liver	2.15	20 × 15 × 10	1.4×10^7	13	–/–‡	+
Lung	1.56	20 × 15 × 10	4.0×10^7	17–18	–/–‡	+
Francisella tularensis Schu S4, n = 3						
Spleen	1.50	15 × 15 × 10	9.3×10^9	13	–/–§	+
Liver	2.29	25 × 13 × 11	9.5×10^7	13	–/–¶	+
Lung	1.30	15 × 13 × 11	4.3×10^8	13	–/–¶	+
Yersina pestis CO92, n = 3						
Spleen	0.96	15 × 10 × 8	1.4×10^{10}	13	–/–§	+
Liver	2.09	30 × 15 × 10	1.1×10^9	13	–/–¶	+
Lung	1.81	25 × 20 × 15	7.0×10^8	13	–/–¶	+

*≥4 guinea pigs were infected with 1 Select Agent. Tissues were excised and then measured, weighed, and plated for CFU. Tissues were fixed in 10% neutral buffered formalin for the indicated time, rinsed for 30 min in phosphate-buffered saline, and then homogenized. +/– indicates presence or absence of growth in broth/on plates.
†100% of sample tested.
‡50% of sample tested.
§90% of 1 sample tested, 10% of others tested.
¶10% of sample tested.

Table 3. Electron microscopy fixation of infected spleen, liver, and lung tissue from guinea pigs in study of inactivation of bacterial Tier 1 Select Agents*

Infectious agent, tissue type	Maximum tissue weight, g	Maximum tissue size, mm	Maximum CFU/g	Fixation time, d	Sample inactivation	Positive control inactivation
Bacillus anthracis Ames (inhalational and intramuscular), n = 3						
Spleen	0.15	10 × 3 × 2	1.1×10^9	6	–/–†	+
Liver	0.18	9 × 5 × 2	9.8×10^7	6	–/–†	+
Lung	0.08	10 × 4×x 2	2.1×10^8; 5.5×10^4 (heated)	6	–/–†	+
Burkholderia pseudomallei 1026b, n = 4						
Spleen	0.09	8 × 4 × 2	7.5×10^8	7	–/–‡	+
Liver	0.16	10 × 6 × 2	1.4×10^7	7	–/–‡	+
Lung	0.09	10 × 4 × 2	4.0×10^7	7	–/–‡	+
Francisella tularensis Schu S4, n = 3						
Spleen	0.15	6 × 6 × 1	9.3×10^9	6	–/–§	+
Liver	0.15	11 × 5 × 1	9.5×10^7	6	–/–¶	+
Lung	0.08	7 × 6 × 1	4.3×10^8	6	–/–¶	+
Yersina pestis CO92, n = 3						
Spleen	0.11	7 × 5 × 1	1.4×10^{10}	6 or 8	–/–§	+
Liver	0.07	7 × 4 × 1	1.1×10^9	6 or 8	–/–¶	+
Lung	0.07	7 × 6 × 1	7.0×10^8	6 or 8	–/–¶	+

*≥4 guinea pigs were infected with 1 Select Agent. Tissues were excised and then measured, weighed, and plated for CFU. Tissues were fixed in EM fixative for the indicated time, rinsed for 30 min in phosphate-buffered saline, and then homogenized. +/– indicates presence or absence of growth in broth/on plates.
†100% of sample tested.
‡50% of sample tested.
§90% of 1 sample tested, 10% of others tested.
¶10% of sample tested.

(*25*). In a separate iteration, rabbits were exposed to aerosolized *B. anthracis* Ames spores and lung samples were obtained through tissue sharing.

B. pseudomallei 1026b (*26*), *F. tularensis* Schu S4 (*27*), and *Y. pestis* CO92 (*28*) were grown until mid-log phase. Bacterial doses and the infection routes used were based on previous studies (Table 4) (*26*,*29*–*31*). To minimize animal pain or distress, we administered meloxicam/buprenorphine (*32*). Animals were observed at least twice daily, and when they were moribund, they were euthanized with pentobarbital (Vortech Pharmaceuticals, Ltd., http://www.vortechpharm.com).

In compliance with the Animal Welfare Act, Public Health Service policy, and other federal statutes and regulations pertaining to animals and experiments involving animals, we conducted our research under an Institutional Animal Care and Use Committee–approved protocol. The facility where this research was conducted is accredited by the Association for Assessment and Accreditation of Laboratory Animal Care, International and adheres to principles stated in the Guide for the Care and Use of Laboratory Animals, National Research Council, 2011 (https://www.aaalac.org; https://grants.nih.gov/grants/olaw/guide-for-the-care-and-use-of-laboratory-animals.pdf).

Inactivation Procedures and Viability Testing

Skin injection sites from guinea pigs infected with Ames spores were incubated in fixative (1:10 wt/vol) at ambient temperature. Lungs, livers, and spleens from euthanized or recently dead guinea pigs and rabbits were excised, divided into several pieces per tissue type, and submerged in fixative for various times. To remove excess fixative, we

Table 4. Routes of infection and delivered doses of Select Agents used to infect guinea pigs and rabbits for tissue collection in study of inactivation of bacterial Tier 1 Select Agents

Bacteria	Route of infection	Delivered dose, CFU	Animal model	Time of collection	Tissue collected
Bacillus anthracis Ames (spores)	Intradermal	2.7×10^8	Guinea pigs-Hartley	2 h after challenge	Skin
	Inhalational and/or intramuscular, respiratory	4.9×10^6 and 1.0×10^3 respiratory	Guinea pigs-Strain 13	Late-stage disease	Lung, liver, spleen
	Inhalational	1.0×10^7	Rabbits-New Zealand White	24 h after challenge	Lung
Burkholderia pseudomallei 1026b	Intraperitoneal	9.0×10^2	Guinea pigs-Strain 13	Late-stage disease	Lung, liver, spleen
Francisella tularensis Schu S4	Subcutaneous	8.6×10^2	Guinea pigs-Strain 13	Late-stage disease	Lung, liver spleen
Yersina pestis CO92	Subcutaneous	7.0×10^4	Guinea pigs-Strain 13	Late-stage disease	Lung, liver, spleen

Table 5. Effect of residual formaldehyde in tissue from guinea pigs on the growth of *Bacillus anthracis* Sterne in study of inactivation of bacterial Tier I Select Agents*

Tissue type, no. samples	Fixation time, d	Incubation time for tissue in PBS/water	Sample inactivation†	Positive control inactivation†
Skin, 2	2	45 min	–/–	+/+
Skin, 2	14	45 min	–/–	+/+
Skin, 2	21	45 min	–/–	+/+
Ears, 2	2	45 min	–/–	+/+
Ears, 2	14	45 min	–/–	–/–
Ears, 2	21	45 min	–/–	–/–
Spleen, 3	2	45 min	–/–	+/+
Spleen, 3	17	45 min	–/–	–/–
Spleen, 3	17	24 h	–/–	+/+
Liver, 3	2	45min	–/–	+/+
Liver, 3	17	45 min	–/–	+/+‡
Liver, 3	17	24 h	–/–	+/+

*Different fixation times (2, 14, 17, or 21 d) and wash times (45 min or 24 h) for skin, outer ear pinna, spleen, and liver result in the different ability of Sterne spores to germinate and grow in broth used for viability testing. +/– indicates presence and/or absence of growth in broth/on plates; PBS, phosphate-buffered saline.
†50% of tissue tested.
‡Of 3 samples, 2 were positive for growth and 1 was inhibited by residual formaldehyde.

soaked fixed tissues for 30 min and homogenized them. The entire homogenate volume was subjected to 7-day broth-to-plate viability testing, as previously described. To provide a positive control, we inoculated an additional sample with spores.

For *B. pseudomallei* 1026b, half of the homogenate was subjected to viability testing and the other half was reinoculated with live organism to serve as a positive control. Most tissue homogenates of *Francisella* and *Yersinia* were tested by using 10% of samples because of the necessary dilution in 10 L of broth for growth; however, spleen tissues with the highest bacterial load were further tested by using 90% of the samples in that volume (10% was reinoculated for positive control). *Burkholderia*, *Francisella*, and *Yersinia* homogenates were incubated in broth and then incubated on solid medium at the appropriate temperature for 3–4 days each.

Results

Spores were able to germinate and grow in the presence of fixed skin or liver when the tissue was washed for a short time (45 min) (Table 5). In contrast, growth did not occur in ears or spleens fixed for a longer time (14–21 d) but washed for a short time. When washing was extended for a longer time (24 h), spleen tissue again permitted growth (Tables 5, 6), suggesting that the fixative was able to adequately diffuse out of the tissue with longer washing.

An alternative way to neutralize formaldehyde in fixed tissue is sufficient dilution in the broth used for viability testing. Thus, we determined the broth volume to which formaldehyde could be adequately diluted to permit growth of *B. anthracis* Sterne, *B. pseudomallei* 82, *F. tularensis* live vaccine strain, and *Y. pestis* Pgm–/pPst–. The growth of these non–Select Agents, used as surrogates, in broth containing 1%–0.001% formaldehyde, is shown in Table 7. Of note is the higher inoculum for *F. tularensis* live vaccine strain necessary to seed the broth cultures for growth. In contrast, substantially less inoculum was required for the other agents. *B. pseudomallei* 82 (a purine auxotroph) required longer incubation (5 d) before a turbidity increase was evident. Therefore, we also performed the formaldehyde sensitivity assay with the virulent strain 1026b. These data indicate that formaldehyde can be washed out or adequately diluted in broth to permit a small number of live organisms, which may be present, to proliferate.

The skin is a difficult tissue for formaldehyde to infiltrate (*16*). Because of this property, along with the resistant nature of spores, to generate a time course of organism killing, we chose skin tissues infected with *B. anthracis* Ames spores. Spores in skin sections fixed for 14 or 21 days were completely inactivated (Table 1). In contrast, 7-day fixation was not adequate; growth occurred in 1 of 3 tissues. To maximize our dataset for inactivation of spore-containing

Table 6. Effect of residual electron microscopy fixative in tissue from guinea pigs on the growth of *Bacillus anthracis* Sterne in study of inactivation of bacterial Tier I Select Agents*

Tissue type, no. samples	Fixation time, d	Incubation time for tissue in PBS/water, h	Sample inactivation†	Positive control inactivation†
Spleen, 3	14	24	–/–	+/+
Spleen, 3	21	24	–/–	+/+
Liver, 3	14	24	–/–	+/+
Liver, 3	21	24	–/–	+/+

*Spleen and liver tissues fixed for 14 or 21 d and washed for 24 h permitted Sterne spores to germinate and grow in broth used for viability testing. +/– indicates presence and/or absence of growth in broth/on plates. PBS, phosphate-buffered saline.
†50% of tissue tested.

Table 7. Growth of *Bacillus, Burkholderia, Francisella,* and *Yersinia* species in diluted formaldehyde in study of inactivation of bacterial Tier I Select Agents*

Strain	CFU/volume	Growth condition	Time, d	NBF concentration, %	Growth
Bacillus anthracis Sterne	5 (bacilli)/500 mL	BHI, 37°C	1	0.1	–
				0.01	+
				0.001	+
Burkholderia pseudomallei 82	10/500 mL	LB + 4% glycerol, 37°C	5	0.1	–
				0.01	–
				0.001	+
B. pseudomallei 1026b	5/500 mL	LB + 4% glycerol, 37°C	3	0.1	–
				0.01	+
				0.001	+
Francisella tularensis LVS	1.4×10^5/100 mL	BHI + 1% IsoVitaleX, 37°C	4	0.1	–
				0.01	–
				0.001	+
Yersina pestis Pgm$^-$/pPst$^-$	10/100 mL	HI + 0.2% xylose, 28°C	3	0.1	–
				0.01	–
				0.001	+

*5 CFU *B. anthracis* Sterne (bacilli), 10 CFU *B. pseudomallei* 82, 5 CFU *B. pseudomallei* 1026b, 1.4×10^5 CFU *F. tularensis* live vaccine strain and 10 CFU *Y. pestis* Pgm–/pPst– bacteria were inoculated into their respective broths containing 0.1%, 0.01%, and 0.001% NBF and grown at the indicated temperature. Time listed is when broth cultures reached turbidity. + /– indicates presence and/or absence of growth in broth.
BHI, brain heart infusion; HI, heart infusion; LB, Lennox broth; LVS, live vaccine strain; NBF, neutral buffered formalin.

tissues, we also fixed lung tissues from rabbits infected with *B. anthracis* Ames spores. Of 3 lung samples, 2 were inactivated at 13 days and the third was inactivated at 20 days (Table 8).

The tissues that we commonly collect and fix for histopathologic analysis are spleen, liver, and lung. Organisms in all infected spleen, liver, and lung samples fixed for various times were inactivated (Table 2). Specifically, we found complete inactivation in spleens infected with the highest load of *B. anthracis* Ames, *F. tularensis* Schu S4, or *Y. pestis* CO92, tested by using either 90% or 100% of the samples. This inactivation includes *B. anthracis* Ames–infected lung tissue from guinea pigs, which also contained heat-resistant spores. Also completely inactivated were *B. pseudomallei* 1026b–infected spleen and other tissues, tested by using 50% of the samples. Similar to formaldehyde-fixed tissues, tissues incubated in EM fixative were also inactivated (Table 3).

Discussion

We examined the effectiveness of formaldehyde, by itself and with glutaraldehyde, to inactivate tissues infected with Select Agents. We found that 14 days in formaldehyde and 7 days in EM fixative are generally sufficient to completely inactivate most infected tissues described in this report, including tissues containing high numbers of resistant spores and hard-to-infiltrate tissues like skin. One exception was a rabbit lung in which B. *anthracis* spores were only partially inactivated at 13 days of fixation but inactivated at 20 days. Although we show that inactivation can probably be achieved in less time, to ensure an adequate safety margin, no change in our institutional standard operating procedure of 21 days fixation will be made.

At the study's inception, we experimented with injecting Select Agents into tissues collected from euthanized animals. However, this ex vivo approach failed because the tissues did not retain the inoculum. Of note, this attempt did not recapitulate in vivo diseased tissue, where organisms are probably distributed more homogeneously. Although we were fortunate to obtain rabbit lung tissues from an ongoing study, other already infected tissues were not readily available. Thus, we infected animals specifically for this work. In addition to infecting with the Select Agents we commonly work with, we also validated different tissue types such as skin and lung, tissues in which a substantial amount of ungerminated spores would remain after exposure. We specifically examined the number of ungerminated spores in rabbit and guinea pig tissues because the chemical sensitivities of spores and bacilli differ greatly.

For this study, we used tissues ≤10 mm thick in 1 dimension. Although it is possible to excise and fix tissue

Table 8. Formaldehyde fixation of infected lung tissue from rabbits exposed to aerosolized *Bacillus anthracis* Ames spores in study of inactivation of bacterial Tier I Select Agents*

Rabbit no.	Tissue weight, g	Tissue size, mm	Total CFU recovered/g	Heat-resistant CFU recovered/g	Time of inactivation		Positive control
					13 d	20 d	
1	0.72	10 × 10 × 10	1.2×10^7	1.5×10^6	–/–†	ND	+/+
2	0.74	10 × 10 × 10	4.4×10^5	4.3×10^5	–/–†	ND	+/+
3	0.71/0.75	10 × 10 × 10	2.6×10^6	1.0×10^6	+/+†	–/–†	+/+

*Infected lung tissues from 3 rabbits were fixed for 13 or 20 d in 4% paraformaldehyde, rinsed for 30 min in phosphate-buffered saline, and then homogenized. Listed are the tissue weight, size, and CFU recovered. +/– indicates presence and/or absence of growth in broth/on plate. ND, not done.
†50% of sample tested.

>10 mm thick, this practice is discouraged because it hampers fixative infiltration into the deep recesses of the tissue; these areas probably also undergo putrefaction before becoming fixed (*10*). Infiltration is already slowed in tissues such as skin and fat (*16*,*17*), so exceeding the limit set forth here (10 mm) will probably lengthen the time needed to inactivate. Exceeding the organ bacterial burdens greater than those stated (Tables 2,3) would also require reevaluation (*23*) because these could require more time to inactivate. Other institutions may use this work as a guide to conduct and develop their own testing to comply with the policy. Furthermore, these methods may be useful in the processing and inactivation of tissues from patients infected with Select Agents for diagnostic testing by state public health laboratories and CDC.

This work was funded by the US Department of Defense.

About the Author

Dr. Chua is a microbiologist/cell biologist who specializes in microscopy. Her research interest includes infectious diseases and microbial pathogenesis.

References

1. Bozue JA, Cote CK, Glass PJ, editors. Medical aspects of biological warfare. Fort Sam Houston (TX): Borden Institute, Office of the Surgeon General of the United States Army; 2018.
2. US Department of Defense. Inadvertent shipment of live. *Bacillus anthracis* spores by DoD: 2015 July 13 [cited 2019 Jan 13]. www.defense.gov/Portals/1/features/2015/0615_lab-stats/Review-Committee-Report-Final.pdf
3. Cote CK, Buhr T, Bernhards CB, Bohmke MD, Calm AM, Esteban-Trexler JS, et al. A standard method to inactivate *Bacillus anthracis* spores to sterility using gamma-irradiation. Appl Environ Microbiol. 2018;84:AEM.00106-18. http://dx.doi.org/10.1128/AEM.00106-18
4. Centers for Disease Control and Prevention, Department of Health and Human Services. Possession, use and transfer of select agents and toxins; biennial review of the list of select agents and toxins and enhanced biosafety requirements. Final rule. Fed Regist. 2017; 82:6278–94.
5. Blum F. Der Formaldehyd als Antisepticum. Münchener medicinische Wochenschrift. 1893;32:601–2.
6. Sabatini DD, Bensch K, Barrnett RJ. Cytochemistry and electron microscopy. The preservation of cellular ultrastructure and enzymatic activity by aldehyde fixation. J Cell Biol. 1963;17:19–58. http://dx.doi.org/10.1083/jcb.17.1.19
7. Fox CH, Johnson FB, Whiting J, Roller PP. Formaldehyde fixation. J Histochem Cytochem. 1985;33:845–53. http://dx.doi.org/10.1177/33.8.3894502
8. Jones D. Reactions of aldehydes with unsaturated fatty acids during histological fixation. Histochem J. 1972;4:421–65. http://dx.doi.org/10.1007/BF01012533
9. Kunkel GR, Mehrabian M, Martinson HG. Contact-site cross-linking agents. Mol Cell Biochem. 1981;34:3–13. http://dx.doi.org/10.1007/BF02354846
10. Thavarajah R, Mudimbaimannar VK, Elizabeth J, Rao UK, Ranganathan K. Chemical and physical basics of routine formaldehyde fixation. J Oral Maxillofac Pathol. 2012;16:400–5. http://dx.doi.org/10.4103/0973-029X.102496
11. Sompuram SR, Vani K, Messana E, Bogen SA. A molecular mechanism of formalin fixation and antigen retrieval. Am J Clin Pathol. 2004;121:190–9. http://dx.doi.org/10.1309/BRN7CTX1E84NWWPL
12. Phillips GB, Novak F, Hanel E Jr. Germicidal effectiveness of formaldehyde fixatives and preservatives against *Bacillus anthracis* in animal tissue. Am J Med Technol. 1955;21:89–91.
13. Malinina ZE, Isupov IV, Dudkova VK. Bactericidal action of formalin on the causative agent of plague [in Russian]. Arkh Patol. 1979;41:80–2.
14. Brantner CA, Hannah RM, Burans JP, Pope RK. Inactivation and ultrastructure analysis of *Bacillus* spp. and *Clostridium perfringens* spores. Microsc Microanal. 2014;20:238–44. http://dx.doi.org/10.1017/S1431927613013949
15. Chafin D, Theiss A, Roberts E, Borlee G, Otter M, Baird GS. Rapid two-temperature formalin fixation. PLoS One. 2013;8:e54138. http://dx.doi.org/10.1371/journal.pone.0054138
16. Buesa RJ, Peshkov MV. How much formalin is enough to fix tissues? Ann Diagn Pathol. 2012;16:202–9. http://dx.doi.org/10.1016/j.anndiagpath.2011.12.003
17. Bauer DR, Stevens B, Chafin D, Theiss AP, Otter M. Active monitoring of formaldehyde diffusion into histological tissues with digital acoustic interferometry. J Med Imaging (Bellingham). 2016;3:017002. http://dx.doi.org/10.1117/1.JMI.3.1.017002
18. Setlow P. Spores of *Bacillus subtilis*: their resistance to and killing by radiation, heat and chemicals. J Appl Microbiol. 2006;101:514–25. http://dx.doi.org/10.1111/j.1365-2672.2005.02736.x
19. Leighton TJ, Doi RH. The stability of messenger ribonucleic acid during sporulation in *Bacillus subtilis.* J Biol Chem. 1971;246:3189–95.
20. Green BD, Battisti L, Koehler TM, Thorne CB, Ivins BE. Demonstration of a capsule plasmid in *Bacillus anthracis.* Infect Immun. 1985;49:291–7.
21. Cote CK, Van Rooijen N, Welkos SL. Roles of macrophages and neutrophils in the early host response to *Bacillus anthracis* spores in a mouse model of infection. Infect Immun. 2006;74:469–80. http://dx.doi.org/10.1128/IAI.74.1.469-480.2006
22. Chua J, Fisher NA, Falcinelli SD, DeShazer D, Friedlander AM. The Madagascar hissing cockroach as an alternative non-mammalian animal model to investigate virulence, pathogenesis, and drug efficacy. J Vis Exp. 2017;129:e56491. PMID: 29286449
23. Centers for Disease Control and Prevention. Revised FSAP policy statement: inactivated *Bacillus anthracis* and *Bacillus cereus* biovar anthracis. 2017 August 14 [cited 2019 Jan 13]. http://www.selectagents.gov/policystatement_bacillus.html
24. Hartings JM, Roy CJ. The automated bioaerosol exposure system: preclinical platform development and a respiratory dosimetry application with nonhuman primates. J Pharmacol Toxicol Methods. 2004;49:39–55. http://dx.doi.org/10.1016/j.vascn.2003.07.001
25. Bozue JA, Parthasarathy N, Phillips LR, Cote CK, Fellows PF, Mendelson I, et al. Construction of a rhamnose mutation in *Bacillus anthracis* affects adherence to macrophages but not virulence in guinea pigs. Microb Pathog. 2005;38:1–12. http://dx.doi.org/10.1016/j.micpath.2004.10.001
26. DeShazer D, Brett PJ, Woods DE. The type II O-antigenic polysaccharide moiety of *Burkholderia pseudomallei* lipopolysaccharide is required for serum resistance and virulence. Mol Microbiol. 1998;30:1081–100. http://dx.doi.org/10.1046/j.1365-2958.1998.01139.x
27. Chance T, Chua J, Toothman RG, Ladner JT, Nuss JE, Raymond JL, et al. A spontaneous mutation in *kdsD*, a biosynthesis gene for 3 deoxy-D-manno-octulosonic acid, occurred in a ciprofloxacin resistant strain of *Francisella tularensis* and caused a high level of attenuation in murine models of tularemia. PLoS One. 2017;12:e0174106. http://dx.doi.org/10.1371/journal.pone.0174106

28. Bozue J, Cote CK, Chance T, Kugelman J, Kern SJ, Kijek TK, et al. A *Yersinia pestis tat* mutant is attenuated in bubonic and small-aerosol pneumonic challenge models of infection but not as attenuated by intranasal challenge. PLoS One. 2014;9:e104524. http://dx.doi.org/10.1371/journal.pone.0104524
29. Hood AM. Virulence factors of *Francisella tularensis.* J Hyg (Lond). 1977;79:47–60. http://dx.doi.org/10.1017/S0022172400052840
30. Samoilova SV, Samoilova LV, Yezhov IN, Drozdov IG, Anisimov AP. Virulence of pPst+ and pPst- strains of *Yersinia pestis* for guinea-pigs. J Med Microbiol. 1996;45:440–4. http://dx.doi.org/10.1099/00222615-45-6-440
31. Jenkins A, Cote C, Twenhafel N, Merkel T, Bozue J, Welkos S. Role of purine biosynthesis in *Bacillus anthracis* pathogenesis and virulence. Infect Immun. 2011;79:153–66. http://dx.doi.org/10.1128/IAI.00925-10
32. Stevens KA, Wilson RP, Suckow MA, editors. The Laboratory Rabbit, Guinea Pig, Hamster, and other Rodents. 1st ed. Boston: Academic Press (Elsevier); 2012.

Address for correspondence: Jennifer Chua or Christopher K. Cote, USAMRIID, 1425 Porter St, Frederick, MD 21702, USA; email: jennifer.chua.ctr@mail.mil or christopher.k.cote.civ@mail.mil

Risk Factors for MERS-CoV Seropositivity among Animal Market and Slaughterhouse Workers, Abu Dhabi, United Arab Emirates, 2014–2017

Ahmed Khudhair,[1] Marie E. Killerby,[1] Mariam Al Mulla, Kheir Abou Elkheir, Wassim Ternanni, Zyad Bandar, Stefan Weber, Mary Khoury, George Donnelly, Salama Al Muhairi, Abdelmalik I. Khalafalla, Suvang Trivedi, Azaibi Tamin, Natalie J. Thornburg, John T. Watson, Susan I. Gerber, Farida Al Hosani,[2] Aron J. Hall[2]

Camel contact is a recognized risk factor for Middle East respiratory syndrome coronavirus (MERS-CoV) infection. Because specific camel exposures associated with MERS-CoV seropositivity are not fully understood, we investigated worker–camel interactions and MERS-CoV seroprevalence. We assessed worker seroprevalence in 2 slaughterhouses and 1 live-animal market in Abu Dhabi, United Arab Emirates, during 2014–2017 and administered an epidemiologic survey in 2016 and 2017. Across 3 sampling rounds during 2014–2017, we sampled 100–235 workers, and 6%–19% were seropositive for MERS-CoV at each sampling round. One (1.4%) of 70 seronegative workers tested at multiple rounds seroconverted. On multivariable analyses, working as a camel salesman, handling live camels or their waste, and having diabetes were associated with seropositivity among all workers, whereas handling live camels and either administering medications or cleaning equipment was associated with seropositivity among market workers. Characterization of high-risk exposures is critical for implementation of preventive measures.

Middle East respiratory syndrome (MERS) coronavirus (MERS-CoV) was first identified as a cause of severe respiratory tract infections in Saudi Arabia in October 2012 (*1*). The clinical spectrum of MERS ranges from asymptomatic infection to acute respiratory distress syndrome and death (*2*). As of April 3, 2019, a total of 2,374 laboratory-confirmed cases of infection have been reported by 27 countries to the World Health Organization (WHO); the reported case-fatality rate is 35% (*2*). All reported cases have an epidemiologic link to the Arabian Peninsula, and imported cases have been reported in Europe, Asia, North America, and Africa. The United Arab Emirates has reported the third-highest number of MERS cases since 2012 (*3*).

MERS-CoV is a zoonotic virus, and dromedaries (camels) are recognized as a major virus reservoir for spillover to humans (*4*). Multiple studies have isolated MERS-CoV or MERS-CoV RNA from camels across the Arabian Peninsula and Africa (*5–11*). Serologic studies of camels in the Middle East and Africa have revealed MERS-CoV seroprevalence of >90%–97% (*8,11–13*). In natural infection, camels have been found to shed MERS-CoV in respiratory secretions and to a lesser extent in stool (*14,15*). Evidence of virus RNA has also been found in milk collected by traditional milking procedures, which involve calf suckling as a stimulus for milk letdown (*15*).

Epidemiologic links between infected camels and human MERS-CoV infections have been shown, with identical or nearly identical MERS-CoV genomes found in human cases and in camels with which they had direct contact (*16–18*). Also, a case–control study identified exposure to camels as a risk factor for human MERS-CoV infection (*19*). Human seroprevalence studies also support the association between MERS-CoV infection and camel contact; in Saudi Arabia MERS-CoV seroprevalence was found to be 15 times greater in camel shepherds and 23 times greater in slaughterhouse workers compared with the

Author affiliations: Abu Dhabi Department of Health, Abu Dhabi, United Arab Emirates (A. Khudhair, M. Al Mulla, K.A. Elkheir, W. Ternanni, Z. Bandar, F. Al Hosani); Sheikh Khalifa Medical City, Abu Dhabi (M.E. Killerby, S. Weber, M. Khoury, G. Donnelly); Centers for Disease Control and Prevention, Atlanta, Georgia, USA (M.E. Killerby, S. Trivedi, A. Tamin, N.J. Thornburg, J.T. Watson, S.I. Gerber, A.J. Hall); Abu Dhabi Food Control Authority, Abu Dhabi (S. Al Muhairi, A.I. Khalafalla)

DOI: https://doi.org/10.3201/eid2505.181728

[1]These authors contributed equally to this article.

[2]These authors contributed equally to this article.

general population (*20*). Further studies have also shown high seroprevalence in specific occupational groups with various camel exposures (e.g., seropositivity was detected in 6.8% of a cohort of 294 camel workers in Qatar [*21*] and in 53% of a cohort of 30 camel workers in Saudi Arabia [*22*]).

Although multiple lines of evidence suggest camel exposure is associated with human MERS-CoV infection, the exact mechanisms of transmission are not fully understood. Information on specific risk factors relating to camel interactions are needed to further understand how the virus might be transmitted from camels to humans and to guide interventions to prevent zoonotic transmission, including changes to camel management practices. Because MERS-CoV vaccines are currently in development and have reported success in phase I clinical trials (*23*), knowledge of groups at risk for MERS-CoV infection might also be useful when considering future vaccine use. Our study aimed to identify risk factors for MERS-CoV seropositivity among live-animal market and slaughterhouse workers.

Methods

Study Site and Population

The study sites consisted of an open-air animal market and 2 slaughterhouses (1 commercial and 1 public). All 3 facilities housed camels, goats, sheep, and cattle (Figure 1). Typically during the study period, approximately 460 persons worked at the market, 101 at the public slaughterhouse, and 29 at the commercial slaughterhouse. The market investigated in this study was linked to a human MERS case in 2015 (*24*). Prior investigation showed a large diversity of MERS-CoVs circulating among camels at the market; 109 (29%) of 276 screened camels had detectable MERS-CoV RNA in nasal swab specimens in the spring of 2015 (*25*).

Serum Sampling and Data Collection

We conducted 3 rounds of worker serum sampling. The first round was conducted during May 11–14, 2014, and the second round during March 23–April 1 and May 7–13, 2015. During the first 2 rounds of sampling, all available workers at the market and public slaughterhouse were requested to provide a serum sample as part of a public health investigation. We conducted a third round of serum sampling during September 22–October 5, 2016, and March 20–23, 2017. The third round of sampling included workers at the market, public slaughterhouse, and the newly opened commercial slaughterhouse. All available workers were requested to provide serum samples, although participation was voluntary. Some, but not all, workers were repeatedly sampled, when feasible, during multiple rounds.

We administered an epidemiologic survey to all workers only during the third round of serum sampling in 2016 and 2017. No surveys were administered in 2014 or 2015. The survey consisted of questions covering worker demographics; occupational history; contact with various animal species; travel history; medical history; consumption of raw camel milk, raw camel meat, and camel urine; specific tasks performed with camels; types of personal protective equipment (PPE) worn; and handwashing practices (Appendix 1, https://wwwnc.cdc.gov/EID/article/25/5/18-1728-App1.pdf). Separate lists of questions covering specific camel tasks performed were asked of market and slaughterhouse workers because of the different nature of camel tasks among occupational groups. Interviews were conducted in Arabic by staff from the Abu Dhabi Department of Health.

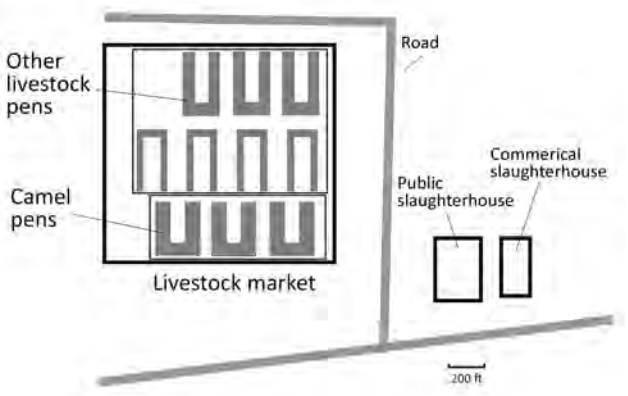

Figure 1. Diagram of study site indicating market and slaughterhouse settings, Abu Dhabi, United Arab Emirates.

Laboratory Testing

Human serum samples were tested for MERS-CoV antibodies at the US Centers for Disease Control and Prevention (CDC) by using indirect ELISAs for nucleocapsid (N) and spike (S) proteins, followed by a confirmatory microneutralization test, as previously described (*26*). Samples were initially tested by using both N and S ELISAs as screening assays with serum diluted to 1:400. All serum samples with optical densities above assay cutoff were diluted serially, 4-fold, from 1:100 to 1:6,400, and used for endpoint titer determinations. Serum samples that were positive by N or S ELISA with titers at 1:400, 1:1600, or 1:6,400, plus 10% of samples negative by N or S ELISA at these titers, were tested by using microneutralization with live MERS-CoV performed in a Biosafety Level 3 laboratory, as previously described (*26*). In addition, we conducted confirmatory microneutralization tests on seronegative samples from any persons who showed a change in seropositivity status over time to confirm changes in seropositivity status. Samples were considered positive if positive on N and S ELISA or if positive on microneutralization. Specimens near the limits of detection but not consistently above or below these limits were considered indeterminate. For the epidemiologic analysis, persons with an indeterminate result were considered seronegative.

Data Analyses

We used Epi Info 7 (https://www.cdc.gov/epiinfo) for data entry and R version 3.3.1 (https://cran.r-project.org/bin/windows/base/old/3.3.1) for data analysis. We performed comparisons between prevalence of work practices by setting (market vs. slaughterhouse) by using the Pearson χ^2 square test. We used univariable logistic regression to estimate odds ratios, 95% CIs, and p values (Wald test) for all associations between potential risk factors and seropositivity. We assessed associations between demographics, occupational history, contact with various animal species, consumption of camel products, travel history, and medical history with seropositivity for all workers. We separately tested associations between specific interactions with camels, types of PPE worn, and handwashing practices with seropositivity for stratified subgroups of market and slaughterhouse workers because of the different nature of work setting and standard practices between these 2 populations. We then performed additional exploratory data description by occupation on the basis of results of univariable analyses.

We developed 3 multivariable logistic models to identify associations between risk factors and seropositivity. First, we constructed a model of risk factors common to all workers and then constructed occupationally stratified models (i.e., separate models for market workers and slaughterhouse workers) to model specific interactions with camels, PPE use, and handwashing practices. We combined or eliminated highly correlated variables, which were determined by condition indices and variance decomposition proportions. We reduced categorical variables to binary options if small group size was observed. We performed initial variable selection by using least absolute shrinkage and selection operator (LASSO) and then tested person-variable significance by using the likelihood ratio test with a cutoff of $p<0.05$ within an ordinary logistic regression model. We then included age and number of years worked at current setting as potential confounders in all 3 final models. We excluded persons with missing data at the LASSO stage but included them for the final logistic regression model.

For the stratified market worker and slaughterhouse models, we also included variables significant in the all workers model but not directly relating to camel interactions (e.g., reported underlying conditions) in the final occupationally stratified models. We did not include significant variables directly relating to camel exposures in the all workers model in the stratified models because more specific camel risk practices were assessed in the stratified models. For market and slaughterhouse models, we tested interactions between significant risk practices and select PPE use and handwashing practices for a protective effect.

Results

Serum Sample Results

We sampled 100 workers in round 1 (2014), 151 workers in round 2 (2015), and 235 workers in round 3 (2016 and 2017); overall MERS-CoV seroprevalence was 6% for round 1, 19% for round 2, and 17% for round 3. Twenty-one persons had specimens taken at rounds 1 and 2, twenty-three at rounds 2 and 3, thirteen at rounds 1 and 3, and twenty-two at all 3 rounds (Figure 2). Of 70 persons who were seronegative at their first sample, only 1 (1.4%, 95% CI 0.1%–8.8%) seroconverted: a 30-year-old man who was a cleaner at the public slaughterhouse tested negative at round 1 and positive at round 2. Of 8 persons who were seropositive at their first sample, 1 (13%) was later found to be seronegative: a 28-year old man who was an administrative supervisor at the market was resampled between rounds 1 and 3. This person did not report handling camels or their waste and did not perform any tasks directly relating to camels. One additional person who had a positive serologic result at their first and second samples and an indeterminate result at their third sample was not subsequently evaluated for change in seropositive status. Because some study participants might have had different medical record numbers across the 3 sampling rounds, we could not determine all potential seroconversions or losses of seropositivity, although we also performed matching by name and age. We compiled serologic results for all participants who ever tested positive (Appendix 2, https://wwwnc.cdc.gov/EID/article/25/5/18-1728-App2.pdf).

Epidemiologic Survey Results

In total, 235 persons both completed the epidemiologic survey and were sampled during round 3. One additional person completed the epidemiologic survey but refused serum sampling and was not included in any analyses. All 235 workers were men, and their median age was 35 years (range 19–64 years). The median number of years worked at the current settings was 6 (range 0.2–15 years). We observed no significant effect of age ($p = 0.26$) or years worked ($p = 0.18$) on seropositivity on univariable analysis.

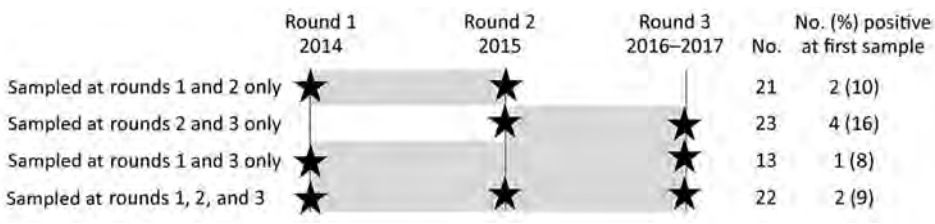

Figure 2. Number of workers sampled during >1 round of sampling (N = 79), Abu Dhabi, United Arab Emirates. Black stars indicate when serum samples were taken; gray shading indicates follow-up periods.

Worker occupations were categorized into animal handlers (n = 16), camel salesmen (n = 37), other animal salesmen (n = 41), animal or waste transporters (n = 27), butchers (n = 65), cleaners (n = 26), veterinarians (n = 9), and other (e.g., supervisor, cashier, and tourist guide) (n = 14). Salesmen only worked in the market, and butchers only worked in the slaughterhouses. The remaining occupations were found in both settings, but each person could only work at a slaughterhouse or the market. None of the workers reported working at any other job outside of the market or slaughterhouses, and the only animals reported present at home were poultry and stray cats.

Overall, 64 (44%) of 145 market workers had daily contact with camels or their waste, compared with 47 (52%) of 90 slaughterhouse workers (p = 0.28). Certain PPE use and handwashing were more frequently reported by slaughterhouse workers than market workers. Among slaughterhouse workers, 99% reported wearing a dust mask (equivalent to a surgical mask), compared with 21% of market workers (p<0.01). Only 37% of slaughterhouse workers reported taking their work clothes home, compared with 97% of market workers (p<0.01). Eighty-one percent of slaughterhouse workers reported washing their hands before and after each animal-related task, compared with 21% of market workers (p<0.01). Ninety-three percent of slaughterhouse workers reported washing their hands at the beginning and end of the day, compared with only 56% of market workers (p<0.01).

Univariable Analyses

Rates of seropositivity were higher among market workers (29 [20%] of 145) than among slaughterhouse workers (11 [12%] of 90), although this difference was not statistically significant on univariable analysis (p = 0.17). By occupation, camel salesmen and animal or waste transporters had significantly higher odds of seropositivity than the reference group of other salesmen (Table 1).

Univariable analyses showed that several characteristics were associated with seropositivity among all workers (Table 1), including handling camels or their waste daily. Not all seropositive workers reported handling camels or

Table 1. Characteristics of 235 market and slaughterhouse workers, by MERS-CoV serostatus, Abu Dhabi, United Arab Emirates*

Characteristic	Total no. participants	No. (%) participants		OR (95% CI)	p value
		Seronegative, n = 195	Seropositive, n = 40		
Work >50 h/wk	132	103 (78.0)	29 (22.0)	2.35 (1.14–5.17)	0.025
Worked another job in previous year	30	25 (83.3)	5 (16.7)	0.97 (0.31–2.53)	0.956
Occupation					
Other salesman	41	40 (97.6)	1 (2.4)	Ref	Ref
Animal handler	16	15 (93.8)	1 (6.3)	2.67 (0.1–70.37)	0.498
Butcher	65	56 (86.2)	9 (13.8)	6.43 (1.14–120.92)	0.083
Camel salesman	37	19 (51.4)	18 (48.6)	37.89 (7.03–707.16)	0.001
Cleaner	26	22 (84.6)	4 (15.4)	7.27 (1–147.06)	0.084
Animal or waste transporter	27	21 (77.8)	6 (22.2)	11.43 (1.79–223.48)	0.029
Veterinarian	9	8 (88.9)	1 (11.1)	5.00 (0.18–135.74)	0.272
Other	14	14 (100.0)	0	NA	0.990
Nationality					
Afghani	27	15 (55.6)	12 (44.4)	Ref	Ref
Bangladeshi	38	30 (78.9)	8 (21.1)	0.33 (0.11–0.97)	0.048
Pakistani	97	92 (94.8)	5 (5.2)	0.07 (0.02–0.21)	<0.001
Sudanese	38	25 (65.8)	13 (34.2)	0.65 (0.23–1.79)	0.404
Other	35	33 (94.3)	2 (5.7)	0.08 (0.01–0.32)	0.002
Contact with					
Camels or waste daily	111	78 (70.3)	33 (29.7)	7.07 (3.14–18.15)	<0.001
Cattle or waste daily	58	50 (86.2)	8 (13.8)	0.73 (0.29–1.61)	0.452
Goats or waste daily	88	79 (89.8)	9 (10.2)	0.43 (0.18–0.91)	0.036
Sheep or waste daily	89	80 (89.9)	9 (10.1)	0.42 (0.18–0.89)	0.031
Drank raw camel milk	25	18 (72.0)	7 (28.0)	2.09 (0.76–5.21)	0.129
Ate raw camel meat†	2	1 (50.0)	1 (50.0)	4.95 (0.19–126.94)	0.262
Travel					
To Saudi Arabia	4	4 (100.0)	0	NA	0.990
Within UAE	67	55 (82.1)	12 (17.9)	1.09 (0.5–2.25)	0.819
Underlying conditions					
Asthma	1	0	1 (100.0)	NA	0.985
Diabetes	9	5 (55.6)	4 (44.4)	4.22 (1–16.71)	0.038
Hypertension	12	9 (75.0)	3 (25.0)	1.68 (0.36–5.93)	0.455
Sought care for respiratory illness	45	36 (80.0)	9 (20.0)	1.28 (0.54–2.84)	0.555
Contact with anyone with respiratory illness	2	1 (50.0)	1 (50.0)	1.38 (0.09–7.84)	0.731
Had chest radiograph	13	10 (76.9)	3 (23.1)	1.5 (0.32–5.18)	0.552

*MERS-CoV, Middle East respiratory syndrome coronavirus; NA, not applicable; OR, odds ratio; Ref, referent; UAE, United Arab Emirates.
†Total seronegative was 194 because answer from 1 person was missing. No workers ever contacted the following species: dogs, cats, bats, rodents, birds, and other animals; 1 worker reported rarely contacting horses.

their waste; 7 workers initially claimed they never handled camels or their waste, although 3 of these later reported that they contacted either camel equipment, viscera, or waste within the slaughterhouse. For the subgroup of market workers, univariable analyses revealed multiple camel exposures to be associated with seropositivity and 2 handwashing practices that were inversely associated with seropositivity (Table 2). For the subgroup of slaughterhouse workers, no individual risk factors were associated with seropositivity (Table 3).

Because camel salesmen had the highest odds of MERS-CoV seropositivity, we summarized their frequency of specific camel exposures separately (Figure 3). Direct observation of camel salesmen in the market showed that most of their time was spent in the camel pens, including while they ate and rested, and direct handling of the animals occurred frequently (data not shown).

Multivariable Analyses

For the multivariable model evaluating risk factors associated with seropositivity in all workers, the following variables remained in the final logistic regression model: handling camels or their waste daily (adjusted odds ratio [aOR] 4.2, 95% CI 1.7–11.8), working as a camel salesman (aOR 4.0, 95% CI 1.6–10.1), and self-reported diabetes (aOR 6.2, 95% CI 1.2–30.3). All 3 factors significantly increased odds of seropositivity.

For market workers, multivariable analysis resulted in a final model in which the following variables were each independently associated with seropositivity: handling live camels (aOR 12.2, 95% CI 3.2–62.9), administering medications to camels (aOR 3.4, 95% CI 1.1–11.2), and self-reported diabetes (aOR 20.9, 95% CI 1.6–341.3). Cleaning equipment was also significantly associated with seropositivity (aOR 3.3, 95% CI 1.1–10.3); substituted for administering medication to camels, this factor produced a model with a near-identical fit along with the other risk factors. Given that administering medications to camels was highly correlated with cleaning equipment, the statistical significance of both factors was lost if both factors were included in the model because of collinearity ($\rho = 0.65$). None of the select PPE and handwashing practices evaluated as interactions with risk practices showed a significant protective effect. No individual risk factors were significantly associated with slaughterhouse workers by multivariable analysis.

Table 2. Comparison of practices among 145 MERS-CoV seronegative and seropositive market workers, Abu Dhabi, United Arab Emirates*

Characteristic	Total no. participants	No. (%) participants		OR (95% CI)	p value
		Seronegative, n = 116	Seropositive, n = 29		
Handle live camels	66	40 (60.6)	26 (39.4)	16.47 (5.38–72.06)	<0.001
Feed camels	51	31 (60.8)	20 (39.2)	6.09 (2.57–15.44)	<0.001
Clean camels	39	22 (56.4)	17 (43.6)	6.05 (2.56–14.83)	<0.001
Clean camel housing	37	19 (51.4)	18 (48.6)	8.35 (3.47–21.11)	<0.001
Handle camel waste	33	16 (48.5)	17 (51.5)	8.85 (3.63–22.56)	<0.001
Clean equipment	33	16 (48.5)	17 (51.5)	8.85 (3.63–22.56)	<0.001
Milk camels	18	12 (66.7)	6 (33.3)	2.26 (0.72–6.49)	0.138
Assist with camel birthing	27	18 (66.7)	9 (33.3)	2.45 (0.94–6.16)	0.060
Give medications to camels	35	18 (51.4)	17 (48.6)	7.71 (3.2–19.34)	<0.001
Contact with ill camel	37	20 (54.1)	17 (45.9)	6.8 (2.85–16.83)	<0.001
Wear dust mask and gloves	25	23 (92.0)	2 (8.0)	0.3 (0.05–1.1)	0.117
Wear respirator	0	0 (NA)	0 (NA)	NA	NA
Wear coveralls	15	13 (86.7)	2 (13.3)	0.59 (0.09–2.3)	0.500
Wear boots	3	3 (100.0)	0 (0.0)	NA	0.991
Who washes your clothes?					
Self	84	69 (82.1)	15 (17.9)	Ref	Ref
Household member	5	4 (80.0)	1 (20.0)	1.15 (0.06–8.49)	0.904
Other worker	56	43 (76.8)	13 (23.2)	1.39 (0.6–3.21)	0.439
Take work clothes home	141	113 (80.1)	28 (19.9)	0.74 (0.09–15.34)	0.801
Wash work clothes at home	89	73 (82.0)	16 (18.0)	0.72 (0.32–1.67)	0.444
Wash work clothes at workplace	6	3 (50.0)	3 (50.0)	4.35 (0.77–24.67)	0.082
Wash work clothes at laundry	63	50 (79.4)	13 (20.6)	1.07 (0.47–2.43)	0.867
Wash hands before and after each animal-related task	40	30 (75.0)	10 (25.0)	1.51 (0.61–3.56)	0.355
Wash hands at mealtimes	145	116 (80.0)	29 (20.0)	NA	NA
Wash hands at bathroom times	145	116 (80.0)	29 (20.0)	NA	NA
Wash hands at prayer times	145	116 (80.0)	29 (20.0)	NA	NA
Wash hands at beginning and end of day	81	70 (86.4)	11 (13.6)	0.4 (0.17–0.92)	0.033
Wash hands at toilets	143	114 (79.7)	29 (20.3)	NA	0.989
Wash hands at restaurant	64	50 (78.1)	14 (21.9)	1.23 (0.54–2.8)	0.616
Wash hands at mosque	69	55 (79.7)	14 (20.3)	1.04 (0.45–2.35)	0.934
Wash hands at barn	4	1 (25.0)	3 (75.0)	13.27 (1.63–274.19)	0.028

*MERS-CoV, Middle East respiratory syndrome coronavirus; NA, not applicable; OR, odds ratio.

Discussion

Our study investigated risk factors for MERS-CoV seropositivity in animal market and slaughterhouse workers at a site previously associated with zoonotic transmission of MERS-CoV. Given the large number of camels present, including many young camels, and the mixing of camels from multiple sources, this site probably facilitates MERS-CoV transmission among camels. Our results demonstrated a relatively high MERS-CoV seroprevalence in workers at this site, ranging from 6% to 19% at each round across all occupations. Because we did not record occupation and other risk factors during the first 2 sampling rounds, we were unable to further assess reasons for the different seropositivity rates between sampling rounds.

We found particularly high seroprevalence in specific occupational groups, namely camel salesmen (49%) and animal or waste transporters (22%). Previous studies of workers with occupational exposure to camels have reported either lower seropositivity rates (e.g., 6.8% of 294 workers with occupational camel contact seropositive in Qatar [*21*] and 2.3% of 87 camel shepherds seropositive in Saudi Arabia [*20*]) or comparable seropositivity (e.g., 53% of camel workers positive in Saudi Arabia [*22*]). Our rates of seropositivity might underestimate actual exposure to MERS-CoV. Previous studies have demonstrated that examining MERS-CoV–specific T cells from MERS patients is more sensitive than examining serum antibodies alone (*27*). To examine T-cell responses, peripheral blood mononuclear cells must be collected, which was beyond the scope of our study.

On multivariable analysis, we found that contact with camels or their waste, working as a camel salesman, and self-reported diabetes were all independently associated with seropositivity in all workers. Because of small stratum size, belonging to other occupational groups could not be meaningfully explored as risk factors. Diabetes has previously been shown to be a commonly reported underlying condition in MERS cases (*28*), has been associated with risk for infection in a case–control study (*19*), and has been associated with increased risk for death in MERS patients (*29*). We found an association between diabetes and MERS-CoV seropositivity in a cohort with occupational exposure to camels. Although persons with diabetes might be at increased risk for MERS-CoV infection, the association between diabetes, MERS-CoV infection, and the resulting antibody response is still not fully understood.

Table 3. Comparison of practices among 90 MERS-CoV seronegative and seropositive slaughterhouse workers, Abu Dhabi, United Arab Emirates*

Characteristic	Total no. participants	No. (%) participants		OR (95% CI)	p value
		Seronegative, n = 79	Seropositive, n = 11		
Handle live camels	56	49 (87.5)	7 (12.5)	1.07 (0.3–4.37)	0.918
Perform antemortem exam of camels	6	5 (83.3)	1 (16.7)	1.48 (0.07–10.5)	0.732
Remove hide from camels†	52	46 (88.5)	6 (11.5)	0.83 (0.23–3.12)	0.780
Remove or handle viscera of camels‡	55	48 (87.3)	7 (12.7)	1.51 (0.39–7.4)	0.573
Clean equipment	68	58 (85.3)	10 (14.7)	3.62 (0.63–68.47)	0.233
Handle camel waste	57	50 (87.7)	7 (12.3)	1.01 (0.28–4.15)	0.982
Prepare cuts of camel meat	52	45 (86.5)	7 (13.5)	1.32 (0.37–5.39)	0.675
Conduct postmortem exam of camels	3	2 (66.7)	1 (33.3)	3.85 (0.17–43.92)	0.288
Slaughter camels	41	36 (87.8)	5 (12.2)	1 (0.27–3.57)	0.994
Contact with ill camel	3	2 (66.7)	1 (33.3)	3.85 (0.17–43.92)	0.288
Wear dust mask and gloves	88	77 (87.5)	11 (12.5)	NA	NA
Wear respirator	0	0	0	NA	NA
Wear coveralls	85	74 (87.1)	11 (12.9)	NA	NA
Wear boots	85	74 (87.1)	11 (12.9)	NA	NA
Who washes your clothes					
Self	30	28 (93.3)	2 (6.7)	Ref	Ref
Household member	2	0	2 (100.0)	NA	NA
Other worker	58	51 (87.9)	7 (12.1)	1.92 (0.43–13.49)	0.434
Take work clothes home	33	29 (87.9)	4 (12.1)	0.99 (0.24–3.55)	0.982
Wash work clothes at home	31	27 (87.1)	4 (12.9)	1.1 (0.27–3.98)	0.886
Wash work clothes at workplace	58	51 (87.9)	7 (12.1)	0.96 (0.27–3.93)	0.952
Wash work clothes at laundry	2	2 (100.0)	0	NA	NA
Wash hands before and after each animal-related task	73	64 (87.7)	9 (12.3)	1.05 (0.24–7.39)	0.949
Wash hands at mealtimes	89	78 (87.6)	11 (12.4)	NA	NA
Wash hands at bathroom times	90	79 (87.8)	11 (12.2)	NA	NA
Wash hands at prayer times	88	78 (88.6)	10 (11.4)	0.13 (0–3.41)	0.158
Wash hands at beginning and end of day	84	75 (89.3)	9 (10.7)	0.24 (0.04–1.9)	0.127
Wash hands at toilets	86	76 (88.4)	10 (11.6)	0.39 (0.05–8.4)	0.440
Wash hands at restaurant	0	0	0	NA	NA
Wash hands at mosque	3	3 (100.0)	0	NA	NA
Wash hands at basin	47	43 (91.5)	4 (8.5)	0.48 (0.12–1.71)	0.268

*Exam, examination; MERS-CoV, Middle East respiratory syndrome coronavirus, NA, not applicable; OR, odds ratio.
†Total seronegative was 78 because answer from 1 person was missing.
‡Total seropositive was 10 because answer from 1 person was missing.

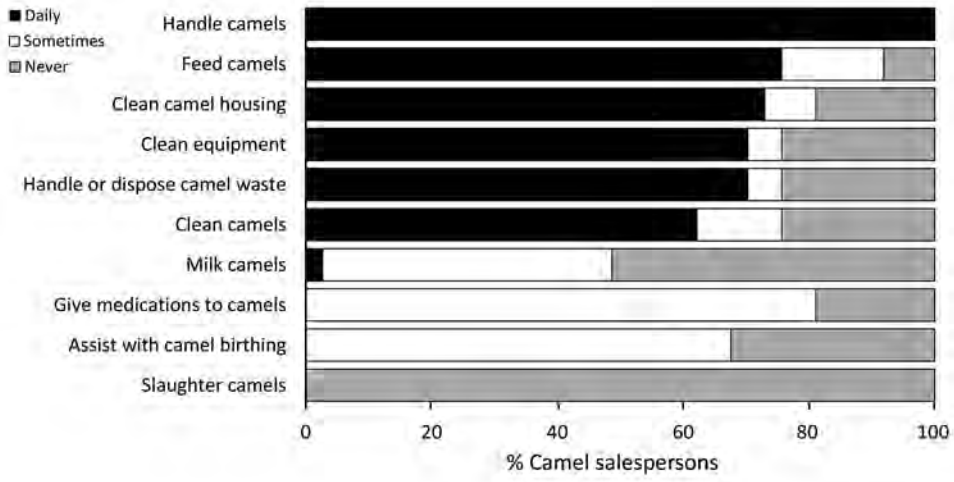

Figure 3. Frequency of tasks performed by camel salesmen (N = 37) in market, Abu Dhabi, United Arab Emirates.

However, because persons with diabetes are considered at high risk for developing severe disease from MERS-CoV infection, WHO recommends these persons take precautions when visiting farms or markets where camels are present, including avoiding contact with camels (*3*).

Among market workers, handling live camels and either administering medications to camels or cleaning equipment were practices associated with significantly increased risk for MERS-CoV seropositivity. Given that administering medications to camels was highly correlated with cleaning equipment, neither factor was statistically significant if both were included in the model. The biological importance of these associations might therefore be difficult to interpret, because either or both risk factors could be statistically associated with MERS-CoV seropositivity and have an undefined strength of association. Practices potentially associated with camel calves, such as milking or assisting with camel birth, were not associated with MERS-CoV seropositivity despite a higher prevalence of viral RNA in camels <1 year of age compared with other ages (*30*) and a previously reported association between milking camels frequently and seropositivity (*31*). However, these practices were not commonly reported by market workers in our study, limiting the power to detect an association with seropositivity.

No specific work practices were found to be associated with seropositivity among slaughterhouse workers. Compared with market workers, slaughterhouse workers had less exposure to live camels and a higher self-reported prevalence of potentially protective practices such as PPE use and frequent handwashing. Although our multivariable analysis did not show a significant association between PPE use (e.g., wearing a dust mask and gloves) or handwashing practices and seropositivity, the small sample size might have restricted the power to detect interactions between PPE and camel exposures. Because camel-to-human transmission of MERS-CoV is not fully understood, WHO recommends broad preventive measures for slaughterhouse and market workers, including wearing facial protection when feasible, washing hands before and after each animal-related task, and washing soiled work clothes and shoes at the work place to avoid exposing family members to soiled work clothing (*3*). Where feasible, increased use of such measures could be encouraged, particularly in market workers, to decrease risk for infection.

Because only a single human MERS case has been reported in connection with the study site, our reported rates of seroprevalence suggest unrecognized transmission (and potentially unrecognized illness) at this site. However, because the length of time MERS-CoV antibodies persist is unknown (*32*), the time and place these infections might have occurred is unknown; transmission potential also exists in the United Arab Emirates outside of markets and slaughterhouses. Whether infections were symptomatic is also unknown. Participants were asked whether they had seen a healthcare provider for respiratory illness in the previous 12 months, but such reported illness was not associated with seropositivity, and multiple pathogens other than MERS-CoV could be responsible for any reported respiratory illness. Despite these limitations, MERS-CoV was detected in camels at the market during our study period (*25*), and an interim seroconversion was noted in 1 worker, suggesting active zoonotic transmission. Taken collectively, our findings suggest an underestimated prevalence of human MERS-CoV infection in settings where the virus is circulating among camels, probably resulting from camel-to-human transmission.

Our study had additional limitations, including the overall sample size and limited number of subjects within specific substrata. Concentration of camel interactions within particular occupational groups limited our ability to differentiate risk among specific camel interactions, despite our use of multivariable analysis. Furthermore, because most persons reported interactions either daily or never, determining whether increased risk was associated with increased frequency of individual tasks was not possible. Also, some MERS-CoV infections might not result in detectable

antibodies, particularly when the infections are asymptomatic or mild (*32*). Persistence of detectable MERS-CoV antibodies after infection is not well-defined, limiting the ability of serologic testing to define previous infection. Finally, because of incomplete linkage of study participants by medical record numbers across the 3 sampling periods, not all potential seroconversions or losses of seropositivity could be determined.

In summary, our study found significantly increased odds of MERS-CoV seropositivity in persons with exposure to camels, in particular among those who handle live camels. Odds of seropositivity were also significantly higher for camel salesmen, suggesting that preventive measures such as PPE use could focus on specific occupational groups, in addition to individual work practices. Determining groups at highest risk for zoonotic MERS-CoV infection could also inform future vaccine trials in geographic regions where MERS-CoV is known to circulate.

Acknowledgments

We thank Yassir Eltahir for critical input during the conceptualization and implementation of this study.

CDC and the Abu Dhabi Department of Health in the United Arab Emirates funded this study.

This investigation was considered a public health response by the Abu Dhabi Department of Health and CDC.

About the Author

Dr. Khudair is a senior officer in the Communicable Disease Control and Management Section of the Abu Dhabi Department of Health. His research interests include MERS-CoV and tuberculosis. Dr. Killerby is an epidemiologist in the Division of Viral Diseases, National Center for Immunization and Respiratory Diseases, CDC. Her research interests include respiratory viruses such as MERS-CoV, human coronaviruses, and adenoviruses.

References

1. Zaki AM, van Boheemen S, Bestebroer TM, Osterhaus ADME, Fouchier RAM. Isolation of a novel coronavirus from a man with pneumonia in Saudi Arabia. N Engl J Med. 2012;367:1814–20. http://dx.doi.org/10.1056/NEJMoa1211721
2. World Health Organization. Middle East respiratory syndrome coronavirus (MERS-CoV) [cited 2019 Apr 3]. http://www.who.int/emergencies/mers-cov
3. World Health Organization. WHO MERS-CoV global summary and assessment of risk, 21 July 2017 [cited 2018 Aug 7]. https://www.who.int/emergencies/mers-cov/risk-assessment-july-2017.pdf
4. Mohd HA, Al-Tawfiq JA, Memish ZA. Middle East respiratory syndrome coronavirus (MERS-CoV) origin and animal reservoir. Virol J. 2016;13:87. http://dx.doi.org/10.1186/s12985-016-0544-0
5. Omrani AS, Al-Tawfiq JA, Memish ZA. Middle East respiratory syndrome coronavirus (MERS-CoV): animal to human interaction. Pathog Glob Health. 2015;109:354–62. http://dx.doi.org/10.1080/20477724.2015.1122852
6. Miguel E, Chevalier V, Ayelet G, Ben Bencheikh MN, Boussini H, Chu DK, et al. Risk factors for MERS coronavirus infection in dromedary camels in Burkina Faso, Ethiopia, and Morocco, 2015. Euro Surveill. 2017;22:30498. http://dx.doi.org/10.2807/1560-7917.ES.2017.22.13.30498
7. Chu DKW, Hui KPY, Perera RAPM, Miguel E, Niemeyer D, Zhao J, et al. MERS coronaviruses from camels in Africa exhibit region-dependent genetic diversity. Proc Natl Acad Sci U S A. 2018;115:3144–9. http://dx.doi.org/10.1073/pnas.1718769115
8. Alagaili AN, Briese T, Mishra N, Kapoor V, Sameroff SC, Burbelo PD, et al. Middle East respiratory syndrome coronavirus infection in dromedary camels in Saudi Arabia. MBio. 2014;5:e00884–14. http://dx.doi.org/10.1128/mBio.01002-14
9. Yusof MF, Eltahir YM, Serhan WS, Hashem FM, Elsayed EA, Marzoug BA, et al. Prevalence of Middle East respiratory syndrome coronavirus (MERS-CoV) in dromedary camels in Abu Dhabi Emirate, United Arab Emirates. Virus Genes. 2015;50:509–13. http://dx.doi.org/10.1007/s11262-015-1174-0
10. Haagmans BL, Al Dhahiry SHS, Reusken CBEM, Raj VS, Galiano M, Myers R, et al. Middle East respiratory syndrome coronavirus in dromedary camels: an outbreak investigation. Lancet Infect Dis. 2014;14:140–5. http://dx.doi.org/10.1016/S1473-3099(13)70690-X
11. Chu DK, Oladipo JO, Perera RA, Kuranga SA, Chan SM, Poon LL, et al. Middle East respiratory syndrome coronavirus (MERS-CoV) in dromedary camels in Nigeria, 2015. Euro Surveill. 2015;20:30086. http://dx.doi.org/10.2807/1560-7917.ES.2015.20.49.30086
12. Meyer B, Müller MA, Corman VM, Reusken CB, Ritz D, Godeke GJ, et al. Antibodies against MERS coronavirus in dromedary camels, United Arab Emirates, 2003 and 2013. Emerg Infect Dis. 2014;20:552–9. http://dx.doi.org/10.3201/eid2004.131746
13. Reusken CB, Messadi L, Feyisa A, Ularamu H, Godeke GJ, Danmarwa A, et al. Geographic distribution of MERS coronavirus among dromedary camels, Africa. Emerg Infect Dis. 2014;20:1370–4. http://dx.doi.org/10.3201/eid2008.140590
14. Hemida MG, Chu DK, Poon LL, Perera RA, Alhammadi MA, Ng HY, et al. MERS coronavirus in dromedary camel herd, Saudi Arabia. Emerg Infect Dis. 2014;20:1231–4. http://dx.doi.org/10.3201/eid2007.140571
15. Reusken CB, Farag EA, Jonges M, Godeke GJ, El-Sayed AM, Pas SD, et al. Middle East respiratory syndrome coronavirus (MERS-CoV) RNA and neutralising antibodies in milk collected according to local customs from dromedary camels, Qatar, April 2014. Euro Surveill. 2014;19:20829. http://dx.doi.org/10.2807/1560-7917.ES2014.19.23.20829
16. Memish ZA, Cotten M, Meyer B, Watson SJ, Alsahafi AJ, Al Rabeeah AA, et al. Human infection with MERS coronavirus after exposure to infected camels, Saudi Arabia, 2013. Emerg Infect Dis. 2014;20:1012–5. http://dx.doi.org/10.3201/eid2006.140402
17. Farag EA, Reusken CB, Haagmans BL, Mohran KA, Stalin Raj V, Pas SD, et al. High proportion of MERS-CoV shedding dromedaries at slaughterhouse with a potential epidemiological link to human cases, Qatar 2014. Infect Ecol Epidemiol. 2015;5:28305. http://dx.doi.org/10.3402/iee.v5.28305
18. Paden C, Yusof M, Al Hammadi Z, Queen K, Tao Y, Eltahir Y, et al. Zoonotic origin and transmission of Middle East respiratory syndrome coronavirus in the UAE. Zoonoses Public Health. 2017.
19. Alraddadi BM, Watson JT, Almarashi A, Abedi GR, Turkistani A, Sadran M, et al. Risk factors for primary Middle East Respiratory syndrome coronavirus illness in humans, Saudi Arabia, 2014. Emerg Infect Dis. 2016;22:49–55. http://dx.doi.org/10.3201/eid2201.151340

20. Müller MA, Meyer B, Corman VM, Al-Masri M, Turkestani A, Ritz D, et al. Presence of Middle East respiratory syndrome coronavirus antibodies in Saudi Arabia: a nationwide, cross-sectional, serological study. Lancet Infect Dis. 2015;15:559–64. http://dx.doi.org/10.1016/S1473-3099(15)70090-3
21. Reusken CB, Farag EA, Haagmans BL, Mohran KA, Godeke GJ V, Raj S, et al. Occupational exposure to dromedaries and risk for MERS-CoV infection, Qatar, 2013–2014. Emerg Infect Dis. 2015;21:1422–5. http://dx.doi.org/10.3201/eid2108.150481
22. Alshukairi AN, Zheng J, Zhao J, Nehdi A, Baharoon SA, Layqah L, et al. High prevalence of MERS-CoV infection in camel workers in Saudi Arabia. MBio. 2018;9:e01985–18. http://dx.doi.org/10.1128/mBio.01985-18
23. Inovio Pharmaceuticals I. Inovio's MERS vaccine generates high levels of antibodies and induces broad-based T Cell responses in phase 1 study [cited 2018 Aug 24]. http://ir.inovio.com/news-and-media/news/press-release-details/2018/Inovios-MERS-Vaccine-Generates-High-Levels-of-Antibodies-and-Induces-Broad-based-T-Cell-Responses-in-Phase-1-Study/default.aspx
24. Sample I. Man in Germany dies of complications stemming from Mers virus. 2015 Jun 16 [cited 2018 Aug 7]. https://www.theguardian.com/science/2015/jun/16/mers-virus-man-dies-germany
25. Yusof MF, Queen K, Eltahir YM, Paden CR, Al Hammadi ZMAH, Tao Y, et al. Diversity of Middle East respiratory syndrome coronaviruses in 109 dromedary camels based on full-genome sequencing, Abu Dhabi, United Arab Emirates. Emerg Microbes Infect. 2017;6:e101. http://dx.doi.org/10.1038/emi.2017.89
26. Trivedi S, Miao C, Al-Abdallat MM, Haddadin A, Alqasrawi S, Iblan I, et al. Inclusion of MERS-spike protein ELISA in algorithm to determine serologic evidence of MERS-CoV infection. J Med Virol. 2018;90:367–71. http://dx.doi.org/10.1002/jmv.24948
27. Zhao J, Alshukairi AN, Baharoon SA, Ahmed WA, Bokhari AA, Nehdi AM, et al. Recovery from the Middle East respiratory syndrome is associated with antibody and T-cell responses. Sci Immunol. 2017;2:eaan5393. http://dx.doi.org/10.1126/sciimmunol.aan5393
28. Assiri A, Al-Tawfiq JA, Al-Rabeeah AA, Al-Rabiah FA, Al-Hajjar S, Al-Barrak A, et al. Epidemiological, demographic, and clinical characteristics of 47 cases of Middle East respiratory syndrome coronavirus disease from Saudi Arabia: a descriptive study. Lancet Infect Dis. 2013;13:752–61. http://dx.doi.org/10.1016/S1473-3099(13)70204-4
29. Choi WS, Kang CI, Kim Y, Choi JP, Joh JS, Shin HS, et al.; Korean Society of Infectious Diseases. Clinical presentation and outcomes of Middle East respiratory syndrome in the Republic of Korea. Infect Chemother. 2016;48:118–26. http://dx.doi.org/10.3947/ic.2016.48.2.118
30. Wernery U, Corman VM, Wong EY, Tsang AK, Muth D, Lau SK, et al. Acute Middle East respiratory syndrome coronavirus infection in livestock dromedaries, Dubai, 2014. Emerg Infect Dis. 2015;21:1019–22. http://dx.doi.org/10.3201/eid2106.150038
31. Sikkema RS, Farag EABA, Himatt S, Ibrahim AK, Al-Romaihi H, Al-Marri SA, et al. Risk factors for primary Middle East respiratory syndrome coronavirus infection in camel workers in Qatar during 2013–2014: a case-control study. J Infect Dis. 2017;215:1702–5. http://dx.doi.org/10.1093/infdis/jix174
32. Choe PG, Perera RAPM, Park WB, Song K-H, Bang JH, Kim ES, et al. MERS-CoV antibody responses 1 year after symptom onset, South Korea, 2015. Emerg Infect Dis. 2017;23:1079–84. http://dx.doi.org/10.3201/eid2307.170310

Address for correspondence: Marie E. Killerby, Centers for Disease Control and Prevention, 1600 Clifton Road NE, Mailstop H24-5, Atlanta, GA 30329-4027, USA; email: lxo9@cdc.gov

Outcomes of Bedaquiline Treatment in Patients with Multidrug-Resistant Tuberculosis

Lawrence Mbuagbaw, Lorenzo Guglielmetti, Catherine Hewison, Nyasha Bakare, Mathieu Bastard, Eric Caumes, Mathilde Fréchet-Jachym, Jérôme Robert, Nicolas Veziris, Naira Khachatryan, Tinatin Kotrikadze, Armen Hayrapetyan, Zaza Avaliani, Holger J. Schünemann, Christian Lienhardt

Bedaquiline is recommended by the World Health Organization for the treatment of multidrug-resistant (MDR) and extensively drug-resistant (XDR) tuberculosis (TB). We pooled data from 5 cohorts of patients treated with bedaquiline in France, Georgia, Armenia, and South Africa and in a multicountry study. The rate of culture conversion to negative at 6 months (by the end of 6 months of treatment) was 78% (95% CI 73.5%–81.9%), and the treatment success rate was 65.8% (95% CI 59.9%–71.3%). Death rate was 11.7% (95% CI 7.0%–19.1%). Up to 91.1% (95% CI 82.2%–95.8%) of the patients experienced ≥1 adverse event, and 11.2% (95% CI 5.0%–23.2%) experienced a serious adverse event. Lung cavitations were consistently associated with unfavorable outcomes. The use of bedaquiline in MDR and XDR TB treatment regimens appears to be effective and safe across different settings, although the certainty of evidence was assessed as very low.

Author affiliations: St. Joseph's Healthcare Hamilton, Hamilton, Ontario, Canada (L. Mbuagbaw); Centre for the Development of Best Practices in Health, Yaoundé, Cameroon (L. Mbuagbaw); McMaster University, Hamilton (L. Mbuagbaw, H.J. Schünemann); Centre d'Immunologie et des Maladies Infectieuses, INSERM, Paris (L. Guglielmetti, E. Caumes, J. Robert, N. Veziris); Centre Hospitalier de Bligny, Bris-sous-Forges, France (L. Guglielmetti, M. Fréchet-Jachym); Sorbonne Université, Paris, France (L. Guglielmetti, J. Robert, N. Veziris); Médecins Sans Frontières, Paris (C. Hewison); Janssen Research & Development, LLC, Titusville, New Jersey, USA (N. Bakare); Epicentre, Paris (M. Bastard); Hôpitaux Universitaires de l'Est Parisien, Paris (N. Veziris); Médecins Sans Frontières, Yerevan, Armenia (N. Khachatryan); Médecins Sans Frontières, Tbilisi, Georgia (T. Kotrikadze); National Tuberculosis Control Centre, Yerevan (A. Hayrapetyan); National Centre for Tuberculosis and Lung Disease, Tbilisi (Z. Avaliani); World Health Organization, Geneva, Switzerland (C. Lienhardt); Université de Montpellier, Montpellier, France (C. Lienhardt)

DOI: https://doi.org/10.3201/eid2505.181823

In 2017, there were ≈10 million (range, 9.0–11.1 million) new cases of tuberculosis (TB) worldwide, of which ≈558,000 were rifampin-resistant TB (RR TB) or multidrug-resistant TB (MDR TB) (*1*). MDR TB refers to resistance to isoniazid and rifampin, 2 of the most powerful TB drugs, with or without resistance to other first-line drugs. Extensively drug-resistant tuberculosis (XDR TB), a more severe form of drug-resistant TB, is defined as MDR TB with additional resistance to any fluoroquinolone and to any of the 3 second-line injectables (amikacin, capreomycin, or kanamycin) (*2*). Treatment outcomes in patients with MDR TB are generally poor, with treatment success in about half of those who receive treatment (56.4%), and much worse in patients with XDR TB (*3*). In 2017, MDR TB and RR TB caused ≈230,000 deaths (*1*). The treatment of MDR and XDR TB is complex and expensive, requiring the use of ≥4 medications considered to be active in longer regimens (18–20 months) (*4*–*6*), and is fraught with many adverse events that can be debilitating or life threatening (*7*,*8*).

Bedaquiline is a new compound belonging to the diarylquinoline class used to treat MDR TB; cure and culture conversion rates using bedaquiline are promising (*9*,*10*). A recent cost-effectiveness analysis showed that bedaquiline added to a background MDR TB regimen would improve health outcomes and reduce costs in high TB burden countries (*11*). Bedaquiline received accelerated approval in the United States in 2012 for the treatment of pulmonary MDR TB as part of an appropriate combination therapy in adult patients with resistance or intolerability to other treatment regimens. However, in 2013, limited data and concerns about higher death rates among patients who received bedaquiline in the phase II randomized controlled trial (*10*) led the World Health Organization (WHO) to issue an interim conditional recommendation on its use under specific conditions: proper patient inclusion, signed informed consent, adherence to the WHO-recommended principles of designing an MDR TB regimen, close monitoring, and active pharmacovigilance (*12*). Since 2013, many countries

have introduced bedaquiline as part of their management strategy for MDR TB, and in 2018, WHO updated its guidance for the use of bedaquiline in MDR TB, including children ≥6 years of age (*6*).

In 2016, to update the interim guidance, the WHO Guideline Development Group (GDG) conducted a review of newly available data on the use of bedaquiline in the treatment of MDR TB (*13*). After the publication of the GDG report, further outcome data were retrieved from cohorts in Armenia and Georgia. We report the results of the updated analysis from 5 cohorts of patients with MDR TB treated with bedaquiline, taking into account both study-level and patient-level characteristics on outcomes, including deaths. We also report on the use of bedaquiline in research and nonresearch settings and on adverse events.

Materials and Methods

Data Sources

We pooled data from 5 cohorts of patients with MDR or XDR TB treated with bedaquiline as part of compassionate use, programmatic use, expanded access, or research programs. The processes and methods used to search, screen, and select studies have been reported previously (*13*). In brief, studies and datasets were considered only if they met the following inclusion criteria: participants received a diagnosis of MDR TB and were treated with bedaquiline for ≥6 months as part of an anti-TB regimen. We excluded studies of bedaquiline-only therapy, studies not providing details of the background regimens, studies not providing outcome information, and studies with <10 participants. We contacted national TB programs, nongovernmental organizations, and the drug manufacturer, Janssen Therapeutics (https://www.janssen.com), for unpublished data that fit the criteria.

Our search retrieved 674 studies, of which only 5 were eligible. The 5 datasets that were finally included for the individual patient data (IPD) meta-analyses originated from Médecins Sans Frontières, which contributed 2 cohorts on behalf of the national TB programs of Armenia and Georgia; the national TB program of South Africa; the Hospital of Bligny, France; and Janssen Therapeutics. All the cohort studies have been published in complete form (*14*–*17*) (Table 1).

Data Management

We invited the investigators of each study to provide data on the basis of a formal data sharing agreement. We used only anonymized data in this study. We cleaned, recoded, and merged data from the 5 cohorts and saved the data on a secure server at the biostatistics unit of St Joseph's Healthcare Hamilton/McMaster University (Hamilton, Ontario, Canada). We contacted investigators of each study to ensure accuracy after recoding. We modified categorical variables to match the most commonly used format to ensure consistency across studies. For example, for data from chest radiography, the presence or absence of lung cavitation was the most commonly reported format for findings, so we collapsed data pertaining to the site of the cavitation (left or right lung) or the number of cavitations. We corrected QT intervals for heart rate using the Fridericia formula (QTcF) (*18*). We categorized drug resistance in order of increasing severity as MDR TB (resistance to isoniazid and rifampin, with or without resistance to other first-line drugs), MDR TB + FLQ (additional resistance to fluoroquinolones), MDR TB + INJ (additional resistance to second-line injectables), and XDR (resistance to at least isoniazid and rifampin, and to any fluoroquinolone, and to any second-line injectables).

Outcomes

Using standard WHO definitions, we measured the following treatment outcomes: cure, treatment completion, treatment success (the sum of cure and treatment completion), loss to follow-up, and death (*19*). We computed culture conversion at 6 months as 2 consecutive cultures, taken ≥30 days apart, found to be negative before or at the end of the sixth month of treatment. Adverse event severity and seriousness were defined as by the US Food and Drug Administration (*20*), or as reported by investigators. We measured the following adverse event outcomes: any adverse event, any serious adverse event, number of adverse events by body system, and QT interval prolongation (highest recorded QTcF value and increase from baseline).

Statistical Methods

We summarized baseline data as mean (± SD) for continuous variables and frequency (%) for categorical variables.

Table 1. Characteristics of cohorts in study of bedaquiline treatment for multidrug-resistant tuberculosis

Cohort	Design	Location	Sample size	Inception date	Type of care
Pym 2013 (*14*)	Phase II, single-arm open-label trial	31 sites, 11 countries*	233	2009 Aug	Research
Guglielmetti 2017 (*15*)	Retrospective cohort	France	45	2010 Jan	Expanded access
Ndjeka 2018 (*16*)	Prospective cohort	South Africa	195	2013 Mar	Compassionate use
Hewison 2018 (*17*)	Prospective cohort	Armenia	62	2013 Apr	Compassionate use
	Prospective cohort	Georgia	30		Compassionate use (20), programmatic use (10)

*China, Estonia, Republic of Korea, Latvia, Peru, Philippines, Russian Federation, South Africa, Thailand, Turkey, Ukraine.

We conducted a random effects meta-analysis of proportions in the first instance to pool effect sizes for effectiveness and safety. The random effects model incorporates the heterogeneity between studies and redistributes the weights of the studies based on this heterogeneity. We assessed statistical heterogeneity using the I^2 statistic, a measure of heterogeneity between studies. We reported variables and outcomes with various levels of completeness and highlighted them where appropriate. For example, we computed culture conversion only if cultures were examined at the sixth month and not later. Similarly, we used baseline QTcF data only if data were collected within 1 month of starting bedaquiline. We used generalized estimation equations to model the effect of individual- and study-level characteristics on outcomes. We built separate models for the dependent binary (yes/no) variables, culture conversion at 6 months, treatment success, and death, using an unstructured correlation matrix and the logit link. The independent variables (age, sex, HIV status, presence of lung cavitations, severity of drug resistance, and previous use of second-line drugs) are all known to affect outcomes in TB (*21*,*22*). We assessed model fit using the quasi-likelihood under independence model criterion and set the level of statistical significance at $\alpha = 0.05$. We used different numbers of patients for each analysis because of variations in completeness and availability of data. Samples used for each analysis are shown in Appendix Table 1 (https://wwwnc.cdc.gov/EID/article/25/5/18-1823-App1.pdf).

Certainty Evaluation

We assessed the certainty of the evidence using the Grading of Recommendations, Assessment, Development, and Evaluation (GRADE) approach, which categorizes each outcome by how confident we are that the effect estimate is close to the quantity of interest (*23*). Using this approach, the certainty rating across studies can be high, moderate, low, or very low. We summarized the results and certainty as evidence profiles.

Results

We included a total of 537 participants in the data analysis. Baseline characteristics are shown in detail by cohort and overall in Table 2. The mean age was 36.4 years (SD 11.8). Two thirds of the participants were men (342; 63.7%); 138 (25.7%) were HIV positive; 341 (99.7%) had pulmonary TB, 253 (73.9%) with lung cavities; and 188 (35.0%) had XDR TB. The key differences between the datasets were a higher proportion of male participants in the cohorts from France and Armenia; 63.1% participants having concurrent HIV in the South Africa cohort; and complete outcome data being available from only 51% of all participants because others were still receiving treatment at the time we collected data. Of note, 36 (6.7%) patients received bedaquiline for ≥6 months.

The baseline regimens we used in the cohorts varied according to local treatment guidelines, drug susceptibility results, or both. Lamivudine, nevirapine, efavirenz, and tenofovir were the most frequently used drugs

Table 2. Baseline characteristics of participants in study of bedaquiline treatment for multidrug-resistant tuberculosis*

Variable	Cohort					Total, n = 537
	South Africa, n = 195	France, n = 45	Janssen, n = 205	Armenia, n = 62	Georgia, n = 30	
Mean age, y (SD)	35.8 (11.2)	37.4 (12.1)	34.9 (12.2)	41.6 (12.6)	38.7 (11.9)	36.4 (11.8)
Sex, no. (%)						
M	98 (50.3)	36 (80.0)	132 (64.4)	55 (88.7)	21 (70.0)	342 (63.7)
F	97 (49.7)	9 (20.0)	73 (35.6)	7 (11.3)	9 (30.0)	195 (36.3)
Mean no. months on BDQ (SD)	5.8 (1.2)	12.3 (7.0)	5.9 (1.1)	5.6 (1.6)	6.0 (1.3)	6.37 (2.3)
No. on BDQ >6 mo (%)	4 (2.1)	32 (71.1)	0.0	0.0	0.0	36 (6.7)†
Mean total treatment duration, mo (SD)	14.9 (6.7)	19.4 (4.7)	21.8 (7.6)	20.2(7.4)	14.0 (6.1)	18.47 (6.9)†
No. (%) with treatment outcome available	101 (51.8)†	45 (100.0)	205 (100.0)	62 (100.0)	30 (100.0)	443 (82.5)
No. (%) HIV positive‡	120 (63.1)	2 (4.4)	8 (4.0)	4 (6.5)	1 (3.3)	135 (25.1)
No. (%) on antiretroviral therapy	110 (56.4)	2 (4.4)	0.0	0	0	112 (20.9)
Type of TB, no. (%)						
Pulmonary	NR	44 (97.8)	205 (100.0)	62 (100.0)	30 (100.0)	341 (99.7)
Extrapulmonary	NR	8 (17.8)	0	0	0	8 (2.3)
No. (%) with previous TB treatment	NR	34 (75.6)	193 (94.1)	62 (100.0)	29 (96.7)	271 (79.2)
No. (%) with previous second-line TB treatment	NR	27 (60.0)	177 (86.3)	62 (100.0)	29 (96.7)	295 (86.3)
No. (%) with lung cavities on chest radiograph	NR	39 (86.7)	135 (65.8)	55 (88.7)	24 (80.0)	253 (73.9)
Resistance profile, no. (%)§						
MDR TB	0	7 (15.6)	93 (45.4)	6 (9.7)	0	100 (18.6)
MDR TB + FQ	73 (37.4)	8 (17.8)	31 (15.1)	26 (41.9)	5 (16.7)	147(27.3)
MDR TB + INJ	29 (14.9)	6 (13.3)	13 (6.3)	7 (11.3)	0	55 (10.2)
XDR TB	77 (39.5)	24 (53.3)	37 (18.0)	23 (37.1)	25 (83.3)	188 (35.0)

*BDQ, bedaquiline; FQ, fluoroquinolone; INJ, injectable; MDR, multidrug resistant; NR, not reported; TB, tuberculosis; XDR, extensively drug resistant.
†Missing data: South Africa = 15.
‡Missing data: South Africa = 17; Janssen (drug manufacturer) = 7.
§Missing data: South Africa = 16; Janssen (drug manufacturer) = 31.

Table 3. Multivariable analyses for key outcomes in study of bedaquiline treatment for MDR TB*

	Culture conversion at 6 mo, n = 318		Success, n = 325		Death, n = 325	
Covariate	Adjusted OR (95% CI)	p value	Adjusted OR (95% CI)	p value	Adjusted OR (95% CI)	p value
Male sex	1.25 (0.65–2.41)	0.499	1.27 (0.74–2.15)	0.382	0.60 (0.24–1.47)	0.264
Age, y	1.01 (0.99–1.04)	0.342	0.99 (0.98–1.01)	0.550	1.05 (1.01–1.09)	0.010
HIV positive	0.42 (0.13–1.39)	0.155	0.35 (0.12–0.99)	0.050	0.97 (0.09–10.05)	0.982
Resistance profile†	0.57 (0.43–0.76)	<0.001	0.84 (0.68 –1.04)	0.110	1.14 (0.73–1.79)	0.562
Presence of lung cavitation	0.30 (0.13–0.70)	0.004	0.38 (0.21–0.68)	0.001	5.31 (1.25–22.52)	0.023
Previous use of second-line drugs	0.67 (0.22–2.01)	0.437	0.73 (0.33–1.59)	0.423	1.22 (0.29–5.15)	0.783

*Absence of data on cavitation precluded use of data from South Africa. MDR, multidrug resistant; TB, tuberculosis; XDR, extensively drug resistant.
†Resistance profiles used in this study were MDR TB (reference), MDR TB plus fluoroquinolone, MDR TB plus injectable drugs, and XDR TB.

among the patients on antiretroviral therapy (Appendix Tables 2, 3).

We computed culture conversion at 6 months only for patients who had a positive sputum culture at baseline and 2 consecutive culture readings ≥30 days apart, the last taken at the end of the sixth month. Thirty-seven patients did not have sufficient culture data. Of 406 patients with sufficient culture data, the overall culture conversion rate at 6 months was 78.0% (95% CI 73.5%–81.9%; $I^2 = 46\%$). A total of 443/537 (82.5%) participants had end-of-treatment outcome data: cure, 60.1% (95% CI 50.2%–69.2%; $I^2 = 66\%$); treatment success, 65.8% (95% CI 59.9%–71.3%; $I^2 = 38\%$); death, 11.7% (95% CI 7.0%–19.1%; $I^2 = 71\%$); treatment failure, 5.1% (95% CI 1.6%–14.8%; $I^2 = 73\%$); and loss to follow-up, 14.8% (95% CI 11.6%–18.7%; $I^2 = 7\%$).

Safety data were available from a total of 565 participants, including an additional 28 participants from the Janssen cohort who were not eligible for efficacy analyses because they were missing a confirmation of

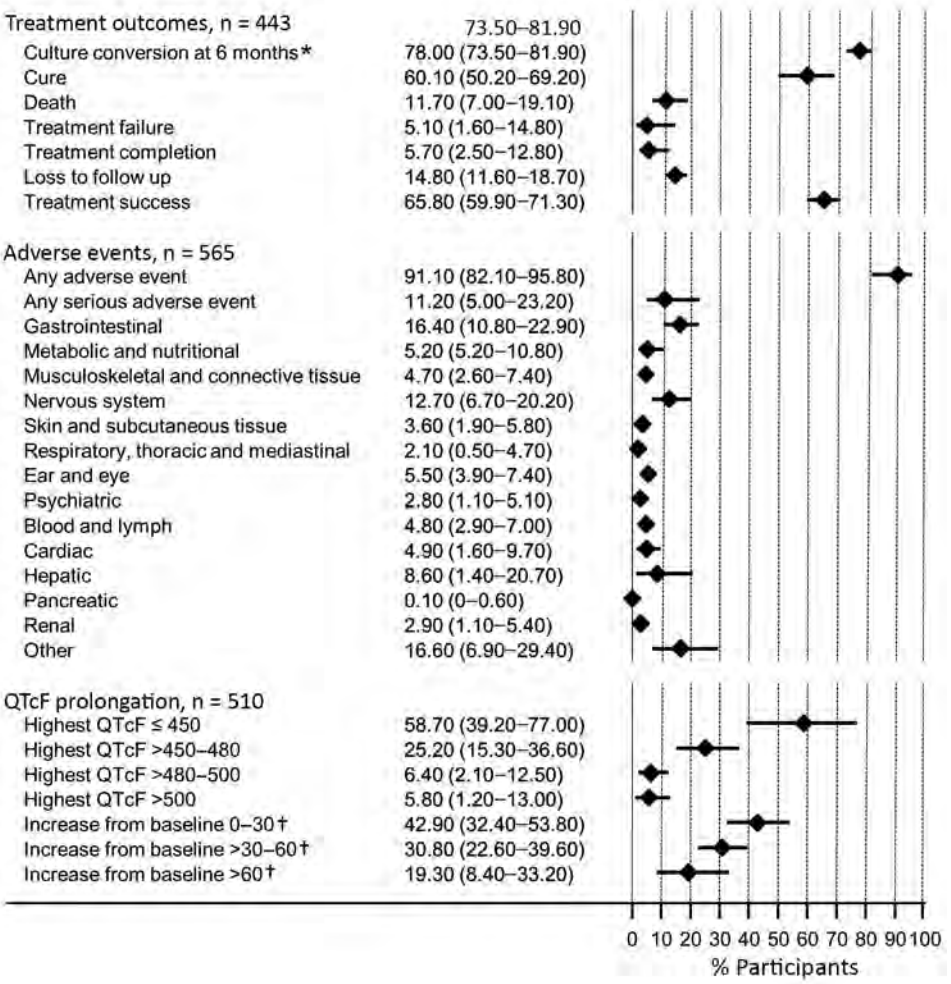

Figure. Summary of treatment outcomes and adverse events in study of bedaquiline treatment for multidrug-resistant tuberculosis. Values are shown as percent with 95% CI, shown in the graph as horizontal bars. QTcF indicates QT intervals corrected for heart rate using the Fridericia formula. *A total of 406 study participants with culture data at the 6-month point; † a total of 509 participants with baseline QTcF data.

MDR (n = 3) or a positive culture at baseline (n = 25). Of these participants, 91.1% (95% CI 82.2%–95.8%) experienced occurrence of any adverse event and 11.2% (5.0%–23.2%) occurrence of any serious adverse event. The most frequent adverse events were gastrointestinal (16.4%; 95% CI 10.8%–22.9%), nervous system (12.7; 95% CI 6.7%–20.2%), and hepatic (8.6%; 95% CI 1.4%–20.7%) (Figure).

We found that 5.8% of 510 participants (95% CI 1.2%–13.0%; I^2 = 84%) had a highest QTcF >500 ms and 19.3% of 509 (95% CI 8.4%–33.2%; I^2 = 93%) had an increase in QTcF from baseline of more >60 ms. Despite the small sample of patients receiving bedaquiline for a prolonged period (i.e., >6 months), data seem to indicate an absence of effect of exposure to bedaquiline for >6 months on QTc prolongation >500 ms.

Adjusted Analyses

Culture conversion at 6 months was less likely in patients with a more severe resistance profile (aOR 0.57, 95% CI 0.43–0.76; p<0.001) and with lung cavitations (aOR 0.30, 95% 0.13–0.70; p = 0.004). Treatment success was less likely in patients with lung cavitations (aOR 0.38, 95% CI 0.21–0.68; p = 0.001) and in those with HIV infection (aOR 0.35, 95% CI 0.12–0.99; p = 0.05). The presence of lung cavitations was associated with death (aOR 5.31, 95% 1.25–22.52; p = 0.023) (Table 3).

The GRADE evidence profile is reported in Appendix Table 4. The GDG judged evidence for all outcomes to be of very low certainty; reasons were the risk for bias (lack of control data), risk for inconsistency (considerable statistical heterogeneity), imprecision (wide confidence intervals), and indirectness (variations in adverse event definition) (*13*).

Discussion

Inclusion of bedaquiline for ≥6 months in the treatment regimen was associated with good outcomes in these cohorts, with 78% culture conversion at 6 months and a 65.8% treatment success rate, indicating a favorable efficacy of this medicine. Observed death rate was 11.7%. Although almost all patients experienced at least an adverse event (91.1%), only 11.2% experienced a serious one. Only 5.8% of patients had a highest recorded value of QTcF >500 ms and 19.3% had an increase QT from baseline of more than 60 ms. Being older, having a more severe resistance profile, concurrent HIV, and lung cavitation were associated with unfavorable outcomes.

Such results compare favorably with those observed in large cohorts of patients with MDR TB in the prebedaquiline era (with success rates of 54%–58% and death rates of 13.8%–15%) (*7*,*24*), thus indicating a beneficial effect of the addition of bedaquiline to background MDR/XDR TB regimens. Our findings are in line with those from a large South Africa cohort in which the additional use of bedaquiline reduced the risk for death in patients with MDR TB, compared with standard regimens (*25*). In a matched subset of patients from the South Africa cohort, switching from second-line injectables (because of intolerance) to bedaquiline led to fewer unfavorable outcomes (death, loss to follow-up, or treatment failure) (*26*). Likewise, an individual patient data meta-analysis of 50 studies (including this study's cohort data from France, South Africa, and Janssen Therapeutics) reported lower odds of death with the use of bedaquiline (*27*). The lower mortality rate we observed strengthens the case for the use of bedaquiline in patients with MDR TB. On the basis of data cumulated since 2012 from various observational and programmatic studies, including the South Africa cohort (*25*), WHO has now consolidated its recommendation for the use of bedaquiline, now proposed as a Group A drug (medicines to be prioritized) in longer MDR TB regimens (*6*).

Very few patients in our study had a highest recorded value of QTcF >500 ms. Other studies have found similarly low rates of cardiotoxicity (*28*). This finding could therefore alleviate some of the concerns around the risk for cardiotoxicity related with the use of bedaquiline (*28*).

Our study adds some information about the use of bedaquiline in persons living with HIV and indicates that favorable outcomes may be more challenging to achieve in these patients, bearing in mind that not all of them were on antiretroviral therapy as recommended by WHO. This information is important for countries with a high prevalence of HIV/TB co-infection. However, other reports indicate that the reductions in number of deaths are similar or better in persons living with HIV (*13*,*25*).

Our findings are similar to those observed in other large multicenter studies in terms of success, death, and adverse events (*4*), although higher culture conversion rates at 6 months were reported from studies in Belarus and Germany (*29*,*30*). Our findings should be interpreted with due consideration of the severity of illness in this cohort, in which up to 35% of patients had XDR TB, 86.3% previous second-line treatment, and 73.9% lung cavitations, suggesting that a success rate of 65.8% is probably higher than would otherwise be expected.

Currently, WHO does not recommend the routine use of bedaquiline for longer than 6 months (*6*). However, WHO acknowledges that "clinicians and national TB programs may be compelled to use [bedaquiline] beyond 24 weeks in selected MDR TB patients (including those with additional drug resistance), if the regimen is unlikely to achieve cure or poses a risk [of] creating additional drug resistance" (*31*). We were unable to properly investigate the effect of prolonged bedaquiline use in this study, given the small number of patients (6.7%) who received the

medicine for >6 months and the risk for bias by indication (bedaquiline offered to patients with more severe disease). However, we found no correlation between QTcF prolongation and extended bedaquiline use.

Overall, our data confirm that bedaquiline should be a Group A drug in the treatment of MDR TB, as currently recommended by WHO (*6*), for not only its additive value in culture conversion and treatment success, but also its safety in varied settings.

This study has some limitations. First, cohorts differed greatly in completeness and quality of data, because they were not all initially designed for research purposes. Some variables were defined differently and the timing and number of follow-up visits varied. To maximize the use of data, we tried to work with variables that were reported across all datasets. These methodological differences, in addition to baseline differences by settings (prevalence of HIV infection, provision of baseline regimens and antiretroviral therapy), probably caused high levels of heterogeneity reflected in the meta-analyses. Second, the absence of certain variables from given datasets precluded their use in the adjusted analyses. For example, at the time of these analyses, data on pulmonary cavitation or prior use of second-line drugs were not available from the South Africa cohort, and we had end-of-treatment data for only 51.8% of those patients. Third, the absence of comparative data from patients who did not receive bedaquiline limits the inferences that can be drawn from these data. Finally, we were unable to report a causality assessment of the adverse events. Because of these limitations, the certainty of evidence was rated by the independent GDG as very low for all outcomes for the purpose of GRADE evaluation in the June 2016 meeting (*13*). Although these concerns appear to limit the credibility of these findings, they represent a real-world picture of the use of bedaquiline under programmatic conditions, outside of research settings.

The strength of this work lies in the use of patient-level data and in the random effects approach used for analyses that embraces the heterogeneity across cohorts. Our results represent data from many countries with different income levels, suggesting that the findings are generalizable. However, whereas heterogeneity is duly accounted for, it is not fully explained, and I^2 values >50% warrant further investigation (*32*). Some study-level characteristics may contribute to the high levels of heterogeneity, such as the prevalence of HIV, extent of drug resistance, delivery of care, and data quality. Another strength of this work is the detailed information on adverse events by system, particularly the QTcF measurements, which are not usually captured in large databases and registries.

Despite the study strengths, some questions still remain unanswered, such as the role of prolonged use of bedaquiline and how best to report safety data on ECG measurements, given the heterogeneity in timing of QTcF measurements. Further studies including data on patients using bedaquiline for >6 months are warranted, as well as studies on the use of bedaquiline in shorter treatment regimens.

In conclusion, these pooled data from 5 cohorts of patients treated with bedaquiline suggest that this drug is effective and safe across different modalities of delivery and in different settings, when added to standard background regimens. Outcomes are less favorable, however, in patients with lung cavitations and more severe drug resistance. The overall certainty of the evidence is very low.

Acknowledgments

We thank L. Thabane, M. Loeb, J. Beyene, and D. Mertz for their guidance on statistics and reporting. We thank Nobert Ndjeka, Francesca Conradie, and Kate Schnippel for supporting the acquisition and transfer of data from the South Africa cohort.

For their contributions to data collection and patient care, we thank L. Yegiazaryan, T. Aydinyan, N. Saribekyan, H. Atchemyan, O. Kirakosyan, N. Danielyan, A. Melikyan, O.Petrosyan, A. Serobyan, N. Kiria, K. Barbakadze, L. Mikiashvili, M. Oniani, N. Chumburidze, M. Kikvidze, M. Gergedava, G. Salia, G. Zaridze, and A. Gegeshidze.

Part of this study was carried out under YODA project no. 2016-0734, using data obtained from the Yale University Open Data Access Project, which has an agreement with Janssen Research & Development, LLC. The interpretation and reporting of research using these data are solely the responsibility of the authors and does not necessarily represent the official views of the Yale University Open Data Access Project or Janssen Research & Development, LLC. The Bill and Melinda Gates Foundation supported this study as part of the WHO guidelines development process through grant project no. OPP1126615.

Conflict of interest: L.G., J. R., and N.V. work in a laboratory that has received grants from Johnson & Johnson to perform preclinical studies on bedaquiline. N.B. is an employee of Johnson & Johnson, the manufacturer of bedaquiline.

Authors' contributions: L. M. contributed to data acquisition, data analyses, interpretation; wrote and revised the manuscript; and approved the final version. L.G., C.H., N.B., M.B., M.F.J., J.R., N.V., N.K., T.K., A.H., and Z.A. contributed to data acquisition from the primary studies, interpretation of data, manuscript writing, and approval of the final version. H.J.S. and C.L. contributed to the conception and design of this study, interpretation of the data, and review and approval of the final version. All authors agree to be accountable for all aspects of the work in ensuring that questions related to the accuracy or integrity of any part of the work are appropriately investigated and resolved.

About the Author

Dr. Mbuagbaw is an assistant professor in the department of health research methods, evidence, and impact at McMaster University and a research methods scientist at St Joseph's Healthcare Hamilton. His primary research interests are infectious diseases and health research methods.

References

1. World Health Organization. Global tuberculosis report 2018. 2018 [cited 2018 Dec 11]. https://www.who.int/tb/publications/global_report
2. World Health Organization. Drug-resistant TB: totally drug-resistant TB FAQ. 2018 [cited 2018 12 Feb]. http://www.who.int/tb/areas-of-work/drug-resistant-tb/totally-drug-resistant-tb-faq
3. Bonnet M, Bastard M, du Cros P, Khamraev A, Kimenye K, Khurkhumal S, et al. Identification of patients who could benefit from bedaquiline or delamanid: a multisite MDR-TB cohort study. Int J Tuberc Lung Dis. 2016;20:177–86. http://dx.doi.org/10.5588/ijtld.15.0962
4. Borisov SE, Dheda K, Enwerem M, Romero Leyet R, D'Ambrosio L, Centis R, et al. Effectiveness and safety of bedaquiline-containing regimens in the treatment of MDR- and XDR TB: a multicentre study. Eur Respir J. 2017;49:1700387. http://dx.doi.org/10.1183/13993003.00387-2017
5. Falzon D, Schünemann HJ, Harausz E, González-Angulo L, Lienhardt C, Jaramillo E, et al. World Health Organization treatment guidelines for drug-resistant tuberculosis, 2016 update. Eur Respir J. 2017;49:1602308. http://dx.doi.org/10.1183/13993003.02308-2016
6. World Health Organization. WHO treatment guidelines for multidrug- and rifampicin-resistant tuberculosis 2018 update. 2018 [cited 2019 Jan 15]. https://www.who.int/tb/publications/2018/WHO.2018.MDR-TB.Rx.Guidelines.prefinal.text.pdf
7. Ahuja SD, Ashkin D, Avendano M, Banerjee R, Bauer M, Bayona JN, et al.; Collaborative Group for Meta-Analysis of Individual Patient Data in MDR-TB. Multidrug resistant pulmonary tuberculosis treatment regimens and patient outcomes: an individual patient data meta-analysis of 9,153 patients. PLoS Med. 2012;9:e1001300. http://dx.doi.org/10.1371/journal.pmed.1001300
8. Nathanson E, Gupta R, Huamani P, Leimane V, Pasechnikov AD, Tupasi TE, et al. Adverse events in the treatment of multidrug-resistant tuberculosis: results from the DOTS-Plus initiative. Int J Tuberc Lung Dis. 2004;8:1382–4.
9. Diacon AH, Dawson R, Von Groote-Bidlingmaier F, Symons G, Venter A, Donald PR, et al. Randomized dose-ranging study of the 14-day early bactericidal activity of bedaquiline (TMC207) in patients with sputum microscopy smear-positive pulmonary tuberculosis. Antimicrob Agents Chemother. 2013;57:2199–203. http://dx.doi.org/10.1128/AAC.02243-12
10. Diacon AH, Pym A, Grobusch MP, de los Rios JM, Gotuzzo E, Vasilyeva I, et al.; TMC207-C208 Study Group. Multidrug-resistant tuberculosis and culture conversion with bedaquiline. N Engl J Med. 2014;371:723–32. http://dx.doi.org/10.1056/NEJMoa1313865
11. Lu X, Smare C, Kambili C, El Khoury AC, Wolfson LJ. Health outcomes of bedaquiline in the treatment of multidrug-resistant tuberculosis in selected high burden countries. BMC Health Serv Res. 2017;17:87. http://dx.doi.org/10.1186/s12913-016-1931-3
12. World Health Organization. The use of bedaquiline in the treatment of multidrug-resistant tuberculosis: interim policy guidance. 2013 [cited 2018 Mar 19]. http://apps.who.int/iris/bitstream/10665/84879/1/9789241505482_eng.pdf
13. World Health Organization. Report of the Guideline Development Group Meeting on the use of bedaquiline in the treatment of multidrug-resistant tuberculosis 2016 [cited 2018 Mar 19]. http://apps.who.int/iris/bitstream/10665/254712/1/WHO-HTM-TB-2017.01-eng.pdf
14. Pym AS, Diacon AH, Tang SJ, Conradie F, Danilovits M, Chuchottaworn C, et al.; TMC207-C209 Study Group. Bedaquiline in the treatment of multidrug- and extensively drug-resistant tuberculosis. Eur Respir J. 2016;47:564–74. http://dx.doi.org/10.1183/13993003.00724-2015
15. Guglielmetti L, Jaspard M, Le Dû D, Lachâtre M, Marigot-Outtandy D, Bernard C, et al.; French MDR-TB Management Group. Long-term outcome and safety of prolonged bedaquiline treatment for multidrug-resistant tuberculosis. Eur Respir J. 2017;49:1601799. http://dx.doi.org/10.1183/13993003.01799-2016
16. Ndjeka N, Schnippel K, Master I, Meintjes G, Maartens G, Romero R, et al. High treatment success rate for multidrug-resistant and extensively drug-resistant tuberculosis using a bedaquiline-containing treatment regimen. Eur Respir J. 2018;52:1801528. http://dx.doi.org/10.1183/13993003.01528-2018
17. Hewison C, Bastard M, Khachatryan N, Kotrikadze T, Hayrapetyan A, Avaliani Z, et al. Is 6 months of bedaquiline enough? Results from the compassionate use of bedaquiline in Armenia and Georgia. Int J Tuberc Lung Dis. 2018;22:766–72. http://dx.doi.org/10.5588/ijtld.17.0840
18. Vandenberk B, Vandael E, Robyns T, Vandenberghe J, Garweg C, Foulon V, et al. Which QT correction formulae to use for QT monitoring? J Am Heart Assoc. 2016;5:e003264. http://dx.doi.org/10.1161/JAHA.116.003264
19. World Health Organization. Companion handbook to the 2011 WHO guidelines for the programmatic management of drug-resistant tuberculosis. 2014 [cited 2018 Mar 16]. http://www.who.int/tb/publications/pmdt_companionhandbook/
20. US Food and Drug Administration. Code of Federal Regulations Title 21. 2017 [cited 2018 Mar 16]. https://www.accessdata.fda.gov/scripts/cdrh/cfdocs/cfCFR/CFRSearch.cfm?fr=312.32
21. Ali MK, Karanja S, Karama M. Factors associated with tuberculosis treatment outcomes among tuberculosis patients attending tuberculosis treatment centres in 2016–2017 in Mogadishu, Somalia. Pan Afr Med J. 2017;28:197.
22. Guglielmetti L, Le Dû D, Jachym M, Henry B, Martin D, Caumes E, et al.; MDR-TB Management Group of the French National Reference Center for Mycobacteria and the Physicians of the French MDR-TB Cohort. Compassionate use of bedaquiline for the treatment of multidrug-resistant and extensively drug-resistant tuberculosis: interim analysis of a French cohort. Clin Infect Dis. 2015;60:188–94. http://dx.doi.org/10.1093/cid/ciu786
23. Guyatt G, Oxman AD, Akl EA, Kunz R, Vist G, Brozek J, et al. GRADE guidelines: 1. Introduction—GRADE evidence profiles and summary of findings tables. J Clin Epidemiol. 2011;64:383–94. http://dx.doi.org/10.1016/j.jclinepi.2010.04.026
24. Cegielski JP, Kurbatova E, van der Walt M, Brand J, Ershova J, Tupasi T, et al.; Global PETTS Investigators. Multidrug-resistant tuberculosis treatment outcomes in relation to treatment and initial versus acquired second-line drug resistance. Clin Infect Dis. 2016;62:418–30.
25. Schnippel K, Ndjeka N, Maartens G, Meintjes G, Master I, Ismail N, et al. Effect of bedaquiline on mortality in South African patients with drug-resistant tuberculosis: a retrospective cohort study. Lancet Respir Med. 2018;6:699–706. http://dx.doi.org/10.1016/S2213-2600(18)30235-2
26. Zhao Y, Fox T, Manning K, Stewart A, Tiffin N, Khomo N, et al. Improved treatment outcomes with bedaquiline when substituted for second-line injectable agents in multidrug-resistant tuberculosis: a retrospective cohort study. Clin Infect Dis. 2018

Aug 24 [Epub ahead of print]. https://doi.org/10.1093/cid/ciy727
27. Ahmad N, Ahuja SD, Akkerman OW, Alffenaar JC, Anderson LF, Baghaei P, et al.; Collaborative Group for the Meta-Analysis of Individual Patient Data in MDR-TB treatment–2017. Treatment correlates of successful outcomes in pulmonary multidrug-resistant tuberculosis: an individual patient data meta-analysis. Lancet. 2018;392:821–34. http://dx.doi.org/10.1016/S0140-6736(18)31644-1
28. Guglielmetti L, Tiberi S, Burman M, Kunst H, Wejse C, Togonidze T, et al. QT prolongation and cardiac toxicity of new tuberculosis drugs in Europe: a Tuberculosis Network European Trialsgroup (TBnet) study. Eur Respir J. 2018;52:1800537. http://dx.doi.org/10.1183/13993003.00537-2018
29. Skrahina A, Hurevich H, Falzon D, Zhilevich L, Rusovich V, Dara M, et al. Bedaquiline in the multidrug-resistant tuberculosis treatment: Belarus experience. Int J Mycobacteriol. 2016;5 (Suppl 1):S62–3. http://dx.doi.org/10.1016/j.ijmyco.2016.11.014
30. Olaru ID, Heyckendorf J, Andres S, Kalsdorf B, Lange C. Bedaquiline-based treatment regimen for multidrug-resistant tuberculosis. Eur Respir J. 2017;49:1700742. http://dx.doi.org/10.1183/13993003.00742-2017
31. World Health Organization. WHO best-practice statement on the off-label use of bedaquiline and delamanid for the treatment of multidrug-resistant tuberculosis. 2017 [cited 2018 May 28]. http://apps.who.int/iris/bitstream/handle/10665/258941/WHO-HTM-TB-2017.20-eng.pdf
32. Higgins JPT, Thompson SG, Deeks JJ, Altman DG. Measuring inconsistency in meta-analyses. BMJ. 2003;327:557–60. http://dx.doi.org/10.1136/bmj.327.7414.557

Address for correspondence: Lawrence Mbuagbaw, St. Joseph's Healthcare, The Research Institute, Biostatistics Unit, 50 Charlton Ave E, 3rd Fl, Martha Wing, Room H321, Hamilton, Ontario L8N 4A6, Canada; email: mbuagblc@mcmaster.ca

Phylogenetic Analysis of *Francisella tularensis* Group A.II Isolates from 5 Patients with Tularemia, Arizona, USA, 2015–2017

Dawn N. Birdsell,[1] Hayley Yaglom,[1] Edwin Rodriguez, David M. Engelthaler, Matthew Maurer, Marlene Gaither, Jacob Vinocur, Joli Weiss, Joel Terriquez, Kenneth Komatsu, Mary Ellen Ormsby, Marette Gebhardt, Catherine Solomon, Linus Nienstadt, Charles H.D. Williamson, Jason W. Sahl, Paul S. Keim, David M. Wagner

We examined 5 tularemia cases in Arizona, USA, during 2015–2017. All were caused by *Francisella tularensis* group A.II. Genetically similar isolates were found across large spatial and temporal distances, suggesting that group A.II strains are dispersed across long distances by wind and exhibit low replication rates in the environment.

Francisella tularensis, a Tier 1 select agent (*1*), has 3 subspecies: *tularensis* (type A), *holarctica* (type B), and *mediasiatica* (Appendix 1 Figure, https://wwwnc.cdc.gov/EID/article/25/5/18-0363-App1.pdf). In humans, disease is caused by type A and type B. Type B is found throughout the Northern Hemisphere, type A only in North America, and *mediasiatica* only in central Asia (*2*). Type A is divided into 2 distinct subgroups, A.I and A.II (Appendix 1 Figure), that have little geographic overlap (*3*,*4*). A.II is found primarily in the mountainous region of western North America (*3*,*4*) and A.I throughout the central eastern regions and along the West Coast (*3*–*5*). Observational human data and limited experimental mouse data suggest A.II is less virulent than A.I but potentially more virulent than type B (*6*,*7*). Here, we describe 5 patients in Arizona, USA, during 2015–2017 with cases of tularemia (1 fatal), all caused by A.II (Appendix 2, https://wwwnc.cdc.gov/EID/article/25/5/18-0363-App2.xlsx).

The Study

Case-patient 1 was a 57-year-old previously healthy man who sought treatment July 12, 2015, for chills and an acute onset of fever >40°C. Five days before symptom onset, while camping at the northern rim of Grand Canyon National Park, he noted a small wound at the lateral aspect of his left elbow consistent with an insect bite. Cellulitis with regional lymphadenopathy developed on his left forearm, extending to the left axillary region. After surgical irrigation, debridement of the wound (August 8), and oral doxycycline treatment upon discharge, the patient fully recovered.

Case-patient 2 was a 55-year-old previously healthy woman who sought treatment on July 20, 2015, for sore throat and an acute onset of fever >40°C. She reported no outdoor activity except being in a Coconino County park 4 days before symptom onset. Despite receiving treatment with amoxicillin, her fever persisted; she returned 4 days later with myalgia, fatigue, headaches, and emesis. Her therapy was switched to sulfamethoxazole/trimethoprim, amoxicillin/clavulanate, and ceftriaxone. A 2-day hospitalization revealed left axillary lymphadenopathy with associated cellulitis in her left chest wall and breast. Her fever resolved with intravenous ceftriaxone and gentamicin. She received oral doxycycline upon discharge and fully recovered.

Case-patient 3 was a 73-year-old Coconino County woman with previous health conditions. She sought treatment in the summer of 2016 and died several days later (Appendix 2 Table). Details about this case-patient are presented elsewhere (*8*).

Case-patient 4 was a 24-year-old previously healthy woman from Navajo County who sought treatment in November 2016. A cat bite was the suspected source of infection, but the cat was euthanized without testing. Severe

Author affiliations: Northern Arizona University, Flagstaff, Arizona, USA (D.N. Birdsell, C.H.D. Williamson, J.W. Sahl, P.S. Keim, D.M. Wagner); Arizona Department of Health Services, Phoenix, Arizona, USA (H. Yaglom, J. Weiss, K. Komatsu); Navajo County Public Health Services District, Show Low, Arizona, USA (E. Rodriguez, C. Solomon); Translational Genomics Research Institute, Flagstaff (D.M. Engelthaler); Coconino County Public Health Services District, Flagstaff (M. Maurer, M. Gaither, M.E. Ormsby, M. Gebhardt); Northern Arizona Healthcare, Flagstaff (J. Vinocur, J. Terriquez, L. Nienstadt)

DOI: https://doi.org/10.3201/eid2505.180363

[1]These authors contributed equally to this article.

swelling and lymphadenopathy developed at the site of the bite; the patient was treated with antimicrobial drugs and recovered.

Case-patient 5 was a 52-year-old man who resided and traveled between both Coconino County and Pinal County. He sought treatment for dizziness, nausea, chills, headache, and body aches in June 2017. He was initially treated with antipyretics but returned to the hospital 2 days later. At this visit, he received treatment with several antimicrobial drugs and recovered. The source of his infection is unknown.

All illnesses were classified as ulceroglandular tularemia except the one in case-patient 3, which was classified as respiratory tularemia. Recovered isolates from all 5 patients tested positive for *F. tularensis* group A.II by PCR (Appendix 2 Table).

Comparisons of whole-genome sequencing and geographic data (Appendix 1) for these 5 isolates and 9 other A.II isolates (Appendix 2 Table) revealed 2 patterns. First, the 5 cases in humans during 2015–2017 were caused by isolates from distinct clades (Figure, panel A). The isolates in case-patients 2 and 3, who probably acquired the infection in the same city, were assigned to 2 different major phylogenetic clades (A.II.2 and A.II.8), suggesting distinct clades co-occur locally in the environment, a finding similar to that observed with type B and group A.I (*9*,*10*). Second, some closely related isolates were distant in geographic and temporal space (Figure, panels A, B). Isolates from case-patients 3 and 4 are highly similar, differing by just 1 single-nucleotide polymorphism (SNP) across the core genome, despite being isolated >150 km and 5 months apart; they also differ by just 3–4 SNPs from a case that occurred in another location 9 years previous in 2007 (no. 8; Figure). Likewise, isolates from case-patients 2 and 5 differ by just 4 SNPs, despite being isolated from distant locations 2 years apart.

The geographic pattern suggests *F. tularensis* group A.II might be capable of long-distance dispersal, perhaps by wind, as has been suggested for type B (*9*,*11*). The temporal pattern, which also has been observed for type B (*9*,*11*), is consistent with a low evolutionary rate for A.II strains in the environment. This pattern suggests group A.II strains may persist in the environment in a dormant state, such as the viable but nonculturable state that has been described for type B (*12*).

Consistent with a low evolutionary rate in the environment, groups A.I and A.II appear to be highly monomorphic and have much less genetic variation than type B (Appendix 1 Figure). Type B was previously described as being less genetically diverse than type A as a whole when groups A.I and A.II were considered together (*2*). However, A.I and A.II are separated by large SNP distances with no intermediate lineages (Appendix 1 Figure), verifying these groups as highly distinct and warranting their analysis as separate groups.

In this study, just 309 SNPs were discovered among 14 A.II isolates separated by considerable geographic

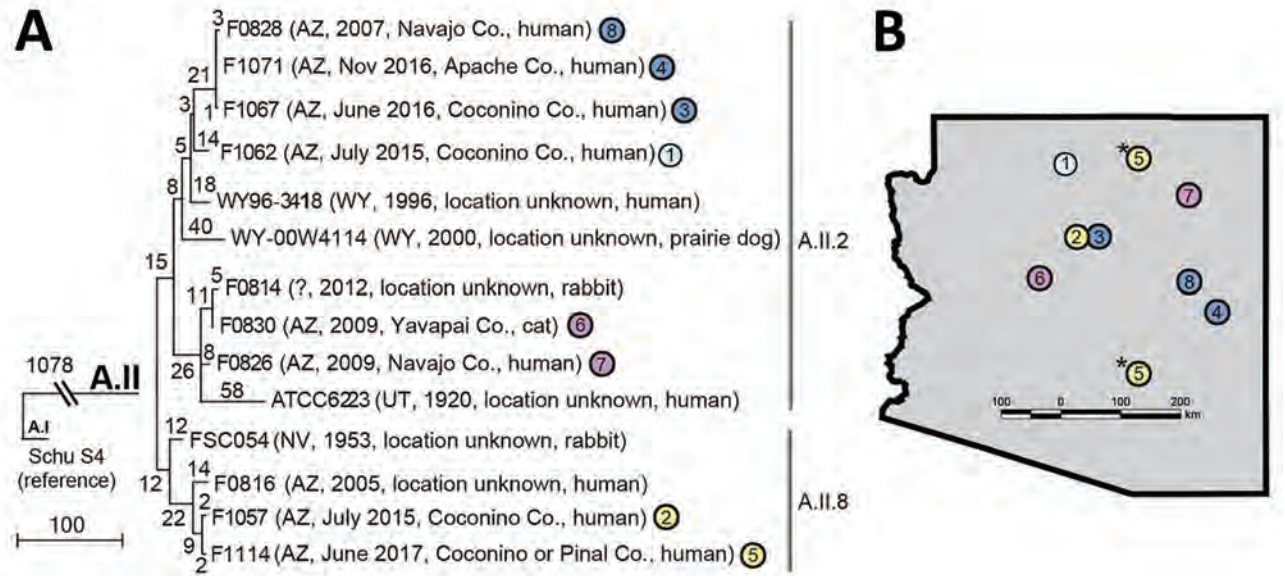

Figure. Phylogeny and geographic distribution of *Francisella tularensis* isolates, Arizona, 2005–2017. A) Maximum-parsimony tree of 14 *F. tularensis* subsp. *tularensis* A.II isolates from humans and other mammals constructed by using single-nucleotide polymorphisms (SNPs) discovered by whole-genome sequencing. The tree is rooted on A.I strain Schu S4. Scale bar indicates number of SNPs. Numbers along branches also indicate the number of SNPs the branches represent. Closely related isolates are indicated with circles of the same color (also indicated in panel B). Numbers within circles correspond to the identification numbers in Appendix 2 Table (https://wwwnc.cdc.gov/EID/article/25/5/18-0363-App2.xlsx. B) Known or suspected geographic origins of tularemia cases in Arizona. *Case 5 is represented twice to reflect the 2 possible geographic sources of this infection. Co., county.

(maximum >1,000 km) and temporal (maximum 96 years) distances (Figure, panel A). In a previous study (*13*), just 295 SNPs were discovered among 14 A.I isolates separated by similar temporal distances (maximum 65 years) and an even greater geographic distance (maximum >2,800 km). In contrast, type B exhibits much more diversity across smaller geographic and temporal scales. For example, 735 SNP differences were found in an analysis of 10 isolates from a respiratory tularemia outbreak in Sweden (*9*), even though the temporal (maximum 1 year) and geographic (maximum ≈201 km) distances among these isolates were much smaller. The patterns observed with group A.II isolates suggest that, as has been suggested for type B (*9*,*11*), both group A.I and A.II strains might also persist long term in the environment in a dormant state where replication is nonexistent or greatly arrested.

A.II appears to be the main and perhaps only group of *F. tularensis* present in the environment in Arizona, although group A.I and type B are known to be present in neighboring states (*14*). However, all available archival isolates from human and wildlife sources in Arizona (Appendix 2 Table) were assigned to the A.II group (Appendix 1), consistent with other reports, indicating the presence of only group A.II from animal and human sources from Arizona (*3*,*4*). In 2000, type B isolates were obtained from captive animals in an Arizona zoo, but these infections were suspected to be imported rather than locally acquired (*2*).

Conclusions

In summary, we report 5 cases of tularemia in humans (including 1 fatality) that occurred in Arizona during 2015–2017, and all were caused by A.II isolates. Phylogeographic patterns suggest *F. tularensis* A.II strains might persist in the environment in a dormant state and be dispersed long distances, perhaps by wind.

This work was funded through Northern Arizona University via the Cowden Endowment and the State of Arizona Technology and Research Initiative Fund administered by the Arizona Board of Regents.

About the Author

Dr. Birdsell is an associate director at the Pathogen and Microbiome Institute, Northern Arizona University, in Flagstaff, Arizona. Her primary research interests are the evolution and phylogeography of *F. tularensis*.

References

1. Rotz LD, Khan AS, Lillibridge SR, Ostroff SM, Hughes JM. Public health assessment of potential biological terrorism agents. Emerg Infect Dis. 2002;8:225–30. http://dx.doi.org/10.3201/eid0802.010164
2. Vogler AJ, Birdsell D, Price LB, Bowers JR, Beckstrom-Sternberg SM, Auerbach RK, et al. Phylogeography of *Francisella tularensis*: global expansion of a highly fit clone. J Bacteriol. 2009;191:2474–84. http://dx.doi.org/10.1128/JB.01786-08
3. Farlow J, Wagner DM, Dukerich M, Stanley M, Chu M, Kubota K, et al. *Francisella tularensis* in the United States. Emerg Infect Dis. 2005;11:1835–41. http://dx.doi.org/10.3201/eid1112.050728
4. Staples JE, Kubota KA, Chalcraft LG, Mead PS, Petersen JM. Epidemiologic and molecular analysis of human tularemia, United States, 1964–2004. Emerg Infect Dis. 2006;12:1113–8. http://dx.doi.org/10.3201/eid1207.051504
5. Keim P, Johansson A, Wagner DM. Molecular epidemiology, evolution, and ecology of *Francisella.* Ann N Y Acad Sci. 2007; 1105:30–66. http://dx.doi.org/10.1196/annals.1409.011
6. Molins CR, Delorey MJ, Yockey BM, Young JW, Sheldon SW, Reese SM, et al. Virulence differences among *Francisella tularensis* subsp. *tularensis* clades in mice. PLoS One. 2010;5:e10205. http://dx.doi.org/10.1371/journal.pone.0010205
7. Kugeler KJ, Mead PS, Janusz AM, Staples JE, Kubota KA, Chalcraft LG, et al. Molecular epidemiology of *Francisella tularensis* in the United States. Clin Infect Dis. 2009;48:863–70. http://dx.doi.org/10.1086/597261
8. Yaglom H, Rodriguez E, Gaither M, Schumacher M, Kwit N, Nelson C, et al. Notes from the field: fatal pneumonic tularemia associated with dog exposure—Arizona, June 2016. MMWR Morb Mortal Wkly Rep. 2017;66:891. http://dx.doi.org/10.15585/mmwr.mm6633a5
9. Johansson A, Lärkeryd A, Widerström M, Mörtberg S, Myrtännäs K, Ohrman C, et al. An outbreak of respiratory tularemia caused by diverse clones of *Francisella tularensis*. Clin Infect Dis. 2014;59:1546–53. http://dx.doi.org/10.1093/cid/ciu621
10. Birdsell DN, Johansson A, Öhrman C, Kaufman E, Molins C, Pearson T, et al. *Francisella tularensis* subsp. *tularensis* group A.I, United States. Emerg Infect Dis. 2014;20:861–5. http://dx.doi.org/10.3201/eid2005.131559
11. Dwibedi C, Birdsell D, Lärkeryd A, Myrtennäs K, Öhrman C, Nilsson E, et al. Long-range dispersal moved *Francisella tularensis* into Western Europe from the East. Microb Genom. 2016; 2:e000100.
12. Forsman M, Henningson EW, Larsson E, Johansson T, Sandström G. *Francisella tularensis* does not manifest virulence in viable but non-culturable state. FEMS Microbiol Ecol. 2000;31: 217–24. http://dx.doi.org/10.1111/j.1574-6941.2000.tb00686.x
13. Birdsell DN, Johansson A, Öhrman C, Kaufman E, Molins C, Pearson T, et al. *Francisella* tularensis subsp. *tularensis* group A.I, United States. Emerg Infect Dis. 2014;20:861–5. http://dx.doi.org/10.3201/eid2005.131559
14. Petersen JM, Carlson JK, Dietrich G, Eisen RJ, Coombs J, Janusz AM, et al. Multiple *Francisella tularensis* subspecies and clades, tularemia outbreak, Utah. Emerg Infect Dis. 2008;14: 1928–30. http://dx.doi.org/10.3201/eid1412.080482

Address for correspondence: David M. Wagner, Pathogen and Microbiome Institute, Northern Arizona University, Flagstaff, AZ 86011-4073, USA; email: dave.wagner@nau.ed

Anthrax Epizootic in Wildlife, Bwabwata National Park, Namibia, 2017

Caitlin M. Cossaboom, Siegfried Khaiseb, Bernard Haufiku, Puumue Katjiuanjo, Apollinaris Kannyinga, Kaiser Mbai, Thompson Shuro, Jonas Hausiku, Annety Likando, Rebekka Shikesho, Kofi Nyarko, Leigh Ann Miller, Simon Agolory, Antonio R. Vieira, Johanna S. Salzer, William A. Bower, Lindsay Campbell, Cari B. Kolton, Chung Marston, Joy Gary, Brigid C. Bollweg, Sherif R. Zaki, Alex Hoffmaster, Henry Walke

In late September 2017, Bwabwata National Park in Namibia experienced a sudden die-off of hippopotamuses and Cape buffalo. A multiorganizational response was initiated, involving several ministries within Namibia and the US Centers for Disease Control and Prevention. Rapid interventions resulted in zero human or livestock cases associated with this epizootic.

Anthrax, caused by *Bacillus anthracis*, is a naturally occurring zoonotic disease of veterinary and public health importance. Anthrax has been reported in wildlife and domestic animals worldwide and can spill over to humans (*1*,*2*). Anthrax epizootics in hippopotamuses have been documented in several countries of southern Africa, including Zambia, Zimbabwe, and South Africa (*3*–*5*). Anthrax is also well documented in wildlife in Etosha National Park, Namibia (*6*). Human infections related to wildlife anthrax typically result from consumption of meat from infected carcasses, causing ingestion anthrax, or direct contact, causing cutaneous anthrax (*5*). Anthrax epizootics in southern Africa are often associated with dry seasons, which typically occur during May–October (*2*,*7*).

A massive dieoff of hippopotamuses and Cape buffalo began in late September 2017 along the Kavango River in Bwabwata National Park (BNP), within the Kavango East region of northeastern Namibia. We report on the multiorganizational response that addressed this event.

The Study

On September 25, 2017, Namibia's Ministry of Environment and Tourism (MET) learned of 2 hippopotamus carcasses found on the western side of BNP. During unrelated aerial surveillance in the area on October 1, MET observed 10 hippopotamus carcasses and on October 7 observed an additional 107 hippopotamus and 20 Cape buffalo carcasses. MET then notified the Ministry of Agriculture, Water, and Forestry and the Ministry of Health and Social Services (MOHSS), which together established a joint action plan. The presumptive diagnosis was anthrax based on clinical and microscopic evidence; however, culture confirmation was not initially possible because of sample collection and laboratory challenges. The US Centers for Disease Control and Prevention (CDC) was consulted for assistance with the investigation.

To address possible human exposure, MOHSS developed a questionnaire and administered it beginning on October 12 to identify persons living in communities adjacent to BNP who were exposed to the carcasses (Figure 1). In total, 1,050 persons were identified as having contact with or consuming meat from the carcasses and were immediately provided with postexposure prophylaxis (PEP) in the form of 2 weeks of ciprofloxacin and symptom monitoring (*8*). MOHSS returned 2 weeks later to assess PEP adherence among exposed community members and reported successful PEP adherence and no severe adverse events associated with taking PEP. Field workers performing carcass disposal continued PEP use until 2 weeks after activities concluded. MOHSS led community education to raise awareness of the ongoing outbreak, communicate the importance of not having contact with or consuming meat from animals found dead, and urge persons to seek healthcare if exposed or symptomatic. No human anthrax cases were associated with this outbreak.

Author affiliations: Centers for Disease Control and Prevention, Atlanta, Georgia, USA (C.M. Cossaboom, A.R. Vieira, J.S. Salzer, W.A. Bower, C.B. Kolton, C. Marston, J. Gary, B.C. Bollweg, S.R. Zaki, A. Hoffmaster, H. Walke); Republic of Namibia Ministry of Agriculture, Water, and Forestry, Windhoek, Namibia (S. Khaiseb, K. Mbai, T. Shuro); Republic of Namibia Ministry of Health and Social Services, Windhoek (B. Haufiku, P. Katjiuanjo, A. Likando, R. Shikesho, K. Nyarko); Republic of Namibia Ministry of Environment and Tourism, Windhoek (A. Kannyinga, J. Hausiku); Centers for Disease Control and Prevention, Windhoek (L.A. Miller, S. Agolory); University of Florida, Vero Beach, Florida, USA (L. Campbell)

DOI: https://doi.org/10.3201/eid2505.180867

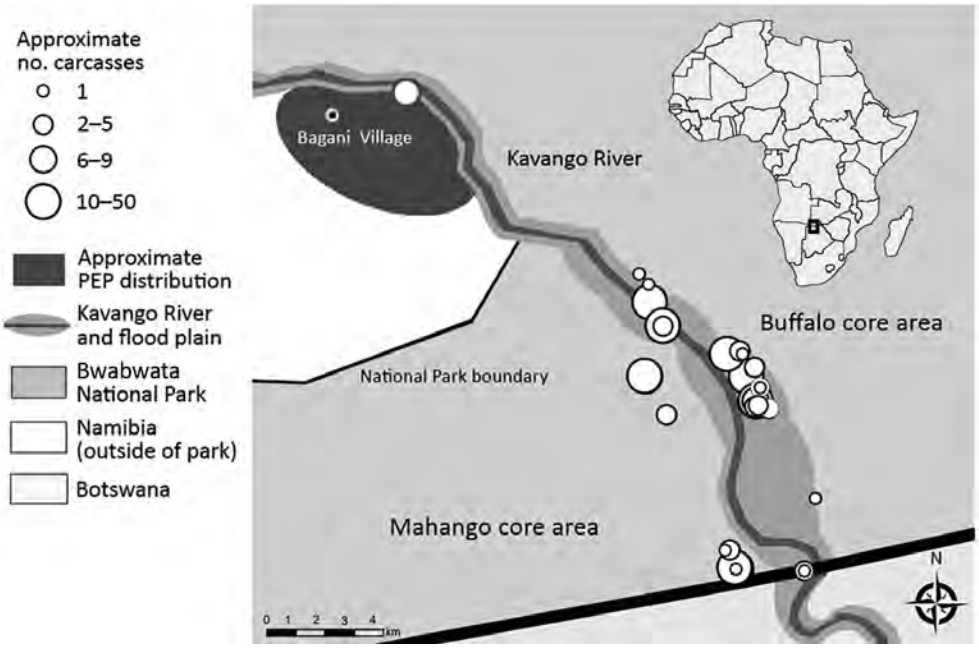

Figure 1. Anthrax investigation points of interest within and directly adjacent to Bwabwata National Park, Namibia, 2017. Inset shows location of park in Africa.

CDC developed a protocol to collect specimens from affected wildlife carcasses. A field team collected several paired samples from 7 carcasses: ear and eyelid tissue biopsy samples and swab specimens of the nasal cavity, rectum, and other pooled blood when available. We recorded geographic coordinates by using a Garmin Montana 650 GPS unit at carcass locations for eventual geospatial analysis (Figure 1).

To test samples, we used the InBios Active Anthrax Detect (AAD) Rapid Test (InBios, http://www.inbios.com), a lateral flow assay that detects capsular polypeptide of *B. anthracis*. This novel assay was developed as a point-of-care diagnostic aid for human inhalation anthrax and is available for investigational or research use only (*9*). A laboratory evaluation conducted on animal tissues by CDC before deployment indicated that the test had 98% specificity and 95% sensitivity (C.B. Kolton, unpub. data). Use of the AAD Rapid Test under field conditions is beneficial because the test requires only a small sample volume, provides results within 15 minutes, and does not require refrigeration.

We performed the AAD Rapid Test in the field on tissue and swab samples collected from wildlife carcasses, following standard protocol provided by InBios (S. Raychaudhuri, InBios, pers. comm., 2016 May 10). We suspended tissue samples in 600 μL of sterile phosphate-buffered saline (PBS) and vortexed the suspension for 10 seconds. After pipetting repeatedly, we applied 10 μL to the AAD Rapid Test cassette. For swabbed exudate samples, we transferred 10 μL of fluid to the cassette without PBS.

We subsequently confirmed *B. anthracis* infection by using culture, real-time reverse transcription PCR (rRT-PCR), and immunohistochemistry (IHC). We processed tissue and swab samples and inoculated them into sheep blood agar or heart infusion broth, then incubated at 37°C for 24 h. We performed DNA extractions on specimens by using the QIAGEN Blood Mini Kit (https://www.qiagen.com) and tested the resulting DNA by using the Laboratory Response Network's rRT-PCR for *B. anthracis* (*10*). We processed formalin-fixed tissue samples from 3 Cape buffalo and 3 hippopotamuses, embedded them in paraffin, and stained them with hematoxylin and eosin, Lillie-Twort Gram stain, and Warthin-Starry silver stain.

The vessels within the dermis of the ear biopsy in 1 Cape buffalo and ear and eyelid biopsies of 3 hippopotamuses contained large, gram-variable bacilli. We performed IHC assays using mouse monoclonal antibodies targeting the *B. anthracis* cell wall and capsule by using an immunoalkaline phosphatase polymer system, as previously described (*11*,*12*), and highlighted bacterial antigen and full bacilli within the vessels of 2 buffalo and all 3 hippopotamuses (Table; Figure 2). All 6 anthrax-suspected carcasses tested positive by AAD Rapid Test and were confirmed positive for *B. anthracis* by culture, rRT-PCR, and/or IHC. A carcass of a buffalo that died from a vehicle collision was included as a negative control and tested negative by all assays (Table).

Livestock vaccination is an effective means to prevent anthrax infection in domestic animals and subsequent transmission to humans (*13*) and is required annually in Namibia. The Ministry of Agriculture, Water, and Forestry secured

Table. Summary of laboratory diagnostic testing results, by carcass sampled, after an anthrax epizootic in wildlife, Bwabwata National Park, Namibia, 2017*

Carcass ID	Species	AAD Rapid Test	Culture	LRN rRT-PCR	Immunohistochemistry	
					Cell wall	Capsule
001	Cape buffalo	+	+	NA	–	+
002	Cape buffalo†	–	–	NA	–	–
005	Cape buffalo	+	+	NA	+	+
007	Hippopotamus	+	+	+	+	+
008	Hippopotamus	+	–	+	+	+
009	Hippopotamus	+	+	+	+	+
012	Hippopotamus	+	+	+	NA	NA

*AAD Rapid Test, InBios Active Anthrax Detect Rapid Test (InBios, http://www.inbios.com); LRN rRT-PCR, Laboratory Response Network real-time reverse transcription PCR; NA, not available; +, positive; –, negative.
†This Cape buffalo carcass served as a negative control. The animal died as a result of a vehicle collision, and anthrax infection was not suspected as cause of death.

≈10,000 doses of livestock anthrax vaccine to prevent spillover of anthrax from wildlife into susceptible domestic animals and will enforce future annual vaccination in the affected area. MET organized vaccination of wildlife. No cases of anthrax in livestock were associated with this outbreak.

Incineration is the recommended disposal method in cases where reducing the carcass to ashes is possible to enable complete destruction of any viable spores (*8*). However, because of the large size and number of carcasses, burial was an alternative method of disposal. We recommended limiting the distance that carcasses were moved for burial to decrease dissemination of spores and ensuring a depth of ≥2 m was reached to prevent scavenger disruption to carcasses (*1*). Spraying the carcass and burial site with 10% formaldehyde minimized external contamination (*1*,*8*).

By early December, the wildlife deaths subsided, and 155 hippopotamus and 86 Cape buffalo carcasses had been disposed of in the Mahango and Buffalo core areas of BNP (Figure 1). MET conducted an aerial survey in the same areas in September 2017 that recorded 588 hippopotamuses and 2,216 Cape buffalo; roughly 26.4% and 3.8% of each population were affected, respectively (*14*).

Conclusions

Our investigation highlights a successful public health outcome with zero human or livestock cases after an anthrax outbreak in wildlife in BNP. We demonstrated the successful use of the AAD Rapid Test for presumptive diagnosis of anthrax in wildlife under field conditions and the use of culture and IHC for confirmation of *B. anthracis* in hippopotamuses and Cape buffalo. The AAD Rapid Test has the potential to improve the ability of low-resource countries to quickly diagnose and effectively manage anthrax epizootics, thus reducing the risk for transmission to humans.

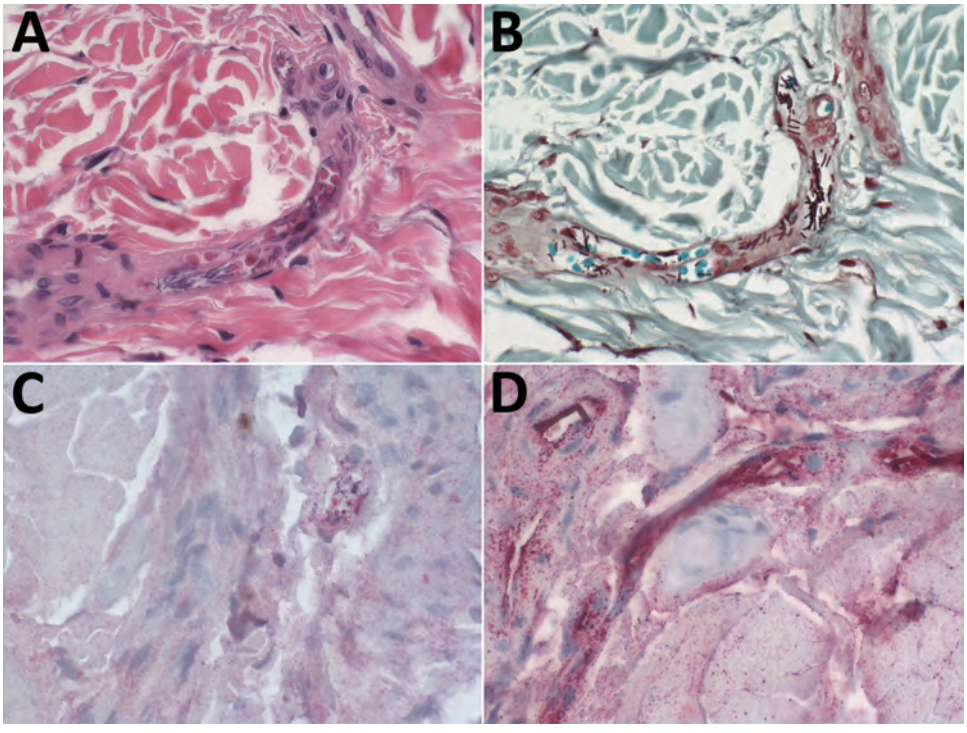

Figure 2. Photomicrographs showing hematoxylin and eosin stain and immunohistochemical findings, using assays targeting the cell wall and capsule of *Bacillus anthracis*, in ear-punch biopsy specimens from a hippopotamus infected with *B. anthracis*, Bwabwata National Park, Namibia, 2017. A) Hematoxylin and eosin stain showing large bacilli evident in vessel lumen. Original magnification × 40. B) Gram stain showing gram-variable rods evident in vessels. Original magnification × 40. C) Immunohistochemical stain of *B. anthracis* cell wall showing antigen evident in vessels (red). Original magnification × 40. D) Immunohistochemical stain of *B. anthracis* capsule showing bacilli evident in vessels (red), and bacterial antigen. Original magnification × 63.

Swift response in organizing PEP dissemination, community education, livestock vaccination, and carcass disposal contributed to the prevention of anthrax transmission to humans and livestock. Our investigation emphasizes the importance of a multiagency coordinated response for zoonotic disease outbreaks and continued efforts to raise awareness of the risks of consuming meat from animal carcasses in anthrax-endemic areas.

Acknowledgments

The authors acknowledge the efforts of the Namibia Ministry of Health and Social Services, Field Epidemiology and Laboratory Training Program staff and residents, and staff of the Andara Hospital who administered questionnaires to assess exposure status, coordinated antibiotic administration, and performed follow-up assessments of exposed community members. We also acknowledge the efforts of the staff of the Namibia Ministry of Environment and Tourism, supported by the Namibia Police Air Wing and the NamParks IV Project and co-financed by the government of Namibia and KfW from the government of Germany. We acknowledge the efforts of the staff of the Namibia Ministry of Agriculture, Water, and Forestry, who performed carcass surveillance and disposal and livestock vaccination during the epizootic and months following. We also thank the staff of the Namibia Institute for Pathology in the Rundu State Hospital and Andara Hospital for providing supplies necessary to the work in the field. Finally, we thank Syamal Raychaudhuri for providing the AAD lateral flow cassettes.

About the Author

Dr. Cossaboom is an Epidemic Intelligence Service officer assigned to the Bacterial Special Pathogens Branch, Division of High-Consequence Pathogens and Pathology, National Center for Emerging and Zoonotic Infectious Diseases, Centers for Disease Control and Prevention, Atlanta, Georgia, USA. Her primary research interests include epidemiology and outbreak response of zoonotic diseases of public health importance.

References

1. Hugh-Jones ME, de Vos V. Anthrax and wildlife. Rev Sci Tech. 2002;21:359–83. http://dx.doi.org/10.20506/rst.21.2.1336
2. Munang'andu HM, Banda F, Siamudaala VM, Munyeme M, Kasanga CJ, Hamududu B. The effect of seasonal variation on anthrax epidemiology in the upper Zambezi floodplain of western Zambia. J Vet Sci. 2012;13:293–8. http://dx.doi.org/10.4142/jvs.2012.13.3.293
3. Pienaar UD. Epidemiology of anthrax in wild animals and the control of anthrax epizootics in the Kruger National Park, South Africa. Fed Proc. 1967;26:1496–502.
4. Clegg SB, Turnbull PC, Foggin CM, Lindeque PM. Massive outbreak of anthrax in wildlife in the Malilangwe Wildlife Reserve, Zimbabwe. Vet Rec. 2007;160:113–8. http://dx.doi.org/10.1136/vr.160.4.113
5. Lehman MW, Craig AS, Malama C, Kapina-Kany'anga M, Malenga P, Munsaka F, et al. Role of food insecurity in outbreak of anthrax infections among humans and hippopotamuses living in a game reserve area, rural Zambia. Emerg Infect Dis. 2017;23:1471–7. http://dx.doi.org/10.3201/eid2309.161597
6. Lindeque PM, Turnbull PC. Ecology and epidemiology of anthrax in the Etosha National Park, Namibia. Onderstepoort J Vet Res. 1994;61:71–83.
7. Mendelsohn J, Roberts C, Hines C. An environmental profile and atlas of Caprivi. Windhoek (Namibia): Directorate of Environmental Affairs; 1997.
8. World Health Organization. Anthrax in humans and animals. 4th ed. Geneva: The Organization; 2008. p. 84–92.
9. Gates-Hollingsworth MA, Perry MR, Chen H, Needham J, Houghton RL, Raychaudhuri S, et al. Immunoassay for capsular antigen of *Bacillus anthracis* enables rapid diagnosis in a rabbit model of inhalational anthrax. PLoS One. 2015;10:e0126304. http://dx.doi.org/10.1371/journal.pone.0126304
10. Hoffmaster AR, Meyer RF, Bowen MD, Marston CK, Weyant RS, Thurman K, et al. Evaluation and validation of a real-time polymerase chain reaction assay for rapid identification of *Bacillus anthracis.* Emerg Infect Dis. 2002;8:1178–82. http://dx.doi.org/10.3201/eid0810.020393
11. Guarner J, Jernigan JA, Shieh WJ, Tatti K, Flannagan LM, Stephens DS, et al.; Inhalational Anthrax Pathology Working Group. Pathology and pathogenesis of bioterrorism-related inhalational anthrax. Am J Pathol. 2003;163:701–9. http://dx.doi.org/10.1016/S0002-9440(10)63697-8
12. Bollweg BC, Silva-Flannery L, Spivey P, Hale GL. Optimization of commercially available Zika virus antibodies for use in a laboratory-developed immunohistochemical assay. J Pathol Clin Res. 2017;4:19–25. http://dx.doi.org/10.1002/cjp2.84
13. Turnbull PC. Anthrax vaccines: past, present and future. Vaccine. 1991;9:533–9. http://dx.doi.org/10.1016/0264-410X(91)90237-Z
14. Beytell PC. Wetland survey of the Bwabwata Okavango Ramsar site, September 2017. Windhoek (Namibia): Directorate of Scientific Services; 2018.

Address for correspondence: Caitlin M. Cossaboom, Centers for Disease Control and Prevention, 1600 Clifton Rd NE, Mailstop A-30, Atlanta, GA 30329-4027, USA; email: nrm9@cdc.gov

Zika Virus in Rectal Swab Samples

Camila Helena Aguiar Bôtto-Menezes, Armando Menezes Neto, Guilherme Amaral Calvet, Edna Oliveira Kara, Marcus Vinícius Guimarães Lacerda, Marcia da Costa Castilho, Ute Ströher, Carlos Alexandre Antunes de Brito, Kayvon Modjarrad, Nathalie Broutet, Patrícia Brasil, Ana Maria Bispo de Filippis, Rafael Freitas Oliveira Franca, ZIKABRA Study Team[1]

We detected Zika virus RNA in rectal swab samples from 10 patients by using real-time reverse transcription PCR, and we isolated the virus from 1 patient. The longest interval from symptom onset to detection was 14 days. These findings are applicable to diagnosis and infection prevention recommendations.

In early 2015, Zika virus was identified in Brazil and spread across nearly the whole continent, affecting thousands of persons (*1*). This outbreak was associated with microcephaly and other congenital abnormalities resulting from infection of the mother during pregnancy (*2*). For different periods after infection, Zika virus RNA can be found in diverse body fluids such as saliva, amniotic fluid, urine, cerebrospinal fluid, blood, semen, and tears (*3*); the longest period of viral RNA shedding has been identified in semen (>1 year after symptom onset) (*4*).

Although Zika virus RNA has been detected in different body fluids, we found only 1 report of Zika virus elimination through feces from 1 naturally infected person (*5*). Experimentally, Zika virus is able to infect mice and adult macaques (*6*) through the anorectal mucosa, leading to detectable viremia with subsequent testicular damage and congenital defects in the offspring of pregnant mice (*5*). These findings indicate that the anorectal mucosa may represent an infection route for Zika virus. However, whether Zika virus can be detected in the anorectal mucosa of naturally infected human patients remains largely unknown. To clarify the kinetics of Zika virus infection across biological compartments and to devise rational measures for preventing transmission of the virus, in July 2017 we began a cohort study of men and women ≥18 years of age with Zika virus infection in Brazil; the study will continue until mid-2020. Written informed consent was obtained from all enrolled participants.

The Study

To assess the persistence of Zika virus in different body fluids of persons with confirmed infection, we conducted a multicenter prospective cohort study (the ZIKABRA Study). Laboratory confirmation of infection was based on real-time reverse transcription PCR (rRT-PCR) performed on samples (urine, blood, or both) from persons in whom a rash developed ≤48 hours after initial symptom onset. We also invited household contacts or sex partners to participate in the study and enrolled those with positive rRT-PCR results for Zika virus. Full details about the study protocol, including ethics approval, are described by Calvet et al. (*7*).

We collected samples (saliva, blood, urine, vaginal, and rectal swabs) at specific intervals from patients identified as Zika virus positive after the screening visit (Figure). Vaginal and rectal swab samples were diluted in 1 mL of sterile Hank's Balanced Salt Solution (ThermoFisher Scientific, https://www.thermofisher.com) and stored at −80°C until processing. After collection, specimens were kept refrigerated and transported within 2 hours to the laboratory, where they were maintained at −80°C. Zika virus detection was performed by rRT-PCR by processing 200 μL of each specimen for RNA extraction through an automated nucleic acid purification platform by using the Maxwell 16 Viral Total Nucleic Acid Purification Kit (Promega Corporation, https://www.promega.com) in a final volume of 70 μL. For rRT-PCR, we used the commercially available ZDC Kit from Instituto de Tecnologia em Imunobiológicos Biomanguinhos, approved by Agência Nacional de Vigilância Sanitária/

Author affiliations: Amazonas State University, Manaus, Brazil (C.H.A. Bôtto-Menezes); Tropical Medicine Foundation Doctor Heitor Vieira Dourado, Manaus (C.H.A. Bôtto-Menezes, M.V.G. Lacerda, M. da Costa Castilho); Institute Aggeu Magalhães, Recife, Brazil (A.M. Neto, C.A. Antunes de Brito, R.F.O. Franca); Evandro Chagas National Institute of Infectious Diseases, Rio de Janeiro, Brazil (G.A. Calvet, P. Brasil); World Health Organization, Geneva, Switzerland (E.O. Kara, U. Ströher, N. Broutet); Oswaldo Cruz Foundation, Manaus (M.V.G. Lacerda); Walter Reed Army Institute of Research, Silver Spring, Maryland, USA (K. Modjarrad); Oswaldo Cruz Institute, Rio de Janeiro (A.M. Bispo de Filippis)

DOI: https://doi.org/10.3201/eid2505.180904

[1]Team members are listed at the end of the article.

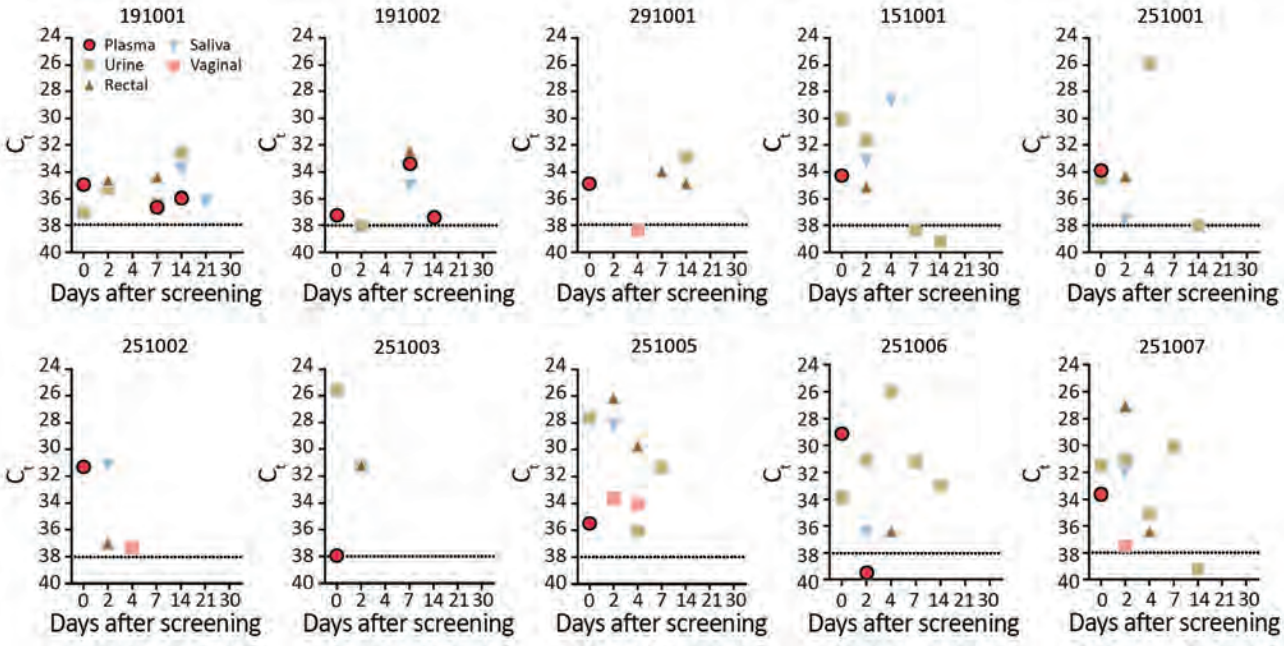

Figure. Detection of Zika virus RNA in human biological specimens from 8 patients, according to C_t and days after disease onset. Patient identification numbers above charts correspond to numbers in the Table. Horizontal dashed lines indicate real-time reverse transcription PCR cutoff C_t of 38. Disease onset is day 0 (screening visit), defined after interviewing patients about symptoms. C_t, cycle threshold.

ANVISA (registry no. 80142170032; https://www.bio.fiocruz.br). We considered positive those samples that displayed positive amplification in the ZDC Kit internal control reaction (which consists of an RNA virus–like particle individually added to each specimen before RNA extraction) and those samples in which the target amplification was detected within 38 amplification cycles, as previously described (*8*).

We report 10 Zika virus–infected patients from 2 locations in Brazil. Of these, 3 patients were identified in Recife, northeastern Brazil, and 7 were from Manaus, northern Brazil. The targeted Zika virus amplicons were found in the plasma of 9 patients and in the urine of 7 patients, all tested at screening visits. We also tested all plasma and urine samples for dengue and chikungunya virus by rRT-PCR; results were negative. Of the 10 Zika virus–infected patients, 9 were symptomatic and 1 (a Zika virus–positive household contact) was asymptomatic at enrollment but subsequently reported muscular weakness and irritability on day 5 and arthralgia on day 7 after Zika virus identification. Median patient age was 31.5 years; 7 patients were nonpregnant women, and 3 were men (Table). All patients were negative for HIV-1, hepatitis B and C, and syphilis.

For all patients, Zika virus RNA was detected >1 time in different body fluids. The longest interval for Zika virus–positive results by rRT-PCR in plasma and urine was 14 days after symptom onset; median cycle threshold value (C_t) was 34.92 in plasma (interquartile range [IQR] 33.57–36.78) and 31.57 in urine (IQR 30.34–34.92). The longest duration of persistence in saliva was 21 days. Zika virus RNA was detected in rectal swab samples from all patients (median C_t 34.36 [IQR 30.08–36.07]); positive results were obtained at >1 time for 4 patients. Vaginal swab sample results were positive for 2 patients (Figure). We attempted virus isolation in Vero E6 cells from all rectal swab specimens positive by rRT-PCR. After filtering samples through a 0.22-μm syringe filter, a rectal swab sample from patient 191002 (at 7 days after symptom onset) was positive in Vero E6 cells, inducing cytopathic effect and returning a C_t of 28.77 after 6 days of incubation at 37°C.

Conclusions

Our detection of Zika virus RNA in human rectal swab samples demonstrates the presence of virus RNA in the anorectal mucosa of naturally infected patients. Because the anorectal mucosa is a major entry site for HIV-1 and other sexually transmitted disease organisms (*9*), this finding may have implications for Zika virus transmission. Direct contact with infected mucosa could present a risk for virus transmission. Moreover, recovery of infectious Zika virus from anorectal mucosa samples may be associated with active virus replication in this body compartment, implicating its permissiveness to Zika virus infection.

Table. Clinical signs and symptoms reported at enrollment visit in study of persistence of Zika virus in different body fluids of persons with confirmed infection, Brazil*

Patient ID	Age, y/sex	Symptoms at enrollment
191001	21/M	None (asymptomatic household contact)
191002	25/M	Erythema and vesicular rash, nasal congestion, sweating, upper limb muscle spasms
291001	22/F	Itchy macular rash, conjunctival hyperemia, prostration, chills, taste alteration, lower back pain, arthralgia, periarticular edema, nausea, irritability
151001	38/M	Itchy macular rash, headache, photophobia, retro-orbital pain, burning eyes, arthralgia (wrists, metacarpals, and phalanges), tingling hands
251001	31/F	Itchy macular rash, conjunctival hyperemia, anorexia
251002	36/F	Itchy macular rash, headache, conjunctival hyperemia, arthralgia (shoulders, elbows, wrists, knees, ankles), abdominal pain, periarticular edema (ankles)
251003	43/F	Itchy macular rash, photophobia, retro-orbital pain, oropharyngeal pain, arthralgia (elbows and ankles)
251005	19/F	Itchy macular rash, fever, headache, photophobia, conjunctival hyperemia, retro-orbital pain, muscle weakness, numbness, irritability, appetite loss, nausea
251006	65/F	Itchy macular rash, fever, headache, photophobia, arthralgia (wrists, phalanges, heel, cervical spine), muscle weakness, prostration, numbness, tingling, drowsiness, abdominal pain, nausea
251007	32/F	Itchy macular rash, fever, headache, retro-orbital pain, photophobia

*Reported signs and symptoms were registered after an initial rash episode following laboratory confirmation of Zika virus infection. All signs and symptoms were registered ≤2 d after the initial rash (except for 1 asymptomatic contact patient). Fever (≥38°C) was any febrile episode reported within 30 d before the medical examination. ID, identification.

Recently, 2 studies explored the mucosa as an experimental entry site for Zika virus. Macaques exposed to high doses of the virus by direct inoculation on palatine tonsils, nasal mucosa, and conjunctival mucosa became infected, whereas virus-naive animals exposed to saliva from Zika virus–infected macaques, containing a 20-fold lower virus concentration, remained uninfected (*6*). In mice, intra-anal inoculation resulted in viremia, replication in multiple organs, and Zika virus RNA detection in feces (*5*). However, it seems that high viral loads are required for successful experimental infection through mucosal tissues. In humans, a report of a man infected through anal intercourse implies that the anorectal mucosa is an entry site for Zika virus (*10*). Also, a rapidly progressive fatal case, with secondary nonsexual transmission to a close contact who reported having had no contact with blood or other body fluids except tears from the original patient, raised the hypothesis of Zika virus transmission through mucosa (*11*). Although mucosal tissues have been extensively explored as a potential site of Zika virus infection, the amount of infectious particles in these tissues remains unclear.

In patients with yellow fever, mucocutaneous bleeding with virus presence has been reported (*12*). However, no mucosal bleeding was observed in the patients we report, despite extensive medical examination. In addition, in 5 of 9 patients, the virus had already cleared from the blood at the time of anorectal detection, which supports the concept of local virus replication. Our finding of Zika virus in the anorectal mucosa of naturally infected persons may influence the recommendations for prevention of Zika virus transmission. We suggest the use of rectal swabbing, a noninvasive method, for diagnosing infection with Zika virus, among other emerging viruses (*13*).

ZIKABRA Study Team members (in alphabetical order): André Luiz de Abreu, Adele Schwartz Benzaken, Ximena Pamela Diaz Bermudez, Camila Helena Aguiar Bôtto-Menezes, Patrícia Brasil, Carlos Alexandre Antunes Brito, Nathalie Jeanne Nicole Broutet, Guilherme Amaral Calvet, Marcia da Costa Castilho, Ana Maria Bispo de Filippis, Rafael Freitas Oliveira Franca, Silvana Pereira Giozza, Ndema Habib, Edna Oliveira Kara, Marcus Vinicius Guimarães Lacerda, Sihem Landoulsi, Morganna Costa Lima, Noemia Lima, Maeve Brito de Mello, Ana Izabel Costa de Menezes, Robyn Meurant, Kayvon Modjarrad, Armando Menezes Neto, Cristina Pimenta, Casey Storme, Ute Ströher, Anna Thorson, Lydie Trautman.

Acknowledgments

We thank all patients for their willingness to participate in the study and all collaborating staff for their invaluable help in designing the protocol.

The research leading to these results received funding from Wellcome Trust grant no. 206522/Z/17/Z, World Health Organization (UNDP-UNFPA-UNICEF-WHO-World Bank Special Programme of Research, Development and Research Training in Human Reproduction), World Health Emergency Programme Organization, Brazilian Ministry of Health (Convênio no. 837059/2016, Processo 25000162039201616), US National Institutes of Health National Institute of Allergy and Infectious Diseases (award no. R21AI139777). This work was supported by a cooperative agreement (W81XWH-18-2-0040) between the Henry M. Jackson Foundation for the Advancement of Military Medicine and the US Department of the Army. The work was funded by the US Defense Health Agency (0130602D16). The funders had no role in study design, data collection, analysis, decision to publish, or preparation of the manuscript.

About the Author

Dr. Bôtto-Menezes is a research associate at Fundacao de Medicina Tropical Doutor Heitor Vieira Dourado and professor at Amazonas State University. Her research interests are tropical medicine, infectious diseases, and epidemiology.

References

1. Faria NR, Azevedo RDSDS, Kraemer MUG, Souza R, Cunha MS, Hill SC, et al. Zika virus in the Americas: early epidemiological and genetic findings. Science. 2016;352:345–9.
2. Miranda-Filho DB, Martelli CMT, Ximenes RA, Araújo TV, Rocha MA, Ramos RC, et al. Initial description of the presumed congenital Zika syndrome. Am J Public Health. 2016;106:598–600. http://dx.doi.org/10.2105/AJPH.2016.303115
3. Paz-Bailey G, Rosenberg ES, Doyle K, Munoz-Jordan J, Santiago GA, Klein L, et al. Persistence of Zika virus in body fluids–preliminary report. N Engl J Med. 2017;379:1234–43.
4. Barzon L, Percivalle E, Pacenti M, Rovida F, Zavattoni M, Del Bravo P, et al. Virus and antibody dynamics in travelers with acute Zika virus infection. Clin Infect Dis. 2018;66:1173–80. http://dx.doi.org/10.1093/cid/cix967
5. Li C, Deng Y-Q, Zu S, Quanquin N, Shang J, Tian M, et al. Zika virus shedding in the stool and infection through the anorectal mucosa in mice. Emerg Microbes Infect. 2018;7:169. http://dx.doi.org/10.1038/s41426-018-0170-6
6. Haddow AD, Nalca A, Rossi FD, Miller LJ, Wiley MR, Perez-Sautu U, et al. High infection rates for adult macaques after intravaginal or intrarectal inoculation with Zika virus. Emerg Infect Dis. 2017;23:1274–81. http://dx.doi.org/10.3201/eid2308.170036
7. Calvet GA, Kara EO, Giozza SP, Bôtto-Menezes CHA, Gaillard P, de Oliveira Franca RF, et al.; ZIKABRA Study Team. Study on the persistence of Zika virus (ZIKV) in body fluids of patients with ZIKV infection in Brazil. BMC Infect Dis. 2018;18:49. http://dx.doi.org/10.1186/s12879-018-2965-4
8. Lanciotti RS, Kosoy OL, Laven JJ, Velez JO, Lambert AJ, Johnson AJ, et al. Genetic and serologic properties of Zika virus associated with an epidemic, Yap State, Micronesia, 2007. Emerg Infect Dis. 2008;14:1232–9. http://dx.doi.org/10.3201/eid1408.080287
9. Workowski KA, Bolan GA; Centers for Disease Control and Prevention. Sexually transmitted diseases treatment guidelines, 2015. MMWR Recomm Rep. 2015 Jun 5;64(RR-03):1–137.
10. Deckard DT, Chung WM, Brooks JT, Smith JC, Woldai S, Hennessey M, et al. Male-to-male sexual transmission of Zika virus—Texas, January 2016. MMWR Morb Mortal Wkly Rep. 2016;65:372–4. http://dx.doi.org/10.15585/mmwr.mm6514a3
11. Swaminathan S, Schlaberg R, Lewis J, Hanson KE, Couturier MR. Fatal Zika virus infection with secondary nonsexual transmission. N Engl J Med. 2016;375:1907–9. http://dx.doi.org/10.1056/NEJMc1610613
12. Monath TP. Yellow fever: an update. Lancet Infect Dis. 2001; 1:11–20. http://dx.doi.org/10.1016/S1473-3099(01)00016-0
13. Uyeki TM, Mehta AK, Davey RT Jr, Liddell AM, Wolf T, Vetter P, et al.; Working Group of the U.S.–European Clinical Network on Clinical Management of Ebola Virus Disease Patients in the U.S. and Europe. Clinical management of Ebola virus disease in the United States and Europe. N Engl J Med. 2016;374:636–46. http://dx.doi.org/10.1056/NEJMoa1504874

Address for correspondence: Rafael F.O. Franca, Oswaldo Cruz Foundation–FIOCRUZ, Department of Virology and Experimental Therapy, Av. Professor Moraes Rego, s/n–Campus da UFPE, Cidade Universitária Recife, Pernambuco 50740-465, Brazil; email: rafael.franca@cpqam.fiocruz.br

Bombali Virus in *Mops condylurus* Bat, Kenya

Kristian M. Forbes,[1] Paul W. Webala, Anne J. Jääskeläinen, Samir Abdurahman, Joseph Ogola, Moses M. Masika, Ilkka Kivistö, Hussein Alburkat, Ilya Plyusnin, Lev Levanov, Essi M. Korhonen, Eili Huhtamo, Dufton Mwaengo, Teemu Smura, Ali Mirazimi, Omu Anzala, Olli Vapalahti, Tarja Sironen

Bombali virus (genus *Ebolavirus*) was identified in organs and excreta of an Angolan free-tailed bat (*Mops condylurus*) in Kenya. Complete genome analysis revealed 98% nucleotide sequence similarity to the prototype virus from Sierra Leone. No Ebola virus–specific RNA or antibodies were detected from febrile humans in the area who reported contact with bats.

The virus family *Filoviridae* is divided into 5 genera: *Cuevavirus, Marburgvirus, Ebolavirus, Striavirus,* and *Thamnovirus* (https://talk.ictvonline.org/taxonomy). Six distinct members of *Ebolavirus* have been described; 4 are known to cause human disease (*1*,*2*). These include highly lethal pathogens capable of producing large outbreaks, namely Bundibugyo, Sudan, and Zaire Ebola viruses, the last responsible for the devastating 2013–2016 outbreak in West Africa and an ongoing extended outbreak in the Democratic Republic of the Congo (*1*,*3*,*4*). Although the natural reservoirs of Ebola viruses remain unconfirmed, considerable evidence supports a role for bat species, particularly fruit bats, analogous to findings implicating *Rousettus aegypticus* fruit bats as a reservoir for Marburg virus (*1*,*5*,*6*).

The most recent Ebola virus to be identified is named Bombali virus (BOMV) and was reported in August 2018 in mouth and fecal swabs collected from free-tailed insectivorous bat species (family Molossidae) *Mops condylurus* and *Chaerephon pumilus* in Sierra Leone (*2*). Although BOMV is not known to infect humans, its envelope glycoprotein shares the same NPC1 receptor as other filoviruses and is capable of mediating BOMV pseudotype virus entry into human cells (*2*). We describe the presence of BOMV in tissues and excreta of an Angolan free-tailed bat (*M. condylurus*) captured near the Taita Hills in southeastern Kenya, the easternmost distributional range of this bat species (*7*), >5,500 km from the original BOMV identification site in Sierra Leone (Figure 1). We also screened human serum samples collected from febrile patients in the Taita Hills area for markers of BOMV infection.

We identified BOMV in an adult female bat (B241) by reverse transcription PCR and next-generation sequencing. This bat was captured along with 15 others in mist nets in savannah habitat near a small river in May 2018; only this bat was BOMV positive (6% prevalence). Viral RNA was present in lung, spleen, liver, heart, intestine, mouth swab, and fecal samples but absent from the brain, kidney, urine, and a few fleas found on the bat; viral loads were especially high in the lung (Appendix, https://wwwnc.cdc.gov/EID/article/25/5/18-1666-App1.pdf). These tissue-positive findings confirm that BOMV can infect *M. condylurus* and is not an artifact of its insect diet, which could not be discounted from the previous analysis on the basis of mouth and fecal swabs (*2*). We also screened lung samples of sympatric *C. pumilus* bats (n = 13) and other bat species (Appendix Table 2) captured from the same area in February 2016 and May 2018; all were negative for BOMV RNA. Serologic analysis revealed antibodies against BOMV in the blood of the tissue-positive bat (Appendix Figure), but specific antibodies were not found in blood from the other bats (Appendix).

Our tissue-positive findings provide a strong host association between BOMV and *M. condylurus* bats; it is possible that BOMV–positive findings from other bat species result from local spillover or contamination. Moreover, phylogenetic analysis of the full BOMV genome from the bat lung revealed 98% nucleotide sequence similarity with the prototype reported in Sierra Leone (GenBank accession no. MK340750) (Figure 2). Considering the high sequence similarity between the 2 locations and that *M. condylurus* bats, like most insectivorous bats, are believed to travel only short distances (*8*), BOMV is likely to be distributed throughout much of sub-Saharan Africa

Author affiliations: University of Helsinki, Helsinki, Finland (K.M. Forbes, A.J. Jääskeläinen, I. Kivistö, H. Alburkat, I. Plyusnin, L. Levanov, E.M. Korhonen, E. Huhtamo, T. Smura, O. Vapalahti, T. Sironen); Maasai Mara University, Narok, Kenya (P.W. Webala); Helsinki University Hospital, Helsinki (A.J. Jääskeläinen, O. Vapalahti); Public Health Agency of Sweden, Stockholm, Sweden (S. Abdurahman, A. Mirazimi); University of Nairobi, Nairobi, Kenya (J. Ogola, M.M. Masika, D. Mwaengo, O. Anzala); Karolinska University Hospital, Stockholm (A. Mirazimi); National Veterinary Institute, Uppsala, Sweden (A. Mirazimi)

DOI: https://doi.org/10.3201/eid2505.181666

[1]Current affiliation: University of Arkansas, Fayetteville, Arkansas, USA.

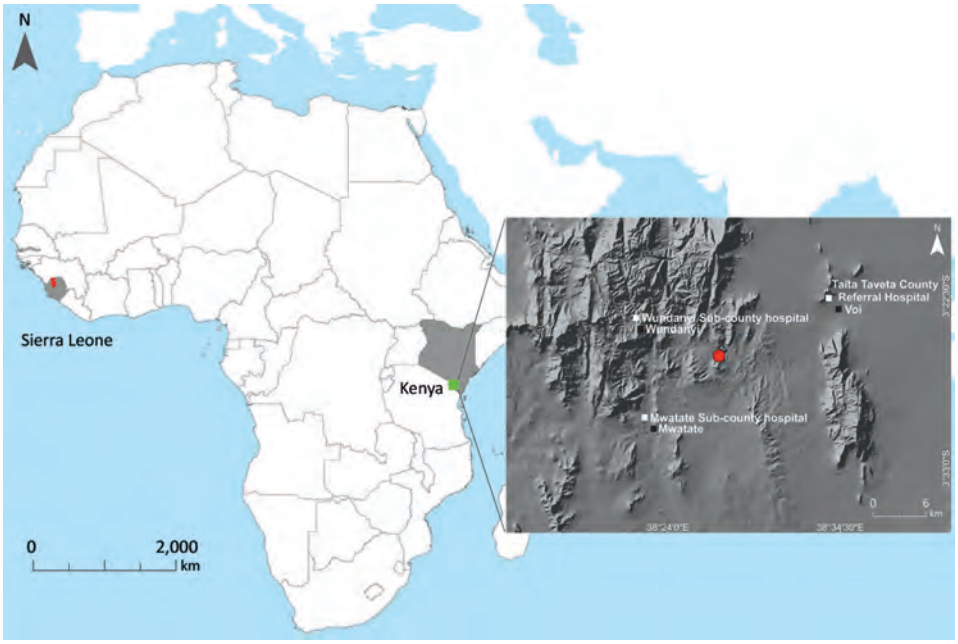

Figure 1. Locations of Bombali Ebola virus infection in Sierra Leone (gray shading at left; Bombali district in red) and Kenya (gray shading at right; Taita Hills area in green). Inset map shows collection site of the Bombali virus–positive bat (red dot) in Kenya, clinics in which human serum samples were collected (white squares), and the closest towns (black squares).

(*7*). However, further monitoring of *M. condylurus* and *C. pumilus* bats and other sympatric species across Africa is required to support this hypothesis.

Because *M. condylurus* bats commonly roost in human structures, such as house roofs (*8*,*9*), human exposure to this species is more likely than for many other bat species. Therefore, we screened for markers of human infection with BOMV by studying serum samples collected from febrile patients who sought treatment at clinics in the Taita Hills area during April–August 2016. Clinics are located in the surrounding areas, all within 15 km of the BOMV–infected bat collection site (Figure 1). We screened patients for filovirus RNA (n = 81) and Ebola virus–specific IgG (n = 250) by an immunofluorescence assay using Zaire Ebola virus VP40–transfected VeroE6 cells as antigen (Appendix). Many samples, including

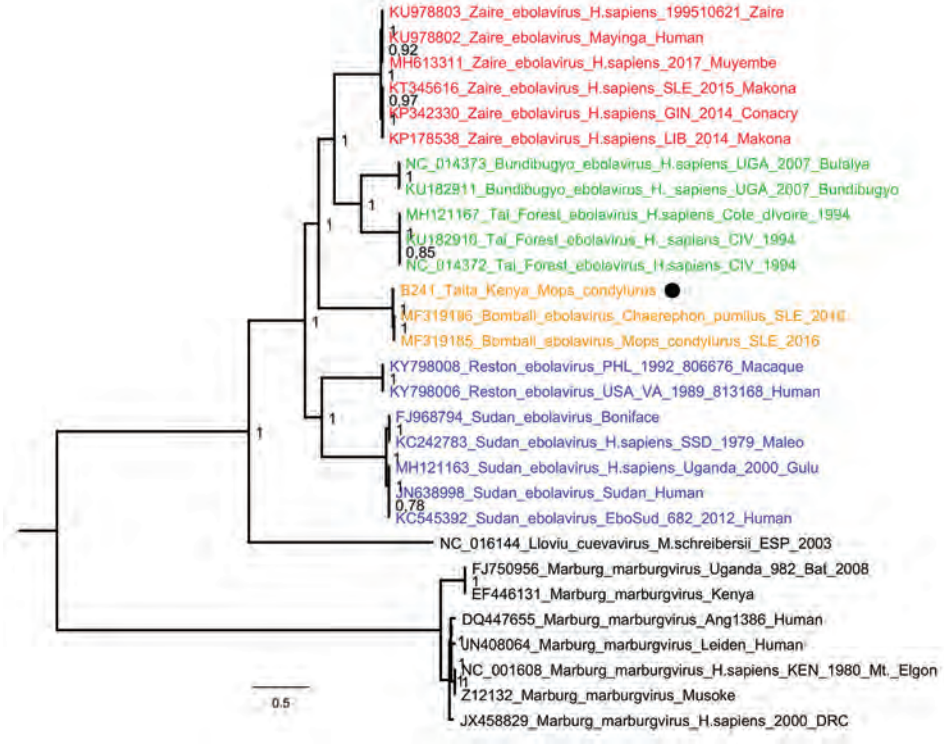

Figure 2. Phylogenetic tree of complete filovirus genomes (18,795–19,115 nt), including Bombali Ebola virus in Sierra Leone and now Kenya (19,026 nt; black dot). Representative sequences were retrieved from the Virus Pathogen Database and Analysis Resource and aligned with a MAFFT online server (http://mafft.cbrc.jp/alignment/software). The tree was built using the Bayesian Markov Chain Monte Carlo method, using a general time-reversible model of substitution with gamma-distributed rate variation among sites allowing the presence of invariable sites. Posterior probabilities are shown at the nodes. Scale bar indicates genetic distance.

all those screened for filovirus RNA, were from patients who reported contact with bats in the home or workplace. We found no evidence of filovirus infection by either screening method, providing no support that BOMV easily infects humans or is a common cause of febrile illness in the area. Ongoing surveillance is nonetheless necessary, and we cannot exclude the possibility that Bombali virus was a recent introduction to the Taita Hills area.

Our results markedly expand the distributional range of this new Ebola virus to eastern Africa and confirm the *M. condylurus* bat as a competent host. Like Goldstein et al. (*2*), we stress that the virus is not known to infect humans, a premise supported by our screening of febrile patients in the Taita Hills area. Potential efforts to eradicate bats are unwarranted and may jeopardize their crucial ecosystem roles and human health (*10*,*11*).

Acknowledgments

We thank Joni Uusitalo and Michael Bartonjo for fieldwork assistance; Johanna Martikainen, Mira Utriainen, and Fathiah Zakham for laboratory assistance; and Ruut Uusitalo for preparing the figure map. We also thank the clinicians who recruited patients for the human study and the staff at the University of Helsinki Taita Research Station and its director, Petri Pellikka, for facilitating this work.

This research was supported by the Finnish Cultural Foundation, the Jenny and Antti Wihuri Foundation, the Academy of Finland (grant no. 318726), Helsinki University Hospital Funds, and the Jane and Aatos Erkko Foundation. A.J.J., S.A., L.L., A.M., O.V., and T.S. are part of the EbolaMoDRAD consortium, which has received funding to develop diagnostic methods for filoviruses from the Innovative Medicine Initiative 2 Joint Undertaking under grant agreement no. 115843. This Joint Undertaking receives support from the European Union's Horizon 2020 research and innovation program and the European Federation of Pharmaceutical Industries and Associations (EFPIA). Bat trapping and sample collections were carried out under permits from the National Commission for Science, Technology, and Innovation (permit no. NACOSTI/P/18/76501/22243) and the Kenya Wildlife Service (permit no. KWS/BRM/500). The Finnish Food Safety Authority (Evira) approved the importation of samples (permit nos. 4250/0460/2016 and 2809/0460/2018). Kenyatta National Hospital and the University of Nairobi Ethics and Research Committee approved the human study (permit no. P707/11/2015).

About the Author

Dr. Forbes is a disease ecologist and assistant professor at the Department of Biological Sciences, University of Arkansas. His research interests include the maintenance and transmission of rodentborne and batborne zoonotic pathogens in nature and the effects of anthropogenic environmental changes on these processes.

References

1. Olival KJ, Hayman DTS. Filoviruses in bats: current knowledge and future directions. Viruses. 2014;6:1759–88. http://dx.doi.org/10.3390/v6041759
2. Goldstein T, Anthony SJ, Gbakima A, Bird BH, Bangura J, Tremeau-Bravard A, et al. The discovery of Bombali virus adds further support for bats as hosts of ebolaviruses. Nat Microbiol. 2018;3:1084–9. http://dx.doi.org/10.1038/s41564-018-0227-2
3. Piot P, Muyembe JJ, Edmunds WJ. Ebola in west Africa: from disease outbreak to humanitarian crisis. Lancet Infect Dis. 2014;14:1034–5. http://dx.doi.org/10.1016/S1473-3099(14)70956-9
4. Nkengasong JN, Onyebujoh P. Response to the Ebola virus disease outbreak in the Democratic Republic of Congo. Lancet. 2018;391:2395–8. https://doi.org/10.1016/S0140-6736(18)31326-6
5. Towner JS, Amman BR, Sealy TK, Carroll SA, Comer JA, Kemp A, et al. Isolation of genetically diverse Marburg viruses from Egyptian fruit bats. PLoS Pathog. 2009;5:e1000536. http://dx.doi.org/10.1371/journal.ppat.1000536
6. Leroy EM, Kumulungui B, Pourrut X, Rouquet P, Hassanin A, Yaba P, et al. Fruit bats as reservoirs of Ebola virus. Nature. 2005;438:575–6. http://dx.doi.org/10.1038/438575a
7. Happold M. Tadarida condylura Angolan free-tailed bat. In: Happold M, Happold D, editors. Mammals of Africa (hedgehogs, shrews, and bats). Vol. 4. London: Bloomsbury; 2013. p. 505–7.
8. Noer CL, Dabelsteen T, Bohmann K, Monadjem A. Molossid bats in an African agro-ecosystem select sugarcane fields as foraging habitat. Afr Zool. 2012;47:1–11. http://dx.doi.org/10.3377/004.047.0120
9. Bronrier GN, Maloney SK, Buffenstein R. Survival tactics within thermally-challenging roosts: heat tolerance and cold sensitivity in the Angolan free-tailed bat, Mops condylurus. S Afr Zool. 1999;34:1–10. http://dx.doi.org/10.1080/02541858.1999.11448481
10. Kunz TH, Braun de Torrez E, Bauer D, Lobova T, Fleming TH. Ecosystem services provided by bats. Ann N Y Acad Sci. 2011; 1223:1–38. http://dx.doi.org/10.1111/j.1749-6632.2011.06004.x
11. Amman BR, Nyakarahuka L, McElroy AK, Dodd KA, Sealy TK, Schuh AJ, et al. Marburgvirus resurgence in Kitaka Mine bat population after extermination attempts, Uganda. Emerg Infect Dis. 2014;20:1761–4. http://dx.doi.org/10.3201/eid2010.140696

Address for correspondence: Kristian M. Forbes, University of Arkansas, Department of Biological Sciences, SCEN Bldg, 850 W Dickson St, Fayetteville, AR 16801, USA; email: kmforbes@uark.edu

Genetic Characterization of Middle East Respiratory Syndrome Coronavirus, South Korea, 2018

Yoon-Seok Chung, Jeong Min Kim, Heui Man Kim, Kye Ryeong Park, Anna Lee, Nam-Joo Lee, Mi-Seon Kim, Jun Sub Kim, Chi-Kyeong Kim, Jae In Lee, Chun Kang

We evaluated genetic variation in Middle East respiratory syndrome coronavirus (MERS-CoV) imported to South Korea in 2018 using specimens from a patient and isolates from infected Caco-2 cells. The MERS-CoV strain in this study was genetically similar to a strain isolated in Riyadh, Saudi Arabia, in 2017.

Between 2012 and the end of August 2018, a total of 2,248 laboratory-confirmed cases of Middle East respiratory syndrome coronavirus (MERS-CoV) infection and 798 associated deaths (case-fatality rate 35.3%) were reported in 27 countries (*1*). Most of these cases (83%) were reported in Saudi Arabia (1,871 cases, including 724 related deaths, for a case-fatality rate of 38.7%).

The 2015 MERS-CoV outbreak in South Korea resulted in 186 laboratory-confirmed cases and 38 deaths. MERS-CoV spread via intrahospital and interhospital transmission at 16 clinics and hospitals across South Korea (*2*). This outbreak was recorded as the largest MERS outbreak outside of the Middle East (*3*).

In August 2018, eight laboratory-confirmed cases of MERS-CoV infection were reported in Saudi Arabia, with 4 associated deaths; 1 case in a person who had travel history to the Arabian Peninsula was reported in the United Kingdom (*4*). In September 2018, a man in South Korea with a history of travel to the Middle East became ill and was suspected of having MERS-CoV infection. We report the investigation of this case and genetic characterization of the virus on the basis of variation and phylogenetic analyses of the spike (S) gene and the full-length genome from patient specimens and isolates from Caco-2 cells.

Author affiliations: Korea Centers for Disease Control and Prevention, Cheongju, South Korea (Y.-S. Chung, J.M. Kim, H.M. Kim, K.R. Park, A. Lee, N.-J. Lee, M.-S. Kim, J.S. Kim, C.-K. Kim, C. Kang); Seoul Institute of Public Health and Environment, Seoul, South Korea (J.I. Lee)

DOI: https://doi.org/10.3201/eid2505.181534

The Study

On September 7, 2018, a 61-year-old man who had moved from Kuwait to South Korea visited the hospital with diarrhea and fever (*5*). The patient had a history of visiting the Middle East and was suspected of MERS-CoV infection; accordingly, he was transferred to a hospital with a national isolation ward.

On September 8, we collected nasopharyngeal swab and sputum samples from the patient and transported them to the Seoul Provincial Institute of Public Health and Environment (Seoul, South Korea). Real-time reverse transcription PCR showed that the sputum was positive for the upstream regions of the E protein (*upE*) and *orf1a* genes (*6*). Later the same day, we collected nasopharyngeal swab, throat swab, and sputum samples from the patient for further confirmation. The Korea Centers for Disease Control and Prevention (KCDC) confirmed that throat swabs and sputum samples were positive for *upE* and *orf1a*.

We added throat swab and sputum samples from the patient to a monolayer of Caco-2, Huh 7, and Vero E6 cells, which we incubated at 37°C in 5% CO_2. We observed a cytopathic effect on the third day after inoculation in Caco-2 cells and confirmed viral replication of MERS-CoV in the supernatant of the infected cells by real-time reverse transcription PCR.

We extracted viral RNA from the specimens and the supernatant of the Caco-2 cells using the Viral RNA Mini Kit (QIAGEN, http://www.qiagen.com). We performed cDNA synthesis using the Superscript IV First-Strand synthesis system (Thermo Fisher Scientific, http://www.thermofisher.com) with random hexamers. We amplified cDNA by overlapping PCR to generate products of 600–1,100 bp covering the entire S gene and the full-length genome; we sequenced the resulting PCR amplicons by Sanger sequencing using an ABI 3730 Analyzer (Applied Biosystems, http://www.thermofisher.com).

We used ClustalW (http://www.clustal.org) to align the S gene sequences of the isolates from the patient, MERS-CoV/KOR/KCDC/001_2018/SP-1 (from sputum sample), TS-1 (from throat swab sample), and TSVi (from Caco-2 processing), with those of 157 other MERS-CoV strains from GenBank and the MERS-CoV sequence database (https://www.ncbi.nlm.nih.gov/

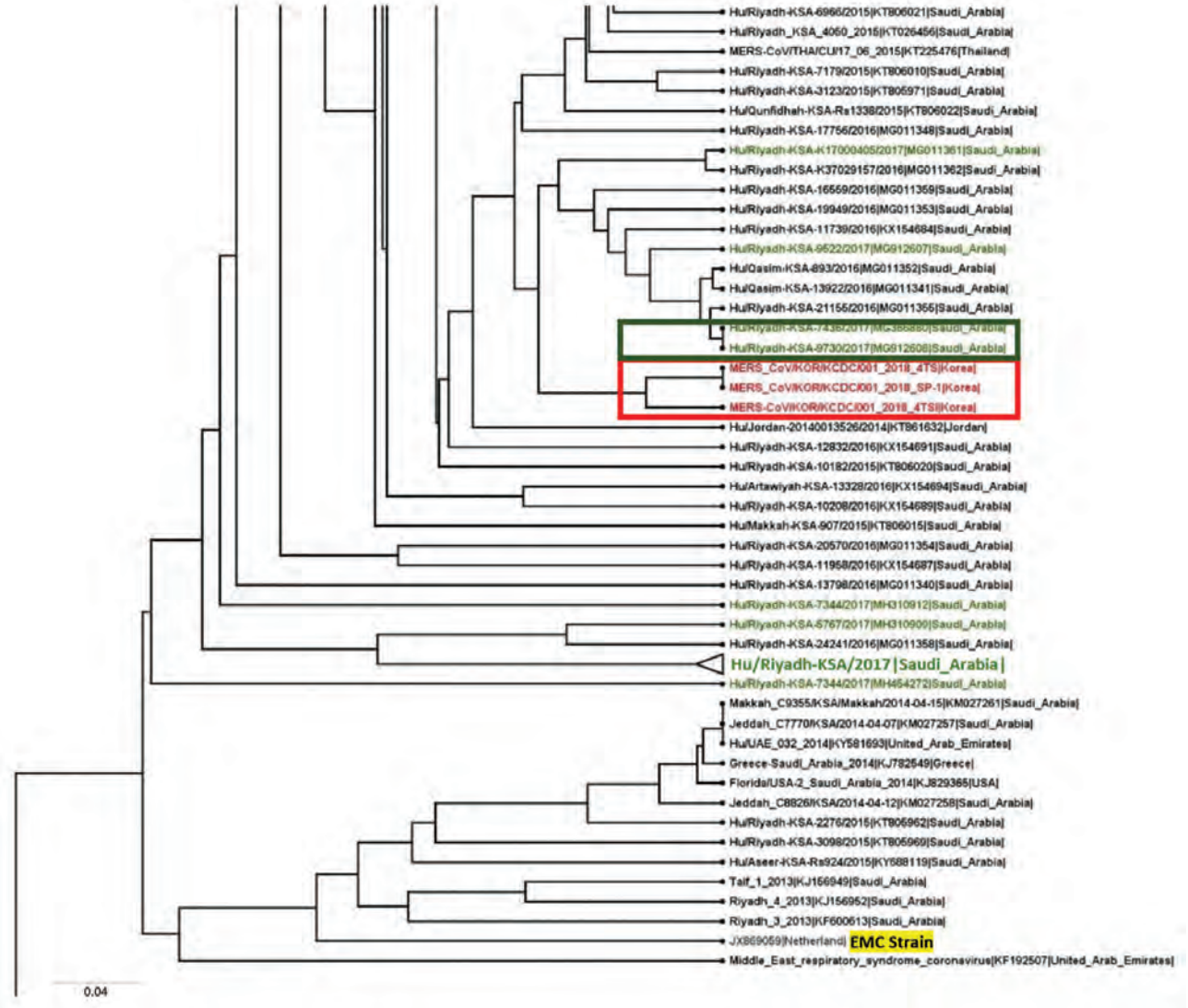

Figure 1. A portion of the molecular phylogenetic tree and coding region variants for the spike (S) glycoprotein gene of MERS-CoV isolates from South Korea, September 2018, and reference sequences. Phylogenetic analysis of 157 S sequences was performed using MEGA7 (https://www.megasoftware.net), with tree visualization using FigTree version 1.4.3 (http://tree.bio.ed.ac.uk/software/figtree). The taxonomic positions of circulating strains from the outbreak in South Korea and Riyadh, Saudi Arabia, are indicated. Boldface indicates compressed major clades of MERS-CoV. Bootstrap values (>70%) on nodes are shown as percentages based on 1,000 replicates. Red indicates South Korea 2018 isolates, blue indicates South Korea 2015 isolates, and green indicates Saudi Arabia 2017 isolates. The highlighted strain, from 2012, is the prototype strain used as the reference. EMC, Erasmus Medical Center; MERS-CoV, Middle East respiratory syndrome coronavirus. Scale bar indicates nucleotide substitutions per site. An expanded version of this figure showing the full phylogenetic tree is available online (https://wwwnc.cdc.gov/EID/article/25/5/18-1534-F1.htm).

genomes/VirusVariation/Database/nph-select.cgi?cmd=database&taxid=1335626), deposited up to August 2018. We sequenced and analyzed the full-length genome of MERS-CoV/KOR/KCDC/001_2018/TSVi and 39 other MERS-CoV strains. We constructed phylogenetic trees by the maximum-likelihood method with 1,000 bootstrap replicates using MEGA7 (*7*) and RAxML (https://github.com/stamatak/standard-RAxML). We constructed phylogenetic trees from the MERS-CoV S genes (4,062 bp) (Figure 1) and the full-length genome (30,150 bp) of the virus (Figure 2) obtained from the patient in this study and the most similar human MERS-CoV sequences from other countries (*4*).

We submitted viral S gene sequences MERS-CoV/KOR/KCDC/001_2018_SP-1, TS-1, TSVi from the patient to GenBank under accession nos. MH978886, MH978887, and MH978888. MERS-CoV/KOR/KCDC/001_2018 SP-1, TS, and TSVi were most closely related (99.85%–99.90% nucleotide identity) to a human MERS-CoV strain isolated in Riyadh, Saudi Arabia, in 2017 (Hu-Riyadh-KSA-9730_2017; GenBank accession no. MG912608).

KOR/KCDC/2018 SP-1 and TS had 5 nucleotide substitutions (C309T, T519C, C2928T, T3375C, and T3598C) compared with a MERS-CoV strain found in Riyadh in 2017, whereas MERS-CoV/KOR/KCDC/001_2018 TSVi had 3 nucleotide substitutions (C309T, C2928T, and T3375C) compared with the same strain. There were no substitutions in the N terminal domain (NTD) and receptor-binding domain (RBD) of the S gene in the same comparison (Table). We submitted the full-length genome sequences from MERS-CoV/KOR/KCDC/001_2018_TSVi, obtained from cell isolates, to GenBank under accession no. MK129253. In a phylogenetic analysis, the virus was located in a lineage of locally endemic 2016 and 2017 Saudi Arabia strains (lineage 5 in Figure 2) but was distinguished from 2015 South Korea strains.

Conclusions

We characterized the S gene and full-length genome of MERS-CoV imported to South Korea from the Middle East using sputum and throat swab specimens from

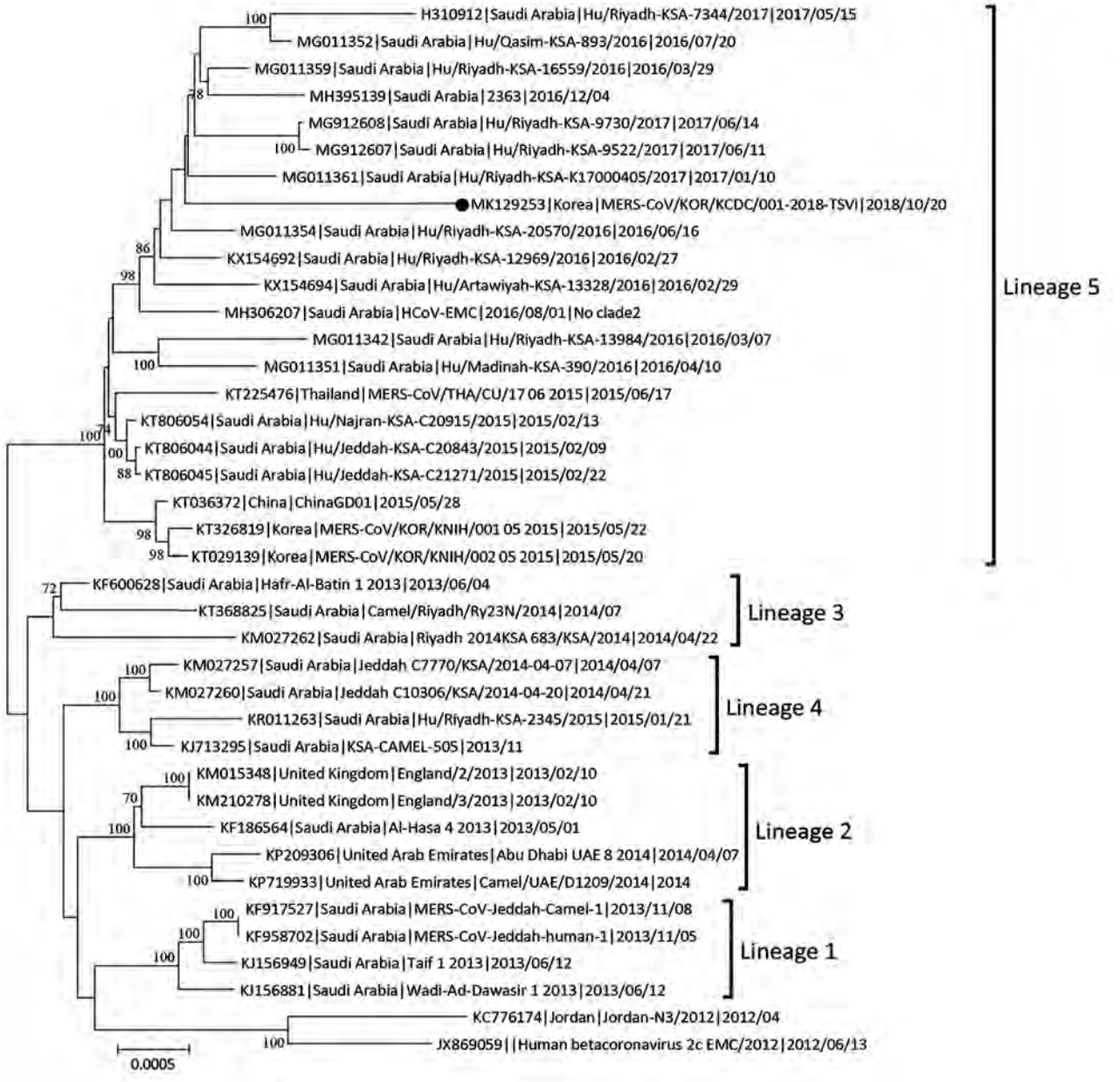

Figure 2. Maximum-likelihood tree showing MERS-CoV isolates from South Korea, September 2018 (black dot), and reference MERS-CoV genomes. Tree estimated using RAxML values (https://github.com/stamatak/standard-RAxML) on branches are shown as percentages based on 1,000 bootstrap replicates from the nucleotide sequences. MERS-CoV, Middle East respiratory syndrome coronavirus. Scale bar indicates nucleotide substitutions per site.

Table. Comparison of spike glycoprotein gene sequence variants for a MERS-CoV isolates from a patient in South Korea, 2018, and reference strains*

	Nucleotide (amino acid) positions								
	NTD			RBD			Other regions		
MERS-CoV strain	183 (61)	258 (86)	409 (137)	1586 (529)	1588 (530)	1848 (616)	1886 (629)	3177 (1059)	3267 (1089)
JX869059_HCoV-EMC_2012†	C (G)	T (V)	A (S)	T (I)	G (V)	T (V)	G (R)	T (D)	C (S)
KR011266_KSA_Hu/Riyadh-KSA-2049/2015		C (V)							
KR011263_KSA_Hu/Riyadh-KSA-2345/2015		C (V)							
KR011264_KSA_Hu/Riyadh-KSA-2343/2015		C (V)							
KR011265_KSA_Hu/Riyadh-KSA-2466/2015		C (V)							
KT026453_KSA_Hu/Riyadh-KSA-2959/2015		C (V)							
KT026454_KSA_Hu/Riyadh_KSA_4050/2015		C (V)							
KX154690_Hu_Jeddah-KSA-161RS1146_2016		C (V)							
KX154684_Hu-Riyadh-KSA-11739_2016		C (V)							
KX154694_Hu-Artawiyah-KSA-13328_2016		C (V)							
MG011361_Hu-Riyadh-KSA-K17000405_2017		C (V)							
MG011360_Hu-Riyadh-KSA-K17000887_2017		C (V)							
MG912608_Hu-Riyadh-KSA-9730_2017		C (V)							
MERS-CoV/KOR/KNIH/001_05_2015		C (V)		C (T)				C (D)	T (S)
KT029139-MERS-CoV/KOR/KNIH/002_05_2015		C (V)	C (R)		C (L)			C (D)	T (S)
MERS-CoV/KOR/KNIH/009_05_2015		C (V)				C (V)		C (D)	T (S)
KT006149-ChinaGD01_2015	G (G)	C (V)				C (V)		C (D)	T (S)
MERS-CoV/KOR/KNIH/012_05_2015		C (V)		C (T)		C (V)		C (D)	T (S)
MERS-CoV/KOR/KNIH/013_05_2015		C (V)		C (T)		C (V)		C (D)	T (S)
MERS-CoV/KOR/KNIH/015_05_2015		C (V)		C (T)		C (V)	A (H)	C (D)	T (S)
MERS-CoV/KOR/KNIH/042_04_2015		C (V)						C (D)	T (S)
MERS-CoV/KOR/KCDC/001_2018_2SP-1		C (V)							
MERS-CoV/KOR/KCDC/001_2018_4TS		C (V)							
MERS-CoV/KOR/KCDC/001_2018_4TSVi		C (V)							

*Only variations from the reference strain are shown. Boldface indicates the South Korea isolates and the most similar strain identified in this study. MERS-CoV, Middle East respiratory syndrome coronavirus; NTD, N-terminal domain; RBD, receptor-binding domain.
†Reference MERS-CoV strain.

a patient and from Caco-2 cells exposed to throat swab samples from the patient (*8*,*9*). A comparative genetic analysis of 157 strains isolated in 27 countries including South Korea demonstrated that the imported MERS-CoV we isolated showed the highest identity (99.85%–99.90%) with a strain recently isolated in Saudi Arabia in 2017 (*1*,*10*). These strains differed at 2 positions (C309T and T519C). We detected no variation in NTD or RBD, which are the major functional sites of the S protein (*11*). In addition, the strains involved in the outbreak in South Korea in 2015 had 12 nt substitutions (NTD, 1 site; RBD, 2 or 3 sites), implying that the imported case in 2018 involved a different virus (*4*).

Despite 110 laboratory-confirmed cases of MERS-CoV reported globally during 2018, no genetic information has been obtained to date. Therefore, we could not compare the genetic relationships between the strain we isolated and MERS-CoV strains in the Middle East (*12*).

In summary, we obtained genetic information about a MERS-CoV strain in South Korea in 2018 that was probably imported from the Middle East. We expect the sequence data we identified to support future epidemiologic investigations of MERS-CoV, particularly to fill the need for recent data. Furthermore, the results of this study improve our understanding of the evolution of MERS-CoV and highlight the need for enhanced surveillance, especially for persons traveling to the Middle East.

This research was supported by a fund (4834-303-210-13) of the Korea Centers for Disease Control and Prevention.

Author contributions: Y.S.C. and C.K. designed the study; J.I.L., N.-J.L., M.-S.K., and A.L collected samples and contributed to diagnosis; J.M.K., H.M.K., and K.R.P. performed sequencing; J.M.K., H.M.K., and J.S.K. analyzed data; J.M.K., H.M.K., and Y.-S.C. prepared the table and figures; and J.M.K., H.M.K., and Y.-S.C. wrote the article.

About the Author

Dr. Chung is a deputy director at the Division of Viral Diseases, Korea Centers for Disease Control and Prevention, Cheongju, South Korea. His research interests include the molecular characterization and pathogenesis of influenza and respiratory viruses.

References

1. Corman VM, Ithete NL, Richards LR, Schoeman MC, Preiser W, Drosten C, et al. Rooting the phylogenetic tree of Middle East respiratory syndrome coronavirus by characterization of a conspecific virus from an African bat. J Virol. 2014;88:11297–303. http://dx.doi.org/10.1128/JVI.01498-14
2. Lee JY, Kim YJ, Chung EH, Kim DW, Jeong I, Kim Y, et al. The clinical and virological features of the first imported case causing MERS-CoV outbreak in South Korea, 2015. BMC Infect Dis. 2017;17:498–507. http://dx.doi.org/10.1186/s12879-017-2576-5
3. Kim KH, Tandi TE, Choi JW, Moon JM, Kim MS. Middle East respiratory syndrome coronavirus (MERS-CoV) outbreak in South

Korea, 2015: epidemiology, characteristics and public health implications. J Hosp Infect. 2017;95:207–13. http://dx.doi.org/10.1016/j.jhin.2016.10.008
4. Plipat T, Buathong R, Wacharapluesadee S, Siriarayapon P, Pittayawonganon C, Sangsajja C, et al. Imported case of Middle East respiratory syndrome coronavirus (MERS-CoV) infection from Oman to Thailand, June 2015. Euro Surveill. 2017;22:30598. http://dx.doi.org/10.2807/1560-7917.ES.2017.22.33.30598
5. World Health Organization. Middle East respiratory syndrome coronavirus (MERS-CoV) infection—Republic of Korea. 2018 Sep 12 [cited 2018 Dec 28]. http://www.who.int/csr/don/12-september-2018-mers-republic-of-korea/en
6. World Health Organization. Laboratory testing for Middle East respiratory syndrome coronavirus: interim guidance (revised). 2018 Jan [cited 2018 Dec 28]. http://www.who.int/csr/disease/coronavirus_infections/mers-laboratory-testing/en
7. Kumar S, Stecher G, Tamura K. MEGA7: Molecular Evolutionary Genetics Analysis version 7.0 for bigger datasets. Mol Biol Evol. 2016;33:1870–4. http://dx.doi.org/10.1093/molbev/msw054
8. Muth D, Corman VM, Meyer B, Assiri A, Al-Masri M, Farah M, et al. Infectious Middle East respiratory syndrome coronavirus excretion and serotype variability based on live virus isolates from patients in Saudi Arabia. J Clin Microbiol. 2015;53:2951–5. http://dx.doi.org/10.1128/JCM.01368-15
9. Drosten C, Muth D, Corman VM, Hussain R, Al Masri M, HajOmar W, et al. An observational, laboratory-based study of outbreaks of Middle East respiratory syndrome coronavirus in Jeddah and Riyadh, kingdom of Saudi Arabia, 2014. Clin Infect Dis. 2015;60:369–77. http://dx.doi.org/10.1093/cid/ciu812
10. Kossyvakis A, Tao Y, Lu X, Pogka V, Tsiodras S, Emmanouil M, et al. Laboratory investigation and phylogenetic analysis of an imported Middle East respiratory syndrome coronavirus case in Greece. PLoS One. 2015;10:e0125809. http://dx.doi.org/10.1371/journal.pone.0125809
11. Kim DW, Kim YJ, Park SH, Yun MR, Yang JS, Kang HJ, et al. Variations in spike glycoprotein gene of MERS-CoV, South Korea, 2015. Emerg Infect Dis. 2016;22:100–4. http://dx.doi.org/10.3201/eid2201.151055
12. Tsiodras S, Baka A, Mentis A, Iliopoulos D, Dedoukou X, Papamavrou G, et al. A case of imported Middle East respiratory syndrome coronavirus infection and public health response, Greece, April 2014. Euro Surveill. 2014;19:20782. http://dx.doi.org/10.2807/1560-7917.ES2014.19.16.20782

Address for correspondence: Chun Kang, Korea Centers for Disease Control and Prevention—Division of Viral Diseases, Center for Laboratory Control of Infectious Diseases, Korea 187, Osongsaengmyeong 2-ro, Osong-eup, Heungdeok-gu, Cheongju-si, Chungcheongbuk-do 28159, South Korea; email: kangchun@korea.kr

Novel Picornavirus in Lambs with Severe Encephalomyelitis

Leonie F. Forth, Sandra F.E. Scholes, Patricia A. Pesavento, Kenneth Jackson, Adrienne Mackintosh, Amanda Carson, Fiona Howie, Kore Schlottau, Kerstin Wernike, Anne Pohlmann, Dirk Höper, Martin Beer

Using metagenomic analysis, we identified a novel picornavirus in young preweaned lambs with neurologic signs associated with severe nonsuppurative encephalitis and sensory ganglionitis in 2016 and 2017 in the United Kingdom. In situ hybridization demonstrated intralesional neuronotropism of this virus, which was also detected in archived samples of similarly affected lambs (1998–2014).

In 2016 in Scotland, and in 2017 in Wales, progressive neurologic signs were observed in young lambs. These cases were associated with nonsuppurative encephalomyelitis predominantly involving gray matter, including neuronal necrosis/neuronophagia and ganglionitis consistent with lesions caused by a neuronotropic viral infection. The target sites included cerebellar roof nuclei in the Purkinje molecular layer of the cerebellum, caudal brainstem nuclei (red nuclei and vestibular complex), and all levels of spinal cord examined (cervical, thoracic, and lumbar segments) located mainly in the ventral horns and dorsal root ganglia (Figure 1, panels A, B). Severe lesions were found consistently in the spinal cord. Louping ill virus, a common etiologic agent of nonsuppurative encephalitis in ruminants in Great Britain, was ruled out on the basis of the clinicopathological presentations and neuropathology, as well as serology. The observed lesion distribution and age of affected sheep were inconsistent with other possible neurotropic viral infections, such as Borna disease virus (*1*).

Author affiliations: Friedrich-Loeffler-Institut, Greifswald-Insel Riems, Germany (L.F. Forth, K. Schlottau, K. Wernike, A. Pohlmann, D. Höper, M. Beer); SRUC Veterinary Services, Edinburgh, Scotland, UK (S.F.E. Scholes, F. Howie); University of California–Davis, Davis, California, USA (P.A. Pesavento, K. Jackson); APHA Veterinary Investigation Centre, Carmarthen, Wales, UK (A. Mackintosh); APHA Veterinary Investigation Centre, Penrith, UK (A. Carson)

DOI: https://doi.org/10.3201/eid2505.181573

The Study

In 2016, we subjected a sample from an affected lamb's cerebrum to metagenomic analysis (Appendix, http://wwwnc.cdc.gov/EID/article/25/5/18-1573-App1.pdf) with read classification using RIEMS (*2*). From the resulting dataset (2 million reads), 99.97% were classified, but only 1 read was reliably classified as a viral sequence. This 326-bp read showed the highest sequence identity with the 5′ untranslated region (UTR) of the genome of human rhinovirus (81.3%), belonging to the family *Picornaviridae*, genus *Enterovirus*. For further validation and sample screening, this viral read was used to design a quantitative reverse transcription PCR (qRT-PCR) assay (Appendix). Using this qRT-PCR, we analyzed lambs that, in 2017, received diagnoses of nonsuppurative encephalomyelitis and ganglionitis typical of neuronotropic viral infection; all 3 animals tested positive (Table 1). We detected the highest viral loads in the cerebellum and spinal cord (PCR quantification cycle [C_q] 18–21), where the most severe lesions were also observed. We detected lower loads in the cerebrum (C_q 30), ileum (C_q 29–32), tonsil (C_q 32–36), and mesenteric lymph node (C_q 34–36). Lung and spleen samples were negative, as were CNS samples from 2 additional lambs from the Scotland flock with compressive spinal cord lesions and no evidence of nonsuppurative encephalitis (Table 1).

We subjected spinal cord samples from selected lambs affected in the 2017 lambing season to metagenomic analysis (Appendix), which yielded datasets with 2.4 million reads each. RIEMS analysis classified 99.9% of the reads, with 900 and 406 reads as sequences related to *Picornaviridae* (genera *Enterovirus* and *Sapelovirus*), and several unclassified species with relatively low sequence identities (64.8%–96.8%). Several reads were classified only after translation into amino acid sequences and comparison to the protein database. We found no evidence of other pathogens that could have resulted in the neuropathological manifestations.

De novo assembly of reads related to *Picornaviridae* generated a complete genome of a novel virus, tentatively named ovine picornavirus (OvPV). The obtained 7.5 kb OvPV genome is only very distantly related to known picornaviruses, with nucleotide sequence identities of 59% with a bovine picornavirus (International Nucleotide Sequence Data Collaboration [INSDC] accession no. LC006971) (*3*) and 55% with a canine picornavirus (accession no. KU871312) (*4*). The OvPV genome comprises a 5′ UTR, a predicted

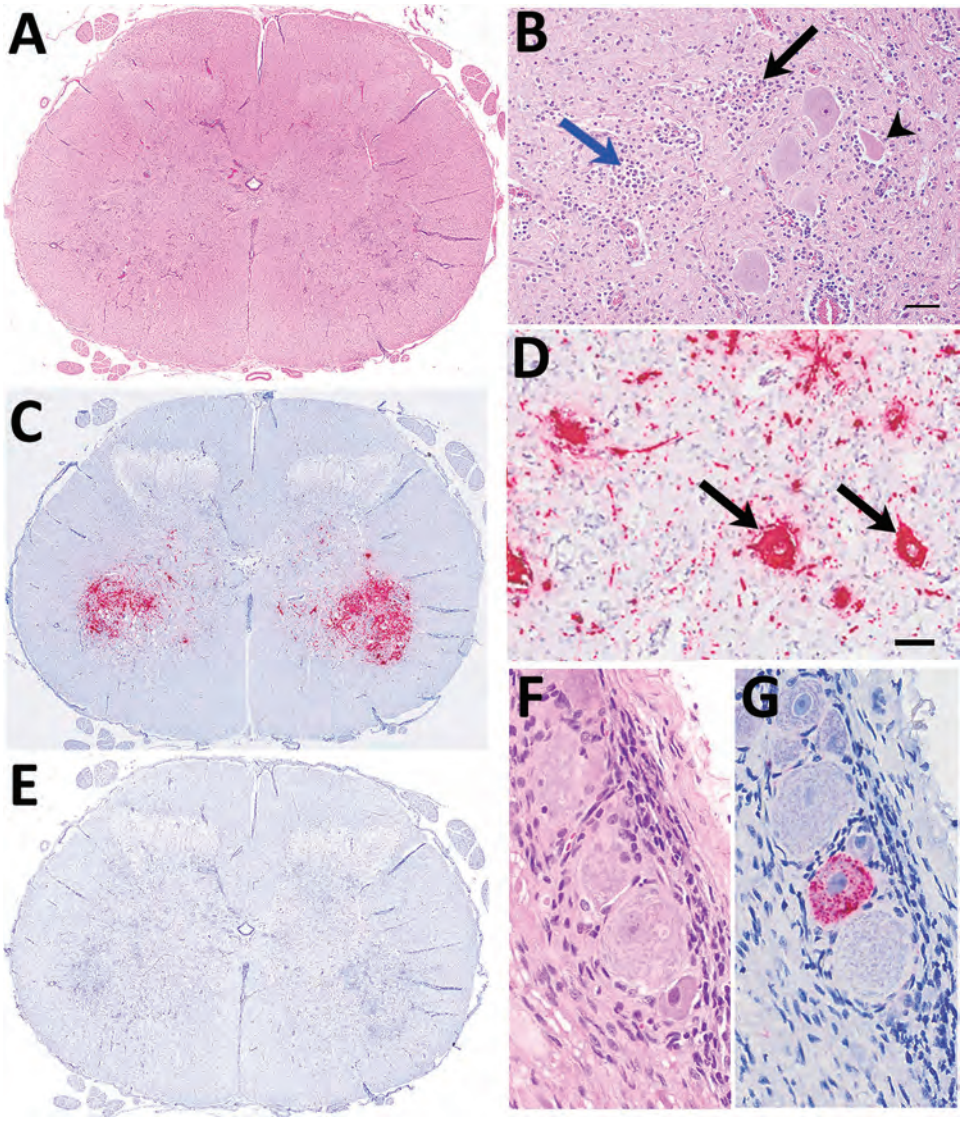

Figure 1. Histologic and in situ hybridization findings in cervical segment 7 of the spinal cord of 3-week-old lamb in Scotland in study of picornavirus in lambs with severe encephalomyelitis. A) Transverse segmental view with hematoxylin and eosin stain under low power. B) Hematoxylin and eosin stain under high power. Nonsuppurative myelitis is oriented on the ventral horn involving neuronal degeneration with satellitosis (black arrow), neuronophagia (arrowhead), and glial nodule formation (blue arrow), accompanied by perivascular mononuclear cell accumulation and gliosis. Scale bar indicates 60 μm. C) By in situ hybridization, ovine picornavirus (OvPV) probe hybridization (red) predominates in the region of ventral horn poliomyelitis. D) Viral probe hybridization is dense in neuronal cytoplasm (black arrows) and within presumed neuronal extensions within the neuropil. Scale bar indicates 60 μm. E) Using an unrelated probe, no hybridization is detectable. F, G) Probe hybridization within scattered individual neurons within a spinal ganglion (F, hematoxylin and eosin stain; G, OvPV probe in situ hybridization). Original magnification ×400.

6,885-nt open reading frame encoding the polyprotein with 2,294 aa, a 3′ UTR, and a poly(A)-tail. The putative structure of the polyprotein is similar to sapeloviruses with the characteristic order 5′-L-1ABCD-2ABC-3ABCD-3′; 3 consecutive methionins in frame could act as start codons of the polyprotein. The translation initiation site is proposed to be the third, because it is contained in the best Kozak context (*5*). Pairwise amino acid identities with P1, P2, and P3 of related picornaviruses are <58% (Appendix Table). Within the family *Picornaviridae*, together with other unclassified viruses (*4*,*6*), OvPV forms a putative new genus that is closest related to the genera *Sapelovirus*, *Rabovirus*, and *Enterovirus* (Figure 2; Appendix Figure). All whole-genome sequences we identified are available from the INSDC databases (accession no. PRJEB28719).

We attempted virus propagation from selected samples of affected animals on various mammalian cell lines (Appendix); however, virus could not be isolated. This result is consistent with other described unsuccessful attempts of viral propagation of related picornaviruses in cell culture (*4*,*7*).

To investigate whether the newly detected virus emerged in 2016 or was present previously, we examined archived cases from sheep in England with nonsuppurative encephalomyelitis oriented on gray matter that had tested negative for Louping ill virus by immunohistochemistry. Although the impaired RNA extracted from formalin-fixed paraffin-embedded (FFPE) material proved to be challenging for sequencing and amplification, we identified several additional cases of OvPV infection using reverse transcription PCR, and we generated whole-genome sequences from selected cases (Table 2). We detected OvPV in lambs of different breeds ≤3–4 weeks of age with neurologic signs; the earliest case identified dated back to 1998 (Table 2). Compared with the 2017 cases in Wales, the full OvPV

Table 1. Investigations of neurologic signs in lambs Scotland and Wales, 2016 and 2017*

Year	Flock	Case information	Case no.	EM	Tested tissue	C_q	OvPV reads, no. (%)†
2016	I	Progressive neurologic signs including tetraparesis, recumbency, ataxia, and death were observed in several lambs beginning at 2–3 weeks of age in a flock of 200 ewes that was accredited free of maedi-visna virus. The lamb submitted for investigation (S012722-2) was being artificially reared. Additional lambs showed similar clinical signs, but they recovered apart from residual slight paresis in one limb.	S012722–1	–	Cerebrum	NA	0
			S012722-2	+	Cerebrum	29.2	1 (0.00005)
2017	I	Neurologic signs resulting from spinal cord compression by a vertebral abscess.	S014148	–	Cerebrum	NA	NP
					Spinal cord	NA	NP
2017	II	Approximately one third of a group of 60 young pet lambs (mainly orphan lambs or triplet lambs because of insufficient milk to rear 3 lambs) being artificially reared were affected in a flock of 650 ewes. Clinical signs reported were stiff back legs, tremors that became exaggerated on handling, progressing to lateral recumbency, terminal seizures, and death or euthanasia. One lamb with mild clinical signs recovered.	S014175	+	Cerebrum	28.1	NP
					Spinal cord	18.2	1,383 (0.06)
			S014176	+	Cerebrum	26.1	NP
					Spinal cord	27.6	NP
			S014177	+	Cerebrum	27.9	NP
					Spinal cord	19.7	590 (0.02)

*Testing by quantitative reverse transcription PCR for ovine picornavirus and by metagenomics. C_q, PCR cycle quantification; EM, encephalomyelitis; NA, not applicable (C_q value in RT-qPCR >45); NP, not performed; OvPV, ovine picornavirus; +, confirmed nonsuppurative encephalomyelitis and ganglionitis; –, no evidence of nonsuppurative encephalomyelitis and ganglionitis; instead, compressive lesions in the spinal cord.
† Number of OvPV reads in the metagenomics dataset, total (proportion).

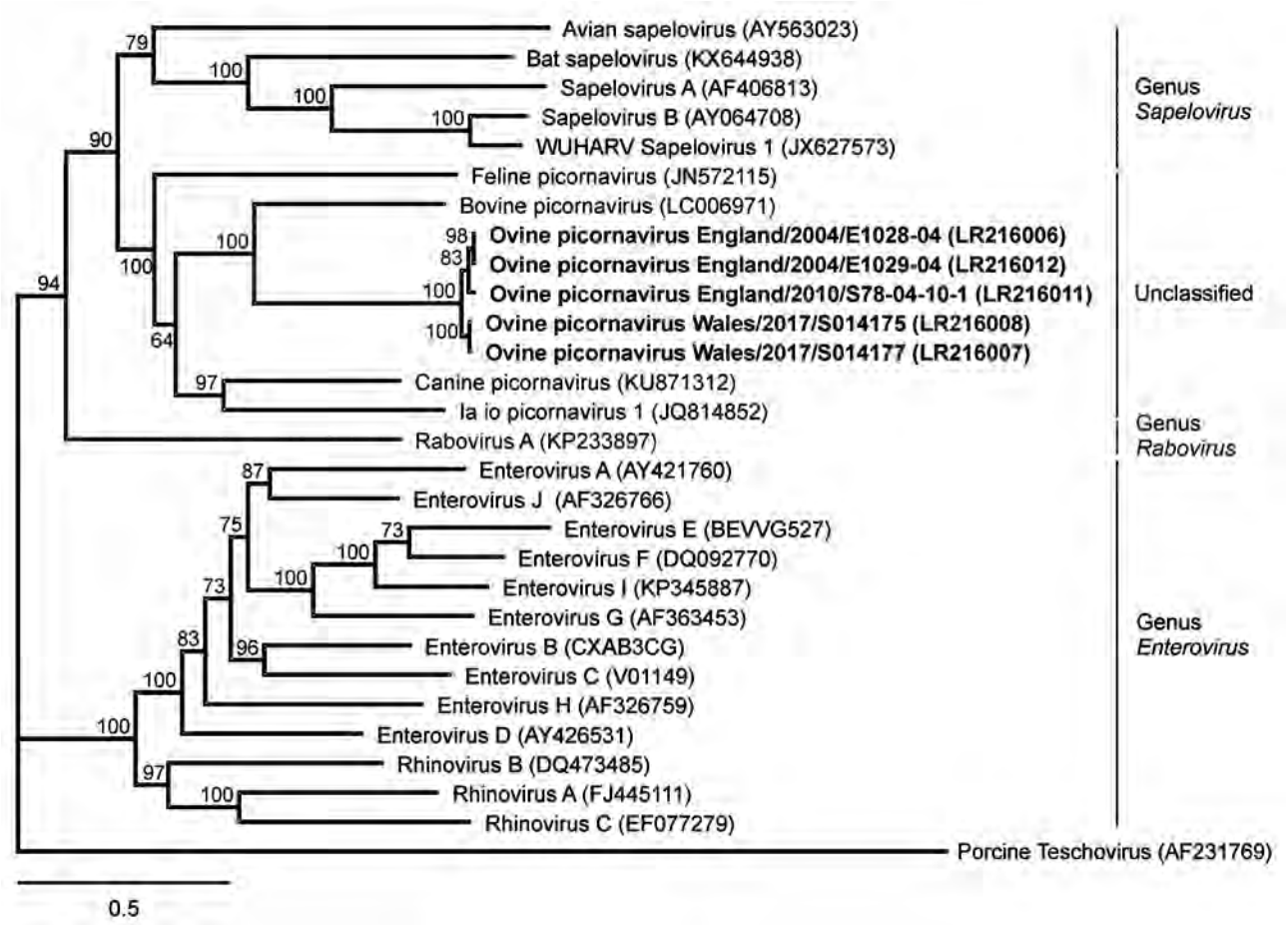

Figure 2. Phylogenetic relation of ovine picornavirus to other picornaviruses of the genera *Sapelovirus*, *Rabovirus*, and *Enterovirus*, as well as unclassified picornaviruses. The maximum-likelihood phylogenetic tree is based on complete coding sequences and calculated by IQ-TREE version 1.6.5 (http://www.iqtree.org) with the best-fit model general time reversible plus empirical base frequencies plus free rate model 5. Teschovirus was included as an outgroup. Statistical supports of 100,000 ultrafast bootstraps are indicated at the nodes. Bold indicates sequences generated in this study; INSDC or GenBank accession numbers are provided. Scale bar indicates nucleotide substitutions per site.

Table 2. Clinical history of lambs in England with nonsuppurative encephalomyelitis and results of testing of archived samples for presence of OvPV in spinal cord and brain*

Year	Signalment (case reference)	Case information	RT-PCR†	OvPV reads, no. (%)‡	Reference coverage§	Nucl. seq. identity§
1998	3-week-old mule lamb (1454/98)	Clinical signs of head tilt, rolling eyes and star gazing, and rapid onset of ataxia, recumbency, and paddling; no response to antimicrobial drugs, multivitamins including B1. Negative for Louping ill virus antibodies in cerebrospinal fluid and serum.	Positive	570 (0.003)	92%	90%–96%
2000	2–4-week-old milking breed lamb (960/00)	One of ≈12 lambs fed artificial colostrum (snatched at birth to prevent transmission of maedi-visna virus) that developed neurologic signs at ≈2 weeks of age, first weak in forelimbs, then hindlimbs, and by the second day, tremor and incoordination.	C_q 35	1061 (0.01)	98%	95%–96%
2004	Two 7–8-day-old triplet lambs (E1028/04 and E1029/04)	Triplets fed proprietary powdered colostrum because the ewe had insufficient milk. Signs of fine tremor progressing to recumbency; the third triplet developed similar neurologic signs at 3 weeks of age (not submitted for investigation).	C_q 32; positive	747,777 (3.02); 238,627 (1.11)	Full; full	95%; 95%
2008	2-week-old Texel X Swaledale (S313-04-08-1)	Neurologic signs not otherwise specified.	C_q 36	242 (0.0006)	89%	93%–95%
2010	1-week-old mule X female lamb (S78-04-10-1)	Approximately 25 lambs have been similarly affected. Portions of fixed juvenile ovine brain were submitted from field postmortem examination with history of suspected neurologic disease before euthanasia.	C_q 24	18,572 (0.07)	Full	95%
2014	Breed and age not known (S247-04-14)	Preweaned lamb with neurologic signs. Field postmortem samples submitted with clinical history of "suspect swayback," thus likely clinical signs of ataxia and paresis.	C_q 34	NP	NP	NP

*C_q, PCR quantification cycle; NP, not performed; nucl. seq., nucleotide sequence; OvPV, ovine picornavirus; RT-PCR, reverse transcription PCR; qRT-PCR, quantitative RT-PCR.
†RT-PCR was performed as prescreening for sample selection for high-throughput sequencing. Where feasible, C_q values of the qRT-PCR are indicated; positive means positive in semi-nested PCR.
‡Number (proportion) of OvPV reads in the complete high-throughput sequencing dataset.
§Genome coverage and nucleotide sequence identity of the full genome or several contigs in relation to the OvPV reference genome strain OvPV/Wales/2017/S014175 (International Nucleotide Sequence Data Collaboration accession no. LR216008).

genomes of the archive cases had ≈90%–96% sequence identity at the nucleotide level but up to 99% sequence identity at the amino acid level.

We performed in situ hybridization on OvPV PCR-positive FFPE tissues, with a subset of neurons within the brain and spinal cord as hybridization targets (Figure 1). In the spinal cord, OvPV in situ hybridization–positive neuronal soma and their projections were dense in the ventral horn in regions of neuronal degeneration and gliosis (Figure 1, panel C). Where dorsal root ganglia were in section, probe hybridization was detected in individual neurons (Figure 1, panels D, G). No hybridization was detected in sequential sections of OvPV-positive tissues under probing with an unrelated probe (Figure 1, panel E), and matched sections of uninfected animals were consistently negative (not shown).

Complete clinical data were not available for all of the archived cases; however, information was available for 5 flocks. In 4 of these flocks, the affected lambs were being fed artificially, usually because of maternal death or insufficient colostrum. Therefore, insufficient colostral antibody intake may predispose to development of neurologic disease similar to that proposed for porcine teschovirus, but this remains unproven. On the basis of the finding that OvPV has already been present in Wales, Scotland, and England for ≥20 years, we suspect that OvPV could be present in the intestinal tract commonly, similar to porcine teschovirus and porcine sapelovirus (*8*,*9*), but only occasionally causing disease in neonatal and early juvenile lambs.

Conclusions

In this study, we report identification of a novel neuroinvasive picornavirus associated with severe nonsuppurative encephalomyelitis and sensory ganglionitis in sheep. The virus has been associated with encephalomyelitis for ≥20 years, affecting sheep in Scotland, Wales, and England in a range of sheep breeds and management systems, but solely young lambs to date. These findings could suggest that OvPV infection is usually subclinical and self-limiting, particularly in older animals. For some cases, particularly those involving multiple affected lambs in a single flock over 1 lambing season, the clinical histories of snatching at birth or artificial feeding of orphan or pet lambs indicated likely failure of transfer of colostral antibodies. The resulting colostrum deficiency may have acted as a predisposing factor. Further research is needed to determine geographic distribution, disease burden, transmission route, and other factors; a serologic assay is also needed to further analyze the distribution in the field. However, OvPV should be considered in the differential diagnosis

of ovine nonsuppurative encephalomyelitis oriented on gray matter, particularly in young lambs with sensory ganglionitis.

Acknowledgments

We gratefully acknowledge Patrick Zitzow, Jenny Lorke, Bianka Hillmann, Joyce Wood, Maria Walker, and Beth Armstrong for their excellent technical assistance.

This work was supported by the German Federal Ministry of Education and Research within the project DetektiVir (grant no. 13N13783). SRUC Veterinary Services is funded in part by the Scottish Government's Veterinary Services Programme. The Animal and Plant Health Agency (APHA) Livestock Disease Surveillance System is funded by the UK Department for Environment, Food, and Rural Affairs.

About the Author

Ms. Forth is a biochemist and PhD student at the Friedrich-Loeffler-Institut, Greifswald-Insel Riems, Germany. Her research interests include novel and emerging viruses, metagenomics, and high-throughput sequencing.

References

1. Watson PJ, Scholes SF. Polioencephalomyelitis of unknown aetiology in a heifer. Vet Rec. 2004;154:766–7.
2. Scheuch M, Höper D, Beer M. RIEMS: a software pipeline for sensitive and comprehensive taxonomic classification of reads from metagenomics datasets. BMC Bioinformatics. 2015;16:69. http://dx.doi.org/10.1186/s12859-015-0503-6
3. Nagai M, Omatsu T, Aoki H, Kaku Y, Belsham GJ, Haga K, et al. Identification and complete genome analysis of a novel bovine picornavirus in Japan. Virus Res. 2015;210:205–12. http://dx.doi.org/10.1016/j.virusres.2015.08.001
4. Woo PCY, Lau SKP, Choi GKY, Huang Y, Sivakumar S, Tsoi HW, et al. Molecular epidemiology of canine picornavirus in Hong Kong and Dubai and proposal of a novel genus in Picornaviridae. Infect Genet Evol. 2016;41:191–200. http://dx.doi.org/10.1016/j.meegid.2016.03.033
5. Kozak M. An analysis of 5′-noncoding sequences from 699 vertebrate messenger RNAs. Nucleic Acids Res. 1987;15:8125–48. http://dx.doi.org/10.1093/nar/15.20.8125
6. Pankovics P, Boros A, Reuter G. Novel picornavirus in domesticated common quail (*Coturnix coturnix*) in Hungary. Arch Virol. 2012;157:525–30. http://dx.doi.org/10.1007/s00705-011-1192-8
7. Lau SK, Woo PC, Yip CC, Choi GK, Wu Y, Bai R, et al. Identification of a novel feline picornavirus from the domestic cat. J Virol. 2012;86:395–405. http://dx.doi.org/10.1128/JVI.06253-11
8. Chiu SC, Hu SC, Chang CC, Chang CY, Huang CC, Pang VF, et al. The role of porcine teschovirus in causing diseases in endemically infected pigs. Vet Microbiol. 2012;161:88–95. http://dx.doi.org/10.1016/j.vetmic.2012.07.031
9. Schock A, Gurrala R, Fuller H, Foyle L, Dauber M, Martelli F, et al. Investigation into an outbreak of encephalomyelitis caused by a neuroinvasive porcine sapelovirus in the United Kingdom. Vet Microbiol. 2014;172:381–9. http://dxdoi.org/10.1016/j.vetmic.2014.06.001

Address for correspondence: Martin Beer, Friedrich-Loeffler-Institut, Institute of Diagnostic Virology, Südufer 10, 17493 Greifswald-Insel Riems, Germany; email: martin.beer@fli.de

Severe Myasthenic Manifestation of Leptospirosis Associated with New Sequence Type of *Leptospira interrogans*

Matthias Tomschik,[1] Inga Koneczny,[1] Anna-Margarita Schötta, Sebastian Scharer, Merima Smajlhodzic, Paloma Fernandes Rosenegger, Martin Blüthner, Romana Höftberger, Fritz Zimprich, Gerold Stanek, Mateusz Markowicz

We report the rapid development of a myasthenic crisis as the first-time manifestation of myasthenia gravis. The symptoms developed in the course of acute leptospirosis associated with a new sequence type of *Leptospira interrogans*. Antibiotic treatment led to rapid amelioration of myasthenia.

Leptospirosis is a global zoonotic disease, endemic in tropical areas, and caused by spirochetes of the genus *Leptospira* (*1*). Involvement of the nervous systems is rare, and only single cases involving aseptic meningitis, encephalitis, movement disorders, neuritis, and polymyositis, among others (*2*,*3*), have been reported. We report a case of leptospirosis leading to a myasthenic crisis and subsequent diagnosis of a rare form of myasthenia gravis (MG) in a previously healthy traveler returning to Austria from Southeast Asia.

In August 2017, a previously healthy man, 32 years of age, visited an emergency department in Vienna, Austria, because of generalized weakness, malaise, double vision, and a 2-day history of fever and diarrhea. His medical history was unremarkable, and he was not taking any medication. Three days before the onset of symptoms, he had returned from a 4-week vacation in Vietnam and Thailand, where he swam in a waterfall pool and came into contact with indigenous animals. In particular, he helped to wash elephants in northern Thailand 1 week before his return. He reported feeling well upon arrival in Austria and even went white-water rafting in an alpine area the next day without experiencing weakness or malaise. However, 1 day later he noticed fatigability in his legs when walking up stairs, and nonbloody diarrhea developed. The diarrhea subsided, but other symptoms progressively worsened until he had trouble swallowing and walking.

A physical examination at the emergency department revealed elevated temperature (38.0°C), pulse (138 bpm), and blood pressure (146/104 mm Hg). The patient displayed typical myasthenic symptoms, including bilateral ptosis, Cogan's lid twitch signs, bilateral weakness of ocular movements, and dysarthria. Symptoms worsened with prolonged talking, including dysphagia and myasthenic weakness of all limbs, such that the patient was dependent on a wheelchair and unable to raise his arms.

Laboratory diagnostic tests revealed elevated C-reactive protein (27.72 mg/dL [reference <0.50 mg/dL]) and gamma-glutamyl-transferase (491 U/L [reference <60 U/L]), with left shift of leukocytes and proteinuria. Other laboratory parameters were within reference limits. In cerebrospinal fluid, cell counts and protein concentration were within reference limits, but intrathecal IgG production was evident.

Real-time PCR on EDTA blood targeting the gene for the major outer membrane protein lip L32 of human pathogenic *Leptospira* spp. showed positive results. We then subjected the sample strain to multilocus sequence typing (MLST) (*4*) to investigate its relationship with other *L. interrogans* strains and determine whether the infection was acquired during the patient's stay in Southeast Asia. In MLST analysis, we sequenced and analyzed 7 housekeeping genes of *Leptospira* spp. (*glmU*, *pntA*, *sucA*, *tpiA*, *pfkB*, *mreA*, and *caiB*). Among these, we found 2 new alleles (for *mreA* and *tpiA*), which resulted in a new sequence type (ST), 247. We constructed a phylogenetic tree for all 147 currently available *L. interrogans* STs, including ST247 (Figure 1) (*5*). The analysis showed that the isolate we obtained clusters with strains from Asia; however, the MLST database comprises strains predominantly from Asia. Further MLST analysis using eBURST (http://eburst.mlst.net) showed that linking STs were still missing. Further research in this field is required before a convincing phylogeographic conclusion can be reached.

Author affiliation: Medical University of Vienna, Vienna, Austria (M. Tomschik, I. Koneczny, A.-M. Schötta, S. Scharer, M. Smajlhodzic, P.F. Rosenegger, R. Höftberger, F. Zimprich, G. Stanek, M. Markowicz); Medizinisches Versorgungszentrum Labor PD Dr. Volkmann und Kollegen GbR, Karlsruhe, Germany (M. Blüthner)

DOI: https://doi.org/10.3201/eid2505.181591

[1]These authors contributed equally to this article.

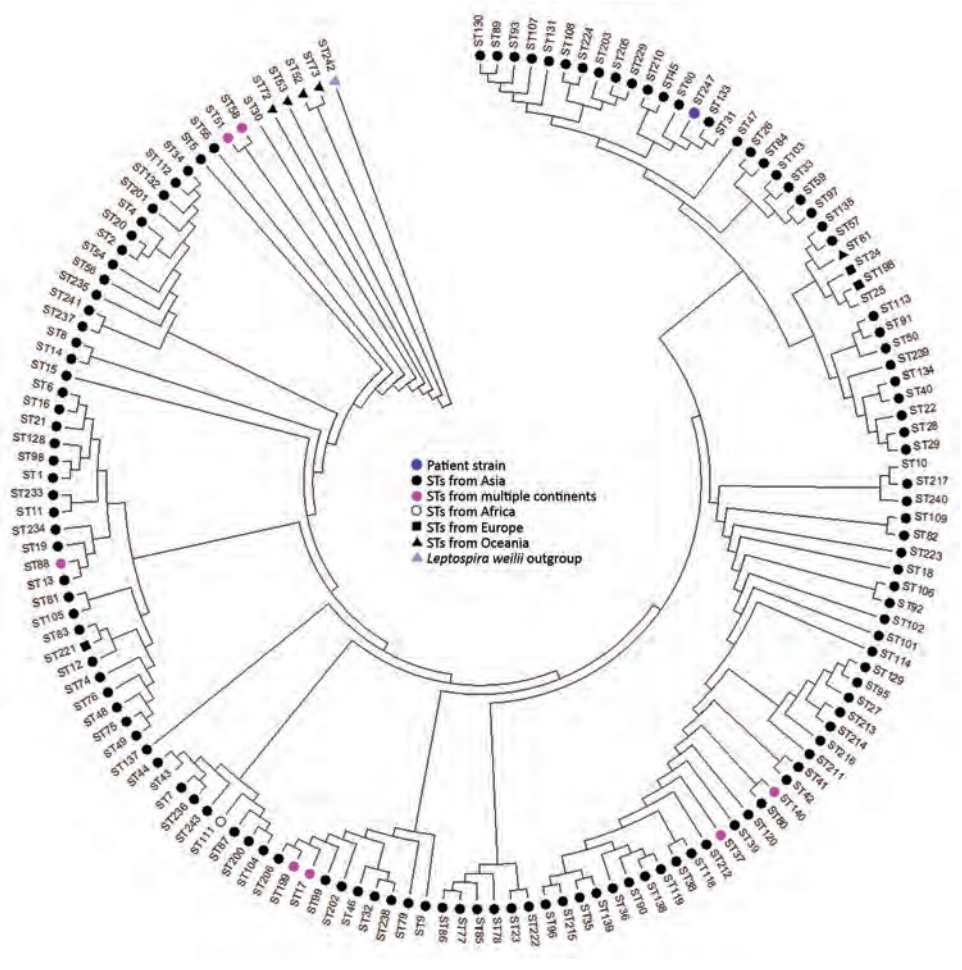

Figure 1. Phylogenetic tree showing only the topology for all *Leptospira interrogans* STs and their continent of origin. The isolate obtained from the patient in this study with severe myasthenic manifestation of leptospirosis is indicated by a blue dot (ST247). Tree was constructed using the maximum-likelihood method with MEGA version 7.0 (*5*). ST, sequence type.

No leptospiral DNA was found in the patient's cerebrospinal fluid; no *Leptospira* spp. IgG or IgM were detected by ELISA (Virion/Serion, https://www.serion-diagnostics.de). Several days later, a second serum sample showed high levels of IgM (>100 U/mL).

The neurologic examination suggested MG, which was corroborated by pathologic decrements in compound muscle action potentials in the orbicularis oculi (-15%) and trapezius (−46%) muscles on repetitive nerve stimulation at 3 Hz. Administration of the acetylcholinesterase inhibitor edrophonium resulted in strong and immediate improvement of ptosis, bulbar symptoms, and limb weakness. Nerve conduction studies revealed prolonged latency in the left medianus nerve, compatible with carpal tunnel syndrome. All other results were unremarkable, largely ruling out peripheral nerve or muscular disorders.

We consequently made a diagnosis of MG and acute leptospirosis and initiated treatment with pyridostigmine bromide and intravenous ceftriaxone. We withheld immunosuppressive therapy because of the acute leptospirosis. After 3 days, the patient demonstrated increased strength without further dysphagia or dysarthria. After 7 days, C-reactive protein levels normalized, proteinuria resolved, and gamma-glutamyltransferase levels decreased to 373 U/L. Ceftriaxone was discontinued after 10 days. Repetitive nerve stimulation was repeated 1 week after the initial test without prior ingestion of pyridostigmine and showed improved function of the neuromuscular junction.

We did not detect antibodies against acetylcholine receptors (AChRs) and muscle-specific tyrosine kinase (MuSK). However, testing for antibodies against low-density lipoprotein receptor-related protein 4 (LRP4) gave weakly positive results in a cell-based indirect immunofluorescence assay in an independent external laboratory (Medizinisches Versorgungszentrum Labor Volkmann Karlsruhe, Karlsruhe, Germany).

Pyridostigmine was discontinued, and the patient was discharged symptom-free and in good health. At follow-up 1 month later, examination of the patient found only minor ocular weakness. Repetitive nerve stimulation of the orbicularis oculi and trapezius muscles yielded normal results. At 4- and 6-month follow-up visits, minor fatigability of

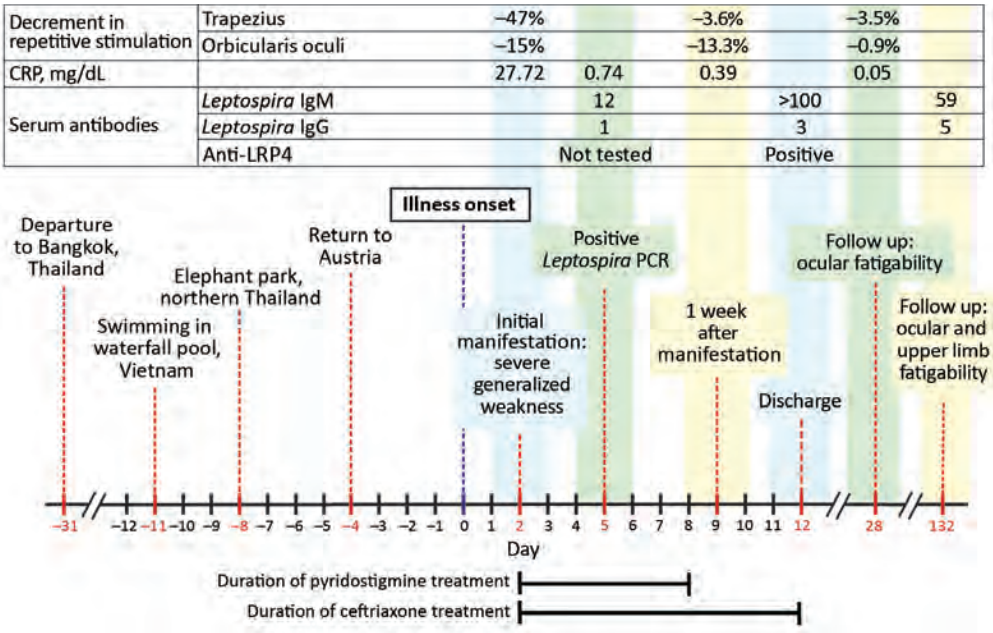

Figure 2. Timeline of medical history for patient with severe myasthenic manifestation of leptospirosis, including results of relevant neurologic and laboratory investigations. Decrement in repetitive stimulation denotes the maximum decrease in amplitude of the fourth or fifth compound muscle action potential waveform during supramaximal repetitive nerve stimulation at 3 Hz. A decrement >10% is regarded as pathologic (*6*). *Leptospira* ELISA cutoff values: IgG, <10 U/mL negative, 15 U/mL positive; IgM, <15 U/mL negative, >20 U/mL positive. CRP, C-reactive protein; LRP4, lipoprotein receptor-related protein 4.

the lateral rectus muscle and the upper extremities was observed, but these effects did not impair the patient's performance in a physically demanding profession and did not require medication. The timeline of the patient's medical history is summarized in Figure 2.

MG is an acquired, antibody-mediated autoimmune disease of the neuromuscular junction causing muscle weakness and increased fatigability. Treatment consists of symptomatic relief with acetylcholinesterase inhibitors. Immunosuppression is often required for disease control. Approximately 85% of MG patients have AChR and MuSK antibodies (*7*); among the remaining patients, anti-LRP4 autoantibodies can be detected in 1.4%–50% of patients, depending on the detection method (*8*,*9*). Cell-based assays with live cells appear associated with lower frequencies compared with fixed-cell assays or with ELISA. Samples from the patient we describe tested negative for AChR and MuSK antibodies, but testing against LRP4 antibodies gave positive results in an external laboratory and borderline positive results in an in-house live cell-based assay (*10*).

Our results should be interpreted cautiously. We were unable to reproduce them with remaining serum samples in the in-house live cell-based assay or ELISA at a later time.

Case series suggest an association of viral infections with the development of MG, although a causal link has yet to be shown (*11*,*12*). Worsening of preexisting MG is often triggered by an infection. A registry study in Spain found life-threatening events related to MG in up to 10% of patients, with infection being the most common cause (*13*).

The patient we report had a myasthenic crisis associated with a new ST of *L. interrogans*. Only 1 other case of leptospirosis with involvement of the neuromuscular junction has been described (*14*), but without direct identification of the pathogen and with symptoms occurring after the leptospiremic phase in the presence of *Leptospira*-specific antibodies; no myasthenic antibodies were tested for, and no diagnosis of MG was made.

In contrast, the patient we describe experienced more severe weakness at a much earlier point, and his serum sample tested positive for LRP4 autoantibodies, suggesting an association between MG and the acute leptospirosis. Reports of leptospirosis-associated, immune-mediated manifestations ranging from mononeuritis and Guillain-Barré–like syndromes to postinfectious autoimmune epilepsy (*3*,*15*) raise the question of whether *Leptospira* infections might precipitate or aggravate autoimmunity.

Acknowledgments

We thank Angela Vincent, David Beeson, and Lin Mei for use of their LRP4 plasmids.

I.K. was funded by a Hertha Firnberg Fellowship (project no. T996-B30) from the Austrian Science Fund.

About the Authors

Dr. Tomschik has been a resident in clinical neurology at the Medical University of Vienna since 2016 whose research currently focuses on neuromuscular diseases, particularly myasthenia gravis. Dr. Koneczny is a molecular biologist and project leader at the Medical University of Vienna whose research currently focuses on MG.

References

1. Levett PN. Leptospirosis. Clin Microbiol Rev. 2001;14:296–326. http://dx.doi.org/10.1128/CMR.14.2.296-326.2001
2. Bharucha NE. Infections of the nervous system. In: Bradley's neurology in clinical practice. Bradley DR, Fenichel GM, editors. Butterworth Heinemann: Boston; 1991. p. 1074–5.
3. Panicker JN, Mammachan R, Jayakumar RV. Primary neuroleptospirosis. Postgrad Med J. 2001;77:589–90. http://dx.doi.org/10.1136/pmj.77.911.589
4. Boonsilp S, Thaipadungpanit J, Amornchai P, Wuthiekanun V, Bailey MS, Holden MT, et al. A single multilocus sequence typing (MLST) scheme for seven pathogenic *Leptospira species.* PLoS Negl Trop Dis. 2013;7:e1954. http://dx.doi.org/10.1371/journal.pntd.0001954
5. Kumar S, Stecher G, Tamura K. MEGA7: Molecular Evolutionary Genetics Analysis version 7.0 for bigger datasets. Mol Biol Evol. 2016;33:1870–4. http://dx.doi.org/10.1093/molbev/msw054
6. AAEM Quality Assurance Committee. American Association of Electrodiagnostic Medicine. Literature review of the usefulness of repetitive nerve stimulation and single fiber EMG in the electrodiagnostic evaluation of patients with suspected myasthenia gravis or Lambert-Eaton myasthenic syndrome. Muscle Nerve. 2001;24:1239–47. http://dx.doi.org/10.1002/mus.1140
7. Vincent A, Huda S, Cao M, Cetin H, Koneczny I, Rodriguez-Cruz P, et al. Serological and experimental studies in different forms of myasthenia gravis. Ann N Y Acad Sci. 2018;1413:143–53. http://dx.doi.org/10.1111/nyas.13592
8. Yan M, Xing GL, Xiong WC, Mei L. Agrin and LRP4 antibodies as new biomarkers of myasthenia gravis. Ann N Y Acad Sci. 2018;1413:126–35. http://dx.doi.org/10.1111/nyas.13573
9. Zisimopoulou P, Evangelakou P, Tzartos J, Lazaridis K, Zouvelou V, Mantegazza R, et al. A comprehensive analysis of the epidemiology and clinical characteristics of anti-LRP4 in myasthenia gravis. J Autoimmun. 2014;52:139–45. http://dx.doi.org/10.1016/j.jaut.2013.12.004
10. Rodríguez Cruz PM, Al-Hajjar M, Huda S, Jacobson L, Woodhall M, Jayawant S, et al. Clinical features and diagnostic usefulness of antibodies to clustered acetylcholine receptors in the diagnosis of seronegative myasthenia gravis. JAMA Neurol. 2015;72:642–9. http://dx.doi.org/10.1001/jamaneurol.2015.0203
11. Leis AA, Szatmary G, Ross MA, Stokic DS. West Nile virus infection and myasthenia gravis. Muscle Nerve. 2014;49:26–9. http://dx.doi.org/10.1002/mus.23869
12. Molko N, Simon O, Guyon D, Biron A, Dupont-Rouzeyrol M, Gourinat AC. Zika virus infection and myasthenia gravis: report of 2 cases. Neurology. 2017;88:1097–8. http://dx.doi.org/10.1212/WNL.0000000000003697
13. Ramos-Fransi A, Rojas-García R, Segovia S, Márquez-Infante C, Pardo J, Coll-Cantí J, et al.; Myasthenia NMD-ES Study Group. Myasthenia gravis: descriptive analysis of life-threatening events in a recent nationwide registry. Eur J Neurol. 2015;22:1056–61. http://dx.doi.org/10.1111/ene.12703
14. Pradhan S, Tandon R, Kishore J. Combined involvement of muscle, nerve, and myoneural junction following *Leptospira* infection. Neurol India. 2012;60:514–6. http://dx.doi.org/10.4103/0028-3886.103202
15. Makhija P, Gopinath S, Kannoth S, Radhakrishnan K. A case of post-leptospirosis autoimmune epilepsy presenting with sleep-related hypermotor seizures. Epileptic Disord. 2017; 19:456–60.

Address for correspondence: Matthias Tomschik, Medical University of Vienna, Department of Neurology, Spitalgasse 23, 1090 Vienna, Austria; email: matthias.tomschik@meduniwien.ac.at

Neonatal Conjunctivitis Caused by *Neisseria meningitidis* US Urethritis Clade, New York, USA, August 2017

Cecilia B. Kretz,[1] Genevieve Bergeron,[1] Margaret Aldrich, Danielle Bloch, Paula E. Del Rosso, Tanya A. Halse, Belinda Ostrowsky, Qinghuan Liu, Edimarlyn Gonzalez, Enoma Omoregie, Ludwin Chicaiza, Greicy Zayas, Bun Tha, Angela Liang, Jade C. Wang, Michael Levi, Scott Hughes, Kimberlee A. Musser, Don Weiss, Jennifer L. Rakeman

We characterized a case of neonatal conjunctivitis in New York, USA, caused by *Neisseria meningitidis* by using whole-genome sequencing. The case was a rare occurrence, and the isolate obtained belonged to an emerging clade (*N. meningitidis* US nongroupable urethritis) associated with an increase in cases of urethritis since 2015.

Neonatal conjunctivitis caused by *Neisseria meningitidis* is a rare occurrence. Using whole-genome sequencing, we analyzed an isolate of *N. meningitidis* from a 3-day-old infant in New York, USA, who was given a diagnosis of unilateral conjunctivitis.

The Study

On August 31, 2017, a 3-day-old infant was given a diagnosis of unilateral conjunctivitis caused by *Neisseria meningitidis*. The infant was born in a New York City, New York, USA, hospital to a healthy mother by cesarean section performed for prolonged rupture of membranes. A conjunctival swab specimen isolated *N. meningitidis*, which was identified by real-time PCR as nongroupable *N. meningitidis*. Nongroupable *N. meningitidis* lacks capsule production, which is a major virulence factor in causing invasive meningococcal disease. The infant received erythromycin gonococcal ophthalmic prophylaxis according to standard care guidelines and bacitracin/polymyxin ointment for empiric treatment of conjunctivitis and was discharged to home.

When *N. meningitidis* was identified on day 4 of life, the infant was hospitalized and underwent a sepsis workup that included blood and cerebrospinal fluid cultures (both showed negative results). Upon review of the limited literature available on primary meningococcal conjunctivitis, we determined that, although the conjunctivitis had improved, a 5-day course of therapy with parenteral ceftriaxone was warranted. The infant was discharged on day 8 of life.

N. meningitidis is a rare but known cause of conjunctivitis in newborns. A case of *N. meningitidis* perinatal transmission linked to genital and nasopharyngeal parental colonization has been described (*1*). In the case-patient described in our study, early onset of illness suggests that the infant might have acquired the infection intrapartum from maternal *N. meningitidis* vaginal colonization.

Because of concerns for parental *N. meningitidis* colonization and possible future transmission to the newborn, we offered meningococcal postexposure chemoprophylaxis to the parents. The mother received 1 dose of ciprofloxacin, which is one of the options for meningococcal postexposure chemoprophylaxis. Maternal nasopharyngeal and vaginal cultures were obtained 3 weeks after the infant's diagnosis and maternal chemoprophylaxis, at which time the mother was able to be evaluated. Maternal cultures showed negative results. The infant's father declined to provide screening cultures.

Whole-genome sequencing performed at the New York City Public Health Laboratory showed that the conjunctival isolate had specific molecular characteristics found in the emerging US *N. meningitidis* nongroupable urethritis clade associated with an increase in cases of urethritis in Ohio, Michigan (*2*,*3*), and other locations (*4*). This novel clade belongs to sequence type 11/clonal complex 11, a hyperinvasive lineage that has caused large meningococcal outbreaks (*5*,*6*).

Author affiliations: Centers for Disease Control and Prevention, Atlanta, Georgia, USA (C.B. Kretz, G. Bergeron); New York City Department of Health and Mental Hygiene, Queens, New York, USA (C.B. Kretz, G. Bergeron, M. Aldrich, D. Bloch, P.E. Del Rosso, Q. Liu, E. Gonzalez, E. Omoregie, L. Chicaiza, G. Zayas, B. Tha, A. Liang, J.C. Wang, S. Hughes, D. Weiss, J.L. Rakeman); Montefiore Medical Center, Bronx, New York, USA (M. Aldrich, B. Ostrowsky, M. Levi); New York State Department of Health, Albany, New York, USA (T.A. Halse, K.A. Musser)

DOI: https://doi.org/10.3201/eid2505.181631

[1]These authors contributed equally to this article.

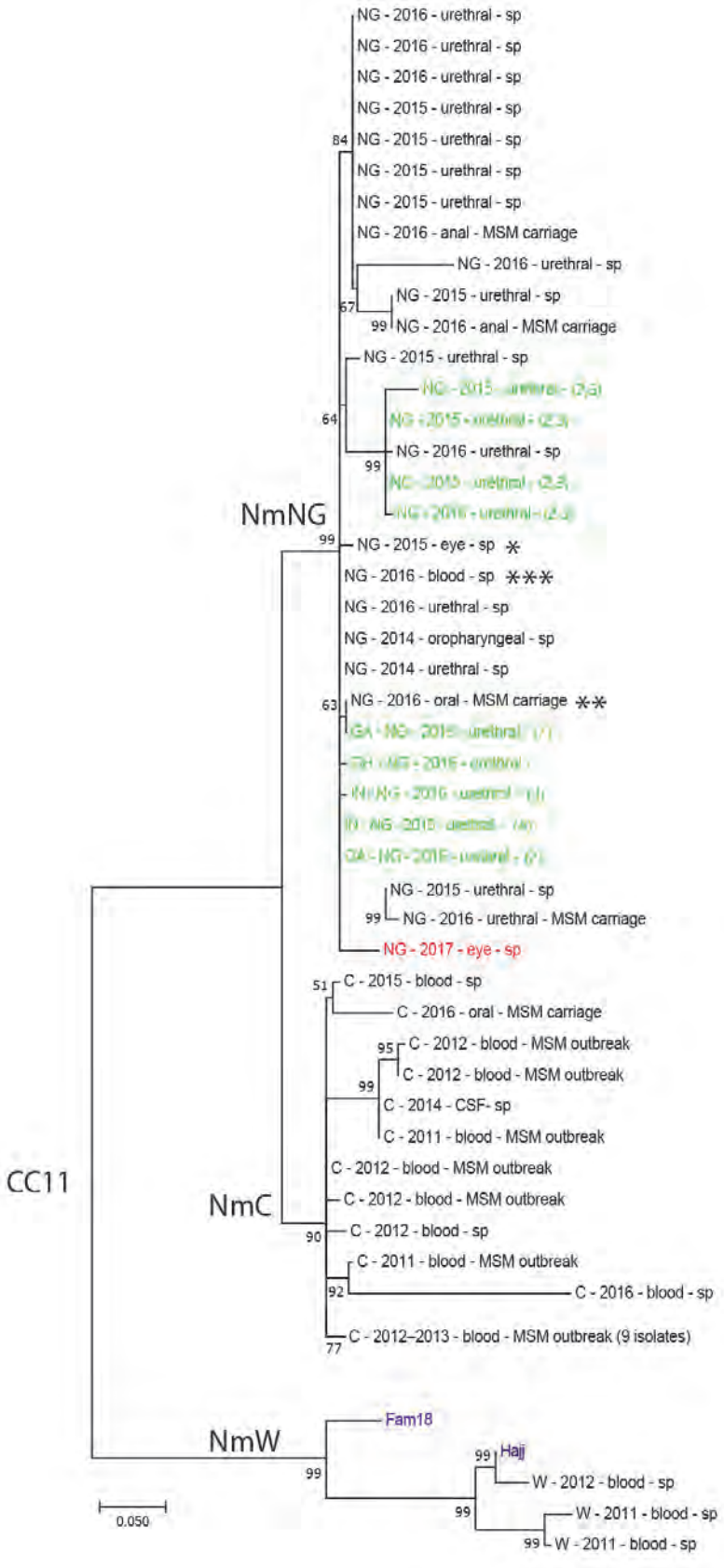

Figure. Molecular phylogenetic analysis of *Neisseria meningitidis* based on whole-genome sequence data from New York City, New York, USA, and publicly available sequences belonging to the multilocus sequence typing group cc11. Isolates are listed with serogroup, year of isolation, source, and study (sp, MSM carriage [for isolates obtained during the 2016 MSM carriage study in New York City], or reference from where they were obtained). *N. meningitidis* reference sequences are labeled in blue (Hajj and Fam18), *N. meningitidis Nm* urethritis clade references in green, and the 2017 conjunctivitis isolate in red. *2015 eye isolate; **oropharyngeal isolate from the MSM carriage study; ***invasive isolate from 2016. Numbers along branches are bootstrap values. The tree is drawn to scale with branch lengths measured in number of nucleotide substitutions per site. Internal nodes are labeled with bootstrap values (500 iterations). Branches are labeled with associated serogroups. Scale bar is based on 10,760 positions in the core single-nucleotide polymorphism matrix. cc, clonal complex; CSF, cerebrospinal fluid; MSM, men who have sex with men; *Nm*C, *N. meningitidis* serogroup C; *Nm*W, *N. meningitidis* serogroup W; *Nm*NG, *N. meningitidis* nongroupable; sp, sporadic case.

Some specific characteristics found in urethritis-associated *N. meningitidis* genomes include multigene deletion at the capsule locus, causing its nongroupable phenotype, and complete acquisition of a functional *nor*B–*ani*A gene cassette, a gonococcal-acquired gene suspected to enable survival in anaerobic environments (*7*). The *ani*A gene is commonly found in *N. meningitidis*. However, many meningococcal strains have frameshift mutations in the operon.

We performed antimicrobial drug susceptibility tests for the isolate by using Etest and obtained results similar to those for other isolates of the *N. meningitidis* urethritis clade (*3*). The isolate was sensitive to azithromycin, cefotaxime, ceftriaxone, chloramphenicol, ciprofloxacin, levofloxacin, meropenem, minocycline, rifampin, and trimethoprim/sulfamethoxazole and had intermediate susceptibility to penicillin and ampicillin.

We used whole-genome–based single-nucleotide polymorphism (SNP) to compare the isolate from the infant with 9 publicly available *N. meningitidis* urethritis sequences (PubMLST, https://pubmlst.org) (*4*,*8*) and 48 meningococcal sequences from New York City that belonged to sequence type 11. These sequences were from isolates obtained from invasive cases detected by surveillance: nonsterile sources, such as urethral, anal, and oropharyngeal specimens obtained during a men who have sex with men (MSM) carriage study conducted in 2016.

Genomic analyses confirmed that the conjunctivitis isolate was phylogenetically part of the *N. meningitidis* urethritis clade previously described (*2*,*4*,*7*) (Figure) because it clustered with available sequences that had only 20–50 SNP differences. This clade was composed mostly of urethral and anal isolates. However, 1 other conjunctivitis-associated isolate from 2015 that was identified from an immunosuppressed 43-year-old woman in New York City (Figure) and an oropharyngeal isolate collected during the MSM carriage study in 2016 (S. Ngai et al., pers. comm.) (Figure) were also part of the *N. meningitidis* urethritis clade. One isolate from the *N. meningitidis* urethritis clade had caused invasive meningococcal disease in a healthy, previously vaccinated, non-MSM man who had a history of childhood meningitis (Figure).

These findings are unusual because only a few invasive isolates have been described as part of the *N. meningitidis* US nongroupable urethritis clade (*8*). These observations demonstrate that strains belonging to this clade can cause invasive disease. However, additional information on these cases to characterize risk factors is limited. Although surveillance of *N. meningitidis* is primarily focused on invasive disease, *N. meningitidis* has been reported from noninvasive sites, such as urethral and oropharyngeal sites. In addition, few cases of primary meningococcal conjunctivitis are reported in the literature.

Conclusions

Our study showed that an *N. meningitidis* isolate belonging to the sequence type 11/clonal complex 11 clade with multigene deletion at the capsule locus has likely caused neonatal conjunctivitis in this child. Strains from this clade have the genetic potential to cause invasive meningococcal disease. The organism was not recovered from the infant's mother. However, she was not tested until 3 weeks after identification of the *N. meningitidis* isolate and after postexposure prophylaxis. The infant's infection might have been healthcare associated, but was more likely acquired by maternal genitourinary colonization ascending to the amniotic fluid during the period of prolonged rupture of membranes.

Modes of transmission are not fully understood for the *N. meningitidis* US nongroupable urethritis clade. Given its potential to cause invasive disease, more studies are needed to increase our understanding and to inform control and prevention measures. A better understanding of *N. meningitidis* noninvasive disease, including conjunctivitis in newborns and urethritis, will improve our understanding of the clinical manifestation, transmission modes, and epidemiologic evolution of *N. meningitidis* strains.

Acknowledgments

We thank Justine Edwards and the Bacterial Meningitis Laboratory, Meningitis and Vaccine Preventable Disease Branch, Division of Bacterial Diseases, National Center for Immunization and Respiratory Diseases, and the Antimicrobial Resistance and Characterization Laboratory, Division of Healthcare Quality Promotion, National Center for Emerging and Zoonotic Infectious Diseases, Centers for Disease Control and Prevention for participating in this study.

This study was supported by an Epidemiology and Laboratory Capacity for Infectious Diseases Cooperative Agreement from the Centers for Disease Control and Prevention.

About the Author

Dr. Kretz is a molecular microbiologist, bioinformatician and laboratory leadership service fellow at the Centers for Disease Control and Prevention who is assigned to the New York City Department of Health and Mental Hygiene, Queens, NY. Her primary research interests are molecular characterization and comparative genomics, using whole-genome sequencing, of respiratory pathogens, such as *N. meningitidis* and *Legionella* spp.

References

1. Chacon-Cruz E, Alvelais-Palacios JA, Rodriguez-Valencia JA, Lopatynsky-Reyes EZ, Volker-Soberanes ML, Rivas-Landeros RM. Meningococcal neonatal purulent conjunctivitis/sepsis and asymptomatic carriage of *N. meningitidis* in mother's vagina and both parents' nasopharynx. Case Rep Infect Dis. 2017; 2017:6132857. http://dx.doi.org/10.1155/2017/6132857

2. Bazan JA, Peterson AS, Kirkcaldy RD, Briere EC, Maierhofer C, Turner AN, et al. Notes from the field: increase in *Neisseria meningitidis*–associated urethritis among men at two sentinel clinics—Columbus, Ohio, and Oakland County, Michigan, 2015. MMWR Morb Mortal Wkly Rep. 2016;65:550–2. http://dx.doi.org/10.15585/mmwr.mm6521a5
3. Bazan JA, Turner AN, Kirkcaldy RD, Retchless AC, Kretz CB, Briere E, et al. Large cluster of *Neisseria meningitidis* urethritis in Columbus, Ohio, 2015. Clin Infect Dis. 2017;65:92–9. http://dx.doi.org/10.1093/cid/cix215
4. Toh E, Gangaiah D, Batteiger BE, Williams JA, Arno JN, Tai A, et al. *Neisseria meningitidis* ST11 complex isolates associated with nongonococcal urethritis, Indiana, USA, 2015–2016. Emerg Infect Dis. 2017;23:336–9. http://dx.doi.org/10.3201/eid2302.161434
5. Deghmane A-E, Parent du Chatelet I, Szatanik M, Hong E, Ruckly C, Giorgini D, et al. Emergence of new virulent *Neisseria meningitidis* serogroup C sequence type 11 isolates in France. J Infect Dis. 2010;202:247–50. http://dx.doi.org/10.1086/653583
6. Folaranmi TA, Kretz CB, Kamiya H, MacNeil JR, Whaley MJ, Blain A, et al. Increased risk for meningococcal disease among men who have sex with men in the United States, 2012–2015. Clin Infect Dis. 2017;65:756–63. http://dx.doi.org/10.1093/cid/cix438
7. Tzeng Y-L, Bazan JA, Turner AN, Wang X, Retchless AC, Read TD, et al. Emergence of a new *Neisseria meningitidis* clonal complex 11 lineage 11.2 clade as an effective urogenital pathogen. Proc Natl Acad Sci U S A. 2017;114:4237–42. http://dx.doi.org/10.1073/pnas.1620971114
8. Retchless AC, Kretz CB, Chang HY, Bazan JA, Abrams AJ, Norris Turner A, et al. Expansion of a urethritis-associated *Neisseria meningitidis* clade in the United States with concurrent acquisition of *N. gonorrhoeae* alleles. BMC Genomics. 2018; 19:176. http://dx.doi.org/10.1186/s12864-018-4560-x

Address for correspondence: Cecilia B. Kretz, Centers for Disease Control and Prevention, 1600 Clifton Rd NE, Mailstop D11, Atlanta, GA 30329-4027, USA; email: kpj2@cdc.gov

Fatal Meningitis in Patient with X-Linked Chronic Granulomatous Disease Caused by Virulent *Granulibacter bethesdensis*

Mafalda Rebelo,[1] Li Ding,[1] Ana Isabel Cordeiro, Conceição Neves, Maria João Simões, Adrian M. Zelazny, Steven M. Holland,[2] João Farela Neves[2]

Granulibacter bethesdensis is a pathogen reported to cause recurrent lymphadenitis exclusively in persons with chronic granulomatous disease. We report a case of fatal meningitis caused by a highly virulent *G. bethesdensis* strain in an adolescent in Europe who had chronic granulomatous disease.

Chronic granulomatous disease (CGD) is a primary immunodeficiency characterized by a deficient nicotinamide adenine dinucleotide phosphate oxidative burst that impairs phagocyte superoxide formation and killing of certain pathogens. Mutations can occur in any of the 5 subunits of nicotinamide adenine dinucleotide phosphate oxidase. Most cases are inherited as X-linked defects (gp-91^{phox}), but they also can occur in an autosomal recessive manner (*1*). Increased susceptibility develops to recurrent infections of the skin, lymph nodes, lungs, and other organs (*2*), mostly caused by bacteria and fungi, including *Staphylococcus aureus*, *Serratia marcescens*, *Burkholderia cepacia*, *Salmonella* spp., *Nocardia* spp., and *Aspergillus* spp. (*2*). Emerging organisms, such as *Granulibacter bethesdensis* and other methylotrophs, occur almost exclusively in CGD patients (*3*,*4*).

G. bethesdensis was first described in 2006, when it was isolated in a CGD patient with lymphadenitis (*4*). It is a gram-negative, aerobic, oxidase-negative, catalase-positive, nonmotile coccobacillus to rod-shaped bacterium belonging to the *Acetobacteraceae* family (*5*,*6*). *G. bethesdensis* was the first of these *Acetobacteraceae* family bacteria with proven pathogenicity in humans, causing invasive disease in CGD patients and mice (*4*). It has been mostly linked to indolent nonfatal lymphadenitis and deep neck infections in patients in North America. The infection can recur over several years by reactivation of the same strain or reinfection with different strains (*3*,*7*–*9*). The first fatal infection was reported in a 10-year-old boy from Spain, who died of fulminant sepsis (*10*). In vitro, *G. bethesdensis* shows extensive resistance to various antimicrobial drugs, although its slow growth makes susceptibility testing difficult. Ceftriaxone, aminoglycosides, doxycycline, and trimethoprim/sulfamethoxazole showed activity in vitro (*7*).

We report a case of *G. bethesdensis* meningitis in a patient with X-linked CGD. We also report animal data comparing this *G. bethesdensis* strain with the strain recovered from recurrent lymphadenitis in a US CGD patient.

The Study

The patient was a 16-year-old boy whose X-linked CGD (CYBB exon 13 deletion) was diagnosed when he was 2 years old. His disease had been well-controlled with cotrimoxazole, itraconazole, and interferon-γ. In September 2014, he was hospitalized with a deep cervical abscess (Figure 1, panel A) and received a 5-week course of intravenous ciprofloxacin, doxycycline, and ceftriaxone that resulted in complete clinical and radiologic resolution, followed by 6 weeks of oral amoxicillin/clavulanic acid, doxycycline, and ciprofloxacin along with his usual prophylaxis. No pathogen was identified despite blood cultures, bronchoalveolar lavage, and lymph node biopsy cultures and broad-range bacterial PCR.

After this regimen was completed, the boy was readmitted for 8 weeks with pneumonia with pleural effusion (Figure 1, panel B). Full 16S rRNA gene sequencing (≈1,500 bp) identified *Cupriavidus* spp. in pleural fluid. He received meropenem, amikacin, ciprofloxacin, teicoplanin, doxycycline, and voriconazole, and his condition improved. However, 2 weeks later, fever returned, along with splenomegaly, hemodynamic instability, pancytopenia,

Author affiliations: Hospital Dona Estefânia—Centro Hospitalar de Lisboa Central, Entidade Publica Empresarial, Lisbon, Portugal (M. Rebelo, A.I. Cordeiro, C. Neves, J.F. Neves); National Institute of Allergy and Infectious Diseases of the National Institutes of Health, Bethesda, Maryland, USA (L. Ding, A.M. Zelazny, S.M. Holland); National Institute of Health Dr. Ricardo Jorge, Lisbon (M.J. Simões); Chronic Diseases Research Center, NOVA Medical School, Lisbon (J.F. Neves)

DOI: https://doi.org/10.3201/eid2505.181505

[1]These authors contributed equally to this article.

[2]These authors contributed equally to this article.

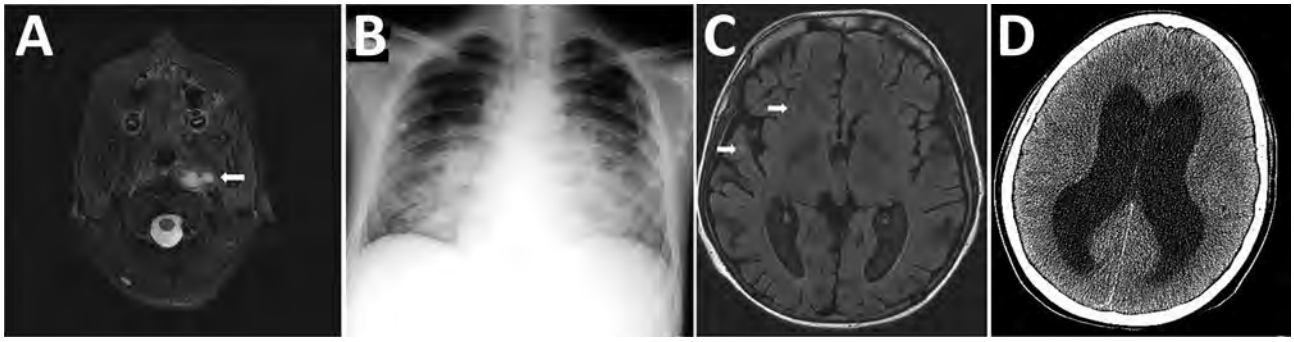

Figure 1. Most relevant imaging results from a 16-year-old boy with X-linked chronic granulomatous disease who died of meningitis caused by a virulent *Granulibacter bethesdensis* strain. A) Computed tomography image showing deep cervical abscess (arrow), July 2012. B) Radiograph showing pneumonia with pleural effusion, October 2012. C) Cranial magnetic resonance image showing multiple intraparenchymal brain abscesses (arrows), December 2012. D) The patient died of obstructive hydrocephalus (shown) and multiorgan failure, April 2013.

hypofibrinogenemia, hyperferritinemia, and elevated soluble CD25. He received intravenous immunoglobulin and dexamethasone for this inflammatory condition and fully recovered. Neck and lung computed tomography images and positron emission tomography performed 1 month later showed no signs of active infection.

Nevertheless, a few days later, the patient sought care for altered mental status, hallucinations, aggressiveness, and respiratory instability requiring admission to the pediatric intensive care unit. He had extensive bilateral pneumonia and multiple intraparenchymal brain abscesses (Figure 1, panel C). Meropenem, ciprofloxacin, amikacin, doxycycline,

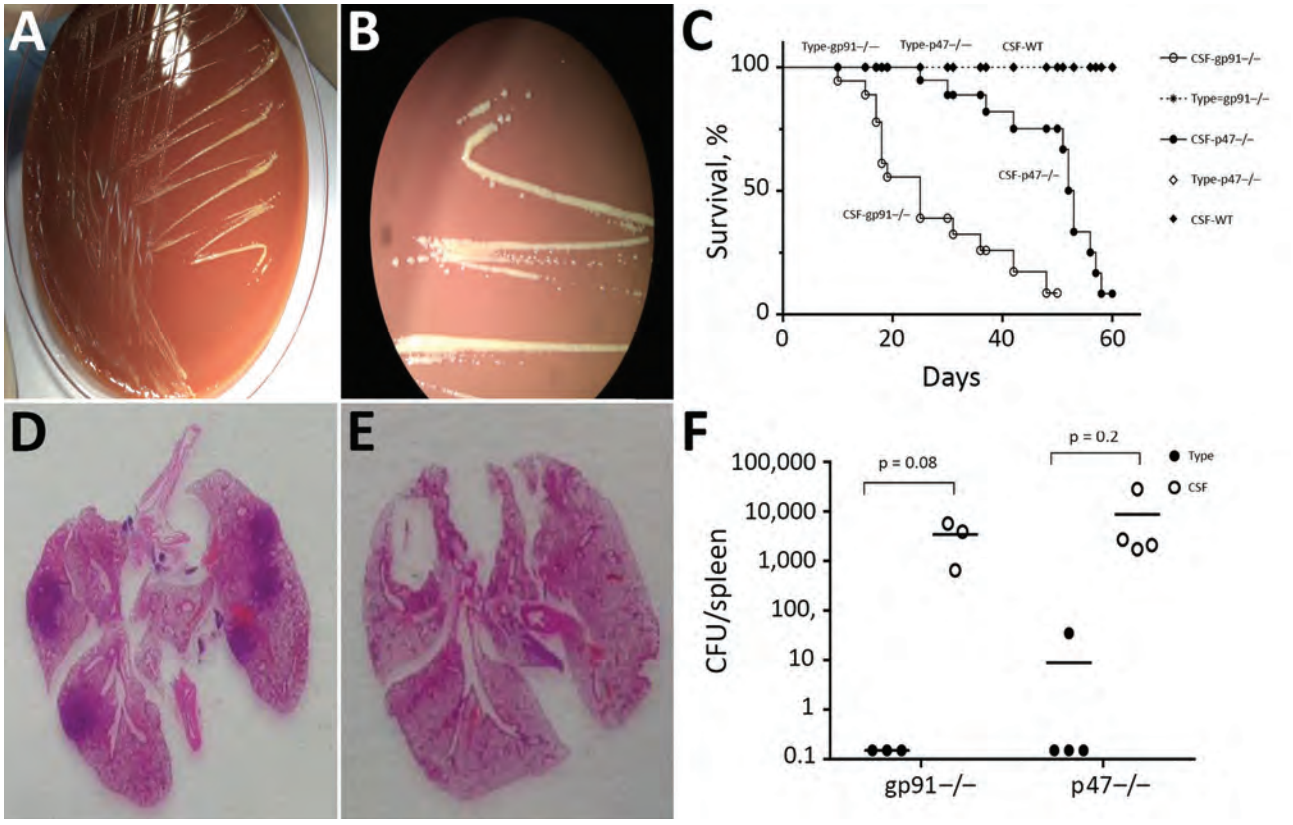

Figure 2. *Granulibacter bethesdensis* colonies and pathology results after inoculation on mouse models. A, B) CSF on chocolate agar for 4 days showed slowly growing brown-yellow, shiny colonies 2–4 mm in diameter. Full 16S RNA sequencing (≈1,500 bp) led to identification of *G. bethesdensis* (with 99.7% match). C) Survival of gp91/p47 KO mice after inoculation of different *G. bethesdensis* strains. D) Pathology images of gp91 KO mouse lung after CSF strain infection. E) Pathology images of gp91 KO mouse lungs after type strain infection. F) Quantification of *G. bethesdensis* strains in spleens of gp91/p47 KO mice after inoculation. CSF, cerebrospinal fluid; type, National Institutes of Health type strain; WT, wild type.

Table. Bacterial culture from blood and brain samples of gP91 KO mouse infected with *Granulibacter bethesdensis* after 4 weeks*

Mouse	Strain	Sample	
		Blood	Brain
gp91$^{-/-}$, n = 10	Type, USA	0	0
gp91$^{-/-}$, n = 10	**CSF, Portugal**	**5**	**2**
p47$^{-/-}$, n = 5	Type	0	0
p47$^{-/-}$, n = 5	CSF	0	0
WT, n = 9	CSF, Portugal	0	ND

*Bold indicates the results of the inoculation of CSF strain in the gp91 KO mouse. CSF, cerebrospinal fluid; ND, not done; WT, wild type.

teicoplanin, and voriconazole were started; results of cerebrospinal fluid (CSF) and lung biopsy samples were unremarkable. Teicoplanin was switched to linezolid and voriconazole to caspofungin and liposomal amphotericin B because of toxicity concerns. Four weeks later, he was discharged from the intensive care unit. One month later, fever, vomiting, and focal neurologic deficits developed. CSF showed pleocytosis and hypoglycorrhachia with elevated protein levels. Cerebral imaging confirmed leptomeningitis. Isoniazid, clarithromycin, and rifampin were added to his treatment regimen, but his neurologic status continued to deteriorate. Obstructive hydrocephalus (Figure 1, panel D) and multiorgan failure developed, and he died 3 months later.

CSF cultures yielded yellow-brown, shiny, small colonies (2–4 mm) on chocolate agar after 4 days' incubation. (Figure 2, panels A, B). Full 16S RNA sequencing (≈1,500 bp) showed 99.7% match to the type strain of *G. bethesdensis* CGDNIH1T (ATCC BAA-1260T, DSM 17861T) from North America and 100% match to a previously reported *G. bethesdensis* strain from Spain. Nonstandardized susceptibility test using Etest, performed in Mueller Hinton agar supplemented with 5% sheep blood agar with an overnight air incubation at 37°C, showed resistance to doxycycline (MIC 24 mg/L) and ceftriaxone (MIC >32 mg/L).

We used mouse models of CGD to determine whether differences existed in immune response, pathogenicity, or severity of disease between the European (CSF strain) and the US (type strain) strains. We intraperitoneally infected gp91$^{phox-/-}$ mice with 10^7 CFU of *G. bethesdensis* type strain and p47$^{phox-/-}$ mice intraperitoneally with 10^7 CFU of CSF strain and monitored moribundity during infection. We euthanized gp91$^{phox-/-}$ mice 4 weeks and p47$^{phox-/-}$mice 8 weeks after infection and collected brain, spleen, lung, lymph nodes, and blood for culture, bacterial enumeration, and histopathologic examination. Plasma cytokines were assayed.

Although we observed differences between gp91$^{phox-/-}$ and p47$^{pho-/-}$ mice, both CGD mice models showed high rates of death when infected with CSF strain. No deaths occurred in mice infected with type strain, nor did CSF strain cause disease in wild-type mice (Figure 2, panel C). CSF strain–infected mice showed more severe pathologic organ changes than did type strain–infected mice (Figure 2, panels D, E; Appendix Figure 1, https://wwwnc.cdc.gov/EID/article/25/5/18-1505-App1.pdf). We performed quantitative cultures to assess bacterial load in the spleens of inoculated mice. CSF strain CFUs were 100–1,000 times higher than those of type strain 4 and 8 weeks after infection. (Table; Figure 2, panel F). In addition, infection with CSF strain yielded 100–1,000 times higher CFUs in spleens of CGD mice than in wild-type mice 4 and 8 weeks after infection. (Appendix Figure 2). CSF strain showed faster growth on solid and in liquid media and a higher optimal growth temperature (37°C) than previously described North America lymph node isolates (Appendix Figure 3). CGD mice infected with CSF strain showed higher plasma interleukin-1β, tumor necrosis factor–α, and interleukin-6 than those infected with type strain 4 and 8 weeks after infection, which correlated with differences in tissue bacterial load. Cytokine levels did not increase in wild-type mice infected with CSF strain (Appendix Figure 4).

Conclusions

G. bethesdensis is an emerging pathogen shown to cause infection exclusively in CGD patients and has a spectrum of disease severity ranging from chronic and recurrent infections to fulminant sepsis, central nervous system infection, and death (*3*,*7*,*10*). Until recently, all reported North America cases were nonfatal chronic infections; 1 case from Europe (Spain) was fatal. Recently, Mayer et al. reported an X-linked CGD patient in the United States who died of fulminant infection with an organism with 100% identity to 500 bp of *G. bethesdensis* 16S (*11*). Unfortunately, that *G. bethesdensis* isolate was not available for analysis and comparison with other *G. bethesdensis* strains. The previous strain from Europe was highly resistant to antimicrobial agents, including colistin, most β-lactams, and quinolones (*10*).

We found that a CSF *G. bethesdensis* strain, showing an identical 16S sequence to a previously described fulminant strain from Europe, was more virulent and lethal in a mouse model than the *G. bethesdensis* US type strain and more virulent in gp91$^{phox-/-}$ than in p47 $^{phox-/-}$ mice. A fatal case of *G. bethesdensis* infection in the United States suggests that heterogeneity might exist among North America *G. bethesdensis* strains. Bacterial genome sequencing may identify discrete virulence factors. *G. bethesdensis* must be included as a cause of fatal disseminated infection in CGD.

This work was supported through the Division of Intramural Research, National Institute of Allergy and Infectious Diseases, National Institutes of Health.

About the Author

Dr. Rebelo is a pediatrics resident in Hospital Dona Estefânia, Centro Hospitalar de Lisboa Central. Her primary research interests are clinical immunology, primary immunodeficiencies, and infectious diseases

References

1. Holland SM. Chronic granulomatous disease. Hematol Oncol Clin North Am. 2013;27:89–99, viii. http://dx.doi.org/10.1016/j.hoc.2012.11.002
2. Gennery A. Recent advances in understanding and treating chronic granulomatous disease. F1000 Res. 2017;6:1427. http://dx.doi.org/10.12688/f1000research.11789.1
3. Falcone EL, Petts JR, Fasano MB, Ford B, Nauseef WM, Neves JF, et al. Methylotroph infections and chronic granulomatous disease. Emerg Infect Dis. 2016;22:404–9. http://dx.doi.org/10.3201/eid2203.151265
4. Greenberg DE, Ding L, Zelazny AM, Stock F, Wong A, Anderson VL, et al. A novel bacterium associated with lymphadenitis in a patient with chronic granulomatous disease. PLoS Pathog. 2006;2:e28. http://dx.doi.org/10.1371/journal.ppat.0020028
5. Greenberg DE, Porcella SF, Stock F, Wong A, Conville PS, Murray PR, et al. *Granulibacter bethesdensis* gen. nov., sp. nov., a distinctive pathogenic acetic acid bacterium in the family *Acetobacteraceae*. Int J Syst Evol Microbiol. 2006;56:2609–16. http://dx.doi.org/10.1099/ijs.0.64412-0
6. Greenberg DE, Porcella SF, Zelazny AM, Virtaneva K, Sturdevant DE, Kupko JJ III, et al. Genome sequence analysis of the emerging human pathogenic acetic acid bacterium *Granulibacter bethesdensis*. J Bacteriol. 2007;189:8727–36. http://dx.doi.org/10.1128/JB.00793-07
7. Greenberg DE, Shoffner AR, Zelazny AM, Fenster ME, Zarember KA, Stock F, et al. Recurrent *Granulibacter bethesdensis* infections and chronic granulomatous disease. Emerg Infect Dis. 2010;16:1341–8. http://dx.doi.org/10.3201/eid1609.091800
8. Zarember KA, Marshall-Batty KR, Cruz AR, Chu J, Fenster ME, Shoffner AR, et al. Innate immunity against *Granulibacter bethesdensis*, an emerging gram-negative bacterial pathogen. Infect Immun. 2012;80:975–81. http://dx.doi.org/10.1128/IAI.05557-11
9. Chu J, Song HH, Zarember KA, Mills TA, Gallin JI. Persistence of the bacterial pathogen *Granulibacter bethesdensis* in chronic granulomatous disease monocytes and macrophages lacking a functional NADPH oxidase. J Immunol. 2013;191:3297–307. http://dx.doi.org/10.4049/jimmunol.1300200
10. López FC, de Luna FF, Delgado MC, de la Rosa II, Valdezate S, Nieto JA, et al. *Granulibacter bethesdensis* isolated in a child patient with chronic granulomatous disease. J Infect. 2008;57:275–7. http://dx.doi.org/10.1016/j.jinf.2008.04.011
11. Mayer EFF, Gialanella P, Munjal I, Cunningham-Rundles C, Dara J. Fulminant sepsis due to *Granulibacter bethesdensis* in a 4-year-old boy with X-linked chronic granulomatous disease. Pediatr Infect Dis J. 2017;36:1165–6. http://dx.doi.org/10.1097/INF.0000000000001659

Address for correspondence: João Farela Neves, Primary Immunodeficiencies Unit, Hospital Dona Estefânia, Rua Jacinta Marto, 1145, Lisbon, Portugal; email: joao.farelaneves@chlc.min-saude.pt

Diagnosis of Imported Monkeypox, Israel, 2018

Noam Erez,[1] Hagit Achdout,[1] Elad Milrot, Yuval Schwartz, Yonit Wiener-Well, Nir Paran, Boaz Politi, Hadas Tamir, Tomer Israely, Shay Weiss, Adi Beth-Din, Ohad Shifman, Ofir Israeli, Shmuel Yitzhaki, Shmuel C. Shapira, Sharon Melamed, Eli Schwartz

We report a case of monkeypox in a man who returned from Nigeria to Israel in 2018. Virus was detected in pustule swabs by transmission electron microscopy and PCR and confirmed by immunofluorescence assay, tissue culture, and ELISA. The West Africa monkeypox outbreak calls for increased awareness by public health authorities worldwide.

Monkeypox is a zoonotic disease caused by monkeypox virus, an orthopoxvirus closely related to variola virus, the causative agent of smallpox. Human cases were first described in 1970; in subsequent decades, sporadic outbreaks were reported in Africa. Mortality rates are 1%–10% (*1*,*2*). The 2 clades, Congo-Basin and West African, each cause disease; the West African clade is considered to be less virulent and is associated with a lower mortality rate (*3*). Nevertheless, this clade is responsible for the largest documented monkeypox outbreak in West Africa (132 confirmed cases in Nigeria) (*4*). Human infection with monkeypox occurred in the United States in 2003, when imported animals from Africa infected pet prairie dogs (*5*). In September 2018 in the United Kingdom, 2 imported cases of monkeypox were detected in persons from Nigeria (*6*); a healthcare worker (HCW) acquired nosocomial infection from 1 of those patients. We report a case of monkeypox in Israel.

The Study

On October 4, 2018, a 38-year-old man sought care for generalized rash and fever at the Department of Emergency Medicine at Shaare-Zedek Medical Center, Jerusalem, Israel. This Israel resident had returned from Port Harcourt, Rivers State, Nigeria, where he had worked a desk job for the previous 10 years. On September 17, during his last trip to Nigeria, he had disposed of 2 rodent carcasses at his residence. He returned to Israel on September 23 and on September 29 noticed 2 itchy lesions on his penis shaft. The next day, he had fever (38.8°C) and chills and started self-medicating with nonsteroidal antiinflammatories and oral penicillin. On October 1, an erythematous rash appeared first on his face and later on his trunk and extremities.

Examination at Shaare-Zedek Medical Center on October 4 revealed that the patient was febrile and had a nonblanching maculopapular rash on his face (Figure 1, panel A), neck, trunk, and lower and upper extremities; several lesions on his palms and soles; 2 ulcers with an erythematous base on his penis shaft; and bilateral enlarged and tender lymph nodes in his groin. Blood test results indicated moderate thrombocytopenia (98,000 platelets/μL) and mild hepatitis. One lesion on the posterior aspect of his left arm (Figure 1, panel B) was suspected to be an eschar, raising the possibility of rickettsialpox. The patient was therefore hospitalized and administered oral doxycycline. His condition improved, and the next day he was discharged with doxycycline and instructions to remain isolated at home.

At a follow-up visit 2 days later (October 7), he was afebrile. The rash was locally synchronous and had progressed from maculopapular to vesicular and pustular; some lesions displayed black umbilication and crusting (Figure 1, panels C, D). Oral examination revealed bilateral tonsillar enlargement and ulcers in the posterior pharynx. Serology results were positive for varicella IgG (past infection) and negative for *Coxiella burnetii*, *Rickettsia conori*, *Rickettsia typhi*, *Brucella* spp., *Treponema pallidum*, and antigen/antibody combination for HIV. Pustular samples were negative for herpes simplex virus by PCR. Because of the rash characteristics and the patient's travel history, monkeypox was suspected.

Samples were sent to the Israel Institute for Biological Research, Ness-Ziona, Israel, and processed in Biosafety Level 3 laboratories. The pustule sample was processed for PCR analysis and transmission electron microscopy. Vero cells were infected for immunofluorescence assay and monitored for cytopathic effect. For transmission electron microscopy, particles were enriched by using a Beckman Airfuge (https://www.beckman.com) before negative staining with phosphotungstic acid.

Authorship affiliations: Israel Institute for Biological Research, Ness-Ziona, Israel (N. Erez, H. Achdout, E. Milrot, N. Paran, B. Politi, H. Tamir, T. Israely, S. Weiss, A. Beth-Din, O. Shifman, O. Israeli, S. Yitzhaki, S.C. Shapira, S. Melamed); Shaare-Zedek Medical Center, Jerusalem, Israel (Y. Schwartz, Y. Wiener-Well); Tel Aviv University, Tel Aviv, Israel (E. Schwartz)

DOI: https://doi.org/10.3201/eid2505.190076

[1]These authors contributed equally to this article.

The sample exhibited numerous brick-shaped particles, characteristic of orthopoxviruses. Particles were observed to be in clusters (up to 10 virions in each cluster) embedded in skin tissue and as single virions (Figure 2, panels A, B). Viral particle dimensions (± SD) were 281 ± 18 nm × 220 ± 17 nm (n = 24), in accordance with previously reported dimensions for monkeypox virus (*5*).

PCR diagnosis was based on specific primers to discriminate between the West African (581 bp) and the Congo-Basin (832 bp) clades by product size (*7*). The PCR product size corresponded to that of the West African clade currently circulating in Nigeria (*8*). This finding was confirmed by high-throughput sequencing.

Within 24 hours of infection, cytopathic effect was observed in Vero cells, exhibiting typical monolayer separation and cell rounding (Figure 2, panel C). The result of immunofluorescence assay with a specific antibody against orthopoxviruses was positive; some cells exhibited viral factories, typical for orthopoxvirus infection (Figure 2, panel D) (*9*).

The patient was instructed to remain isolated in his residence until he had fully recovered. Days after he returned home, the pustules turned to scabs (0.3–0.8 mm in diameter) and were shed (Figure 1, panels E, F). Concomitant with recovery, antibodies against orthopoxvirus and a neutralizing antibody titer (50% plaque reduction neutralization test titer = 134) developed, comparable to those of smallpox-vaccinated humans (*10*). Of note, scabs collected from the patient during recovery, then homogenized and tested for monkeypox virus, contained viable viral loads of 10^5–10^7 PFU/scab.

All of the patient's contacts in Israel (5 household members and 11 HCWs) were offered smallpox vaccination, but only 1 HCW agreed. All contacts were followed up for 21 days; no virus transmission was detected.

Figure 1. Dermal manifestations of monkeypox on patient in Israel, 2018. Maculopapular rash was apparent on the face (A) and body on the day of hospital admission. A lesion on the left proximal extremity (B) was suspected to be a rickettsial eschar. After 3 days, the rash changed into vesicles and pustules on the face (C) and body (D). Skin resolution was apparent 13 days after admission; pustules and vesicles crusted and were shed (E, F). G) Timeline of disease progression.

Conclusions

Since the first documented case of human monkeypox in 1970, sporadic outbreaks have been reported, especially in the Congo Basin and West Africa. Contributing to the increased frequency of such occurrences were discontinued vaccination against smallpox, increased interaction with wildlife because of deforestation and population movement, consumption of bushmeat, and increased population density (*11*,*12*). Although most infections are acquired from wildlife, human-to-human transmission has been reported, as in the 1996–1997 outbreak in the Democratic Republic of the Congo (*13*) and the current outbreak in West Africa (*8*). The availability and speed of international transportation combined with the natural progression of the disease (long incubation and prodromal periods, up to 21 days combined) increase the risk for monkeypox spread from rural regions into urban areas and to countries outside Africa. Indeed, during September and October 2018, monkeypox was diagnosed in the United Kingdom and Israel (*6*,*14*).

Thus far, all imported cases of monkeypox in humans (United States in 2003, United Kingdom and Israel in 2018) have involved the West African clade of the virus (*3*,*6*). After a similar incubation period (12 days), all patients had fever and chills, lymphadenopathy, and skin lesions (*5*,*6*). Although the patient in Israel had numerous vesiculopustules on his face and body, the patients involved in the US outbreak had substantially fewer (1–50) and reported a

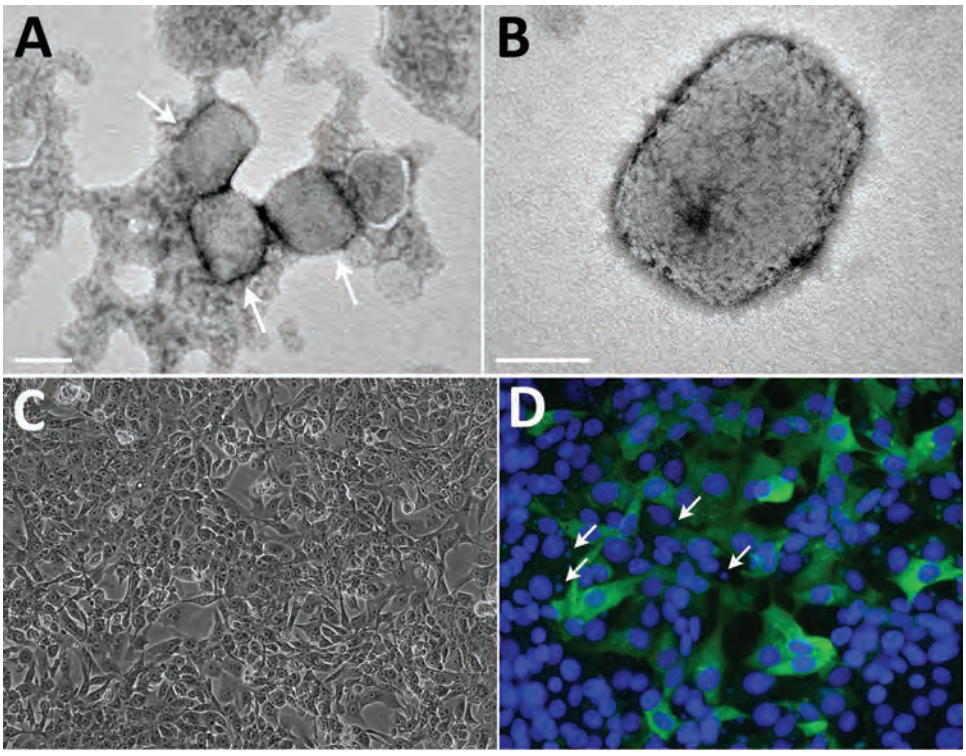

Figure 2. Transmission electron microscopy and cell culture–based diagnosis of monkeypox in patient in Israel, 2018. Virus particles were detected in lesion samples as either virion aggregates (arrows) (A) or individual virions (B) with a typical brick shape. Infected Vero cells depicted typical cytopathic effect, exhibiting cell detachment and rounding. Scale bar in A indicates 0.2 μm; scale bar in B indicates 100 nm. C) Infected Vero cells depicting typical cytopathic effect: cell detachment and rounding. Original magnification ×10. D) Immunofluorescent staining of infected Vero cells: DNA (DAPI [4′,6-diamidino-2-phenylindole] stain, blue) and monkeypox virus (green); viral factories are evident (arrows). Original magnification ×25.

persistent cough, which the patient from Israel did not report. Of note, the first sign noted by the Israel and UK patients was groin lesions (*6*). Although past reports considered the Congo-Basin clade to be more virulent (*2*,*3*,*12*), recent reports show that the West African clade can also cause disseminated disease and can be transmitted from human to human (*4*,*8*).

For this study, we used multiple diagnostic approaches. The virus was detected in pustule swab specimens by transmission electron microscopy and PCR within 3 hours of sample arrival and confirmed by immunofluorescence assay, tissue culture, and ELISA for orthopoxvirus antigens.

The very high virus titers contained by pustules and scabs, as demonstrated in this case, increase the risk for human-to-human transmission and environmental spread. To prevent further transmission, HCWs should implement safety practices and local authorities should map contacts and consider use of smallpox vaccines or antiviral drugs (*14*,*15*), according to risk assessment.

Acknowledgment

We thank Itai Glinert for help with the manuscript.

About the Author

Drs. Erez and Achdout are researchers at the Department of Infectious Diseases, Israel Institute for Biological Research, Ness-Ziona, Israel. Their research interests include immune response to vaccines and viral infections.

References

1. Di Giulio DB, Eckburg PB. Human monkeypox: an emerging zoonosis. Lancet Infect Dis. 2004;4:15–25. http://dx.doi.org/10.1016/S1473-3099(03)00856-9
2. Breman JG, Kalisa-Ruti, Steniowski MV, Zanotto E, Gromyko AI, Arita I. Human monkeypox, 1970–79. Bull World Health Organ. 1980;58:165–82.
3. Likos AM, Sammons SA, Olson VA, Frace AM, Li Y, Olsen-Rasmussen M, et al. A tale of two clades: monkeypox viruses. J Gen Virol. 2005;86:2661–72. http://dx.doi.org/10.1099/vir.0.81215-0
4. Petersen E, Abubakar I, Ihekweazu C, Heymann D, Ntoumi F, Blumberg L, et al. Monkeypox— enhancing public health preparedness for an emerging lethal human zoonotic epidemic threat in the wake of the smallpox post-eradication era. Int J Infect Dis. 2019;78:78–84. http://dx.doi.org/10.1016/j.ijid.2018.11.008
5. Reed KD, Melski JW, Graham MB, Regnery RL, Sotir MJ, Wegner MV, et al. The detection of monkeypox in humans in the Western Hemisphere. N Engl J Med. 2004;350:342–50. http://dx.doi.org/10.1056/NEJMoa032299
6. Vaughan A, Aarons E, Astbury J, Balasegaram S, Beadsworth M, Beck CR, et al. Two cases of monkeypox imported to the United Kingdom, September 2018. Euro Surveill. 2018;23. http://dx.doi.org/10.2807/1560-7917.ES.2018.23.38.1800509
7. Shchelkunov SN, Gavrilova EV, Babkin IV. Multiplex PCR detection and species differentiation of orthopoxviruses pathogenic to humans. Mol Cell Probes. 2005;19:1–8. http://dx.doi.org/10.1016/j.mcp.2004.07.004
8. Yinka-Ogunleye A, Aruna O, Ogoina D, Aworabhi N, Eteng W, Badaru S, et al. Reemergence of human monkeypox in Nigeria, 2017. Emerg Infect Dis. 2018;24:1149–51. http://dx.doi.org/w10.3201/eid2406.180017
9. Smith GL, Vanderplasschen A, Law M. The formation and function of extracellular enveloped vaccinia virus. J Gen Virol. 2002;83:2915–31. http://dx.doi.org/10.1099/0022-1317-83-12-2915

10. Orr N, Forman M, Marcus H, Lustig S, Paran N, Grotto I, et al.; Vaccinia Study Group, Medical Corps, Israel Defense Force; Vaccinia Study Group, Israel Institute for Biological Research. Clinical and immune responses after revaccination of Israeli adults with the Lister strain of vaccinia virus. J Infect Dis. 2004;190:1295–302. http://dx.doi.org/10.1086/423851
11. Nolen LD, Osadebe L, Katomba J, Likofata J, Mukadi D, Monroe B, et al. Introduction of monkeypox into a community and household: risk factors and zoonotic reservoirs in the Democratic Republic of the Congo. Am J Trop Med Hyg. 2015;93:410–5. http://dx.doi.org/10.4269/ajtmh.15-0168
12. McCollum AM, Damon IK. Human monkeypox. Clin Infect Dis. 2014;58:260–7. http://dx.doi.org/10.1093/cid/cit703
13. Centers for Disease Control and Prevention. Human monkeypox—Kasai Oriental, Democratic Republic of Congo, February 1996–October 1997. MMWR Morb Mortal Wkly Rep. 1997;46:1168–71.
14. Angelo KM, Petersen BW, Hamer DH, Schwartz E, Brunette G. Monkeypox transmission among international travelers—serious monkey business? J Travel Med. 2019. http://dx.doi.org/10.1093/jtm/taz002
15. Melamed S, Israely T, Paran N. Challenges and achievements in prevention and treatment of smallpox. Vaccines (Basel). 2018;6:E8. http://dx.doi.org/10.3390/vaccines6010008

Address for correspondence: Sharon Melamed, Israel Institute for Biological Research, Department of Infectious Diseases, Ness-Ziona 74100, POB 019, Israel; email: sharonm@iibr.gov.il

Population-Based Estimate of Melioidosis, Kenya

Esther M. Muthumbi, Nicola C. Gordon, George Mochamah, Sammy Nyongesa, Emily Odipo, Salim Mwarumba, Neema Mturi, Anthony O. Etyang, David A.B. Dance, J. Anthony G. Scott, Susan C. Morpeth

Melioidosis is thought to be endemic, although underdiagnosed, in Africa. We identified 5 autochthonous cases of *Burkholderia pseudomallei* infection in a case series in Kenya. Incidence of *B. pseudomallei* bacteremia in Kenya's Kilifi County is low, at 1.5 cases per million person-years, but this result might be an underestimate.

Burkholderia pseudomallei, the causative agent of melioidosis, is a gram-negative bacillus endemic particularly in northern Australia and South and Southeast Asia. Worldwide, *B. pseudomallei* causes ≈165,000 cases of disease and ≈89,000 deaths annually (*1*). The presence of *B. pseudomallei* in Africa has been demonstrated by sporadic cases of melioidosis reported in travelers returning from countries including Kenya (*2*). Indigenous culture-confirmed cases have been reported in only 4 countries in Africa, mainly from research centers with diagnostic laboratory facilities (*3*).

The first case of melioidosis linked to Kenya was diagnosed in 1982 in a tourist from Denmark who had visited Nyali (an area of Mombasa City), ≈50 km south of the town of Kilifi (*2*). Follow-up clinical surveillance in Nairobi and environmental surveillance from other regions in Kenya yielded no *B. pseudomallei* isolates (*4*). However, growing concerns over possible underestimation of the disease in potentially endemic areas, including in tropical Africa, have led to calls for improved surveillance (*5*).

In 2010, at Kilifi County Hospital (KCH), we isolated *B. pseudomallei* from the blood culture of a 3-year-old child after a near-drowning accident in a seasonal river. The identity of the isolate was confirmed by real-time PCR targeting the type III secretion system genes of *B. pseudomallei* (*6*), and the isolate was later sequenced for a study of geographic dissemination of *B. pseudomallei* (*7*). After this identification, we conducted a retrospective analysis of archived blood culture isolates collected during 1994–2012 to investigate possible missed cases of invasive *B. pseudomallei* infection.

Author affiliations: KEMRI–Wellcome Trust Research Programme, Kilifi, Kenya (E.M. Muthumbi, N.C. Gordon, G. Mochamah, S. Nyongesa, E. Odipo, S. Mwarumba, N. Mturi, A.O. Etyang, J.A.G. Scott, S.C. Morpeth); London School of Hygiene & Tropical Medicine, London, UK (N.C. Gordon, D.A.B. Dance, J.A.G. Scott, S.C. Morpeth); Lao-Oxford-Mahosot Hospital–Wellcome Trust Research Unit, Vientiane, Laos (D.A.B. Dance); University of Oxford, Oxford, UK (D.A.B. Dance, J.A.G. Scott, S.C. Morpeth)

DOI: https://doi.org/10.3201/eid2505.180545

The Study

During 1994–1998, blood culture was performed on all febrile patients admitted to the pediatric wards at KCH. Since 1998, all pediatric patients <15 years of age admitted, except those having trauma, burns, or elective surgery, have had blood samples drawn for culture. Surveillance for patients ≥15 years of age began in 2007; blood samples are drawn at admission for cultures on patients meeting clinical criteria for possible invasive bacterial disease. Since 2002, hospitalization events have been linked to the Kilifi Health and Demographic Surveillance System (KHDSS), which monitors the population of ≈280,000 over an area of 891 km^2 (*8*). Informed consent is obtained from all patients participating in the surveillance, including for storage of isolates and future use of clinical data.

Blood samples for bacterial cultures were collected in BACTEC Peds Plus or BACTEC Plus Aerobic/F bottles (Becton Dickinson, https://www.bd.com) and incubated on a BACTEC FX 9050 Automated Blood Culture instrument (Becton Dickinson). Nonfastidious, oxidase-positive, gram-negative bacilli were identified by using API 20NE test kits (bioMérieux, https://www.biomerieux.com). We reviewed all gentamicin-resistant, glucose-nonfermenting, gram-negative rods, with the exception of *Pseudomonas aeruginosa*, even if the API 20NE identification was acceptable, to account for difficulties in speciating *Burkholderia* spp. with biochemical methods.

A total of 86,582 patients <15 years of age were admitted during 1994–2012 and 18,864 patients ≥15 years of age during 2007–2012. Surveillance identified 33 gentamicin-resistant, glucose-nonfermenting bacilli in 14,235 positive blood cultures from patients <15 years of age and 5 gentamicin-resistant, glucose-nonfermenting bacilli in 705 positive blood cultures from patients ≥15 years of age (Figure). We retrieved all 38 isolates from storage for PCR, which we performed using published primer and probe sequences (*6*).

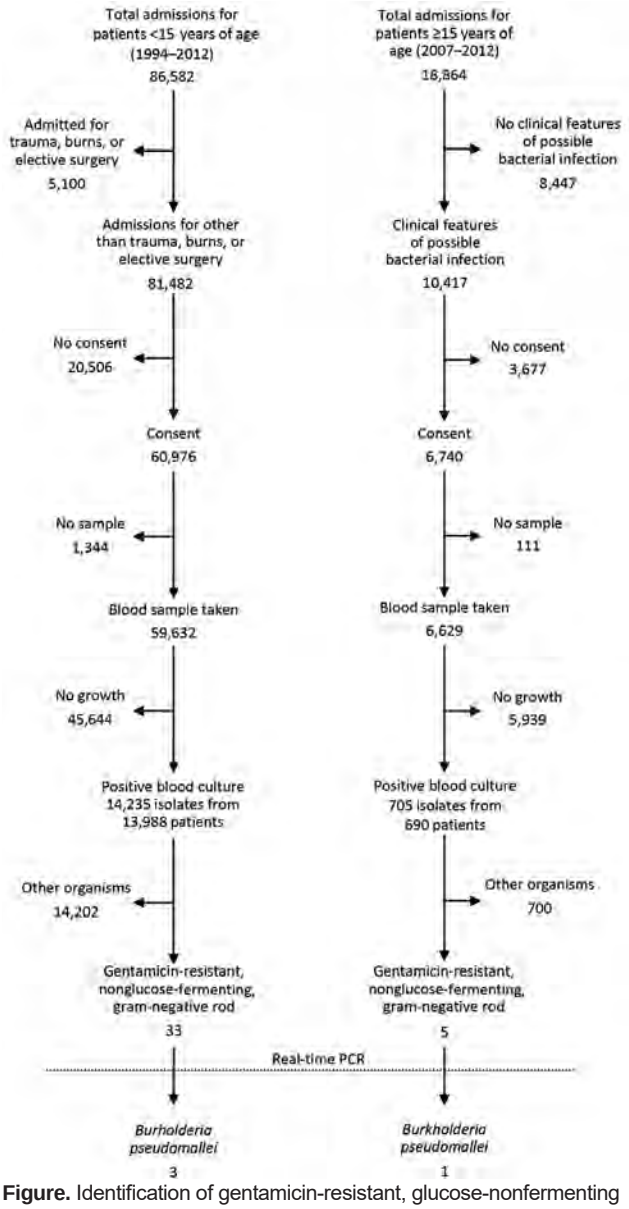

Figure. Identification of gentamicin-resistant, glucose-nonfermenting bacilli and *Burkholderia pseudomallei* from isolates collected from patients at Kilifi County Hospital, Kilifi, Kenya, 1994–2012.

We identified 4 isolates as *B. pseudomallei* by PCR, including the index isolate from 2010 (Table 1; Appendix, https://wwwnc.cdc.gov/EID/25/5/18-0545-App1.pdf). One isolate was previously identified as *B. cepacia*, and 2 were previously labeled as *Pseudomonas* species. We identified a fifth *B. pseudomallei* case in July 2014 in a 68-year-old female patient with diabetes mellitus and bilateral cervical abscesses (Table 1; Appendix). Blood culture results were negative, but aspirated pus grew *B. pseudomallei*, identified by API 20NE and confirmed by PCR.

None of the case-patients had any history of travel outside Kilifi County. Three died during the course of their admission. No further information is available for the 2 case-patients who survived because they were not residents of the area surveyed by KHDSS.

To estimate the incidence of melioidosis bloodstream infection, we divided the number of invasive *B. pseudomallei* cases among KHDSS residents by the sum of the annual midyear population counts during 2002–2012 for those <15 years of age and during 2007–2012 for those ≥15 years of age. We also adjusted for the sensitivity of the surveillance to account for the proportion of patients not consenting to the surveillance study and those who did not have a blood culture drawn. For the period before 2002, we extrapolated age-specific population estimates by using a log-linear model of age-specific population data based on subsequent enumerations. The estimated incidence was 1.3 cases/1 million person-years of observation for those <15 years of age and 2 cases/1 million person-years of observation for those ≥15 years of age (Table 2).

Conclusions

We identified 5 cases of melioidosis from a single surveillance site in Kenya. Despite reports suggesting that melioidosis is endemic but underdetected in the region (*5*), we demonstrated low incidence in this part of Kenya. Even so, *B. pseudomallei* has emerged as an underdiagnosed cause of sepsis in Kilifi County. The empirical treatment used for sepsis, ampicillin and gentamicin, does not cover *B. pseudomallei*. The lack of pathognomonic clinical features makes it difficult to detect melioidosis clinically, especially in areas to which the disease is not endemic. In the series we report, 2 case-patients died before receiving definitive treatment, and only 1 case-patient received antimicrobial drugs recommended to treat melioidosis.

The integrated, population-based bacterial surveillance system in Kilifi County provides a unique opportunity to estimate incidence. Routine blood culture sampling of all admitted patients <15 years of age and eligible patients ≥15 years of age eliminates reliance on clinical suspicion for bacteremic melioidosis. The use of molecular methods on isolates suspected to be *B. pseudomallei* will probably enhance case detection because *B. pseudomallei* is commonly misidentified or unidentified by culture (*9*). Only 2 isolates in our study were identified by using standard techniques, despite the reported good discriminatory performance of API 20NE in distinguishing *B. pseudomallei* and *B. cepacia* (*10*).

Our reported incidence rates might still be underestimated. Our data do not account for KHDSS residents who do not go to KCH. For example, ≈64% of deaths in children <5 years of age in the KHDSS area occur at home or in other healthcare facilities (*8*). Furthermore, as

Table 1. Clinical summary of patients with positive *Burkholderia pseudomallei* isolates, Kilifi, Kenya, 2002–2014*

Year	Age/sex	Clinical features	Risk factors	Diagnosis†	Culture source	Antimicrobial sensitivity					Days in hospital	Outcome
						AMC	STX	TET	CAZ	IMI		
2002	8 d/M	Fever, jaundice, respiratory distress	None identified	Neonatal sepsis	Blood	S	S	S	S	S	3	Died
2008	7 d/M	Respiratory distress	None identified	Severe pneumonia, neonatal sepsis	Blood	S	S	S	S	S	3	Survived
2010	3 y/F	Fever, respiratory distress	Near-drowning	Severe pneumonia, septic shock	Blood	S	S	S	S	S	6	Died
2011	52 y/M	Persistent fever and night sweats of unknown duration	None identified	Acute renal failure, meningitis	Blood	S	S	S	S	S	5	Died
2014	68 y/F	Fever, bilateral cervical neck swellings	Diabetes mellitus	Diabetes, cervical lymphadenitis	Pus swab	S	S	S	S	S	40	Survived

*AMC, amoxicillin/clavulanic acid; CAZ, ceftazidime; IMI, imipenem; S, susceptible; STX, sulfamethoxazole/trimethoprim; TET, tetracycline.
†Diagnosis at time of admission.

demonstrated by the fifth case, the incidence of nonbacteremic infection might be higher because non–blood culture samples are not systematically collected. Only 50%–75% of patients with melioidosis are bacteremic (*11*), and culture has an estimated sensitivity of 60.2% for melioidosis (*12*). In addition, our screening method excluded gentamicin-susceptible isolates. If gentamicin-susceptible *B. pseudomallei* is as common in Kenya as reported in other areas (*13*), additional surveillance that includes these organisms could increase the reported incidence rates. Finally, melioidosis often is unevenly distributed within endemic areas, as noted in Thailand (*14*). Despite these factors, our results suggest that, although *B. pseudomallei* is present in tropical Africa, the incidence of invasive melioidosis is surprisingly low.

The differences in disease incidence in Africa and Asia are striking. Host factors, such as diabetes mellitus, might contribute, but environmental factors and agricultural practices, such as rice farming, are probably more important in permitting exposure to and environmental persistence and proliferation of the organism. Nonetheless, Kenya has been identified as environmentally suitable for *B. pseudomallei* because of its soil type, agricultural practices, and rainfall (*1*). Our study demonstrates the presence of *B. pseudomallei* in Kenya. Changes in climate and agricultural practices might lead to future increases in melioidosis, and ongoing surveillance is necessary.

Acknowledgments

We thank the nursing, clinical, and clerical staff of Kilifi County Hospital and the patients and their families.

The surveillance work was funded by the Wellcome Trust (core support to KEMRI–Wellcome Trust Research Program grant no. 203077) and by Gavi, the Vaccine Alliance, through support for a study of pneumococcal vaccine impact. J.A.G.S. is supported by a Wellcome Trust clinical research fellowship (no. 098532) and D.A.B.D. is funded by Wellcome grant no. 106698/Z/14/Z.

E.M.M. is supported through the DELTAS Africa Initiative [DEL-15-003]. The DELTAS Africa Initiative is an independent funding scheme of the African Academy of Sciences' (AAS) Alliance for Accelerating Excellence in Science in Africa and supported by the New Partnership for Africa's Development Planning and Coordinating Agency (NEPAD Agency) with funding from the Wellcome Trust, [107769/Z/10/Z] and the government of the United Kingdom. The views expressed in this publication are those of the authors and not necessarily those of AAS, NEPAD Agency, Wellcome Trust, or the UK government.

This paper is published with the approval of the director of the Kenya Medical Research Institute.

About the Author

Dr. Muthumbi is a medical epidemiologist at the KEMRI–Wellcome Trust Research Programme in Kenya. She is a doctoral student in infectious disease epidemiology.

Table 2. Incidence of melioidosis in Kilifi County Hospital, Kilifi, Kenya, 1994–2012*

Patient age group	No. cases	No. case-patients residing in KHDSS area	Study period	Person-years of observation	Crude incidence† (95% CI)	Adjusted incidence† (95% CI)
<15 y	3	2	1994–2012	2,026,781	1.0 (0.12–3.56)	1.3 (0.17–5.17)
≥15 y	1	1	2007–2012	782,373	1.3 (0.03–7.1)	2.0 (0.08–15.6)
Overall	4	3	NA	2,809,154	1.1 (0.22–3.12)	1.5 (0.35–5.0)

*KHDSS, Kilifi Health and Demographic Surveillance System; NA, not applicable.
†Incidence per 10^6 person-years of observation, adjusted for nonconsenters and missing blood cultures among eligible consenters.

References

1. Limmathurotsakul D, Golding N, Dance DAB, Messina JP, Pigott DM, Moyes CL, et al. Predicted global distribution of *Burkholderia pseudomallei* and burden of melioidosis. Nat Microbiol. 2016;1:15008 http://dx.doi.org/10.1038/nmicrobiol.2015.8
2. Bremmelgaard A, Bygbjerg I, Høiby N. Microbiological and immunological studies in a case of human melioidosis diagnosed in Denmark. Scand J Infect Dis. 1982;14:271–5. http://dx.doi.org/10.3109/inf.1982.14.issue-4.05
3. Birnie E, Wiersinga WJ, Limmathurotsakul D, Grobusch MP. Melioidosis in Africa: should we be looking more closely? Future Microbiol. 2015;10:273–81. http://dx.doi.org/10.2217/fmb.14.113
4. Batchelor BI, Paul J, Trakulsomboon S, Mgongo M, Dance DAB. Melioidosis survey in Kenya. Trans R Soc Trop Med Hyg. 1994;88:181. http://dx.doi.org/10.1016/0035-9203(94)90286-0
5. Currie BJ, Dance DAB, Cheng AC. The global distribution of *Burkholderia pseudomallei* and melioidosis: an update. Trans R Soc Trop Med Hyg. 2008;102(Suppl 1):S1–4. http://dx.doi.org/10.1016/s0035-9203(08)70002-6
6. Novak RT, Glass MB, Gee JE, Gal D, Mayo MJ, Currie BJ, et al. Development and evaluation of a real-time PCR assay targeting the type III secretion system of *Burkholderia pseudomallei*. J Clin Microbiol. 2006;44:85–90. http://dx.doi.org/10.1128/jcm.44.1.85-90.2006
7. Chewapreecha C, Holden MT, Vehkala M, Valimaki N, Yang Z, Harris SR, et al. Global and regional dissemination and evolution of *Burkholderia pseudomallei*. Nat Microbiol. 2017;2:16263. http://dx.doi.org/10.1038/nmicrobiol.2016.263
8. Scott JAG, Bauni E, Moisi JC, Ojal J, Gatakaa H, Nyundo C, et al. Profile: the Kilifi Health and Demographic Surveillance System (KHDSS). Int J Epidemiol. 2012;41(3):650–7. http://dx.doi.org/10.1093/ije/dys062
9. Amornchai P, Chierakul W, Wuthiekanun V, Mahakhunkijcharoen Y, Phetsouvanh R, Currie BJ, et al. Accuracy of *Burkholderia pseudomallei* identification using the API 20NE system and a latex agglutination test. J Clin Microbiol. 2007;45:3774–6. http://dx.doi.org/10.1128/jcm.00935-07
10. Kiratisin P, Santanirand P, Chantratita N, Kaewdaeng S. Accuracy of commercial systems for identification of *Burkholderia pseudomallei* versus *Burkholderia cepacia*. Diagn Microbiol Infect Dis. 2007;59:277–81. http://dx.doi.org/10.1016/j.diagmicrobio.2007.06.013
11. Wiersinga WJ, Virk HS, Torres AG, Currie BJ, Peacock SJ, Dance DAB, et al. Melioidosis. Nat Rev Dis Primers. 2018;4:17107. http://dx.doi.org/10.1038/nrdp.2017.107
12. Limmathurotsakul D, Jamsen K, Arayawichanont A, Simpson JA, White LJ, Lee SJ, et al. Defining the true sensitivity of culture for the diagnosis of melioidosis using Bayesian latent class models. PLoS ONE. 2010;5:e12485. http://dx.doi.org/10.1371/journal.pone.0012485.
13. Podin Y, Sarovich DS, Price EP, Kaestli M, Mayo M, Hii K, et al. *Burkholderia pseudomallei* isolates from Sarawak, Malaysian Borneo, are predominantly susceptible to aminoglycosides and macrolides. Antimicrob Agents Chemother. 2014;58(1):162–6. https://dx.doi.org/10.1128/aac.01842-13
14. Vuddhakul V, Tharavichitkul P, Na-Ngam N, Jitsurong S, Kunthawa B, Noimay P, et al. Epidemiology of *Burkholderia pseudomallei* in Thailand. Am J Trop Med Hyg. 1999;60:458–61. http://dx.doi.org/10.4269/ajtmh.1999.60.458

Address for correspondence: Esther M. Muthumbi, KEMRI–Wellcome Trust Research Programme, PO Box 230, Kilifi, Kenya; email: emuthumbi@kemri-wellcome.org

Originally published in November 2009

etymologia revisited

Burkholderia

[burk″hol-dēr′e-ə]

This genus of gram-negative, rod-shaped bacteria comprising animal and plant pathogens was named for American plant pathologist Walter H. Burkholder. Dr. Burkholder first described a particular species of this genus, later called *Burkholderia cepacia* (Latin for "like onion"), after an outbreak of infection in vegetable growers in New York State in 1949. Previously known to cause disease in onion bulbs, these organisms are now recognized as major bacterial lung pathogens in patients with cystic fibrosis. *B. mallei* causes glanders in horses, and *B. pseudomallei* is the etiologic agent of melioidosis in humans and animals. Dr. Burkholder is recognized for helping establish the role of bacteria as plant pathogens.

Source: Dorland's illustrated medical dictionary, 31st edition. Philadelphia: Saunders; 2007; De Soyza A, Silipo A, Lanzetta R, Govan JR, Molinaro A. Chemical and biological features of *Burkholderia cepacia* complex lipopolysaccarides. Innate Immunity. 2008;14:127.

https://wwwnc.cdc.gov/eid/article/15/11/e1-1511_article

Novel Method for Rapid Detection of Spatiotemporal HIV Clusters Potentially Warranting Intervention

Arthur G. Fitzmaurice, Laurie Linley, Chenhua Zhang, Meg Watson, Anne Marie France, Alexandra M. Oster

Rapid detection of increases in HIV transmission enables targeted outbreak response efforts to reduce the number of new infections. We analyzed US HIV surveillance data and identified spatiotemporal clusters of diagnoses. This systematic method can help target timely investigations and preventive interventions for maximum public health benefit.

Despite innovations in HIV prevention and treatment, HIV outbreaks do occur in the United States. Local public health staff identified >200 persons with HIV resulting from an injection drug use (IDU)–associated outbreak in 2015 in Scott County, Indiana (*1*). The multipronged outbreak response included the establishment of Indiana's first syringe services program. The number of cases might have been worse without intervention, suggesting the value of rapidly detecting and responding to increases in HIV transmission, whether related to IDU or other transmission modes.

The Centers for Disease Control and Prevention (CDC) recently began using HIV nucleotide sequence data from the National HIV Surveillance System (NHSS) to identify clusters of recent and rapid HIV transmission (*2*). Sequences are generated through HIV drug resistance testing routinely conducted as part of clinical care, but sequence reporting to health departments and CDC can be delayed or incomplete (*3*). Case surveillance data (i.e., reported diagnoses), which are timelier and more complete than sequence data, can be used to detect spatiotemporal increases in diagnoses.

CDC has not previously used systematic methods to analyze HIV case surveillance data to detect outbreaks as they occur. We developed a method to identify spatiotemporal clusters of increased diagnoses. Our proposed method enables efficient analysis at local and national levels to generate spatiotemporal alerts representing concentrated increases that require further investigation.

Author affiliations: Centers for Disease Control and Prevention, Atlanta, Georgia, USA (A.G. Fitzmaurice, L. Linley, M. Watson, A.M. France, A.M. Oster); ICF International, Atlanta (C. Zhang)

DOI: https://doi.org/10.3201/eid2505.180776

The Study

We reviewed non–HIV outbreak detection literature and methods employed by disease and syndromic surveillance programs at CDC and in several state and local health departments. Methods generally inferred outbreaks from statistically significant increases above historical baselines (*4*–*6*). We tested analytic parameters on NHSS data to adapt existing methodologies. For example, HIV symptom onset and diagnosis can be delayed compared with other infectious diseases, so we varied frames for batching data and manually compared method outputs to determine optimal parameters based on epidemiologists' assessments of the most concerning clusters. This systematic method detects increases in HIV diagnoses above expected baselines (i.e., alerts) in specified geographic areas.

We applied this method to NHSS data reported from all 50 US states and the District of Columbia, examining the numbers of cases by state and county or countyequivalent (e.g., borough, parish; hereafter, collectively referred to as "county" and including the District of Columbia). For each state or county, we determined the total number of diagnoses during the most recent 12 months (January–December 2016) on the basis of residence address at time of HIV diagnosis (Figure 1). We calculated the baseline as mean diagnoses in the 3 prior 12-month periods (calendar years 2013, 2014, and 2015). An alert was generated in a geographic area when the total number of cases during the most recent 12 months was >2 SD and >2 diagnoses greater than the baseline mean. The latter criterion eliminates alerts resulting from small diagnosis levels (e.g., baseline of 0 alerting with only 1 diagnosis). We repeated these analyses limiting to IDU-related diagnoses, excluding men who reported both male-to-male sexual contact and IDU.

State-level alerts occurred for 4 (8%) of 50 states (Midwest 3, South 1); county-level alerts occurred for 143 (5%) of 3,142 counties nationwide (Table). A median of 2 and mean of 4 counties per state had alerts. Using the exact Pearson test for homogeneity, we determined that alerting counties were disproportionately located in the Northeast

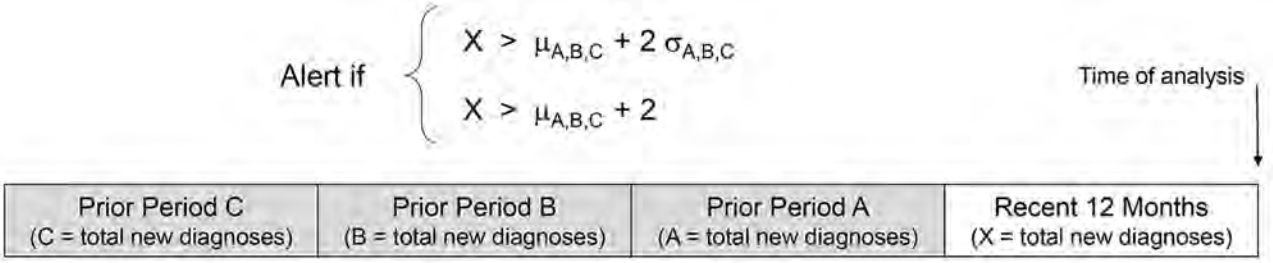

Figure 1. Alert criteria used in method for identifying spatiotemporal clusters of HIV diagnoses. For each cluster, the total number of cases (X) in a specified geographic area during the most recent 12 months exceeds the baseline mean (μ) of the previous 3 12-month periods by >2 SD (σ) and >2 diagnoses.

(15%; p<0.001) and South (59%; p<0.001), compared with nonalerting counties in the Northeast (7%) and South (45%). Among cases with reported IDU risk, alerts occurred for 2 states in the Midwest, 1 state in the West, and 21 counties, which were located mostly in the South (38%) and Midwest (29%). Baseline rates for county-level IDU alerts averaged 0.3–9 diagnoses per year.

Discussion

We aimed to develop a spatiotemporal cluster detection method that could efficiently be used and adapted to identify potential increases in HIV transmission in different local contexts. We identified significant increases in HIV diagnoses across all regions, capturing alerts from counties with small, medium, and large baseline numbers of HIV diagnoses. Some counties had small increases in the number of diagnoses and large percentage increases; others had larger increases in numbers but smaller increases in percentages (Figure 2). IDU-attributable diagnoses constitute a small proportion of total diagnoses, so the ability to identify potential IDU transmission clusters by analyzing IDU-attributable diagnoses separately is a strength of this method. Transmission through sexual and other risk networks might cross arbitrary geographic boundaries, but this method uses administrative boundaries aligned with existing data systems, so surveillance staff at state and local levels can automate monthly data analyses. States can conduct analyses at intermediary levels between state and county (e.g., regions within a state), and state or local health departments can analyze smaller areas (e.g., census tracts); national analyses will be vital for identifying spatiotemporal clusters across state boundaries.

We discussed our results with several state and local health departments that expressed interest in a robust, systematic method for routine identification of spatiotemporal clusters. They confirmed that this method identified alerts where they had recently begun responding and that new alerts provided actionable information regarding concerning HIV transmission increases.

Small median and mean numbers of alerts suggest reasonable investigative loads for this method. Batching data into moving 12-month frames reduces alerts resulting from seasonal variability and data noise. The chronic nature of HIV infection means that related cases might not be diagnosed until months or years after infection, so the 12-month analysis frame might not capture all related diagnoses, but it does account for delays between diagnosis and reporting to surveillance systems. These delays need to be addressed differently across states (*8*). State and local health departments with longer delays should improve reporting processes or analyze preliminary data; others can adapt the method by lagging or contracting the analysis frame.

Further investigation is needed to determine whether spatiotemporal clusters repre sent true increases in HIV transmission. Alerts might result from programmatic arti-

Table. Distribution of spatiotemporal clusters of HIV diagnoses among counties in 50 states and the District of Columbia, 2016

Characteristic	All diagnoses			Diagnoses attributable to injection drug use		
	Counties with alerts, no. (%)*	Counties without alerts, no. (%)	p value	Counties with alerts, no. (%)*	Counties without alerts, no. (%)	p value
Region (*7*)						
Northeast	21 (15)	196 (7)	0.0002	3 (14)	214 (7)	0.18
Midwest	27 (19)	1,028 (34)	0.0001	6 (29)	1,049 (34)	0.63
South	84 (59)	1,338 (45)	0.0009	8 (38)	1,414 (45)	0.51
West	11 (8)	437 (15)	0.022	4 (19)	444 (14)	0.53
Baseline mean annual HIV diagnoses, 2013–2015						
<3	52 (36)	2,128 (71)	$<10^{-4}$	13 (62)	2,176 (69)	0.46
3–9	40 (28)	463 (15)	$<10^{-4}$	8 (38)	495 (16)	0.0056
>9	51 (36)	408 (14)	$<10^{-4}$	0	459 (15)	0.057
Total counties	143 (100)	2,999 (100)		21 (100)	3,121 (100)	

*An alert occurred when the number of diagnoses in 2016 increased by >2 SD and >2 diagnoses compared with the mean annual baseline over the preceding 3 years (2013–2015).

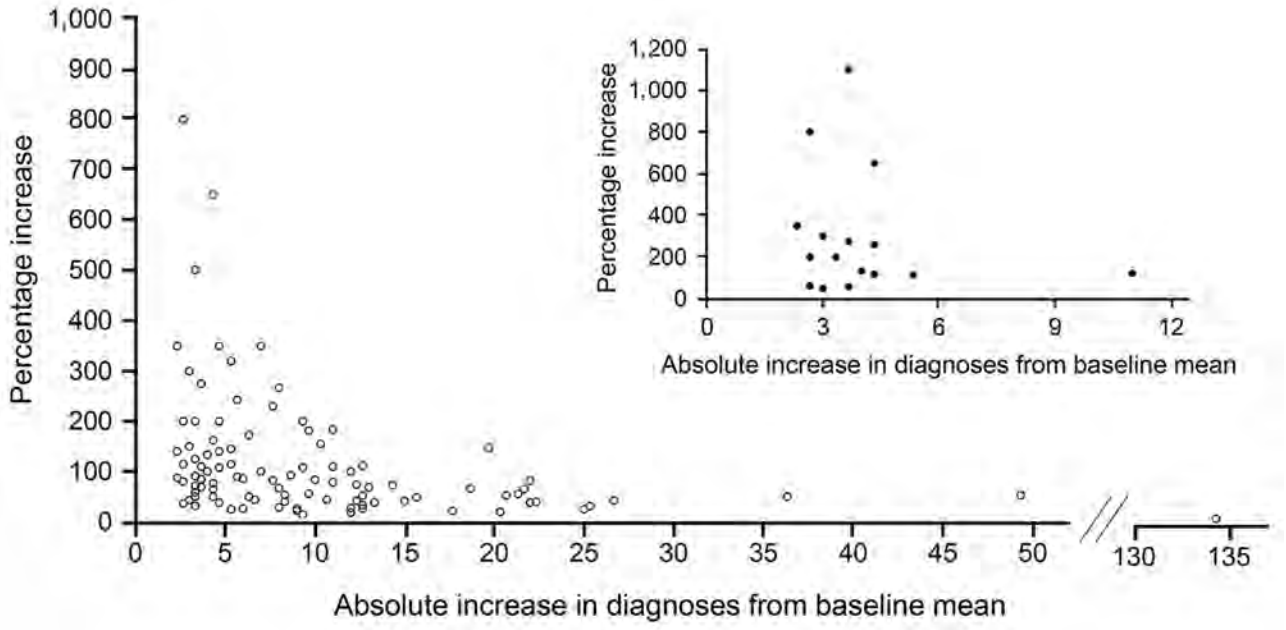

Figure 2. Percentage and absolute increases in annual HIV diagnoses above 3-year baseline means used in method for identifying spatiotemporal clusters of HIV diagnoses. Alerts are shown for 138 counties, as well as 21 county alerts attributable to injection drug use (inset). Five county alerts with 0 baseline diagnoses not shown (infinite percentage increase).

facts, although local epidemiologists would be aware of such programmatic influences (e.g., testing campaigns resulting in increased diagnoses not representing recent transmission). Reviewing testing history, partner services, contact tracing, and molecular data might help determine whether alerts represent clusters of recent infections that warrant investigation. Future evaluation will assess the extent to which this method identifies recent transmission and whether modifications might improve the method for different contexts.

The ideal cluster and outbreak detection system would use both case surveillance and molecular sequence-based approaches. Each method might help overcome the other's limitations. Although some alerts occurred in counties with large baseline HIV numbers, this method is less sensitive for these areas and might not capture all meaningful clusters. Analysis of sequence data is crucial for identifying transmission clusters in areas with larger numbers of cases and those distributed over broader geographic areas. However, this method is timelier than molecular methods and can provide state and local health officials with actionable data for early investigation. This factor might be particularly necessary for identifying increases in transmission associated with IDU, given increasing opioid use and the potential for rapid spread of HIV among vulnerable populations (*1*,*9*–*11*).

Conclusions

In summary, we developed a systematic method to identify spatiotemporal clusters of HIV diagnoses. Routine use of this method in near real-time can automate detection of increases in HIV diagnoses meriting further investigation, helping state and local health departments prioritize and target HIV prevention and outbreak response efforts for maximum public health benefit.

About the Author

Dr. Fitzmaurice currently serves in East Africa as senior data use advisor with the Division of Global HIV & TB, Center for Global Health, Centers for Disease Control and Prevention. His primary research interests include HIV prevention and treatment of vulnerable populations and social and behavioral determinants of health.

References

1. Peters PJ, Pontones P, Hoover KW, Patel MR, Galang RR, Shields J, et al.; Indiana HIV Outbreak Investigation Team. HIV infection linked to injection use of oxymorphone in Indiana, 2014–2015. N Engl J Med. 2016;375:229–39. http://dx.doi.org/10.1056/NEJMoa1515195
2. Oster AM, France AM, Panneer N, Bañez Ocfemia MC, Campbell E, Dasgupta S, et al. Identifying clusters of recent and rapid HIV transmission through analysis of molecular surveillance data. J Acquir Immune Defic Syndr. 2018;79:543–50. http://dx.doi.org/10.1097/QAI.0000000000001856
3. Dasgupta S, France AM, Brandt MG, Reuer J, Zhang T, Panneer N, et al. Estimating effects of HIV sequencing data completeness on transmission network patterns and detection of growing HIV transmission clusters. AIDS Res Hum Retroviruses. 2018 Dec 20 [cited 2018 Dec 20]. http://dx.doi.org/10.1089/AID.2018.0181.

4. Chen D, Cunningham J, Moore K, Tian J. Spatial and temporal aberration detection methods for disease outbreaks in syndromic surveillance systems. Ann GIS. 2011;17:211–20. http://dx.doi.org/10.1080/19475683.2011.625979
5. Hutwagner L, Browne T, Seeman GM, Fleischauer AT. Comparing aberration detection methods with simulated data. Emerg Infect Dis. 2005;11:314–6. http://dx.doi.org/10.3201/eid1102.040587
6. Wong WK, Moore M, Cooper G, Wagner M. What's strange about recent events (WSARE): an algorithm for the early detection of disease outbreaks. J Mach Learn Res. 2005; 6:1961–98.
7. US Census Bureau. Geography. 2015 Jul 28 [cited 2018 Feb 23]. https://www.census.gov/geo/reference/webatlas/regions.html
8. Rosinska M, Pantazis N, Janiec J, Pharris A, Amato-Gauci AJ, Quinten C; ECDC HIV/AIDS Surveillance Network. Potential adjustment methodology for missing data and reporting delay in the HIV Surveillance System, European Union/European Economic Area, 2015. Euro Surveill. 2018;23. http://dx.doi.org/10.2807/1560-7917.ES.2018.23.23.1700359
9. Rudd RA, Aleshire N, Zibbell JE, Gladden RM. Increases in drug and opioid overdose deaths—United States, 2000–2014. MMWR Morb Mortal Wkly Rep. 2016;64:1378–82. http://dx.doi.org/10.15585/mmwr.mm6450a3</jrn>
10. Substance Abuse and Mental Health Services Administration. Key substance use and mental health indicators in the United States: results from the 2016 National Survey on Drug Use and Health; 2017 Sep [cited 2018 Feb 23]. https://www.samhsa.gov/data/sites/default/files/NSDUH-FFR1-2016/NSDUH-FFR1-2016.htm#opioid1
11. Van Handel MM, Rose CE, Hallisey EJ, Kolling JL, Zibbell JE, Lewis B, et al. County-level vulnerability assessment for rapid dissemination of HIV or HCV infections among persons who inject drugs, United States. J Acquir Immune Defic Syndr. 2016; 73:323–31. http://dx.doi.org/10.1097/QAI.0000000000001098

Address for correspondence: Arthur G. Fitzmaurice, Centers for Disease Control and Prevention, 1600 Clifton Rd NE, Mailstop E-93, Atlanta, GA 30329-4027, USA; email: afitzmaurice@cdc.gov

Rickettsia japonica and Novel *Rickettsia* Species in Ticks, China

Xiang-Rong Qin, Hui-Ju Han, Fu-Jun Han, Fu-Ming Zhao, Zhen-Tang Zhang, Zai-Feng Xue, Dong-Qiang Ma, Rui Qi, Min Zhao, Li-Jun Wang, Li Zhao, Hao Yu, Jian-Wei Liu, Xue-Jie Yu

PCR amplification indicated the minimum infection rate of *Rickettsia* spp. was 0.66% in *Haemaphysalis longicornis* ticks collected from Shandong Province, China. Phylogenetic analysis based on the *rrs*, *gltA, ompA*, and *ompB* genes indicated that the ticks carried *R. japonica*, *Candidatus* Rickettsia longicornii, and a novel *Rickettsia* species related to *R. canadensis*.

Rickettsia species are gram-negative obligate intracellular bacteria that infect humans and a variety of vertebrates through the bite of arthropod vectors. Hard-body ticks are the primary vector of spotted fever group (SFG) rickettsiae; recently, several emerging and reemerging SFG rickettsiae were found to infect humans (*1*). *Rickettsia japonica* is the pathogenic agent of Japanese spotted fever that has been reported in Japan, South Korea, and Thailand since 1984 (*2*–*4*). Japanese spotted fever is a severe zoonosis and develops abruptly with headache, fever, shaking chills, skin eruptions, tick bite eschars, and malaise (*2*). *R. canadensis* was initially isolated from ticks in Canada; a serologic study indicated the presence of *R. canadensis* antibodies in febrile patients (*5*). The presence of *Rickettsia* species and their distributions in China are not very clear. In this study, we analyzed *Rickettsia* species in *Haemaphysalis longicornis* ticks collected from Shandong Province, China, and found *R. japonica*, *Candidatus* Rickettsia longicornii, and a novel *Rickettsia* species closely related to *R. canadensis* in the ticks.

The Study

We collected questing ticks by flagging during April–July 2013–2015. We collected them in Jiaonan County (35°35′–36°8′ N and 119°30′–120°11′E), Shandong Province, China. Jiaonan County is located on the Pacific coast of China and has a maritime monsoon-type climate. We identified tick species individually by morphology and confirmed by PCR amplification and DNA sequencing of the 16S rRNA gene of 2 nymphs and 2 adult ticks of each species as described previously (*6*,*7*).

For detection of *Rickettsia* DNA, we pooled ticks according to their developmental stages, with each pool consisting of 20 nymphs or 10 adult ticks. We homogenized them with Tissue Lyser II (QIAGEN, http://www.qiagen.com). We extracted total nucleic acids from the tick suspension using the AllPrep DNA/RNA Mini Kit (QIAGEN).

Initially, in all the tick pools, we amplified nucleic acid preparations with rickettsial universal primers targeting *rrs*, *gltA*, and *ompB* (B1–B4). We further amplified *Rickettsia* clones in the tick pools closely related to *R. japonica* with primers of *ompA*, an SFG rickettsia unique gene. The clones positive with *rrs* and *gltA* gene primers but negative with *ompB* primers (B1–B4) we further amplified with primers Cand-1 to Cand-4, which were designed from the *R. canadensis ompB* gene because the *Rickettsia* clones from these tick pools were closely related to *R. canadensis* on the basis of the *rrs* and *gltA* gene sequences (Table). We used distilled water as a negative control in each run.

We performed electrophoresis on the PCR products in 1.2% agarose gels, stained them with ethidium bromide, and visualized them under UV light. DNA bands with the expected size were excised and extracted by Gel Extraction Kit (Omega Bio-tek, https://www.omegabiotek.com). We cloned the purified PCR products into pMD19-T vector (Takara, https://www.takara-bio.com) and engaged Sangon Biotech (Shanghai, China) (https://www.life-biotech.com) to conduct sequencing on both strands. We compared nucleotide sequences with BLAST (http://blast.ncbi.nlm.nih.gov/Blast.cgi) and constructed a phylogenetic tree using the maximum-likelihood method with MEGA version 6.0 (https://www.megasoftware.net). We deposited the *Rickettsia* genes obtained in this study in GenBank under accession nos. MF496152–MF496168 (*rrs*), MF496169–MF496185 (*gltA*), MF496186–MF496199 (*ompB*), and MK102707–MK102720 (*ompA*).

Author affiliations: Wuhan University, Wuhan, China (X.-R. Qin, H.-J. Han, R. Qi, M. Zhao, L.-J. Wang, J.-W. Liu, X.-J. Yu); Huangdao District Center for Disease Control and Prevention, Qingdao City, China (F.-J. Han, F.-M. Zhao, Z.-T. Zhang, Z.-F. Xue, D.-Q. Ma); Shandong University, Jinan, China (L. Zhao); Fudan University, Shanghai, China (H. Yu)

DOI: https://doi.org/10.3201/eid2505.171745

Table. Primer sequences and PCR conditions used in study of *Rickettsia* species, China

Target gene	Primer name	Sequence, 5′ → 3′	Amplicon size, bp	Annealing temp, °C	Reference
rrs	S1	TGATCCTGGCTCAGAACGAAC	1,486	55	(*8*)
	S2	TAAGGAGGTAATCCAGCCGC			
	S3	AACACATGCAAGTCGRACGG	1,371	55	
	S4	GGCTGCCTCTTGCGTTAGCT			
gltA	gltA1	GATTGCTTTACTTACGACCC	1,087	52	(*9*)
	gltA2	TGCATTTCTTTCCATTGTGC			
	gltA3	TATAGACGGTGATAAAGGAATC	667	53	
	gltA4	CAGAACTACCGATTTCTTTAAGC			
ompB	B1	ATATGCAGGTATCGGTACT	1,355	56	(*9*)
	B2	CCATATACCGTAAGCTACAT			
	B3	GCAGGTATCGGTACTATAAAC	843	56	
	B4	AATTTACGAAACGATTACTTCCGG			
ompB	Cand-1	CCGGACTTTGCGGTGTAGAT	1,136	52	This study
	Cand-2	AAAGCCAGAAGGTGAGGCTG			
	Cand-3	ACCGCACTTGTATCGGTAGT	874	50	
	Cand-4	AAGCAGGTGGTGTAGTCGGA			
ompA	Rr190.70p	ATGGCGAATATTTCTCCAAAA	631	50	(*10*)
	Rr190.701n	GTTCCGTTAATGGCAGCATCT			
Tick mitochondrial 16S RNA	Forward	AGTATTTTGACTATACAAAGGTATTG	408	55	(*7*)
	Reverse	GTAGGATTTTAAAAGTTGAACAAACTT			

We collected a total of 2,560 *H. longicornis* ticks, 2,080 nymphs and 480 adults. PCR amplification indicated that 14 tick pools were positive with *rrs*, *gltA*, and *ompB* (B1–B4) primers and further positively amplified by PCR with *ompA* primers. In addition, 3 clones were positive with *rrs*, *gltA*, and *ompB* (Cand-1 to Cand-4) primers. The minimum infection rate of *Rickettsia* in the ticks was 0.66% (17/2,560), assuming 1 tick was positive in each positive pool of ticks.

Sequence analysis indicated that 3 clones (J84, J85, and J217) detected from the tick pools were closely related to *R. canadensis*, showing sequence homology of 98.7%–99.1% for *rrs*, 97.8%–98.4% for *gltA* and 94.8%–95.1% for *ompB*. One clone (J244) was highly homologous to *Candidatus* Rickettsia longicornii, showing sequence homology of 99.2% for *rrs*, 100% for *gltA*, and 99.7% for *ompA*. The remaining 13 clones were homologous to each other and to *R. japonica*, showing sequence homology of 99. 2%–100% for *rrs*, 99.1%–100% for *gltA*, 99.3%–99.4% for *ompB*, and 97%–97.3% for *ompA* of a variety strains of *R. japonica* (Appendix Tables 1–4, https://wwwnc.cdc.gov/EID/article/25/5/17-1745-App1.xlsx).

Phylogenetic analysis based on the concatenated sequences of *rrs*, *gltA*, *ompB*, and *ompA* showed that *Rickettsia* clones (J84, J85, and J217) were clustered in the same clade with, but distinct from, *R. canadensis*; clone J244 was in the same clade as *Candidatus* Rickettsia longicornii; the remaining 13 clones were in the same clade as *R. japonica*. These results indicated that clones J84, J85, and J217 were a novel *Rickettsia* species; clone 244 was *Candidatus* Rickettsia longicornii; and other clones were *R. japonica* (Figure).

Conclusions

In this study, we demonstrated that *H. longicornis* ticks from China were infected with multiple *Rickettsia* species, including *R. japonica*, *Candidatus* Rickettsia longicornii, and a novel *Rickettsia* species. We named the novel species *Candidatus* Rickettsia jiaonani after the sampling site. The exact classification of *Candidatus* Rickettsia jiaonani needs to be further studied by sequencing the whole genomes of the organisms.

R. japonica infection in humans has been reported recently in Anhui Province in central China (*11*), suggesting that *R. japonica* is widely distributed in China and its epidemiology needs to be further investigated. *Candidatus* Rickettsia longicornii was previously detected in *H. longicornis* ticks collected from South Korea (*12*). *Candidatus* Rickettsia jiaonani is closely related to *R. canadensis*, which was first isolated from *H. leporispalustris* ticks removed from rabbits in Ontario, Canada, in 1963 and then from a *H. leporispalustris* tick removed from a black-tailed jackrabbit in California in 1980 (*13*).

H. longicornis ticks are native to East Asia, including China, Korea, and Japan, and they were introduced into Oceania, including Australia, New Zealand, Fiji, and Hawaii, through cattle importation (*6*). Recently, this tick species was found in 8 states in the eastern United States (*14*). This study and previous studies demonstrated that *H. longicornis* ticks carry *R. japonica*, *Candidatus* Rickettsia longicornii, *Candidatus* Rickettsia jiaonani, *Anaplasma phagocytophilum*, *Ehrlichia*, and severe fever with thrombocytopenia syndrome virus (*12*,*15*). These pathogens need to be monitored in countries in East Asia in which the *H. longicornis* tick is native and in the countries that this tick species has invaded.

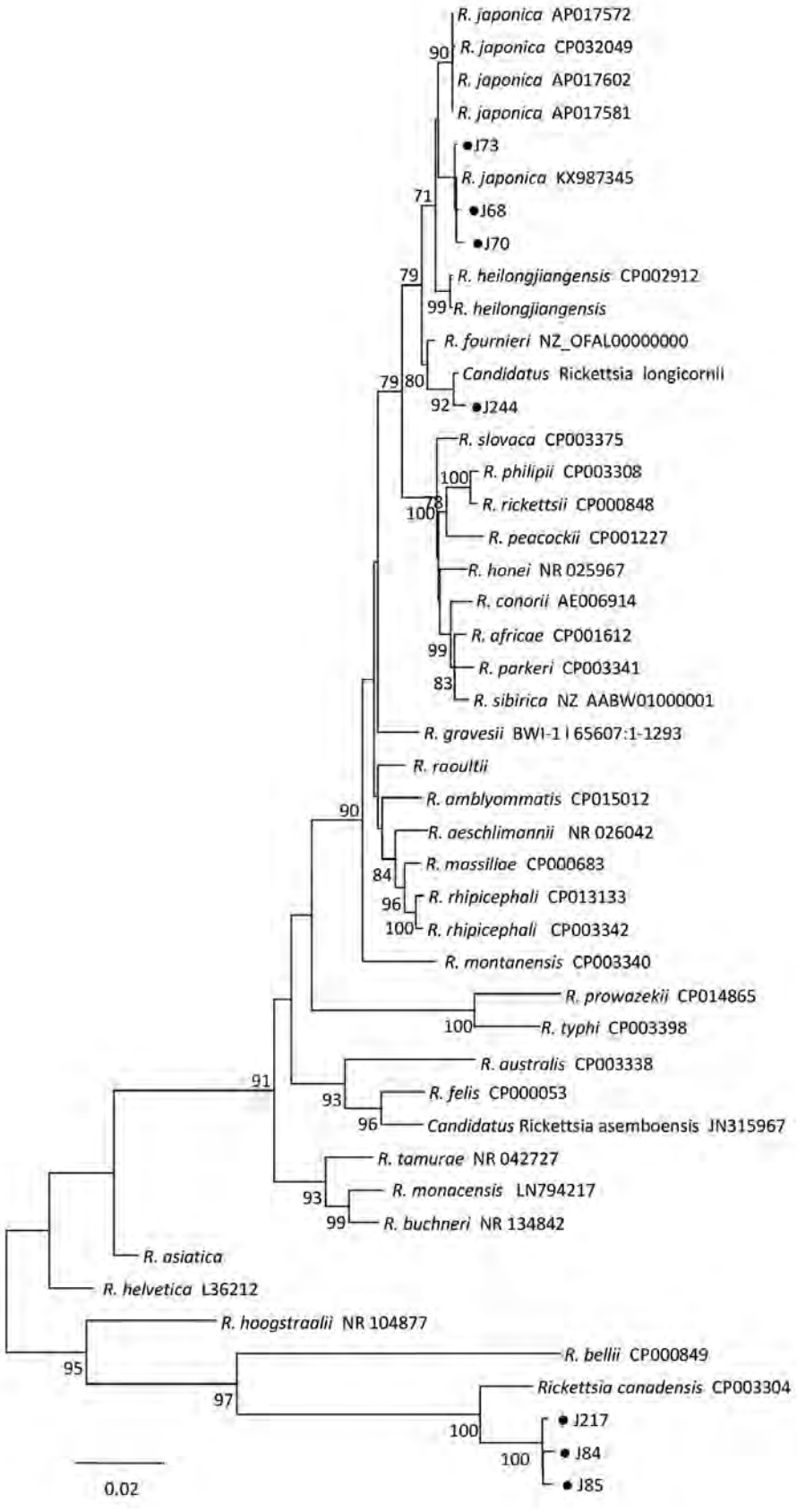

Figure 1. Phylogenetic tree of isolates from study of *Rickettsia* species in China (black dots) and comparison isolates. The tree was generated using the concatenated sequences of *rrs*, *gltA*, *ompB*, and *ompA* of *Rickettsia* species by the maximum-likelihood method in MEGA6 software (http://www.megasoftware.net) with 1,000 replicates for bootstrap testing. Numbers (>70) above or below branches are posterior node probabilities. Dots indicate rickettsial sequences obtained in this study. *Rickettsia* clones J69, J70, and J73 represent 13 similar clones in the phylogenetic analysis. Scale bar indicates nucleotide substitutions per site. The *Rickettsia* species name and complete genome GenBank accession no. appear on each line. For the *Rickettsia* species without complete genome sequences, the GenBank accession nos. in the order of *rrs*, *gltA*, *ompB* and *ompA* are NR_074469, KT899087, and AY280712, AF179362 for *R. heilongjiangensis*; KY474575, KX963389, KU310593, and KX506738 for *R. raoultii*; MG906672, MG906678, and MG906676,0020 for *Candidatus* Rickettsia longicornii; and AF394906, AF394901 and DQ110870 for *R. asiatica*.

This study was supported by a grant from the National Natural Science Funds of China (no. 31570167).

About the Author

Ms. Qin is a PhD student in the School of Health Sciences of Wuhan University. Her research interest is infectious disease epidemiology.

References

1. Parola P, Paddock CD, Socolovschi C, Labruna MB, Mediannikov O, Kernif T, et al. Update on tick-borne rickettsioses around the world: a geographic approach. Clin Microbiol Rev. 2013;26:657–702. http://dx.doi.org/10.1128/CMR.00032-13
2. Mahara F. Japanese spotted fever: report of 31 cases and review of the literature. Emerg Infect Dis. 1997;3:105–11. http://dx.doi.org/10.3201/eid0302.970203
3. Gaywee J, Sunyakumthorn P, Rodkvamtook W, Ruang-areerate T, Mason CJ, Sirisopana N. Human infection with *Rickettsia* sp. related to *R. japonica*, Thailand. Emerg Infect Dis. 2007;13:657–9. http://dx.doi.org/10.3201/eid1304.060585
4. Chung MH, Lee SH, Kim MJ, Lee JH, Kim ES, Lee JS, et al. Japanese spotted fever, South Korea. Emerg Infect Dis. 2006;12:1122–4. http://dx.doi.org/10.3201/eid1207.051372
5. Bozeman FM, Elisberg BL, Humphries JW, Runcik K, Palmer DB Jr. Serologic evidence of *Rickettsia canada* infection of man. J Infect Dis. 1970;121:367–71. http://dx.doi.org/10.1093/infdis/121.4.367
6. Teng K, Jiang Z. Economic insect fauna of China Fasc 39 Acari: *Ixodidae*. Fauna Sinica Beijing: Science Press. 1991.
7. Luo LM, Zhao L, Wen HL, Zhang ZT, Liu JW, Fang LZ, et al. *Haemaphysalis longicornis* ticks as reservoir and vector of severe fever with thrombocytopenia syndrome virus in China. Emerg Infect Dis. 2015;21:1770–6. http://dx.doi.org/10.3201/eid2110.150126
8. Huang Y, Zhao L, Zhang Z, Liu M, Xue Z, Ma D, et al. Detection of a novel *Rickettsia* from *Leptotrombidium scutellare* mites (Acari: *Trombiculidae*) from Shandong of China. J Med Entomol. 2017;54:544–9. http://dx.doi.org/10.1093/jme/tjw234
9. Igolkina YP, Rar VA, Yakimenko VV, Malkova MG, Tancev AK, Tikunov AY, et al. Genetic variability of *Rickettsia* spp. in *Ixodes persulcatus/Ixodes trianguliceps* sympatric areas from Western Siberia, Russia: identification of a new *Candidatus* Rickettsia species. Infect Genet Evol. 2015;34:88–93. http://dx.doi.org/10.1016/j.meegid.2015.07.015
10. Roux V, Fournier PE, Raoult D. Differentiation of spotted fever group rickettsiae by sequencing and analysis of restriction fragment length polymorphism of PCR-amplified DNA of the gene encoding the protein rOmpA. J Clin Microbiol. 1996;34:2058–65.
11. Li J, Hu W, Wu T, Li HB, Hu W, Sun Y, et al. Japanese spotted fever in eastern China, 2013. Emerg Infect Dis. 2018;24:2107–9. http://dx.doi.org/10.3201/eid2411.170264
12. Jiang J, An H, Lee JS, O'Guinn ML, Kim HC, Chong ST, et al. Molecular characterization of *Haemaphysalis longicornis*–borne rickettsiae, Republic of Korea and China. Ticks Tick Borne Dis. 2018;9:1606–13. http://dx.doi.org/10.1016/j.ttbdis.2018.07.013
13. Philip RN, Casper EA, Anacker RL, Peacock MG, Hayes SF, Lane RS. Identification of an isolate of *Rickettsia canada* from California. Am J Trop Med Hyg. 1982;31:1216–21. http://dx.doi.org/10.4269/ajtmh.1982.31.1216
14. Haddow AD. The consequences of medically important invasive arthropods: the longhorned tick, *Haemaphysalis longicornis.* Clin Infect Dis. 2019;68:530–1.
15. Qin XR, Han FJ, Luo LM, Zhao FM, Han HJ, Zhang ZT, et al. *Anaplasma* species detected in *Haemaphysalis longicornis* tick from China. Ticks Tick Borne Dis. 2018;9:840–3. http://dx.doi.org/10.1016/j.ttbdis.2018.03.014

Address for correspondence: Jian-Wei Liu or Xue-Jie Yu, Wuhan University School of Health Sciences, Donghulu No. 115, Wuhan 250012, China; email: liujianwei@whu.edu.cn; email: yuxuejie@whu.edu.cn

Value of PCR, Serology, and Blood Smears for Human Granulocytic Anaplasmosis Diagnosis, France

Yves Hansmann, Benoit Jaulhac, Pierre Kieffer, Martin Martinot, Elisabeth Wurtz, Régis Dukic, Geneviève Boess, André Michel, Christophe Strady, Jean François Sagez, Nicolas Lefebvre, Emilie Talagrand-Reboul, Xavier Argemi, Sylvie De Martino

We prospectively examined the effectiveness of diagnostic tests for anaplasmosis using patients with suspected diagnoses in France. PCR (sensitivity 0.74, specificity 1) was the best-suited test. Serology had a lower specificity but higher sensitivity when testing acute and convalescent samples. PCR and serology should be used in combination for anaplasmosis diagnosis.

Human granulocytic anaplasmosis (HGA) is a tickborne intracellular bacterial infection caused by *Anaplasma phagocytophilum*. The disease is present in North America, Europe, and northern Asia, areas with *Ixodes ricinus* ticks, the primary vector for transmission to humans (*1*,*2*). Clinical manifestations of disease include acute fever, headache, and myalgia occurring 2–3 weeks after tick bite. Diagnosis requires the isolation of *A. phagocytophilum* in blood culture, the presence of morulae in polymorphonuclear cells after May Grünwald-Giemsa staining of peripheral blood smears, positive serologic results (seroconversion or high titer of specific antibodies), or a positive *A. phagocytophilum* PCR result. The May Grünwald-Giemsa stain test has a low sensitivity (*3*); PCR and serology are more widely available, but their diagnostic value is not well established. The aim of our study was to compare the diagnostic values of the available microbiological tests in a prospectively selected series of patients with clinical signs and symptoms consistent with an HGA diagnosis.

Author affiliations: Université de Strasbourg, Strasbourg, France (Y. Hansmann, B. Jaulhac, E. Talagrand-Reboul, S. De Martino); Hôpitaux Universitaires de Strasbourg, Strasbourg (Y. Hansmann, N. Lefebvre, X. Argemi); Centre National de Référence des *Borrelia*, Strasbourg (B. Jaulhac, S. De Martino); Centre Hospitalier Emile Muller, Mulhouse, France (P. Kieffer); Centre Hospitalier Pasteur, Colmar, France (M. Martinot); Centre Hospitalier Saverne, Saverne, France (E. Wurtz); Centre Hospitalier de Haguenau, Haguenau, France (R. Dukic); Centre Hospitalier de Guebwiller, Guebwiller, France (G. Boess); Centre Hospitalier de Wissembourg, Wissembourg, France (A. Michel); Polyclinique Saint André, Reims, France (C. Strady); Centre Hospitalier Sélestat, Sélestat, France (J.F. Sagez)

DOI: https://doi.org/10.3201/eid2505.171751

The Study

In this prospective, multicenter study, we enrolled symptomatic patients living in Alsace, a region of northeastern France where tickborne diseases are highly endemic. Patients gave written, informed consent to participate in our study, which was approved by the ethics committee of the University Hospital of Strasbourg (Strasbourg, France).

We included patients if they had 1 of the following combinations of signs and symptoms occurring no more than 4 weeks after a tick bite: 1) fever or other symptom presumed related to a tick bite, 2) fever plus thrombocytopenia with or without leukopenia or elevated liver enzyme levels, 3) thrombocytopenia with or without leukopenia, or 4) elevated liver enzyme levels without fever. The first visit included clinical and epidemiologic evaluations and the collection of blood samples for *A. phagocytophilum* serology, May Grünwald-Giemsa staining, and *A. phagocytophilum*–specific PCR. We did not culture for *A. phagocytophilum*. An etiologic investigation was also conducted to obtain a differential diagnosis. After ≥4 weeks, a second visit was scheduled to obtain a clinical evaluation, *A. phagocytophilum* serology, and (if necessary) a complete differential diagnosis.

We stratified patients into 3 groups on the basis of their diagnosis. One group included controls, who were patients with a clinical and microbiologically confirmed non-anaplasmosis diagnosis. The second group included anaplasmosis patients defined by ≥1 if the following criteria: intraleukocyte morulae on blood smears, a positive PCR result for *Anaplasma*, a 4-fold increased antibody titer for *A. phagocytophilum* in the follow-up sample or a seroconversion (i.e., change in antibody titer from negative in first sample to ≥1:64 in second sample), or a high antibody titer for *Anaplasma* (≥1:256) by indirect immunofluorescence antibody assay. The third group were patients without any diagnosis.

We performed DNA extraction, PCR, and serologic testing blinded to sample identification as previously described (*4*). The PCR targeted the *A. phagocytophilum msp2/p44* gene. We performed serologic testing using the *Anaplasma phagocytophilum* IFA IgG assay (Focus Diagnostics, http://www.focusdx.com) (*4*). Trained staff examined May Grünwald-Giemsa–stained smear preparations of whole blood samples for intracellular morulae. We collected data by using EpiData version 3.1.2701.2008 (http://epidata.dk) and extracted data to Excel spreadsheets (Microsoft, https://www.microsoft.com) for analysis. After patient stratification, we estimated the sensitivity and specificity of the different diagnostic tests.

During May 2010–July 2012, we enrolled 155 patients into the study, 25 of whom did not complete the second visit. None of these 25 patients had a positive PCR result or an antibody titer ≥1:256 at the first visit. The remaining 130 patients completed both study visits and were thus included in the study evaluation. Of these 130 patients, 19 had confirmed anaplasmosis diagnoses and 36 were controls with confirmed nonanaplasmosis diagnoses (infections with *Borrelia burgdorferi*, Epstein-Barr virus, cytomegalovirus, HIV, tick-borne encephalitis virus, *Leptospira* spp., *Babesia* spp., parvovirus B19, hantavirus, *Francisella tularensis*, *Plasmodium* spp., and *Aeromonas* spp.). Of the patients with HGA, 84.2% (16/19) met the serologic criteria and 73.7% (14/19) met the PCR criteria (Table; Figure). Fever, the most frequent symptom (89%), was associated with joint and muscle pain. Cytopenia of platelets, neutrophils, or both (74%) and elevated liver enzyme levels (63%) were frequently present.

Calculations of the diagnostic value of each test method showed that PCR had a sensitivity of 0.74 and a specificity of 1 and blood smear staining had a sensitivity of 0.21 and a specificity of 1. Seroconversion or a 4-fold increase of antibody titer had a sensitivity of 0.32 and specificity of 0.97, an antibody titer ≥1:256 had a sensitivity of 0.58 and specificity of 0.97, and overall serology had a sensitivity of 0.84 and specificity of 0.94.

The interval between the first and second serologic tests for most patients in the anaplasmosis group was 4–8 weeks (mean 49.8 days). Five patients had the second test >8 weeks after the first. Of these patients, 2 seroconverted, 1 experienced a substantial decrease in antibody titer, 1 experienced a substantial increase at week 12, and 1 had a stable antibody titer.

Our study confirms PCR as the gold standard for diagnosis of HGA; this test enabled rapid diagnosis during the acute stage of infection with good sensitivity and excellent specificity. However, the absence of a gold standard diagnostic test to compare our results with is a limitation to our study. *A. phagocytophilum* culture is the reference test for HGA diagnosis (*5*,*6*) but is not well suited for routine use because culturing is time-consuming and not widely performed. The diagnosis of anaplasmosis often involves assessing for the presence of morulae, but this test has low sensitivity (*3*). In our study, this test was of limited value for HGA diagnosis because whenever morulae were detected on blood smears ≥1 of the other diagnostic tests was positive. However, May Grünwald-Giemsa staining is the quickest test to do, and when performed by trained staff, positive results are helpful for physicians.

In clinical practice, diagnosis of HGA often relies on serology (*7*–*9*), but 2 limitations are associated with this method: a risk for false-negative results during the acute stage of infection because *A. phagocytophilum* antibodies are detected on average 11.5 days after symptom onset and a risk for false-positive results because *Anaplasma* antibodies are detectable in 86.4% of patients for 6–10 months and in 40% of patients up to 2 years after the initial infection (*10*). Positive serologic criteria are seroconversion, a 4-fold increase in antibody titer, or a stable and high antibody titer

Table. *Anaplasma phagocytophilum* diagnostic test results of patients with nonanaplasmosis and human granulocytic anaplasmosis diagnoses, France, May 2010–July 2012

Test result	Control group, no./total	*Anaplasma* group, no./total
Positive blood smear	0/36	4/19
Positive by serology	2/36	16/19
Seroconversion* or 4-fold rise in antibody titer	1/36†	6/19‡§
Antibody titer ≥1:256 at first visit	1/36¶	11/19§
Positive PCR	0/36	14/19

*Seroconversion is defined as a change in antibody titer from negative in the first sample obtained during acute illness to ≥1/64 in the second sample acquired ≥4 weeks later.
†One patient had a seroconversion with a microbiologically confirmed diagnosis of parvovirus B19 infection.
‡Only 1 patient had a 4-fold increase in antibody titer, but the titer at the first study visit was already high enough to establish the diagnosis (increase from 1:512 to 1:2,048).
§One patient had a seroconversion with an *A. phagocytophilum* antibody titer ≥1:256 at the second visit (patient counted once in both serology categories). All other patients with seroconversion had an antibody titer <1:256.
¶One patient with microbiologically confirmed leptospirosis had an *A. phagocytophilum* antibody titer of 1:256 at the first visit that decreased to 1:64 at the second visit.

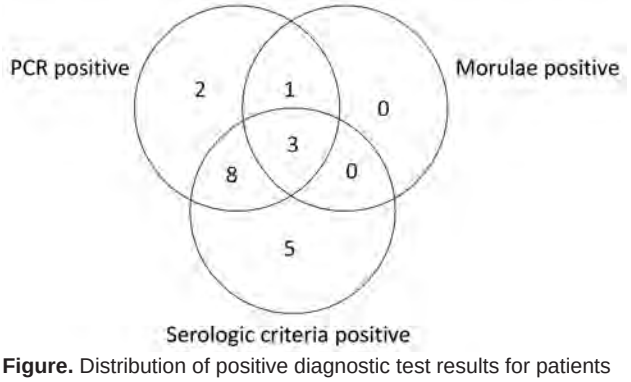

Figure. Distribution of positive diagnostic test results for patients with confirmed human granulocytic anaplasmosis, France, May 2010–July 2012.

(*11*,*12*). In our study, we observed that each of these criteria can lead to misdiagnosis at the beginning of infection, as previously reported (*13*).

PCR is considered the most effective diagnostic method during early stage *A. phagocytophilum* infection (*14*,*15*). Our results confirm this belief, despite our limitation of a small study population. However, if PCR is use alone, HGA might be underdiagnosed.

Conclusions

The presentation of fever in a patient with a history of tick bite does not qualify for an anaplasmosis diagnosis; microbiological tests need to be performed. For anaplasmosis, PCR testing appears to be the most effective diagnostic tool. However, the sensitivity of PCR is <100%, and combining PCR with serologic testing at the first visit appears to be the best strategy for early diagnosis of acute anaplasmosis. In cases of high suspicion for HGA in patients without any diagnosis at the first visit, a second serologic test ≥4 weeks later can be helpful. A multiplex approach could also be used in such cases to look for differential diagnoses.

This study was supported by the French Hospital Clinical Research Program (PHRC HUS 2007–3960).

About the Author

Dr. Hansmann is head of the Infectious Disease Department at Strasbourg University Hospital, Strasbourg, France; a member of the Borreliosis group of the European Society of Clinical Microbiology and Infectious Diseases; and involved in designing the tickborne disease national diagnosis and health plan for France. His research interests are tickborne diseases and diagnosis.

References

1. Strle F. Human granulocytic ehrlichiosis in Europe. Int J Med Microbiol. 2004;293(Suppl 37):27–35.
2. Dedkov VG, Simonova EG, Beshlebova OV, Safonova MV, Stukolova OA, Verigina EV, et al. The burden of tick-borne diseases in the Altai region of Russia. Ticks Tick Borne Dis. 2017;8:787–94. http://dx.doi.org/10.1016/j.ttbdis.2017.06.004
3. Bakken JS, Dumler JS. Human granulocytic anaplasmosis. Infect Dis Clin North Am. 2015;29:341–55. http://dx.doi.org/10.1016/j.idc.2015.02.007
4. Koebel C, Kern A, Edouard S, Hoang AT, Celestin N, Hansmann Y, et al. Human granulocytic anaplasmosis in eastern France: clinical presentation and laboratory diagnosis. Diagn Microbiol Infect Dis. 2012;72:214–8. http://dx.doi.org/10.1016/j.diagmicrobio.2011.12.005
5. Goodman JL, Nelson C, Vitale B, Madigan JE, Dumler JS, Kurtti TJ, et al. Direct cultivation of the causative agent of human granulocytic ehrlichiosis. N Engl J Med. 1996;334:209–15. http://dx.doi.org/10.1056/NEJM199601253340401
6. Wormser GP, Aguero-Rosenfeld ME, Cox ME, Nowakowski J, Nadelman RB, Holmgren D, et al. Differences and similarities between culture-confirmed human granulocytic anaplasmosis and early Lyme disease. J Clin Microbiol. 2013;51:954–8. http://dx.doi.org/10.1128/JCM.02929-12
7. Yeh MT, Mather TN, Coughlin RT, Gingrich-Baker C, Sumner JW, Massung RF. Serologic and molecular detection of granulocytic ehrlichiosis in Rhode Island. J Clin Microbiol. 1997;35:944–7.
8. Kocianová E, Kost'anová Z, Stefanidesová K, Spitalská E, Boldiš V, Hucková D, et al. Serologic evidence of *Anaplasma phagocytophilum* infections in patients with a history of tick bite in central Slovakia. Wien Klin Wochenschr. 2008;120:427–31. http://dx.doi.org/10.1007/s00508-008-1000-y
9. Aguero-Rosenfeld ME, Kalantarpour F, Baluch M, Horowitz HW, McKenna DF, Raffalli JT, et al. Serology of culture-confirmed cases of human granulocytic ehrlichiosis. J Clin Microbiol. 2000;38:635–8.
10. Lotric-Furlan S, Avsic-Zupanc T, Petrovec M, Nicholson WL, Sumner JW, Childs JE, et al. Clinical and serological follow-up of patients with human granulocytic ehrlichiosis in Slovenia. Clin Diagn Lab Immunol. 2001;8:899–903.
11. Bakken JS, Haller I, Riddell D, Walls JJ, Dumler JS. The serological response of patients infected with the agent of human granulocytic ehrlichiosis. Clin Infect Dis. 2002;34:22–7. http://dx.doi.org/10.1086/323811
12. Brouqui P, Bacellar F, Baranton G, Birtles RJ, Bjoërsdorff A, Blanco JR, et al.; ESCMID Study Group on Coxiella, Anaplasma, Rickettsia and Bartonella; European Network for Surveillance of Tick-Borne Diseases. Guidelines for the diagnosis of tick-borne bacterial diseases in Europe. Clin Microbiol Infect. 2004;10:1108–32. http://dx.doi.org/10.1111/j.1469-0691.2004.01019.x
13. Lotrič-Furlan S, Rojko T, Jelovšek M, Petrovec M, Avšič-Županc T, Lusa L, et al. Comparison of clinical and laboratory characteristics of patients fulfilling criteria for proven and probable human granulocytic anaplasmosis. Microbes Infect. 2015;17:829–33. http://dx.doi.org/10.1016/j.micinf.2015.09.017
14. Dumler JS, Madigan JE, Pusterla N, Bakken JS. Ehrlichioses in humans: epidemiology, clinical presentation, diagnosis, and treatment. Clin Infect Dis. 2007;45(Suppl 1):S45–51. http://dx.doi.org/10.1086/518146
15. Weil AA, Baron EL, Brown CM, Drapkin MS. Clinical findings and diagnosis in human granulocytic anaplasmosis: a case series from Massachusetts. Mayo Clin Proc. 2012;87:233–9. http://dx.doi.org/10.1016/j.mayocp.2011.09.008

Address for correspondence: Yves Hansmann, Hôpitaux Universitaires de Strasbourg, Médecine Interne et Maladies Infectieuses et Tropicales 1, Place de l'Hôpital, Strasbourg 67091, France; email: yves.hansmann@chru-strasbourg.fr

Lassa and Crimean-Congo Hemorrhagic Fever Viruses, Mali

Jan Baumann,[1] Mandy Knüpfer,[1] Judicael Ouedraogo, Brehima Y. Traoré, Asli Heitzer, Bourama Kané, Belco Maiga, Mariam Sylla, Bouréma Kouriba,[2] Roman Wölfel[2]

We report detection of Lassa virus and Crimean-Congo hemorrhagic fever virus infections in the area of Bamako, the capital of Mali. Our investigation found 2 cases of infection with each of these viruses. These results show the potential for both of these viruses to be endemic to Mali.

Numerous viral hemorrhagic fevers are endemic to countries in Africa. Despite the underlying pathogens originating from diverse virus families, clinical features of hemorrhagic fevers are similar, including fever, malaise, abdominal pain, vomiting, headache, and myalgia (*1*). These nonspecific symptoms and their similarity to other infectious diseases common in West Africa, such as malaria, complicate the differential diagnosis. In regions where surveillance data are limited and healthcare workers are less aware of viral hemorrhagic diseases, the possibility for misdiagnosis is high.

Lassa virus (LASV; species *Lassa mammarenavirus*, genus *Arenaviridae*) is the causative agent of Lassa fever. The multimammate rat, *Mastomys* spp., is the natural host of LASV and sheds the virus in urine and droppings. Transmission of LASV to humans usually occurs through contact with the excreta of infected rodents or with body fluids from persons with symptomatic illness.

Lassa fever is known to be endemic in parts of West Africa; most cases are reported from Guinea, Liberia, Sierra Leone, and Nigeria. LASV species in these geographic regions are related genetically, suggesting an ongoing exchange between LASV-endemic regions (*2*). People living in rural areas of West Africa are most at risk for Lassa fever. In recent years, an increasing trend in the number of Lassa fever cases has been observed in countries of West Africa. Annually, ≈300,000 persons are infected with LASV in virus-endemic areas, and ≈5,000 die. Because LASV infections can be asymptomatic, case numbers likely are underestimated (*3*). Although some reports describe serologic evidence that LASV is endemic to Mali (*4*,*5*), few surveillance studies have been conducted. One such study identified a distinct LASV clade in rodents 280 km south of Bamako, the capital of Mali (*6*). In addition, a young man traveling in the border region of Mali and Burkina Faso died from an acute LASV infection in 2009 after returning to the United Kingdom (*7*).

Another prominent pathogen causing hemorrhagic fever, Crimean-Congo hemorrhagic fever virus (CCHFV; family *Nairoviridae*, genus *Orthonairovirus*), is endemic to many regions, including Eurasia, Central America, and parts of Europe and Africa. To date, reports of acute CCHFV infections in West Africa are limited to Senegal (*8*) and Mauritania (*9*). Nevertheless, recent studies confirmed the incidence of CCHFV in *Hyalomma* spp. ticks collected from domestic cattle in southern Mali (*10*). In addition, serologic studies show evidence for human contact with CCHFV (*11*). However, no human cases of acute infection with CCHFV have been identified in Mali. We describe 2 cases of LASV infection and 2 cases of CCHFV infection detected in hospitalized pediatric patients in Bamako.

The Study

During April 2016–May 2017, we screened malaria-negative blood samples collected at the pediatric department of the University Hospital Gabriel Touré and the pediatric ward of Hôpital du Mali, both located in Bamako. We included febrile patients 3 months to 14 years of age in the study. We obtained ethics approval from the Research Ethics Institutional Review Board, University of Bamako, Mali (no. 2016/01/CE/FMPOS).

We screened 489 samples for various bacterial and viral pathogens, including LASV and CCHFV. We extracted total nucleic acid using the QIAamp viral RNA kit (QIAGEN, https://www.qiagen.com) and amplified viral RNA by using LASV reverse transcription PCR (*12*) and CCHFV reverse transcription quantitative PCR (*13*) protocols.

We detected LASV RNA in blood samples from 2 patients, a 5-year-old boy and a 13-year-old girl. Both children were treated for episodes of high fever during

Author affiliations: Bundeswehr Institute of Microbiology, Munich, Germany (J. Baumann, M. Knüpfer, A. Heitzer, R. Wölfel); Centre d'Infectiologie Charles Mérieux du Mali, Bamako, Mali (J. Ouedraogo, B.Y. Traoré, B. Kouriba); Hôpital du Mali, Bamako (B. Kané); Centre Hospitalier Universitaire Hospital Gabriel Touré, Bamako (B. Maiga, M. Sylla)

DOI: https://doi.org/10.3201/eid2505.181047

[1]These authors contributed equally to this article.

[2]These authors were co–principal investigators.

September–October 2016 at the Hôpital du Mali. The Centre d'Infectiologie Charles Mérieux du Mali in Bamako performed conventional reverse transcription PCR and gel electrophoresis on the LASV. Isolated DNA fragments were shipped to the Bundeswehr Institute of Microbiology (Munich, Germany) for further investigation.

Diagnostic amplicons of the LASV small (S) RNA segment, 278 nt from the boy and 276 nt from the girl, were sequenced by Sanger sequencing (GenBank accession nos. MH473586–7). Sequence analysis of the viral S segment showed that 1 patient was infected by a LASV strain that clusters genetically with viruses belonging to lineage IV (Figure 1). Because lineage IV strains previously were not reported to circulate in wildlife in Mali, we suspect this virus reached the country through regional migratory activity of wildlife. Nevertheless, epidemiologic data about LASV in Mali are limited, and frequent exchange between the LASV lineages in West Africa is possible.

The second identified Lassa fever case was caused by a LASV strain belonging to the Mano River clade with 91% similarity to Lassa Soromba R (GenBank accession no. KF478765) (Figure 1). This virus was first isolated in 2010 from rodents near the village Soromba at the southern tip of Mali (*6*). Additional laboratory characterization at that time revealed a relatively mild pathogenicity in macaques (*14*). However, Lassa

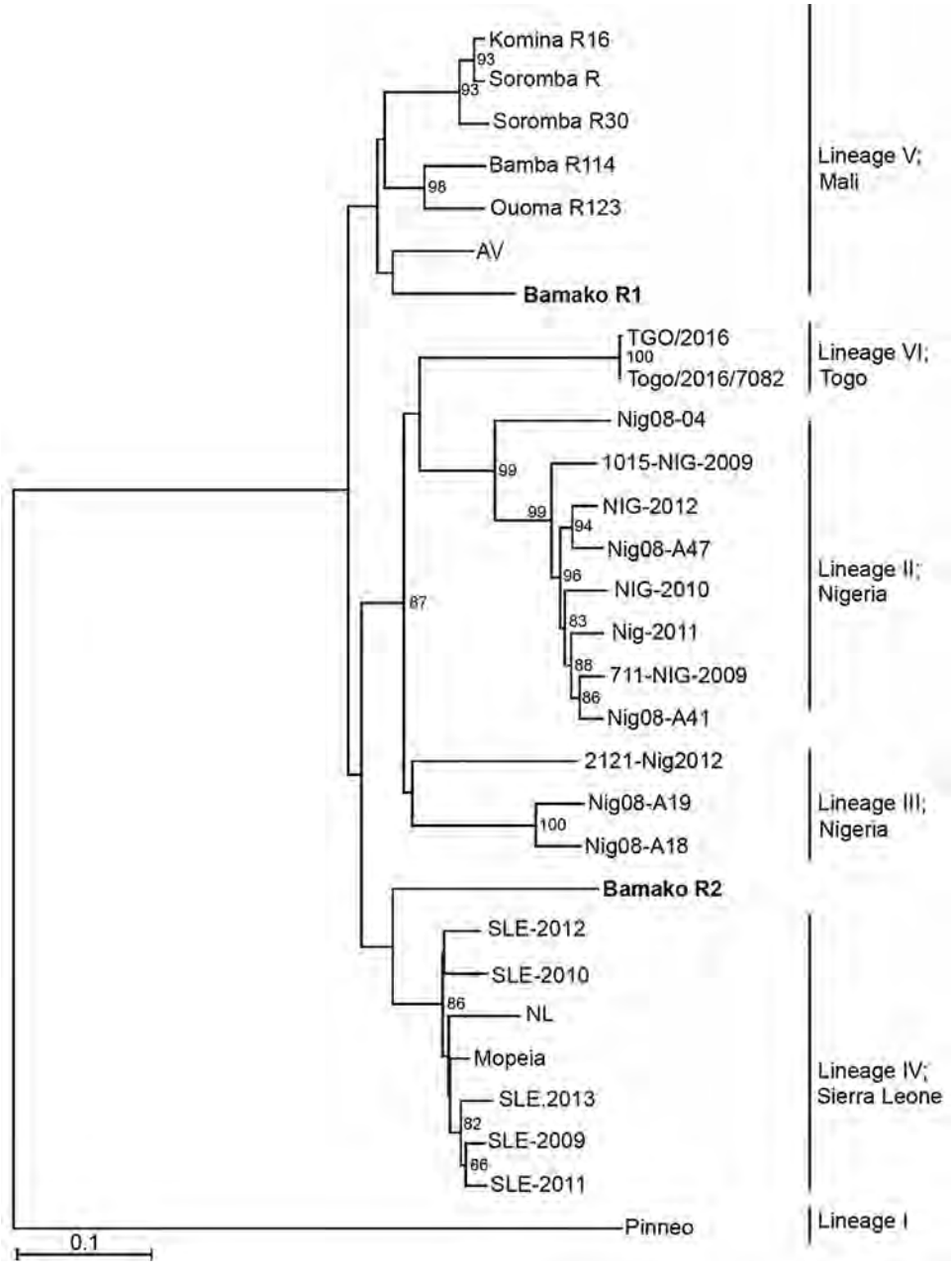

Figure 1. Phylogenetic analysis of representative Lassa virus (LASV) isolates identified in Mali in 2016 (bold) and reference isolates. The tree was constructed by using full-length sequences of the small RNA segment and the neighbor-joining method with bootstrapping to 10,000 iterations. Partial sequences were compared by using the pairwise deletion method. The tree is drawn to scale. Evolutionary analyses were conducted in MEGA7 (https://www.megasoftware.net). Scale bar indicates nucleotide substitutions per site.

Soromba R is closely related to the AV strain (GenBank accession no. FR832711) that caused a fatal infection in a young man who returned to Germany after traveling to Ghana, Côte d'Ivoire, and Burkina Faso in 2000 (*15*) and is related to a strain from a patient in the United Kingdom who likely was infected in the border region between Mali and Burkina Faso in 2009 (*7*). Because the case we identified originated in a district of Bamako, we believe LASV could be more widely distributed in southern Mali than previously believed.

We also detected CCHFV, which previously was not known to circulate in the population of Mali. Using reverse transcription quantitative PCR, we detected acute CCHFV infection in 2 patients hospitalized at Hospital Gabriel Touré in April 2017, a 1-year-old boy (cycle threshold 32.74) and a 2-year-old boy (cycle threshold 36.95). We obtained sequence data from the viral S segment for the 1-year-old boy. Phylogenetic analysis showed that this virus is related to CCHFV strain ArD39554 from Mauritania and CCHFV sequence (GenBank accession no. KF793333) recently detected in ticks collected only 25 km from Bamako (*10*) (Figure 2). We were unable to extract sufficient genomic material to perform sequencing on samples from the second case-patient.

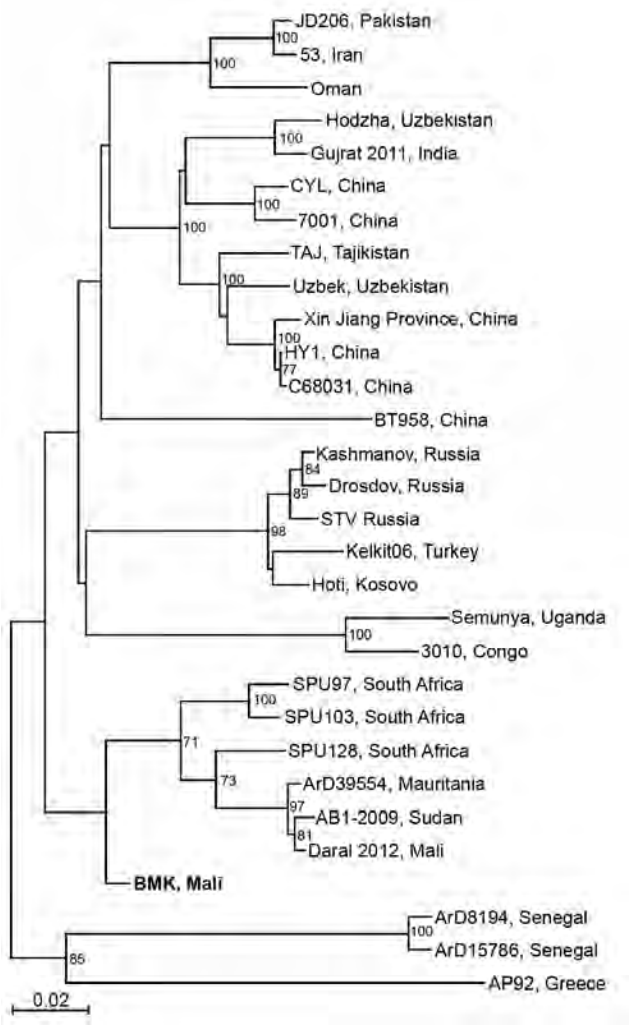

Figure 2. Phylogenetic analysis of representative Crimean-Congo hemorrhagic fever virus (CCHFV) isolates identified in Mali in 2017 (bold) and reference isolates. The tree was constructed by using full-length sequences of the small RNA segment and the neighbor-joining method with bootstrapping to 10,000 iterations. Partial sequences were compared by using the pairwise deletion method. The tree is drawn to scale. Evolutionary analyses were constructed in MEGA7 (https://www.megasoftware.net). Scale bar indicates nucleotide substitutions per site.

Conclusions

In summary, our study detected 2 cases of infection with LASV in Bamako, Mali, indicating a broader distribution of LASV in Mali than previously known. This finding raises serious public health concerns for future LASV infection in cities in Mali. We also identified 2 human cases of infection with CCHFV in Mali, suggesting an extended CCHFV-endemic region in Africa. Our results underline the need for LASV and CCHFV surveillance programs in sub-Saharan regions of Mali, Burkina Faso, and Niger, which have similar ecology.

Acknowledgments

We thank the patients and their parents for participating in this study, as well as Erna Fleischmann and Kathrin Baumann for skillful technical assistance, and multiple host-country investigators for their hard work and dedication.

This study was funded through the German Biosecurity Program under grant no. OR12-01-370.43-BIOS-IMB-MLI and by the Medical Biodefense Research Program of the German Bundeswehr Medical Service.

About the Author

Dr. Baumann is a research scientist at the Bundeswehr Institute of Microbiology. He is interested in improving viral disease diagnostic capacities in the G5-Sahel region and his research interest focuses on the epidemiology of hemorrhagic fever viruses.

References

1. World Health Organization. Lassa fever. March 2016 [cited 5 Mar 2018]. http://www.who.int/mediacentre/factsheets/fs179
2. Sogoba N, Feldmann H, Safronetz D. Lassa fever in West Africa: evidence for an expanded region of endemicity. Zoonoses Public Health. 2012;59(Suppl 2):43–7. http://dx.doi.org/10.1111/j.1863-2378.2012.01469.x
3. McCormick JB, Fisher-Hoch SP. Lassa fever. Curr Top Microbiol Immunol. 2002;262:75–109. http://dx.doi.org/10.1007/978-3-642-56029-3_4
4. Richmond JK, Baglole DJ. Lassa fever: epidemiology, clinical features, and social consequences. BMJ. 2003;327:1271–5. http://dx.doi.org/10.1136/bmj.327.7426.1271

5. Sogoba N, Rosenke K, Adjemian J, Diawara SI, Maiga O, Keita M, et al. Lassa virus seroprevalence in Sibirilia Commune, Bougouni District, southern Mali. Emerg Infect Dis. 2016; 22:657–63. http://dx.doi.org/10.3201/eid2204.151814
6. Safronetz D, Lopez JE, Sogoba N, Traoré' SF, Raffel SJ, Fischer ER, et al. Detection of Lassa virus, Mali. Emerg Infect Dis. 2010;16:1123–6. http://dx.doi.org/10.3201/eid1607.100146
7. Atkin S, Anaraki S, Gothard P, Walsh A, Brown D, Gopal R, et al. The first case of Lassa fever imported from Mali to the United Kingdom, February 2009. Euro Surveill. 2009;14:1–3. https://doi.org/10.2807/ese.14.10.19145-en
8. Tall A, Sall AA, Faye O, Diatta B, Sylla R, Faye J, et al. Two cases of Crimean-Congo hemorrhagic fever (CCHF) in two tourists in Senegal in 2004 [in French]. Bull Soc Pathol Exot. 2009;102:159–61.
9. Nabeth P, Cheikh DO, Lo B, Faye O, Vall IO, Niang M, et al. Crimean-Congo hemorrhagic fever, Mauritania. Emerg Infect Dis. 2004;10:2143–9. http://dx.doi.org/10.3201/eid1012.040535
10. Zivcec M, Maïga O, Kelly A, Feldmann F, Sogoba N, Schwan TG, et al. Unique strain of Crimean-Congo hemorrhagic fever virus, Mali. Emerg Infect Dis. 2014;20:911–3. http://dx.doi.org/10.3201/eid2005.131641
11. Safronetz D, Sacko M, Sogoba N, Rosenke K, Martellaro C, Traoré S, et al. Vectorborne infections, Mali. Emerg Infect Dis. 2016;22:340–2. http://dx.doi.org/10.3201/eid2202.150688
12. Olschläger S, Lelke M, Emmerich P, Panning M, Drosten C, Hass M, et al. Improved detection of Lassa virus by reverse transcription-PCR targeting the 5′ region of S RNA. J Clin Microbiol. 2010;48:2009–13. http://dx.doi.org/10.1128/JCM.02351-09
13. Atkinson B, Chamberlain J, Logue CH, Cook N, Bruce C, Dowall SD, et al. Development of a real-time RT-PCR assay for the detection of Crimean-Congo hemorrhagic fever virus. Vector Borne Zoonotic Dis. 2012;12:786–93. http://dx.doi.org/10.1089/vbz.2011.0770
14. Safronetz D, Strong JE, Feldmann F, Haddock E, Sogoba N, Brining D, et al. A recently isolated Lassa virus from Mali demonstrates atypical clinical disease manifestations and decreased virulence in cynomolgus macaques. J Infect Dis. 2013;207:1316–27. http://dx.doi.org/10.1093/infdis/jit004
15. Günther S, Emmerich P, Laue T, Kühle O, Asper M, Jung A, et al. Imported Lassa fever in Germany: molecular characterization of a new Lassa virus strain. Emerg Infect Dis. 2000;6:466–76. http://dx.doi.org/10.3201/eid0605.000504

Address for correspondence: Roman Wölfel, Bundeswehr Institute of Microbiology, Neuherbergstrasse 11, 80937 Munich, Germany; email: romanwoelfel@instmikrobiobw.de

Nipah Virus Sequences from Humans and Bats during Nipah Outbreak, Kerala, India, 2018

Pragya D. Yadav, Anita M. Shete, G. Arun Kumar, Prasad Sarkale, Rima R. Sahay, Chandni Radhakrishnan, Rajen Lakra, Prachi Pardeshi, Nivedita Gupta, Raman R. Gangakhedkar, V.R. Rajendran, Rajeev Sadanandan, Devendra T. Mourya

We retrieved Nipah virus (NiV) sequences from 4 human and 3 fruit bat (*Pteropus medius*) samples from a 2018 outbreak in Kerala, India. Phylogenetic analysis demonstrated that NiV from humans was 96.15% similar to a Bangladesh strain but 99.7%–100% similar to virus from *Pteropus* spp. bats, indicating bats were the source of the outbreak.

Nipah virus (NiV) was first reported from Malaysia in 1999 (*1*). Additional NiV outbreaks have occurred in Bangladesh (*2–4*) and India (*5*,*6*). NiV is a negative-sense enveloped RNA encoding for 6 genes (nucleocapsid, phosphoprotein, matrix, fusion protein, glycoprotein, and polymerase) (*7*,*8*). Two NiV clades have been proposed: B genotype, predominantly found circulating in Bangladesh, and M genotype in Malaysia and Cambodia (*9*). NiV-positive fruit bats (*Pteropus medius*) were found in West Bengal, Assam, and Haryana states in India, posing a possible source of NiV infection in humans (*10–12*).

The Study

In May 2018, the Indian Council of Medical Research–National Institute of Virology (ICMR-NIV; Pune, India) received clinical specimens (throat swab, urine, and serum) from 3 persons from Kozhikode district, Kerala state, who were suspected to have NiV infection. Their clinical signs and symptoms were moderate to high-grade fever, headache, vomiting, myalgia, cough, and rapidly progressing breathlessness. Neurologic symptoms included altered sensorium and seizures. Details of the index case-patient and all secondary case-patients have been described (*13*).

We tested clinical samples from 9 secondary case-patients (Table 1, https://wwwnc.cdc.gov/EID/article/25/5/18-1076-T1.htm) for NiV using quantitative reverse transcription PCR (RT-PCR), nested RT-PCR, and IgM and IgG ELISA (*4*,*5*,*11–14*). The nested RT-PCR amplification was performed using first set primers NipahNF31166 5′-CGTGGTTATCTTGAACCTATGTACTTCAG-3′ and Nipahreverse1771 5′-CGCAACTTTAATGTAATTGGTCCCTTAGTG-3′ and nested set primers NipahNF45–1342 5′-CAGAGAAGCTAAATTTGCTGCAGGAGG-3′ and NipahN16845-5′-TCACACATCAGCTCTGACAAAGTCAAG-3′. These reactions were conducted using SuperScript III Single-Step RT-PCR system with PlatinumTaq High-fidelity (https://www.thermofisher.com).

We attempted to isolate virus from 26 specimens from 9 Nipah-confirmed case-patients and 1 NiV-negative patient by processing throat swab, lung tissue, urine, and serum specimens in the Biosafety Level 4 laboratory of ICMR-NIV, as described previously (*14*) (Table 1). We inoculated 100 μL of each sample into a 24-well culture plate of Vero (ATCC, CCL-81) cells in 1 ml of Eagle minimal essential growth medium containing 10% fetal calf serum in each well. The culture plate was incubated at 37°C with 5% CO_2. All culture fluid was passaged 4 times, irrespective of showing cytopathic effect. We adjusted urine sample pH to 7.4 using 1N sodium hydroxide before proceeding to virus isolation.

To determine the possible role of bats in NiV transmission in this outbreak, we captured bats from the area near the index case-patient's house using specialized nets, 21–30 days after illness onset in the index case-patient. Two species of bats, the fruit bat (*Pteropus medius*; n = 52) and Leschenault's rousette (*Rousettus leschenaulti*; n = 12), as well as 5 birds, were trapped. We euthanized them, collected rectal and throat swab specimens in the field, then transported these animals in a liquid nitrogen transport container to ICMR-NIV. The animals were dissected in the containment laboratory, and organs (lung, spleen/liver, kidney, intestine, brain) were collected. All specimens were tested by quantitative and nested RT-PCR.

We conducted next-generation sequencing (NGS) for each positive sample with a minimum volume of 250 μL, if available. We followed a library preparation method as

Author affiliations: Indian Council of Medical Research–National Institute of Virology, Pune, India (P.D. Yadav, A.M. Shete, P. Sarkale, R.R. Sahay, R. Lakra, P. Pardeshi, D.T. Mourya); Manipal Centre for Virus Research, Manipal, India (G.A. Kumar); Government Medical College Kozhikode, Kozhikode, India (C. Radhakrishnan, V.R. Rajendran); Indian Council of Medical Research, New Delhi, India (N. Gupta, R.R. Gangakhedkar); Health & Family Welfare, Kerala (R. Sadanandan)

DOI: https://doi.org/10.3201/eid2505.181076

described previously (*15*) and analyzed the paired-end reads from Illumina Miniseq (Illumina, https://www.illumina.com) using CLC Genomics Workbench software (QIAGEN, https://www.qiagen.com). We performed reference-based mapping to retrieve the NiV genome.

Only 1 throat swab sample (MCL-18-H-1088) inoculated in Vero CCL81 cells showed significant cellular morphologic changes, beginning at 8 h into 1 day postinfection (dpi) of passage 2 (Figure 1). We observed cell fusion and syncytial formation, and the frequency of the giant multinucleated cells increased as infection progressed. At 48 h, cells with dendritic-like projections appeared, and at 64 h, extensive cell damage occurred, and cells were detached. There was no obvious cell lysis, but we observed apoptosis such as nuclear invagination and membrane blebbing. The NiV isolate (MH523642) obtained showed a cycle threshold of 15.

Throat and rectal swab specimens from 13 (25%) *Pteropus* sp. bats were positive for NiV; cycle threshold ranged from 28 to 37. Of these positive bats, liver, spleen, or both of 3 bats was also NiV positive (product size 342 bp) by nested RT-PCR for partial nucleocapsid (N) gene. The product was sequenced and compared with Kerala human NiV sequences.

We retrieved 4 complete protein encoding regions of NiV using NGS from a secondary case-patient's throat swab sample (MH396625), lung tissue of a secondary case-patient (MH523640), and throat swab sample of a recovered case-patient (MH523641) and from a NiV isolate (from a throat swab specimen; MH523642) (Table 1). Approximately 18,100 nt of the NiV genome was retrieved, encoding nucleocapsid, phosphoprotein, matrix, fusion, glycoprotein, and RNA polymerase protein. We tried NGS on positive NiV bat tissues/specimens, but attempts were unsuccessful.

We compared the retrieved genome sequence with the sequences available in GenBank and generated a

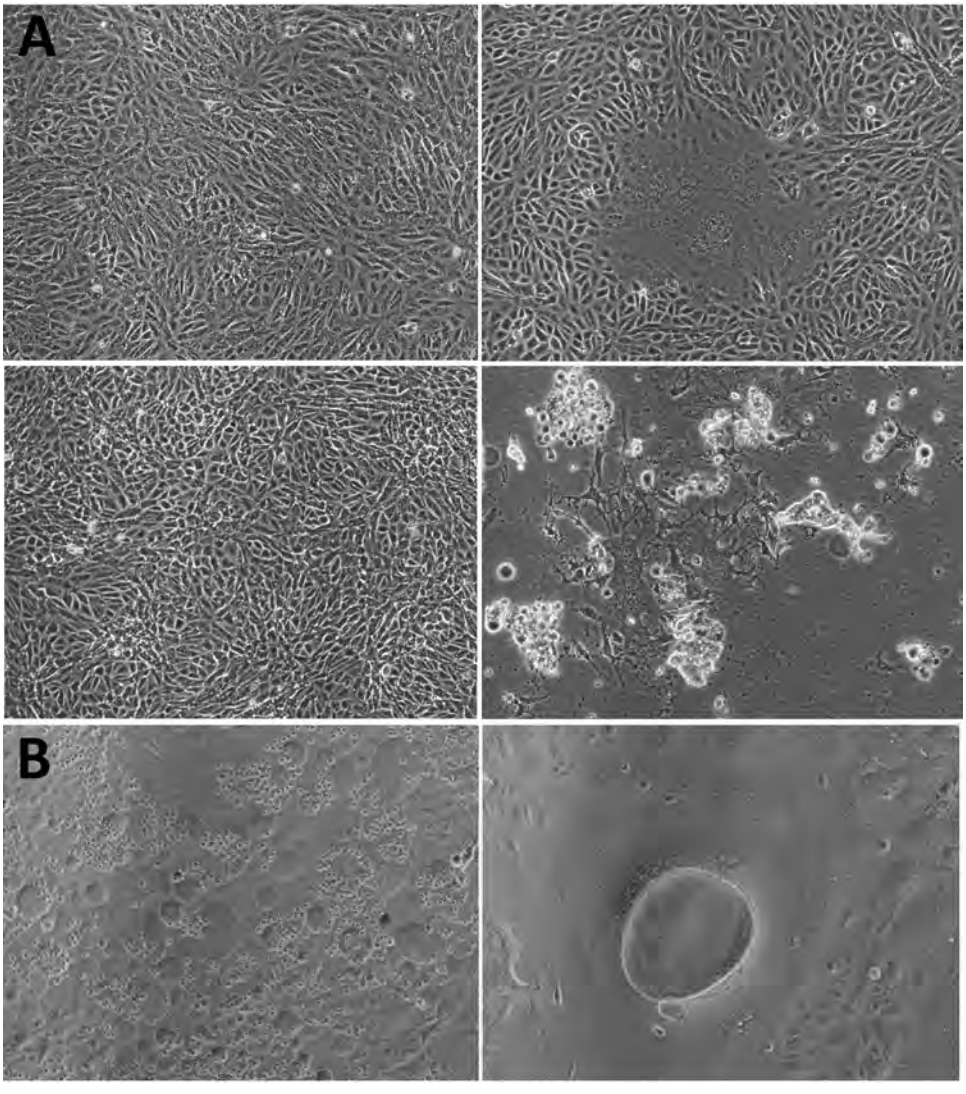

Figure 1. Cytopathic effect (CPE) of Nipah virus from throat swab samples of a patient in Kerala, India, 2018. Virus was inoculated into Vero CCL81 cells. A) CPE at postinfection days 1 (top) and 2 (bottom). Left panels depict the control cell; right panels depict the NiV-infected cell. B) NiV-infected cells. Original magnification ×10.

maximum-likelihood tree using the Tamura-Nei model on the complete coding region and a 316-nt region of the nucleocapsid region (Figure 2). Kerala NiV sequences from humans and bats clustered with the B clade, circulating in Bangladesh. The Nadia NiV sequence (GenBank accession no. FJ513078.1) showed higher similarity to and clustering with the Bangladesh viruses. However, the bat N gene sequences matched more closely with human sequences from Kerala than with others; Kerala human NiV sequences were 99.7%–100.0% homologous with the bat NiV sequences. The complete NiV genome of the Kerala strain had 85.14%–96.15% similarity with M and B NiV genotype. Despite having 96.15% similarity to the Bangladesh strain, Kerala NiV strain forms a separate cluster (Table 2, https://wwwnc.cdc.gov/EID/article/25/5/18-1076-T2.htm; Appendix Table, https://wwwnc.cdc.gov/EID/article/25/5/18-1076-App1.pdf).

Conclusions

In this outbreak, NGS helped identify the circulating NiV in Kerala as B genotype. We found the highest similarity between human NiV complete sequences from Kerala and NiV N gene sequences from *Pteropus* spp. fruit bats (99.7%–100%), compared with NiV sequences reported from Malaysia, Cambodia, and Bangladesh (85.14%–96.15%). This finding indicates that *Pteropus* spp. bats were most likely the source for human infection in this outbreak.

Distinct clustering of Kerala sequences suggests that this strain may be circulating locally in bats and some evolution might exist that differentiates it from the northern Bangladesh/West Bengal strain. It may also suggest that the colony of bats sampled in this outbreak had active infection, but additional epidemiologic studies in bats may be needed to support this. Freeze–thawing of organs, lack of collection of fresh tissue samples in the field, or preserving tissues in virus transport medium might be the reasons for failure to retrieve the complete genome from bats.

Because of the lack of effective specific treatment or preventive vaccines for NiV infection, emphasis should be placed on containment of this virus. Strict isolation; biorisk mitigation; and hospital infection control policies, including the explicit use of personal protective equipment as a part of risk mitigation by healthcare workers, needs to be strengthened. Effective close contact and suspected NiV case surveillance will help in early diagnosis and isolation, thereby preventing secondary transmission (*4*).

Ingestion of fruit coming in contact with the saliva of bats or inhalation of tiny droplets produced from the infected urine or saliva of the bats residing at the tops of trees can be an important mode of transmission of NiV to humans. Even though the route of infection of the index case-patient in this outbreak was unknown, further

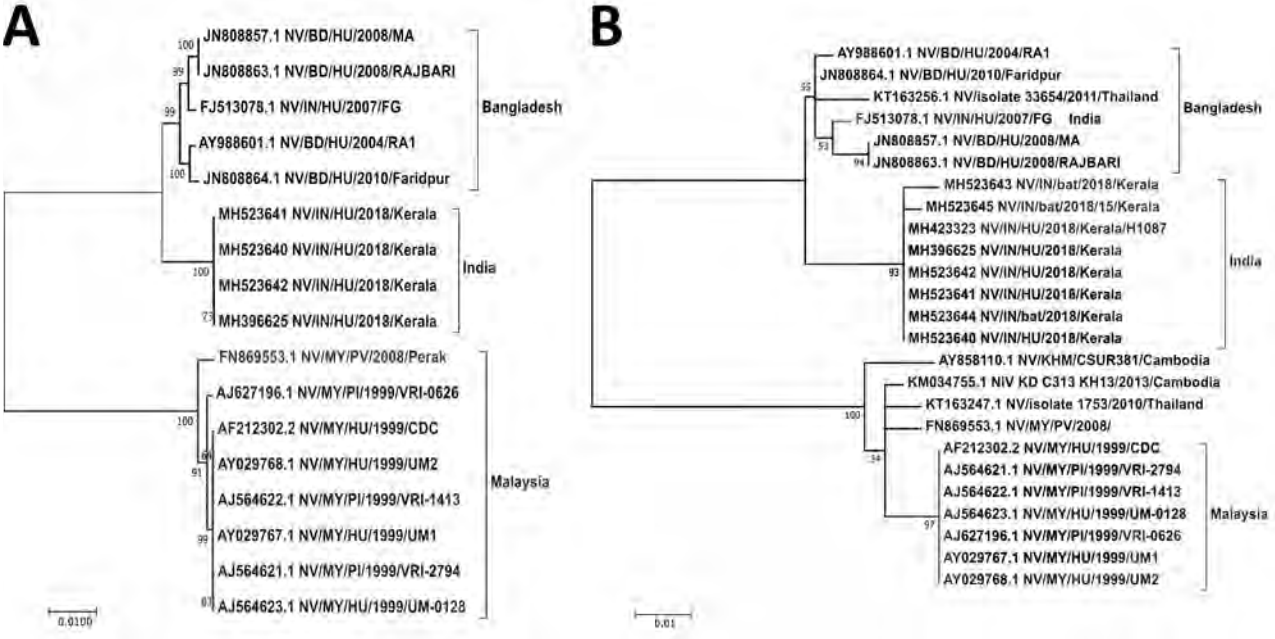

Figure 2. Maximum-likelihood phylogenetic tree of the nucleocapsid gene (region 1293–1608) of Nipah virus from Kerala, India, 2018, and reference sequences. A) Complete coding region. The evolution distance for 17 complete sequences was generated using the Tamura-Nei model plus gamma distance using different isolates. Bootstrap replication of 500 replication cycles was used for the statistical assessment of the generated tree. B) Partial nucleocapsid gene. The evolution distance for 25 nucleocapsid gene sequences of length 316 nt was generated using the Tamura-Nei model plus gamma distance using different isolates. Bootstrap replication of 500-replication cycle was used for the statistical assessment of the generated tree. GenBank accession numbers are provided for all sequences. Scale bars indicate nucleotide substitutions per site.

investigation is needed to determine how contaminated fruit can be a route of NiV transmission. High positivity in bats shows the epizootic of NiV infection. Health education and community awareness are needed to break the chain of NiV transmission.

Acknowledgments

We gratefully acknowledge the encouragement and support extended by Balram Bhargava. We also thank K.G. Sajeeth Kumar for coordinating and sending clinical samples of NiV case-patients. We thank the dedicated staff of the Biosafety Level 4 facility at ICMR-NIV, especially Sreelekshmy Mohandas, Shilpi Jain, T.P. Majumdar, Savita Patil, Sanjay Gopale, P. Kore, Ganesh Chopade, A. Srivastava, Sheetal Melag, Yogita Chopade, Swapnil Patil, and Vinod Kumar Soman, for their technical support and R. Laxminarayanan for administrative support during the study.

Financial support was provided by intramural funding of the ICMR-NIV.

About the Author

Dr. Yadav is a group leader for the maximum containment laboratory, ICMR-NIV, Pune, India. Her primary research interests include new pathogen discovery and emerging and reemerging zoonotic diseases of high-risk viruses, including Crimean-Congo hemorrhagic fever, Kyasanur Forest disease, and Nipah.

References

1. Chan YP, Chua KB, Koh CL, Lim ME, Lam SK. Complete nucleotide sequences of Nipah virus isolates from Malaysia. J Gen Virol. 2001;82:2151–5. http://dx.doi.org/10.1099/0022-1317-82-9-2151
2. Lo MK, Lowe L, Hummel KB, Sazzad HMS, Gurley ES, Hossain MJ, et al. Characterization of Nipah virus from outbreaks in Bangladesh, 2008–2010. Emerg Infect Dis. 2012;18:248–55. http://dx.doi.org/10.3201/eid1802.111492
3. Rahman MA, Hossain MJ, Sultana S, Homaira N, Khan SU, Rahman M, et al. Date palm sap linked to Nipah virus outbreak in Bangladesh, 2008. Vector Borne Zoonotic Dis. 2012;12:65–72. http://dx.doi.org/10.1089/vbz.2011.0656
4. Sazzad H. Nipah outbreak in Faridpur District, Bangladesh, 2010. Health Sci Bull. 2010;8:6–11.
5. Chadha MS, Comer JA, Lowe L, Rota PA, Rollin PE, Bellini WJ, et al. Nipah virus–associated encephalitis outbreak, Siliguri, India. Emerg Infect Dis. 2006;12:235–40. http://dx.doi.org/10.3201/eid1202.051247
6. Arankalle VA, Bandyopadhyay BT, Ramdasi AY, Jadi R, Patil DR, Rahman M, et al. Genomic characterization of Nipah virus, West Bengal, India. Emerg Infect Dis. 2011;17:907–9. http://dx.doi.org/10.3201/eid1705.100968
7. Kawada J, Okuno Y, Torii Y, Okada R, Hayano S, Ando S, et al. Identification of viruses in cases of pediatric acute encephalitis and encephalopathy using next-generation sequencing. Sci Rep. 2016;6:33452. http://dx.doi.org/10.1038/srep33452
8. Harcourt BH, Tamin A, Ksiazek TG, Rollin PE, Anderson LJ, Bellini WJ, et al. Molecular characterization of Nipah virus, a newly emergent paramyxovirus. Virology. 2000;271:334–49. http://dx.doi.org/10.1006/viro.2000.0340
9. Luby SP, Hossain MJ, Gurley ES, Ahmed BN, Banu S, Khan SU, et al. Recurrent zoonotic transmission of Nipah virus into humans, Bangladesh, 2001–2007. Emerg Infect Dis. 2009;15:1229–35. http://dx.doi.org/10.3201/eid1508.081237
10. Epstein JH, Prakash V, Smith CS, Daszak P, McLaughlin AB, Meehan G, et al. Henipavirus infection in fruit bats (*Pteropus giganteus*), India. Emerg Infect Dis. 2008;14:1309–11. http://dx.doi.org/10.3201/eid1408.071492
11. Yadav PD, Raut CG, Shete AM, Mishra AC, Towner JS, Nichol ST, et al. Detection of Nipah virus RNA in fruit bat (*Pteropus giganteus*) from India. Am J Trop Med Hyg. 2012;87:576–8. http://dx.doi.org/10.4269/ajtmh.2012.11-0416
12. Yadav P, Sudeep A, Gokhale M, Pawar S, Shete A, Patil D, et al. Circulation of Nipah virus in *Pteropus giganteus* bats in northeast region of India, 2015. Indian J Med Res. 2018;147:318–20. http://dx.doi.org/10.4103/ijmr.IJMR_1488_16
13. Arunkumar G, Chandni R, Mourya DT, Singh SK, Sadanandan R, Sudan P, et al.; NIPAH: Nipah Investigators People And Health. Outbreak investigation of Nipah virus disease in Kerala, India, 2018. J Infect Dis. 2018;:26; Epub ahead of print.
14. Chua KB, Bellini WJ, Rota PA, Harcourt BH, Tamin A, Lam SK, et al. Nipah virus: a recently emergent deadly paramyxovirus. Science. 2000;288:1432–5. http://dx.doi.org/10.1126/science.288.5470.1432
15. Yadav PD, Albariño CG, Nyayanit DA, Guerrero L, Jenks MH, Sarkale P, et al. Equine encephalosis virus in India, 2008. Emerg Infect Dis. 2018;24:898–901. http://dx.doi.org/10.3201/eid2405.171844

Address for correspondence: Devendra T. Mourya, Indian Council of Medical Research–National Institute of Virology, 20-A, Dr. Ambedkar Road, Pune, Maharashtra, Pin 411001, India; email: dtmourya@gmail.com

Infections among Contacts of Patients with Nipah Virus, India

C.P. Girish Kumar, Attayur P. Sugunan, Pragya Yadav, Karishma Krishna Kurup, Renjith Aarathee, Ponnaiah Manickam, Tarun Bhatnagar, Chandni Radhakrishnan, Bina Thomas, Akhilesh Kumar, V. Jayasree, Beena Philomina Jose, K.G. Sajeeth Kumar, N.K. Thulaseedharan, Nivedita Gupta, V.R. Rajendran, R.L. Saritha, Devendra T. Mourya, Raman R. Gangakhedkar, Manoj V. Murhekar

We conducted a serosurvey of 155 healthcare workers and 124 household and community members who had close contact with 18 patients who had laboratory-confirmed Nipah virus infections in Kerala, India. We detected 3 subclinical infections; 2 persons had IgM and IgG and 1 only IgM against Nipah virus.

Nipah virus (NiV) infection is an emerging zoonotic disease that has the potential to cause severe disease in both animals and humans (*1*). Fruit bats of the *Pteropus* genus (family *Pteropodidae*) are the natural hosts of NiV (*2*). Outbreaks of NiV have been reported from Malaysia, Singapore, Bangladesh, and eastern India; mortality rates are 40%–70% (*3*–*5*). In an outbreak in Malaysia, pigs were intermediate hosts and most human infections occurred from close contact with infected pigs (*6*), whereas during outbreaks in Bangladesh, ingestion of date palm sap contaminated with saliva or excreta from infected fruit bats was the main spillover route (*7*). During outbreaks in Bangladesh (*4*) and West Bengal, India (*5*), person-to-person transmission occurred among close contacts, including healthcare workers (HCWs), after initial spillover of NiV into humans.aDuring May 2018, an NiV outbreak occurred in the Kozhikode and Malappuram districts of Kerala, India (*8*). The initial case-patient was hospitalized on May 3, 2018, but his blood sample could not be collected for laboratory confirmation of NiV. During May 3–29, NiV infection was confirmed in another 18 patients, linked to the initial probable case-patient, through detection of NiV RNA by reverse transcription PCR of throat swab, urine, or blood samples. Sixteen patients with laboratory-confirmed NiV infection died (case-fatality rate 89%). Although the source of infection for the initial case remained unknown, all subsequent cases occurred by person-to-person transmission through close contact with NiV patients.

As part of contact tracing, district health authorities identified ≈2,600 contacts of laboratory-confirmed NiV patients. Contacts were classified into 5 categories depending on the type of exposure they had with patients, similar to the scheme of classification followed during Ebola outbreaks (*9*). Contacts were monitored for 21 days postexposure for development of febrile illness.

Although 17 of the 18 laboratory-confirmed NiV patients exhibited acute neurologic or respiratory symptoms, 1 had mild, uncomplicated febrile illness. This patient had a history of close contact with another laboratory-confirmed patient and survived after being treated with ribavirin and supportive therapy. Laboratory-confirmed infection in a NiV patient with only mild febrile illness raised a question of whether additional, mildly symptomatic or asymptomatic NiV infections might also occur among close contacts in this outbreak. To address this question, we conducted a cross-sectional study during July 2–13, 2018 (60–71 days after the initial case was hospitalized), of persons with high-risk exposure to NiV patients to estimate the seroprevalence of NiV-specific IgM and IgG.

The Study

We used a line list of high-risk exposure contacts of the initial 18 laboratory-confirmed NiV patients, including 235 HCWs and 191 household and community contacts. We needed to survey 300 contacts (150 HCW and 150 household and community contacts) because our assumption was that 5% of contacts would have asymptomatic infection develop, and absolute precision of the estimate would be 2.5% for a 95% confidence level. The Institutional Human Ethics Committee of the ICMR–National Institute of Epidemiology, Chennai (approval no. NIE/IHEC/201806-01) and the Government Medical College, Kozhikode (approval no. GMCKKD/RP2018/IEC/97) approved the study protocol.

Author affiliations: ICMR National Institute of Epidemiology, Chennai, India (C.P.G. Kumar, K.K. Kurup, R. Aarathee, P. Manickam, T. Bhatnagar, M.V. Murhekar); ICMR–Regional Medical Research Centre, Port Blair, India (A.P. Sugunan); ICMR–National Institute of Virology, Pune, India (P. Yadav, D.T. Mourya); Directorate of Health Services, Government of Kerala, Kerala (R. Aarathee, A. Kumar, V. Jayasree, R.L. Saritha); Government Medical College, Kozikhode, India (C. Radhakrishnan, B. Thomas, B.P. Jose, K.G.S. Kumar, N.K. Thulaseedharan, V.R. Rajendran); Indian Council of Medical Research, New Delhi, India (N. Gupta, R.R. Gangakhedkar)

DOI: https://doi.org/10.3201/eid2505.181352

We approached the contacts at their residences or workplaces and interviewed them using a structured questionnaire. We collected sociodemographic information, data on the type and frequency of contact with ≥1 NiV patient, and history of febrile illness after contact with NiV patients. For each person who consented to participate, we collected a 3-mL blood sample, separated serum, and transported samples to the National Institute of Virology (Pune, India), where they were tested for human IgM and IgG against NiV.

We collected 279 blood samples from 155 HCWs and 124 household and community contacts. The median age for HCWs was 37 years (interquartile range 29–48 years) and for household and community contacts was 39 years (interquartile range 30–51 years). Thirty-two HCWs and 36 household contacts reported exposure to body fluids of NiV patients; 123 (79.4%) HCWs and 88 (71.0%) household contacts reported physical contact with ≥1 NiV patient (Table 1).

We performed ELISA on samples with reagents provided by the US Centers for Disease Control and Prevention (Atlanta, GA, USA) and tested serum at 4 dilutions: 1:100, 1:400, 1:1,600, and 1:6,400. For IgM assays, we considered samples positive when the sum of the optical density for all 4 dilutions was >0.45 (*10*). For IgG assays, we considered samples positive when the sum of the optical density for all dilutions was >0.95.

Of the 279 serum samples tested, 2 had IgM and IgG and 1 had only IgM against NiV. We calculated the overall seroprevalence of NiV as 1.08% (95% CI 0.37–3.11). None of the seropositive persons reported having a febrile illness after their last contact with an NiV patient, indicating subclinical infections. Two seropositive persons were family members of a laboratory-confirmed patient, and the third was a HCW in the emergency medicine department. All 3 had a history of exposure to body fluids of ≥1 NiV patient (Table 2).

The risk for subclinical infection was higher among the contacts who had exposure to body fluids (3/68, 4.4% [95% CI 1.5%–12.2%]) than for those who only had physical contact with ≥1 NiV patient (0/211, 0% [95% CI 0%–1.8%]; p = 0.007). The epidemiologic association between exposure and seropositivity suggests our results are accurate. Applying the proportion of asymptomatic infection found in our sample of 279 to all 426 persons exposed to laboratory-confirmed NiV infection yields an expected total of 23 NiV infections among contacts, including 5 (21.7%) asymptomatic cases.

Conclusions

Although NiV is known to cause subclinical infections, the extent of these infections among close contacts varies during outbreaks. For instance, no subclinical infections have been reported from outbreaks in Bangladesh (*11*), but 1%–15% of infections were subclinical during outbreaks in Malaysia (*12*–*15*). Parashar et al. reported clinically undetected NiV infection in 6% of 166 community-farm controls and in 11% of 178 case-farm controls (*12*). Another study of household contacts of hospitalized NiV patients indicated that 8% had subclinical infections (*13*). In an outbreak in Singapore, infections were reported in 2 (4.6%) of 43 asymptomatic abattoir workers (*14*). Another study conducted in Singapore among 1,460 HCWs having contact with NiV patients identified antibodies specific for NiV in 22 (1.5%), 10 of whom were asymptomatic (*15*). These studies suggest that infection with the Malaysian strain of NiV causes less severe illness, a lower case-fatality rate, and higher prevalence of asymptomatic infections compared with outbreaks involving the Bangladesh strain. Studies in African green monkeys also suggest the Bangladesh strain of NiV is more pathogenic than the Malaysian strain (*1*). The NiV strain responsible for the Kerala outbreak was closer to the Bangladesh strain and was more

Table 1. Distribution of contacts of patients with laboratory-confirmed Nipah virus by selected characteristics, Kerala, India, 2018

Characteristic	Healthcare workers, no. (%), n = 155	Household and community contacts, no. (%), n = 124
Age, y		
<15	0	3 (2.4)
15–45	103 (66.4)	72 (58.1)
>45	52 (33.6)	49 (39.5)
Sex		
M	39 (25.2)	91 (73.4)
F	116 (74.8)	33 (26.6)
Type of exposure		
In patient's room	123 (79.4)	113 (91.1)
Contact with patient, no contact with body fluids	123 (79.4)	88 (71.0)
Exposure to body fluids*	32 (20.6)	36 (29.0)
Saliva	5 (3.2)	28 (22.6)
Cough	15 (9.7)	16 (12.9)
Vomit	6 (3.9)	14 (11.3)
Blood	10 (6.5)	0

*Contacts reported exposure to >1 type of body fluid.

Table 2. Details of Nipah virus seropositive samples among close patient contacts, Kerala, India, 2018

Characteristic	Contact 1*	Contact 2*	Contact 3
Age, y	58	60	49
Sex	M	F	M
Date of contact	22 May 2018	22 May 2018	5 May 2018
Time between exposure and blood sample collection	49 d	49 d	63 d
Laboratory findings			
IgM against Nipah virus (optical density)	Positive (0.55)	Positive (0.77)	Positive (0.46)
IgG against Nipah virus (optical density)	Positive (0.85)	Positive (1.86)	Negative (0.09)
Time of exposure			
During patient's illness	Yes	Yes	Yes
On day of patient's death	Yes	Yes	No
After patient's death (e.g., funeral rituals)	Yes	Yes	No
Type of exposure			
Touched patient	Yes	Yes	Yes
Had contact with a patient's body fluids	Yes	Yes	Yes
Spent >1 day with a patient in same room or ward	Yes	Yes	No
Fed patient with hands	No	Yes	No
Changed patient's bed linen	No	Yes	No
Changed patient's clothes	No	Yes	No
Washed patient's bed linen	No	Yes	No
Washed patient's clothes	No	Yes	No

*Family member of patient with Nipah virus.

pathogenic (*8*). Although previous studies did not show any subclinical infections during NiV outbreaks with the Bangladesh strain, our study suggested that NiV strain of Kerala outbreak generated asymptomatic infections. Our study also found that IgM could be detected ≤2 months after NiV infection and the immunoglobulin class switch to IgG could occur beyond 2 months.

Our study had 1 limitation. Although we approached all line-listed contacts, we collected samples from only 124 of 191 household and community members. The remaining contacts were either unavailable (17%) or declined to give a blood sample (18%). However, this limitation is unlikely to affect overall seroprevalence because nonparticipation in the survey was not based on exposure status.

Our findings indicate that subclinical infections occurred among close contacts of patients during an NiV outbreak in Kerala, India, but were infrequent. In addition, we found the risk for subclinical infections was higher among persons with a history of exposure to body fluids of NiV patients than for those with only physical contact.

Acknowledgments

We gratefully acknowledge Balram Bhargava and Rajeev Sadanandan for their guidance and administrative support. We thank the hospital and peripheral health workers of the district health services of Kozhikode and Malappuram districts and principal and trainees of Health and Family Welfare Training Centre, Kozhikode, for providing support in conducting the survey. We thank Seethu Ponnu Thampi, Aarti Krishnan, Reshma Ranjan, P.P. Ajeeba, Jangmi Derapi, Anu Elizabeth, Abdul Sathar, S.S. Roshni, S.S. Ageesh, A.S. Anju, and G. Alan for their fieldwork support. We also thank Annamma Jose and Anita Aich for providing laboratory support.

The study was conducted through the extramural funding received from the Indian Council of Medical Research, New Delhi.

About the Author

Dr. Kumar is a public health microbiologist with the ICMR National Institute of Epidemiology, Chennai, India. His research interests include disease surveillance, emerging infectious diseases, and antimicrobial resistance.

References

1. Ang BSP, Lim TCC, Wang L. Nipah virus infection. J Clin Microbiol. 2018; 56:e01875-17. PubMed http://dx.doi.org/10.1128/JCM.01875-17
2. Yob JM, Field H, Rashdi AM, Morrissy C, van der Heide B, Rota P, et al. Nipah virus infection in bats (order Chiroptera) in peninsular Malaysia. Emerg Infect Dis. 2001;7:439–41. http://dx.doi.org/10.3201/eid0703.017312
3. Goh KJ, Tan CT, Chew NK, Tan PS, Kamarulzaman A, Sarji SA, et al. Clinical features of Nipah virus encephalitis among pig farmers in Malaysia. N Engl J Med. 2000;342:1229–35. http://dx.doi.org/10.1056/NEJM200004273421701
4. Rahman M, Chakraborty A. Nipah virus outbreaks in Bangladesh: a deadly infectious disease. WHO South East Asia J Public Health. 2012;1:208–12. http://dx.doi.org/10.4103/2224-3151.206933
5. Chadha MS, Comer JA, Lowe L, Rota PA, Rollin PE, Bellini WJ, et al. Nipah virus-associated encephalitis outbreak, Siliguri, India. Emerg Infect Dis. 2006;12:235–40. http://dx.doi.org/10.3201/eid1202.051247
6. Chua KB. Nipah virus outbreak in Malaysia. J Clin Virol. 2003; 26:265–75. http://dx.doi.org/10.1016/S1386-6532(02)00268-8
7. Luby SP, Hossain MJ, Gurley ES, Ahmed BN, Banu S, Khan SU, et al. Recurrent zoonotic transmission of Nipah virus into humans, Bangladesh, 2001–2007. Emerg Infect Dis. 2009;15:1229–35. http://dx.doi.org/10.3201/eid1508.081237
8. Arunkumar G, Chandni R, Mourya DT, Singh SK, Sadanandan R, Sudan P, et al.; NIPAH: Nipah Investigators People And Health. Outbreak investigation of Nipah virus disease in Kerala, India, 2018. J Infect Dis. 2018. http://dx.doi.org/10.1093/infdis/jiy612

9. World Health Organization. Ebola and Marburg virus disease epidemics: preparedness, alert, control and evaluation. 2014 [cited 2018 Dec 8]. http://apps.who.int/iris/bitstream/handle/10665/130160/WHO_HSE_PED_CED_2014.05_eng.pdf
10. Wong KT, Shieh WJ, Kumar S, Norain K, Abdullah W, Guarner J, et al.; Nipah Virus Pathology Working Group. Nipah virus infection: pathology and pathogenesis of an emerging paramyxoviral zoonosis. Am J Pathol. 2002;161:2153–67. http://dx.doi.org/10.1016/S0002-9440(10)64493-8
11. Hsu VP, Hossain MJ, Parashar UD, Ali MM, Ksiazek TG, Kuzmin I, et al. Nipah virus encephalitis reemergence, Bangladesh. Emerg Infect Dis. 2004;10:2082–7. http://dx.doi.org/10.3201/eid1012.040701
12. Parashar UD, Sunn LM, Ong F, Mounts AW, Arif MT, Ksiazek TG, et al. Case-control study of risk factors for human infection with a new zoonotic paramyxovirus, Nipah virus, during a 1998–1999 outbreak of severe encephalitis in Malaysia. J Infect Dis. 2000;181:1755–9. http://dx.doi.org/10.1086/315457
13. Tan KS, Tan CT, Goh KJ. Epidemiological aspects of Nipah virus infection. Neurol J Southeast Asia 1999;4:77–81.
14. Chew MH, Arguin PM, Shay DK, Goh KT, Rollin PE, Shieh WJ, et al. Risk factors for Nipah virus infection among abattoir workers in Singapore. J Infect Dis. 2000;181:1760–3. http://dx.doi.org/10.1086/315443
15. Chan KP, Rollin PE, Ksiazek TG, Leo YS, Goh KT, Paton NI, et al. A survey of Nipah virus infection among various risk groups in Singapore. Epidemiol Infect. 2002;128:93–8. http://dx.doi.org/10.1017/S0950268801006422

Address for correspondence: Manoj V. Murhekar, ICMR–National Institute of Epidemiology, R127 TNHB, Ayapakkam, Chennai 600077, India; email: mmurhekar@gmail.com

etymologia

Nipah Virus [ne'-pə vī'-rəs]

Ronnie Henry

In 1994, a newly described virus, initially called equine morbillivirus, killed 13 horses and a trainer in Hendra, a suburb of Brisbane, Australia. The reservoir was subsequently identified as flying foxes, bats of the genus *Pteropus* (Greek *pteron* ["wing"] + *pous* ["foot"]). In 1999, scientists investigated reports of febrile encephalitis and respiratory illness among workers exposed to pigs in Malaysia and Singapore. (The pigs were believed to have consumed partially eaten fruit discarded by bats.)

The causative agent was determined to be closely related to Hendra virus and was later named for the Malaysian village of Kampung Sungai Nipah. The 2 viruses were combined into the genus *Henipavirus*, in the family *Paramyxoviridae*. Three additional species of *Henipavirus*—Cedar virus, Ghanaian bat virus, and Mojiang virus—have since been described, but none is known to cause human disease. Outbreaks of Nipah virus occur almost annually in India and Bangladesh, but *Pteropus* bats can be found throughout the tropics and subtropics, and henipaviruses have been isolated from them in Central and South America, Asia, Oceania, and East Africa.

Spectacled flying fox (*Pteropus conspicullatus*) feeding on nectar of unidentified flowers. The natural reservoir for Hendra virus is believed to be flying foxes (bats of the genus *Pteropus*) found in Australia. The natural reservoir for Nipah virus is still unknown, but preliminary data suggest that these bats are also reservoirs for Nipah virus in Malaysia. CDC/Brian W.J. Mahy.

Sources

1. Centers for Disease Control and Prevention. Outbreak of Hendra-like virus—Malaysia and Singapore, 1998–1999. MMWR Morb Mortal Wkly Rep. 1999;48:265–9.
2. Selvey LA, Wells RM, McCormack JG, Ansford AJ, Murray K, Rogers RJ, et al. Infection of humans and horses by a newly described morbillivirus. Med J Aust. 1995;162:642–5.

Address for correspondence: Ronnie Henry, Centers for Disease Control and Prevention, 1600 Clifton Rd NE, Mailstop E28, Atlanta, GA 30329-4027, USA; email: boq3@cdc.gov

DOI: https://doi.org/10.3201/eid2505.ET2505

Estimating Risk to Responders Exposed to Avian Influenza A H5 and H7 Viruses in Poultry, United States, 2014–2017

Sonja J. Olsen, Jane A. Rooney, Lenee Blanton, Melissa A. Rolfes, Deborah I. Nelson, Thomas M. Gomez, Steven A. Karli, Susan C. Trock, Alicia M. Fry

In the United States, outbreaks of avian influenza H5 and H7 virus infections in poultry have raised concern about the risk for infections in humans. We reviewed the data collected during 2014–2017 and found no human infections among 4,555 exposed responders who were wearing protection.

In late 2014 and early 2015, highly pathogenic avian influenza (HPAI) A(H5N2), A(H5N1), and A(H5N8) viruses were detected in poultry and wild birds in the United States and Canada. A fully Eurasian A/goose/Guangdong/1/1996-lineage (gs/GD/96) HPAI H5N8 clade 2.3.4.4 virus was detected along with reassortants of gs/GD/96 H5N8 with North American wild bird lineage low pathogenicity avian influenza (LPAI) viruses (reassortants H5N2 and H5N1). The gs/GD/96 H5N8 virus was detected sporadically along the Pacific flyway with few detections of the reassortant H5N2 virus in poultry. However, shortly after the reassortant H5N2 virus was detected in the Midwest, it rapidly spread, infected domestic poultry flocks in 15 states, and required a massive response effort to depopulate >50 million birds (*1*). Although ample data regarding potential public health impacts were available for the gs/GD/96 H5N1 virus, less was known about the more recent subclades (H5 2.3.4.4). Since 2003, gs/GD/96 had been reported to have caused 860 human infections in 16 countries (*2*). Furthermore, reported illness from the gs/GD/96 H5 virus infections has been severe; this virus caused deaths in 53% of persons infected (*3*).

On the basis of the theoretical risk for transmission from poultry to humans, in 2015 the Centers for Disease Control and Prevention (CDC) and the US Department of Agriculture (USDA) Animal and Plant Health Inspection Service (APHIS) drafted monitoring recommendations for persons potentially exposed to low pathogenicity and highly pathogenic H5 and H7 viruses as a part of the official USDA APHIS response efforts in the United States (Table 1). The recommendations were phased in during late 2015 and called for active monitoring for illness in persons exposed to virus through these response activities (e.g., handling infected birds or carcasses or working in a virus-contaminated environment) during and for 10 days after the last exposure. We reviewed the data and proposed a revision to the recommendations for monitoring.

The Study

The objective of this evaluation was to estimate the risk for infection in persons responding to outbreaks by using data retrospectively obtained during December 2014–September 2017. We used several sources of data. We identified the domestic poultry detection events that were reported to USDA. Then, to identify the number of persons exposed during a response (i.e., responders), we used USDA reports from each incident and limited to persons who were deployed to the field. For the numerator, we used state reports to CDC of any ill responders and testing results. Specimens were tested for influenza viruses by reverse transcription PCR. We calculated the percent positive among exposed official responders and estimated 95% binomial CIs.

We found 264 detections of H5 or H7 viruses in poultry across 20 states; most (≈92%) were during the outbreak of infection with gs/GD H5 HPAI virus during 2014–2015, and 4,555 responders were potentially exposed to a virus (Table 2). Responders were from 3 main groups: USDA, USDA contractors, and state/local agriculture. All responders were recommended to receive seasonal influenza vaccine and were assumed to have properly worn adequate personal protective equipment (PPE) (*4*); no data were systematically collected on PPE breaches. CDC did not recommend antiviral chemoprophylaxis for persons using proper PPE. The APHIS Health and Safety and PPE Guidance for HPAI and APHIS-CDC monitoring guidance applied to all responders. Twenty-three persons became ill and were tested; no human infections with avian influenza viruses were detected. The risk for infection

Author affiliations: Centers for Disease Control and Prevention, Atlanta, Georgia, USA (S.J. Olsen, L. Blanton, M.A. Rolfes, S.C. Trock, A.M. Fry); US Department of Agriculture, Riverdale, Maryland, USA (J.A. Rooney, D.I. Nelson, T.M. Gomez, S.A. Karli)

DOI: https://doi.org/10.3201/eid2505.181253

Table 1. Information on monitoring guidelines for persons responding to an outbreak of avian influenza in poultry, United States, 2014–2017*

Area of information	Guidance
Definition of active monitoring	Active monitoring indicates that someone contacted each responder daily to assess responder health status. Monitoring for signs of illness was recommended for the duration of the exposure and for 10 d after the last exposure.
Responders asked to report if they had new onset or worsening of any of the following signs and symptoms	Fever or feeling feverish/chills; cough; sore throat; runny or stuffy nose; eye tearing, redness, irritation (pink eye); sneezing; difficulty breathing; shortness of breath; fatigue (feeling tired); muscle or body aches; headaches; nausea; vomiting; diarrhea; seizures; rash
Specimen	Respiratory or conjunctival
Who monitored	
Mobilized responders	USDA/APHIS safety officers or contractor safety officers performed daily monitoring on-site
Demobilized responders	State or local health department officials made contact with demobilized responders at least twice, upon arrival and at the end of the 10-d period
Who performs testing	State health department
Who is tested	Decision based on recommendations of state health department after assessing clinical illness, exposure, and use/breach of personal protective equipment

*USDA/APHIS, US Department of Agriculture Animal and Plant Health Inspection Service.

with avian influenza for responders was low, although our power to make this statement with confidence varied by year and virus because there was a wide range (74–3,962) of number of persons involved in each response. The data were most robust during the outbreaks of infection with gs/GD/96 H5N8 and reassortant HPAI H5N2 viruses in poultry during 2014–2015.

These results complement data previously published for outbreaks in the United States during 2014–2015, which found no avian influenza infections in 164 persons mostly exposed while not wearing PPE (*5*). Animal model data also support these epidemiologic data. The gs/GD/96 H5N8 and reassortant HPAI H5N2 viruses can replicate efficiently in the respiratory tract of ferrets, but illness was mild and did not transmit through direct contact between ferrets (*6*). North American lineage H7N8 virus also replicated in ferrets, and pathogenicity was greater for HPAI viruses than for LPAI viruses. Limited transmission in ferrets through direct contact was observed only for the LPAI virus (*7*). Similarly, North American lineage LPAI H7N9 viruses demonstrated limited transmissibility through direct contact in ferrets (*8*). The viruses from each of these events were evaluated by using the Influenza Risk Assessment Tool (*9*), which is used to assess the potential pandemic risk. The North American H7N8 and H7N9 viruses had low risk, and the gs/GD H5N8 and reassortant H5N2 and H5N1 viruses had low to moderate risk.

Table 2. Influenza virus detection in poultry and persons potentially exposed, ill and tested, United States, 2014–2017*

Time	No. states	Virus	No. premises	No. domestic poultry	Total responders potentially exposed (by affiliation)	No. ill persons positive for avian influenza/no. tested (95% CI)	Other pathogens detected
Dec 2014–Jun 2015	15	H5N2, H5N8, H5N1†	242: all HPAI	50.4 million	3,962 (3,009 contractors, 773 USDA; 180 state/local)	0/5 (0–0.001)	Not systematically collected
Jan 2016‡	1	H7N8	9: 1 HPAI, 8 LPAI	414,000	519§ (374 contractors; 78 USDA; 67 state/local)	0/16¶ (0–0.007)	1 coronavirus OC43, 1 rhino/enterovirus
Mar 2017	4	H7N9	13: 2 HPAI, 11 LPAI	272,000	74# (45 USDA; 29 state/local)	0/2** (0–0.001)	1 coronavirus, 1 influenza B virus

*HPAI, highly pathogenic avian influenza; LPAI, low pathogenicity avian influenza; USDA, US Department of Agriculture.
†There were no data on persons potentially exposed in response to detection of reassortant H5N1 virus in wild birds. We were not able to differentiate the number of responders exposed to each virus separately.
‡https://www.cdc.gov/mmwr/volumes/67/wr/mm6748a2.htm.
§In response to the outbreak of infection with North American wild bird lineage H7N8 virus (LPAI that mutated to HPAI on 1 premise) in poultry in the United States during 2016. Median time a responder was on a premise was 14 d (range 1 d–44 d).
¶All 16 responders reported ≥1 sign or symptom: 2 had fever, 11 cough, 6 conjunctivitis, 7 sore throat, 4 rhinorrhea, 3 muscle ache, and 2 difficulty breathing. Of 11 with information, 9 (82%) were tested within 2 d of illness onset.
#In response to the outbreak of infection with North American wild bird lineage H7N9 virus (LPAI with 1 mutation to HPAI) in poultry in the United States during 2017. Median time a responder was on a premise was 5 d (range 2 d–41 d).
**One responder infected with coronavirus reported coughing and sneezing. One responder infected with influenza B virus reported having a fever. No other signs or symptoms were reported from responders.

Conclusions

On the basis of these data, CDC and USDA revised the recommendations for monitoring illness in responders (https://www.cdc.gov/flu/avianflu/h5/infected-birds-exposure.htm). When responding to H5 or H7 viruses similar to those previously encountered in the United States to date, we recommend passive monitoring (i.e., self-report if ill) for persons wearing adequate PPE. For response personnel with inadequate or no PPE, or after experiencing a breach of PPE, we continue to recommend active monitoring. If personnel are responding to an avian influenza virus of unknown origin, we recommend active monitoring during exposure and for 10 days postexposure, regardless of PPE use. The change in procedure will substantially reduce the workload for safety officers and public health officials, and shift much of the reporting responsibility to the individual.

A limitation to this report is the lack of information regarding breaches in PPE. It is likely that breaches occurred, which, in turn, might have increased the risk for transmission. PPE noncompliance had been well-documented in the healthcare setting (*10*). The fact that we were unable to detect such a transmission event while actively monitoring, combined with what we know about the genetic and receptor binding characteristics of these viruses and the animal studies (*7*–*9*,*11*), might suggest that the viruses are not well adapted to humans. Another limitation was the challenge to follow-up responders after they returned to their home states. These data further support the rationale for revising the current monitoring recommendations. In contrast, if infection causes mild illness, it might have been missed. It is possible that in revising the monitoring recommendations we will risk missing a human infection. However, we might expect to detect an illness severe enough that the person seeks medical care and is tested for influenza.

The gs/GD/96 lineage clade 2.3.4.4 HPAI H5 viruses continue to cause outbreaks in poultry and wild birds in other parts of the world (*12*). One report from Canada monitored 50 household members or animal caretakers on affected farms potentially exposed to gs/GD/96 reassortant H5N2 or H5N1 viruses during 2014–2015, and no infections were identified (*13*). A recent study of 23 countries in Europe on outbreaks of infection with gs/GD/96 H5N8 virus in poultry during 2016–2017 reported no infections among 524 exposed persons who were monitored by a mixture of active and passive monitoring (*14*). Globally, many more persons have likely been exposed, but no human infections with gs/GD/96 H5N8 clade 2.3.4.4 viruses have been reported. Novel influenza virus infections in persons are reportable to the World Health Organization through the International Health Regulations (*15*). Given the nature of influenza viruses, we will continue to monitor the epidemiology and the viruses. Going forward, CDC and USDA should prospectively collect data on exposure and PPE use to better define the risk for responders exposed to avian influenza viruses.

Acknowledgments

We thank Todd Davis and Mia Torchetti for reviewing and making comments on the manuscript.

This study was supported by the US government.

About the Author

Dr. Olsen is an epidemiologist in the Influenza Division, National Center for Immunization and Respiratory Diseases, Centers for Diseases Control and Prevention, Atlanta, GA. Her research interests include novel influenza virus outbreaks and global influenza surveillance and response.

References

1. US Department of Agriculture. 2014–2015 HPAI outbreak; 2016 [cited 2018 Mar 30]. https://www.aphis.usda.gov/aphis/ourfocus/animalhealth/animal-disease-information/avian-influenza-disease/defend-the-flock/2014-2015-hpai-outbreak
2. World Health Organization. Cumulative number of confirmed human cases for avian influenza A(H5N1) reported to WHO, 2003–2018; 2018 [cited 2018 Mar 30]. http://www.who.int/influenza/human_animal_interface/2018_03_02_tableH5N1.pdf?ua=1
3. Abdel-Ghafar AN, Chotpitayasunondh T, Gao Z, Hayden FG, Nguyen DH, de Jong MD, et al.; Writing Committee of the Second World Health Organization Consultation on Clinical Aspects of Human Infection with Avian Influenza A (H5N1) Virus. Update on avian influenza A (H5N1) virus infection in humans. N Engl J Med. 2008;358:261–73. http://dx.doi.org/10.1056/NEJMra0707279
4. US Department of Agriculture. Highly pathogenic avian influenza standard operating procedures: 8. health and safety and personal protective equipment; 2014 [cited 2019 Jan 28]. https://www.aphis.usda.gov/animal_health/emergency_management/downloads/sop/sop_hpai_health_safety.pdf
5. Arriola CS, Nelson DI, Deliberto TJ, Blanton L, Kniss K, Levine MZ, et al.; H5 Investigation Group. Infection risk for persons exposed to highly pathogenic avian influenza A H5 virus–infected birds, United States, December 2014–March 2015. Emerg Infect Dis. 2015;21:2135–40. http://dx.doi.org/10.3201/eid2112.150904
6. Pulit-Penaloza JA, Sun X, Creager HM, Zeng H, Belser JA, Maines TR, et al. Pathogenesis and transmission of novel highly pathogenic avian influenza H5N2 and H5N8 viruses in ferrets and mice. J Virol. 2015;89:10286–93. http://dx.doi.org/10.1128/JVI.01438-15
7. Sun X, Belser JA, Pulit-Penaloza JA, Zeng H, Lewis A, Shieh WJ, et al. Pathogenesis and transmission assessments of two H7N8 influenza A viruses recently isolated from turkey farms in Indiana using mouse and ferret models. J Virol. 2016;90:10936–44. http://dx.doi.org/10.1128/JVI.01646-16
8. Belser JA, Brock N, Sun X, Jones J, Zanders N, Hodges E, et al. Mammalian pathogenesis and transmission of avian influenza A(H7N9) viruses, Tennessee, USA, 2017. Emerg Infect Dis. 2018;24:149–52. http://dx.doi.org/10.3201/eid2401.171574
9. Centers for Disease Control and Prevention. Summary of influenza risk assessment tool (IRAT) results; 2018 [cited 2018 Mar 30]. https://www.cdc.gov/flu/pandemic-resources/monitoring/irat-virus-summaries.htm

10. Hinkin J, Gammon J, Cutter J. Review of personal protection equipment used in practice. Br J Community Nurs. 2008;13:14–9. http://dx.doi.org/10.12968/bjcn.2008.13.1.27978
11. Kaplan BS, Russier M, Jeevan T, Marathe B, Govorkova EA, Russell CJ, et al. Novel highly pathogenic avian A(H5N2) and A(H5N8) influenza viruses of clade 2.3.4.4 from North America have limited capacity for replication and transmission in mammals. mSphere. 2016;1:pii:e00003–16.
12. Bodewes R, Kuiken T. Changing role of wild birds in the epidemiology of avian influenza A viruses. Adv Virus Res. 2018;100:279–307. http://dx.doi.org/10.1016/bs.aivir.2017.10.007
13. Murti M, Skowronski D, Lem M, Fung C, Klar S, Bigham M, et al. Public health response to outbreaks of avian influenza A(H5N2) and (H5N1) among poultry—British Columbia, December 2014–February 2015. Can Commun Dis Rep. 2015; 41:69–72. http://dx.doi.org/10.14745/ccdr.v41i04a01
14. Adlhoch C, Dabrera G, Penttinen P, Pebody R; Country Experts. Protective measures for humans against avian influenza A(H5N8) outbreaks in 22 European Union/European Economic Area countries and Israel, 2016–17. Emerg Infect Dis. 2018;24:1–8. http://dx.doi.org/10.3201/eid2410.180269
15. World Health Organization. International health regulations (2005). [cited 2019 Jan 28]. http://www.who.int/ihr/publications/9789241580496/en/

Address for correspondence: Sonja J. Olsen, Centers for Disease Control and Prevention, 1600 Clifton Rd NE, Mailstop H24-7, Atlanta, GA 30329-4027, USA; email: sco2@cdc.gov

Mycobacterium obuense Bacteremia in a Patient with Pneumonia

Bruno Ali López Luis, Paulette Díaz-Lomelí, Livier Patricia Gómez-Albarrán, Areli Martínez-Gamboa, Alfredo Ponce-de-León

Author affiliation: Instituto Nacional de Ciencias Médicas y Nutrición Salvador Zubirán, Mexico City, Mexico

DOI: https://doi.org/10.3201/eid2505.180208

Mycobacterium obuense is a pigmented, rapidly growing mycobacterium. Because it has been considered nonpathogenic, *M. obuense* is being investigated in clinical trials of cancer immunotherapy and bioremediation. We report a case of bacteremia caused by *M. obuense* in a patient with pneumonia, showing its potential pathogenicity.

Approximately 75 species of rapidly growing mycobacteria (RGM) have been isolated from soil, animals, and water (*1*). The RGM *Mycobacterium obuense*, an environmental pigmented mycobacterium, is mobile and easily adaptable to the environment and possesses oxygenases that enable it to degrade organic compounds and dechlorinate methoxychlor-based insecticides (*2*). Until recently, *M. obuense* has been considered nonpathogenic. We report a case of bacteremia caused by *M. obuense*.

A 29-year-old man from a rural community in Puebla, Mexico, arrived at an emergency department in Mexico City reporting a 2-day history of chest pain, dyspnea, and fever. On physical examination, his heart rate was 94 bpm, blood pressure 175/88 mm Hg, temperature 38.5°C, and peripheral oxygen saturation 70%. Chest auscultation revealed bibasilar fine crackles and signs of pleural effusion.

The patient was a farmer; had been in close contact with pigs, sheep, and cows; and reported consuming unpasteurized dairy products. He had a history of diabetes mellitus with chronic kidney disease categorized as stage G4 A3 (glomerular filtration rate 16.7 mL/min/1.73 m^2; proteinuria >2.8 g/d) of the KDIGO classification (Kidney Disease: Improving Global Outcomes, https://kdigo.org) without replacement therapy. He reported taking metformin, amlodipine, furosemide, and iron sulfate.

At admission, laboratory test results included leukocyte count, 11,900 cells/μL with 88.2% neutrophils; C-reactive protein, 250 mg/L; procalcitonin, 17 ng/mL; creatinine, 4.0 mg/dL; and arterial blood gases, pH 7.24, pO_2 40.8 mm Hg, pCO_2 34.8 mm Hg, lactate 2.9 mmol/L, HCO_3 14.6 mmol/L, and sO_2 71% on ambient air. Findings of a computed tomography scan of the chest suggested that the patient had a lung infection (Figure).

The patient began empirical treatment for community-acquired pneumonia with ceftriaxone and clarithromycin. No respiratory samples were obtained because the patient was unable to produce sputum. We performed blood cultures in Aerobic/F medium (Becton Dickinson, https://www.bd.com). After a 7-day incubation period, we detected growth and observed gram-positive bacilli in the gram stain (Appendix Figure, panel A, http://wwwnc.cdc.gov/EID/article/25/5/18-0208-App1.pdf). We made subcultures on sheep blood, chocolate, and Sabouraud agar and performed Kinyoun and Ziehl-Neelsen stains, in which we observed partially acidic alcohol-resistant coccobacilli (Appendix Figure, panels B,C). After 2 weeks of incubation at 35°–37°C, we observed rough, mucoid colonies (Appendix Figure, panels D,E).

We attempted to identify the bacilli by using GenoType Mycobacterium (Hain Lifescience, https://www.hain-lifescience.de) but were unsuccessful because no species-specific probe is available. We performed amplification and sequencing of the 16S rRNA gene (498 bp) and *hsp65* gene (400 bp). Pairwise sequence aligned 100% with 16S rRNA and 99.6% with *hsp65* to the sequences of *M. obuense* strain CIP 106803 (GenBank accession no. AF547954.1).

The patient was started on intravenous amikacin, clarithromycin, and moxifloxacin as soon as we notified clinicians of RGM isolated from his blood cultures. We conducted susceptibility testing by broth microdilution, which showed susceptibility to all antimicrobial drugs tested except tobramycin (intermediate susceptibility) (Appendix) (*3*).

The patient completed 2 weeks of intravenous moxifloxacin, amikacin, and clarithromycin and was discharged. He received 4 additional weeks of oral azithromycin and moxifloxacin and experienced complete resolution.

M. obuense, first described as a scotochromogenic RGM species isolated primarily from soil >40 years ago in Obu, Japan, is a catalase-positive, peroxidase-negative bacillus that can degrade salicylates, forming a black product (*4*,*5*). In culture, *M. obuense* has 2 morphotypes, smooth and rough variants. In the smooth variants, its cell wall contains long-chain saturated fatty acids that enable it to colonize the environment and are responsible for the pleomorphism observed on the surface of solid agars (*6*). Although this species was later isolated from sputum samples from patients with apparent pulmonary disease, no additional clinical data were reported, and thus, no evidence of pathogenicity was established (*4*,*7*).

Phylogenetic analysis of *M. obuense* shows close association with *M. chubuense* (81.3% identity) and *M. rufum* (92.2% identity) (*7*). Its genome consists of 5,576,960 bp

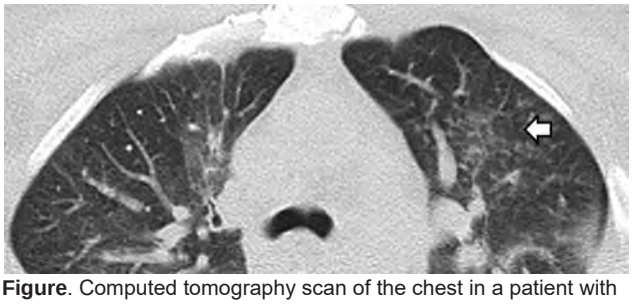

Figure. Computed tomography scan of the chest in a patient with *Mycobacterium obuense* pneumonia, Mexico, showing air space infiltration in the left parahilar and a tree bud pattern in the left upper lobe (arrow), as well as bilateral interstitial thickening and ground glass opacities.

(of which 133,713 bp are of plasmid origin with 68% GC content) and 800 unique genes, more than related species, such as *M. chubuense.* Although these mycobacteria are considered nonpathogenic, they have homologous genes to mammalian cell entry that encode proteins involved in virulence and cell invasion. In addition, *M. obuense* contains genes involved in antimicrobial resistance, such as *marA*, aminoglycoside-resistance protein kinase, β-lactamases, and monooxygenases, which confer *M. obuense* with intrinsic rifampin resistance (*2*,*7*).

Establishing etiology in this case was challenging because current nucleic acid probe assays cannot identify *M. obuense* correctly. Clinicians should avoid discarding RGM or misclassifying these isolates as colonizers until definitive species identification confirms etiology.

M. obuense has been evaluated as an adjuvant immunotherapy in phase I and II trials on patients with melanoma, pancreatic cancer, and colorectal cancer, with promising results. This treatment consists of an intradermal application of a suspension of heat-killed whole cell *M. obuense* (*8*–*10*).

The isolation of *M. obuense* from blood cultures of a patient with community-acquired pneumonia suggests its capacity for virulence and invasiveness in humans. Because *M. obuense* might become an adjuvant in cancer therapy, researchers should ensure implementation of proper, standardized inactivation protocols.

About the Author

Dr. Luis is a fellow in infectious diseases and Dr. Ponce-de-Leon is a senior researcher at the National Institute of Medical Science and Nutrition Salvador Zubiran, Mexico City. Their research fields are mycobacterial diseases and clinical microbiology.

References

1. Brown-Elliott BA, Philley JV. Rapidly growing mycobacteria. Microbiol Spectr. 2017;5. http://dx.doi.org/10.1128/microbiolspec.TNMI7-0027-2016
2. Das S, Pettersson BM, Behra PR, Ramesh M, Dasgupta S, Bhattacharya A, et al. Characterization of three *Mycobacterium* spp. with potential use in bioremediation by genome sequencing and comparative genomics. Genome Biol Evol. 2015;7:1871–86. http://dx.doi.org/10.1093/gbe/evv111
3. Clinical and Laboratory Standards Institute. Susceptibility testing of *Mycobacteria, Nocardiae,* and other aerobic actinomycetes. Approved standard. 2nd edition. Document M24–A2. Wayne (PA): The Institute; 2011.
4. Tsukamura M, Mizuno S. *Mycobacterium obuense,* a rapidly growing scotochromogenic mycobacterium capable of forming a black product from *p*-aminosalicylate and salicylate. J Gen Microbiol. 1971;68:129–34. http://dx.doi.org/10.1099/00221287-68-2-129
5. Tsukamura M, Mizuno S, Tsukamura S. Numerical analysis of rapidly growing scotochromogenic mycobacteria, including *Mycobacterium obuense* sp. nov., nom. rev., *Mycobacterium rhodesiae* sp. nov., nom. rev., *Mycobacterium aichiense* sp. nov., nom. rev., *Mycobacterium chubuense* sp. nov., nom. rev., and *Mycobacterium tokaiense* sp. nov., nom. rev. Int J Syst Bacteriol. 1981;31:263–75. http://dx.doi.org/10.1099/00207713-31-3-263
6. Agustí G, Astola O, Rodríguez-Güell E, Julián E, Luquin M. Surface spreading motility shown by a group of phylogenetically related, rapidly growing pigmented mycobacteria suggests that motility is a common property of mycobacterial species but is restricted to smooth colonies. J Bacteriol. 2008;190:6894–902. http://dx.doi.org/10.1128/JB.00572-08
7. Greninger AL, Cunningham G, Hsu ED, Yu JM, Chiu CY, Miller S. Draft genome sequence of *Mycobacterium obuense* strain UC1, isolated from patient sputum. Genome Announc. 2015;3:e00612-15. http://dx.doi.org/10.1128/genomeA.00612-15
8. Fowler D, Dalgleish A, Liu W. A heat-killed preparation of *Mycobacterium obuense* can reduce metastatic burden in vivo. J Immunother Cancer. 2014;2(Suppl 3):P54. http://dx.doi.org/10.1186/2051-1426-2-S3-P54
9. Stebbing J, Dalgleish A, Gifford-Moore A, Martin A, Gleeson C, Wilson G, et al. An intra-patient placebo-controlled phase I trial to evaluate the safety and tolerability of intradermal IMM-101 in melanoma. Ann Oncol. 2012;23:1314–9. http://dx.doi.org/10.1093/annonc/mdr363
10. Costa Neves M, Giakoustidis A, Stamp G, Gaya A, Mudan S. Extended survival after complete pathological response in metastatic pancreatic ductal adenocarcinoma following induction chemotherapy, chemoradiotherapy, and a novel immunotherapy agent, IMM-101. Cureus. 2015;7:e435.

Address for correspondence: Alfredo Ponce-de-León, Laboratory of Clinical Microbiology, Department of Infectious Diseases, Instituto Nacional de Ciencias Médicas y Nutrición Salvador Zubirán, Avenida Vasco de Quiroga No.15, Colonia Belisario Domínguez Sección XVI, Delegación Tlalpan, 14080, Mexico City, Mexico; email: alf.poncedeleon@gmail.com

Gordonia bronchialis–Associated Endophthalmitis, Oregon, USA

Rene Choi, Luke Strnad, Christina J. Flaxel, Andreas K. Lauer, Eric B. Suhler

Author affiliations: Casey Eye Institute, Portland, Oregon, USA (R. Choi, C.J. Flaxel, A.K. Lauer, E.B. Suhler); Oregon Health and Science University, Portland (L. Strnad); Veterans Administration Portland Health Care System, Portland (E.B. Suhler)

DOI: https://doi.org/10.3201/eid2505.180340

Gordonia bronchialis is an aerobic actinomycetes that rarely causes infections in humans. Few reports describe *Gordonia* spp. causing eye-related infections. We report a case of chronic infectious endophthalmitis in Oregon, USA, associated with infection by *G. bronchialis.*

Gordonia bronchialis is an aerobic bacteria that rarely causes infections in humans. We report a case of chronic infectious endophthalmitis caused by infection with *G. bronchialis.*

A 63-year-old woman was referred to a uveitis service in Portland, Oregon, USA, because of a 10-month history of decreased vision in the left eye caused by 3 recurrences of anterior and intermediate uveitis that was refractory to topical corticosteroids. Her ocular history included cataract surgery with intraocular lens implants placed bilaterally 2.5 years before symptom onset. Her medical history included chronic obstructive pulmonary disease, diabetes mellitus type 2, and hypertension. A complete review of systems, including fevers, chills, night sweats, weight loss, or history of contacts with ill persons, was unremarkable.

Her visual acuity was 20/20, and she had hand motion vision at 2 feet in the right and left eyes. No afferent pupillary defect was appreciated, and intraocular pressures were normal bilaterally. In the left eye, anterior segment examination showed 4+ anterior chamber cell with a hypopyon and a diffuse white granular sheet along the posterior face of the intraocular lens implant. Visualization of the left fundus was precluded by 4+ vitreous cell and haze. B-scan ultrasonography showed extensive vitreous opacities and an attached retina (Figure).

Laboratory test results were negative for rapid plasma reagin, fluorescent treponemal antibody absorption, tuberculosis (Quantiferon-Gold TB; Quest Diagnostics, https://www.questdiagnostics.com), angiotensin-converting enzyme, rheumatoid factor, antinuclear antibody, and human leukocyte antigen B27. We obtained standard results for a complete blood count with differential counts, erythrocyte sedimentation rate, complete metabolic panel, and chest radiography.

The patient was given a diagnosis of presumptive chronic infectious endophthalmitis and underwent a pars plana vitrectomy and intraocular lens implant removal of the left eye. A vitreous sample was sent for pan-culture, cytologic analysis, flow cytometry, and broad-range PCR

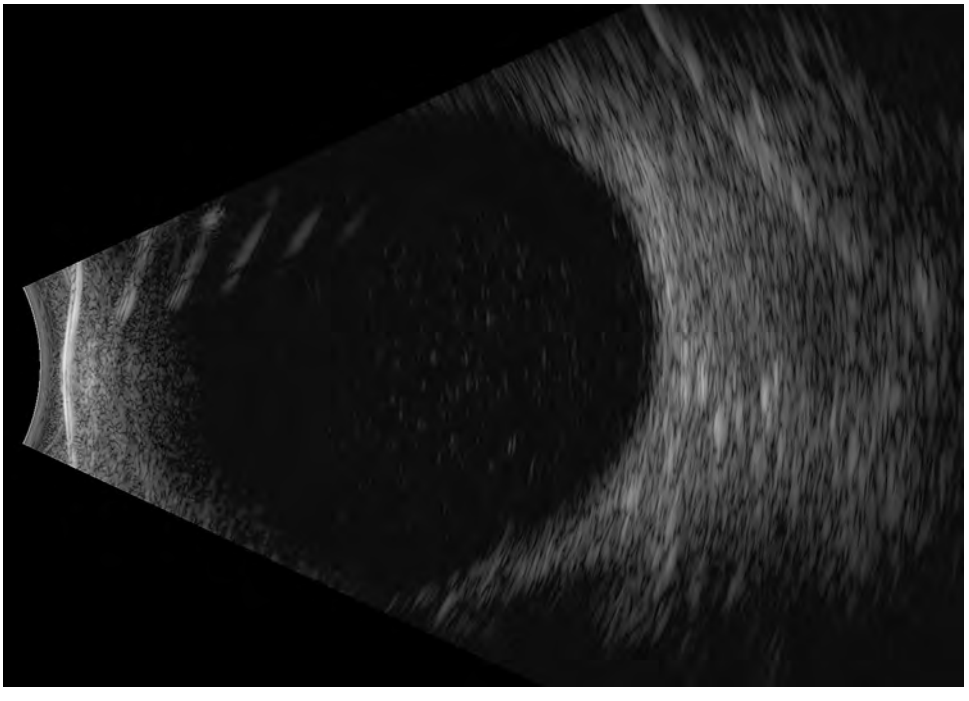

Figure. B-scan ultrasonography of the left eye of a 63-year-old woman with *Gordonia bronchialis*–associated endophthalmitis, Oregon, USA, showing dense opacities in the vitreous space.

analyses with 16S rRNA gene sequencing. Results of cytology analysis and flow cytometry were negative for neoplastic processes. Culture analysis showed gram-positive bacilli but did not identify the species.

The 16S rRNA gene sequencing yielded positive results for *G. bronchialis*. We confirmed the bacterium to be *G. bronchialis* by using matrix-assisted laser desorption/ionization time-of-flight mass spectrometry. Antimicrobial susceptibility testing showed favorable MICs for amikacin, ceftriaxone, amoxicillin/clavulanic acid, and ciprofloxacin. Subsequently, the patient was treated with an intravitreal injection of 400 μg of amikacin to the left eye.

Two weeks after this intervention, visual acuity had improved to 20/100 in the left eye and ocular inflammation had resolved. However, 3 weeks later, the patient returned because of worsening symptoms, hand motion vision, and severe symptomatic recurrent anterior chamber and vitreous inflammation in the left eye. Intravitreal ceftazidime (2.25 mg) was administered to the left eye, and a 21-day course of oral moxifloxacin (400 mg/d) was prescribed. One week after completing her moxifloxacin regimen, her symptoms had improved, her best corrected visual acuity had improved to 20/40 in the left eye, and intraocular inflammation had resolved.

Gordonia spp. are gram-positive, weakly acid-fast aerobic actinomycetes that are ubiquitous in the environment; 29 species have been identified (*1*). Human infections are rare, although a few case reports of sternal wound infections, bloodstream and intravascular catheter related infections, and skin abscesses have been published (*2*). Optimal antimicrobial drug treatment for infection with *Gordonia* spp. is unknown. However, the organisms are generally believed to be susceptible to cephalosporins, aminoglycosides, and fluoroquinolones (*3*).

One previous case of *Gordonia* spp. playing a pathogenic role in an eye-related infection in a case of traumatic endophthalmitis secondary to infection with *G. sputi* has been reported (*4*). In contrast, the peculiarity of our case was the lack of obvious mode of transmission for *G. bronchialis* into the intraocular space. Seeding of the intraocular lens implant at the time of cataract surgery is possible, but unlikely, given the time lapse of 2.5 years between surgery and onset of symptoms. The patient also had no risk factors or history suggesting seeding from the bloodstream.

The course of our patient was of particular interest because the eye initially improved after vitrectomy and administration of intravitreal amikacin. However, a robust recurrence of inflammation occurred 3 weeks later, probably caused by incomplete treatment during initial therapy.

Although previously accurate identification of *Gordonia* spp. by using traditional culturing techniques has been challenging, advent of molecular biology techniques, such as 16S rRNA sequencing and matrix-assisted laser desorption/ionization time-of-flight mass spectrometry, has improved identification of aerobic actinomycetes (*3*–*8*). Because the organism was partially identified by culture and fully identified by multiple molecular techniques and responded clinically to targeted antimicrobial drugs, we believe this case was a pathogenic infection and not a nonpathogenic contaminant/colonizer.

We report a case of chronic infectious endophthalmitis caused by infection with *G. bronchialis.* Molecular methods have enabled successful identification of this organism, which is generally considered to have low virulence and be highly susceptible to antimicrobial drugs. A combination approach of pars plana vitrectomy and intraocular lens explantation with intravitreal and oral antimicrobial drugs might lead to a successful outcome.

This study was supported by core grant P30 EY010572 (to the Casey Eye Institute) from the National Institutes of Health and an unrestricted grant to the Casey Eye Institute from Research to Prevent Blindness (New York, NY)

About the Author

Dr. Choi is a vitreoretinal surgery fellow at the Casey Eye Institute at Oregon Health and Science University, Portland, OR. His primary research interest is in elucidating the mechanisms that govern infectious and noninfectious causes of uveitis.

References

1. Sukackiene D, Rimsevicius L, Kiveryte S, Marcinkeviciene K, Bratchikov M, Zokaityte D, et al. A case of successfully treated relapsing peritoneal dialysis-associated peritonitis caused by *Gordonia bronchialis* in a farmer. Nephrol Ther. 2017.
2. Ramanan P, Deziel PJ, Wengenack NL. *Gordonia* bacteremia. J Clin Microbiol. 2013;51:3443–7. http://dx.doi.org/10.1128/JCM.01449-13
3. Blaschke AJ, Bender J, Byington CL, Korgenski K, Daly J, Petti CA, et al. *Gordonia* species: emerging pathogens in pediatric patients that are identified by 16S ribosomal RNA gene sequencing. Clin Infect Dis. 2007;45:483–6. http://dx.doi.org/10.1086/520018
4. Fang W, Li J, Cui HS, Jin X, Zhai J, Dai Y, et al. First identification of Gordonia sputi in a post-traumatic endophthalmitis patient: a case report and literatures review. BMC Ophthalmol. 2017;17:190. http://dx.doi.org/10.1186/s12886-017-0573-5
5. Verma P, Brown JM, Nunez VH, Morey RE, Steigerwalt AG, Pellegrini GJ, et al. Native valve endocarditis due to *Gordonia polyisoprenivorans*: case report and review of literature of bloodstream infections caused by *Gordonia* species. J Clin Microbiol. 2006;44:1905–8. http://dx.doi.org/10.1128/JCM.44.5.1905-1908.2006
6. Gil-Sande E, Brun-Otero M, Campo-Cerecedo F, Esteban E, Aguilar L, García-de-Lomas J. Etiological misidentification by routine biochemical tests of bacteremia caused by *Gordonia terrae* infection in the course of an episode of acute cholecystitis. J Clin Microbiol. 2006;44:2645–7. http://dx.doi.org/10.1128/JCM.00444-06
7. Wang T, Kong F, Chen S, Xiao M, Sorrell T, Wang X, et al. Improved identification of *Gordonia*, *Rhodococcus* and *Tsukamurella* species by 5′-end 16S rRNA gene sequencing.

Pathology. 2011;43:58–63. http://dx.doi.org/10.1097/PAT.0b013e328340e431
8. Rodriguez-Lozano J, Pérez-Llantada E, Agüero J, Rodríguez-Fernández A, Ruiz de Alegria C, Martinez-Martinez L, et al. Sternal wound infection caused by *Gordonia bronchialis*: identification by MALDI-TOF MS. JMM Case Rep. 2016;3: e005067.

Address for correspondence: Rene Choi, Department of Ophthalmology, Casey Eye Institute, Oregon Health and Science University, 3375 SW Terwilliger Blvd, Portland, OR 97239, USA; email: choir@ohsu.edu

Rickettsiales in Ticks Removed from Outdoor Workers, Southwest Georgia and Northwest Florida, USA

Elizabeth R. Gleim,[1] L. Mike Conner, Galina E. Zemtsova, Michael L. Levin, Pamela Wong, Madeleine A. Pfaff, Michael J. Yabsley

Author affiliations: Joseph W. Jones Ecological Research Center at Ichauway, Newton, Georgia, USA (E.R. Gleim, L.M. Conner); Oxford College of Emory University, Oxford, Georgia, USA (E.R. Gleim, P. Wong); University of Georgia, Athens, Georgia, USA (E.R. Gleim, M.A. Pfaff, M.J. Yabsley); Centers for Disease Control and Prevention, Atlanta, Georgia, USA (G.E. Zemtsova, M.L. Levin)

DOI: https://doi.org/10.3201/eid2505.180438

We determined the prevalence of selected Rickettsiales in 362 ticks removed from outdoor workers in southwest Georgia and northwest Florida, USA. Persons submitted an average of 1.1 ticks/month. We found *Ehrlichia chaffeensis* in an *Amblyomma maculatum* tick, and Panola Mountain *Ehrlichia* sp. in 2 *A. maculatum* ticks and 1 *Dermacentor variabilis* tick.

The southeastern United States has multiple tick species that can transmit pathogens to humans. The most common tick species, *Amblyomma americanum*, is the vector for the causative agents of human ehrlichioses and southern tick-associated rash illness, among others (*1*). *Dermacentor variabilis* ticks can transmit the causative agent of Rocky Mountain spotted fever, and *Ixodes scapularis* ticks can transmit the causative agents of Lyme disease, babesiosis, and human granulocytic anaplasmosis (*1*). Although less common in the region, *A. maculatum* ticks are dominant in specific habitats and can transmit the causative agent of *Rickettsia parkeri* rickettsiosis (*1*).

Persons who have occupations that require them to be outside on a regular basis might have a greater risk for acquiring a tickborne disease (*2*). Although numerous studies have been conducted regarding risks for tickborne diseases among forestry workers in Europe, few studies have been performed in the United States (*2*,*3*). The studies that have been conducted in the United States have focused on forestry workers in the northeastern region (*2*). However, because of variable phenology and densities of ticks, it is useful to evaluate tick activity and pathogen prevalence in various regions and ecosystems.

Burn-tolerant and burn-dependent ecosystems, such as pine (*Pinus* spp.) and mixed pine forests commonly found in the southeastern United States, have unique tick dynamics compared with those of other habitats (*4*). The objective of this study was to determine the tick bite risk and tickborne pathogen prevalence in ticks removed from forestry workers working in pine and mixed pine forests in southwest Georgia and northwest Florida, USA.

During June 2009–December 2011, forestry workers in southwestern Georgia (7 counties) and northwestern Florida (1 county) submitted ticks crawling on or attached to them. We identified ticks and tested them for selected pathogens (Appendix, https://wwwnc.cdc.gov/EID/article/25/5/18-0438-App1.pdf). Immature forms of the same species from the same day and person were pooled (≤5 nymphs and ≤20 larvae) for testing.

A total of 53 persons submitted 362 ticks (Table). Excluding larvae, the most common tick species submitted was *A. maculatum*, followed by *A. americanum*, *I. scapularis*, and *D. variabilis*. On 4 occasions, 1 person submitted *A. tuberculatum* ticks (3 batches of larvae and 1 batch of nymphs) from a longleaf pine site in Baker County, Georgia. Average submissions per person were 2.6 ticks (median 1 tick), but 1 person submitted 100 ticks. A total of 24 persons submitted ticks more than once, and they submitted an average of 0.08–6.5 ticks/month (overall average submission rate of 1.1 ticks/month). Three ticks were engorged (1 *D. variabilis* adult, 1 *A. americanum* nymph, and 1 *Amblyomma* sp. nymph); only the *Amblyomma* sp. nymph was positive for a pathogen (*R. amblyommatis*).

Rickettsia spp. prevalence was 36.4% in adult, 27.9% in nymphal, and 20% in larval *A. americanum* ticks; *R. amblyommatis* was the only species identified (Table). *Rickettsia* spp. were detected in 23% of *A. maculatum* adults; *R. amblyommatis* was most common (6.0%), followed by

[1]Current affiliation: Hollins University, Roanoke, Virginia, USA.

Table. Prevalence of *Ehrlichia chaffeensis,* PME, and *Rickettsia* spp. in ticks submitted by outdoor workers, southwestern Georgia and northwestern Florida, USA*

Tick species and stage	Months submitted	No. positive ticks/no. tested (%)			*Rickettsia* spp.†
		E. chaffeensis	PME	*Rickettsia* spp.	
Amblyomma americanum, adults	Feb–Sep	0/11 (0)	0/11 (0)	4/11 (36.4)	2 *R. amblyommatis*
A. americanum nymphs‡	Mar–Sep	0/43 (0)	0/43 (0)	12/43 (27.9)	9 *R. amblyommatis*
A. americanum larvae‡	Apr and Oct	0/5 (0)	0/5 (0)	1/5 (20.0)	1 *R.amblyommatis*
Amblyomma sp. nymphs	Jun and Oct	0/3 (0)	0/3 (0)	1/3 (33.3)	1 *R. amblyommatis*§
Amblyomma sp. larvae	Oct	0/5 (0)	0/5 (0)	0/5 (0)	
A. maculatum adults	May–Oct	1/83 (1.2)	2/83 (2.4)¶	18/83 (21.7)	5 *R. amblyommatis*,§ 4 *R. parkeri*,§ 1 *Rickettsia* sp. TR-39/TX125, 2 *Candidatus* R. andeanae
A. tuberculatum nymphs‡	Apr	0/5 (0)	0/5 (0)	1/5 (5.0)	1 novel SFG *Rickettsia* sp.
A. tuberculatum larvae‡	Feb#	0/182 (0)	0/182 (0)	10/182 (5.5)**	10 novel SFG *Rickettsia* sp.**
Dermacentor variabilis adults	Jun–Aug	0/10 (0)	1/10 (10.0)	2/10 (20.0)	1 *R. amblyommatis*§
Ixodes scapularis adults	Oct–Mar	NT	0/15 (0)	7/15 (46.7)	4 *Rickettsia* sp. TR-39, 3 *R. buchneri*

*All *Rickettsia* spp. were identified by sequencing unless otherwise noted. NT, not tested; PME, Panola Mountain *Ehrlichia* sp., SFG, spotted fever group.
†*Rickettsia* spp. for whom amplicons did not provide high-quality bidirectional sequences were categorized as unknown *Rickettsia* spp.
‡Minimum infection prevalence is no. positive tick pools/no. ticks tested.
§The following *R. amblyommatis* samples were identified by restriction fragment length polymorphism analysis: for 1 *D. variabilis* adult, 5 *A. maculatum* adults, and 1 *Amblyomma* sp. nymph; for *A. americanum*, 1 adult, 2 nymphs, and 1 larva. Three *A. maculatum* adults were also identified as containing *R. parkeri* positive by restriction fragment length polymorphism analysis.
¶Data included in Loftis et al. (*5*).
#Date was known only for 1 submission of 20 larvae. Dates for others were not provided when submitted.
**Data included in Zemtsova et al. (*6*).

R. parkeri (4.8%). A previously detected novel *Rickettsia* sp. was identified in 10 of 11 *A. tuberculatum* larval pools and was reported by Zemtsova et al. (*6*). An additional pool of *A. tuberculatum* nymphs was tested in this study and also was positive for the novel *Rickettsia* sp. *E. chaffeensis* was detected in 1 *A. maculatum* adult (prevalence 1.2%), and Panola mountain *Ehrlichia* sp. was detected in 2 *A. maculatum* adults (prevalence 2.4%) and 1 *D. variabilis* adult (prevalence 10%). No ticks were positive for *Borrelia* spp., *E. ewingii,* or *Anaplasma phagocytophilum*.

Thus, forestry workers were found to encounter ticks on a regular basis, and peak encounter rates reflected previously reported tick seasonality in this region (*4*). Only 3 (0.8%) of the ticks submitted were engorged, indicating prompt removal of most ticks and thus low risk for pathogen transmission. *A. maculatum*, a fairly uncommon tick in the southeastern United States, was the most commonly submitted tick. However, *A. maculatum* ticks dominate in regularly burned pine ecosystems (*4*), which is where most of these workers spent their time.

We observed several unique findings related to pathogens during this study. Larvae and nymphs of *A. tuberculatum* ticks were submitted on multiple occasions, a tick rarely reported on humans (*7*). These findings, in conjunction with the identification of a novel *Rickettsia* sp. (*6*), suggest that additional research is warranted. This study also identified *E. chaffeensis* and Panola Mountain *Ehrlichia* in *A. maculatum* ticks. Although *A. americanum* ticks are considered the primary vector of *Ehrlichia* spp., these pathogens have been occasionally reported in questing *A. maculatum* ticks, suggesting that this tick might be involved in their transmission cycles (*5*,*8*). We also detected Panola Mountain *Ehrlichia* in 1 *D. variabilis* tick. Thus, further research regarding these alternative tick species as potential vectors of these pathogens is warranted, particularly in the case of *A. maculatum* ticks, which were a common species on forestry workers and are widespread in this region (*4*).

Acknowledgments

We thank the persons whom submitted ticks for this study and members of the Yabsley and Levin laboratories for providing laboratory assistance.

This study was supported by the Centers for Disease Control and Prevention/University of Georgia (UGA) collaborative grant (#8212, Ecosystem Health and Human Health: Understanding the Ecological Effects of Prescribed Fire Regimes on the Distribution and Population Dynamics of Tick-Borne Zoonoses); the Oxford Research Scholars Program at Oxford College of Emory University; the Joseph W. Jones Ecological Research Center, the Warnell School of Forestry and Natural Resources (UGA); the Southeastern Cooperative Wildlife Disease Study (UGA) through the Federal Aid to Wildlife Restoration Act (50 Statute 917); and Southeastern Cooperative Wildlife Disease Study sponsorship from fish and wildlife agencies of member states.

About the Author

At the time of this study, Dr. Gleim was a research scientist at the University of Georgia, Athens, GA. She is currently a disease ecologist at Hollins University, Roanoke, VA. Her research interests include wildlife and zoonotic diseases with a particular emphasis on tickborne diseases.

References

1. Stromdahl EY, Hickling GJ. Beyond Lyme: aetiology of tick-borne human diseases with emphasis on the south-eastern United States. Zoonoses Public Health. 2012;59(Suppl 2):48–64. http://dx.doi.org/10.1111/j.1863-2378.2012.01475.x
2. Covert DJ, Langley RL. Infectious disease occurrence in forestry workers: a systematic review. J Agromed. 2002;8:95–111. http://dx.doi.org/10.1300/J096v08n02_12
3. Lee S, Kakumanu ML, Ponnusamy L, Vaughn M, Funkhouser S, Thornton H, et al. Prevalence of Rickettsiales in ticks removed from the skin of outdoor workers in North Carolina. Parasit Vectors. 2014;7:607. http://dx.doi.org/10.1186/s13071-014-0607-2
4. Gleim ER, Conner LM, Berghaus RD, Levin ML, Zemtsova GE, Yabsley MJ. The phenology of ticks and the effects of long-term prescribed burning on tick population dynamics in southwestern Georgia and northwestern Florida. PLoS One. 2014;9:e112174. http://dx.doi.org/10.1371/journal.pone.0112174
5. Loftis AD, Kelly PJ, Paddock CD, Blount K, Johnson JW, Gleim ER, et al. Panola Mountain *Ehrlichia* in *Amblyomma maculatum* from the United States and *Amblyomma variegatum* (Acari: Ixodidae) from the Caribbean and Africa. J Med Entomol. 2016;53:696–8. http://dx.doi.org/10.1093/jme/tjv240
6. Zemtsova GE, Gleim E, Yabsley MJ, Conner LM, Mann T, Brown MD, et al. Detection of a novel spotted fever group *Rickettsia* in the gophertortoise tick. J Med Entomol. 2012; 49:783–6. http://dx.doi.org/10.1603/ME11264
7. Goddard J. A ten-year study of tick biting in Mississippi: implications for human disease transmission. J Agromed. 2002;8:25–32. http://dx.doi.org/10.1300/J096v08n02_06
8. Allerdice ME, Hecht JA, Karpathy SE, Paddock CD. Evaluation of Gulf Coast ticks (Acari: Ixodidae) for *Ehrlichia* and *Anaplasma* species. J Med Entomol. 2017;54:481–4.

Address for correspondence: Elizabeth R. Gleim, Department of Biology and Environmental Studies. Hollins University, 8003 Fishburn Dr, PO Box 9615, Roanoke, VA 24020, USA; email: egleim@hollins.edu

Hepatic Brucelloma Diagnosis and Long-Term Treatment, France

Marie Amsilli, Olivier Epaulard, Jean-Paul Brion, Patricia Pavese, Christian Letoublon, Isabelle Pelloux, Max Maurin

Author affiliations: Centre Hospitalier Universitaire de Grenoble, Grenoble, France (M. Amsilli, O. Epaulard, J.-P. Brion, P. Pavese, C. Letoublon, I. Pelloux, M. Maurin); Université Grenoble Alpes, Grenoble (O. Epaulard, C. Letoublon, M. Maurin)

DOI: https://doi.org/10.3201/eid2505.180613

We report a case of hepatic brucelloma in France. This diagnosis may be suspected in any patient who has a liver abscess after traveling to a brucellosis-endemic area. *Brucella* spp. may be detected by PCR in the liver tissue or suppuration. Abscess drainage and prolonged antimicrobial therapy help achieve healing.

Brucellosis is a zoonosis found worldwide (*1*,*2*) caused by gram-negative, facultative intracellular bacteria of the genus *Brucella*. Approximately 500,000 new infections are diagnosed annually, mainly in the Mediterranean basin, the Middle East, Latin America, and Asia (*1*–*3*). Brucellosis is a rare and mainly imported disease in other countries, including France (*1*,*4*). *Brucella* infection usually occurs after contact with infected animals or consumption of contaminated unpasteurized dairy products. Hepatic brucelloma (HB) is a chronic form of brucellosis arising up to 40 years after initial infection (*1*,*3*,*5*). Only 60 cases (1%–2% of all brucellosis infections) have been reported in English-language literature since 1904 (*1*,*3*,*5*,*6*). HB is associated with nonspecific systemic clinical symptoms (e.g., fever, malaise, weight loss, upper abdominal pain), moderate biologic abnormalities, and typical hypodense hepatic lesion with peripheral enhancement and central calcification (*1*–*3*,*5*,*6*).

In April 2015, a previously healthy 55-year-old woman was referred to Grenoble University Hospital after 7 days of fever, asthenia, and weight loss. She had lived in France for 20 years, but had been born in and had traveled every year to Algeria. Her clinical examination was unrevealing. Blood tests showed moderate inflammation and anicteric cholestasis (Table). Hepatic ultrasound (HUS) and computed tomography (CT) confirmed a defect 60 mm in diameter in liver segments IV and VIII with several subcapsular liquid collections and central calcification (Appendix Figure, panel A, https://wwwnc.cdc.gov/EID/article/25/5/18-0613-App1.pdf).

Blood cultures remained sterile. Serologic test results were negative for HIV, amebiasis, and echinococcosis, but positive for *Yersinia enterocolitica* serotype O:9 and *Brucella* sp. (Table). HUS-guided drainage of the abscess yielded thick purulent fluid. Fluid cultures were negative, but we detected *Brucella melitensis* DNA by PCR amplification and sequencing of the 16S rRNA–encoding gene. Histological findings of liver tissue were compatible with a chronic abscess. We confirmed diagnosis on 2 occasions by PCR detection of *Brucella* DNA in the liver abscess, as previously reported (*1*,*3*,*5*–*7*).The serologic profile was suggestive of chronic brucellosis combining low IgM but strong IgG *Brucella* antibody titers (*1*,*3*,*5*,*7*). However, *Brucella* serologic diagnosis is poorly specific, due to antigenic cross-reactions (e.g.,

Table. Diagnostic and blood tests on patient with hepatic brucellosis, Grenoble, France*

Test	Reference value	2015 Apr	2015 Nov	2016 Jan
Rose Bengal plate agglutination test (bioMérieux, https://www.biomerieux.com)	NA	Strongly positive	Positive	Negative
Tube agglutination test (Elitech, https://www.elitechgroup.com)	≥80	160	20	<20
Immunofluorescence IgM (BioRad, http://www.bio-rad.com)	≥40	<20	<20	<20
Immunofluorescence IgG (BioRad)	≥80	160	160	320
Brucella PCR testing of liver tissue biopsies	NA	Positive for 16S rDNA	NA	Positive for *bcsp31* gene
Blood cultures	NA	Negative	Negative	Negative
Liver abscess and tissue cultures† (bacteria, fungi and mycobacteria)	NA	Negative	NA	Negative
C-reactive protein, mg/L	<3	56	5	4
Fibrinogen, g/L	2.1–4.1	6.1		
Leukocyte count, G/L	4–11	8.5	5	4.9
Neutrophil count, G/L	1.6–8.8	5.9	2.5	2.1
Thrombocyte count, G/L	150–400	489	287	284
Bilirubin, μmol/L	3–17	5	5	5
Alkaline phosphatase, IU/L	50–136	158	85	69
γ-glutamyl transferase, IU/L	5–55	107	31	23
Aspartate aminotransferase, IU/L	15–37	20	16	14
Alanine aminotransferase, IU/L	12–78	28	26	22

*NA, not applicable.
†Tissues were cultured for bacteria, fungi, and mycobacteria.

Y. enterocolitica 0:9) and residual antibodies related to past exposure in patients from *Brucella*-endemic areas (*3*). *Brucella* cultures of blood or tissue samples and PCR on serum are usually not contributing factors in chronic focal brucellosis (*1*,*3*,*5*–*7*).

Upon diagnosis of hepatic brucellosis, we administered doxycycline plus rifampin, replacing initial empirical treatment with ceftriaxone and metronidazole for suspected pyogenic abscess. After 2 months of treatment, clinical and biologic abnormalities had regressed. CT with contrast revealed substantial reduction of the abscess, but also thrombosis of the median hepatic vein, infiltration of the gallbladder, and new lesions in segment VIII (Appendix Figure, panel B). We continued the antimicrobial therapy and surgery was recused. After 6 months of treatment, antibody titers were decreasing (Table). Three months later, positron emission tomography highlighted intense focal uptake in segments IV and VIII. Fluid from a second HUS-guided drainage was positive by *Brucella*-specific PCR test (Table). We changed the treatment to trimethoprim/sulfamethoxazole plus doxycycline for another 6 months. At completion, magnetic resonance imaging showed abscess reduction with stable central calcification.

HB patients are difficult to manage because of lack of optimized treatment (*1*,*8*), and clinical course is the only reliable evidence in disease control (*1*,*3*,*9*).Our treatment was conservative, including 15 months of antimicrobial therapy and repeated HUS drainages. We continued treatment despite worsening radiological findings (including onset of cholecystitis and deep vein thrombosis) on the basis of early favorable clinical course and patient compliance (*1*–*3*,*8*,*9*). We monitored the improvement of radiological lesions using positron emission tomography–computed tomography and magnetic resonance imaging, both of which are sensitive for diagnosis although not assessed for monitoring, for 15 months after treatment. Few studies have described the radiological evolution over time in complicated cases (*1*–*3*,*5*,*8*), but persistence of calcifications is usual in HB (*2*,*3*,*9*).

Administration of doxycycline plus rifampin, an aminoglycoside, or both is currently recommended for brucellosis (*1*–*3*); choice and duration of treatment must be individualized to the patient's symptomatology and treatment tolerability (*1*–*3*,*8*,*9*) and the involved tissues (*2*,*8*). Surgical resection and percutaneous drainage of the abscess are both reported as effective adjunctive therapy, with surgery indicated when evacuation of pus is ineffective or clinical symptoms persist despite drainage (*1*–*3*,*5*,*6*). A short course of an aminoglycoside could have been added at the time of radiological diagnosis of complications, as reported in other focal brucellosis with poor clinical evolution (*2*,*8*,*9*), in which a prolonged regimen (6–52 weeks) is also described (*3*,*8*,*9*). As of January 2019, after 2.5 years of treatment and follow-up care, our patient is considered cured. Relapses mainly occur within a few months of treatment completion but may occasionally occur later (*2*,*5*).

Any patient with characteristic liver abscess after traveling in brucellosis-endemic areas should undergo serologic testing for a presumptive diagnosis, and PCR testing of abscess fluid or hepatic tissue for confirmation of brucelloma. A conservative treatment combining long-term antimicrobial therapy and repeated HUS drainage may be effective. Long-term clinical comprehensive follow-up is required.

Acknowledgments

We thank Linda Northrup for English editing. We thank the patient for consenting to publication of her clinical data.

About the Author

Dr. Amsilli is an infectious and tropical diseases physician. Her research interests are emerging infectious diseases and medicine quality.

References

1. Barutta L, Ferrigno D, Melchio R, Borretta V, Bracco C, Brignone C, et al. Hepatic brucelloma. Lancet Infect Dis. 2013;13:987–93. http://dx.doi.org/10.1016/S1473-3099(13)70197-X
2. Franco MP, Mulder M, Gilman RH, Smits HL. Human brucellosis. Lancet Infect Dis. 2007;7:775–86. http://dx.doi.org/10.1016/S1473-3099(07)70286-4
3. Ariza J, Pigrau C, Cañas C, Marrón A, Martínez F, Almirante B, et al. Current understanding and management of chronic hepatosplenic suppurative brucellosis. Clin Infect Dis. 2001;32:1024–33. http://dx.doi.org/10.1086/319608
4. Santé Publique France, Institut National de Veille Sanitaire. Brucellosis—epidemiologic data2016 [in French]. 2016 [cited 2018 Mar 5]. http://invs.santepubliquefrance.fr/Dossiers-thematiques/Maladies-infectieuses/Zoonoses/Brucellose/Donnees-epidemiologiques/Brucellose-Donnees-epidemiologiques-2016
5. de Dios Colmenero J, Queipo-Ortuño MI, Reguera JM, Suarez-Muñoz MA, Martín-Carballino S, Morata P. Chronic hepatosplenic abscesses in Brucellosis. Clinico-therapeutic features and molecular diagnostic approach. Diagn Microbiol Infect Dis. 2002;42(3):159–67. http://dx.doi.org/10.1016/S0732-8893(01)00344-3
6. Heller T, Bélard S, Wallrauch C, Carretto E, Lissandrin R, Filice C, et al. Patterns of hepatosplenic *Brucella* abscesses on cross-sectional imaging: a review of clinical and imaging features. Am J Trop Med Hyg. 2015;93:761–6. http://dx.doi.org/10.4269/ajtmh.15-0225
7. Morata P, Queipo-Ortuño MI, Reguera JM, Miralles F, Lopez-Gonzalez JJ, Colmenero JD. Diagnostic yield of a PCR assay in focal complications of brucellosis. J Clin Microbiol. 2001;39:3743–6. http://dx.doi.org/10.1128/JCM.39.10.3743-3746.2001
8. Al-Tawfiq JA. Therapeutic options for human brucellosis. Expert Rev Anti Infect Ther. 2008;6:109–20.
9. Solera J. Update on brucellosis: therapeutic challenges. Int J Antimicrob Agents. 2010;36(Suppl 1):S18–20. http://dx.doi.org/10.1016/j.ijantimicag.2010.06.015

Address for correspondence: Marie Amsilli, Centre Hospitalier Universitaire Grenoble Alpes—Service de Maladies Infectieuses, BP 217, Grenoble 38043, France; email: marieamsilli@gmail.com

Human Monkeypox in Sierra Leone after 44-Year Absence of Reported Cases

Mary G. Reynolds, Nadia Wauquier, Yu Li, Panayampalli Subbian Satheshkumar, Lansana D. Kanneh, Benjamin Monroe, Jacob Maikere, Gbessay Saffa, Jean-Paul Gonzalez, Joseph Fair, Darin S. Carroll, Amara Jambai, Foday Dafae, Sheik Humarr Khan, Lina M. Moses

Author affiliations: Centers for Disease Control and Prevention, Atlanta, Georgia, USA (M.G. Reynolds, Y. Li, P.S. Satheshkumar, B. Monroe, D.S. Carroll); MRI Global–Global Health Surveillance and Diagnostics, Gaithersburg, Maryland, USA (N. Wauquier); Kenema Government Hospital, Kenema, Sierra Leone (L.D. Kanneh, S.H. Khan); Médecins Sans Frontières, Brussels, Belgium (J. Maikere); Ministry of Health and Sanitation, Bo, Sierra Leone (G. Saffa); Center of Excellence for Emerging Zoonotic and Animal Diseases, Manhattan, Kansas, USA (J.-P. Gonzalez); Texas A&M University Agrilife Research, College Station, Texas, USA (J. Fair); Ministry of Health and Sanitation, Freetown, Sierra Leone (A. Jambai, F. Dafae, S.H. Khan); Tulane University, New Orleans, Louisiana, USA (L.M. Moses)

DOI: https://doi.org/10.3201/eid2505.180832

We note the reemergence of human monkeypox in Sierra Leone following a 44-year absence of reported disease. The persons affected were an 11-month-old boy and, several years later, a 35-year-old man. The reappearance of monkeypox in this country suggests a need for renewed vigilance and awareness of the disease and its manifestations.

Monkeypox, a tropical zoonosis with an estimated death rate of 15% in children, is a resurgent presence in several countries in West and Central Africa (*1*,*2*). Before 2000, only 21 cases of monkeypox had been reported from these regions, including a single case in Sierra Leone in 1970 (*3*). The disease had not been observed in Sierra Leone since then, although a 2007 survey for orthopoxvirus antibodies among populations near Kenema, Sierra Leone, generated evidence to suggest ongoing circulation of orthopoxviruses in the area (*4*).

On March 18, 2014, a resident of Kpetema town in Sierra Leone brought her 11-month-old son to the community health post in nearby Mano village. There, he was evaluated for fever and released. The child failed to improve, and the next day his mother again sought medical care, this time from the community health center (CHC) in Koribondo. At this time, the child remained febrile and was exhibiting a

nascent-stage rash. At the Koribondo CHC the child was given a presumptive diagnosis of early stage chickenpox and sent home.

Within 2 days of the child's evaluation at the Koribondo CHC, pustular, umbilicated lesions had spread to cover his body, including his face, mouth, oral mucosa, trunk, back, palms, and genital area. In addition, the child was experiencing sweats, chills, vomiting, loss of appetite, cough, and pruritus. On March 21, the child was taken to the Médicins sans Frontières Gondama Referral Center and was admitted with fever (body temperature 38.9°C) and disseminated vesiculopustular rash. Notably, lymphadenopathy was absent. On hospital day 4 (day 8 after fever onset), physicians from Médicins sans Frontières working in a pediatric ward at the facility alerted national authorities that they suspected the child might have monkeypox. After consultation with the Directorate of Disease Prevention and Control of the Sierra Leone Ministry of Health and Sanitation, Kenema scientists contacted the Centers for Disease Control and Prevention (CDC) in Atlanta, Georgia, USA.

Diagnostic specimens were collected from the patient on April 1. At that time his rash was desquamating. Lesion crusts and serum samples were obtained, and specimens were shipped to CDC on April 4. On April 8, real-time PCR testing for nonvariola *Orthopoxvirus* and for West African variant monkeypox virus (*5*) yielded weak positive findings from both the lesion and serum specimens. The patient's serum sample also tested positive for the presence of *Orthopoxvirus* IgG and IgM (*6*).

No viable virus was detected in the specimens. Further genetic characterization of the virus was unsuccessful owing to the limited quality and quantity of specimens.

Upon confirmation of monkeypox etiology, investigators from the Bo District Surveillance Office and the Lassa Fever Outreach Program traveled to the child's town (Kpetema; Figure) to interview his parents. By that time, the child had recovered. The child's mother denied that he had had any contact with persons exhibiting a monkeypox-like illness in the 2 weeks before onset of his illness. The mother also denied that the child had had any history of contact with animals. However, both the mother and father of the boy stated that they regularly prepare and consume meat from wild animals. The mother and father also confirmed that small rodents were sometimes present in the family house.

Figure. Locations of monkeypox cases in Sierra Leone from 2014 (Kpetema) and 1970 (Aguebu). Map credits: Esri, HERE, Delorme, MapmyIndia, © OpenStreetMap contributors, and the GIS user community.

On March 25, 2017, a 35-year-old male farmer in Pujehun district came to Pujehun Government Hospital in Sierra Leone with fever, generalized body pain, enlarged cervical lymph nodes, dysphagia, malaise, and macular rash with cropping of papules and macules. Various samples were taken and shipped out of the country for laboratory investigations. Monkeypox was confirmed, and community sensitization was instituted.

The detection of monkeypox virus infection in an 11-month-old child and a 35-year-old man signals the possible reemergence of this disease in Sierra Leone (*3*), from which it had not been reported for 44 years. The reappearance of monkeypox in Sierra Leone suggests a need for renewed vigilance and heightened awareness of the disease and its manifestations. In the early stages of illness, monkeypox can be mistaken for chickenpox, as happened in the case of the child. The confusion led to a delay in diagnosing and reporting the Kpetema case.

Multiple factors are probably driving the resurgence of monkeypox in West and Central Africa. Increasing population susceptibility is likely to be one (*7*). Smallpox vaccine has been shown to confer protection against monkeypox virus infection (*8*). However, routine vaccination ceased worldwide after the declaration by the World Health Organization in 1980 that smallpox had been eradicated. The lack of smallpox vaccination has led to the steady accumulation of poxvirus-susceptible human hosts in the areas of West and Central Africa where humans routinely encounter sylvatic animals, some of which may harbor monkeypox virus. Disease control efforts could be further aided by dedicated surveillance for monkeypox virus among target animal species (*9*).

Acknowledgments

We wish to acknowledge the tragic death of Sheik Humarr Khan, chief physician of the Lassa Fever Research Program at Kenema Government Hospital in Kenema, Sierra Leone, who provided countless hours of compassionate care for Ebola patients until he himself succumbed to the disease on July 29, 2014. We also note with sadness the sudden, recent death of Foday Dafae, who devoted his long professional career to the care and wellbeing of all Sierra Leoneans. We thank Olga Urazova for anti-orthopoxvirus serology.

This investigation received partial funding support from Tulane University's Lassa Fever Project and from Metabiota.

About the Author

Dr. Reynolds is the deputy chief of the Poxvirus and Rabies Branch in the Division of High-Consequence Pathogens and Pathology, National Center for Emerging and Zoonotic Infectious Diseases, at the Centers for Disease Control and Prevention, Atlanta, Georgia, USA. Her research interests include the epidemiology of poxvirus-associated diseases.

References

1. Berthet N, Nakouné E, Whist E, Selekon B, Burguière AM, Manuguerra JC, et al. Maculopapular lesions in the Central African Republic. Lancet. 2011;378:1354. http://dx.doi.org/10.1016/S0140-6736(11)61142-2
2. Learned LA, Reynolds MG, Wassa DW, Li Y, Olson VA, Karem K, et al. Extended interhuman transmission of monkeypox in a hospital community in the Republic of the Congo, 2003. Am J Trop Med Hyg. 2005;73:428–34. http://dx.doi.org/10.4269/ajtmh.2005.73.428
3. Foster SO, Brink EW, Hutchins DL, Pifer JM, Lourie B, Moser CR, et al. Human monkeypox. Bull World Health Organ. 1972;46:569–76.
4. MacNeil A, Abel J, Reynolds MG, Lash R, Fonnie R, Kanneh LD, et al. Serologic evidence of human orthopoxvirus infections in Sierra Leone. BMC Res Notes. 2011;4:465. http://dx.doi.org/10.1186/1756-0500-4-465
5. Li Y, Zhao H, Wilkins K, Hughes C, Damon IK. Real-time PCR assays for the specific detection of monkeypox virus West African and Congo Basin strain DNA. J Virol Methods. 2010;169:223–7. http://dx.doi.org/10.1016/j.jviromet.2010.07.012
6. Karem KL, Reynolds M, Braden Z, Lou G, Bernard N, Patton J, et al. Characterization of acute-phase humoral immunity to monkeypox: use of immunoglobulin M enzyme-linked immunosorbent assay for detection of monkeypox infection during the 2003 North American outbreak. Clin Diagn Lab Immunol. 2005;12:867–72.
7. Reynolds MG, Carroll DS, Karem KL. Factors affecting the likelihood of monkeypox's emergence and spread in the post-smallpox era. Curr Opin Virol. 2012;2:335–43. http://dx.doi.org/10.1016/j.coviro.2012.02.004
8. Jezek Z, Grab B, Paluku KM, Szczeniowski MV. Human monkeypox: disease pattern, incidence and attack rates in a rural area of northern Zaire. Trop Geogr Med. 1988;40:73–83.
9. Doty JB, Malekani JM, Kalemba LN, Stanley WT, Monroe BP, Nakazawa YU, et al. Assessing monkeypox virus prevalence in small mammals at the human–animal interface in the Democratic Republic of the Congo. Viruses. 2017;9:283. http://dx.doi.org/10.3390/v9100283

Address for correspondence: Mary G. Reynolds, Centers for Disease Control and Prevention, 1600 Clifton Rd NE, Mailstop A30, Atlanta, GA 30329, USA; email: nzr6@cdc.gov

Increase in Lassa Fever Cases in Nigeria, January–March 2018

Elsie A. Ilori,[1] Christina Frank,[1] Chioma C. Dan-Nwafor, Oladipupo Ipadeola, Amrei Krings, Winifred Ukponu, Oboma E. Womi-Eteng, Ayodele Adeyemo, Samuel K. Mutbam, Emmanuel O. Musa, Clement L.P. Lasuba, Wondimagegnehu Alemu, Sylvanus Okogbenin, Ephraim Ogbaini, Uche Unigwe, Emeka Ogah, Robinson Onoh, Chukwuyem Abejegah, Olufemi Ayodeji, Chikwe Ihekweazu

Author affiliations: Nigeria Centre for Disease Control, Abuja, Nigeria (E.A. Ilori, C.C. Dan-Nwafor, O. Ipadeola, W. Ukponu, O.E. Womi-Eteng, C. Ihekweazu); Robert Koch Institute, Berlin, Germany (C. Frank, A. Krings); African Field Epidemiology Network, Abuja (C.C. Dan-Nwafor); US Centers for Disease Control and Prevention, Abuja (O. Ipadeola); University of Maryland, Abuja (W. Ukponu); eHealth Africa, Abuja (A. Adeyemo); World Health Organization Abuja Country Office, Abuja (S.K. Mutbam, E.O. Musa, C.L.P. Lasuba, W. Alemu); Irrua Specialist Teaching Hospital, Edo, Nigeria (S. Okogbenin, E. Ogbaini); Federal Teaching Hospital, Abakiliki, Nigeria (U. Unigwe, E. Ogah, R. Onoh); Federal Medical Centre, Owo, Nigeria (C. Abejegah, O. Ayodeji)

DOI: https://doi.org/10.3201/eid2505.181247

We reviewed data pertaining to the massive wave of Lassa fever cases that occurred in Nigeria in 2018. No new virus strains were detected, but in 2018, the outbreak response was intensified, additional diagnostic support was available, and surveillance sensitivity increased. These factors probably contributed to the high case count.

A massive wave of laboratory-confirmed cases of Lassa fever occurred in Nigeria in 2018. Whether this high case count was caused by a new virus variant, increased seasonal incidence, improved case recognition, availability of laboratory diagnostics and therapy, or a combination of these factors is unknown. We set out to determine the factors that contributed to this outbreak using data available through the Nigerian Disease Surveillance System.

Lassa fever is endemic in Nigeria and peaks during the first 12 weeks of the year (January–March; Figure) (https://ncdc.gov.ng/themes/common/files/sitreps/b7cd08c8047e52ceabb09e5318a3b0a7.pdf). A total of 107 laboratory-confirmed cases were reported during the first 12 weeks of 2017 and 394 during the same period in 2018. Among confirmed and probable cases, 50 deaths were reported during the peak season in 2017 and 104 in 2018. In the neighboring states of Edo and Ondo, 45.0% of confirmed cases occurred in 2017 and 66.0% in 2018. These states have access to the long-established and largest Lassa fever treatment center that has Lassa virus diagnostic capabilities in Nigeria. Although Edo and Ondo comprise only 4.6% of Nigeria's population, the population in these states accounted for 74.6% of the increase in confirmed cases during the 2017 and 2018 peak seasons. Another area with a strong increase in case numbers in 2018 was the nonadjacent Ebonyi State, where another laboratory was outfitted to conduct Lassa virus diagnostics by early 2018.

Evidence from sequencing studies yielded no indication that viruses circulating in 2018 were different from those found in previous years (*1*). Phylogenetic data suggest multiple zoonotic infections instead of extensive person-to-person transmission.

The increased case numbers in Edo, Ondo, and Ebonyi could not be accounted for by gross population changes; these states are distant from the refugee emergency in northeastern Nigeria (http://reporting.unhcr.org/node/21275). Studies on climatic and other environmental circumstances (e.g., new agricultural practices or larger harvests) that could have potentially contributed to changes in the way and frequency humans come into contact with the Lassa virus reservoir, *Mastomys natalensis* mice, have not been established. Also, data on rodent abundance are not available.

However, in 2018, many changes occurred in Nigeria regarding Lassa virus surveillance and treatment. Instead of only 1 Lassa virus laboratory for Edo and Ondo and 1 in Lagos, 2 additional laboratories (in Ebonyi and Abuja) started providing diagnostic services in early 2018. Sample transport logistics had improved, and patients' samples were transported and tested without charge. Considering that laboratory confirmation is a prerequisite for counting cases, laboratory capacity building directly affects surveillance case numbers. By early 2018, Lassa fever surveillance had been strengthened by the formulation of standard operating procedures, and rapid response teams provided capacity building and support to affected states 4 weeks earlier than they did in 2017. Clinical cases of Lassa fever need to be treated in isolation facilities, and by 2018, additional treatment centers had been assessed and were being supported by the federal government. At this time, ribavirin was also available to patients without charge, and the media actively advertised this message, encouraging patients to seek medical treatment. In addition, Lassa fever

[1]These first authors contributed equally to this article.

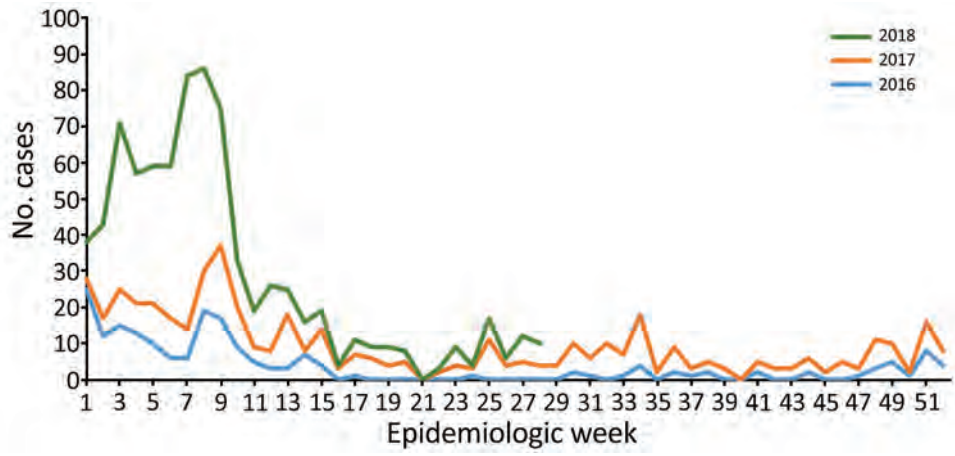

Figure. Weekly trends of confirmed Lassa fever cases, Nigeria, 2016–2018.

received strong media attention in early January 2018 because of an incident in a healthcare facility where 3 of 4 infected healthcare workers died.

Surveillance data are incomplete for 2018, but higher surveillance sensitivity is visible in the available data from the peak 2017 and 2018 seasons. The percentage of suspected Lassa fever cases testing positive decreased from 31.0% in 2017 to 21.6% in 2018 (30.2% decrease). Nosebleed, an indicator of disease severity in nonfatal confirmed cases, was noted on 10.8% of case report forms for surviving patients in 2017, but this frequency declined to 2.6% in 2018 (75.9% decrease), and the case-fatality ratio among confirmed and probable cases declined from 43.9% in 2017 to 25.8% in 2018 (41.2% decrease). Disease severity and case-fatality ratios are also influenced by the timeliness of patients seeking treatment and treatment availability. The decrease in the 3 aforementioned factors (percentage of Lassa virus–positive cases, percentage of nonfatal confirmed cases with nosebleeds, and case-fatality ratio) reflects lowering of the surveillance threshold to detect cases. More patients with comparatively mild disease probably sought treatment because of the increased Lassa fever publicity and communication about available therapy; moreover, additional suspected cases were probably detected in the community through enhanced contact tracing and active case finding.

In conclusion, we cannot exclude that early 2018 represents a particularly active Lassa fever season in Nigeria, especially in Edo, Ondo, and Ebonyi. However, no available evidence indicates that higher case numbers could be attributed to new virus strains. The addition of new laboratories with growing surveillance capacities, an overall intensified response, and increasing surveillance sensitivity are likely major drivers of the high number of Lassa fever cases reported in early 2018. The weekly case numbers reported in early 2019 slightly surpass those from 2018 (https://ncdc.gov.ng/themes/common/files/sitreps/b94e459c79a59ca9d667a55539cda5db.pdf). Improved identification of Lassa fever cases in Nigeria provides the basis for epidemiologic studies of disease and effective disease control. Also, each identified case treated in isolation centers reduces the likelihood of person-to-person transmission.

About the Author

Mrs. Ilori is the national Lassa Fever Technical Working Group team lead at the Nigeria Centre for Disease Control in Abuja, Nigeria. She coordinates the Lassa fever response activities and production of various guidelines for Lassa fever control in Nigeria. Dr. Frank is an epidemiologist at the Robert Koch Institute in Berlin, Germany. Her research interests are emerging infections and zoonoses.

Reference

1. Kafetzopoulou LE, Pullan ST, Lemey P, Suchard MA, Ehichioya DU, Pahlmann M, et al. Metagenomic sequencing at the epicenter of the Nigeria 2018 Lassa fever outbreak. Science. 2019;363:74–7. http://dx.doi.org/10.1126/science.aau9343

Address for correspondence: Chioma C. Dan-Nwafor, Nigeria Centre for Disease Control, Surveillance and Epidemiology, Plot 801 Ebitu Ukiwe St, Jabi, Abuja 0000 Nigeria; email: chioma.dannwafor@ncdc.gov.ng

Rabies Acquired through Mucosal Exposure, China, 2013

Hong Zhao, Jian Zhang, Cong Cheng, Yi-Hua Zhou

Author affiliations: Second Hospital of Nanjing at Southeast University, Nanjing, China (H. Zhao, J. Zhang, C. Cheng); Nanjing University Medical School, Nanjing (Y.-H. Zhou)

DOI: https://doi.org/10.3201/eid2505.181413

In China in 2013, a man acquired rabies after sucking wounds of his son, who had been bitten by a stray dog. The man declined postexposure prophylaxis (hyperimmunoglobulin and vaccine) and died; the son accepted prophylaxis and survived. Physicians should be aware of rabies transmission through mucosal exposure and encourage postexposure prophylaxis.

Rabies, caused by the rabies virus (family *Rhabdoviridae*, genus *Lyssavirus*), is a zoonotic encephalitis with a mortality rate of almost 100%. Although rare in industrialized countries because of mandatory vaccination of dogs and other domestic pets, rabies frequently occurs in developing countries (*1*). In industrialized countries, the virus is transmitted to humans mostly by contact with wild animals; in developing countries, by dog bites (*1*). We report a fatal case of rabies in a man who had sucked the wounds of his son who had been bitten by a stray dog. The study was approved by the institutional ethics review committees of the Second Hospital of Nanjing and Nanjing Drum Tower Hospital, Nanjing, China, and was performed in accordance with the ethics standards in the 1964 Declaration of Helsinki and its later amendments. Written informed consent was obtained from the patient's son.

The patient was a 41-year-old man from a village in northern Jiangsu Province, China. On August 19, 2013, the man's 17-year-old son was bitten on the left leg by a stray dog, leaving bleeding wounds on the lower part of the gastrocnemius muscles. Because of concern about rabies, the man and other family members immediately washed the boy's wounds with water, and the man's neighbors killed and buried the stray dog. While washing his son's wounds, the man made a dramatic scene by crouching down to suck "toxic blood" from his son's wounds and spitting out the blood several times. He then sent his son to a local hospital, where the physicians immediately (within 1 hour after the dog bite) cleaned the wounds by using standard procedures and administered postexposure prophylaxis (rabies hyperimmunoglobulin and the first dose of freeze-dried rabies vaccine for human use [Vero cells]; Liaoning Chengda Biotechnology, http://www.cdbio.cn). The son received another 4 doses of rabies vaccine on days 3, 7, 14, and 28 after the bite. Because the man had sucked the wounds, the physicians also recommended that he receive postexposure prophylaxis (rabies hyperimmunoglobulin and vaccine); however, the man declined because of concern over the relatively high cost and because he considered that he had spat out all the sucked blood and could not have "so bad luck." Thus, the man did not receive any medical treatment.

On September 23, 2013, the man was referred to the Nanjing Second Hospital, the main infectious diseases hospital in Jiangsu, with a 2-day history of general malaise, sleep disturbance, waking in a cold sweat, irritability to air and sound, involuntary contraction of pharyngeal muscles, and choking when drinking and eating. At the time of examination, the patient showed remarkable agitation, delirium, and hallucination. Saliva was collected and tested for rabies viral RNA by reverse transcription PCR; the result was positive for rabies virus. The patient received systemic support and symptomatic therapy but died on September 24. The clinical course of rabies in this patient progressed rapidly; although the incubation period for this patient was 33 days (in agreement with incubation period of 20–60 days for most patients), he died 3 days after the appearance of furious (classical) symptoms. The patient's son remained in good health 5 years later.

The main route for rabies virus transmission is bites of infected dogs and other animals. Unusual transmission routes include mucosal exposure, aerosol inhalation, organ transplantation (*2*–*7*), and contamination of broken skin by blood from wounds of a person bitten by an infected dog (*8*). The most effective way to control rabies in humans is mandatory vaccination of all dogs and other domestic pets, but widespread vaccination is not feasible in China and resource-limited countries. Although China's central and local governments recommend that all domestic pets be vaccinated against rabies, implementation of vaccination is difficult in many rural areas of China. Thus, for preventing rabies in humans in rabies-endemic countries and regions, postexposure prophylaxis is crucial.

The rabies case that we report was acquired after sucking wounds created by the bite of a presumably rabies-infected dog. Evidently, the virus invaded the patient through his oral mucosa. Unfortunately, the patient declined postexposure prophylaxis and died.

This case underscores the possibility of rabies transmission by mucosal exposure, which should be made widely known to the public. To further reduce this disease in

rabies-endemic countries, physicians should emphasize the high likelihood of transmission of rabies virus after mucosal exposure and try to persuade persons at risk to receive postexposure prophylaxis.

About the Author

Dr. Zhao is a chief clinician specializing in the diagnosis and treatment of infectious diseases at the Department of Infectious Diseases, Second Hospital of Nanjing. Her research interests include viral hepatitis and other viral diseases.

References

1. Etheart MD, Kligerman M, Augustin PD, Blanton JD, Monroe B, Fleurinord L, et al. Effect of counselling on health-care-seeking behaviours and rabies vaccination adherence after dog bites in Haiti, 2014-15: a retrospective follow-up survey. Lancet Glob Health. 2017;5:e1017–25. http://dx.doi.org/10.1016/S2214-109X(17)30321-2
2. Kan VL, Joyce P, Benator D, Agnes K, Gill J, Irmler M, et al. Risk assessment for healthcare workers after a sentinel case of rabies and review of the literature. Clin Infect Dis. 2015;60:341–8. http://dx.doi.org/10.1093/cid/ciu850
3. Srinivasan A, Burton EC, Kuehnert MJ, Rupprecht C, Sutker WL, Ksiazek TG, et al.; Rabies in Transplant Recipients Investigation Team. Transmission of rabies virus from an organ donor to four transplant recipients. N Engl J Med. 2005;352:1103–11. http://dx.doi.org/10.1056/NEJMoa043018
4. Vora NM, Basavaraju SV, Feldman KA, Paddock CD, Orciari L, Gitterman S, et al.; Transplant-Associated Rabies Virus Transmission Investigation Team. Raccoon rabies virus variant transmission through solid organ transplantation. JAMA. 2013;310:398–407. http://dx.doi.org/10.1001/jama.2013.7986
5. Ross RS, Wolters B, Hoffmann B, Geue L, Viazov S, Grüner N, et al. Instructive even after a decade: complete results of initial virological diagnostics and re-evaluation of molecular data in the German rabies virus "outbreak" caused by transplantations. Int J Med Microbiol. 2015;305:636–43. http://dx.doi.org/10.1016/j.ijmm.2015.08.013
6. Zhou H, Zhu W, Zeng J, He J, Liu K, Li Y, et al. Probable rabies virus transmission through organ transplantation, China, 2015. Emerg Infect Dis. 2016;22:1348–52. http://dx.doi.org/10.3201/eid2208.151993
7. Chen S, Zhang H, Luo M, Chen J, Yao D, Chen F, et al. Rabies virus transmission in solid organ transplantation, China, 2015–2016. Emerg Infect Dis. 2017;23:1600–2. http://dx.doi.org/10.3201/eid2309.161704
8. Zhu JY, Pan J, Lu YQ. A case report on indirect transmission of human rabies. J Zhejiang Univ Sci B. 2015;16:969–70. http://dx.doi.org/10.1631/jzus.B1500109

Address for correspondence: Yi-Hua Zhou, Nanjing Drum Tower Hospital, Departments of Laboratory Medicine and Infectious Diseases, 321 Zhongshan Rd, Nanjing 210008, China; email: zgr03summer@126.com

Endemic Severe Fever with Thrombocytopenia Syndrome, Vietnam

Xuan Chuong Tran, Yeojun Yun, Le Van An, So-Hee Kim, Nguyen T. Phuong Thao, Phan Kim C. Man, Jeong Rae Yoo, Sang Taek Heo, Nam-Hyuk Cho, Keun Hwa Lee

Author affiliations: The Hue University Hospital and Hue University of Medicine and Pharmacy, Hue, Vietnam (X.C. Tran, L.V. An, N.T.P. Thao, P.K.C. Man); Ewha Womans University, Seoul, South Korea (Y. Yun); The Kyung Hee University, Seoul (S.-H. Kim); The Jeju National University College of Medicine, Jeju, South Korea (J.R. Yoo, S.T. Heo, K.H. Lee); Seoul National University College of Medicine, Seoul (N.-H. Cho)

DOI: https://doi.org/10.3201/eid2505.181463

Severe fever with thrombocytopenia syndrome (SFTS), a tickborne viral disease, has been identified in China, South Korea, and Japan since 2009. We found retrospective evidence of SFTS virus (SFTSV) infection in Vietnam, which suggests that SFTSV infections also occur in Vietnam, where the virus has not been known to be endemic.

Severe fever with thrombocytopenia syndrome virus (SFTSV) is a tickborne virus (genus *Phlebovirus*, family *Phenuiviridae*) that can cause a mild to severe febrile illness similar to hemorrhagic fever (*1*). Phleboviruses have been found in the Americas, Asia, Africa, and the Mediterranean region. For example, Heartland virus (HRTV), another tickborne phlebovirus, was identified in northwestern Missouri, USA, in 2009 (*2*). Malsoor virus, a new bat phlebovirus closely related to SFTSV and HRTV, was identified in western India, and a phlebovirus similar to SFTSV and HRTV was isolated from ticks in Australia (*3*,*4*).

Severe fever with thrombocytopenia syndrome (SFTS) illness was first confirmed in China in 2009. It was retrospectively identified in South Korea in 2010 and the western regions of Japan in 2013 (*1*,*5*,*6*). SFTS is characterized by acute high fever, thrombocytopenia, leukopenia, elevated serum hepatic enzymes, gastrointestinal symptoms, and multiorgan failure and has a death rate of 16.2%–30% (*1*,*6*,*7*). Atypical signs and symptoms and asymptomatic infections also have been identified (*5*,*8*). Most SFTSV infections occur through *Haemaphysalis longicornis* ticks, although SFTSV transmission can also occur through close contact with an infected patient (*8*).

To investigate evidence of SFTSV infections in Vietnam, we collected serum samples from 80 patients with acute febrile illnesses admitted to Hue University Hospital (Hue, Vietnam)

during October 1, 2017–March 31, 2018. The Institutional Review Board of Hue University Hospital approved the study.

For the molecular diagnosis of SFTSV, we extracted RNA from stored patient serum using a QIAamp Viral RNA Mini Kit (QIAGEN, https://www.qiagen.com) and performed real-time reverse transcription PCR (rRT-PCR) to amplify the partial small (S) segment of the viral RNA from the stored serum and confirm SFTSV infection (*9*). rRT-PCR showed 2 positive results, from the stored serum of 2 patients with thrombocytopenia who had been seen at Hue University Hospital during 2017 and who had no history of travel to SFTSV-endemic countries, such as China, South Korea, and Japan. We also detected IgM in the serum of 1 of these patients (Appendix Table, https://wwwnc.cdc.gov/EID/article/25/5/18-1463-App1.pdf) (*8*).

On October 29, 2017, a 29-year-old woman (Hue 06-Vietnam-10-2017) was hospitalized at Hue University Hospital because of headache, vomiting, and gum bleeding. She lived in Hue City and was unaware of having received an insect bite. Her temperature was 38°C, and blood tests showed leukopenia (leukocyte count 1,900 cells/μL [reference 4,000–10,000 cells/μL]), thrombocytopenia (platelet count 125 × 10^3/μL [reference 150–450 × 10^3/μL]), and a low hematocrit level (34.3% [reference 36%–44%]). The patient fully recovered without other complications after 5 days.

On November 2, 2017, a 27-year-old man (Hue 13-Vietnam-11-2017) was hospitalized at Hue University Hospital because of headache and fatigue. He had had dengue fever at 8 years of age. Blood tests showed thrombocytopenia (platelet count 14 × 10^3/μL), normal leukocyte count (7,410 cells/μL), mildly elevated aspartate aminotransferase (84 IU/L [reference 8–38 IU/L]), elevated alanine aminotransferase (98 IU/L [reference 4–44 IU/L]), and mildly elevated hematocrit (47.6% [reference 36%–44%]). He fully recovered without other complications after 7 days.

We sequenced rRT-PCR products from the stored serum samples using a BigDye Terminator Cycle Sequencing kit (Applied Biosystems, http://www.thermofisher.com). We performed phylogenetic analysis of the partial S segment sequences with MEGA6 (https://www.megasoftware.net) and constructed phylogenetic trees using the maximum-likelihood method, which confirmed SFTSV infection (Appendix Figure).

We confirmed 2 SFTSV infections in Hue in 2017 by amplifying the partial S segment of the viral RNA in stored serum from patients with thrombocytopenia; elevated levels of serum hepatic enzymes, including aspartate aminotransferase and alanine aminotransferase; and gastrointestinal symptoms, such as vomiting. The signs and symptoms were milder than the major signs and symptoms of SFTS, which has a high death rate.

H. longicornis, *Amblyomma testudinarium*, and *Ixodes nipponensis* ticks are vectors of SFTSV, and *A. testudinarium* has been found in Vietnam. Migratory birds are known to be long-distance carriers of virus-bearing ticks (*10*). Therefore, virus-bearing *A. testudinarium* ticks and migratory birds may play a role in dispersing SFTSV to Vietnam (*10*).

This study expands the understanding of the distribution of SFTSV in Southeast Asia and suggests that SFTSV may have a much wider global distribution than previously thought. The 2 patients reported here had relatively mild illness, and 1 did not have leukopenia. Therefore, further epidemiologic and clinical research is needed to clarify the epidemiology, geographic distribution, and transmission dynamics of SFTSV in Vietnam and other areas of Southeast Asia. This subject deserves further discussion and might warrant changes in the background description of the disease (*5*,*8*).

Acknowledgments

We thank L. Bakkensen for providing comments on this paper.

This work was supported by the Bio & Medical Technology Development Program of the National Research Foundation (NRF), funded by the South Korean government (grant no. NRF-2016M3A9B6021161), and a grant from the Korean Health Technology R&D Project of the Ministry of Health and Welfare, South Korea (grant no. HI15C2891).

About the Author

Dr. Tran is a professor at the Department of Infectious Diseases, Hue University Hospital and Hue University of Medicine and Pharmacy, Hue, Vietnam. His research interest is infectious diseases.

References

1. Yu XJ, Liang MF, Zhang SY, Liu Y, Li JD, Sun YL, et al. Fever with thrombocytopenia associated with a novel bunyavirus in China. N Engl J Med. 2011;364:1523–32. http://dx.doi.org/10.1056/NEJMoa1010095
2. McMullan LK, Folk SM, Kelly AJ, MacNeil A, Goldsmith CS, Metcalfe MG, et al. A new phlebovirus associated with severe febrile illness in Missouri. N Engl J Med. 2012;367:834–41. http://dx.doi.org/10.1056/NEJMoa1203378
3. Mourya DT, Yadav PD, Basu A, Shete A, Patil DY, Zawar D, et al. Malsoor virus, a novel bat phlebovirus, is closely related to severe fever with thrombocytopenia syndrome virus and Heartland virus. J Virol. 2014;88:3605–9. http://dx.doi.org/10.1128/JVI.02617-13
4. Wang J, Selleck P, Yu M, Ha W, Rootes C, Gales R, et al. Novel phlebovirus with zoonotic potential isolated from ticks, Australia. Emerg Infect Dis. 2014;20:1040–3. http://dx.doi.org/10.3201/eid2006.140003
5. Kim YR, Yun Y, Bae SG, Park D, Kim S, Lee JM, et al. Severe tever with thrombocytopenia syndrome virus infection, South Korea, 2010. Emerg Infect Dis. 2018;24:2103–5. http://dx.doi.org/10.3201/eid2411.170756

6. Takahashi T, Maeda K, Suzuki T, Ishido A, Shigeoka T, Tominaga T, et al. The first identification and retrospective study of severe fever with thrombocytopenia syndrome in Japan. J Infect Dis. 2014;209:816–27. http://dx.doi.org/10.1093/infdis/jit603
7. Li H, Lu QB, Xing B, Zhang SF, Liu K, Du J, et al. Epidemiological and clinical features of laboratory-diagnosed severe fever with thrombocytopenia syndrome in China, 2011–17: a prospective observational study. Lancet Infect Dis. 2018;18:1127–37. http://dx.doi.org/10.1016/S1473-3099(18)30293-7
8. Yoo JR, Heo ST, Park D, Kim H, Fukuma A, Fukushi S, et al. Family cluster analysis of severe fever with thrombocytopenia syndrome virus infection in Korea. Am J Trop Med Hyg. 2016;95:1351–7. http://dx.doi.org/10.4269/ajtmh.16-0527
9. Zhang YZ, He YW, Dai YA, Xiong Y, Zheng H, Zhou DJ, et al. Hemorrhagic fever caused by a novel bunyavirus in China: pathogenesis and correlates of fatal outcome. Clin Infect Dis. 2012;54:527–33. http://dx.doi.org/10.1093/cid/cir804
10. Yun Y, Heo ST, Kim G, Hewson R, Kim H, Park D, et al. Phylogenetic analysis of severe fever with thrombocytopenia syndrome virus in South Korea and migratory bird routes between China, South Korea, and Japan. Am J Trop Med Hyg. 2015; 93:468–74. http://dx.doi.org/10.4269/ajtmh.15-0047

Address for correspondence: Keun Hwa Lee, Jeju National University College of Medicine, Department of Microbiology and Immunology, 15, Aran 13-gil, Jeju 63241, South Korea; email: yomust7@jejunu.ac.kr

Mixed *Mycobacterium tuberculosis* Lineage Infection in 2 Elephants, Nepal

Sarad Paudel,[1] Chie Nakajima,[1] Susan K. Mikota, Kamal P. Gairhe, Bhagwan Maharjan, Suraj Subedi, Ajay Poudel, Mariko Sashika, Michito Shimozuru, Yasuhiko Suzuki, Toshio Tsubota

Author affiliations: Hokkaido University, Sapporo, Japan (S. Paudel, C. Nakajima, M. Sashika, M. Shimozuru, Y. Suzuki, T. Tsubota); Elephant Care International, Hohenwald, Tennessee, USA (S.K. Mikota); Department of National Parks and Wildlife Conservation, Kathmandu, Nepal (K.P. Gairhe); German Nepal Tuberculosis Project, Kathmandu (B. Maharjan); National Trust for Nature Conservation, Lalitpur, Nepal (S. Subedi); Chitwan Medical College, Chitwan, Nepal (A. Poudel)

DOI: https://doi.org/10.3201/eid2505.181898

[1]These first authors contributed equally to this article.

Tuberculosis in elephants is primarily caused by *Mycobacterium tuberculosis*. We identified mixed *M. tuberculosis* lineage infection in 2 captive elephants in Nepal by using spoligotyping and large sequence polymorphism. One elephant was infected with Indo-Oceanic and East African–Indian (CAS-Delhi) lineages; the other was infected with Indo-Oceanic and East Asian (Beijing) lineages.

Mycobacterium tuberculosis is a primary cause of tuberculosis (TB) in elephants (*1*). Culture of trunk wash samples is regarded as the standard method for the diagnosis of TB in elephants; however, this method has many limitations (*2*). We previously reported TB in 3 elephants in Nepal that was caused by *M. tuberculosis* of Indo-Oceanic lineage (*3*). Here, we report on mixed *M. tuberculosis* lineage infection in 2 captive elephants from Chitwan National Park (CNP) in Nepal.

Elephant A was a female elephant ≈65–70 years old. She had been in retirement for 3 years before she died in February 2013. We observed TB-like lesions in the lungs postmortem (Appendix Figure 1, https://wwwnc.cdc.gov/EID/article/25/5/18-1898-App1.pdf). Elephant B was a 32-year-old male. His body condition had substantially deteriorated for several months before he died. We found extensive TB-like lesions in the lungs at postmortem.

We performed the DPP VetTB Assay (Chembio Inc., http://chembio.com), a serologic test, on the postmortem lung fluid (an off-label use) of elephant A and the serum of elephant B; results were reactive in both cases, indicating the presence of antibodies to TB. We processed the suspected lung lesions according to standard guidelines (*4*) and performed culture by using Löwenstein–Jensen media.

We performed genetic analyses on the 2 *M. tuberculosis* isolates by using spoligotyping and large-sequence polymorphism (LSP) as described previously (*5*). We amplified the direct-repeat region with a primer pair and hybridized the PCR products to a set of 43 oligonucleotide probes corresponding to each spacer covalently bound to the membrane. We identified the spoligo-international type by comparing spoligotypes with the international spoligotyping database (SpolDB4) (*6*). We performed LSP on the isolates by using specific primers for respective lineages, as described previously (*7*).

We identified the elephant isolates as a mixture of 2 strains based on uneven spoligotyping color development (suggesting mixture) and LSP detection PCR results (2 bands were observed). The spoligotyping results showed that the elephant A isolate had a new spoligotype that was not found in the international spoligotyping database. The elephant B isolate belonged to the Indo-Oceanic lineage (East African–Indian 5 spoligo-international type 1365) (Table). The prevalence of the Indo-Oceanic lineage among human TB patients in Nepal is only 11.5% (*8*). The drug

Table. Genotypic characteristics of *Mycobacterium tuberculosis* isolates from 2 elephants, Nepal*

Source	Spoligotype† binary code	SIT	Clade	*gyrA*‡
Elephant A	11100001111111111111111001111000010111111111	New§	New§	T231C
Elephant B	00000000000000000000000001111000010111111111	1365	EAI5	T231C

*EAI5, East African–Indian 5; SIT, spoligo-international type.
†Spoligotype was determined as previously described by Brudey et al. (*6*).
‡Mutation in a partial sequence of *gyrA*. The *gyrA* sequence of both elephant isolates had a synonymous single nucleotide polymorphism from T to C at position 231.
§Not found in the international spoligotyping database (SpolDB4).

resistance–associated region sequences *rpoB, katG, inhA* promoter region, and *gyrA* were all wild types in both isolates. Similarly, LSP results showed that elephant A was infected by the Indo-Oceanic and East African–Indian lineages (CAS-Delhi) (Appendix Figure 2), whereas elephant B was infected with the East Asian type (Beijing type) (Appendix Figure 3). The prevalence of CAS-Delhi and Beijing type lineages in Nepal in human TB patients is 40.6% and 32.2%, respectively (*8*). In the *gyrA* sequence, both of the samples showed a mixed peak of T231C, suggesting that the East African–Indian type is a Nepal-specific lineage.

Our study shows that the first elephant was infected with the Indo-Oceanic and East African–Indian (CAS-Delhi) *M. tuberculosis* lineages, whereas the second elephant was infected with the Indo-Oceanic and East Asian (Beijing) lineages. We previously identified the Indo-Oceanic lineage in 3 elephants from Nepal (*3*). We suspect that this lineage might be well adapted in elephants in Nepal.

We diagnosed the mixed lineage infection postmortem in both elephants. However, a successful antemortem diagnosis of mixed infection in a single elephant would enable a precise TB diagnosis and selection of an appropriate anti-TB treatment, which could eventually lead to the control of this disease at the herd level.

The source of these mixed infections is unknown and could be from humans or elephants infected with these lineages. Infected elephant handlers who have daily close contact would be a likely human source. Genotyping of additional isolates from elephants and their handlers will help to determine the source of infection. We recommend regular TB screening of elephant handlers to safeguard human health and help prevent transmission of TB from humans to elephants.

Acknowledgments

We thank Arjun Pandit, Chitra B. Khadka, and Kiran Rijal for helping with the collection of elephant samples; technicians at the German Nepal Tuberculosis Project in Kathmandu for performing the laboratory work; and Yukari Fukushima and Haruka Suzuki for technical support at the Hokkaido University Research Centre for Zoonosis Control.

The National Trust for Nature Conservation Nepal and the Department of National Parks and Wildlife Conservation of Nepal's Ministry for Forests and Soil Conservation supported this work.

About the Author

Mr. Paudel is an assistant professor in the Department of Cell Physiology, Faculty of Medicine and Graduate School of Medicine, Hokkaido University, Sapporo, Japan. His research interests include the mechanism of TB bacteria entry into cells, TB in elephants, and development of TB diagnostic tools for elephants.

References

1. Mikota SK, Lyashchenko KP, Lowenstine L, Agnew D, Maslow JN. Mycobacterial infections in elephants. In: Mukundan H, Chambers MA, Waters WR, Larsen MH, editors. Tuberculosis, leprosy and other mycobacterial diseases of man and animals: the many hosts of mycobacteria. Wallingford (UK): CABI Publishing House; 2015. p. 259–76.
2. Lyashchenko KP, Greenwald R, Esfandiari J, Olsen JH, Ball R, Dumonceaux G, et al. Tuberculosis in elephants: antibody responses to defined antigens of *Mycobacterium tuberculosis*, potential for early diagnosis, and monitoring of treatment. Clin Vaccine Immunol. 2006;13:722–32. http://dx.doi.org/10.1128/CVI.00133-06
3. Paudel S, Mikota SK, Nakajima C, Gairhe KP, Maharjan B, Thapa J, et al. Molecular characterization of *Mycobacterium tuberculosis* isolates from elephants of Nepal. Tuberculosis (Edinb). 2014;94:287–92. http://dx.doi.org/10.1016/j.tube.2013.12.008
4. Groothuis DG, Yates MD. Decontamination, microscopy and isolation. In: Groothius DG, Yates MD, editors. Diagnostic and public health mycobacteriology. 2nd ed. London: Bureau of Hygiene and Tropical Diseases, European Society for Mycobacteriology; 1991. p. 63.
5. Kamerbeek J, Schouls L, Kolk A, van Agterveld M, van Soolingen D, Kuijper S, et al. Simultaneous detection and strain differentiation of *Mycobacterium tuberculosis* for diagnosis and epidemiology. J Clin Microbiol. 1997;35:907–14.
6. Brudey K, Driscoll JR, Rigouts L, Prodinger WM, Gori A, Al-Hajoj SA, et al. *Mycobacterium tuberculosis* complex genetic diversity: mining the fourth international spoligotyping database (SpolDB4) for classification, population genetics and epidemiology. BMC Microbiol. 2006;6:23. http://dx.doi.org/10.1186/1471-2180-6-23
7. Gagneux S, DeRiemer K, Van T, Kato-Maeda M, de Jong BC, Narayanan S, et al. Variable host-pathogen compatibility in *Mycobacterium tuberculosis*. Proc Natl Acad Sci U S A. 2006;103:2869–73. http://dx.doi.org/10.1073/pnas.0511240103
8. Malla B, Stucki D, Borrell S, Feldmann J, Maharjan B, Shrestha B, et al. First insights into the phylogenetic diversity of *Mycobacterium tuberculosis* in Nepal. PLoS One. 2012;7:e52297. http://dx.doi.org/10.1371/journal.pone.0052297

Address for correspondence: Toshio Tsubota, Hokkaido University, Laboratory of Wildlife Biology and Medicine, Graduate School of Veterinary Medicine, Kita 18 Nishi 9, Sapporo, Hokkaido 060-0818, Japan; email: tsubota@vetmed.hokudai.ac.jp

Need for Aeromedical Evacuation High-Level Containment Transport Guidelines

Shawn G. Gibbs, Jocelyn J. Herstein, Aurora B. Le, Elizabeth L. Beam, Theodore J. Cieslak, James V. Lawler, Joshua L. Santarpia, Terry L. Stentz, Kelli R. Kopocis-Herstein, Chandran Achutan, Gary W. Carter, John J. Lowe

Author affiliations: Indiana University School of Public Health, Bloomington, Indiana, USA (S.G. Gibbs, A.B. Le); University of Nebraska Medical Center College of Public Health, Omaha, Nebraska, USA (J.J. Herstein, T.J. Cieslak, C. Achutan, J.J. Lowe); University of Nebraska Medical Center College of Nursing, Omaha (E.L. Beam); University of Nebraska Medical Center College of Medicine, Omaha (J.V. Lawler, J.L. Santarpia); National Strategic Research Institute, Omaha (J.V. Lawler, J.L. Santarpia, G.W. Carter); University of Nebraska–Lincoln Charles W. Durham School of Architectural Engineering and Construction, Lincoln, Nebraska, USA (T.L. Stentz, K.R. Kopocis-Herstein)

DOI: https://doi.org/10.3201/eid2505.181948

Circumstances exist that call for the aeromedical evacuation high-level containment transport (AE-HLCT) of patients with highly hazardous communicable diseases. A small number of organizations maintain AE-HLCT capabilities, and little is publicly available regarding the practices. The time is ripe for the development of standards and consensus guidelines involving AE-HLCT.

During a highly hazardous communicable diseases (HHCD) outbreak, most patients are likely to be treated within the affected region. However, circumstances exist for which aeromedical evacuation high-level containment transport (AE-HLCT) of patients with HHCDs is necessary (e.g., political considerations, resource limitations, armed conflict). Although AE-HLCT has occurred since the 1970s, the 2013–2016 Ebola virus disease (EVD) outbreak in West Africa brought this practice to the forefront of public consciousness (*1*). During that outbreak, at least 33 patients with confirmed or suspected EVD were transported to EVD treatment facilities in the United States and Europe that were capable of high-level isolation. Asymptomatic persons with high-risk exposures (e.g., needle sticks, blood or body fluid splashes) have also been transported for quarantine. In 2016, two patients with Lassa fever were transported by AE-HLCT from Togo, 1 each to the United States and Germany (*2*). Despite the introduction of an EVD vaccine, the Democratic Republic of the Congo is experiencing the second largest EVD outbreak in history; in December 2018, a US citizen exposed to EVD was transported to the University of Nebraska Medical Center for observation before being discharged in January 2019 (*3*). Clearly, AE-HLCT is an ongoing need.

The death rate from certain HHCDs can exceed 70%, as was the case with EVD in parts of West Africa (*4*). Thus, streamlined policies and procedures for efficient, timely AE-HLCT can decrease transmission risk and optimize patient management in flight. Because of the significant risks to crews and receiving communities, HHCD patients must be managed by highly trained teams and organizations, especially considering the uncontrolled environment of AE-HLCT missions and the potential for the rapid deterioration of patient condition. Historically, AE-HLCTs for HHCDs have been conducted by a limited number of military organizations or private corporations contracted by national governments or relief organizations to protect the well-being of their citizens or their volunteer personnel. Providers of AE-HLCT maintain teams of highly trained staff and regularly test, validate, and exercise their systems and procedures to ensure mission readiness. Moreover, these experienced organizations have recently developed systems with the capability of transporting multiple patients of varying levels of acuity during the same operation, expanding the capacity of AE-HLCT missions that historically had been limited to a single patient (*5*,*6*).

Isolation of HHCD patients during aeromedical evacuation is a complex process with numerous requirements related to the preflight, in-flight, and postflight environments, involving highly knowledgeable and trained persons from a variety of professions, as well as specialized equipment and validated infection control processes (Table) (*7*). The safe and successful use of these AE-HLCT systems requires coordination and approval at all levels of government, as well as between governments, given that most AE-HLCT missions will cross international borders. Despite this complexity, no generally accepted standards exist outside the few organizations that have conducted them. Moreover, the processes, operations, and capabilities used, as well as the lessons learned from postmission evaluations, are not found in the peer-reviewed literature. Only a few case studies have been publicly disseminated because of security concerns, a desire to maintain proprietary information, or simply because of the niche field and limited audience. The literature is sparser still regarding the methods associated with the transportation of asymptomatic persons with high-risk exposures. Although we are aware that cooperation between these organizations often occurs, the lack of literature disseminated to the larger academic and practice community remains a problem. Without knowledge of the

Table. Processes to be considered during an aeromedical evacuation high-level containment transport

Environment, process to consider
Preflight
Types of diseases
Decision to aeromedically evacuate
Training/drills
Regulations and legal limitation
Communication plan
Layout/space assessment
Other preparations
In-flight
Personnel
Personal protective equipment
Type of isolation units
Procedures/capabilities inflight
Liquid and solid waste handling
Death in flight
Other contingency procedures
Postflight
Decontamination
Equipment reuse
Waste disposal
Personnel monitoring

science that established these procedures or a broad continual review of such science, an inherent barrier persists for current or future researchers or practitioners attempting to build on ongoing research and experiences.

Finally, the limited amount of information about the processes, procedures, and equipment available from a small number of aeromedical organizations impedes scalability should the need arise. Most of the organizations that have historically conducted AE-HLCT missions often have limited capacity, personnel, or systems to conduct multiple missions, with most only able to conduct 1 or 2 AE-HLCT missions simultaneously. The lack of nonorganizational specific standards and specialization diminishes the ability to transfer such capabilities to other organizations that might have the desire and personnel to assist or to nations that currently lack such capabilities but might have a current or future need for such capabilities. A critical evaluation of the literature would enable the dissemination of lessons learned, thereby enhancing best practices and driving the field forward, ultimately leading to safer outcomes for patients, caregivers, and receiving communities. Because much of this information does not exist within peer-reviewed literature, much would be gained through a conference on the subject that evaluates various procedures and establishes consensus recommendations for best practices, including creation of a verified information exchange mechanism. The time is ripe for the development of standards and consensus guidelines involving AE-HLCT.

About the Author

Dr. Gibbs is executive associate dean and professor of environmental health at Indiana University School of Public Health–Bloomington. His research interests include industrial hygiene and environmental exposure assessment, focusing on environmental microbiology and disrupting transmission of highly infectious diseases.

References

1. Lotz E, Raffin H. Aeromedical evacuation using an aircraft transit isolator of a patient with Lassa fever. Aviat Space Environ Med. 2012;83:527–30. http://dx.doi.org/10.3357/ASEM.3094.2012
2. Woodruff Health Sciences Center. Experimental antiviral combo + immunology [cited 2019 Jan 15]. http://news.emory.edu/stories/2017/06/lassa_kraft_mcelroy
3. Martinez G. American flown to Nebraska hospital after possible Ebola exposure in the Congo [cited 2019 Jan 15]. http://time.com/5490412/ebola-doctor-nebraska-medical-center
4. Uyeki TM, Mehta AK, Davey RT Jr, Liddell AM, Wolf T, Vetter P, et al.; Working Group of the U.S.–European Clinical Network on Clinical Management of Ebola Virus Disease Patients in the U.S. and Europe. Clinical management of Ebola virus disease in the United States and Europe. N Engl J Med. 2016;374:636–46. http://dx.doi.org/10.1056/NEJMoa1504874
5. Wade S. Scott Airmen train on transport isolation system [cited 2018 Apr 15]. http://www.af.mil/DesktopModules/ArticleCS/Print.aspx?PortalId=1&ModuleId=850&Article=562739
6. Phelps D. Ready for the challenge: Dobbins selected as home for new biocontainment system [cited 2018 Nov 8]. https://www.thefreelibrary.com/Ready+for+the+challenge%3A+Dobbins+selected+as+home+for+new+...-a0435001746
7. Thoms WET, Wilson WT, Grimm K, Conger NG, Gonzales CG, DeDecker L, et al. Long-range transportation of Ebola-exposed patients: an evidence-based protocol. American Journal of Infectious Diseases and Microbiology. 2015;2(6A):19–24.

Address for correspondence: Jocelyn J. Herstein, College of Public Health, University of Nebraska Medical Center, 984388 Nebraska Medical Center, Omaha, NE 68198, USA; email: jocelyn.herstein@unmc.edu

Corrections

Vol. 24, No. 10

A grant number was listed incorrectly in Human Pegivirus in Patients with Encephalitis of Unclear Etiology, Poland (I. Bukowska-Ośko et al.). The Polish National Science Center grant number should be 2017/25/B/NZ6/01463. The article has been corrected online (https://wwwnc.cdc.gov/eid/article/24/10/18-0161_article).

Vol. 25, No. 2

The number of cases of West Nile neuroinvasive disease was listed incorrectly in the abstract of Acute and Delayed Deaths after West Nile Virus Infection, Texas, USA, 2002–2012 (D.C.E. Philpott et al.). The article has been corrected online (https://wwwnc.cdc.gov/eid/article/25/2/18-1250_article).

Giovanni Battista Foggini (1652–1725), ***Laocöon*** (detail) (c. 1720). Bronze, 22 1/16 in × 17 5/16 in × 8 5/8 in/56 cm × 44 cm x 21.9 cm. Digital image courtesy of the Getty's Open Content Program, The J. Paul Getty Museum, Los Angeles, CA, USA.

Consequences of Failing to Investigate

Byron Breedlove

High-consequence pathogens cause diseases, such as Ebola virus disease, Rift Valley fever, Nipah virus disease, hantavirus pulmonary syndrome, measles, smallpox, and anthrax. Some such pathogens have the potential to spread rapidly and to cause epidemics. One of the tactics used to control the spread of such pathogens is careful investigation of cases.

Author affiliation: Centers for Disease Control and Prevention, Atlanta, Georgia, USA

DOI: https://doi.org/10.3201/eid2505.AC2505

Knowing where the danger lies, whether assessing the threat for human infection with high-consequence pathogens or defending a besieged city, is crucial to protecting the health and well-being of the public. Perhaps careful investigation might have changed the outcome of the Trojan War, a mythical protracted, bloody Bronze Age conflict pitting the kingdoms of Troy and Mycenaean Greece against one another.

The Trojan War is one of the most celebrated events in Greek mythology, and many incidents from that epic war have proven to be irresistible subjects for artists, who

have reimagined them in sculptures, frescoes, sketches, and paintings. One oft-depicted incident is the ghastly death of the Trojan priest Laocöon and his two sons, Antiphas and Thymbraeus, by serpents.

The reddish-brown bronze statue of Laocöon featured on this month's cover was fashioned by Italian artist Giovanni Battista Foggini. It is one of a series of small bronzes he created for displaying on tabletops or desks. Foggini used his talent and connections to become the leading court artist and architect to Cosimo III de' Medici, the Grand Duke of Tuscany. Foggini frequently drew ideas from events portrayed in ancient classical literature. His bronze statue was inspired by the marble sculpture of Laocöon's death unearthed in Rome in 1506 and later displayed in the Vatican museums.

In this bronze statue, Foggini recreated an event that proved pivotal in ending the war. Following a decade of skirmishes, sieges, counterattacks, and infighting on both sides, the Greek army feigns its withdrawal and leaves a massive, hollow wooden horse near the city's gates as an offering for the gods. Laocöon senses treachery and counsels the Trojans either to investigate what is inside the horse or to burn it. When it seems his argument has swayed the majority, the gods intervene and dispatch a pair of sea serpents to silence Laocöon. In his towering epic poem the *Aeneid*, Virgil describes the serpents' approach:

> Looping in giant spirals; the foaming sea
> Hissed under their motion. And they reached the land,
> Their burning eyes suffused with blood and fire,
> Their darting tongues licking the hissing mouths.

The *Aeneid* tells us that the serpents "squeezed with scaly pressure" and "fastened their fangs in those poor bodies," crushing their victims before vanishing with their bodies. Struggling with his foes, the powerful figure of Laocöon dominants the sculpture. His rippling muscles, flowing hair, and thick beard stand in contrast to his smaller and smooth-limbed sons. The J. Paul Getty Museum, where the sculpture resides today, notes that Foggini is recognized for his "exactitude in anatomical modeling and an equally precise and expert finishing of details."

After witnessing the excruciating deaths of the priest and his sons, the dazed Trojans reason that the wooden horse was intended as a sacred gift for the gods, and they move this trophy inside the walls of Troy. An elite Greek force sequestered in the horse emerges during the night and opens the gates for the Greeks army, which has stealthily returned. The Greeks overwhelm the unprepared Trojans, sack the city, and win the war. Laocöon had properly understood the ruse and his admonition had proven accurate.

Bad decisions and character flaws were not solely responsible for the fall of Troy. The major Greek deities had their own interests in the outcome, and their many intercessions caused death and mayhem on both sides before the final reckoning. Historian Barbara Tuchman explains, "Taking sides and playing favorites, potent but fickle, conjuring deceptive images, altering the fortunes of battles to suit their desires, whispering, tricking, falsifying, even inducing the Greeks through deceit to continue when they are ready to give up and go home, the gods keep the combatants engaged while heroes die and homelands suffer."

Had the Trojan leaders conducting their own careful investigation to see whether the Greek forces had actually retreated and to see what was lurking inside the horse, then the Greeks might not have succeeded in executing perhaps the best-known subterfuge described in literature. Foggini's bronze statue reminds us that the consequences of dismissing admonitions and failing to investigate can be catastrophic.

Bibliography

1. Centers for Disease Control and Prevention. Division of High-Consequence Pathogens and Pathology [cited 2019 Mar 14]. https://www.cdc.gov/ncezid/dhcpp/index.html
2. Centers for Disease Control and Prevention. Division of High-Consequence Pathogens and Pathology Factsheet [cited 2019 Mar 14]. https://www.cdc.gov/ncezid/dhcpp/pdfs/DHCPP-factsheet.pdf
3. Encyclopedia of Art. Laocöon and his sons [cited 2019 Mar 21]. http://www.visual-arts-cork.com/sculpture/Laocöon.htm
4. Fogleman P, Fusco P, Cambarer M. Italian and Spanish sculpture: catalogue of the J. Paul Getty museum collection. Los Angeles: Getty Publications; 2002. p. 250–6.
5. Humphries R, Trans. The Aeneid of Virgil. New York: Charles Scribner's Sons; 1951. p. 32–3, 38–40.
6. Paul Getty Museum J. Laocöon [cited 2019 Mar 1]. http://www.getty.edu/art/collection/objects/1116/giovanni-battista-foggini-Laocöon-italian-about-1720
7. Tuchman BW. The march of folly: from Troy to Vietnam. New York: Random House Trade Paperbacks; 1985. p. 41–4.

Address for correspondence: Byron Breedlove, EID Journal, Centers for Disease Control and Prevention, 1600 Clifton Rd NE, Mailstop H16-2, Atlanta, GA 30329-4027, USA; email: wbb1@cdc.gov

EMERGING INFECTIOUS DISEASES®

Upcoming Issue

- Enhancement of Risk for Lyme Disease by Landscape Connectivity, New York, New York, USA
- Follow-Up of Crimean-Congo Hemorrhagic Fever Enzootic Focus, Spain, 2011–2015
- Mass Die-Off of Saiga Antelopes, Kazakhstan, 2015
- Sequential Emergence and Wide Spread of Neutralization
- Escape Middle East Respiratory Syndrome Coronavirus Mutants, South Korea, 2015
- Assessment of Economic Burden of Concurrent Measles and Rubella Outbreaks, Romania, 2011–2012
- Phenotypic and Genomic Analyses of *Burkholderia stabilis* Clinical Contamination, Switzerland
- Performance of 2 Commercial Serologic Tests for Diagnosis of Zika Virus Infection
- Respiratory Syncytial Virus Seasonality, Beijing, China, 2007–2015
- New Delhi Metallo-β-Lactamase 5–Producing *Klebsiella pneumoniae* Sequence Type 258, Southwest China, 2017
- Scrub Typhus in Continental Chile, 2016–2018
- Increase in Enterovirus D68 Infections in Young Children, United Kingdom, 2006–2016
- Enterovirus A71 Subgenogroup C1 Isolates Associated with Neurologic Disease, France, 2016
- Hepatitis E Virus Infection in European Brown Hares, Germany, 2007–2014
- African Swine Fever Virus in Pork Brought into South Korea by Travelers from China, August 2018
- Infection with New York Orthohantavirus and Associated Respiratory Failure and Multiple Cerebral Complications
- Reemergence of Classical Swine Fever, Japan, 2018
- Hepatitis Rebound after Infection with Yellow Fever Virus
- Comparative Analysis of Whole-Genome Sequence of African Swine Fever Virus Belgium 2018/1

Complete list of articles in the June issue at
http://www.cdc.gov/eid/upcoming.htm

Upcoming Infectious Disease Activities

June 20–24, 2019
ASM Microbe 2019
San Francisco, CA, USA
https://www.asm.org/index.php/asm-microbe-2018

June 23–28, 2019
Biology of Vector-borne Diseases
Six-Day Training Course
Moscow, ID, USA
https://www.uidaho.edu/cals/center-for-health-in-the-human-ecosystem/education/vector-borne-diseases

July 14–17, 2019
STI and HIV 2019 World Congress
Vancouver, Canada
https://stihiv2019vancouver.com

July 20–24, 2019
American Society for Virology
Minneapolis, MN, USA
https://www.asv.org

July 21–24 , 2019
International Aids Society 2019
Mexico City, Mexico
https://www.ias2019.org

August 12–23, 2019
16th International Course on Dengue, Zika and other Emergent Arboviruses
Havana, Cuba
http://instituciones.sld.cu/ipk/16th-international-course-on-dengue-zika-and-other-emergent-arboviruses/

August 28–September 1, 2019
OPTIONS X for the Control of Influenza
Suntec, Singapore
https://www.isirv.org/site/

November 20–24, 2019
ASTMH
American Society of Tropical Medicine and Hygiene
68th Annual Meeting
National Harbor, MD, USA
https://www.astmh.org/

Announcements
Email announcements to EIDEditor (eideditor@cdc.gov). Include the event's date, location, sponsoring organization, and a website. Some events may appear only on EID's website, depending on their dates.

Earning CME Credit

To obtain credit, you should first read the journal article. After reading the article, you should be able to answer the following, related, multiple-choice questions. To complete the questions (with a minimum 75% passing score) and earn continuing medical education (CME) credit, please go to http://www.medscape.org/journal/eid. Credit cannot be obtained for tests completed on paper, although you may use the worksheet below to keep a record of your answers.

You must be a registered user on http://www.medscape.org. If you are not registered on http://www.medscape.org, please click on the "Register" link on the right hand side of the website.

Only one answer is correct for each question. Once you successfully answer all post-test questions, you will be able to view and/or print your certificate. For questions regarding this activity, contact the accredited provider, CME@medscape.net. For technical assistance, contact CME@medscape.net. American Medical Association's Physician's Recognition Award (AMA PRA) credits are accepted in the US as evidence of participation in CME activities. For further information on this award, please go to https://www.ama-assn.org. The AMA has determined that physicians not licensed in the US who participate in this CME activity are eligible for AMA PRA Category 1 Credits™. Through agreements that the AMA has made with agencies in some countries, AMA PRA credit may be acceptable as evidence of participation in CME activities. If you are not licensed in the US, please complete the questions online, print the AMA PRA CME credit certificate, and present it to your national medical association for review.

Article Title

Novel Sequence Type in *Bacillus cereus* Strains Associated with Nosocomial Infections and Bacteremia, Japan

CME Questions

11. You are advising a large hospital in Japan about nosocomial infections. According to the genotyping study by Akamatsu and colleagues, which of the following statements about findings from genotype analysis of *Bacillus cereus* strains isolated from nosocomial infections in Japan in 2006, 2012, 2013, and 2016 is correct?

A. Sequence type (ST) 1428 was a newly identified, novel ST and the dominant ST isolated from nosocomial infection cases
B. ST1420 was the dominant ST isolated from nosocomial infection cases in only 1 of 4 studied locations in Japan in 2006, 2013, and 2016
C. Among strains causing infections in Tokyo in 2013, there were 19 pulsed-field gel electrophoresis (PFGE) cluster types and 11 repetitive PCR (rep-PCR) cluster types, with more than one-third in a single PFGE cluster (cluster e)
D. Rep-PCR fingerprinting analysis of Tokyo strains led to findings different from that of the PFGE analysis

2. According to the genotyping study by Akamatsu and colleagues, which of the following statements about findings from MLST analysis of *B. cereus* strains isolated from recent nosocomial infections in Japan in 2006, 2012, 2013, and 2016 is correct?

A. ST1420 was present among the Tokyo, Tochigi, and Kochi strains
B. *B. cereus* infections at Tokyo and Tochigi likely came from contaminated hospital linens from the same supplier
C. ST167 and ST365 were detected in bacteremia cases in Tottori and Kochi
D. Previous studies of pathogenic *B. cereus* isolates showed that some cases of emetic illness were linked to ST26, and some cases of pneumonia were linked to ST78

3. According to the genotyping study by Akamatsu and colleagues, which of the following statements about findings from phylogenetic analysis of *B. cereus* strains isolated from recent nosocomial infections in Japan in 2006, 2012, 2013, and 2016 is correct?

A. ST1420 strains were located in the Anthracis lineage
B. The Cereus III lineage is much closer to the Anthracis lineage than to Cereus I and II lineages
C. Most of the strains from patients with bacteremia were in the Cereus I lineage
D. Among the Tokyo and Tochigi strains, isolates from patients with bacteremia were classified only into Clade II

Earning CME Credit

To obtain credit, you should first read the journal article. After reading the article, you should be able to answer the following, related, multiple-choice questions. To complete the questions (with a minimum 75% passing score) and earn continuing medical education (CME) credit, please go to http://www.medscape.org/journal/eid. Credit cannot be obtained for tests completed on paper, although you may use the worksheet below to keep a record of your answers.

You must be a registered user on http://www.medscape.org. If you are not registered on http://www.medscape.org, please click on the "Register" link on the right hand side of the website.

Only one answer is correct for each question. Once you successfully answer all post-test questions, you will be able to view and/or print your certificate. For questions regarding this activity, contact the accredited provider, CME@medscape.net. For technical assistance, contact CME@medscape.net. American Medical Association's Physician's Recognition Award (AMA PRA) credits are accepted in the US as evidence of participation in CME activities. For further information on this award, please go to https://www.ama-assn.org. The AMA has determined that physicians not licensed in the US who participate in this CME activity are eligible for AMA PRA Category 1 Credits™. Through agreements that the AMA has made with agencies in some countries, AMA PRA credit may be acceptable as evidence of participation in CME activities. If you are not licensed in the US, please complete the questions online, print the AMA PRA CME credit certificate, and present it to your national medical association for review.

Article Title

Age-Dependent Increase in Incidence of *Staphylococcus aureus* Bacteremia, Denmark, 2008–2015

CME Questions

1. Which of the following statements regarding the demographics of *Staphylococcus aureus* bacteremia (SAB) in the current study by Thorlacius-Ussing and colleagues is most accurate?

A. The median age of patients with SAB was 84 years
B. Most patients with SAB were male
C. SAB was diagnosed with no comorbidity in half of cases
D. Methicillin-resistant *Staphylococcus aureus* accounted for 60% of cases of SAB

2. Which age group experienced the biggest increase in the incidence of SAB between 2008 and 2015 in the current study?

A. Children <5 years old
B. Young adults 18 to 30 years old
C. Middle-aged adults 40 to 60 years old
D. Older adults >80 years old

3. What did the current study find regarding temporal trends in hospitalization for SAB between 2008 and 2015?

A. The proportion of total hospital admissions and hospital days related to SAB increased
B. Hospital admissions for SAB increased, but total hospital days related to SAB did not
C. There was no significant change in the proportion of hospital admissions or hospital days for SAB
D. Hospital admissions for SAB decreased, but total hospital days related to SAB increased

4. Which of the following statements regarding the outcomes of SAB in the current study is most accurate?

A. The proportion of deaths because of SAB increased between 2008 and 2015
B. The mortality rate of SAB for adults >80 years old declined slightly between 2008 and 2015
C. The case fatality rate of SAB increased during the study period
D. Men experienced a higher case fatality rate than women

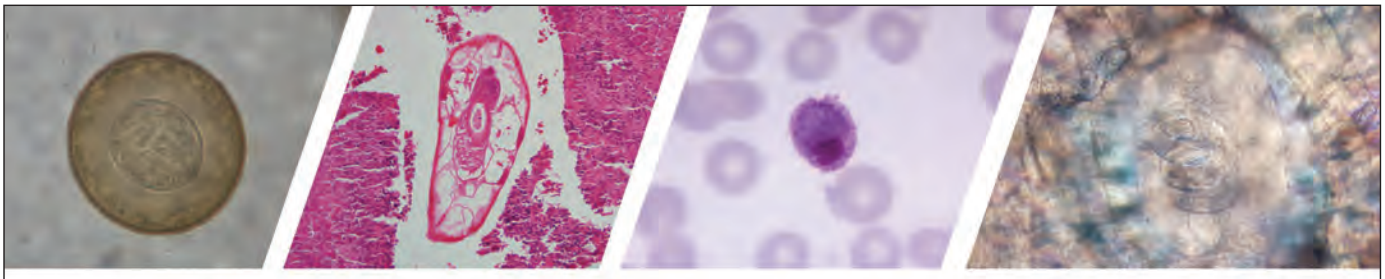

DPDx

Diagnostic Assistance and Training in Laboratory Identification of Parasites

A free service of CDC available to laboratorians, pathologists, and other health professionals in the United States and abroad

- Diagnosis from photographs of worms, histological sections, fecal, blood, and other specimen types
- Expert diagnostic review
- Formal diagnostic laboratory report
- Submission of samples via secure file share

Visit the DPDx website for information on laboratory diagnosis, geographic distribution, clinical features, parasite life cycles, and training via Monthly Case Studies of parasitic diseases.

www.cdc.gov/dpdx
dpdx@cdc.gov

U.S. Department of Health and Human Services
Centers for Disease Control and Prevention

CS272346-DE

Emerging Infectious Diseases is a peer-reviewed journal established expressly to promote the recognition of new and reemerging infectious diseases around the world and improve the understanding of factors involved in disease emergence, prevention, and elimination.

The journal is intended for professionals in infectious diseases and related sciences. We welcome contributions from infectious disease specialists in academia, industry, clinical practice, and public health, as well as from specialists in economics, social sciences, and other disciplines. Manuscripts in all categories should explain the contents in public health terms. For information on manuscript categories and suitability of proposed articles, see below and visit http://wwwnc.cdc.gov/eid/pages/author-resource-center.htm.

Summary of Authors' Instructions

Authors' Instructions. For a complete list of EID's manuscript guidelines, see the author resource page: http://wwwnc.cdc.gov/eid/page/author-resource-center.

Manuscript Submission. To submit a manuscript, access Manuscript Central from the Emerging Infectious Diseases web page (www.cdc.gov/eid). Include a cover letter indicating the proposed category of the article (e.g., Research, Dispatch), verifying the word and reference counts, and confirming that the final manuscript has been seen and approved by all authors. Complete provided Authors Checklist.

Manuscript Preparation. For word processing, use MS Word. Set the document to show continuous line numbers. List the following information in this order: title page, article summary line, keywords, abstract, text, acknowledgments, biographical sketch, references, tables, and figure legends. Appendix materials and figures should be in separate files.

Title Page. Give complete information about each author (i.e., full name, graduate degree(s), affiliation, and the name of the institution in which the work was done). Clearly identify the corresponding author and provide that author's mailing address (include phone number, fax number, and email address). Include separate word counts for abstract and text.

Keywords. Use terms as listed in the National Library of Medicine Medical Subject Headings index (www.ncbi.nlm.nih.gov/mesh).

Text. Double-space everything, including the title page, abstract, references, tables, and figure legends. Indent paragraphs; leave no extra space between paragraphs. After a period, leave only one space before beginning the next sentence. Use 12-point Times New Roman font and format with ragged right margins (left align). Italicize (rather than underline) scientific names when needed.

Biographical Sketch. Include a short biographical sketch of the first author—both authors if only two. Include affiliations and the author's primary research interests.

References. Follow Uniform Requirements (www.icmje.org/index.html). Do not use endnotes for references. Place reference numbers in parentheses, not superscripts. Number citations in order of appearance (including in text, figures, and tables). Cite personal communications, unpublished data, and manuscripts in preparation or submitted for publication in parentheses in text. Consult List of Journals Indexed in Index Medicus for accepted journal abbreviations; if a journal is not listed, spell out the journal title. List the first six authors followed by "et al." Do not cite references in the abstract.

Tables. Provide tables within the manuscript file, not as separate files. Use the MS Word table tool, no columns, tabs, spaces, or other programs. Footnote any use of boldface. Tables should be no wider than 17 cm. Condense or divide larger tables. Extensive tables may be made available online only.

Figures. Submit editable figures as separate files (e.g., Microsoft Excel, PowerPoint). Photographs should be submitted as high-resolution (600 dpi) .tif or .jpg files. Do not embed figures in the manuscript file. Use Arial 10 pt. or 12 pt. font for lettering so that figures, symbols, lettering, and numbering can remain legible when reduced to print size. Place figure keys within the figure. Figure legends should be placed at the end of the manuscript file.

Videos. Submit as AVI, MOV, MPG, MPEG, or WMV. Videos should not exceed 5 minutes and should include an audio description and complete captioning. If audio is not available, provide a description of the action in the video as a separate Word file. Published or copyrighted material (e.g., music) is discouraged and must be accompanied by written release. If video is part of a manuscript, files must be uploaded with manuscript submission. When uploading, choose "Video" file. Include a brief video legend in the manuscript file.

Types of Articles

Perspectives. Articles should not exceed 3,500 words and 50 references. Use of subheadings in the main body of the text is recommended. Photographs and illustrations are encouraged. Provide a short abstract (150 words), 1-sentence summary, and biographical sketch. Articles should provide insightful analysis and commentary about new and reemerging infectious diseases and related issues. Perspectives may address factors known to influence the emergence of diseases, including microbial adaptation and change, human demographics and behavior, technology and industry, economic development and land use, international travel and commerce, and the breakdown of public health measures.

Synopses. Articles should not exceed 3,500 words in the main body of the text or include more than 50 references. Use of subheadings in the main body of the text is recommended. Photographs and illustrations are encouraged. Provide a short abstract (not to exceed 150 words), a 1-line summary of the conclusions, and a brief biographical sketch of first author or of both authors if only 2 authors. This section comprises case series papers and concise reviews of infectious diseases or closely related topics. Preference is given to reviews of new and emerging diseases; however, timely updates of other diseases or topics are also welcome. If detailed methods are included, a separate section on experimental procedures should immediately follow the body of the text.

Research. Articles should not exceed 3,500 words and 50 references. Use of subheadings in the main body of the text is recommended. Photographs and illustrations are encouraged. Provide a short abstract (150 words), 1-sentence summary, and biographical sketch. Report laboratory and epidemiologic results within a public health perspective. Explain the value of the research in public health terms and place the findings in a larger perspective (i.e., "Here is what we found, and here is what the findings mean").

Policy and Historical Reviews. Articles should not exceed 3,500 words and 50 references. Use of subheadings in the main body of the text is recommended. Photographs and illustrations are encouraged. Provide a short abstract (150 words), 1-sentence summary, and biographical sketch. Articles in this section include public health policy or historical reports that are based on research and analysis of emerging disease issues.

Dispatches. Articles should be no more than 1,200 words and need not be divided into sections. If subheadings are used, they should be general, e.g., "The Study" and "Conclusions." Provide a brief abstract (50 words); references (not to exceed 15); figures or illustrations (not to exceed 2); tables (not to exceed 2); and biographical sketch. Dispatches are updates on infectious disease trends and research that include descriptions of new methods for detecting, characterizing, or subtyping new or reemerging pathogens. Developments in antimicrobial drugs, vaccines, or infectious disease prevention or elimination programs are appropriate. Case reports are also welcome.

Research Letters Reporting Cases, Outbreaks, or Original Research. EID publishes letters that report cases, outbreaks, or original research as Research Letters. Authors should provide a short abstract (50-word maximum), references (not to exceed 10), and a short biographical sketch. These letters should not exceed 800 words in the main body of the text and may include either 1 figure or 1 table. Do not divide Research Letters into sections.

Letters Commenting on Articles. Letters commenting on articles should contain a maximum of 300 words and 5 references; they are more likely to be published if submitted within 4 weeks of the original article's publication.

Commentaries. Thoughtful discussions (500–1,000 words) of current topics. Commentaries may contain references (not to exceed 15) but no abstract, figures, or tables. Include biographical sketch.

Another Dimension. Thoughtful essays, short stories, or poems on philosophical issues related to science, medical practice, and human health. Topics may include science and the human condition, the unanticipated side of epidemic investigations, or how people perceive and cope with infection and illness. This section is intended to evoke compassion for human suffering and to expand the science reader's literary scope. Manuscripts are selected for publication as much for their content (the experiences they describe) as for their literary merit. Include biographical sketch.

Books, Other Media. Reviews (250–500 words) of new books or other media on emerging disease issues are welcome. Title, author(s), publisher, number of pages, and other pertinent details should be included.

Conference Summaries. Summaries of emerging infectious disease conference activities (500–1,000 words) are published online only. They should be submitted no later than 6 months after the conference and focus on content rather than process. Provide illustrations, references, and links to full reports of conference activities.

Online Reports. Reports on consensus group meetings, workshops, and other activities in which suggestions for diagnostic, treatment, or reporting methods related to infectious disease topics are formulated may be published online only. These should not exceed 3,500 words and should be authored by the group. We do not publish official guidelines or policy recommendations.

Photo Quiz. The photo quiz (1,200 words) highlights a person who made notable contributions to public health and medicine. Provide a photo of the subject, a brief clue to the person's identity, and five possible answers, followed by an essay describing the person's life and his or her significance to public health, science, and infectious disease.

Etymologia. Etymologia (100 words, 5 references). We welcome thoroughly researched derivations of emerging disease terms. Historical and other context could be included.

Announcements. We welcome brief announcements of timely events of interest to our readers. Announcements may be posted online only, depending on the event date. Email to eideditor@cdc.gov.

In This Issue

Synopsis

Research

Dispatches

ISSN 1080-6040

DEPARTMENT OF HEALTH & HUMAN SERVICES
Public Health Service
Centers for Disease Control and Prevention (CDC)
Mailstop D61, Atlanta, GA 30329-4027

Official Business
Penalty for Private Use $300
Return Service Requested

MEDIA MAIL
POSTAGE & FEES PAID
PHS/CDC
Permit No. G 284